Nanovibrational stimulation for 3D osteogenesis in biphasic 3D scaffold; A new option for bone tissue engineering

Wich Orapiriyakul

M.D., F.R.C.O.S.T.

Submitted in fulfilment of requirements for the degree of Doctor of Philosophy (PhD)

Centre for the Cellular Microenvironment
Institute of Molecular, Cell and Systems Biology
College of Medical, Veterinary and Life Sciences
University of Glasgow
Glasgow, G12 8QQ

January 2020

Abstract

In our centre, we had developed nanovibrational bioreactor generating nanoscale vibration by piezo actuator for bone tissue engineering. Recently, nanovibrational stimulation (NS; 30 nm at 1000 Hz) showed the success of osteogenic induction in mesenchymal stem cells (MSCs) seeded collagen hydrogel without chemical supplement. However, culturing MSCs in the collagen hydrogel for long term NS stimulation in NS bioreactor is challenging due to its mechanical properties. The principle aim of this thesis is to develop the scaffold for nanovibrational bioreactor which is suitable for surgical application. Three strategies including in-gel scaffolds, collagen concentration optimization and genipin crosslinking were trialled which aimed to improve hydrogel stiffness and handleability, possess biocompatibility and allow NS force transmission.

The role of high amplitude stimulation (90 nm at 1000 Hz) on 3D osteogenesis was also studied. Interestingly, increasing NS amplitude successfully enhanced 3D osteogenesis through multiple pathways and it was biologically safe. Metabolomics during NS revealed the evidence of low level of reactive oxygen species production and inflammation which was controlled in physiological level through multiple intracellular signals such as redox balancing, NFκB and MAPK pathways.

To propose the technique how to use NS induced MSCs for clinics, MSCs seeded biphasic scaffolds compositing collagen hydrogels and freeze dried collagen sponges were developed. Cell-hydrogel-sponge composite (CHSC) was reproducible, handleable and biologically safe. CHSC allowed a good fidelity of NS. NS with high amplitude stimulation successfully induced 3D osteogenesis. NS protocol in CHSC was optimized in order to identify a stimulating duration which can induce osteogenesis without phenotypic reversibility. Interestingly, two-week stimulation possibly committed MSCs in the preosteoblast stage.

Table of Contents

List of Tables

List of Figures

Acknowledgement

I sincerely thank Prof. Matthew Dalby and Dr. Penelope M Tsimbouri for their patience, great supervisions and supports and also thank Prof. Stuart Reid for suggestions and supports on nanovibrational bioreactor.

I would like to thank Prof. Richard Oreffo (Bone and Joint Research Group, University of Southampton) for providing MSCs, Prof. Elizabeth K Tanner (Queen Mary University of London) for collagen sponge suggestions, Dr. Peter Childs (University of Glasgow), Dr. Shaun Robertson and Dr. Paul Clampsie (University of Stratclyde) for their suggestions and facilitating on bioreactor.

Also thank Dr. Mathis Riehle and Dr. Catherine Berry (CeMi) for warm welcome and facilitating many things in lab, Dr. Manlio Tassieri for great helps on rheology works, Dr. Marc Antoni Fernandez-Yague (Ireland, Galway) for processing protein antibody microarray, Dr. Gavin Blackburn for Metabolomics help and Ms Carol-Anne Smith for many helps in lab. Moreover, I would like to thank and recognize the supports of my colleagues (Ewan, Jing Li, Tom, Virginia, Nuttaporn, Yinbo) in the CeMi.

I would like to thank the Thai Government and Faculty of Medicine, Prince of Songkla University for giving the opportunity to study at University of Glasgow. I respectfully thank Asst. Prof. Kanyika Chamniprasas M.D. and Assoc. Prof. Puttisak Puttawibul M.D. for all supports and giving opportunities, also thank Dr. Somyot Chirasatitsin and Asst. Prof. Dr. Surapong Chatpun (IBME, PSU), orthopedic staffs (PSU), IBME (PSU) and my family for all helps.

Publication

Tsimbouri PM, Child.PG, Pemberton GD, Yang J, Jayawarna V, Orapiriyakul W, Burgess K, Gonzalez-Garcia.C, Blackburn G, Thomas D, Vallejo-Giraldo C, Biggs MJP, Curtis AG, Salmeron-Sanchez M, Reid S, Dalby MJ. 3D osteogenesis of mesenchymal stem cells stimulated by nanovibrational bioreactor in vitro. Nature Biomedical engineering. Elsevier. 2017;1:758-70.

Awards

Award winner in Medical Science of Anglo-Thai Society Educational Awards for Excellence, 2018.

Presentations

Podium presentations

30th Annual Conference of the European Society for Biomaterials (ESB) 9-13th September 2019, Dresden, Germany

28th Annual Conference of the European Society for Biomaterials (ESB) 4-8th September 2017, Athens, Greece

4th AO Trauma Asia Pacific Scientific Congress 24-25th May 2019, Taipei, Taiwan

Poster presentations

5th TERMIS World Congress 2018, 4-7th September 2018, Kyoto, Japan

29th European Conference on Biomaterials (ESB 2018), 9-13th September 2018, Maastricht, Netherlands.

Glasgow Orthopaedic Research Initiative (GLORI 2018), 23th February 2018, Glasgow, UK.

FEBS Workshop Biological Surfaces and Interfaces: Interface Dynamics, 2nd-7th July 2017, Sant Feliu de Guixols, Catalonia, Spain

10th UK Mesenchymal Stem Cell Meeting, 5th December 2016 York, UK.

British Orthopaedic research Society (BORS), UK, 5-6th September 2016, Glasgow, UK

Author's Declaration

I declare that, this thesis is my own work except where explicit reference is made to the contribution of others and has not been submitted for any other degree.

Wich Orapiriyakul

January 2020

Definition and abbreviations

Abbreviation	Name	Definitions and functions	Chapters
AA	Arachidonic acid	AA is a polyunsaturated omega-6 fatty acid converted from linoleic acid. AA is the precursor of eicosanoids which plays role in inflammation.	5
AC	Adenylate cyclase	Enzyme which is regulated by G proteins and calcium ions.	4
Acetyl-CoA	Acetyl coenzyme A	A molecule which is derived from carbohydrate, and fatty acid metabolism. Acetyl-CoA enters TCA cycle generating NADH and CO_2.	5
ACC1 and 2	Acetyl-CoA carboxylases	Enzyme converts acetyl-CoA to malonyl-CoA for fatty acid synthesis.	5
AKT	Protein kinase B (PKB)	AKT is serine/threonine-specific kinase. AKT controls cell survival, metabolism and NFκB.	5
ALP	Alkaline phosphatase	Enzyme which is present in many tissues including bone. ALP regulates phosphate ion initiating mineralization.	1-6
Atf6	Activating transcription factor 6	Atf6 is an endoplasmic reticulum membrane-bound bZIP transcription factor. Atf6 plays role on osteogenesis by regulating RUNX2.	4
ATGL	Activating adipose triglyceride lipase	Enzyme, found in lipolysis, which breaks down triacylglycerol and promotes fatty acid oxidation.	5
ATP	Adenosine triphosphate	Organic chemical which provides energy. ATP is produced by glycolysis, TCA cycle and ß-oxidation.	1, 5
AMPK	AMP-activated protein kinase	AMPK functions as energy sensor. AMPK activation promotes catabolism producing energy, syntheses anti-oxidants as well as reduces anabolism.	5
BC	ß-catenin	Protein which involves in many cellular pathways. In bone, with canonical Wnt, ß-catenin promotes early phase of osteogenesis.	1, 4, 5
BMP2	Bone morphogenetic protein 2	Protein which plays role in bone development.	1, 4, 5
BMPR1a	Bone morphogenetic protein receptor type 1A	BMPs receptor which plays role in bone and cartilage development.	4

Abbreviation	Name	Definitions and functions	Chapters
ß-oxidation	Beta-oxidation	The process which breakdowns fatty acid to produce acetyl-CoA in turn entering TCA cycle.	5
cAMP	Cyclic adenosine monophosphate	Molecule which is synthesised from ATP by AC. cAMP interacts with protein kinase A regulating TRP channels.	4
CaMKs	Calmodulin-dependent kinase	Enzyme which interacts with Ca^{2+}/calmodulin (CaM) complex. Ca^{2+}/CaM complex binds to CAMKII in turn activating AP-1 to promote osteoblast differentiation.	4
CaSR	Calcium-sensing receptor	G-protein coupled receptor which controls calcium homeostasis and extracellular calcium.	5
CD105	Cluster of differentiation 105 (Endoglin)	CD105 is a co-receptor of TGF-ß and also expresses in endothelial cells.	1
CD11b	Cluster of differentiation 11b (Integrin alpha M)	Expresses in leukocytes.	1
CD14	Cluster of differentiation 14	CD14 is found in neutrophils, dendritic cells, and macrophages.	1
CD19	Cluster of differentiation 19	Expresses in B cell lymphocytes.	1
CD34	Cluster of differentiation 34	CD34 is found in hematopoietic cells, MSCs and endothelial progenitor cells	1
CD45	Cluster of differentiation 45 (protein tyrosine phosphatase receptor type C; PTPRC)	Commonly found in leukocytes.	1
CD73	Cluster of differentiation 73 (5'-nucleotidase; NT5E)	Expressed by stromal cells, dendritic cells and lymphocyte.	1
CD79	Cluster of differentiation 79	Expresses on B cell lymphocytes.	1
CD90	Cluster of differentiation 90	Found in non-lymphoid tissues e.g. neuron cells, fibroblasts, myoblast, and endothelial cells.	1
CDK	Cyclin dependent kinase	Protein kinase plays role in cell cycle regulation. ROS can also activate CDK.	5
Col1A1	Collagen type I alpha 1	ECM protein which is found in cartilage, bone and tendon.	1, 4

Abbreviation	Name	Definitions and functions	Chapters
COX	Cyclooxygenase	Enzyme which catalyses arachidonic acid to prostanoids e.g. thromboxanes and prostaglandins.	5
DAG	diacylglycerol	Secondary messenger which can activate PKC in turn regulating calcium ion channels.	4
DAMPs	Damaged-associated molecular patterns	Molecules which are produced by injured cells for noninfectious inflammatory response.	5
DHA	Docosahexaenoic acid	DHA (omega-3 fatty acid; 22:6(n-3)) is synthesised (by elongation and desaturation) from alpha-linolenic acid. DHA is converted from DPA and EPA.	5
Dlx5	Distal-less homeobox 5	Transcription factor plays role in osteogenesis.	4
DPA	Docopentaenoic acid	Omega-3 fatty acid consists of 22 carbons and 5 double bonds (22:5).	5
ECM	Extracellular matrix	Networks, produced by cells, which provide microenvironment to support cells.	1-6
EPA	Eicosapentaenoic acid	Omega-3 fatty acid consists of 20 carbons and 5 double bonds (20:5). EPA is elongated by Δ5 elongase to produce DPA.	5
ERK1/2	Extracellular signal-regulated kinase 1 and 2	ERK1/2 (MAPK members) is involved in many cellular processes such as proliferation, differentiation and migration.	1, 2, 4, 5
ESCs	Embryonic stem cells	Pluipotent stem cells which are derived from blastocyst after fertilization.	1
FAK	Focal adhesion kinase	Tyrosine kinase which plays role in integrin signaling.	1, 5
Fas	-	Fas or CD95 (APO-1) is a member of TNFs. Fas links to cytoskeleton.	5
FGF2	Fibroblast growth factor 2	Growth factor which is not only involved in many cell activities but also important for bone regeneration.	1
FHL2	Four and a half LIM domains protein 2	Protein which can interact with Wnt/ß-catenin pathway in turn promoting RUNX2 expression.	1

Abbreviation	Name	Definitions and functions	Chapters
FOXO	Forkhead box, class O	Transcription factor which regulates cellular stress and promote anti-oxidation. FOXO is regulated by AMPK-AKT pathway.	5
G3P shuttle	Glycerol-3-phosphate shuttle	Process which produces energy, generates NADH and bypasses complex I in electron transport chain. This shuttle links between glycolysis, lipogenesis and OXPHOS through G3P dehydrogenase (GPDH) enzyme.	5
GLUTs	Glucose transporters	Proteins promoting glucose transportation at cell membrane.	5
GPCRs	G protein coupled receptors	Receptors on cellular membrane which can recognize molecules such as ligands in turn activating intracellular signals.	5
GSH	Glutathione	GSH plays role as anti-oxidant via redox balancing.	5
GSK-3β	Glycogen synthase kinase 3-beta	Serine/threonine kinase which involves in glycogen synthesis. GSK-3β can decrease RUNX2 expression and Wnt/β-catenin.	1
GSSG	Glutathione disulfide	Oxidized form of GSH.	5
Hh	Hedgehog	Protein which plays role in osteoblast differentiation. Hh consists of Shh (sonic), Ihh (indian) and Dhh (desert).	1
HIF1α	Hypoxia-inducible factor 1-alpha	Transcription factor which plays role in MSCs differentiation and is regulated by oxygen condition.	5
HLA-DR	Human leukocyte antigen-DR isotype	Molecules which is found in antigen presenting cells and activated T-cells.	1
HMG-CoA reductase	β-Hydroxy β-methylglutaryl-CoA reductase	Enzyme in mevalonate pathway which involves in cholesterol synthesis.	5
H_2O_2	Hydrogen peroxide	Oxidizer which is used for oxidative stress induction.	5
IDO	Indoleamine 2,3-dioxygenase	Enzyme which promotes tryptophan degradation. IDO reduces inflammatory response and inactivates T-cell function.	5
IGF	Insulin like growth factor	Hormone which involves in proliferation and differentiation (including osteogenesis).	5

Abbreviation	Name	Definitions and functions	Chapters
IκB	Nuclear factor of kappa-light-chain-enhancer of B-cells inhibitor	Protein which binds to NFkB to inhibit NFκB function in resting stage. IκB degradation allows NFκB nuclear translocation.	1
IKKs	IκB kinases	Enzyme of NFκB pathway consists of IKKα, and IKKβ. Phosphorylated IKK complex degrades IκB.	1
IL-1	Interleukin-1	IL-1 plays role in inflammatory response commonly produced by inflammatory cells such as macrophages, monocytes and dendritic cells.	1, 5, 7
IL-6	Interleukin-6	Cytokine which plays role in both pro- and anti-inflammation. MSC can also secrete IL-6 to convert monocytes to M2 macrophages	1, 5, 7
IL-10	Interleukin-10	Cytokine which is produced by macrophage for anti-inflammatory effects.	1, 5
IL-11	Interleukin-11	IL-11 involves in osteoclastogenesis, neurogenesis and hematopoitic effect.	1
IL-18	Interleukin-18	Cytokine which involves in inflammation.	1
IP3	Inositol-1,4,5-triphosphate	IP3 promotes calcium release from endoplasmic reticulum (ER) via IP3 receptor.	4
Igβ1,5	Integrin β1, 5	Cell membrane receptors play role in cell adhesion.	4
iPSCs	Induce pluripotent stem cells	Pluripotent stem cells which are derived from somatic cells through transduction process using Oct, SOX, Klf2 and Myc factors.	1, 7
JAKs	Janus kinases	Tyrosine kinases which play role in bone development.	5
JNKs	c-Jun N-terminal kinases	JNK (MAPK member) responds to oxidative stress.	5
KCNK 2	Potassium channel subfamily K member 2 (TREK1)	Potassium channel which responds to mechanical stimuli.	4
KCNK 4	Potassium channel subfamily K member 4 (TRAAK1)	Potassium channel which is found in neuron relating to mechanical stimulation.	4

Abbreviation	Name	Definitions and functions	Chapters
LC-PUFAs	Long chain polyunsaturated fatty acids	Fatty acids (with 18 carbons or more) consisting of omega 3 and omega 6. LC-PUFAs are precursors of eicosanoids.	5
LINC complex	Linker of nucleus and cytoskeleton complex	Proteins on nuclear membrane which consist of SUN (links to lamin) and nesprin (links to actin).	1
LOX	Lipoxygenase	Enzyme which catalyses AA or LC-PUFAs to eicosanoids such as leukotrienes.	5
LR	Lipid raft	Plasma membrane which is composed of lipids, cholesterol and protein receptors. Clusters of protein receptors in LR provide signals responding to the environment.	5
LRP5 and 6	Low-density lipoprotein-related receptor-5 and -6	Proteins on cellular membrane function as co-receptor of Frizzled receptor. LRPs sense to mechanical stimuli and activate Wnt canonical pathway.	1, 4
MAPK	Mitogen-activated protein kinase	MAPK (protein kinase) involves proliferation, differentiation, inflammation and apoptosis. MAPK consists of ERK1/2, JNK and p38.	1, 4, 5
MKP1	Mitogen-activated protein kinase phosphatase 1	Phosphatase enzyme which can downregulate MAPK signaling. MKP1 plays role in transdifferentiation of preadipocyte to osteoblast.	1
MSCs	Mesenchymal stem cells	Multipotent stem cells which can differentiate to osteoblast, chondrocyte, adipocyte and fibroblast. MSCs can be found in adiposed tissue (AMSCs), bone marrow (BM-MSCs), and cord blood (CB-MSCs).	1-7
Msx2	MSh homeobox 2	Transcription factor which promotes osteogenesis.	4
mTOR	Mammalian target of rapamycin	mTOR is a nutrient sensor for cells. mTOR is regulated by both AMPK and AKT thus balancing catabolic and anabolic pathways. mTOR plays role in growth function and survival.	5
NCX	Na^+/Ca^{2+} exchanger	Ion channel on plasma membrane which allows sodium ion influx exchanged with calcium ion efflux.	4

Abbreviation	Name	Definitions and functions	Chapters
NCKX	Na^+/Ca^{2+}-K^+ exchanger	Ion channel which allows sodium ion influx exchanged with calcium and potassium ion efflux.	4
NFκB	Nuclear factor kappa-light-chain-enhancer of activated B cells	Transcription factor which is known as a stress sensor regulating immune responses and survival pathways.	5
NLRs	NOD-like receptor	Receptor in cytoplasm which recognises PAMPs and DAMPs	5
NLRP3	NOD-like receptor protein 3	Receptor which senses to various inflammasomes and plays a role in immune system.	5
NO	Nitric oxide	Molecule which involves in cell proliferation, apoptosis and bone homeostasis.	5
NOS	Nitric oxide synthase	Enzyme produced endogenous NO. NOS can be found in endothelial cells (eNOS), central nervous system (nNOS), or induced by inflammation (iNOS).	5
NOX	Nicotinamide adenine dinucleotide phosphate oxidase (NADPH oxidase)	Enzyme on plasma membrane which catalyses NADPH to NADP which, in turn, produces ROS.	5
Nrf2	Nuclear factor erythroid 2-related factor2	Transcription factor which promotes anti-oxidative enzyme synthesis such as SOD and heme oxygenase 1(HO-1).	5
OCN	Osteocalcin	OCN is an osteoblast secreted hormone which regulates bone mineralization.	1-6
Omega-3	-	Polyunsaturated fatty acids with 3 double bonds (such as α-linolenic acid and DHA).	5
Omega-6	-	Polyunsaturated fatty acids with 6 double bonds (such as linoleic acid and AA).	5
ON	Osteonectin	ON is an osteogenic marker protein which can bind to collagen and hydroxyapatite to trigger mineralization process.	1-6
OPG	Osteoprotegerin	Protein which can bind to RANKL to inhibit RANK-RANKL interaction.	1
OSX	Osterix	OSX is a transcription factor which can regulate osteoblast commitment.	1-6

Abbreviation	Name	Definitions and functions	Chapters
OPN	Osteopontin	OPN is an extracellular matrix protein which can regulate mineralization and bone remodeling.	1-6
OXPHOS	Oxidative phosphorylation	The process of nutrient metabolism which produces ATP under aerobic condition in mitochondria.	5
P38	-	MAPK member which responds to stress.	1, 4, 5
PAMPs	Pathogen-associated molecular patterns	Molecules on bacteria or endotoxin which can be recognized by TLRs.	5
PC 1	Polycystin 1	PC1 is G-protein coupled receptor on cellular membrane. PC1 senses to fluid shear stress to regulate calcium ion channels.	5
PCL	Polycarpolactone	Biodegradable synthetic polymer which is commonly used in tissue engineering.	1
PDH	Pyruvate dehydrogenase	Enzyme which converts pyruvate to acetyl-CoA.	5
PDK1	Pyruvate dehydrogenase kinase 1	PDK1 is a HIF1α activated enzyme which can inactivate PDH.	5
PGE2	Prostaglandin E2	Inflammatory mediator which is derived from AA.	5
PDGF	Platelet-derived growth factor	Growth factor which plays role in MSC differentiation and angiogenesis. PDGF is found during normal bone healing.	1
PGA	Polyglycolic acid	PGA is a widely used synthetic biomaterial (such as suture). PGA is degradable by hydrolysis.	1
PHDs	Prolyl hydroxylases	Enzyme which inhibits HIF1α.	5
PI3K	Phosphoinositide 3-kinase	PI3Ks is an enzyme involving in cell functions. PI3Ks activates AKT in PI3K/AKT/mTOR pathway.	5
PIP_2	Phosphatidylinositol 4,5 – bisphosphate	PIP2 is a phospholipid of cell membrane. PIP2 is hydrolysed by PLC into DAG and IP3.	4
PKB	Protein kinase B	Refer to AKT.	5
PKC	Protein kinase C	Enzyme which plays role in intracellular calcium signals. PKC is activated by DAG and calcium ions.	1, 4, 5

Abbreviation	Name	Definitions and functions	Chapters
PLA	Polylactic acid	Biodegradable material which is commonly used for 3D printing material.	1
PLC	Phospholipase C	Enzyme which hydrolyses PIP2 to DAG and inositol-1,4,5-triphosphate (IP3).	4
PLGA	Poly (lactide-co-glycolide)	Biodegradable material which is derived from glycolic acid and lactic acid.	1
PMCA	Plasma membrane Ca^{2+} ATPase	PMCA is a plasma membrane protein driving calcium efflux. PMCA plays role in maintaining calcium ion level in cytoplasm.	4
PPARγ	Peroxisome proliferator-activated receptor γ	Master regulator of adipogenesis.	4
PPP	Pentose phosphate pathway	PPP is a glucose pathway which converts glucose-6-phosphate to ribose-5-phosphate and produces NADPH.	5
RANK	Receptor activator of nuclear factor kappa-B	Osteoclast receptor which can bind to RANKL promoting osteoclast differentiation.	5
RANKL	Receptor activator of nuclear factor kappa-B ligand	Membrane protein on osteoblast binds to RANK (on osteoclast) and OPG.	5
Ras	Rat sarcoma	Ras is a protein which regulates cytoskeleton, migration, cell differentiation and proliferation. Ras activates MAPK pathway.	5
RGD	Arg-Gly-Asp motif	Amino acid on ECM (such as fibronectin) which plays role on cell attachment interacting with intergrins.	1
ROCK	Rho-associated kinase	ROCK is a kinase enzyme which plays role in cell migration and cytoskeleton. Rho family consists of Rho, Rac and Cdc42.	1, 4, 5
ROS	Reactive oxygen species	Oxygen derived molecules such as superoxide anion and hydrogen peroxide which is produced at mitochondria or cell membrane (via NADPH oxidase).	1, 4, 5

Abbreviation	Name	Definitions and functions	Chapters
Ror2	Receptor tyrosine kinase-like orphan receptor 2	Tyrosine kinase receptor which plays role in bone homeostasis. Ror2 (on osteoclast) interacts with Wnt5a (from osteoblast) to promote osteoclastogenesis.	1
RUNX2	Runt-related transcription factor 2	Major transcription factor of osteogenesis.	5
RyR	Ryanodine receptors	Calcium ion channel on endoplasmic reticulum which releases calcium ion from storage to cytosol.	4
SERCA	Sarco-endoplasmic reticular Ca^{2+}-ATPase	Ca2+ ATPase allows cytosolic calcium to storage in sarco- or endoplasmic reticulum. SERCA can be found in many cell types such as myocyte (most common), cardiocyte and monocyte.	4
SMAD1/5	-	Proteins which involves in BMP canonical pathway for osteogenesis.	1, 4, 5
SMAD2/3	-	With canonical TGF-β, SMAD2/3 promotes early osteogenesis	1
SOD	Superoxide dismutase	SOD is an anti-oxidant enzyme which is found in cytoplasm (ZnSOD) and mitochondria (MnSOD).	5
Src	Steroid receptor coactivator	Src (intracellular tyrosine kinase) plays many roles in cellular responses. Src activates FAK phosphorylation.	1
STATs	Signal transducer and activator of transcription proteins	STATs are transcription factors regulating bone homeostasis and skeletal development as well as controlling MSC proliferation.	5
SVCT2	Sodium dependent vitamin C transporter 2	SVCT2 is a glycoprotein which plays role in ascorbic acid (vitamin C) transportation.	1
TAZ	Transcriptional coactivator with PDZ-binding motif	TAZ is an effector of Hippo signaling pathway and plays role in mechanical sensing and phenotypic memory.	1, 4, 6
TBC1D1	Tre-2/USP6, BUB2, cdc16 domain family member 1	TBC1D1 is a protein regulating glucose transportation. AMPK increases glucose uptake via TBC1D1 phosphorylation in turn promoting GLUT1 and 4 membrane localization.	5

Abbreviation	Name	Definitions and functions	Chapters
TCA	Tricarboxylic acid cycle	Biochemical pathway which oxidizes Acetyl-CoA in order to generate NADH to enter OXPHOS for ATP production.	5
TGF-β	Transforming growth factor beta	Cytokine which promotes osteoprogenitor proliferation and early osteoblastic differentiation.	5
TLRs	Toll-like receptor	TLRs are membrane receptors on leukocyte. TLRs recognise to PAMPs in turn activating immune responses.	5
TNFα	Tumor necrosis factor alpha	Cytokine which involves inflammatory responses. TNFα inhibits osteoblast and promotes osteoclastogenesis.	5
TRAF6	Tumor necrosis factor receptor associated factor 6	TRAF6 is a mediator of NFκB and MAPKs involving in immunological and inflammatory responses.	1
TRPA1	Transient receptor potential Ankyrin 1	Ion channel which senses to pain and oxidative stress.	4
TRPM	Transient receptor potential melastatin	Ion channel which senses to heat.	4
TRPP	Transient receptor potential polycystin	Refer to polycystin.	4
TRPV1	Transient receptor potential vanilloid type 1	Calcium and sodium ions channel which senses to temperature and pain.	1-5
TXAs	Thromboxanes	Eicosanoids play roles in vasoconstriction and platelet aggregation.	5
VEGF-D	Vascular endothelial growth factor D	Growth factor which plays role in angiogenesis. VEGF-D also promotes osteoblast differentiation.	5
VEGFR3	Vascular endothelial growth factor receptor 3	VEGFR3 is a VEGF receptor which can be found in osteoblast. VEGFR3 can recognise VEGF-D.	5
VGCCs	Voltage-gated calcium channels	Calcium ion channels on cell membrane which allow calcium influx activated by depolarization.	4
VHL	Von Hippel-Lindau ubiquitin ligase	VHL binds to prolyl hydroxylase domain (PHD) and factor inhibiting hypoxia-1 (FIH-1) in order to inhibit HIF-1α under normoxic condition.	5

Abbreviation	Name	Definitions and functions	Chapters
Wnt	Wingless-related integration site	Wnt is a protein which is recognised by Frizzled receptor. Wnt signaling pathway promotes osteogenesis in early phase.	1, 4, 5
YAP	Yes-associated protein	Transcriptional factor which is related to skeleton and phenotypic memory. YAP is regulated by hippo pathway.	4, 6

Chapter 1 Introduction

Chapter 1 Introduction to nanovibrational stimulation

1.1 From Bedside to Bench; What do orthopaedic surgeons want from bone tissue engineering?

Nowadays, introducing tissue engineered bone substitutes for clinical orthopaedic applications is challenging. There are a diversity of indications that could use bone substitutes such as spinal fusion, nonunion, etc (Baldwin et al., 2019). However, the most difficult situation is the segmental bone defect resulting from a traumatic event or bone tumor removal. Because of the large defect complicated with poor surrounding tissue, many orthopaedic patients suffer from the long-term process of treatment, multiple operations and surgical complications (L., C., J., A., & Baldy, 2010).

The most popular and effective surgical technique for large bone defect treatment is the distraction osteogenesis by external ring fixator, invented by Professor GA. Illizarov (Spiegelberg et al., 2010). Distraction osteogenesis provides a successful approach for large bone defect treatments (Aktuglu, Erol, & Vahabi, 2019). However, there are many drawbacks. For instance, awkward, heavy and long-term application of the ring frame makes patients feel uncomfortable. In addition, the external rods and pins may introduce pathogens into the bone which may then develop into a pin track infection and osteomyelitis. Also, the patient's self administered daily distraction adjustment may also lead to unfavorable outcomes (Kempton, McCarthy, & Afifi, 2014; Lascombes, Popkov, Huber, Haumont, & Journeau, 2012; Paley, 1990).

The induced membrane technique (IMT) is a another strategy for treatment of the segmental bone loss proposed by Masquelet et al (Giannoudis, Faour, Goff, Kanakaris, & Dimitriou, 2011; A. C. Masquelet & Begue, 2010). IMT is a two-staged procedure (A. Masquelet, Kanakaris, Obert, Stafford, & Giannoudis, 2019). Polymethyl- methacrylate (PMMA) is implanted at the bone defect in turn allowing the host to create membrane encapsulation. At the second stage, the PMMA spacer is removed. The bone void is filled with autologous bone graft (Giannoudis et al., 2011). Nevertheless, this technique requires an abundance of bone graft which inevitably leads to donor site morbidity, causing fracture and pain (Stafford & Norris, 2010). In large defects, chemical supplements such as BMPs may be required to improve healing (Giannoudis et al., 2011).

Biologically, the induced membrane is comprised of fibroblast, blood vessels and inflammatory cells (Christou, Oliver, Yu, & Walsh, 2014). This membrane produces bone morphogenetic protein-2 (BMP-2), vascular endothelial growth factor (VEGF) and transforming growth factor β1 (TGF-β1) during week 4-6 (Pelissier, Masquelet, Bareille, Pelissier, & Amedee, 2004; X. Wang, Wei, Luo, Huang, & Xie, 2015). However, clinical outcomes of the IMT for bone defect treatment is varied (A. C. Masquelet, 2003; Niccolai, Di Mento, Mocchi, & Berlusconi, 2018; R., M., A., & I., 2017; J. Wang, Yin, Gu, Wu, & Rui, 2019). In the future, a combination of the IMT with stem cells and tissue engineering concepts may potentially improve the outcome of large bone defect treatments (Dilogo, Primaputra, Pawitan, & Liem, 2017; Viateau et al., 2010).

1.2 Bone structure and bone marrow cells niche

Bone structurally consists of cortical bone (compact bone) and cancellous bone (spongy or medullary bone) (Clarke, 2008). Histologically, bone can be classified into woven (immature, disorganized collagen fiber) and lamellar bone (mature, organized collagen fiber) (Tzelepi, Tsamandas, Zolota, & Scopa, 2009).

Cortical bone is an outer and dense part of bone. Cortical bone consists of osteons (or Haversian system) which is a lamellar mineralized matrix. Osteocytes reside in osteons and communicate each other through canaliculi (Hideki Yoshikawa, Tsumaki, & Myoui, 2009). The lamellar structures of osteons surround the haversian canels where mesenchymal stem cells, vessels and nerves are located. Vessels in haversial canels play role on transferring oxygen and nutrients to osteocytes (Khurana & Safadi, 2010).

Endosteum, lining at the inner layer of cortical bone, consists of MSCs, pre-osteoblasts, osteoblasts, fibroblast. Lining osteoblasts play interactive roles with hematopoietic stem cells (HSCs) in medullary canel (Lévesque, Helwani, & Winkler, 2010). Surfaces of lamellar bone are lined with quienscent osteoblasts. Osteoclasts formed a Howship's lacunae on endosteum to resorb bone mineralized matrix for enhancing bone homeostasis and remodelling (Safadi et al., 2009).

Cancellous bone (medullary bone) is trabecular network of lamellar bone (Tzelepi et al., 2009). Cancellous bone is filled with bone marrow (BM) consisting of hematopoietic cells (red marrow) and adipose tissue (yellow marrow). BM consists of osteoprogenitor cells, osteoblast, osteoclast precursor cells, haematopoietic stem cells

(HSCs), stromal cells, MSCs, adipocytes, endothelial cells and nerve cells (Travlos, 2006).

In BM, MSCs plays role not only in bone regeneration but also supporting HSCs (Crippa & Bernardo, 2018; Frenette, Pinho, Lucas, & Scheiermann, 2013). At endosteum (endosteal niche), HSCs interact with osteoblasts, MSCs and adipose tissues affecting on HSCs mobilization, quiescence, and differentiation (Lévesque et al., 2010). BM adipose tissue also links to bone metabolism (Yujue Li, Meng, & Yu, 2019). BM is vascularized by medullary artery, arterioles, capillary and sinusoids. Many cells, e.g. endothelial cells, CXCL12 abundant reticular cells, pericytes and megakaryocytes, are resided nearby sinusoids creating vascular niche. Vascular niche plays important roles on HSCs growth and functions. (Lilly, Johnson, & Bunce, 2011; Tamma & Ribatti, 2017).

1.3 Bone healing: What can we learn from nature?

Bone healing is a dynamic process involving vascularization, cartilage and osteogenic differentiation and then mineralization. Thus, understanding the natural bone healing process could help in developing synthetic bone substitutes. Vascularization, linking to oxygen conditioning (Y. Wang et al., 2007), is a key modulator of bone healing (Drager, Harvey, & Barralet, 2015; Marenzana & Arnett, 2013). Hypoxic condition suits chondrogenic differentiation (Schipani, 2006) while normoxic conditions promotes osteoblast differentiation (Shyh-Chang, Daley, & Cantley, 2013). Considering orthopaedic fixation treatment, fracture reduction and fixation stability affect vascularization and thus fracture healing (Claes, Eckert-Hubner, & Augat, 2003; Lienau, Schell, Muchow, & Duda, 2004). In primary bone healing, internal fixation with fracture compression technique restores blood flow thus enhancing osteogenic differentiation. While in secondary bone healing, relative stability allows interfragmentary micromotion (Perren, 2002). Gaps at the fracture site represent vascular disruption indicating hypoxic conditions (Kunze, Hofstetter, Posalaky, & Winkler, 1981). Hypoxic condition initially promotes chondrogenesis thus enhances enchondral ossification. Osteogenesis and mineralization then occur after intensive vascularization (Claes, Recknagel, & Ignatius, 2012). Bone healing consists of 3 stages, inflammation, reparation and remodelling **(Figure 1.1)**.

1.3.1 Inflammatory phase

The inflammatory phase occurrs within 24 hours to 1 week in order to activate and recruit essential cells such as MSCs and immune cells into the fracture site to enhance regeneration (Jiliang Li, Kacena, & Stocum, 2019). At the fracture site, a hematoma is formed to create a fracture niche. Surrounding injured tissues generate inflammatory signals and cytokines preparing adjacent structures for the healing process such as vasodilation and increase vessel permeability (Ryan E. Tomlinson & Silva, 2013). Inflammatory cytokines such as tumor necrosis factor alpha (TNFα), interleukin-1 (IL-1), IL-6, IL-11 and IL-18 (Giannoudis et al., 2015) are secreted aiming to promote vascularization, and recruit cells to fracture sites such as macrophages (eliminating death cells via phagocytosis) and precursor cells (such as MSCs) which are essential for bone healing and angiogenesis (Giannoudis et al., 2015; Florence Loi et al., 2016).

1.3.2 Reparation phase

The reparation phase is affected by fracture niche including fracture gap (Claes et al., 2003; Meeson et al., 2019), interfragmentary micromotion (Elliott et al., 2016) and vascular supply at fracture site (Marenzana & Arnett, 2013; Ryan E. Tomlinson & Silva, 2013). In the reparation phase, woven bone (immature bone) is developed from a soft (cartilaginous) callus to become a hard (mineralized) callus (J. Li et al., 2019). The fracture characteristics can also influence the applied fracture fixation technique and mode of bone healing.

1.3.2.1 Direct fracture healing

Direct fracture healing (primary bone healing) occurs when the fracture is simple with less periosteal injury, thus preserving periosteal blood supply (Ryan E. Tomlinson & Silva, 2013). This type of fracture can be anatomically reduced and an absolute stability of fixation can be achieved (Perren, 2002). After reduction, the haversian system is restored allowing intraosseous blood flow. Normoxic condition then induces MSC to osteogenic cell fate (Shyh-Chang et al., 2013). Direct fracture healing can be divided into contact healing (gap < 10 μm) and gap healing (gap 800 μm-1 mm) (Marsell & Einhorn, 2011). The process of contact healing involves a direct remodelling process (via the cutting cone (Eriksen, 2010)),

while gap healing generates lamellar bone to fill the gap before bone remodelling (Marsell & Einhorn, 2011).

1.3.2.2 Indirect fracture healing

Indirect bone healing (secondary bone healing) occurs in comminuted fractures where some fixation stability has been achieved (Perren, 2002). This mode of bone healing involves both intramembranous and endochondral bone healing (Marsell & Einhorn, 2011). At the fracture gap, recruited MSCs produce various growth factors such as transforming growth factor beta (TGF-β; involved in chondrogenesis), BMPs (promoting osteogenesis), VEGF (angiogenesis), platelet-derived growth factor (PDGF; cell migration), and fibroblast growth factor 2 (FGF2; angiogenesis) (Ghiasi, Chen, Vaziri, Rodriguez, & Nazarian, 2017). At 2-6 weeks, a soft callus, consisting of blood vessels, cartilage and spongy bone, is formed and, in turn, is mineralized to a hard callus (Holmes, 2017).

1.3.3 Remodelling

After the reparation phase, active osteoclasts remodel woven bone to lamellar bone restoring the harversian system (Eriksen, 2010). Osteoclasts attach on to bone, form a ruffled membrane as well as secreting H^+, ATPase and Cathepsin K in vesicles in order to degrade mineralized bone (Boyle, Simonet, & Lacey, 2003; Rucci, 2008). In this phase, high levels of inflammatory cytokines such as IL-1 and TNFα can be found (Marsell & Einhorn, 2011).

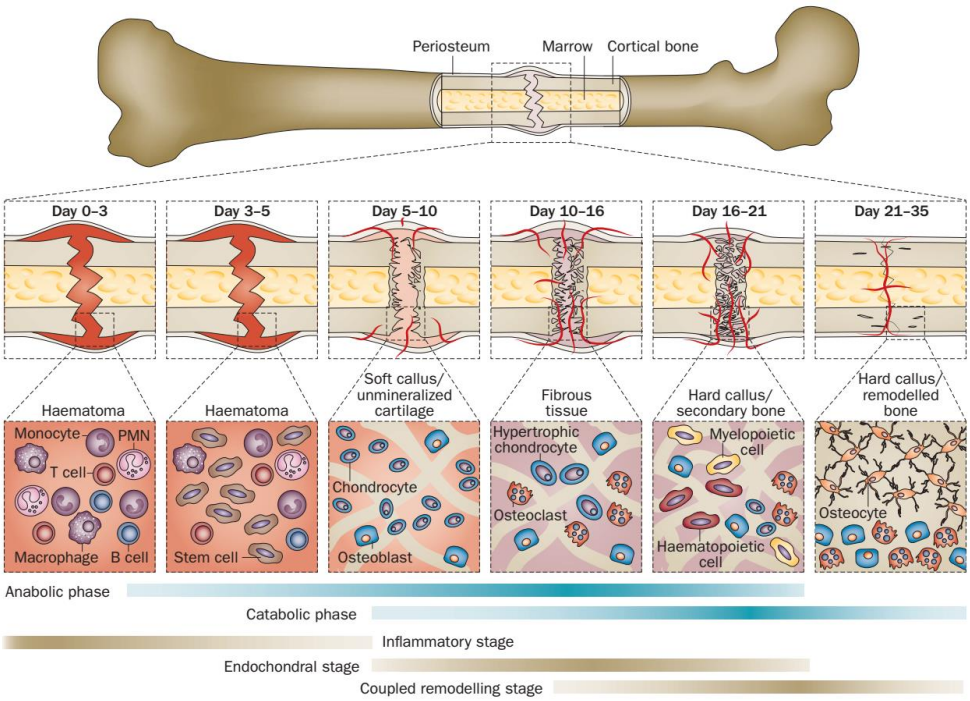

Figure 1.1 Phase of bone healing

In the inflammatory phase, a hematoma is formed. Precursor cells are recruited to the fracture site. After that, granulation tissue is formed, in turn developing soft and hard callus in the reparation phase. Vascularization is also found in this phase. Bone remodelling occurs after hard callus formation. (With permission of Einhorn., et al 2015 (Einhorn & Gerstenfeld, 2015))

1.4 Osteogenic pathways

Diverse osteogenic pathways are orchestrated at specific time points (James, 2013; Javed, Chen, & Ghori, 2010) and the same pathways may provide different functions at different stages of osteoblast development. Major pathways involved in osteogenesis include TGF-β, BMPs, Hedgehog, Wnt and Notch are reviewed below **(Figure 1.2)**.

1.4.1 TGF-β signaling pathway

TGF-β promotes proliferation and osteoblast commitment in mammalian development (G. Chen, Deng, & Li, 2012). TGF-β consists of canonical (using TGF-β ligand via SMAD2/3) and non canonical (via p38; mitogen-activated protein kinase; MAPK pathways (M. Wu, Chen, & Li, 2016)). TGF-ß (e.g. TGF-ß1) coordinates between bone formation and bone remodeling by recruiting MSCs to the resorption area showed in *in vitro* and *in vivo* studies (Y. Tang et al., 2009). TGF-ß also itself induces progenitor cell proliferation and differentiation *in vitro* and *in vivo studies* (Matsunobu et al., 2009; Salkın, Gönen, Ergen, Bahar, & Çetin, 2019). In *in vitro* studies, canonical TGF-ß (via SMADs) promotes early phase osteogenic differentiation but inhibits mineralization and maturation of osteoblasts (S. Maeda, Hayashi, Komiya, Imamura, & Miyazono, 2004; M. Wu et al., 2016). In *in vitro* studies, optimal levels of TGF-ß promote osteoclast migration and differentiation. However, high levels of TGF-ß inhibit osteoclast differentiation (Itonaga et al., 2004; Pilkington, Sims, & Dixon, 2001; M. Wu et al., 2016; Yasui et al., 2011).

1.4.2 BMPs signaling pathway

BMPs are members of the TGF-β superfamily. BMPs relay signals through SMAD-dependent and SMAD–independent (MAPK) pathways to enhance osteogenesis (M. Wu et al., 2016). BMP2 and BMP7 have been commonly used in orthopaedics (Conway, Shabtai, Bauernschub, & Specht, 2014; Cook, Salkeld, Patron, & Rueger, 2000; S.D., T.A., H.S., S.E., & Sofamor, 2002; Suk, 2008) and dentistry (Taşlı, Aydın, Yalvaç, & Şahin, 2014). In *in vitro and in vivo* studies, BMP2 enhances RUNX2 through SMADs 1/5/8 for osteogenesis (Kopf, Petersen, Duda, & Knaus, 2012; Phimphilai, Zhao, Boules, Roca, & Franceschi, 2006; Retting, Song, Yoon, & Lyons, 2009). BMP2 also enhances osteocalcin (OCN) (Jang et al., 2012), osteopontin (OPN) *in vitro* (X. Yang et al., 2009), as well as promoting alkaline phosphatase (ALP) through the MAPK pathway (W. Huang, Yang, Shao, & Li, 2007). In *in vivo* study, BMP7 also enhances osteogenesis (Cook et al., 2000). In *in vitro* studies, BMP 7 promotes ALP and mineralization (Xue et al., 2015; Yeh, Tsai, & Lee, 2002). BMP/SMAD signalling induces early phase osteoblast differentiation while SMAD-independent (MAPK) promotes osteogenic differentiation and bone development by phosphorylating

RUNX2 and thus stimulating osterix (OSX) (Rahman, Akhtar, Jamil, Banik, & Asaduzzaman, 2015; M. Wu et al., 2016).

1.4.3 Hedgehog signaling pathway

Hedgehog (Hh) signaling plays important roles in bone development and osteoblast differentiation in mammals (Jing Yang, Andre, Ye, & Yang, 2015). Hh signaling consists of Sonic hedgehog (Shh), Indian hedgehog (Ihh) and Desert Hedgehog (Dhh). Shh and Ihh play pivotal roles in skeletal development. Shh modulates osteogenic differentiation, bone homeostasis and angiogenesis as well as anti-adipogenesis (James et al., 2010; Lamplot et al., 2013). Ihh is important for enchondral ossification. Ihh triggers both chondrogenesis and osteogenesis during enchondral ossification (Ohba, 2016; Razzaque, Soegiarto, Chang, Long, & Lanske, 2005). Hh and Wnt are reciprocally antagonists (M. Ding & Wang, 2017; Song, Li, Liu, & Zhao, 2015).

1.4.4 Wnt signaling pathway

Wnt signaling is involved in cell proliferation, differentiation and migration (Barbáchano, Larriba, Ferrer-Mayorga, Muñoz, & González-Sancho, 2014). Canonical Wnt signals via β-catenin while non-canonical Wnt activates JNK or Rho pathways linked to the cytoskeleton (in Wnt/planar cell polarity signaling) as well as protein kinase C (in Wnt/Calcium signaling) (Niehrs, 2012). In canonical Wnt signaling, frizzled protein receptors and low-density lipoprotein receptor-related protein 5 (LRP5) senses mechanical stimulation regulating osteoblast differentiation showed in *in vivo* studies (H. Q. Gao et al., 2017; K. S. Kang & Robling, 2015; Y. Wang et al., 2014). Canonical Wnt with LRP5 promotes increase in bone density (Johnson, 2004; Krishnan, Bryant, & Macdougald, 2006; Norwitz, Mota, Misra, & Ackerman, 2019). As showed in *in vitro* and *in vivo* studies, the Wnt pathway promotes osteoblastic differentiation of MSCs in the early phase of osteogenesis but inhibits differentiation into mature osteoblasts (Eijken et al., 2008; Rodda & McMahon, 2006).

Wnt canonical and noncanonical signals also play roles in osteoclast differentiation (Yasuhiro Kobayashi, Shunsuke Uehara, Masanori Koide, & Naoyuki Takahashi, 2015). In *in vivo* and *in vitro* studies, osteoblasts secrete Wnt16 activating Wnt/β-catenin which, in turn, suppresses osteoclast differentiation through the receptor activator of nuclear factor kappa B/osteoprotegerin (RANKL/OPG) axis (Y. Kobayashi, G. J. Thirukonda, et al., 2015; Moverare-Skrtic et al.,

2014). However, non-canonical Wnt promotes osteoclast differentiation. Osteoblasts secrete Wnt5a binding to receptor tyrosine kinase Ror2 (Ror2) in osteoclast precursors promoting RANK in *in vivo* studies (Y. Kobayashi, S. Uehara, M. Koide, & N. Takahashi, 2015; Kobayashi, Uehara, & Udagawa, 2018; K. Maeda et al., 2012). It is noteworthy, however, that Wnt5a can also enhance osteoblast differentiation (via LRP5-6/Wnt/ β-catenin) in *in vitro* study (Okamoto et al., 2014). Noncanonical Wnt links to JNK. In *in vitro* study, Wnt5a/Ror2/JNK signaling suppresses osteoblasts which may prevent over-mineralization (Hasegawa et al., 2018). Wnt can crosstalk to many pathways (Y. Wang et al., 2014) such as BMPs (Y. Chen et al., 2007), Hedgehog (M. Ding & Wang, 2017), and Notch (Collu, Hidalgo-Sastre, & Brennan, 2014).

1.4.5 Notch signaling pathway

Notch signaling modulates osteogenesis, osteoclastogenesis and angiogenesis in mammals (Z. Luo et al., 2019). Notch inhibits differentiation in the early phase of osteogenesis by interacting with β-catenin, RUNX2 and OSX. Notch and RUNX2 are reciprocal antagonists as RUNX2 can inhibit Notch showing in *in vitro* study (Ann et al., 2011). By *in vitro* and *in vivo* study, Notch can also inhibit RUNX2 (through Hes, Hey proteins) maintaining progenitor cells (Hilton et al., 2008) as well as inhibiting Wnt/ β-catenin (Hayward, Kalmar, & Martinez Arias, 2008). However, in some *in vitro* literature studying in MG63, Notch has also been seen to upregulate RUNX2 and OSX (Ongaro et al., 2016). In *in vitro* study, Notch can suppress glycolysis in turn reducing oxidative phosphorylation and inhibiting osteogenic differentiation through lack of metabolic energy (S.-Y. Lee & Long, 2018). In late osteogenesis, activation of Notch in mature osteocytes promotes bone formation and mineralization showed in *in vitro* and *in vivo* studies (P. Liu et al., 2016). Notch promotes osteoclast maturation and bone remodelling in *in vitro* study(Ashley, Ahn, & Hankenson, 2015).

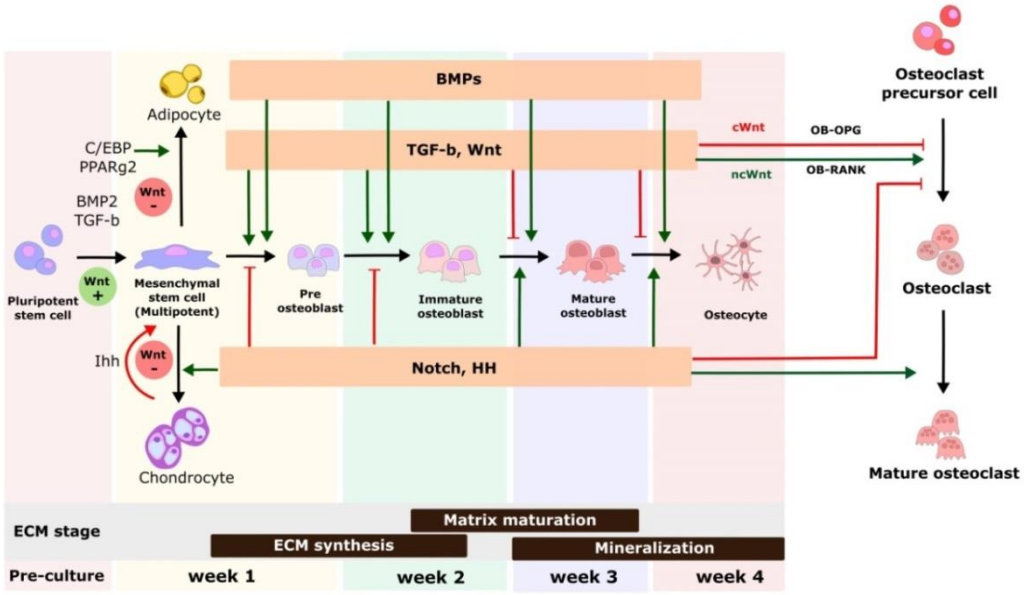

Figure 1.2 Interaction of BMPs, TGF-β, Wnt, Notch and Hedgehog pathways in osteogenesis and osteoclastogenesis

BMPs promote the process of osteogenic differentiation. In the early phase of osteogenesis, Wnt enhances the commitment of MSCs to preosteoblast thus promotes osteogenesis. In the late stage (mineralization), Wnt inhibits the maturation of osteoblasts. Wnt is involved in osteoclast differentiation via the RANK/OPG axis. Notch inhibits differentiation in early the phase of osteogenesis resulting in pooling of osteoblast progenitors. Notch also promotes maturation of osteoclasts. Hh is an antagonist to Wnt (green arrow; activation, red arrow; inhibition) (Eijken et al., 2008; Rahman et al., 2015; Regard, Zhong, Williams, & Yang, 2012; Rodda & McMahon, 2006; M. Wu et al., 2016).

1.5 Stem cell source for bone tissue engineering

Various stem cell types are extensively studied for their potential use in bone tissue engineering. However, driving stem cell based therapy into clinics is challenging. Many obstacles, including immunological responses, ethical issues, patient safety, tumorigenic potency, etc require intensive research before approval. The summary of advantages and disadvantages of available stem cell types is shown in **table 1.1**.

Table 1.1 Comparison the advantages and disadvantages of stem cell type.

	ESCs	IPSCs	BM-MSCs	CB-MSCs	ASCs	Osteoblast
Sources	embryos	Somatic cells	Bone marrow	Cord blood	Fat tissue	Bone graft
Proliferation capacity	Unlimited	Unlimited	Limited	Limited	Limited	Limited
Differentiation potency	Pluripotency	Pluripotency	Multipotent	Multipotent	Multipotent	Osteoblast
Osteogenic differentation capacity	Fair-Good	Fair-Good	Good	Good	Good	Very good
Preparation technique, isolation and expansion problems	Donor safety concern, Difficult isolation	Retroviral problem, Require large expansion	Senescence	Difficult isolation	Senescence, Multiple step of isolation	Senescence
Ethical issue	Yes (Embryo ternination)	No	No	No	No	No
Tumoriginicity	Yes	Yes	No	No	No	No
Immunogenic	Possibly	No (Autologous)	No (Autologous)	No (Autologous)	No (Autologous)	No

1.5.1 Embryonic stem cells

Embryonic stem cells (ESCs) are derived from the blastocytes of embryos. ESCs are pluripotent thus providing benefits of high proliferation (Kargozar et al., 2019). Human embryonic stem cell (hESC) research is growing (W. C. Chen et al., 2013; Kuhn et al., 2014), however, using hESCs in tissue engineering has ethical issues arising from termination of embryos issue and safety of donor oocytes (Lo & Parham, 2009). Moreover, the tumorigenic potency of ESCs is controversial (X. Wang et al., 2012).

ESCs can be osteogenically induced using standard osteogenic media (dexamethasone, ascorbic acid, and β-glycerolphosphate) (Boast & Stern, 2013). However, the osteogenic differentiation potency of ESC derived MSCs is controversial. Some studies showed that osteogenically induced ESCs provided comparable results for osteogenesis with bone marrow derived mesenchymal stem cells (BM-MSCs) (Arpornmaeklong, Brown, Wang, & Krebsbach, 2009). However, some literature reported less effective outcomes of osteogenic induction of ESCs compared to those of BM-MSCs (Brown, Squire, & Li, 2014). At present, hESCs are widely studied in bone tissue engineering (W. C. Chen et al., 2013; Marolt et al., 2012) and fracture healing induction (Undale et al., 2011).

1.5.2 Induced pluripotent stem cells (iPSCs)

Induced pluripotent cells (iPSCs) are derived from genetic reprogramming of somatic cells (such as fibroblasts) by transduction of Yamanaka's factors (Oct, Sox2, Klf4 and Myc) studied in mouse fibroblasts (K. Takahashi & Yamanaka, 2006) and human fibroblasts (K. Takahashi et al., 2007). iPSCs are pluripotent and posses unlimited self-renewal. As somatic cells are derived from an autologous donor, there is no genetic matching problem nor ethical issues (Kargozar et al., 2019; King & Perrin, 2014; Lo & Parham, 2009; Sugarman, 2008; Yousefi et al., 2016). However, there are critical hurdles towards clinical application such as teratogenicity (Gutierrez-Aranda et al., 2010; Mitchell, Wanczyk, Jensen, & Finck, 2019), drawbacks of using retrovirus transfection as well as reproducibility of transfection (Medvedev, Shevchenko, & Zakian, 2010).

There are many techniques for inducing iPSCs towards MSC and osteoprogenitor cells, such as through embryoid body formation or direct differentiation using osteogenic media (dexamethasone,

ascorbic acid, and β-glycerolphosphate) (Bastami et al., 2017; Illich et al., 2011). Osteogenic differentiation potency of iPSCs is comparable to MSCs (Bastami et al., 2017; Fliefel, Ehrenfeld, & Otto, 2018). iPSCs are also studied in many fields of tissue engineering such as cardiac disease treatment (Miyagawa & Sawa, 2018; Musunuru et al., 2018), and organoids (Ogura, Sakaguchi, Miyamoto, & Takahashi, 2018), etc. To introduce iPSCs into clinic in the future, pretreatment such as irradiation to reduce tumorigenesis may be required (Inui et al., 2017).

1.5.3 Mesenchymal stem cells (MSCs)

MSCs are the most popular stem cell source for bone tissue engineering. MSCs are multipotent, differentiating into osteogenic, chondrogenic, reticular and adipogenic lineages. The International Society for Cellular Therapy (Dominici et al., 2006) defined the characteristics of MSCs. MSCs must adhere on to tissue culture plates and be multipotent. Moreover, MSCs should express surface markers – they are positive for CD73, CD90, CD105 and negative for CD14, CD34, CD45 or CD11b, CD79α or CD19 and HLA-DR (Dominici et al., 2006). Stro1, another surface marker, is commonly used for enriching MSCs from the bone marrow (G. Lin et al., 2011; F. J. Lv, Tuan, Cheung, & Leung, 2014). Stro1 selected MSCs can differentiate into osteoblasts, chondrocytes, adipocytes fibroblasts and hematopoietic supporting cells such as vascular smooth muscle cells, thus they are suitable for the studies of osteogenesis together with angiogenesis (Dennis, Carbillet, Caplan, & Charbord, 2002; Melchiorri, Nguyen, & Fisher, 2014). MSCs can be harvested from many tissue sources such as bone marrow (BM-MSCs), adipose tissue (AMSCs) and cord blood (CB-MSCs). Among the three sources, osteogenic differentiation potency is comparable (Heo, Choi, Kim, & Kim, 2016; Rebelatto et al., 2008; Wagner et al., 2005).

1.6 MSC *in vitro* Microenvironments

Microenvironments play important roles in stem cell self-renewal or differentiation (Donnelly, Salmeron-Sanchez, & Dalby, 2018). Stem cell fate is influenced by various factors such as extracellular matrix, secreted factors, cell-to-cell interaction, inflammation, physical

factors (such as shearing and material stiffness) as well as hypoxia and metabolism (Lane, Williams, & Watt, 2014) **(Figure 1.3)**.

In material sciences, extracellular matrix is the keystone of microenvironment fabrication integrating all factors of MSCs niche for bone regeneration. Multiple modalities had been proposed to create MSC niches. For example, ECM physical modifications (such as tuning stiffness and topography) affect cell adhesion, cell cytoskeleton and, in turn, regulating cell growth (Dalby et al., 2007). Furthermore, integrating surface chemistry and growth factors on matrices can also promote cell adhesion and differentiation in *in vitro and in vivo studies* (Llopis-Hernández et al., 2016)(X. Zhao et al., 2017).

Cell-to-cell interaction is a part of the cellular niche. MSCs communicate to neighboring cells through cell adhesion molecules (such as tight junctions, gap junctions, adherens junctions (Hartsock & Nelson, 2008) or cytokines (J.-M. Zhang & An, 2007). Cell-to-cell interaction can occur between cells of the same phenotype or different cell types, for example, osteoblasts require connexin 43 for bone development (Moorer & Stains, 2017). Adhesions amongst different cells are also important in the bone marrow compartment, e.g. osteoblasts promote HSC functions (X. Gao, Xu, Asada, & Frenette, 2018) and osteoclast development (X. Chen et al., 2018; Sharaf-Eldin, Abu-Shahba, Mahmoud, & El-Badri, 2016).

The metabolic and oxygen niche also affect cell lineage. Oxygen links to hypoxic inducible factor 1-alpha (HIF-1α) controlling energy synthesis via balance of glycolysis and oxidative phosphorylation (Drager et al., 2015; Mohyeldin, Garzón-Muvdi, & Quiñones-Hinojosa, 2010). Moreover, inflammation and oxidative stress are also involved in cell differentiation (Bernardo & Fibbe, 2013; Kyurkchiev et al.,

2014). The role of oxygen, metabolism and oxidative stress are discussed in chapter 5.

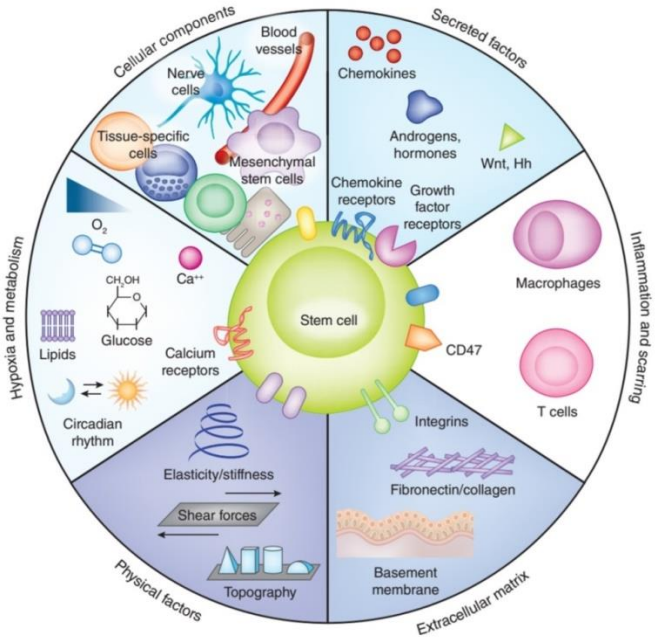

Figure 1.3 The stem cell niche

Stem cell niche consists of complex factors influencing on stem cell function and growth. For example, ECM and physical cues (e.g. topography and external force) involve stem cells through adhesion-cytoskeletal complex. Further, stem cells also interact and communicate to other cell types (via cytokines, etc) maintaining cellular function, and quiescence. Hypoxic condition also affects cellular metabolism and differentiation (With permission of Lane et al., 2014 (Lane et al., 2014)).

1.6.1 Extracellular matrix

Understanding the structure and components of ECM is essential for scaffold design and material selection. The ECM, where cells reside, plays important roles in cellular functions (Lozito, Kolf, & Tuan, 2009). In nature, ECM is composed of soluble factors (such as cytokines, growth factors) and insoluble components (e.g. glycoproteins, proteoglycans and proteins) (Kular, Basu, & Sharma, 2014). The insoluble components play roles in cell-ECM interaction, for example, collagens provide structural support relating to composite stiffness (Kular et al., 2014). Fibronectin, containing the cell binding domain Arg-Gly-Asp (RGD), is important for cell adhesion (J. Xu & Mosher, 2011). Currently, ECM modification for tissue

regeneraton is extensively studied. Designed ECM for bone tissue engineering must allow cell adhesion and should allow transmission of external mechanical signals.

1.6.1.1 Cell adhesion

Adhesion proteins, such as fibronectin and laminin, play pivotal roles in cell adhesion (J. Xu & Mosher, 2011). Cells use integrin to bind peptide motifs of adhesion proteins such as RGD to attach to the ECM. In *in vitro* study, controlling the density and patterning of RGD ligands can regulate the cell signaling pathways of MSC differentiation (Dalby, Gadegaard, & Oreffo, 2014). Another experimental study reported that patterned RGD ligands (distance <70 nm) can cluster integrins and promote focal adhesion formation (J. Huang et al., 2009). At the focal adhesion, integrins connect with actin binding proteins such as talin, vinculin, filamin and focal adhesion kinase (FAK) (Brakebusch & Fassler, 2003). Talin, connected to vinculin, controls the optimal force for maintaining the stability of cell-matrix adhesion (Neumann & Gottschalk, 2016; Yao et al., 2016). Vinculin, linking to actin, induces actin polymerization (Atherton, Stutchbury, Jethwa, & Ballestrem, 2016; Golji & Mofrad, 2013). Activation of FAK controls intracellular mechanotransduction (Lachowski et al., 2018). FAK regulates actin polymerization and organization (Schaller, 2010). The activation of FAK also promotes RhoA and Rho-associated protein kinase (ROCK) which then crosstalks to ERK1/2 (Khatiwala, Kim, Peyton, & Putnam, 2009; Shih, Tseng, Lai, Lin, & Lee, 2011). ERK1/2, in turn, phosphorylates RUNX2 driving osteogenesis (Khatiwala et al., 2009). The focal adhesion formation activates G proteins (e.g. Rac, Cdc42 and Rho) and, in turn, triggers actin-myosin contraction (Lawson & Burridge, 2014; Price, Leng, Schwartz, & Bokoch, 1998). Cell adhesion and contraction link to intracellular tension. High intracellular tension promotes osteogenesis while low tension enhances adipogenesis (Kilian, Bugarija, Lahn, & Mrksich, 2010; McBeath, Pirone, Nelson, Bhadriraju, & Chen, 2004).

1.6.1.2 ECM Stiffness

It is known that two dimensional (2D) ECM stiffness affects MSCs commitment through complex crosstalk networks **(Figure 1.4A)**. A seminal *in vitro* study by Engler et al elucidated how MSCs respond to ECM stiffness (Engler, Sen, Sweeney, & Discher, 2006). Soft stiffness (E~0.1-1 kPa) were considered to drive neurogenic fate of MSCs. Stiffer matrices (E~8-17 kPa) promoted myogenic fate. High stiffness (E~25-40 kPa) promotes osteogenesis, with MSCs spread in polygonal morphologies (Engler et al., 2006). However, the cause of cell fate regulation is still debated whether from substrate stiffness or tethering effects of proteins on the substrate surfaces. Some *in vitro* studies explained that fiber tethering of protein ECM and density of crosslinkers affected cell differentiation (Trappmann et al., 2012). Low collagen fiber density allows ECM fiber deformation resulting in soft feedback while higher fiber density, or high levels of crosslinking, allow cells to generate rigid feedback. Rigid feedback enhances actin polymerization (F. M. Watt & Huck, 2013). After that, Wen et al. argued that protein tethering and substrate porosity did not affect cell differentiation but substrate stiffness was the determining factor in MSC commitment (Wen et al., 2014).

By transferring signals from the ECM to the nucleus, MSCs sense ECM stiffness using integrins as a stiffness sensor. Integrins (such as integrins β3, α2) bind to the extracellular proteins in ECM which in turn form the focal adhesion. Integrins link to actin-myosin complexes. Perinuclear actin is an important key factor affecting nuclear shape (Khatau et al., 2009). LINC complexs (linker of nucleus and cytoskeleton) is a protein complex joining the cytoskeleton and nucleus (nucleoskeleton). LINC complexes consist of SUN and nesprin proteins. Nesprins connect to actin while SUN interacts with lamins and nuclear pore complexs (Dahl, Ribeiro, & Lammerding, 2008). Lamins are intermediate filament proteins consisting of Lamins A-C, located at the inner nuclear membrane. In *in vitro* studies, Lamins interact with chromatin and play a role in coveyance of cytoskeletal forces into the nucleus (S. Cho, Irianto, & Discher, 2017; Dalby et al., 2014). Lamins play roles in control of viscoelastic nuclear properties. In *in vitro* study, Lamin A functions in a viscous manner while lamin B is elastic (Swift et al., 2013). In stiff ECM, lamins are not

phosphorylated, thus their degradations are prevented (S. Cho et al., 2017; Dingal & Discher, 2014) **(Figure 1.4B)**.

Cell interactions with stiff ECM result in increased actin tension, in turn pulling nesprins which activate emerin by Src kinase (S. Cho et al., 2017). In *in vitro* study, phosphorylated emerin controls stress fiber formation (Guilluy et al., 2014). Cytoskeletal tension modulates nuclear pore opening subsequently promoting Yes associated protein (YAP) translocation into nucleus (*in vitro* study)(Elosegui-Artola et al., 2017). Adequate accumulation of YAP in the nucleus, in turn, promotes an irreversible osteogenic phenotype (C. Yang, Tibbitt, Basta, & Anseth, 2014).

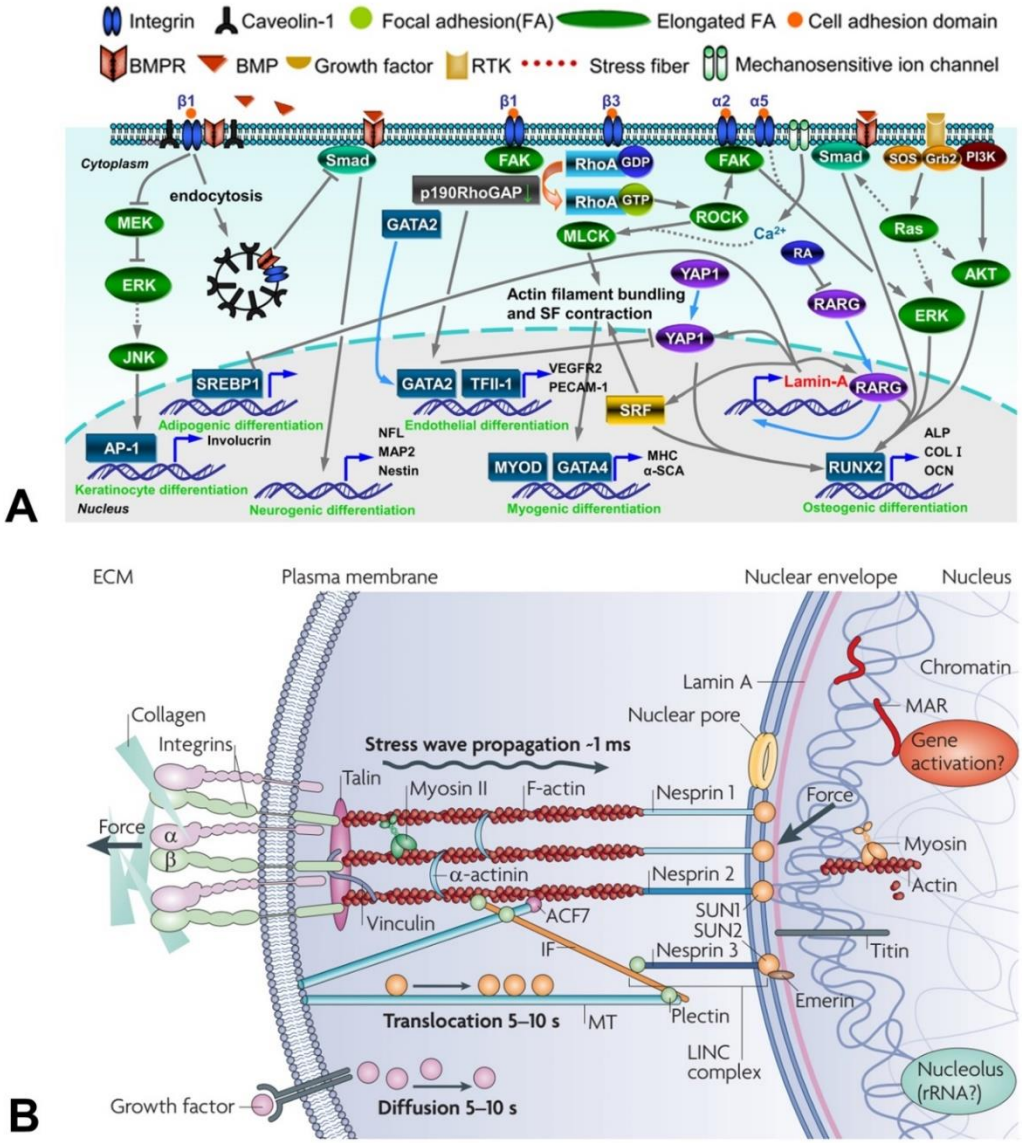

Figure 1.4 Crosstalk network responding to matrix stiffness

A) Crosstalk network responding to matrix stiffness (from soft to stiff matrices; left to right). In soft matrice, BMP/Smad pathway was inhibited promoting neurogenic differentiation. In medium stiffness, myogenic differentiation was enhanced through ROCK-MLCK pathways. In stiff matrice, osteogenic differentiation is enhanced via ROCK-FAK-ERK1/2 and smad 1/5/8 pathways (With permission of Lv et al., 2015 (H. Lv et al., 2015), licensed under Creative Common Attribution License; CC; https://creativecommons.org/licenses/by/4.0/)).
B) Signal transduction from ECM to nucleus. Integrins attach on ECM transferring force through actin. Nesprin is connected actin and SUN. SUN is linked to lamin and chromatin regulating gene positioning (With permission of Wang et al., 2009 (Ning Wang, Tytell, & Ingber, 2009).

1.7 Difference between 2D and 3D cultures: cell physiology and cytoskeleton

In two dimensions (2D), monolayer cells adhere and migrate on planar surfaces **(Figure 1.5A)**. Spread cells in 2D culture have high surface-to-volume ratio, thus, soluble nutrients and growth factors in culture media can interact with receptors on the dorsal cell surface (Meyers, Craig, & Odde, 2006). In three dimensional models (3D), cells are entrapped in 3D-ECM mimicking natural microenvironment of MSCs (Naito et al., 2013) **(Figure 1.5B)**. Focal adhesions distribute in all dimensions thus cells interact with ECM around the cells. In 3D-ECMs, nutrients and molecules unequally distribute across the scaffold depending on diffusion rate, porosity of scaffolds, etc (Cheema et al., 2012; Rouwkema, Koopman, van Blitterswijk, Dhert, & Malda, 2010). Gradients of soluble factors may affect cell functions (Baker & Chen, 2012).

Comparing cellular responses between 2D and 3D culture, in 2D culture, cytoskeleton plays a major role responding to stiffness (McBeath et al., 2004; Provenzano & Keely, 2011). However, the effect of myosin-based cytoskeletal tension on differentiation is controversial in 3D culture (H. Lv et al., 2015). For example, Parekh et al., reported a wider range of stiffness (0.2 kPa-59 kPa) which can induce osteogenesis in MSCs in 3D compared to 2D (20-40 kPa) (Parekh et al., 2011). They also found that material driven 3D osteogenesis did not involve cytoskeletal and ROCK activity (Parekh et al., 2011). Huebsche et al., elucidated that MSCs are driven towards osteogenic

fate by 3D-ECM where the stiffness is 11-30 kPa. The authors also reported that the organization of integrin binding in relation to ECM stiffness was important to osteogenic committment, but cell morphology was not (Huebsch et al., 2010).

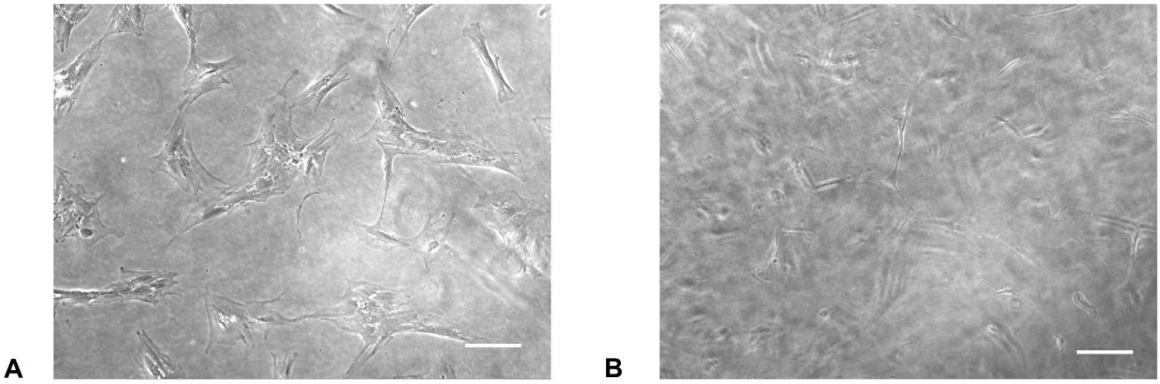

Figure 1.5 Cell characteristics in 2D vs 3D culture

(A) 2D-MSC culture, cells spread on 2D planar surface (10x magnification, scale bar 100 μm). (B) 3D-MSC cuture, cells have satellite and branched shape (10x magnification, scale bar 100 μm)

1.8 Chemically induced osteogenesis

Chemical induction of osteogenesis is a common and widely used approach. Various growth factors (such as BMP2, BMP7) (M. Knippenberg, M. N. Helder, B. Zandieh Doulabi, P. I. J. M. Wuisman, & J. Klein-Nulend, 2006; Marupanthorn, Tantrawatpan, Kheolamai, Tantikanlayaporn, & Manochantr, 2017; Yeh et al., 2002) as well as chemical supplements (such as dexamethasone, ascorbic acid, β-glycerophosphate, statins and calcium phosphates) (Langenbach & Handschel, 2013), are proposed for regulating osteogenic differentiation of MSCs. However, the high cost of growth factors and targeted delivery is challenging. Growth factor coating on material surfaces can reduce the cost of growth factors (Llopis-Hernández et al., 2016). However, drug/growth factor release requires matching to the dynamical changes of the bone healing process and this is hard to achieve (M. Wu et al., 2016).

1.8.1 Chemicals

Currently, many chemicals are used for osteogenic induction. Dexamethasone, the most commonly used agent, induces RUNX2 expression which is a major transcription factor for osteoblastogenesis (Langenbach & Handschel, 2013). Dexamethasone induces Four and a half LIM domains protein 2 (FHL2) which then interacts with Wnt/β-catenin and results in RUNX2 expression (Hamidouche et al., 2008). Moreover, dexamethasone also promotes RUNX2 activity through transcriptional coactivator with PDZ-binding motif (TAZ) upregulation which is a RUNX2 transcription coactivator as well as mitogen-activated protein kinase 1 (MKP1) upregulation promoting RUNX2 transactivation (Langenbach & Handschel, 2013). Some literature shows that glucocorticoids (GC) inhibit the ERK signaling pathway (Bladh, Johansson-Haque, Rafter, Nilsson, & Okret, 2009; Y. Lu, Fukuda, Liu, Kumagai, & Nishida, 2004). However, ERK is required for RUNX2 phosphorylation which, in turn, drives osteogenesis (Arumugam, Vairamani, Partridge, & Selvamurugan, 2017; Ge et al., 2009). Sustained exposure of dexamethasone has been shown to down-regulate collagen type I synthesis and induce maturation of an adipocyte subpopulation within bone marrow stem cell cultures (Porter, Huckle, & Goldstein, 2003). High doses of GC inhibit osteoblast differentiation (Shalhoub et al., 1992; Smith et al., 2000). GC inhibit cytokines such as IL-11 thus reducing osteoblast differentiation (Rauch et al., 2010). In tissue engineering, dexamethasone can be used in many forms, such as direct loading in scaffolds (S. Ding et al., 2013; Tsiapla et al., 2018), loading in calcium phosphate nanoparticles (Ying Chen, Chen, Kawazoe, & Chen, 2018; Y. Chen, Kawazoe, & Chen, 2018) or direct mixing with 3D printed materials (X. Li et al., 2018).

Ascorbic acid (vitamin C) and β-glycerophosphate are commonly used in osteogenic induction cocktails. Ascorbic acid promotes collagen type I and fibronectin secretion which are ECM proteins, as well as integrin β1 expression (F. Wei et al., 2012). The transportation of ascorbic acid into MSCs (via sodium dependent vitamin C transporter 2; SVCT2) also reduces oxidative stress (Sangani et al., 2015). However, high doses of ascorbic acid (5-250 μM) provide toxicity, reducing cell density and changing cell morphology (K. M. Choi et al., 2008). β-glycerophosphate provides an inorganic phosphate source for mineralization (Chung, Golub, Forbes, Tokuoka, & Shapiro, 1992), promotes ERK1/2 phosphorylation and regulates osteopontin (Beck & Knecht, 2003). However, high level of phosphate ions induces

osteoblast apoptosis (Meleti, Shapiro, & Adams, 2000). Ascorbic acid and β-glycerophosphate can be supplemented in composites for bone tissue engineering (Faikrua, Jeenapongsa, Sila-asna, & Viyoch, 2009; T. Liu et al., 2018; C. Wang, Cao, & Zhang, 2017).

Statins or ß-Hydroxy ß-methylglutaryl-CoA (HMG-CoA) reductase inhibitors are commonly used in hyperlipidemia treatment (H. D. Choi & Chae, 2018). In bone, statins upregulate BMP2 and RUNX2 enhancing osteoblastic differentiation and reducing osteoclastogenesis (Oryan, Kamali, & Moshiri, 2015). However, some studies have shown that high doses of statins may induce apoptosis (Izadpanah et al., 2015; Kupcsik, Meurya, Flury, Stoddart, & Alini, 2009). Statins can be used in tissue engineering, for example, simvastatin can be supplemented in form of microspheres (Yu et al., 2017).

1.8.2 Growth factors

BMPs, growth factors inducing bone induction, are widely studied in bone tissue engineering (Jian Yang et al., 2014). BMP2 (Beazley & Nurminskaya, 2014), BMP6 (Akman, Seda Tigli, Gumusderelioglu, & Nohutcu, 2010), BMP7 (Cook et al., 2000) and BMP9 (Dumanian et al., 2017; T. Fu et al., 2019; Tasli, Aydin, Yalvac, & Sahin, 2014) provide potent osteoinductive activity. BMP7 not only promotes osteogenesis but also enhances chondrogenesis (F. Chen et al., 2019; M. Knippenberg, M. N. Helder, B. Zandieh Doulabi, P. I. Wuisman, & J. Klein-Nulend, 2006; Tasli et al., 2014). However, there is much literature reporting clinical complications of BMPs overdosing such as ectropic bone ossification, vertebral osteolysis, radiculitis, etc (Carragee, Hurwitz, & Weiner, 2011; Shimer, Oner, & Vaccaro, 2009). Moreover, BMP protein degradation is rapid (El Bialy, Jiskoot, & Reza Nejadnik, 2017). It is difficult to design scaffolds which can slowly and continuously release BMPs sustaining the growth factor within the safety range. Further, not only clinical complications, but also the cost effectiveness of using BMP-2 is controversial. The use of BMPs for spinal fusion surgery may increase the cost of the procedure to the UK-NHS by about 1.3 million pounds per year and 3.5 million pounds per year in open tibial fractures treatment (Garrison et al., 2007). To reduce this problem, BMP2 nanocoatings on materials has been proposed (Llopis-Hernández et al., 2016). This technique potentially reduces the cost of growth factor using and also diminishes side

effects of high dose BMPs (Z. A. Cheng et al., 2019; Llopis-Hernández et al., 2016).

1.9 Mechanical stimulation, mechanotransduction and osteogenesis

It is known that mechanical stimulation can promote bone healing and bone homeostasis (Bouletreau, Warren, & Longaker, 2002; X. Huang, Das, Patel, & Duc Nguyen, 2018; Steward & Kelly, 2015). In bone tissue engineering, many studies propose techniques to promote osteogenesis using mechanical stimuli such as cyclic stretch (J. Gao et al., 2016; Y. Yang, Wang, Chang, Wan, & Han, 2018), compression (Burger, Klein-Nulend, & Veldhuijzen, 1992), tensile stretch (Grottkau, Yang, Zhang, Ye, & Lin, 2013) and fluid shear (Stolberg & McCloskey, 2009; Yourek, McCormick, Mao, & Reilly, 2010). Even though mechanical osteogenic induction is widely studied, the challenge remains in precisely controlling the stimulus intensity as well as upscaling to industry.

Mechanotransduction is the process that converts extracellular physical stimuli to biological signals resulting in cellular responses such as cell adhesion, proliferation, differentiation and survival. After cells sense the stimuli, mechanical signals are transferred through specific pathways. The MAPK pathway is activated to regulate cellular response (Plotnikov, Zehorai, Procaccia, & Seger, 2011). Intracellular signals also activate nuclear factor kappa B (NFκB) functioning as stress sensor (Ahn & Aggarwal, 2005). Overdose of stimuli may activate cell survival pathways to maintain proper cellular function (T. Wang, Zhang, & Li, 2002). Yes-associated protein (YAP) functions in stress memory (C. Yang et al., 2014). YAP accumulation from adequate dose/duration of mechanical stimuli and, in turn, switches on genes for differentiation (Elosegui-Artola et al., 2017) **(Figure1.6).**

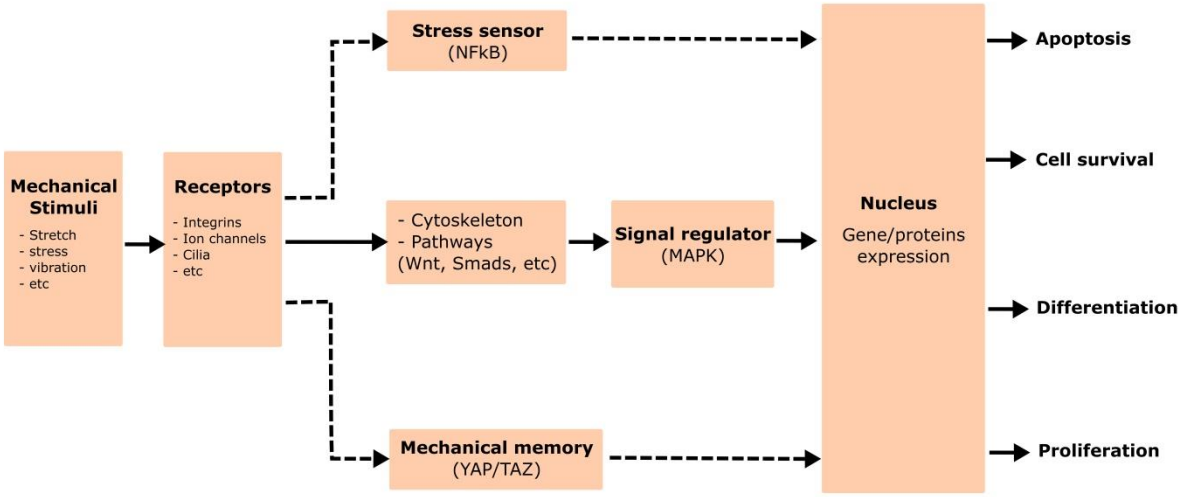

Figure 1.6 Mechanotransduction model; from receptors into nucleus

1.9.1 Mechanical stimuli, sensors and related pathways

As aformentioned, various types of physical stimuli induce osteogenesis, such as tension, compression, fluid shear stress and substrate material properties (Kyle H. Vining & David J. Mooney, 2017). Cells sense mechanical stimuli and environment using mechanosensors such as focal adhesion-cytoskeleton, membrane ion channels, and primary cilia (J. C. Chen & Jacobs, 2013). Single stimuli may activate multiple mechanical sensors. For example, fluid shear stress can involve integrin-dependent pathways and also activates cilia (Yavropoulou & Yovos, 2016). Thus, single mechanical stimulus may activate multiple pathways, such as cyclic stretch which can activate BMP2, Wnt, ROCK, etc (J. Gao et al., 2016; Suzuki, Nemoto, & Shimauchi, 2014; C. Zhao et al., 2017). Examples of stimuli and related pathways are summarized in **Table 1.2-1.3.**

1.9.1.1 Integrin dependent pathway

Integrins are major mechanoreceptors sensing ECM stiffness or topography. Integrins on cell memebranes form focal adhesion complexes. At the focal adhesion, tyrosine kinases (e.g. FAK and Src) in turn regulate G-proteins (e.g. Rho and Rac) and actin microfilaments generating localized signaling for lamellipodia and filopodia formation and cytoskeletal contraction (Burridge & Wennerberg, 2004; Guilluy, Garcia-Mata, & Burridge, 2011). The ROCK/Rho pathway also activates the MAPK pathway (e.g. ERK1/2, JNK) which takes an important role in the integrin dependent pathway controlling MSC growth and differentiation (McMurray et al., 2011; Tsimbouri et al., 2012).

1.9.1.2 Stretch activated ion channels

Mechanical stimuli can also affect mechano-sensitive ion channels on the cell membrane which subsequently allow extracellular calcium influx. Each ion channel senses mechanical stimuli at different intensity of stimuli **(Figure 1.7)** (Bavi et al., 2017). There are two models explaining how mechanosensitive ion channels respond to mechanical stimuli. Tension force may be transferred via the cellular membrane in turn directly opening ion channels thus called “force from membrane”. Another model explains the mode of channel response to stimuli via the tethering effect of intracellular or extra-cellular structures called “force from filament” (Martinac & Poole, 2018).

It is difficult to prove whether ion channels respond directly or indirectly to mechanical stimuli. Some evidence suggested that piezo1 may directly respond to stimuli via membrane tension (Charles D. Cox et al., 2016; Syeda et al., 2016). However, some literature reports the evidence of the channel response via cytoskeletal activation (Albarran-Juarez et al., 2018). Piezo1 can be found in many cell types (Coste et al., 2010). Piezos can sense shear flow (Albarran-Juarez et al., 2018; Jetta, Gottlieb, Verma, Sachs, & Hua, 2019), stiffness (Pathak et al., 2014), tissue tension (Lewis & Grandl, 2015), and sound waves (Coste et al., 2012). Osteoblasts also use piezo1 for mechanical sensing relating to bone formation (W. Sun et al., 2019). Moreover, MSCs respond to mechanical stimuli such as hydrostatic pressure producing BMP2 through piezo1 activation (Asuna Sugimoto et al., 2017). Transient receptor potential vanilloid 4 (TRPV4) is another ion channel that senses mechanical stimuli such as deflection (Rocio

Servin-Vences, Moroni, Lewin, & Poole, 2017) and cell swelling (Becker, Blase, Bereiter-Hahn, & Jendrach, 2005). TRPV4 allows calcium influx which in turn crosstalks with abundant intracellular pathways (Hasan & Zhang, 2018). Increased intracellular calcium may enhance osteogenic differentiation (Boonrungsiman et al., 2012). TRPV4 also plays a role as themosensor and nociceptor (Plant & Strotmann, 2007; Shibasaki, 2016) and may modulate inflammation releasing IL-6 through MAPK pathways (Nayak et al., 2015).

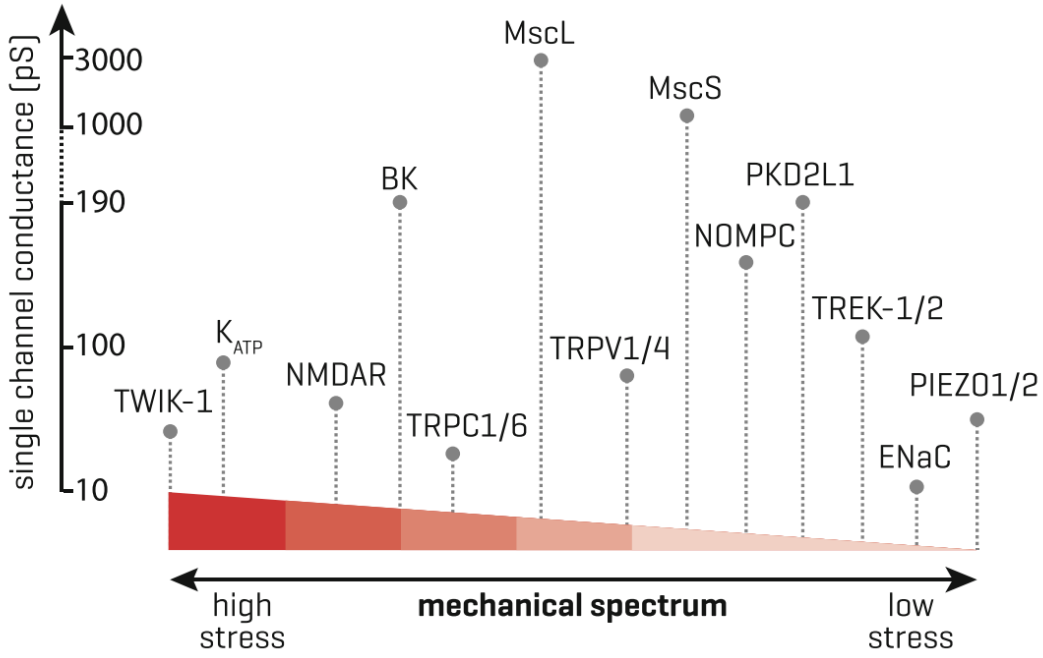

Figure 1.7 The mechanical response spectrum of ion channels stimulated by patch-clamp technique

(With permission of Bavi., et al 2017 (Bavi et al., 2017; C. D. Cox, Bavi, & Martinac, 2017; Morris, 2011; Sachs, 2010)).

1.9.1.3 Primary cilia movement

Osteoblasts use primary cilia to sense fluid flow (Malone et al., 2007) and cyclic tensile strain (J. Bodle et al., 2019). Some literature shows that activation of primary cilia potentially promotes osteogenesis (J. C. Bodle et al., 2013; Hoey, Tormey, Ramcharan, O'Brien, & Jacobs, 2012). Fluid flow induces extracellular calcium influx through cilium-localized Ca^{2+}-permeable channels polycystin-2 (PC-2) and TRPV4 (K. L. Lee et al., 2015). However, Malone et al., showed that primary cilia activation can induce osteogenesis through cilia but does not relate to calcium influx and stretch activated ion channels (Malone et al., 2007).

1.9.1.4 Other

Gap junctions may be considered as mechanical sensors. Gap junctions (such as connexins) allow molecule and ion transportation between cells which may be stimulated during mechanotransduction (Saunders et al., 2003). Connexin 43, for example, plays a role in the osteogenic fate through the glycogen synthase kinase 3-beta (GSK-3β)/β-catenin pathway (F. X. Lin et al., 2018).

Table 1.2 Examples of cyclic stress studies and related pathways

Types	%strain/ frequency/duration	Cell type	Related pathways	2D/3D cellular response	Outcomes	References
Cyclic compression	10%, 0.5 Hz, 4 hr	Pre-osteoblast	BMP2	2D & 3D	Induce BMP2/SMAD5, RUNX2, ALP OCN, ON, OPN and Col1A	Rath et al 2009 (Rath, Nam, Knobloch, Lannutti, & Agarwal, 2008)
Cyclic stretch	3, 5, 10%, 0.016 Hz, 6 hr	Periodontal ligament cells	BMP2	2D	- Increase BMP2 (via ERK1/2, p38 - Induce COX2	Suzuki et al 2013 (Suzuki et al., 2014)
	2 mm, 0.2 Hz,1 hr	BMSCs, rats	Wnt/β catenin	2D	- Increase proliferation - Upregulate ALP, Wnt3a, LRP5, β catenin and RUNX2	Zhao et al 2017 (C. Zhao et al., 2017)
	0-8%, 0.5 Hz, 4 hrs	Human patellar tendon fibroblasts	TGF-β1	2D	- Increase TGF-ß and Col-1 gene expression	Yang et al 2004 (G. Yang, Crawford, & Wang, 2004)
	12%, 24 hrs	MG63	Cytoskeleton (Cofilin)	2D	ALP, OCN, RUNX2, Col-1 upregulation	Gao et al 2016 (J. Gao et al., 2016)
	10%, 0.1 Hz, 24 hrs	HDPLCs	ROCK and YAP	2D	- Increase CTGF and CYR61 (YAP target gene) - YAP links to ROCK pathway	Yang et al 2018 (Y. Yang et al., 2018)
	15%, 1/12 Hz	MC3T3-E1	ERK1/2	2D	- Upregulate ALP and RUNX2 through ERK1/2	Kanno et al 2007 (Kanno, Takahashi, Tsujisawa, Ariyoshi, & Nishihara, 2007)
	15%, 0.5 Hz	Dermal fibroblasts	MAPK	3D	ERK1/2 upregulation at 6 hrs or increase stimuli Incremental stretch increase collagen transcription	Schmidt et al 2016(Schmidt, Chen, & Tranquillo, 2016)
	10%, 1 Hz	Bovine aortic endothelial cells	Cytoskeleton (Rho kinase and mDia)	2D	3% stretch enhance stress fiber orientation	Kaunas et al 2005 (Kaunas, Usami, & Chien, 2006)
	1-5%, 0.01-10 Hz	PMEFs	Cytoskeleton, YAP, MRTF-A	2D	- Cell spreading and stress fiber formation - Increase YAP and MRTF-A nucler localization	Cui et al 2015 (Cui et al., 2015)
	25%, 12 Hz, 1 hr	Satellite cells, rat	Calcium ion channels	2D	- Mechanical sensing and L-VGC channel allow extracellular calcium influx	Hara et al 2012 (Hara et al., 2012)

CYR61; cysteine-rich angiogenic inducer 61, HPDLCs; Human periodontal ligament cells, PMEFs; Primary mouse embryo fibroblast

Table 1.3 Examples of fluid flow, vibration, stiffness studies and related pathways

Types	Intensity/duration	Cell type	Related pathways	2D/3D Cellular response	Outcomes	References
Fluid flow	Primary cilia, 1 Pa, 52.5 ml/min, 1 Hz, 2 hrs	C3H10T1/2 murine MSCs	TRPV4	2D	- TRPV4 localization at primary cilium	Corrigan et al 2018 (Michele A. Corrigan et al., 2018)
	Pulsatile fluid flow, 0.8 Pa, 1-4 hrs	ROS17/2.8 osteoblast	Wnt	2D on 3D scaffold	- Upregulate ALP, LRP5, Wnt3a and β-catenin	Jia et al 2014 (Jia et al., 2014)
	12 dynes/cm^2, 2 hrs	HPDLCs	MAPK	2D	- Upregulate ALP, Col-1, ERK1/2, p38	Tang et al 2014 (M. Tang et al., 2014)
	Shear stress, flow rate 0.274 μL/min, 48 hrs	hMSCs	TAZ	2D	- Upregulation of CTGF and Cyr61 (TAZ related) - Upregulate RUNX2 DLX5 and Msx2	Kim et al 2014 (K. M. Kim et al., 2014)
	9 dynes/cm^2, 24 hrs	hMSCs	BMP2	2D	- Upregulation of BMP2, OPN	Yourek et al 2010 (Yourek et al., 2010)
Vibration	LMHFV, 0.3g, 40 Hz, 50 μm, 15 mins/day	MSCs	MAPK	2D	- Promote adipogenesis (PPARγ) and p38	Zhao et al 2017 (Zhao, Lu, Gan, & Yu, 2017)
	LMHFV, 0.3g, 60 Hz, 1 hr	Rat BMSCs	-	2D	- Decrease osteogenesis and mineralization	Lau et al 2011 (Lau et al., 2011)
	LMHFV,0.3g, 40 Hz, 30 mins/day	Rat BMSCs	Wnt/β-catenin	2D	- Increase fibronectin, integrin, vinculin expression - Upregulate Wnt10B, β-catenin, RUNX2, OSX	Chen et al 2016 (B. Chen et al., 2016)
	LMHFV,0.3g, 45 Hz, 20 mins/day, 5 day/week	MC3T3-E1	Cytoskeleton	2D	- Cell proliferation and Cox2 expression related to estrogen receptor α - Vibration involved ROCK pathway	Haffner-Luntzer et al 2018 (Haffner-Luntzer, Lackner, Liedert, Fischer, & Ignatius, 2018)
stiffness	134, 16 and 1.2 kPa, PDMS	Rat Osteoblast	ROCK	2D	- Soft stiffness decreases RUNX2, OCN which related to ROCK pathway	Zhang et al 2017 (T. Zhang et al., 2017)
	2-20 kPa Polyacrylamide gels	HCT-116 Colorectal cancer cell line	YAP/TAZ	2D	Stiffness increase Lamin A/C regulated by YAP	Tan et al 2017 (F. Tan et al., 2018)
	0.5-1 kPa and 100 kPa Polyacrylamide gels	BMSCs, primary chondrocytes	Wnt/ β-catenin	2D	Stiffness enhance Wnt/ β-catenin pathways and also activate FAK pathway	Du et al 2016 (Du et al., 2016)

LMHFV; low-magnitude high frequency vibration, LRP5; lipoprotein receptor-related protein 5, HPDLCs; Human periodontal ligament cell

1.9.2 Role of nanoscale mechanical stimulation in osteogenesis

The concept of nanoscale mechanical stimuli originates from that size of structures on cellular membranes, such as integrins (Campbell & Humphries, 2011) etc. Thus, nanoscale mechanical stimuli possibly affect proteins or receptors on membranes triggering mechanotranductive signals into the nucleus. Currently, the effect of nanotopography is elucidated that it can promote osteogenesis of MSCs (Dalby et al., 2007), regulate cytoskeletal tension and transcriptional co-activator with PDZ-binding motif (TAZ) (Qian et al., 2017). Various types of nanotopography, such as nanopits (Davison, McMurray, Smith, Dalby, & Meek, 2016), nanowires (H. H. Pan et al., 2015), nanopillars (Sjostrom et al., 2009) and nanorods (Ning et al., 2016) show interaction with the cytoskeleton. Patterning of nanotopography, such as disordered patterns, regulates formation of nanopodia and focal adhesion in turn modulates cytoskeletal tension (Dalby et al., 2014; McNamara et al., 2014). Cytoskeleton links to the LINC complexs, potentially triggering chromosome reorganization (Dalby et al., 2014).

1.9.3 Role of MAPK-NFκB pathways and mechanosensing in physiological and inflammatory conditions

During physiological or inflammatory conditions, MAPK (signal regulator) and NFκB (stress sensor) play a critical role in controlling intracellular signaling to produce proper cellular response to external stimuli such as differentiation or apoptosis (Ahn & Aggarwal, 2005; Chang et al., 2013; Cowan & Storey, 2003; Lawrence, 2009; T. Liu, Zhang, Joo, & Sun, 2017; W. Zhang & Liu, 2002).

The MAPK signaling pathway is the central pathway responding to extracellular stimuli such as stress, cytokines, etc. The MAPK pathway mediates the intracellular signaling pathways of proliferation, differentiation, inflammation and apoptosis. The MAPK pathway consists of extracellular signal regulated kinase (ERK), p38 and c-Jun NH2-terminal kinase (JNK) (Plotnikov et al., 2011; W. Zhang & Liu, 2002).

ERK1/2 upregulation can be induced by various stimuli such as inflammation and stress (Plotnikov et al., 2011). ERK1/2 links to cytoskeletal tension induced osteogenesis through Integrin-FAK-ROCK-ERK1/2 pathways (McBeath et al., 2004; Shih et al., 2011). ERK1/2 is also activated by ion channel activation (Vyklicka, Boukalova, Macikova, Chvojka, & Vlachova, 2017). Moreover, ERK1/2 is also

involved in cell proliferation and apoptosis (Mebratu & Tesfaigzi, 2009).

P38, another member of the MAPK family, also affects osteogenesis by promoting and suppressing relevant proteins. P38 can be activated by stress (Plotnikov et al., 2011) and promotes bone progenitor proliferation and differentiation (Rodriguez-Carballo, Gamez, & Ventura, 2016). Not only ERK1/2, but also p38 can phosphorylate RUNX2 to active bone formation (Rodriguez-Carballo et al., 2016). P38 is also involved in many osteogenesis pathways such as BMP/TGFβ-p38-β-catenin and WNT-p38-β-catenin (Rodriguez-Carballo et al., 2016).

It has been shown that JNK is involved in apoptosis pathways (A. Lin, 2003; Weston & Davis, 2007). Activation of JNK together with AKT and NFκB enhances cell survival (Lamb, Ventura, Hess, Flavell, & Davis, 2003). JNK can be activated by stress and cytokines such as IL-1β and TNFα (Plotnikov et al., 2011; Rodriguez-Carballo et al., 2016). ERK1/2 can directly activate JNK kinase (W. Zhang & Liu, 2002). The role of JNK for osteogenesis is not obviously clear. Some reports have shown that JNK is important for osteoblast function (R. Xu et al., 2017). On the other hand, JNK inhibition may enhance osteogenesis e.g. in stromal cells (Doan et al., 2012).

As aformentioned, optimal mechanical stimulation can enhance osteogenesis (J. C. Chen & Jacobs, 2013; K. H. Vining & D. J. Mooney, 2017). However, high intensity (overdose) mechanical stimulation can induce reactive oxygen species (ROS) or inflammatory response (Biswas, 2016). Theoretically, a low level of inflammation enhances osteogenesis and mineralization as this occurs in the early phase of the normal bone healing process (Knapik et al., 2014). However, high grade inflammation can suppress osteogenesis (H. Huang et al., 2011; Lacey, Simmons, Graves, & Hamilton, 2009). With optimal (low grade) inflammatory response, IL-6 and TNFα (essential inflammatory cytokines) are secreted in the early phase of bone healing. TNFα, a paracrine cytokine, interacts with MAPK and caspases (J. Liu, Minemoto, & Lin, 2004; L. Wang, Du, & Wang, 2008) and activates NFκB (N. Wang et al., 2016). Moreover, TNFα promotes angiogenesis (Kwon et al., 2013) and enhances MSCs to secrete IL-6 (De Cesaris et al., 1998). Sun et al., proposed that IL-6 could then enhance BMP2

production (M. Sun et al., 2017) promoting RUNX2 expression and therefore bone production.

NFκB pathways regulate inflammation and the immune system. NFκB is a stress sensor that is activated for cell survival (Ahn & Aggarwal, 2005). NFκB is involved in proliferation, apoptosis and differentiation (T. Liu et al., 2017). NFκB prevents TNFα-induced apoptosis by suppressing caspases and JNK activation (A. Lin, 2003). NFκB enhances manganese superoxide dismutase (MnSOD) which is a ROS antioxidant enzyme (H. Tanaka et al., 2002). Therefore, an increase of NFκB provides evidence for increased inflammatory response.

Sudha Agarwal's group studied the effect of magnitude of mechanical stimuli on intracellular signaling response and NFκB signaling pathways (Agarwal et al., 2003; Anghelina et al., 2008; Dossumbekova et al., 2007; Knapik et al., 2014; Madhavan et al., 2007; J. Nam, Aguda, Rath, & Agarwal, 2009). At physiological magnitudes, mechanical stimulus activates intracellular signals in which it promotes osteogenesis from pathways such as BMP2/Smad, calcium signaling, ERK1/2, nitric oxide, prostaglandin E2 and Wnt (Knapik et al., 2014). The NFκB pathway is also activated to control oxidative stress (Oeckinghaus & Ghosh, 2009). In oxidative stress conditions induced by mechanical stimuli, NFκB provides anti-oxidative functions such as increasing antioxidants and autophagy, reducing ROS and JNK as well as increasing pro-oxidant genes such as NADPH oxidase (Lingappan, 2018). In conditions where cells are injured by exposure to high magnitude stimulation, NFκB activates high levels of proinflammatory cytokines and signals such as TNFα, IL-1β, NO and ROS resulting in supressed osteogenesis (Anghelina et al., 2008; Dickson, Bhakar, & Barker, 2004; N. Wang et al., 2016). Interestingly, in inflammatory conditions, the physiological magnitude of mechanical stimulation can inhibit the NFκB signaling pathway (by suppressing TRAF6 in turn IKKs and IκB inactivation), thus promoting anti-inflammatory signals (Knapik et al., 2014) **(Figure 1.8)**.

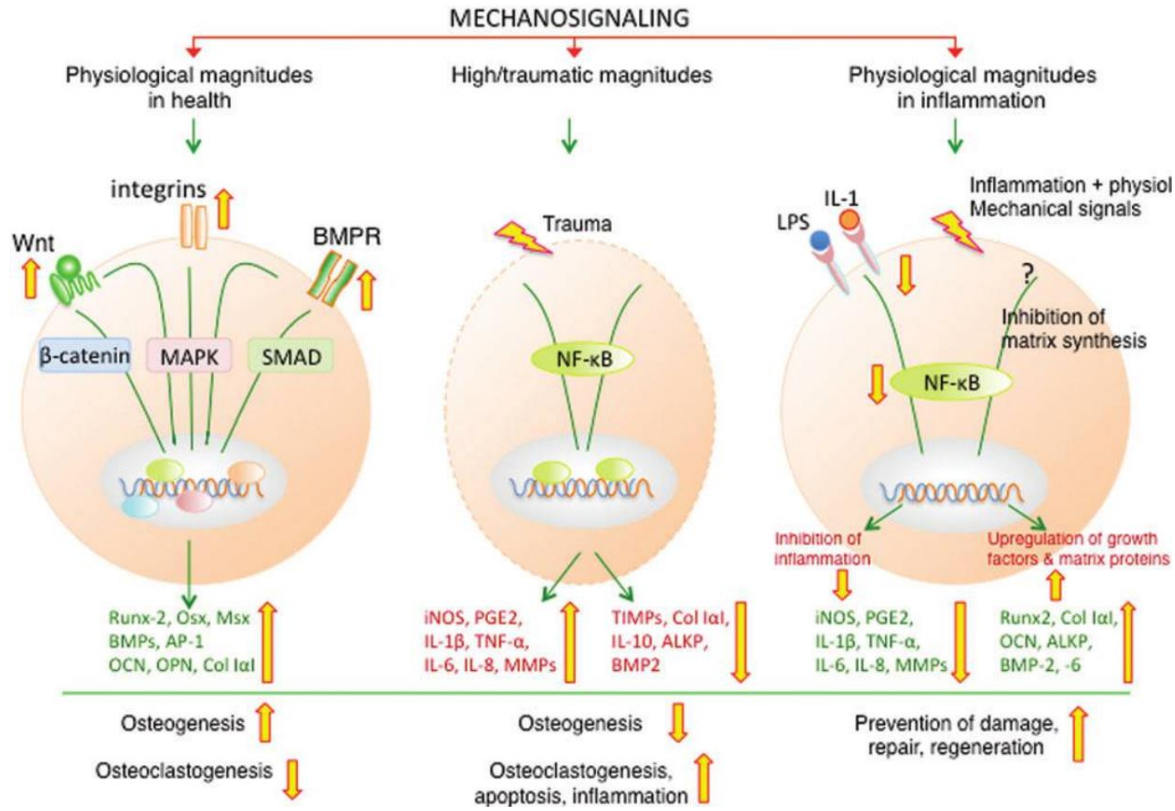

Figure 1.8 Effect of stimulating magnitude on inflammation

In normal conditions (left), physiological magnitudes promote osteogenesis through multiple pathways such as SMADs, MAPK and β-catenin. High magnitude stimulation (middle) activates high levels of NFκB functioning as a pro-inflammatory signal. Osteogenesis is thus suppressed. During inflammatory conditions (right), low grade machanical stimulation inhibits NFκB to promote osteogenesis (With permission of Knapik et al., 2014 under Mary Ann Liebert, Inc, New Rochelle, NY (Knapik et al., 2014)).

1.10 Nanovibrational stimulation; concept and related pathways and rationale of 3D study.

The concept of NS was firstly established by Prof Adam Curtis (1934-2017) as nanoscale stimuli, such as nanotopography, can modulate cell adhesion in turn driving osteogenesis (Dalby et al., 2007). Together with, cells can sense the difference of topography at approximately 8 nm (McNamara et al., 2014). Thus, Prof Curtis proposed that application of controllable and precise external force stimulation on the nanoscale may drive changes in cell response. Further, osteogenic differentiation seemed to be a sensible target because of the adhesion-cytoskeleton relationship (Kilian et al., 2010; McBeath et al., 2004; Nikukar et al., 2013).

The NS bioreactor uses piezo actuators to generate stimulating amplitudes in Z axis which is perpendicular to the base of culture surface (Curtis et al., 2013). In MSCs, NS drove osteogenic induction in both 2D and 3D cultures. In 2D culture, Nikukar et al., found that NS drives osteogenesis through a RhoA-ROCK pathway (Nikukar et al., 2013). To explain the mechanism, the hypothesis of 2D-NS mechanism was that nanovibration (in the Z-axis) possibly oscillated the culture media and attached cells in the culture plate (X-Y plane) resulting in repetitive and fast membrane indentation (Curtis et al., 2013). This pico Newton force, which is of similar magnitude to stimulate hair cells during hearing (Curtis & Tsimbouri, 2014), may flutter the cell membrane (Rappaz et al., 2009) and, in turn, initiates intracellular signals (D. Wu, Ganatos, Spray, & Weinbaum, 2011) through cytoskeletal tension regulation (McBeath et al., 2004), switching on gene expression and driving osteogenesis (Childs et al., 2015).

Moving from 2D towards *in vivo* and clinical studies, the effect of NS in 3D culture were in turn conducted. Recently, Tsimbouri et al., showed successful results of 3D NS in collagen hydrogels and proposed that NS promotes 3D osteogenesis in hMSCs via the TRPV1 ion channel, PKC and β-catenin pathways. Cytoskeleton thus appears to be less involved in 3D culture (Tsimbouri P.M., 2017). Further details are discussed in chapter 4.

1.10.1 Amplitudes, frequencies and acceleration

To mechanically induce cellular differentiation, an adequate dose of mechanical stimulation vibration, is crucial (Elosegui-Artola et al., 2017; Y. Yang et al., 2018). The dose of mechanical stimuli such as cyclic stretch and vibration affecting cell growth depends on various factors including frequency, intensity, and duration (Cui et al., 2015). Currently, the effect of vibrational stimulation on osteogenic induction is intensively studied (Brooke McClarren & Ronke Olabisi, 2018). However, large variations of stimulating amplitude, frequency and duration have been used for osteogenic induction **(Table 1.4-1.5)**. Determining the primary factors of NS, among amplitude (nm), frequency (Hz) or magnitude (g); which one mainly drives osteogenesis, is challenging.

Biologically, the adequate dose of mechanical stimulation allows YAP nuclear translocation, in turn, driving osteogenic differentiation (Elosegui-Artola et al., 2017; Y. Yang et al., 2018). Some *in vitro* 2D studies showed that adequate dose of intensity of cyclic strain can promote cellular reorientation and stress fiber (Cui et al., 2015; Faust et al., 2011). However, the intensity and frequency of stimuli also relate to cellular stress (Chapman et al., 2005; Hong et al., 2015). Optimal strain promotes osteogenesis while over strain decreases osteogenesis (M. Arai, Shibata, Pugdee, Abiko, & Ogata, 2007; Atashi, Modarressi, & Pepper, 2015; Chapman et al., 2005; J. Tan et al., 2015).

Considering the effect of frequency on cell differentiation, some studies showed that increase stimulating frequency affect phenotypic expression. Chen X et al studied the effect of increasing frequency in acoustic-frequency vibratory stimulation (from 0 upto 800 Hz) and reported that higher frequency stimulation (800 Hz) with 0.3 g of magnitude promoted osteogenesis and suppressed adipogenesis (X. Chen, He, Zhong, & Luo, 2015). However, this study did not control the amplitude during stimulation. Interestingly, The stimulating frequency of Chen X et al study was comparable to Nikukar's (Nikukar, 2013) and Tsimbouri's (Tsimbouri P.M., 2017) studies (1000 Hz) for enhancing osteogenesis in MSCs.

Gravity (acceleration) also affects on MSC differentiation. In *in vitro* studies, low gravity condition (e.g. microgravity) induces adipogenesis (Dai, Wang, Ling, Wan, & Li, 2007; M. Zayzafoon, Gathings, & McDonald, 2004) while hypergravity can induce osteogenesis (S. Zhou, Zu, Sun, Zhuang, & Yang, 2015).

Considering the studies using vibrational stimulation to induce osteogenesis in MSCs, low-magnitude high frequency vibration (LMHFV) is commonly investigated. LMHFV is defined by a magnitude less than 1 g with a frequency of 20-90 Hz (Y. Zhou et al., 2011). In our centre, Nikukar et al., (Nikukar, 2013; Nikukar et al., 2013) and Pemberton et al., (G.D., 2015; Pemberton et al., 2015) previously investigated the effect of NS. They found that NS with 20-30 nm amplitude at 1000 Hz frequency enhances osteogenesis. At 20-30 nm, the force is extremely small (0.05-0.12 g). As NS (nanovibrational stimulation or Nanokick) uses ultra low amplitude (in nanoscale) with high frequency (1000 Hz). Thus, term of “ultra low amplitude high frequency vibration (ULAUHFV)” was newly proposed for better classification.

Table 1.4 Examples of low-magnitude high frequency vibration (LMHFV), stimulating dose and outcomes

2D/3D	Cell types	Amplitude, frequency, duration	Outcomes	References
2D	MSCs, rats	0.3 g, 60 Hz, 1 hr/day, 6 days/week	Decrease OSX and mineralization	Lau et al., 2011 (Lau et al., 2011)
3D	MSCs, rats	0.3 g, 40 Hz, ±50 μm, 30 mins/12 hr	Upregulate RUNX2, ALP, Col1, OCN and ERK1/2	Zhou et al., 2011 (Y. Zhou et al., 2011)
3D porous titanium alloy	Primary osteoblast, rabbits	0.5 g, 30 Hz, 6 and 12 weeks	Increase OCN, RUNX2, Wnt3a, Lrp6 and β-catenin	Jing et al., 2015 (Jing et al., 2015)
OP rat, In vivo	HA coated titanium	0.3 g, 40 Hz, ±50 μm, 30 mins/12 hr, 5 days	Upregulate osteoblast differentiation via ERK1/2 and suppress osteoclastogenesis	Zhou et al., 2015 (Y. Zhou et al., 2015)
2D HA coated surface	MSCs, rats	0.3 g, 40 Hz, 30 min /day	Increase FN, RUNX2, OSX, ALP, Col1, OCN	Chen et al., 2016 (B. Chen et al., 2016)
2D	hASCs	0.3 g, 25, 35, 45 Hz	35 Hz promote cartilaginous tissue formation	Marycz et al., 2016 (Marycz et al., 2016)
2D	hASCs	0.3 g, 25, 35, 45 Hz, 10 min 0-3 week	25 Hz, increase differentiation and mineralization	Maredziak et al., 2017 (Marędziak, Lewandowski, Tomaszewski, Kubiak, & Marycz, 2017)
2D	MSCs, rats	0.3 g, 50 μm, 40 Hz, 15 mins/day	Promote adipogenesis via p38	Zhao et al., 2017(Q. Zhao et al., 2017)
2D	MC3T3-E1, mice primary osteoblasts	0.3 g 45 Hz, 20 mins/day, 5days/week	LMHFV depend on estrogen receptor α signaling	Haffner-Luntzer et al., 2018 (Haffner-Luntzer et al., 2018)
3D PEG	hTERT-hMSCs	0.3, 3, 6 g, 0.0149, 0.149, 0.298 mm, 100 Hz, 24 hr	3g promotes but 6 g inhibits osteogenesis	Mehta et al., 2018 (Mehta et al., 2018)

ASCs; adipose derived mesenchymal stem cells, OP; osteoporotic

Table 1.5 Available publication of ultra low magnitude high frequency vibration (ULMHFV)

2D/3D	Cell types	Amplitude, frequency, duration	Outcomes	References
2D	L929, MEFs EEFs, Hela, HUVECs	100 nm , 1000 Hz	Increase filopodia formed cells and gene expression	Ito et al., 2011 (Y. Ito et al., 2011)
2D	hMSCs	0.05 g, 12.57 nm, 1000 Hz	Increase BMP2, RUNX2, FAK and ERK1/2	Nikukar et al., 2013 (Nikukar et al., 2013).
2D nanotopography	Le-2 endothelial cells	20 nm peak to peak, 0.8 $x10^{-7}$ g at 1 Hz, 0.2 x 10^{-3} g at 50 Hz	Increase Kruppel-like factor 2 and cell adhesion	Curtis et al., 2013 (Curtis et al., 2013)
2D nanotopography	hMSCs	~ 0.12 g, 16-30 nm, 1000-5000 Hz	1000 Hz enhance RUNX2, BMP2, OCN, ON and mineralization	Pemberton et al., 2015 (Pemberton et al., 2015)
3D collagen	hMSCs	0.10-0.12 g, 25-30 nm, 1000 Hz, 1-3 weeks	Promote 3D osteogenesis via TRPV1-PKC-β-catenin	Tsimbouri et al., 2017 (Tsimbouri P.M., 2017)
3D collagen	hMSCs	0.36 g, 90 nm, 1000 Hz, 1-3 weeks	Increase osteogenic gene/protein expression, ROS	Orapiriyakul et al., 2019 (In this thesis)

1.11 Nanovibrational bioreactor development

The development of the NS bioreactor aimed to improve the generation of precise amplitudes (and frequencies) and also consider upscaling for industry and clinical application. The first generation NS bioreactor was assembled using single petri dishes attached onto single piezo actuators (Nikukar et al., 2013) **(Figure 1.9A)**. The first version was difficult to assemble and upscale. The second generation (T1000-2000) comprised arrays of piezo actuators assembled on aluminium base block. All piezos stimulated a rigid metallic top plate where tissue culture plates were attached **(Figure 1.9B)**. The third generation (T3000-5000) used a laptop signal generator, thus, the user could adjust to the desired stimulating amplitude simply **(Figure 1.9C).** The fourth generation (NTB version) has bespoke signal generating apparatus with set applitude and frequency (30 nm, 1000 Hz) - i.e. an on/off switch for ease of use. Additionally, handles were designed for convenient transfer in the laboratory **(Figure 1.9D)**. In the fifth generation (NTB version), the piezo-top plate-base block assembly was changed from gluing to screwing with C-clamp in order to improve precision of stimulating amplitude across different areas on top plate and because, with time, it was noted that the glue could fail **(Figure 1.9E)**.

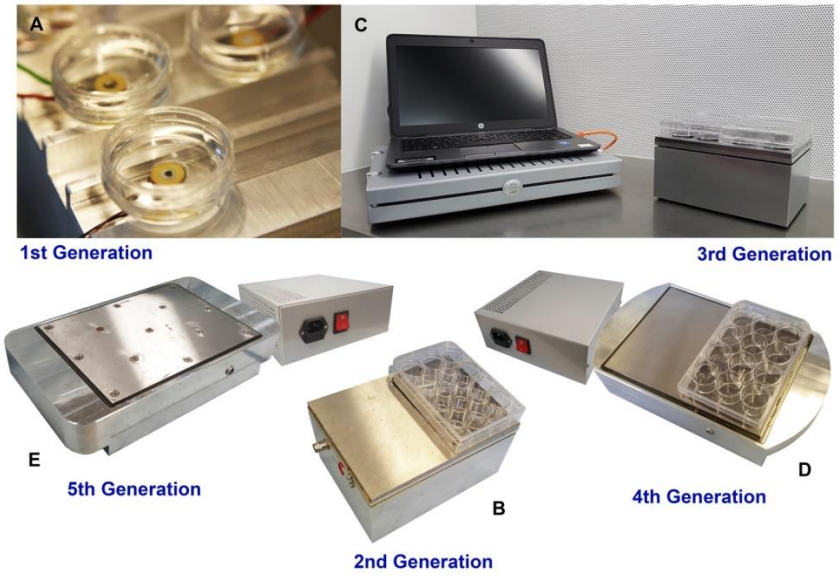

Figure 1.9 NS bioreactor development from 1st to 5th generation.

1.12 Bone tissue engineering

Successful bone healing treatments require osteogenic cells, osteoconductive scaffolds and osteoinductive factors (such as growth factors and mechanical environments) (Giannoudis, Einhorn, & Marsh, 2007). To achieve these goals, biomaterials science is a key consideration in creating cellular microenvironments / scaffolds that can promote osteoconductivity and osteoinductivity (Lane et al., 2014). Materials for bone tissue engineering require biocompatibility, osseointegration and also, optimally, possess biodegradability (Bettina M. Willie & Patrick Strube, 2010). Moreover, bone scaffolds require to be rigid for mechanical support but need to allow nutrients, oxygen and growth factors permeation throughout the scaffolds enhancing cell growth and angiogenesis (Rouwkema et al., 2010; Yousefi, Hoque, Prasad, & Uth, 2015). Thus, integrating the knowledge of material property (e.g. stiffness (Olivares-Navarrete et al., 2017)) and structural architecture (e.g. porosity (Karageorgiou & Kaplan, 2005; Loh & Choong, 2013)) is a fundamental concept to synthesise the scaffold mimicking forms and functions of bone.

1.12.1 Type of materials

Currently, a diverse range of biomaterials are used for bone scaffolds such as polymers, ceramics, etc (Yousefi et al., 2015). Naturally derived polymers (e.g. collagen, gelatin, silk, alginate, etc) are widely used for tissue engineering due to excellent biocompatibility and bioactivity. However, mechanical property modification and reducing degradation time are challenging (Garcia-Gareta, Coathup, & Blunn, 2015). Collagen is the most popular material used in tissue engineering. In human bone, collagen forms a composite with hydroxyapatite providing ductility and stiffness (Swift & Discher, 2014; Swift et al., 2013). Collagen contains the RGD sequence in its peptide chain allowing cells to adhere via integrin binding (Barczyk, Carracedo, & Gullberg, 2010).

Synthetic polymers (e.g. polylactic acid, and polycaprolactone) provide better mechanical support and posses slower degradation (Alizadeh-Osgouei, Li, & Wen, 2018) but require engineering techniques to improve cell adhesion (Serra, Mateos-Timoneda, Planell, & Navarro, 2013).

Ceramic scaffolds (e.g. calcium phosphates (Tripathi & Basu, 2012), bioglass (Q. Z. Chen, Thompson, & Boccaccini, 2006)) are commonly used due to the rigidity. Moreover, calcium phosphate also promotes osteogenesis (John, Varma, & Kumari, 2003; Jung, Park, & Han, 2010; Samavedi, Whittington, & Goldstein, 2013). However, techniques producing interconnective porosity are complex (H. Yoshikawa, Tamai, Murase, & Myoui, 2009). The advantages and disadvantages of common materials are summarized in **table 1.6.**

Table 1.6 Advantages and disadvantages of natural and synthetic polymers for tissue engineering

(Modified from Mottaghitalab et al (Garcia-Gareta et al., 2015; K. Y. Lee & Mooney, 2012; Mottaghitalab et al., 2015; Serra et al., 2013))

Types	Polymers	Advantages	Disadvantages
Natural polymers	Collagen	Excellent biocompatibility, low antigenicity	Poor mechanical properties, Poor cross-linking, high rate of degradation
	Gelatin	Excellent biocompatibility, Biodegradable, cheap, low antigenicity	Poor mechanical properties, high rate of degradation, dissolve at 37°C
	Alginate	Good biocompatibility, low cost, low tissue inflammation response	Non degradable in mammals, limited mechanical stiffness
	Chitosan	Support cell attachment and matrix mineralization, non-toxic	Poor mechanical resistance (hydrogel), toxic if chemical crosslinking
	Silk	Biocompatibility, low infection risk (compared to other protein-based polymer), cost effective	Production time consuming
Synthetic polymers	Polylactic acid (PLA)	FDA approved, excellent biodegradation, biocompatibility	Low mechanical property, low hydrophilicity, tissue inflammation
	Polycarpolactone (PCL)	FDA approved, good mechanical properties	Slow degradation, release of acidic degradation, lack of cell adhesion site
	Polyglycolic acid (PGA)	FDA approved Tunable properties	Lack of cell recognition signals, Inflammatory reactions, high strength and modulus

1.12.2 Scaffold forms and functions

Two common forms of scaffold, hydrogel and rigid, are widely used for tissue engineering. Hydrogels, both natural (e.g. collagen, gelatin) and synthetic (e.g. PEG (Park et al., 2015; Raic, Rödling, Kalbacher, & Lee-Thedieck, 2014)), provide 3D-polymeric networks and hydrophilicity (K. Y. Lee & Mooney, 2001) allowing cell adhesion in 3D niches. Hydrogels provide various advantages such as easy preparation and allowing oxygen and nutrient transportation (Cheema et al., 2012). Hydrogel stiffness is tunable by various techniques (such as crosslinking). However, mechanical properties, syneresis and early degradation remain major hurdles (Scherer, 1989a; Y. K. Zhu et al., 2001).

Rigid scaffolds can be fabricated in various forms such as lattice, fibrous, sponge and woven (Z. Izadifar, X. Chen, & W. Kulyk, 2012). Interporous connection is an important factor. Rigid and dense scaffolds allow slow rates of vascularization, in particular the central area (Rouwkema et al., 2010). Conventional techniques (such as freeze-drying and leaching, etc) are used for fabricating rigid scaffolds together with creating porosity with interporous connections. Nevertheless, these techniques are complex (Loh & Choong, 2013). Solid free-form fabrication (SFF) or rapid prototyping, such as 3D printing, can be used as they can control pore size and porous connectivity by scaffold design (Buj-Corral, Bagheri, & Petit-Rojo, 2018). However, synthetic materials for SFF tend to be hydrophobic resulting in less cell-material affinity and poor cell loading (Shim, Kim, Park, Park, & Cho, 2011).

Biphasic scaffold is an upcoming trend of tissue engineering, combining the advantages of rigid scaffolds and hydrogels together. Hydrogels hold cells within solid scaffold allowing nutrient and growth factor transportation, while porous rigid scaffolds function as structural reinforcement. Currently, there are many techniques for biphasic scaffold production. Rigid scaffolds can be separately prepared and integrated into cell loaded 3D-ECM (Y. Tanaka et al., 2010). Furthermore, the concepts of biphasic scaffolds are also applied in 3D bioprinting. Multiple materials are simultaneously printed for biological and structural support. Synthetic polymer such as PCL is printed as a framework while cells loaded in hydrogel inks function as cellular ECMs

(H. W. Kang et al., 2016; Stanton, Samitier, & Sanchez, 2015) **(Figure 1.10)**.

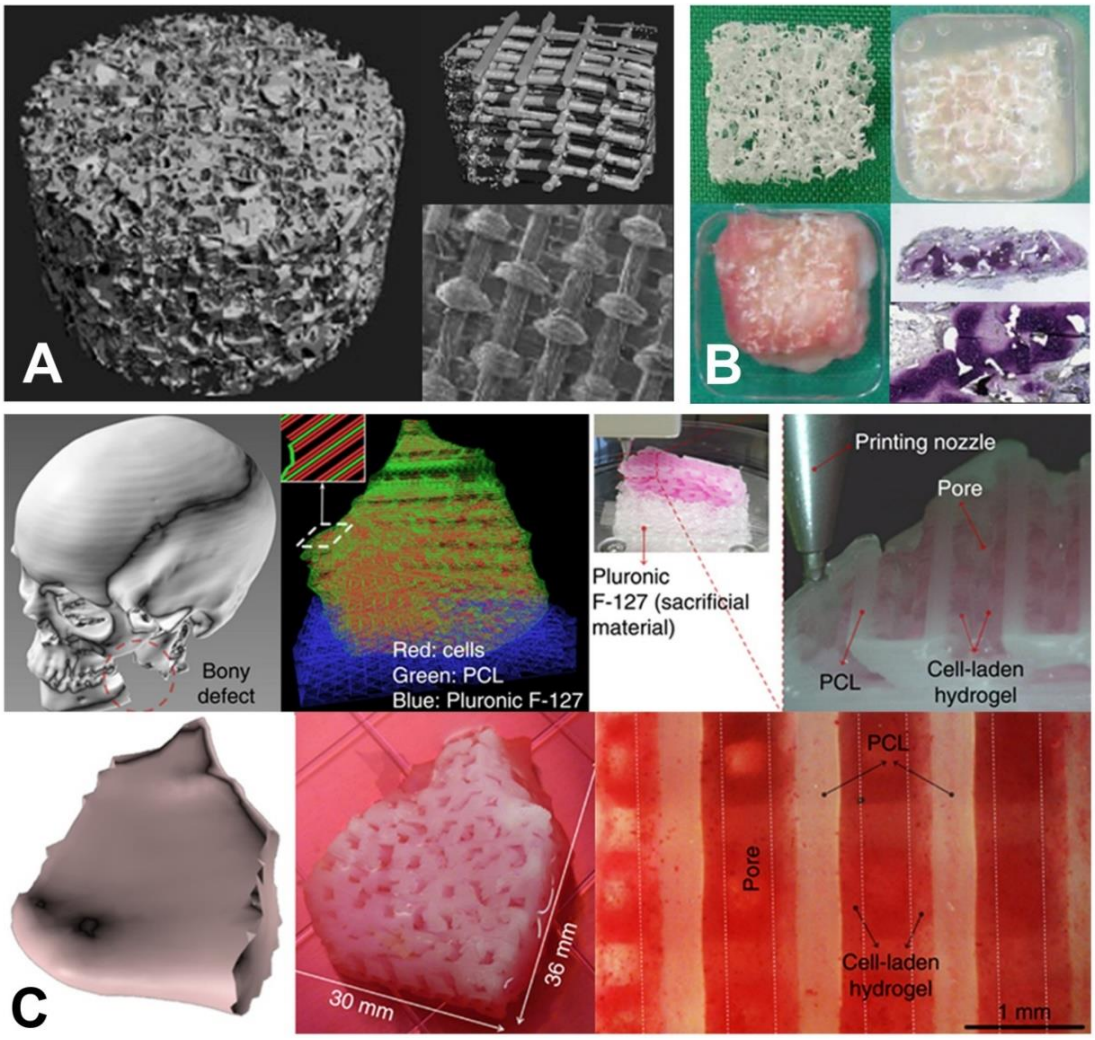

Figure 1.10 Scaffold designs, biphasic scaffold and applications

A) Examples of rigid scaffolds (sponge, fibrous, woven) (With permission of Izadifar et al., 2012 (Z. Izadifar et al., 2012), licensed under Creative Common Attribution License; CC; https://creativecommons.org/licenses/by/4.0/)).
B) Biphasic scaffold - PLLA with sugar leaching technique (0.3 mm pore size, 95% porosity) with atelocollagen (With permission of Tanaka et al., 2010 (Y. Tanaka et al., 2010))
C) Concept of biphasic materials in 3D bioprinting. PCL is a rigid construct functioning as the backbone of scaffolds. Hydrogel

loading with cells is printed between PCL fibers allowing nutrient transportation during cell growth (With permission of Kang et al., 2016 (H. W. Kang et al., 2016)).

1.12.3 Scaffold degradation and host reaction

The bone regeneration process requires long periods of time. Depending on the bone defect size, the bone healing process may be take from 2 months up to a year (Lerner et al., 2005). Corresponding to material degradation by time, implanted bone scaffolds play a role in structural support until mineralization is complete (Amini, Wallace, & Nukavarapu, 2011). Natural polymers possess short term degradation while synthetic polymers provide slower rates of degradation **(Table 1.7)**. In *in vivo* studies, macrophages appear to play role in material degradation (Valentin, Stewart-Akers, Gilbert, & Badylak, 2009). After implantation, the host reacts to scaffolds as foreign body. Inflammation occurs around the scaffold driving fibrosis (Onuki, Bhardwaj, Papadimitrakopoulos, & Burgess, 2008). Thus, synthetic materials such as poly-L-lactic acid (PLLA) and PGA can provide a long-term soft tissue reaction resulting in fluid accumulation, swelling and osteolysis. While natural scaffolds such

as collagen, which possess short term degradation providing less soft tissue reaction (Amini et al., 2011).

Table 1.7 Degradation time of synthetic materials (Modified from Mottaghitalab et al, 2015 (Mottaghitalab et al., 2015))

Materials	Degradation time
Polyglycolic acid (PGA)	6-12 weeks
Polylactic acid (PLA)	12-18 weeks
Poly (lactide-co-glycolide) (PLGA)	1-12 months
Polycaprolactone (PCL)	>24 weeks

1.13 3D Scaffolds for nanovibrational stimulation

In previous studies, the effect of NS on 3D osteogenesis was studied in soft collagen hydrogels (G.D., 2015; Tsimbouri P.M., 2017). However, soft hydrogel contraction is a pivotal problem (as will be described). To develop scaffolds for the NS bioreactor, scaffold stiffness improvement was required to resist the cell pulling force on the ECM as well as providing a benefit to the surgeon regarding handleability. Natural polymers are still the first option due to their better biocompatibility with less cellular reaction (Mottaghitalab et al., 2015). Thus, collagen I used in this thesis is considered in hydrogel and biphasic forms.

1.14 Thesis objectives

1. To develop the implantable 3D-bone scaffolds for nanovibrational bioreactor and propose cell-hydrogel-sponge composite

2. To biologically and mechanically optimise the stimulating amplitude for the proposed 3D scaffold and also study the effect of the high amplitude nanovibrational stimulation on 3D osteogenesis, related biological pathways, metabolomics and inflammatory response.

Chapter 2 Material and Method

Chapter 2 Material and Methods

2.1 Cell isolation and culture

Stro-1 selected MSCs from adult human bone marrow (BM) were obtained from Prof R.O.C. Oreffo, Bone and Joint Research Group, University of Southampton, UK. Cells were cultured in Dulbecco's modified essential medium (DMEM) (Sigma) supplemented with 10% Fetal Bovine Serum (FBS; Sigma), 1% (v/v) L-glutamine (200 mM, Gibco), 1% sodium pyruvate (11 mg/ml; Sigma), 1% MEM NEAA – (amino acids, Gibco) and 2% antibiotics (6.74 U/mL penicillin-streptomycin, 0.2 µg/mL fungizone) (Sigma). Cells were cultured in an incubator set at 37°C with 5% CO_2 environment and subcultured to passage 2-3. Culture media was changed every 3 days. A similar cell culture process and media were used for the MG63 cell line.

2.2 Gel preparation

Collagen hydrogels were prepared by using rat tail collagen type I (2 and 5 mg/ml, First link, UK). 10xDMEM (First link, UK) and FBS (Sigma) were used for cell supplement. 0.1M sodium hydroxide (Fluka, UK) was used for pH titration adjusting to pH 7.7-8.0 by universal lithmus paper and phenol red indicator. The percentage of reagent is shown in **Table 2.1**. After pH titration, MSCs were added in the gel mixture and decanted 2.5 ml into 12 plates. Gelation was allowed in a 37°C incubator for 30 minutes.

Table 2.1 Collagen hydrogel regimens

	0.76 mg/ml hydrogel (final concentration)		1.78 mg/ml hydrogel (final concentration)	
	% V	Vol (ml)	% V	Vol (ml)
Collagen type I (Rat tail, First link UK)	35.7%	8 ml of 2 mg/ml	35.7%	7.5 ml of 5 mg/ml
10xDMEM (First link, UK)	7.14%	1.5 ml	7.14%	1.5 ml
Cells in basal media	7.14%	1.5 ml	7.14%	1.5 ml
FBS (Fisher Scientific)	7.14%	1.5 ml	7.14%	1.5 ml
0.1M NaOH (Fluka, UK)	42.86%	8.5 ml	42.86%	9 ml
Total volume	100%	21 ml	100%	21 ml

2.3 Nanovibrational Bioreactor set up

Selected nanovibrational stimulation (NS) frequencies in .flac file type were operated on Kinsky software (Version 4.3.14). The laptop was connected to the amplifier (Linn amplifier, Sneaky DS, UK) and the signal was transferred to the nanovibrational bioreactor. The nanovibrational bioreactor (T5000 model) incorporating piezo actuators (Thru Ring Actuators; P-010.00H, Physik Instrumente, Germany), was used as the nanovibration-signal effector. To construct the culture plate-bioreactor apparatus, adhesive magnetic sheets (3M, UK) were adhered to the bottom of 6 well- or 12 well- plates (Corning, USA) and attached on the platform of the bioreactor **(Figure 2.1)**.

Figure 2.1 Nanovibrational bioreactor

12 well plates containing collagen hydrogels were attached onto the bioreactor platform. The laptop generating a signal was connected to the amplifier and in turn plugged in the bioreactor for nanovibrational stimulation

2.4 Nanovibration stimulating amplitude measurement by interferometry

Interferometry is used to measure displacement of hydrogel surface or culture plate during NS. The surface displacement is calculated from the interference of 2 split light waves (by a reflecting mirror allowing partially laser reflection as well as passing through) which travel in different optical paths but are generated from a single light source. The phase difference of the 2 waves is analysed with software by Fast Fourier Transform (FFT) algorithm. In our technique, a laser with a known wavelength, is used as a light source. During NS, reflective tape placing on the hydrogel surface reflects a split laser beam back to the detector. NS generates a phase difference of the reflected light waves comparing

to the reference mirror, which in turn is used for the surface displacement amplitude calculation by the software **(Figure 2.2)**.

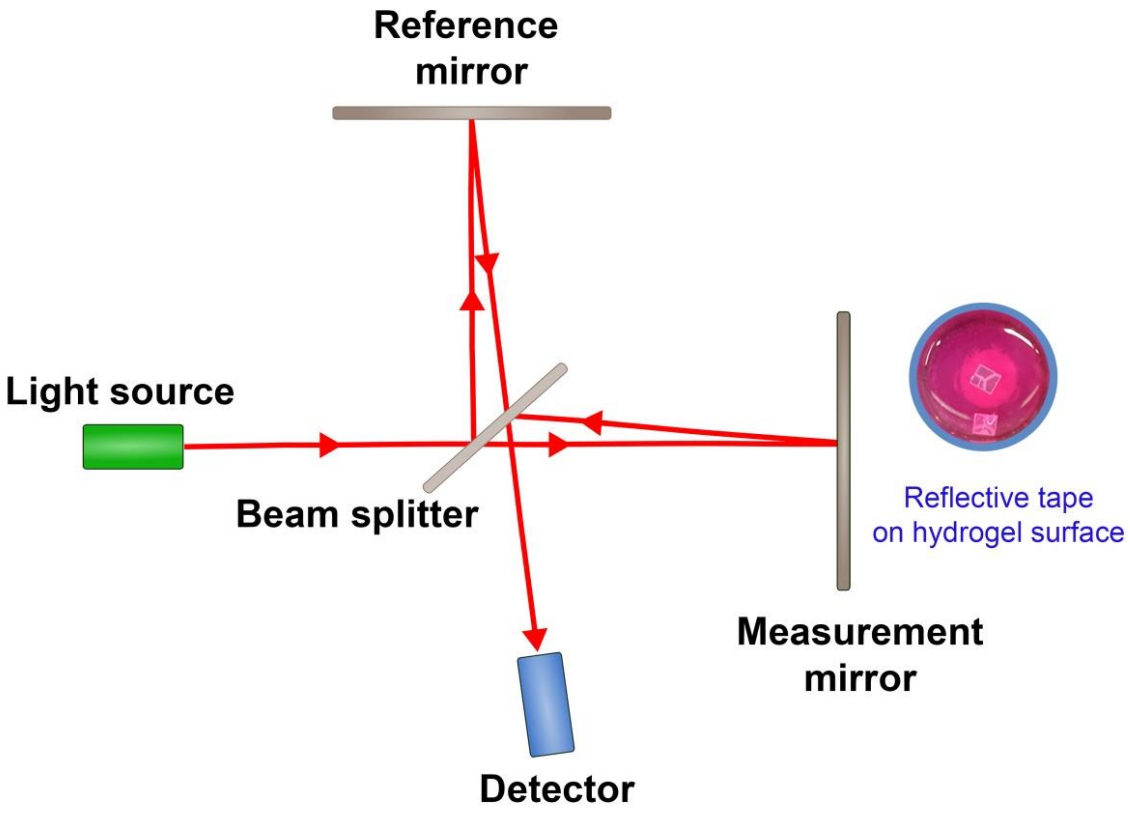

Figure 2.2 Concept of interferometry

In this thesis, 0.8 mg/ml or 1.8 mg/ml collagen hydrogels were prepared. The hydrogel nanovibration was measured by laser interferometric vibrometer (wavelength = 632.8 nm, CW power; 5mW; SIOS, Meßtechnik GmbH, Germany). An oscilloscope (72-6800 model; Tenma, UK) was connected in order to monitor the interferometer. A 3x3 mm of reflective tape was placed on top of the hydrogels underneath 1.5 ml of media to reflect the laser beam. The vibration distance was analysed

using INFAS Vibro 1.8.4 software (SIOS, Meßtechnik GmbH, Germany) **(Figure 2.3)**.

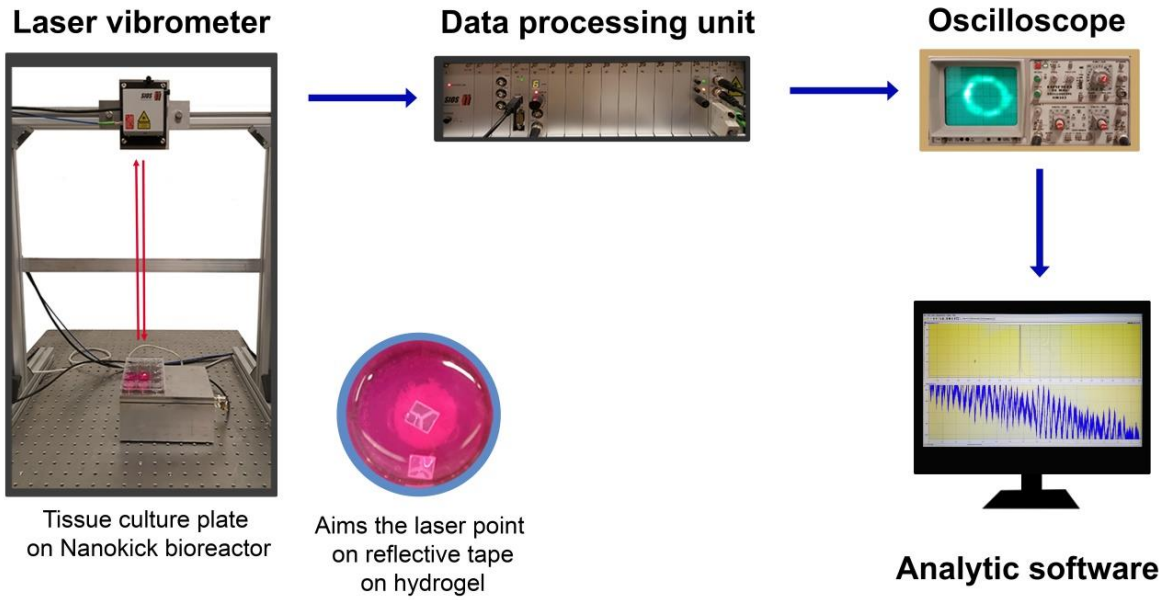

Figure 2.3 Nanovibration measurement by interferometry

Refective tape is placed on the hydrogel surface. A laser beam is aimed to the reflective tape reflecting back to the detector. An oscilloscope was used for signal adjustment. The interferencing signal is analysed by FFT.

2.5 Rheology

Hydrogels were prepared in 6 well plates 24 hours prior to the study. To investigate the quantitative viscoelastic property of the hydrogels, rheology was studied. Hydrogels were placed on the rheology plate **(Figure 2.4)**. Firstly, strain sweep was measured to evaluate the breaking point of the hydrogels and then frequency sweep was used to assess hydrogel stiffness. A modular compact rheometer (MCR 302, Anton

Paar, Austria) was used in this study. To study the rheology of different regimen of hydrogel, the parameters were set as follows;

The study of 0.8 mg/ml hydrogels

The parallel plate method (PP25) was used. The prepared hydrogels were removed from the plate and placed on the rheometer plate. Temperature was set at 23°C. The gap size was 1.5 mm, and normal force compression was 0.01 N. The strain sweep was measured from 0.01% to 1% at 10 rad/sec in order to select the strain which was in linear-viscoelastic regime. Consequently, the frequency sweep test was measured at 1% strain starting from 100-0.1 rad/sec.

The study of 1.8 mg/ml hydrogels

The parallel plate method (PP25) was used. The gap size was 1.4 mm. The samples were placed on 23°C of rheometer plate, and normal force compression was 0.01 N. The strain sweep test was measured from 0.1% to 10% at 10 rad/sec. Consequently, 1% percent strain was selected. Frequency sweep was then measured starting from 100-0.1 rad/sec.

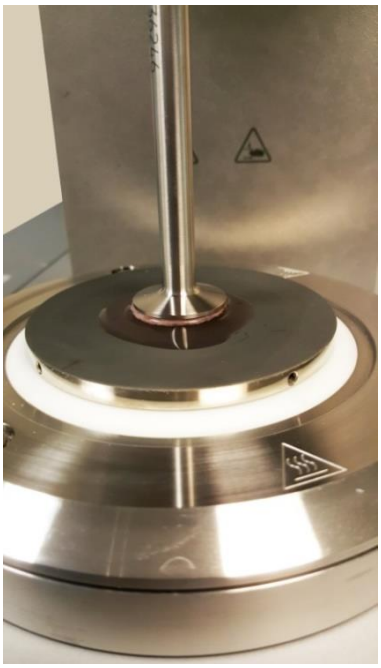

Figure 2.4 Rheology

The hydrogel was transferred onto the rheometer plate. The parallel plate (PP25) was leveled down and touched onto the samples.

To study the stiffness of the hydrogels in specific conditions such as the addition of hydroxyapatite and genipin crosslinking, the parameters were set as shown in **Table 2.2**.

Table 2.2 Rheology parameters set up

Addition of composite	Collagen conc (mg/ml)	Sample volume (ml)	Strain sweep test at 10 rad/sec (%)	Frequency sweep test (rad/s) at 0.1% strain	Gap size (mm.)	Temp (°C)	Pararellel plate diameter (mm.)
HA	0.8	2.5	0.01 -1%	100 – 0.1	1.5	23	25
	1.8	2.5	0.1 - 10%	100 – 0.1	1.5	23	25
Genipin	1.8	2.5	0.1 – 1%	10 – 0.1	2	23	25

2.6 Alamar Blue assay

Stro1 selected MSCs in hydrogels with $4x10^4$ cells/ml density (Tsimbouri P.M., 2017), were used in all of cell viability tests. The process of Alamar Blue assay started by removing the previous culture media. The 10% volume of Alamar Blue resazurin (Bio-Rad, UK) diluted in phenol-red free media (D5030, Sigma) was added into each sample. After further incubation for six hours at 37°C, 5% CO_2, the supernatant containing the up-taken alamar blue was pipetted and transferred into 96 well plates. A microplate reader (Clariostar, Germany) was used to detect light

absorbance at the wavelengths of 570 nm and 600 nm. The percentage of alamar blue reduction was calculated as following;

$$Percentage\ of\ reduction = \frac{(\varepsilon_{ox})\lambda_2 A\lambda_1 - (\varepsilon_{ox})\lambda_1 A\lambda_2}{(\varepsilon_{red}\lambda_1 A'\lambda_2 - (\varepsilon_{red})\lambda_2 A'\lambda_1} x\ 100$$

λ_1	= wavelength 570 nm., λ_2 = wavelength 600 nm.
$(\varepsilon_{ox})\lambda_2$	= molar extinction coefficient of alamarBlue oxidized form of λ_2
$(\varepsilon_{ox})\lambda_1$	= molar extinction coefficient of alamarBlue oxidized form of λ_1
$(\varepsilon_{red})\lambda_1$	= molar extinction coefficient of alamarBlue reduced form of λ_1
$(\varepsilon_{red})\lambda_2$	= molar extinction coefficient of alamarBlue reduced form of λ_2
$A\lambda_1$	Observed absorbance reading for test well
$A\lambda_2$	Observed absorbance reading for test well
$A'\lambda_1$	Observed absorbance reading for negative control well
$A'\lambda_2$	Observed absorbance reading for negative control well

2.7 Live-dead staining

To study cell viability using live-dead staining, $4x10^4$ cells/ml hydrogels were prepared. After the old media were removed, 1%(v/v) calcein AM (Life technology, USA) and 1%(v/v) of ethidium homodimer-1 (Life technology, USA) diluted in 1.5 ml of media and were added in each well. The samples were then re-incubated at 37°C, 5 CO_2 for 2 hours. The 10x magnification microscopic images were taken (Olympus, US) operated on Surveyor software version 9.0.1.4 (Objective Imaging, UK). First and last focusing levels at the center of the hydrogel were recorded. The mid distance of focusing level was selected for the entire XY plane scan. FITC/TRITC channel images were stitched and processed using ImageJ (Version 1.50g, USA) and Photoshop CS4 (Adobe, version11 extended, Ireland).

2.8 qRT-PCR

To assess gene expression changes, $4x10^4$ MSCs/ml in hydrogels were prepared for quantitative RT-PCR (qRT-PCR). The samples were removed from the bioreactor and transferred to falcon tubes. The 2.5 mg/ml of collagenase (Sigma-Aldrich, UK) was added and incubated for 1.5 hours to digest collagen hydrogels. Trizol (Life Technologies) and chloroform

(Sigma-Aldrich, UK) were then added with ratio 5:1 in order to purify nucleic acids. RNA extraction kit (RNeasy extraction Kit, Qiagen) was used to purify RNA. The concentration of purified RNA was measured by a spectrophotometer (Nanodrop 2000c, Thermo scientific, USA). cDNA was then synthesized using the QuantiTect Reverse Transcription Kit (Qiagen). The cycling temperature in each process is shown in **Table 2.3**. Forward and reverse primers for qRT-PCR are shown in **Table 2.4-2.5**. GAPDH, house-keeping gene, was used as the internal control of the analysis. SYBR Green dye was used to target the synthesized cDNA (Quantifast SYBR Green I, Qiagen). Real time PCR was then performed (7500 Real Time PCR system, Applied Biosystem, USA). The $2^{-\Delta\Delta CT}$ method was used for the interpretation (Livak & Schmittgen, 2001). The cycling protocol was run as shown in **Table 2.6**.

Table 2.3 Thermal cycling protocol for cDNA synthesis

Reaction	Temperature	Times (minutes)
Genomic DNA elimination	42°	2
Reverse transcription	42°	30
Inactivation	95°	3

Table 2.4 Primer sequence used in qRT-PCR

	Forward primer	Reverse primer
Alkaline phosphatase	ATGAAGGAAAAGCCAAGCAG	CCACCAAATGTGAAGACGTG
BMP2	CCCACTTGGAGGAGAAACAA	AGCCACAATCCAGTCATTCC
CaSR	CTACGCACCAGAACTCCCTG	CTGTAACAGTGCTGCCTCCA
COL1A1	CCATGTGAAATTGTCTCCCA	GGGGCAAGACAGTGATTGAA
ERK1	CCCTAGCCCAGACAGACATC	GCACAGTGTCCATTTTCTAACAGT
ERK2	TCTGCACCGTGACCTCAA	GCCAGGCCAAAGTCACAG
GAPDH	TCAAGGCTGAGAACGGGAA	TGGGTGGCAGTGATGGCA
Il-6	GATGAGTACAAAAGTCCTGATCCA	CTGCAGCCACTGGTTCTGT
Integrin β5	CTGTGGTCGGTAGCATCCTC	GGATCGCTCGCTCTGAAACT
Integrin β1	GTGCAATGAAGGGCGTGTT	GTTGCACTCACACACACGACA
JNK1	GGGCAGCCCTCTCCTTTA	CATTGACAGACGACGATGATG
JNK2	GAAAGAAGCAAGAATGGTGTTGT	GAGAAGGAGTGGCGTTGCTA
Nestin	GTGGGAAGATACGGTGGAGA	ACCTGTTGTGATTGCCCTTC
NFκB	CAGCTGGCTGAAGATGTGAA	GTGTTTTGGAAGGAGCAGGA
Osteocalcin	CAGCGAGGTAGTGAAGAGACC	TCTGGAGTTTATTTGGGAGCAG
Osteonectin	AGAATGAGAAGCGCCTGGAG	CTGCCAGTGTACAGGGAAGA
Osteopontin	AGCTGGATGACCAGAGTGCT	TGAAATTCATGGCTGTGGAA
Osterix	GGCAAAGCAGGCACAAAGAAG	AATGAGTGGGAAAAGGGAGGG

Table 2.5 Primer sequence used in qRT-PCR (Continue)

	Forward primer	Reverse primer
PPARɣ	TGTGAAGCCCATTGAAGACA	CTGCAGTAGCTGCACGTGTT
Piezo1	TCGCTGGTCTACCTGCTCTT	GGCCTGTGTGACCTTGGA
Piezo2	CCCGGAGTTTGAAAATGAAG	CAGTGCCTCTTCTGAATCAATTT
RUNX2	GGTCAGATGCAGGCGGCCC	TACGTGTGGTAGCGCGTGGC
STAT3	GGCATTCGGGAAGTATTGTCG	GGTAGGCGCCTCAGTCGTATC
SMAD1	CCACTATAAGAGAGTAGAAAGCCC TGT	AAGTTACGGAACTGAGCTAAGAGG
SMAD5	GGGTGCCATGGAGGAACTGGA	AATCCGGCCAGCGCCAAACA
TNFα	CAGCCTCTTCTCCTTCCTGAT	GCCAGAGGGCTGATTAGAGA
TRPA	TGGACACCTTCTTCTTGCATT	TCTTCTCCATTAGCTCAATTTGG
TRPV1	AGAGTCACGCTGGCAACC	GGCAGAGACTCTCCATCACAC

Table 2.6 qRT-PCR cycling protocol

Stage	Ramp rate (%)	Temperature	Time (mins:sec)
Holding stage	100	50	2:00
	100	95	10:00
Cycling stage (40 cycles) Starting cycle 2	100	95	00:15
	100	50	1:00
Melting curve stage	100	95	00:15
	100	60	1:00
	1	95	00:30
	100	60	00:15

2.9 Western blot

The $4x10^4$ MSCs/ml containing hydrogels were prepared for western blot study. To harvest the samples, the collagen hydrogels were digested with 2.5mg/ml collagenase D (Roche) and centrifuged at 200g for 4 minutes. After the supernatant was discarded, the cell pellets were lysed by RIPA lysis buffer containing phosphatase and protease inhibitors (Pierce, Thermo Fisher). BCA assay (Pierce, Thermo Fisher) was used to quantify the protein concentration. The samples were subsequently run on pre-cast 4-12% Bis-Tris gel system (NOVEX, Invitrogen, 12 -well) and transfer onto membrane (Immobilon F, Millipore). The blots were incubated in 5% BSA, 0.1%TBS, tween20 and, subsequently, in primary antibodies **(shown in Table 2.7)**. Vinculin and GAPDH were used as the housekeeping proteins (Bhardwaj et al., 2015; Bhardwaj et al., 2014; D.-Q. Li et al., 2011; Matsumoto et al., 2013; Riera-Borrull et al., 2017). Primary antibodies, prepared in working concentration, were incubated at 4ºC overnight. The blots were washed in 0.1% TBST on a shaker for 5 minutes. Li-COR secondary antibodies (1:10,000) were used and blots were incubated at room temperature for 1 hour. The blots were then washed 3 times for 5 minutes with 0.1% TBST, and the signal was detected using the LICOR system (LICOR Odyssey Sa, UK). Band densitometry was measured by ImageJ software (Version 1.50g, USA).

Table 2.7 Antibodies used in western blot

Antibodies	Brand	Lot No.	Species	Working concentration
pRUNX2	Orb 4788, Biorbyt	A5186	Rabbit	1:2000
RUNX2	Sc-390715, Santa cruz	D1817	Mouse	1:1000
OPN	Sc-21742 Santa cruz	K0217	Mouse	1:1000
GAPDH	Sc32233, Santa cruz	D3018	Mouse	1:1000
Vinculin	V9264, Sigma	086M4757V 047M4795V	Mouse	1:1000
pTRPV1	PA5-64860, Invitrogen	TI2641194	Rabbit	1:1000
TRPV1	H00007442-M01, Abnova	E128A-1F5	Mouse	1:1000
pERK1/2 (P-p44/42)	197G2, Cell signaling, No.4377S	10,15	Rabbit	1:1000
ERK1/2 (p44/42)	137F5, Cell signaling No.4695S	14	Rabbit	1:1000
β-catenin	07-1653, Milipore	2976288	Rabbit	1:1000
Active β-catenin	05-665, Millipore	3102364	Mouse	1:1000

2.10 In-Cell Western

Monolayer Stro1 selected MSCs, seeded at $1x10^4$ MSCs/well density in 24 well plates, were prepared for this study. Samples were fixed with the fixative solution for 15 minutes. The 150 µl of permeabilisation buffer was added and incubated at 4°C for 5 minutes. After that, 150 µl of 1%

milk in PBS was added and incubated for 1.5 hours at room temperature. The 150 µl of primary antibody was then added and incubated at 4˚C overnight on a shaker (pRUNX2; biorbyt, 1:200, RUNX2; Santa cruz, 1:100; diluted in 1% milk blocking buffer). The primary antibodies were removed. The samples were washed 5 times with washing buffer for 5 minutes each at room temperature on a shaker. The 150 µl of secondary antibody against primary antibody (1: 800, Li-cor, in 1% milk blocking buffer) was added for 1 hour on a shaker at room temperature. Secondary antibodies were removed and washed with washing buffer for 5 times, 5 minutes each on a shaker at room temperature. After completing the washing process, samples were dried at room temperature. The samples were read at 680 and 800 nm. The reagents and buffer recipes were shown in **Table 2.8**.

2.11 Immunofluorescent staining

The samples were rinsed with 1xPBS and fixed with fixative at 37˚C for 15 minutes. After that, permeabilisation buffer was added and incubated at 4˚C for 5 minutes. The samples were then blocked with 1% BSA in PBS at 37˚C for 5 minutes. Primary antibody (P-myosin light chain 2, cell signaling, 3671S, rabbit, 1:50) and rhodamine-phalloidin (Invitrogen, Thermo fisher, 1:500) diluted in 1% BSA in PBS were added and incubated at 37˚C for 1 hour. The samples were then washed with 0.5% PBST for 3 times (5 minutes each). Biotinylated secondary antibody (anti-rabbit; Vector Laboratories, USA, 1:50) diluted in 1% BSA in PBS was added and incubated at 37˚C for 1 hour. The samples were washed again with 0.5% PBST for 3 times. Streptavidin-FITC (Vector Laboratories, USA, 1:50) diluted in 1% BSA in PBS was incubated at 4˚C for 30 minutes. The samples were washed for 3 times. A small drop of DAPI (4’,6-diamidino-2 phenylindole, Vectashield) was placed onto the samples and covered with coverslips. FITC/TRITC channel images were taken (Olympus, US) operated on Surveyor software version 9.0.1.4 (Objective Imaging, UK). The images were processed using ImageJ (Version 1.50g, USA) and Photoshop CS4 (Adobe, version11 extended, Ireland). The reagents and buffer recipes were shown in **Table 2.8**.

Table 2.8 Reagents and buffers of In cell western and Immunoflurescent staining

Buffers	Chemicals	Quantities (unit)
Fixatives	Formadehyde	10 ml
	PBS	90 ml
	Sucrose	2 g
Permeabilisation buffer (pH 7.2)	Sucrose	10.3 g
	NaCl	0.292 g
	MgCl2	0.006 g
	Hepes	0.476 g
	Triton X	0.5 ml
1% milk or BSA (Blocking buffer)	Milk or BSA	0.5 g
	PBS	50 ml
0.1% Tween 20 (Washing buffer)	Tween 20	1 ml
	PBS	1000 ml
0.5% Tween 20 (Washing buffer)	Tween 20	5 ml
	PBS	1000 ml

2.12 Protein Inhibitory study

After the experiment was set up **(in chapter 5, section 5.4.5-5.4.7)**, inhibitors which were diluted in basal media as working concentration, were added at day 2 (List of inhibitors and used concentration are shown in **Table 2.9**). Culture media with diluted inhibitor was changed every 2 days.

Table 2.9 List of inhibitors and working concentration

Function	Inhibitors	Cat No./Batch	Working concentration
ERK inhibitor	U126, Tocris	1144/5	10 μM
P38 inhibitor	SB 202190, Tocris	1264/5	5 μM
JNK inhibitor	SP600125, Tocris	1496/10	25 μM
NFkB inhibitor	TPCA-1, Tocris	2559/5	5 μM
TNF alpha	R 7050, Tocris	5432/1	2 μM
ROCK inhibitor	Y-27632, Tocris	1254/35	10 μM
ROS inhibitor	N-acetyl cysteine, Sigma Aldrich	WXBC4028V	10 μM

2.13 Protein antibody microarray

The 4x 10^4 cells/ml of Stro1 selected MSCs in 1.8 mg/ml collagen hydrogels were stimulated with N30 and N90. After stimulation for 1 and 2 weeks, hydrogel samples were digested with collagenase. Total protein amounts were quantified using micro-BCA kit (Pierce, Thermo Fisher). The samples were then transferred to Dr. Marc Antoni Fernandez-Yague (Centre for Research in Medical devices, National University of Ireland, Galway) to process on the protein microarray. β-actin was used as an internal protein control. Data were analysed by Excels. Heatmaps were generated by Hierarchical Clustering Explorer v3.0 (http://www.cs.umd.edu/hcil/hce/hce3.html **(Appendix I)**.

2.14 Statistics

To compare the means of samples more than two groups, One-way ANOVA with Tukey's post hoc test was used in qRT-PCR, ROS measurement and AlamarBlue assay. Two-way ANOVA with Tukey's post hoc test was used to analyse hydrogel and CHSCs contraction by times. To compare the data between 2 groups, two tailed, paired t- test were used in Alamar Blue Assay of CHSCs. Two tailed, Mann-Whitney U test was used in interferometric measurement, rheology western blot and qRT-PCR. Biological sample population with 4 replicates were always used. All results are shown in mean ± standard deviation with 95%, 99% and 99.9% of accuracy (* $P \leq 0.5$, ** $P \leq 0.01$, *** $P \leq 0.001$).

Chapter 3 Strategies to deal with hydrogel contraction for nanovibrational bioreactor

Chapter 3 Strategies to deal with hydrogel contraction for nanovibrational bioreactor

3.1 Introduction

At present, diverse techniques and materials fabrication of 3D scaffolds for bone tissue engineering have been studied (Loh & Choong, 2013). Collagen, a natural ECM protein, is a major component of bone and is thus commonly used for bone tissue engineering (Ferreira, Gentile, Chiono, & Ciardelli, 2012); collagen can enhance MSC adhesion and growth (C. Somaiah et al., 2015). Collagen based scaffolds can be prepared in many forms such as rigid forms (e.g. freeze dried technique (Al-Munajjed & O'Brien, 2009; Kane & Roeder, 2012), electrospinning (Jha et al., 2011; Law, Liau, Saim, Yang, & Idrus, 2017; Matthews, Wnek, Simpson, & Bowlin, 2002)) and hydrogel form (Hesse et al., 2010; M. Liu et al., 2017).

In our previous publication, we recently elucidated that NS can drive 3D osteogenesis in MSCs. The 0.8 mg/ml rat tail collagen type I hydrogels was used as an ECM for MSCs cultured in the NS bioreactor. This soft hydrogel was selected to avoid hydrogel itself inducing an osteogenicity by the effect of stiff ECM (Engler et al., 2006; Tsimbouri P.M., 2017). These studies were performed using bought MSCs. However, when switch to Stro-1 selected MSCs in my PhD, the fresher, less expanded cells were seen to be able to detach gels from the well plates due to increased contractility (data not shown). The contraction and detachment of collagen hydrogel is a critical problem disrupting long-term 3D cell culture in the NS bioreactor. This chapter aims to develop a strategy dealing with hydrogel contraction while maintaining the concept of NS conducting in MSCs within a soft ECM.

Considering cell-material interaction, integrins recognize adhesive ligands in hydrogels, subsequently allowing cytoskeletal contraction (Hoffman, Grashoff, & Schwartz, 2011; Ning Wang et al., 2009). Cell pulling force interacts with ECM leading to syneresis (Scherer, 1989a; Tranquillo, Durrani, & Moon, 1992). Syneresis is a process by which

hydrogels loose fluid and in turn reduce gel size (Scherer, 1989a). Factors inducing collagen hydrogel syneresis are physical cues such as gel-container interaction, ECM factors as well as biological cues e.g. cellular contraction.

The interaction between the gel-container may resist hydrogel contraction force and thus extend the starting time of hydrogel contraction. In the wells, hydrogel has a meniscus shape which indicates that it adheres to the side walls of the well plate and the bonding (adhesion between the hydrogel and cultureware) is stronger than the cohesive force between particles of hydrogel itself (Marshall, Bayne, Baier, Tomsia, & Marshall, 2010). Generally, the culture well surface was pre-treated (e.g. corona-gas treatment, Coroning CellBIND surface) to promote cell adhesion thus the cultureware surface is hydrophilic and negatively charged (Webb, Hlady, & Tresco, 1998). Hydrophilicity helps hydrogels to adhere onto container surfaces (Webb et al., 1998). A well attached gel may resist cell pulling forces better (Y. K. Zhu et al., 2001). Even though the interaction between hydrogel and cultureware can resist hydrogel contraction, theorectically, syneresis did not depend on the interfacial free energy but may depend on hydrogel permeability, viscoelastic property, hydrogel shape and size (Scherer, 1989a, 1989b).

Hydrogel properties, including hydrogel stiffness, fiber density, hydrogel permeability and viscoelastic property also affect hydrogel syneresis rate (Bell, 2000; Scherer, 1989a). Loose fibers allow water to be squeezed out through pores, while dense fibers hold water inside the hydrogel thus reduce syneresis rate (Scherer, 1989b).

Cellular factors such as cell-seeding number, cell proliferation and differentiation rate (Chieh et al., 2010) are crucial factors of cell induced syneresis. Cells generate traction forces to migrate through the collagen fibers resulting in collagen network deformation, compaction of fibrils and squeezing of water from the hydrogel pores, therefore, inducing syneresis (Tranquillo et al., 1992) **(Figure 3.1).**

In this chapter, the first strategy to deal with hydrogel contraction was aimed at mechanical modification. Polylactic acid (PLA) rings were fabricated by 3D printing and implanted into hydrogels to re-balance the

hydrogel contraction force and cell pulling force. This ring-in-gel concept maintained the soft ECM property using a standard 0.8 mg/ml collagen hydrogel formulation used in previous studies with bought-in MSCs (Tsimbouri P.M., 2017). PLA is the widely used for bone tissue engineering as it is rigid, biodegradable, biocompatible and approved by the FDA (Lopes, Jardini, & Maciel, 2012).

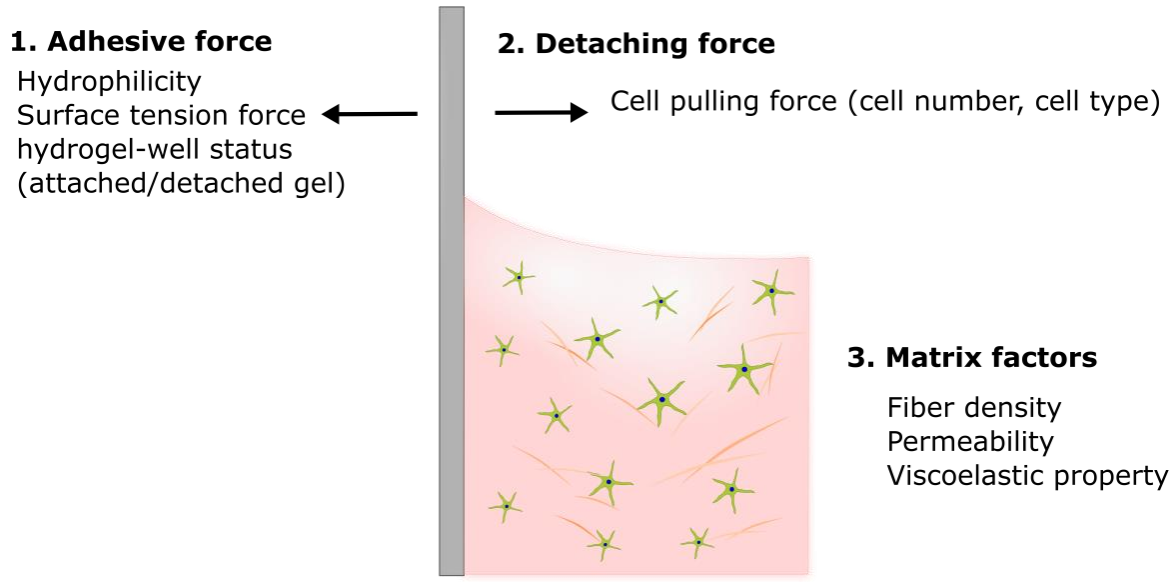

Figure 3.1 Factors related to hydrogel contraction

1) Hydrogels attached to the side wall of a tissue culture well by adhesive surface tension force together with hydrophilicity resisting cell pulling force. Hydrogel syneresis rate can be affected by various factors. 2) A high number of seeded cells accelerates gel contraction. 3) Dense fibers, stiffer ECM and poor liquid permeability (small pores) decrease the syneresis rate. Gel detachment allows adhesive forces to fully contract the hydrogel.

The second strategy was aimed at ECM modification without extra-chemical use based on the concept that stiffer ECM (increasing viscoelastic properties) may reduce syneresis rate. Theoretically, many physicochemical factors have an effect on collagen hydrogel

polymerization such as ratio of collagen mass per total volume (Doyle, 2016), pH, temperature and ionic strength (Achilli & Mantovani, 2010). These factors influence collagen hydrogel fibrillary microstructure, matrix pores, and stiffness (Achilli & Mantovani, 2010). In 2D culture, where MSCs are seeded onto ECM after e.g. gelation, some publications showed successful osteogenic induction of MSCs by the use of physicochemical modifications. For example, collagen hydrogels which are polymerized at 4°C produce long and low fiber stiffness and possibly, in turn, promote cell spreading and focal adhesion formation thus enhancing osteogenic differentiation (Xie, Bao, Bruekers, & Huck, 2017). Furthermore, gelation at 4°C and pH 10 provides a high compressive modulus (Achilli & Mantovani, 2010). On the other hand, achieving these mechanical advantages by using extreme environments (low temperature and high alkaline pH) may be impossible for 3D culture due to poor biocompatibility.

To prepare cells in 3D collagen hydrogels, cells are added into collagen hydrogels and gelation is then initiated. Thus, cells are directly exposed to pH and temperature conditions which can have strongly adverse effects on cell viability and osteogenic differentiation (Achilli & Mantovani, 2010; Fliefel et al., 2016; Monfoulet et al., 2014). Increasing collagen concentration is, therefore, an option for improving stiffness without the addition of chemicals in 3D culture (Y. K. Zhu et al., 2001).

Further to these approaches, crosslinking techniques are widely used to improve collagen hydrogel viscoelastic properties. Many crosslinking techniques had been proposed including chemical (e.g. enzymatic induced, Diels-Alder click reaction) and physical (e.g. ionic, thermal, hydrogel bonding) crosslinking (Hu, Wang, Xiao, Zhang, & Wang, 2019) **(Table 3.1)**. The next strategy in the endeavor to improve collagen hydrogel properties to prevent contraction was thus conducted by using the genipin crosslinker. Genipin ($C_{11}H_{14}O_5$), a naturally derived substance has been widely used for crosslinking hydrogels made from e.g. collagen and chitosan due to low cytotoxicity (Muzzarelli, El Mehtedi, Bottegoni, Aquili, & Gigante, 2015). Genipin, extracted from *Genipa Americana* and *Gardenia jasminoides Ellis*, reacts to primary amines of biopolymers to form crosslinks (and gives a resultant blue colour) (Butler, Ng, & Pudney,

2003), thus increasing stiffness (Fessel, Cadby, Wunderli, van Weeren, & Snedeker, 2014; Sundararaghavan et al., 2008).

3.2 Aims and objectives

1. To assess the feasibility of the “ring in gel; biphasic scaffold” for clinical application in the aspect of gel contraction.
2. To study the effects of increasing collagen concentration on hydrogel handleability, hydrogel contraction and NS force transmission.
3. To investigate the effects of genipin crosslinking collagen in mechanical properties and biological response of MSCs.

Table 3.1 Example of techniques for collagen hydrogel modification

Collagen	Co-polymer	Modification Techniques	Cells	Cell-ECM preparation	Cell response	References
Type I, bovine cornea	-	Crosslinking by EDC, glutaraldehyde	Immortalized human corneal epithelial cells	Separate	2D	Duan et al., 2006 (X. Duan & Sheardown, 2006)
NM	Chitosan	Crosslinking by Glutaraldehyde	preadipocyte	Separate	IC	Wu et al., 2006 (X. Wu, Black, Santacana-Laffitte, & Patrick, 2007)
Type I, atelo, Porcine	Chitosan	PEG stabilized, crosslinking by carbodiimide	Immortalized human corneal epithelial cells	Separate, seed ontop	2D	Rafat et al., 2008 (Rafat et al., 2008)
Type I,	2-methacryl oyloxyethyl phosphoryl choline	Crosslinking by ethanol-water, EDC, NHS	L929 (mouse fibroblast)	Separate	2D	Nam et al., 2010 (K. Nam, Kimura, Funamoto, & Kishida, 2010a, 2010b)
Type I, Rat tail	-	Non-enzymatic Glycation (Ribose)	Bovine aortic endothelial cells (spheroids)	Mixed together	3D	Mason et al., 2013 (Mason, Starchenko, Williams, Bonassar, & Reinhart-King, 2013)
Type I, Bovine	-	Aldehyde-functionalized dextran, oxidizing dextran with sodium periodate	COS-7, L929, Hela cells	Separate, seed on top	2D	Zhang et al., 2014 (X. Zhang, Yang, Yao, Shao, & Chen, 2014)
Calf skin	-	Crosslinking by Glutaraldehyde	-	Separate	-	Tian et al., 2016 (Tian, Liu, & Li, 2016)

EDC; 1-ethyl-3-(3 dimethylaminopropyl)-1-carbodiimide hydrochloride, NHS; N-hydroxysuccinimide, NM =not mentioned, IC = inconclusive

3.3 Methodology and experimental design

Composite optimizations of all hydrogel modification strategies were studied. Mechanical validations including hydrogel contraction, handleability, interferometry, rheology as well as MSCs viability were conducted shown in **Figure 3.2**.

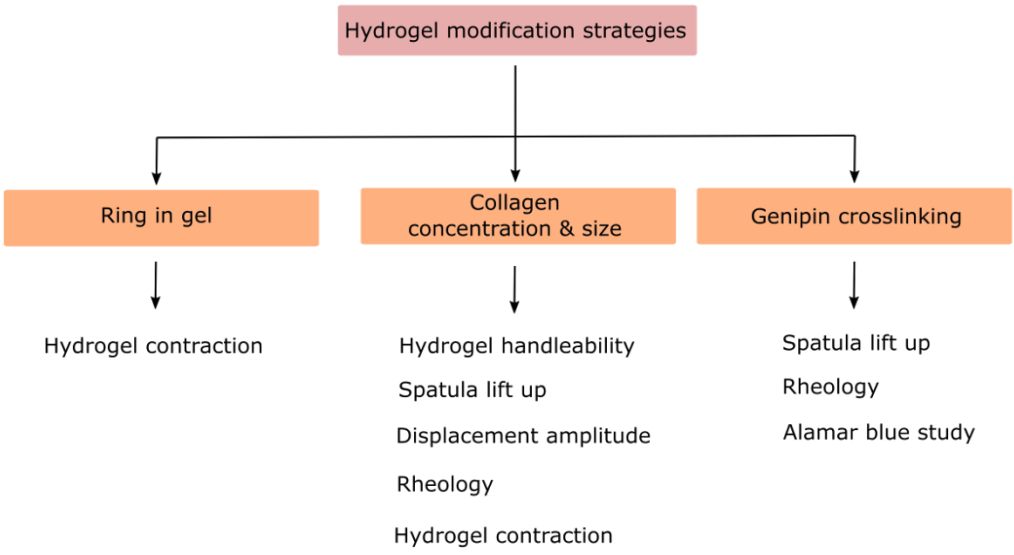

Figure 3.2 Diagram of hydrogel modification strategies and optimization in Chapter 3

The optimization of three strategies; Ring-in-gel, collagen concentration optimization and genipin crosslinking were studied.

3.3.1 'Ring in gel' biphasic scaffold

To engineer the hydrogel supporting structure, ring shape scaffolds were designed (AutoCAD 2016 software, Autodesk, USA) and printed

by 3D printer using polylactic acid (PLA). Two generation ring designs are shown in **Figure 3.3**.

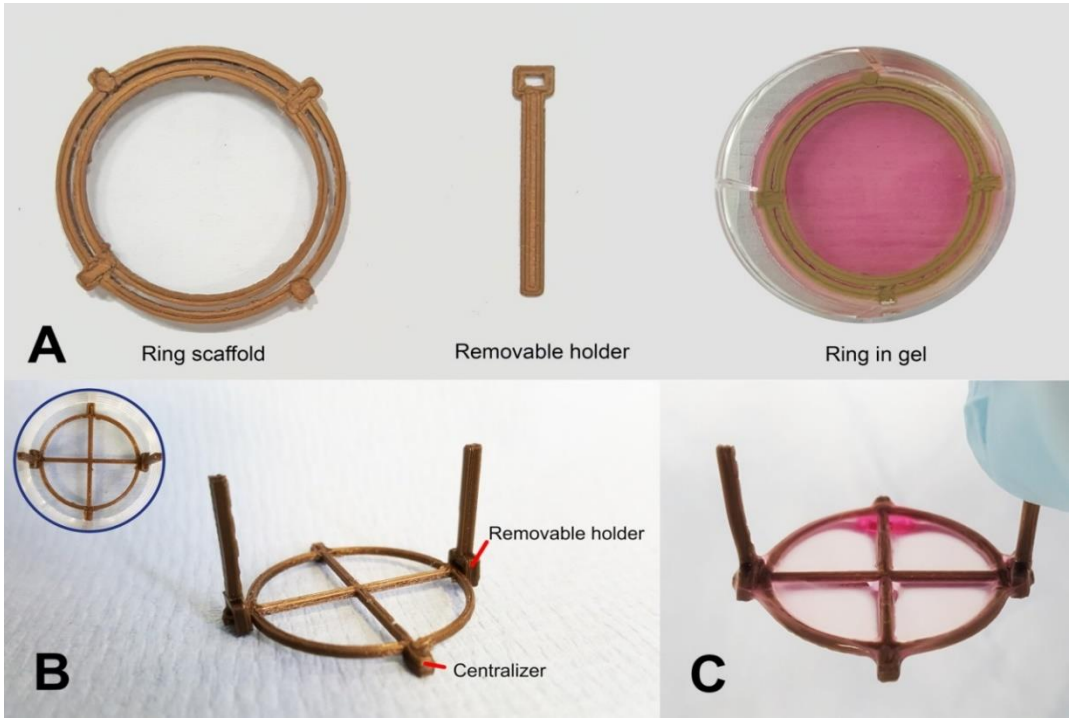

Figure 3.3 PLA ring design

A) The first-generation ring scaffold design. The 4-notches function as a centralizer of the PLA ring. The notches can be attached to removable holders aiming to remove the Ring-gel composite.
B) The second-generation ring scaffold design: Cross hair design attached with removable holder for six well plates.
C) Long term culture ring-gel composite. MG63 seeded in 0.8 mg/ml collagen hydrogel with the second-generation ring scaffold. At day 65, hydrogel attached to the ring. The gel-ring composite can be transferred from the 6-well plate using a holder.

3.3.2 Collagen concentration

The 0.8 and 1.8 mg/ml (final collagen concentration) of collagen hydrogels were prepared using rat tail collagen type I (2 and 5 mg/ml of commercialized concentration, First link, UK) as shown in chapter 2, section 2.

3.3.3 Genipin crosslinking

The sterile 1x PBS was used to prepare 20 mM of genipin stock solution (Sigma Aldrich, UK). The genipin stock was then diluted to 0.5 mM, 1 mM and 10 mM using basal media. After completing the gelation process, 1.5 ml of genipin solution was added onto the gels and incubated at 37°C for 12 hours.

3.3.4 Rheology

Rheology was performed as shown in Chapter 2, section 2.5. The 0.8 and 1.8 mg/ml hydrogel and genipin crosslinking hydrogels were prepared in 6 well plate, 24 hours prior to the testing. Rheology parameters was shown in **Table 3.3.**

Table 3.2 Rheology parameter set up

Experiments	Collagen conc (mg/ml)	Sample volume (ml)	Strain sweep test at 10 rad/sec (%)	Frequency sweep test (rad/s) at 1% strain	Gap size (mm.)	Temp (°C)	Pararellel plate diameter (mm.)
Conc test	0.8	2.5	0.01 -1%	100 – 0.1	1.5	23	25
	1.8	2.5	0.1 - 10%	100 – 0.1	1.5	23	25
Genipin test	1.8	3.5	0.1 – 1%	10 – 0.1	2	23	25

3.3.5 Hydrogel contraction

In order to monitor the hydrogel contraction without NS, percentage of hydrogel contraction comparing to initial size was quantified by the use of gel diameter or gel surface area in top view. To measure the hydrogel diameter, the diameters of 6 and 12 well plates were used as references. The center of the hydrogel was identified and the shortest diameter of the hydrogel was selected for measurement using a scientific ruler. An average of three repeated measurements was recorded at each time point, every 3-4 days. To quantify the hydrogel top view area, the hydrogel image was taken in top view every 3-4

days. The hydrogel surface areas in top view were measured and analysed by ImageJ software.

3.4 Results

3.4.1 Ring in gel strategy

3.4.1.1 The first-generation ring-in-gel contraction

To study the efficacy of the first-generation ring design, Stro1 selected hMSCs seeded in 0.8 mg/ml rat tail collagen type I hydrogels were prepared and trialled with a range of culture plates in order to study whether different culturewares could improve hydrogel adhesion. Thus, four conditions were prepared in two commercial 6-well plates (A; CytoOne, USA Scientific, B; Corning, Costar, Sigma-Aldrich): group1; brand A with ring, group2; brand A with no ring, group 3; brand B with ring and group 4; brand B with no ring. Hydrogel contraction was observed for 4 weeks.

After 4 weeks of hydrogel observation (**Figure 3.4**), plain collagen hydrogels in plate B (no ring group) showed less gel contraction compared to hydrogels in plate A. At day 17, the percentage of remaining hydrogel diameter (compared to time 0), where no ring scaffold was used, was significantly smaller than where a ring was used in plate A. However, there were no significant difference in plate B with/without the use of a ring. The results indicated that plate B provided better hydrogel adhesion to side wall of wells than that of plate A. Furthermore, the first-generation PLA ring could not prevent hydrogel contraction.

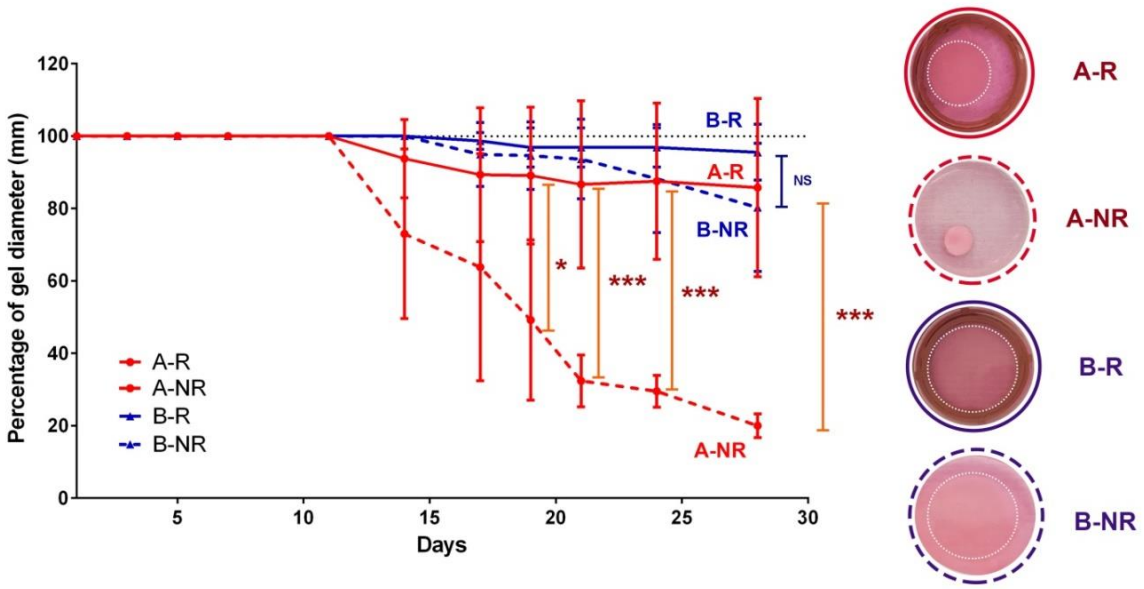

Figure 3.4 Hydrogel contraction in different brand of cultureware

Comparison of the percentage of gel diameter remaining, from time 0 (starting diameter), between Stro1 selected MSCs in 0.8 mg/ml gels seeded into 6 well plates from brand A (CytoOne, USA Scientific) and brand B (Corning, Costar, Sigma-Aldrich) with/without the first-generation ring scaffold. Hydrogel contraction in plate A with ring was greater than plate B with ring. However, it was not seen to prevent gel contraction in both culturewares. Gel contraction in plate A was significantly higher than that in plate B. (n=3, * P≤ 0.05, ** P≤ 0.01, *** P≤ 0.001, Two way ANOVA, Tukey's post hoc test, A; Brand A; B; Brand B, R; ring, NR; no ring).

3.4.1.2 The second-generation ring-in-gel contraction

The second-generation PLA ring was designed with a cross hair pattern aiming to reduce cell pulling force. To study the efficacy of hydrogel contraction reduction of the second design ring, MG63 seeded in 0.8 mg/ml collagen hydrogels were prepared (n=3). Hydrogel contraction was observed for 4 weeks. The results showed that the new design of ring scaffold prevented the gel contraction **(Figure 3.3B).** However, the hydrogel still detached from the 6-well plate. The significant

difference of percentage gel diameter remaining between ring and no ring groups began at day 6.

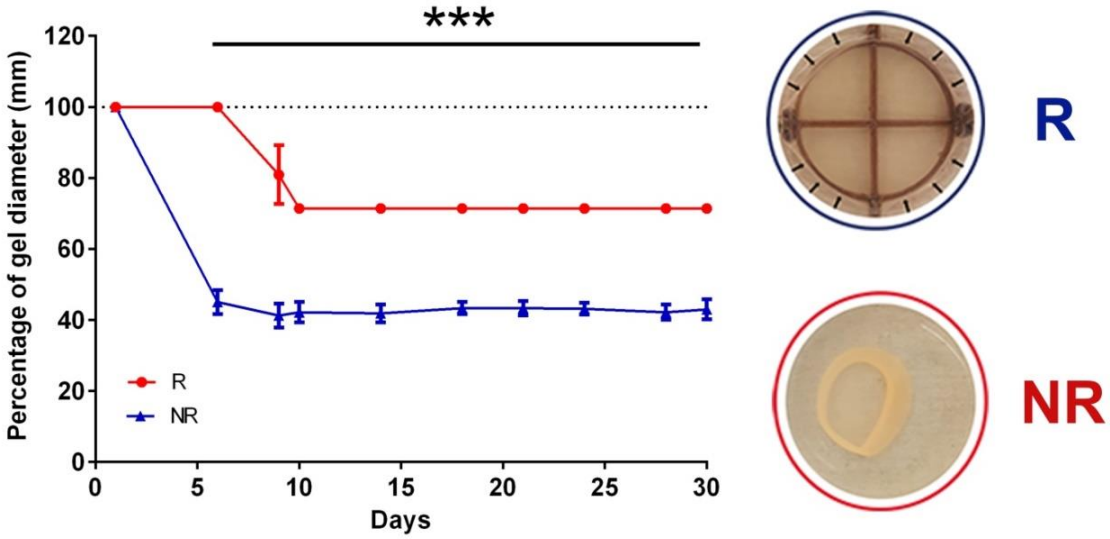

Figure 3.5 Hydrogel contraction in the second-generation ring-gel composite.

Comparison of the percentage of gel diameter by time between groups with/without the second-generation rings for cells seeded into 0.8 mg/ml collagen hydrogels. The second-generation ring design can prevent further hydrogel contraction after day 10. (*n=3, P≤ 0.05, ** P≤ 0.01, *** P≤ 0.001, R; ring, NR; no ring, 2-way ANOVA, Sidak's post hoc tests)

3.4.2 Collagen concentration and diameter

It is considered that the ring-in-gel approach might be problematic for future clinical use. Thus, physicochemical modulation of hydrogels was the next strategy to be trialed. Hydrogel diameter and collagen concentration were considered. Previously, 0.8 mg/ml collagen hydrogels (2.5 ml) seeded with MSCs in 6 well plates were used in 3D NS-induced osteogenesis (Tsimbouri P.M., 2017). However, the collagen hydrogel is too thin and difficult to handle in clinical use. To improve handleability for clinical application, hydrogel use of 12 well plate rather than 6 well plate was trialed (**Figure 3.6**). Interferometry

showed that changing the well plate diameter did not reduce the nanovibration amplitude **(Figure 3.7)**.

Increasing collagen concentration from 0.8 mg/ml to 1.8 mg/ml appeared to improve hydrogel handleability **(Figure 3.9)**, improve stiffness **(Figure 3.10)** and extend the starting date of hydrogel contraction **(Figure 3.11)** while still allowing good vibrational fidelity **(Figure 3.12).**

3.4.2.1 Hydrogel diameter validation

Considering intended clinical use, a thin and flat hydrogel, seeded in a 6 well plate, is difficult to fill the bone defect. Furthermore, dividing the scaffold into small pieces, e.g. using a scalpel, could potentially injure the nanovibration stimulated MSCs. Comparing well plate diameter to human bone morphology, a 12 well plate diameter was approximately a transverse diameter of human humerus (Murdoch, Mathias, & Smith, 2002) which is a moderate long bone size. Whereas, a 24 well plate diameter is approximately the diameter of human phalanges (Ash & Unsworth, 2000). Therefore, in this thesis, 12 well culture plates (22.1 mm well diameter) were selected for 3D hydrogel size regarding size and handlability. Moreover, it is an optimal scaffold size to fill long bone defect where the common sites of injury are tibia, femur and humerus (Kironde, Sekimpi, Kajja, & Mubiri, 2019).

3.4.2.2 Hydrogel handleability and spatula lift test

By preparing hydrogels with the 2.5 ml volume in 6 well plates, hydrogel diameter was larger than finger diameter of the user **(Figure 3.6A)**. These large, soft and thin characteristics resulted in a floppy hydrogel that was difficult to handle. It can be suggested that the 12 well plate size hydrogel (2.5 ml volume) therefore provides a better handleability **(Figure 3.6B)**.

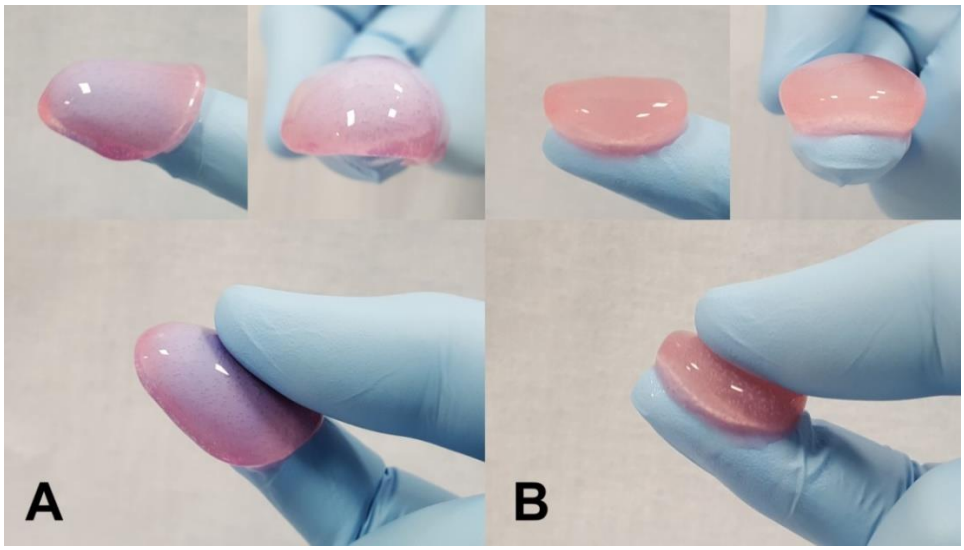

Figure 3.6 Hygrogel handleability

6 well plate (A) and 12 well plate (B) sized hydrogels. (6 and 12 well plate diameter; 35 mm and 22.1 mm respectively, 2.5 ml/ wells). 6 well plate diameter is not suitable for surgeon handleability.

3.4.2.3 Hydrogel surface displacement amplitude measurement of 6 and 12 well plates

The efficacy of nanovibrational transmission through the hydrogels in the different sizes of tissue culture plate was then investigated. All hydrogels were prepared in 6 and 12 wells plates and measured at the centre point by interferometry. There was no significant difference in surface displacement amplitudes comparing between hydrogels in the 6 well and 12 well plates (**Figure 3.7A**); at 1000 Hz, NS provided a good fidelity of displacement amplitudes in both plates. Hydrogels in 12 well plates showed greater average amplitude at resonant frequency than those in 6 well plates, but this resonant frequency was clear at cell stimulating frequency of this study (1000 Hz) (**Figure 3.7B**). Thus, changing from 6 well to 12 well plate diameter did not have an effect on NS force transmission at 1000 Hz.

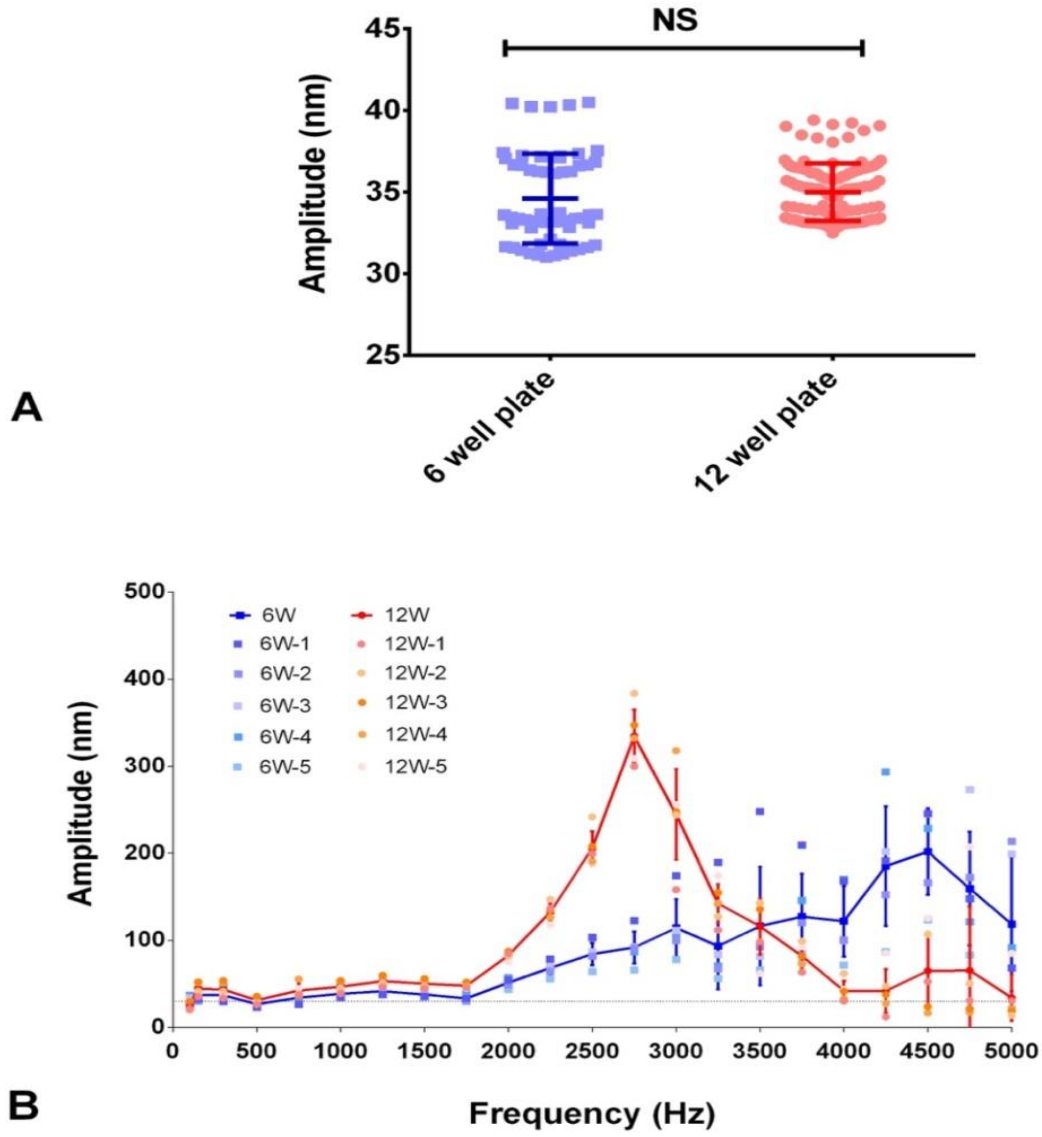

Figure 3.7 NS amplitude comparison between 6 and 12 well plates

A) The NS amplitude comparison of hydrogels (at the centre point) prepared in 6 and 12 well plate and stimulating at 1000 Hz, no significant difference were noted (6 wells; mean =55.36 nm, SD=5.21 nm, 12 wells; mean 61.87 nm, SD 21.90 nm, * P≤ 0.05, ** P≤ 0.01, *** P≤ 0.001, n=12-24, Mann-Whitney test, T5000, Voltage peak to peak 19.69).

B) Frequency-amplitude plot showed that NS provided reliable amplitude at 1000 Hz in hydrogels both in 6 and 12 well plates. The resonant frequency was noted between 1500-3000 Hz resulting in amplitude amplification thus providing unreliable stimulating amplitudes.

3.4.2.4 The homogenicity of stimulating amplitude across the wells on the NS bioreactor

The comparison of the 6 and 12 well plates showed that the NS bioreactor generated reliable amplitudes through all wells in both 6 and 12 well plates. Thus, changing from the 6 to 12 well culture plate did not affect NS (**Figure 3.8**).

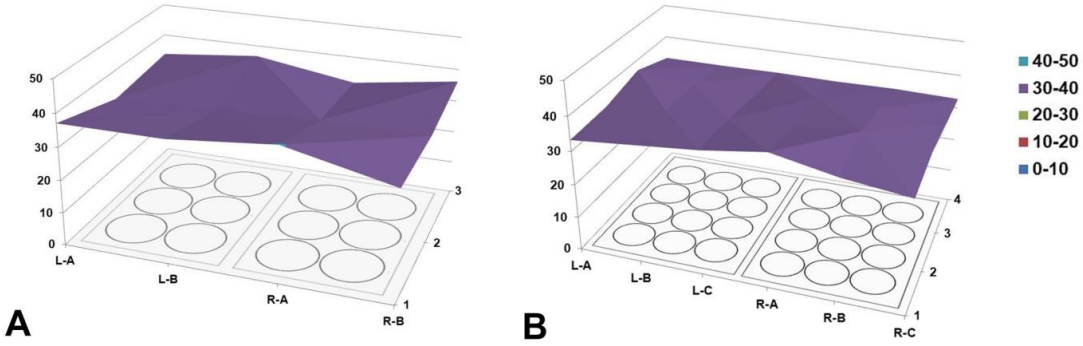

Figure 3.8 NS stimulating amplitude across the 6 and 12 culture wells

The 3D surface plot showed hydrogel displacement amplitude measured at the centre of hydrogels in all wells of the plates. During NS at 1000 Hz, the NS bioreactor generated reliable NS amplitudes across the 6 (A) and 12 (B) well plates. (6 wells, n=12 gels, mean 34.6 nm, SD 2.85 nm; 12 wells, n=24 gels, mean= 34.99 nm, SD=1.78 nm, third generation bioreactor, PSU4003).

3.4.2.5 Collagen concentration

It is known that increasing collagen concentration can increase hydrogel stiffness (Swift & Discher, 2014), thus potentially extending the starting date of hydrogel contraction (Chieh et al., 2010). Increasing collagen concentration is interesting as it is simple and free of additional chemical crosslinking, maintaining 3D cellular response and still using collagen, which is the naturally derived extracellular matrix. To investigate the effect of collagen concentration, mechanical properties including hydrogel characteristics and stiffness, hydrogel contraction and gel displacement during NS were measured.

3.4.2.5.1 Spatula lift test

The spatula lift test was performed for simple hydrogel inspection. The 0.8 mg/ml hydrogel is very soft while the 1.8 mg/ml hydrogel was more handleable and could maintain its shape during the lift up **(Figure 3.9)**.

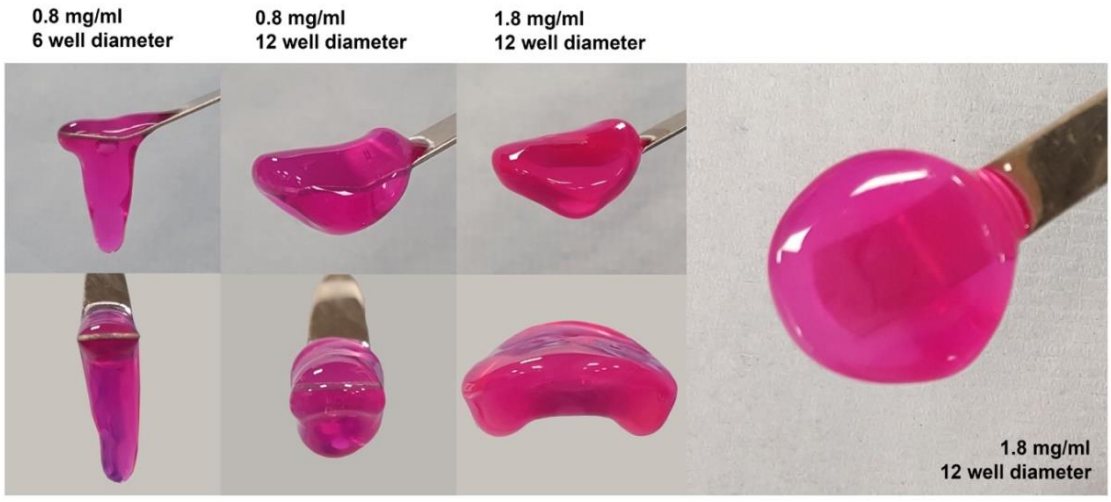

Figure 3.9 Hydrogel characteristics at 2 week.

The 0.8 mg/ml hydrogel in 6 well plate (2.5 ml collagen hydrogel) is very soft. The 0.8 mg/ml hydrogel in the 12 well appears floppy while the 1.8 mg/ml hydrogel can maintain its shape.

3.4.2.5.2 Hydrogel stiffness

As discussed, to improve hydrogel handleability, the final collagen concentration of the hydrogels was increased from 0.8 mg/ml to 1.8 mg/ml. The hydrogel viscoelastic property was measured by the rheometer. Frequency sweep test was conducted to study the viscoelasticity of polymer architecture or crosslinking (Zuidema, Rivet, Gilbert, & Morrison, 2014). Comparing storage (G') and loss (G") modulus of the hydrogels, 1.8 mg/ml collagen hydrogel had a higher storage modulus (G'= 161.27 Pa; SD 15.17 Pa) than that of the 0.8 mg/ml hydrogel (G'= 25.67 Pa; SD 2.91 Pa) **(Figure 3.10)**. Even though 1.8 mg/ml hydrogel was still soft, it was handleable.

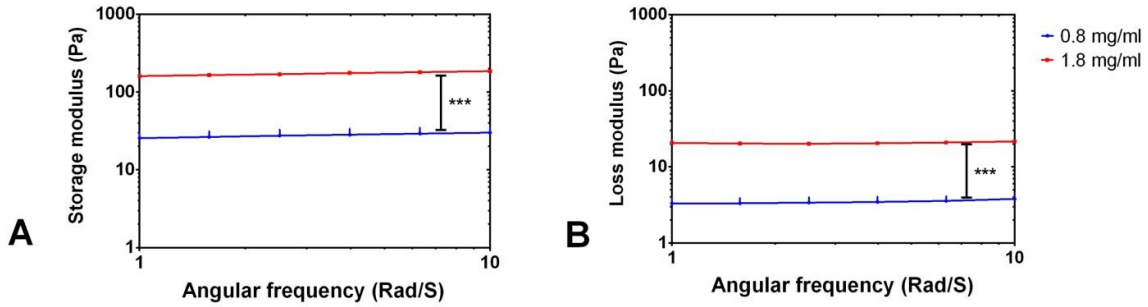

Figure 3.10 Hydrogel stiffness measured by rheology

Frequency sweep test with angular frequency (ω) ranging from -20 rad/second of 0.8 vs 1.8 mg/ml collagen concentration studied by rheology (n=3). The 1.8 mg/ml collagen had a higher storage modulus (A), thus, indicating higher elastic modulus than that of 0.8 mg/ml. The elastic modulus was higher than the loss modulus (B) confirming that the properties of both 0.8 and 1.8 mg/ml collagen were hydrogels, rather than liquid (mean±SD, n=4, * P≤ 0.05, ** P≤ 0.01, *** P≤ 0.001, Mann-Whitney test).

3.4.2.5.3 Hydrogel contraction

To study the effect of cell number and collagen concentration on hydrogel contraction, 0.8 and 1.8 mg/ml collagen hydrogels seeded with 40,000 and 80,000 Stro1 selected MSCs/ml were prepared. The surface areas of hydrogels in top view were quantified every 3-4 days. The 0.8 mg/ml cell seeded collagen hydrogels started to contract at day 28 in this experiment. Interestingly, increasing collagen

concentration to 1.8 mg/ml extended the starting date of hydrogel contraction to day 80. Moreover, increasing cell seeding number produced greater hydrogel contraction, but did not accelerate the start date of contraction **(Figure 3.11).**

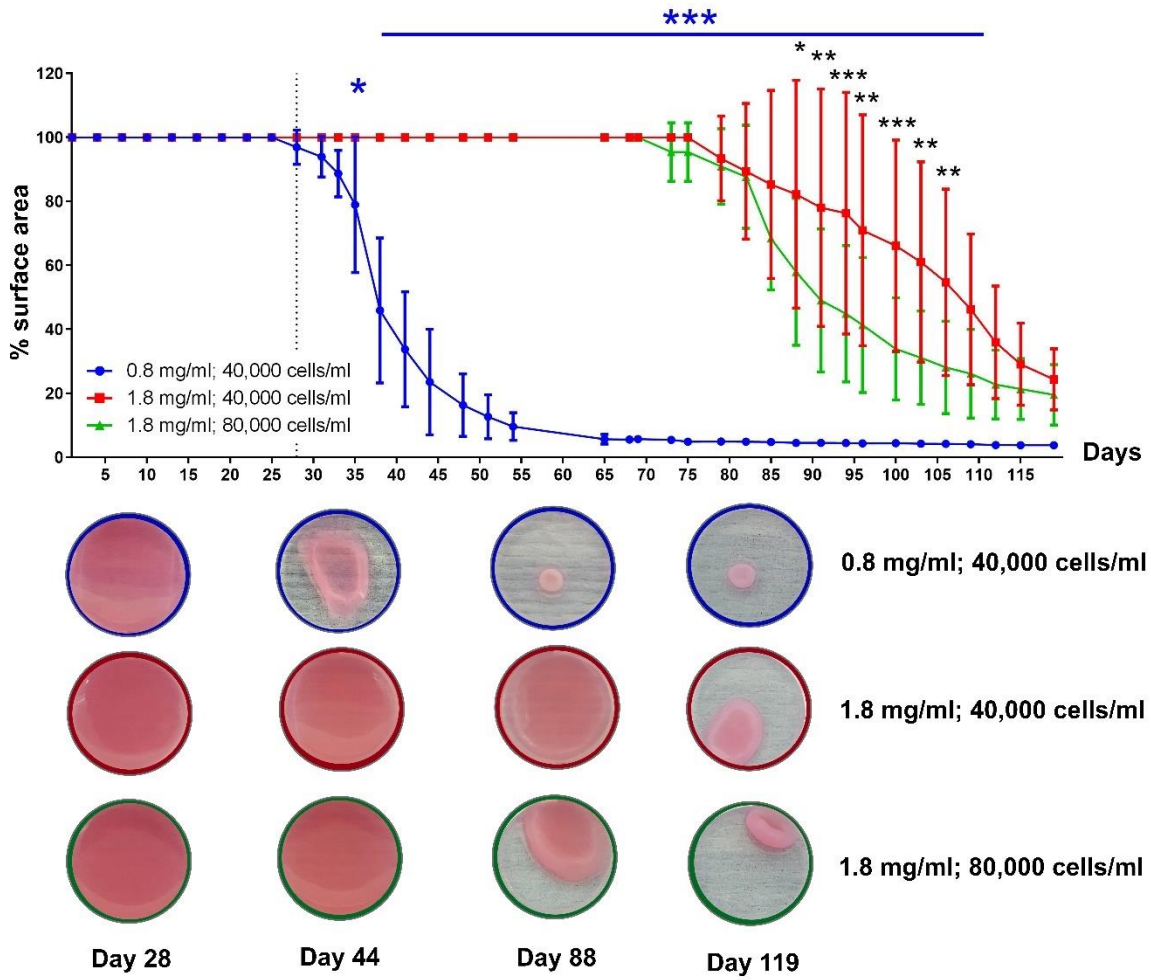

Figure 3.11 Hydrogel contraction observation.

The 0.8 mg/ml hydrogel contraction started at day 28. However, the 1.8 mg/ml hydrogels contracted at day 80. The 1.8 mg/ml collagen hydrogel with 80,000 MSCs/ml contracted more than that with 40,000 MSCs/ml. (mean±SD, n=4, * P≤ 0.05, ** P≤ 0.01, *** P≤ 0.001, Two-way ANOVA, Tukey's post hoc test).

3.4.2.5.4 Interferometry

To investigate the effect of increasing collagen concentration on NS amplitude, the 0.8 and 1.8 mg/ml collagen hydrogels were stimulated at 1000 Hz with 30 nm vibrations. NS amplitude of 1.8 mg/ml collagen

hydrogels (mean 34.99 nm, SD =1.76 nm) were slightly higher than that of 0.8 mg/ml hydrogels (mean 35.83, SD 1.77) (**Figure 3.12A**). Again, the NS bioreactor generated reliable amplitudes at 1000 Hz without resonance (**Figure 3.12B**).

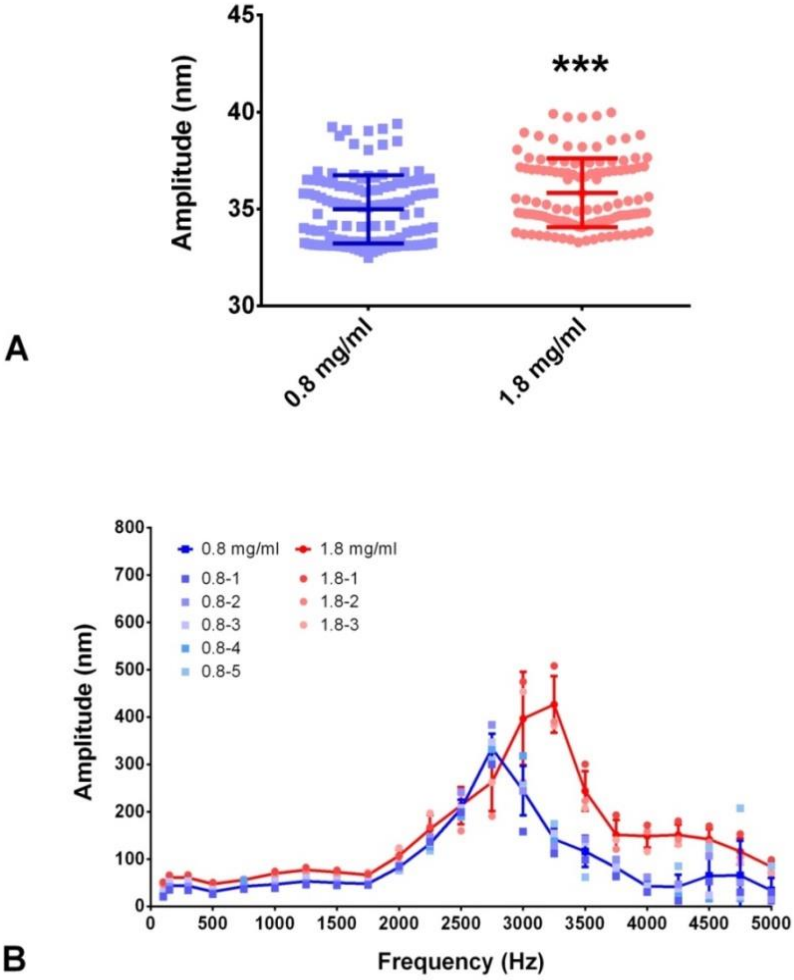

Figure 3.12 Interferometry for 0.8 and 1.8 mg/ml collagen hydrogels in 12 wells plates.

Comparison of 0.8 and 1.8 mg/ml collagen hydrogel in 12 well plates: A) During NS, gel surface displacement of 1.8 mg/ml collagen hydrogel was significantly higher than that of 0.8 mg/ml group (mean±SD, n=24, * P≤ 0.05, ** P≤ 0.01, *** P≤ 0.001, Mann-Whitney test, PSU4003). B) Frequency-amplitude graph showed that both 0.8 and 1.8 mg/ml collagen hydrogels showed good fidelity of NS at 1000 Hz. Resonant frequency of both hydrogel types ranged approximately from 2,750 to 3,250 Hz.

3.4.3 Genipin crosslinking collagen hydrogel

In the previous section, it was shown that increasing collagen concentration can extend the starting date of hydrogel contraction. To achieve better hydrogel stiffness and possibly resist hydrogel degradation *in vivo*, genipin crosslinking was trialed. Mechanical and biological optimisations were studied which are described in this section.

3.4.3.1 Genipin-hydrogel characteristics

To observe hydrogel characteristics after genipin crosslinking, 2.5 ml of 1.8 mg/ml collagen gels were prepared in 12 well plates. All hydrogels were, in turn, crosslinked with 0, 1, 5, 10 mM of genipin. Genipin crosslinking resulted in a gel color change to dark blue, in particular at 5 and 10 mM concentrations. However, 5 and 10 mM genipin crosslinked hydrogels showed better gel handleability by inspection (**Figure 3.13**).

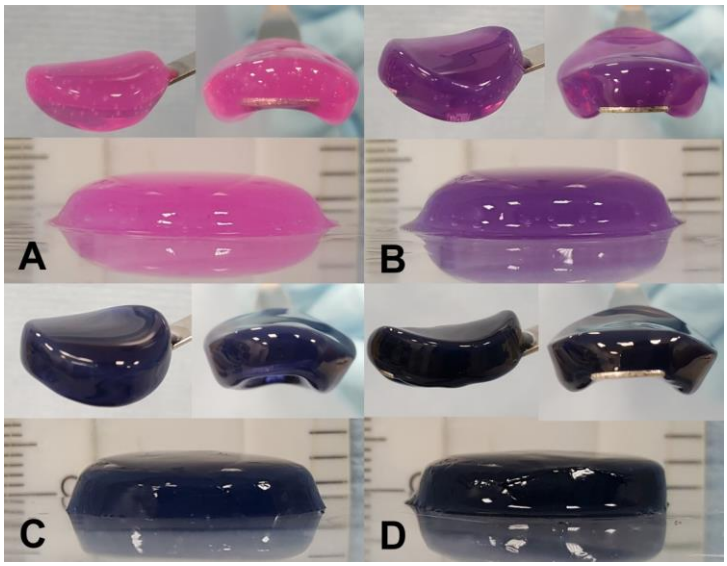

Figure 3.13 Genipin crosslinked hydrogel

The 0, 1, 5 and 10 mM (A to D) of genipin crosslinked 1.8 mg/ml collagen hydrogels (2.5 ml seeded in 12 wells plate). Improved handleability was seen after genipin crosslinking.

3.4.3.2 Genipin-crosslinking and hydrogel stiffness

The 1.8 mg/ml collagen hydrogels crosslinked with 0, 1, 5 and 10 mM of genipin were prepared in 6 well plates. The stiffness of all hydrogels was studied by rheology. The frequency sweep test showed that there was no significant difference in elastic modulus between 0 and 1 mM genipin crosslinking. The 5 and 10 mM genipin crosslinking, however, significantly increased elastic modulus ($P \leq 0.001$) up to 1.03 kPa in the 10 mM genipin group (**Figure 3.14**).

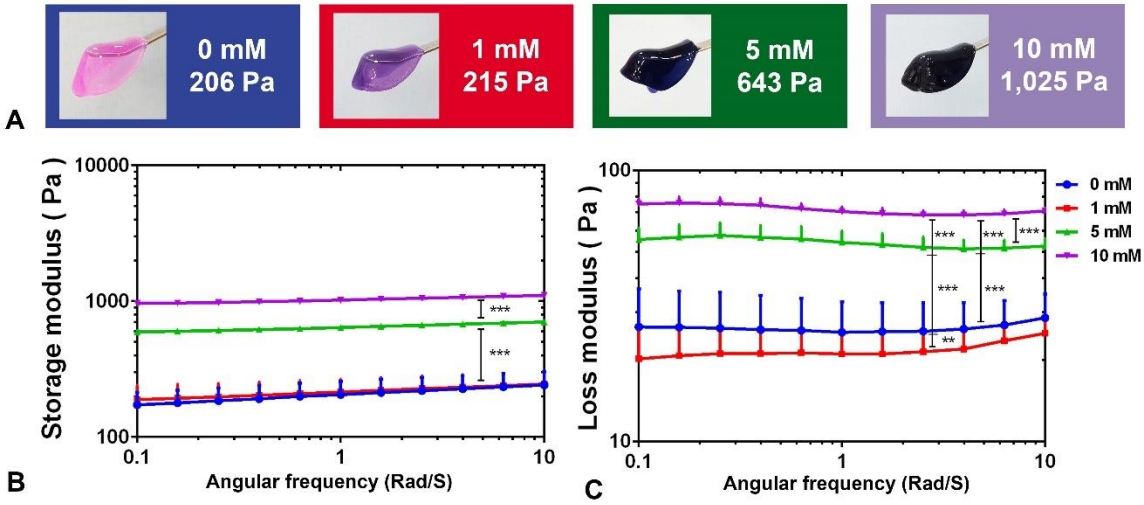

Figure 3.14 Rheological study of genipin crosslinked 1.8 mg/ml collagen hydrogels

The characteristics and colour of genipin crosslinked collagen hydrogels (A); Addition of genipin significantly increased the elastic modulus in the 5 and 10 mM groups (B). (mean±SD, n=3, * P≤ 0.05, ** P≤ 0.01, *** P≤ 0.001, B= storage modulus (G'), C= loss modulus (G"), Two-way ANOVA, Tukey's post hoc test).

Genipin crosslinking can increase the elastic modulus of collagen hydrogels up to > 1 kPa. This is a significant increase, but it is still far from the stiffness required for osteogenic induction (25-40 kPa) (Engler et al., 2006). Dose and time dependent cytotoxicity was next studied.

3.4.3.3 Genipin crosslinked hydrogel interferometry

The surface displacement amplitude of 1.8 mg/ml collagen hydrogels crosslinked with 0, 1, 5 and 10 mM genipin were studied during NS. At 1000 Hz, NS amplitude was significantly reduced in crosslinked hydrogels (**Figure 3.15A and B**). The effect of displacement amplification, causing by resonance frequency, was noted at 3000 Hz in the softer hydrogel (0, 1 mM genipin crosslinked hydrogel) while the stiffer hydrogels (5, 10 mM genipin crosslinked gels) showed less resonance (**Figure 3.15A and C**). At 5000 Hz, stimulating amplitude in all groups was very low **(Figure 3.15A and D)**.

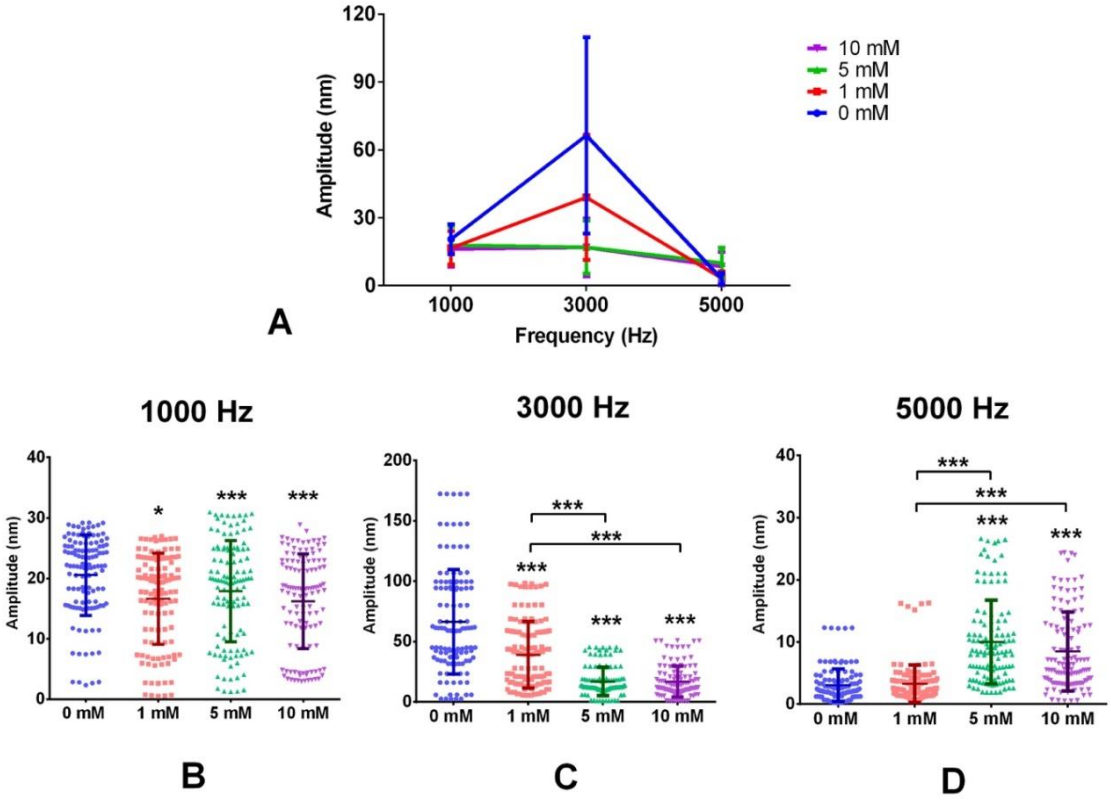

Figure 3.15 Interferometry in genipin crosslinked hydrogels.

(A) Overview comparison of hydrogel displacement at the centre of the hydrogels during NS at 1000, 3000 and 5000 Hz. (B-C) At 1000 and 3000 Hz, hydrogel displacement amplitude was decreased in stiff hydrogels (5 and 10 mM group). (C) At 3000 Hz, the amplitudes exagerated by resonance phenomenon, in particular in the soft hydrogels (0 and 1 mM groups) (mean±SD, n=3, * P≤ 0.05, ** P≤ 0.01, *** P≤ 0.001, One-way ANOVA, Tukey's post hoc test).

3.4.3.4 Genipin crosslinked hydrogel and cell viability studies

To investigate the effect of genipin on cell viability, 0,1, 5 and 10 mM genipin crosslinked hydrogels were prepared. The Alamar blue test and microscopy were performed. Microscopic images showed that cells were poorly spread after genipin crosslinking **(Figure 3.16 A-D)**. The Alamar blue test at 2 week and 4 weeks showed a decreasing trend of viability with increased genipin concentration **(Figure 3.16 E-F)**.

This study showed that genipin crosslinking adversely affected cell viability. Genipin crosslinking can increase the elastic modulus up to 1 kPa using 10 mM concentration (**Figure 3.14**). However, microscopic images showed rounded and poorly spreading cells after exposure to higher concentrations of genipin. Using low concentration of genipin may reduce the cytotoxicity but the advantage of hydrogel stiffness improvement was insufficient. Therefore, the use of genipin crosslinking strategy was discontinued.

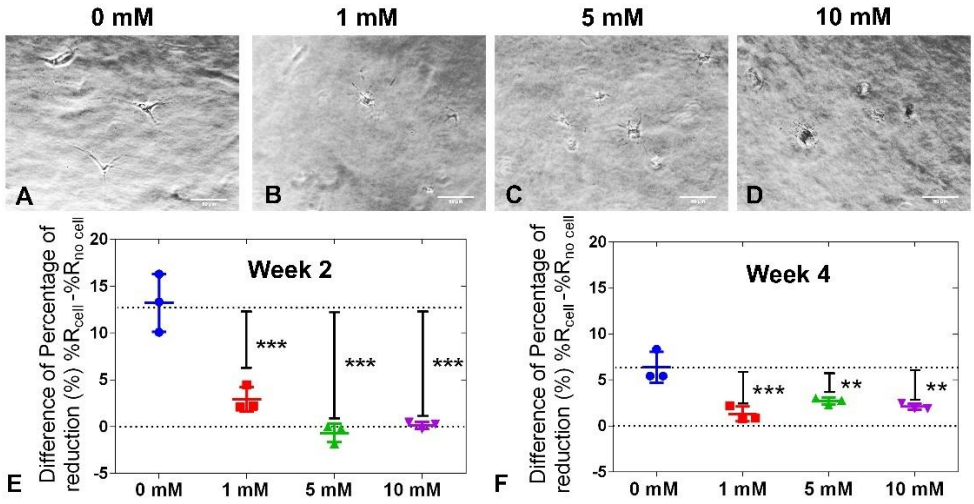

Figure 3.16 Microscopy and Alamar blue study in genipin crosslinking hydrogel

At 2 week, A-D) microscopic images showed poor MSCs spreading in genipin crosslinking groups. E-F) At 2 and 4 week, percentage of Alamar blue reduction was significantly decreased compare to control group (mean±SD, n=3, * P≤ 0.05, ** P≤ 0.01, *** P≤ 0.001, One-way ANOVA, Tukey's post hoc test).

3.5 Discussion

3.5.1 Ring in gel: what can we learn?

The concept of ring-in-gel was originated based on our previous publication that, cells were grown in 3D hydrogel provided with NS gave osteogenic response (Tsimbouri P.M., 2017). However, when we switched from commercial to Stro-1 MSCs, gel contraction suddenly became a problem. The ring-in-gel strategy focused on changing hydrogel supporting structure while preserving hydrogel property.

The first ring design provided an unsatisfactory result. Initially, it was expected that PLA ring inside hydrogel may resist the contraction force at gel-container area. However, the first ring design did not reduce cell pulling force inside the ring (ring-gel surface). Moreover, the PLA ring (in particular without surface treatment such as plasma polymerization) may provide inadequate adhesion between the ring-gel contact surface.

The second-generation of scaffold was designed based on the hypothesis that increasing the ratio of gel-material (ring) contact surface (junction) could possibly dissipate the cell pulling force, in turn, preventing the gel contraction. In order to rebalance cell pulling force and scaffold-gel interface bonding, the internal shape structure was changed to a cross-hair design **(Figure 3.3B)**.

To explain this hypothesis mathematically; the inner circumferential length of PLA ring was calculated using the formula:

$$L = 2\pi r$$

$L1$ = *inner circumferential length of ring*

r = *radius of ring*

π = *3.14*

Thus, the ratio (R1) of volume of "cell in hydrogel" (V1) per contact surface length of material-gel junction (L1) of first ring-gel composite was:

$$R1 = \frac{V1}{2\pi r}$$

$$R1 = \frac{V1}{6.28r}$$

In the cross-hair design, the contact junction length (L2) of each "cell in hydrogel" area was the sum of a quarter of the inner circumferential length of the ring plus with 2 radii, therefore:

$$L2 = \frac{2\pi r}{4} + 2r$$

$$L2 = 3.57r$$

The volume of "cell in hydrogel" was divided into 4 areas, thus:

$$Volume\ per\ each\ area\ (V2) = \frac{V1}{4}$$

Therefore, the ratio (R2) of volume of "cell in hydrogel" (V2) per contact surface length (L2) of cross hair PLA ring was:

$$R2 = \frac{\frac{V1}{4}}{3.57r}$$

$$R2 = \frac{V1}{14.28r}$$

In conclusion, the new design PLA ring increases the contact length of the gel-material interface up to 4 folds (R1/R2). Mechanically, this design possibly shares the cell pulling force in the hydrogel, in turn, reducing hydrogel contraction. Our experiment showed that the second-generation PLA ring can indeed prevent further hydrogel contraction **(Figure 3.3C)**. However, our preliminary study showed that the ring in gel composite was difficult to remove from tissue culture using the ring holder, in particular in short term culture

hydrogels. Moreover, the “ring in gel” composite was difficult to use, for example, when dividing the hydrogels into small pieces to fill small bone defect in clinics. The ring-in-gel concept was, therefore, discontinued as it was considered not suitable for clinical application.

3.5.2 Increasing collagen concentration strategy

Collagen concentration had an effect on viscoelasticity. It is known that high concentration of collagen increases viscoelasticity while low concentration decreases (Swift et al., 2013). Increasing collagen concentration increases fibre density and reduces the pore size of ECM (Wolf et al., 2013) and this reduces syneresis (Chieh et al., 2010; Y. K. Zhu et al., 2001). To solve the hydrogel contraction issue by increasing collagen concentration, hydrogels were gelated at slightly alkaline (approximately pH 7.5-8) and 37°C which is a physiological condition of MSCs. Furthermore, MSCs were not exposed to cytotoxicity of crosslinking chemicals, rendering this technique safe for MSCs.

From our results, the storage modulus of 1.8 mg/ml collagen hydrogel was 161 Pa **(Figure 3.10)** indicating that the hydrogel is soft but handleable **(Figure 3.9).** The 1.8 mg/ml collagen hydrogel allows reliable NS force transmission **(Figure 3.12)**. This soft hydrogel is insufficient to drive osteogenic differentiation (Engler et al., 2006), therefore it can be extrapolated that osteogenic expression after NS was only driven by the effect of NS. Moreover, the storage modulus of this hydrogel is compatible with the stiffness of hematomas at fracture site. Thus, it could mimic 3D niche of the initial phase of bone healing process (Ryan, Mockros, Weisel, & Lorand, 1999).

Considering hydrogel contraction, increase collagen concentration from 0.8 mg/ml to 1.8 mg/ml can extend the starting date of hydrogel contraction significantly in tissue culture which allows an adequate stimulating time to induce MSCs osteoblastic commitment, transfer composite to clinics and possibly maintain their shapes during bone healing process (Claes et al., 2012; Einhorn & Gerstenfeld, 2015) **(Figure 3.11).** Therefore, the concept of cells-gel-sponge composites

were proposed to improve hydrogel structure that suit surgical purposes (see details in chapter 6).

3.5.3 Genipin-crosslinking collagen hydrogel

Genipin had been widely used as a crosslinker for biomaterials and soft tissue grafts such as bovine cardiac tissue (Yoo, Kim, Kim, & Choi, 2011), tracheas (F. Sun et al., 2016), sclera (S. Q. Zhu, Pan, Zheng, Wu, & Xue, 2018; S. Q. Zhu et al., 2016) and scaffolds. However, in most of the literature reporting cell seeded genipin crosslinked 3D scaffolds, cells were seeded after the scaffold crosslinking process (Bi et al., 2011; Campos et al., 2018). In our study, MSCs were mixed with collagen solution before allowing gelation to create 3D cellular niche. Genipin crosslinking was then performed afterwards. MSCs were therefore directly exposed to genipin in the 3D hydrogel. Our result corresponded to the published literature reporting cytotoxicity of genipin **(Figure 3.16)** (Fessel et al., 2014). Genipin affected cell viability by dose- and time-dependence as has been reported previously (Fessel et al., 2014). Furthermore, considering signaling pathways, the literature shows that genipin can activate MAPK pathways and p53 (H. Cao et al., 2010; E. S. Kim, Jeong, & Moon, 2012; X. Yang et al., 2013) as well as promote reactive oxygen species production (B. C. Kim et al., 2005) which, in turn, may activate apoptotic pathways.

Considering the crosslinking mechanism of genipin, genipin possibly crosslinks collagen fibrils at amine groups (Butler et al., 2003). Increasing genipin concentration increases the density of crosslinked sites, in turn, improves hydrogel stiffness (S. Lin & Gu, 2015). Theoretically, crosslinked scaffold may extend the scaffold syneresis (Guo et al., 2019) and reduce scaffold degradation (McGann et al., 2015).

From **Figure 3.15**, the relationship between displacement amplitude and hydrogel stiffness at 1000 and 3000 Hz stimulation possibly was explained by oscillation theory (Garrett, 2017; Kett, 1982). Hydrogel displacement was assumed as moving in a simple harmonic motion and

hydrogel oscillation frequency was equal to stimulated frequency without damping following Hooke's law:

$$F = -kX \qquad (1)$$

F = *force action*
k = *constant factor characteristic of gel (act as spring)*
X = *displacement from equilibrium position*

Following Newton's second law (F = ma) for a hydrogel moving under gravity (g). Thus, at maximum amplitude (X_a):

$$mg = -kX_a \qquad (2)$$

$$-\frac{mg}{k} = X_a \qquad (3)$$

From equation (3), hydrogel stiffness (k) is inversely proportional to amplitude (X_a). Correlating to **Figure 3.15-3.16,** the 5 and 10 mM genipin crosslinked hydrogels had high stiffness (k). Therefore, displacement amplitude was decreased. This trend was departed from at 3000 Hz due to resonant frequency (value was nearly 3000 Hz).

3.6 Conclusion

The first PLA ring design showed an unsatisfactory result. Hydrogel contraction still occurred at the ring-gel junction of both commercial plates. The second-generation ring reduced hydrogel contraction without using chemical crosslinking. In long term culture, hydrogel attached to the ring and thus this composite was transferable (**Figure 3.3C**). However, removing the composite in short term culture was challenging. The ring cut through the hydrogel during lifting with the holder. In clinical application, the design would be difficult to use. The handle removal process is difficult and can also cause composite damage.

To improve hydrogel handleability, the 1.8 mg/ml collagen hydrogel can be prepared in 12 well plates without disturbing NS. Increasing collagen concentration can extend the starting date of collagen

hydrogel contraction without reducing NS, thus, potentially allow long term NS within the NS bioreactor. Following the results in this chapter, the 1.8 mg/ml collagen prepared in 12 well plate was the best strategy to deal with hydrogel contraction, therefore, this strategy is then used in the following chapters for biocompatibility testing, phenotype-pathway studies as well as developing cell-hydrogel-sponge composites.

Genipin crosslinking can increase collagen hydrogel stiffness up to 1 kPa. Biologically, genipin significantly increases cytotoxicity in 3D hydrogels. Therefore, this strategy is not suitable for developing 3D hydrogels for NS.

Chapter 4 The effect of high amplitude nanovibrational stimulation on phenotype and related pathways

Chapter 4 The effect of high amplitude nanovibrational stimulation on phenotype and related pathways

4.1 Introduction

In chapter 3, the 1.8 mg/ml collagen hydrogel was proposed as a suitable extracellular matrix (ECM) for mesenchymal stem cells (MSCs) on the nanovibrational bioreactor. However, no previous study investigated in the effect of NS amplitude in 3D osteogenesis. In this section, a study of the effects of amplitude in 3D was performed. Theories of osteogenic differentiation and phenotype expression were also reviewed. Since Tsimbouri et al recently showed the success of NS induced 3D osteogenesis via transient receptor potential vanilloid type 1 (TRPV1) - protein kinase C (PKC) - extracellular signaling-regulated kinase 1 and 2 (ERK1/2) - β-catenin pathways (Tsimbouri P.M., 2017), understanding of calcium signaling and channels, as well as interplays between calcium signaling, mitogen-activated protein kinase (MAPK) and Wnt signaling may help to unlock the basis of nanovibrational stimulation.

4.1.1 Nanovibrational stimulation; rational for amplitude control.

It has been shown that mechanical stimulations, such as vibration and mechanical strain by stretching, affect cell differentiation. However, the proposed intensities and stimulating durations are diverse and inconclusive in both 2D and 3D culture systems (B. McClarren & R. Olabisi, 2018; Sen et al., 2011).

Based on the concept that if the size of mechanical stimuli is compatible with cellular membrane receptors, it has been proposed that Nanovibrational stimulation (NS) possibly triggered specific mechanotransductive pathways driving osteogenesis. Recently, NS had successfully enhanced 2D and 3D osteogenesis in MSCs using high frequency at 1000 Hz (Nikukar et al., 2013; Tsimbouri P.M., 2017). Nikukar H. and Pemberton G. had studied the osteogenic induction effect of stimulating frequencies. They proposed that NS with 30 nm at 1000 Hz can promote 2D osteogenesis (Nikukar et al., 2013; Pemberton et al., 2015). Following that, Tsimbouri et al again elucidated the success of 3D osteogenesis in MSCs-seeded 0.8 mg/ml

collagen by stimulating at 30 nm (Tsimbouri P.M., 2017). However, most of these studies focused on frequency rather than amplitude.

Considering the cytoskeletal tension effect on MSCs in 2D culture, strain can promote cell spreading and thus in turn switches on osteogenic gene expression (Cui et al., 2015). However, excessive strain reduces actin fiber formation and cell spreading (Cui et al., 2015). In 2D culture, cells spread asymmetrically and interact with the uniplanar ECM (Baker & Chen, 2012). However, in 3D culture, cells spread in 3D multiplanar manner from the centre (nucleus), thus their cellular structure is more symmetrical than that of 2D culture (Beningo, Dembo, & Wang, 2004; Jiang & Grinnell, 2005). Considering these observations, it was hypothesized that MSCs in a 3D niche, where MSCs have lower cytoskeletal tension than that in 2D niche, may require higher NS amplitude to tune cytoskeletal tension. This tension is crucial to reach the threshold level of osteogenic induction in order to trigger mechanotransduction pathways driving gene transcription. Moreover, the new collagen hydrogels in which concentration was increased for gaining higher stiffness were used. Thus, revalidation of NS in the new hydrogels was required.

4.1.2 Progression of the osteoblast phenotype.

Osteogenic genes / proteins provide specific functions at specific time points driving MSC osteocommitment. For example, Runt-related transcription factor 2 (RUNX2) and osterix (OSX) drive osteogenic commitment at the early stage, while osteocalcin (OCN) and osteopontin (OPN) enhance ECM mineralization at late stage (Lian & Stein, 1992; Lian et al., 1991; Stein et al., 1991). Thus, disorder of phenotypic expression may hint at differentiation problems and pathological conditions (W. Liu et al., 2018; Philipp J. Thurner et al., 2010). Temporal study of phenotype correlated to MSCs differentiation stage is illustrated in **Figure 4.1**.

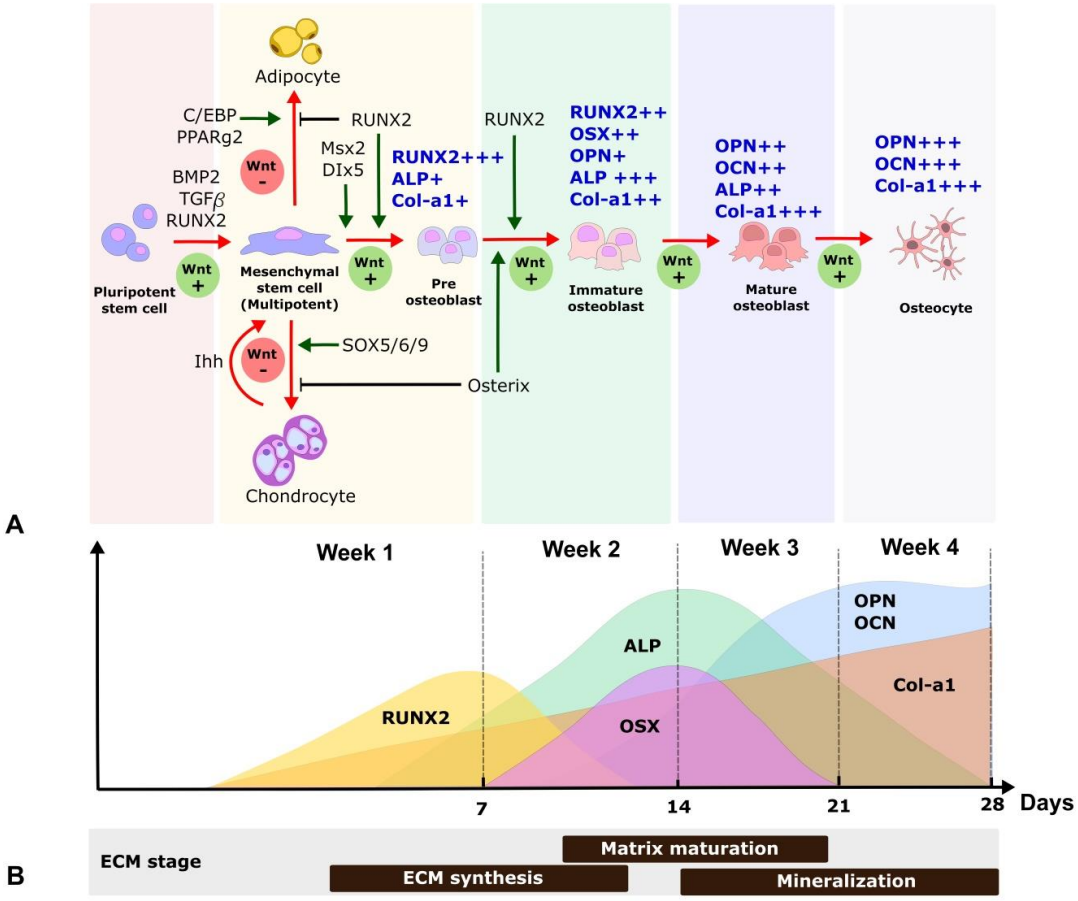

Figure 4.1 Osteogenic differentiation and phenotypes

A) Osteogenic differentiation from MSCs towards osteoblastic differentiation.
B) Temporal phenotypic expression and ECM development. In summary, in the early phase (week 1), RUNX2 mainly commits MSCs to the osteogenic lineage; RUNX2 expression inhibits adipogenesis. After RUNX2 expression, OSX then plays a role to drive immature osteoblast at week 2. Alkaline phosphatase (ALP) and ON promote ECM maturation (week 2 - 3) while OCN and OPN enhance mineralization (week 3 - 4) (Komori, 2010, 2019; Lian & Stein, 1992; Lian et al., 1991; Stein et al., 1991).

In the early phase, RUNX2 and OSX commit MSCs to the osteogenic lineage. RUNX2 is a major transcription factor in early osteogenesis. RUNX2 levels peak at day 5-7 (Hassan et al., 2006; J. L. Yang et al., 2014). RUNX2 is detected in pre-osteoblasts and immature osteoblasts (Komori, 2010) and can regulate OCN, OPN as well as collagen type Iα1 (Col1A1) expression (Bruderer, Richards, Alini, & Stoddart, 2014). Via bone morphogenetic protein 2 (BMP2) stimulation, RUNX2 links to SMAD (Rahman et al., 2015) and non-SMAD pathways (such as the MAPK pathway (Rodriguez-Carballo et al., 2016)). OSX is another

transcription factor that contributes to later stage osteogenesis and bone matrix deposition (Nakashima et al., 2002). OSX levels peak approximately at day 9-14 (J. L. Yang et al., 2014; C. Zhang, 2010). OSX is typically regulated in dependence of RUNX2 (Matsubara et al., 2008). The BMP-2 pathway can also induce osterix expression via Distal-less homeobox 5 (Dlx5) and MSh homeobox 2 (Msx2) transcription factors (M. H. Lee, Kwon, Park, Wozney, & Ryoo, 2003; Matsubara et al., 2008).

Osteonectin (ON; or SPARC) is a bone-specific protein linked to collagen type I and hydroxyapatite. ON is highly upregulated at week 1 (Ardeshirylajimi, Soleimani, Hosseinkhani, Parivar, & Yaghmaei, 2014). ON promotes ECM assembly and collagen fibril formation (Rosset & Bradshaw, 2016). ON may initiate mineralization (Termine et al., 1981) and also support osteoblast differentiation and survival. Kessler et al showed increase of the Notch1 gene (transmembrane receptor regulating adipogenesis and osteogenesis) in ON-null osteoblasts. They also proved that Notch1 is regulated by cAMP, and proposed that increase of Notch1 relates to the decrease of coupling of G proteins to activate adenylyl cyclase (AC) displaying aging phenotypes such as osteopenia and increased adipose deposits (Kessler & Delany, 2007).

Alkaline phosphatase (ALP) promotes matrix maturation and reaches its peak at 2 weeks (Lian & Stein, 1992). ALP is an ectoenzyme found in liver, bone and kidney. ALP plays an important role in mineralization. Chondrocytes or osteoblasts bud matrix vesicles which contain intravesicular calcium (influxed through the annexin channel) and phosphate (influxed by type III Na/Pi cotransporter and PHOSPHO I) (Orimo, 2010). These ions interact with the phosphatase enzyme and in turn produce PO_4 resulting in the deposition of $CaPO_4$ (Anderson, 1995; Orimo, 2010).

In the late phase, OPN and OCN enhance mineralization and peak at week 3-4 (Lian & Stein, 1992; Lian et al., 1991). OPN is a nonspecific glycoprotein secreted by bone, kidney and the epithelial lining. OPN is expressed in osteoblasts and osteoclasts playing the role in bone remodeling by inhibiting the formation of hydroxyapatite (Mazzali et al., 2002). Furthermore, OPN also plays an important role by regulating immune cells during inflammation (Lund, Giachelli, & Scatena, 2009). OCN is an osteoblast specific protein. OCN is defined as a hormone which can control insulin secretion and is thus related to glucose metabolism (J. Wei & Karsenty, 2015). Absence of OCN

increases bone formation in *in vivo* study (Ducy et al., 1996). OCN can bind to hydroxyapatite as well as recruit osteoblasts and osteoclasts for bone resorption and mineralization (Hoang, Sicheri, Howard, & Yang, 2003). OCN is found in mature osteoblasts while OPN is expressed in immature osteoblasts (Komori, 2010). Transitionally, OCN can be found in immature osteoblasts expressing RUNX2 and OPN (Komori, 2010).

4.1.3 Potential mechanism from NS to drive osteogenesis.

To investigate the related pathways of NS and increased/high amplitude NS, understanding the related pathways in NS is important. In this section, the previous NS-induced 3D osteogenesis results (Tsimbouri P.M., 2017) are focussed on to give hints the potential areas to be investigated when the amplitude is increased. Calcium signaling, MAPK and wnt are also reviewed.

4.1.3.1 NS induced 3D osteogenesis

Tsimbouri et al proposed that the success of NS induced 3D osteogenesis was mainly through ion channel activation. At the gene level, NS promoted BMP2, ALP, OPN and OCN in the early phase **(Figure 4.2A)**. In the early phase **(**day 5-7, **Figure 4.2B)**, NS activated ions channels such as piezo1/2 (tension) and TRPV1 (temperature, pain) (Tsimbouri P.M., 2017). Data suggested that TRPV1 is possibly indirectly activated by a cytoskeleton dependent pathway as TRPV1 was effected by ROCK and myosin inhibition (Tsimbouri P.M., 2017). However, ROCK and myosin did not affect osteogenesis **(Figure 4.2C)** (Tsimbouri P.M., 2017). Next, the related pathways were investigated at the protein level, and, again, no evidence of cytoskeletal tension (FAK, myosin, ERK1/2) and BMP2 (SMAD1/5) pathways involvement was found for 3D osteogenesis; this is different to 2D NS osteogenesis where tension has been implicated (Nikukar et al., 2013). However, it is known that the ion channel TRPV1 can act via protein kinase C (PKC) to effect β-catenin (canonical Wnt) (Tsimbouri P.M., 2017). It was shown that inhibition of TRPV1 (and PKC) reduced active β-catenin and reduced osteogenesis in 3D NS (Tsimbouri P.M., 2017) **(Figure 4.3 D-E)**.

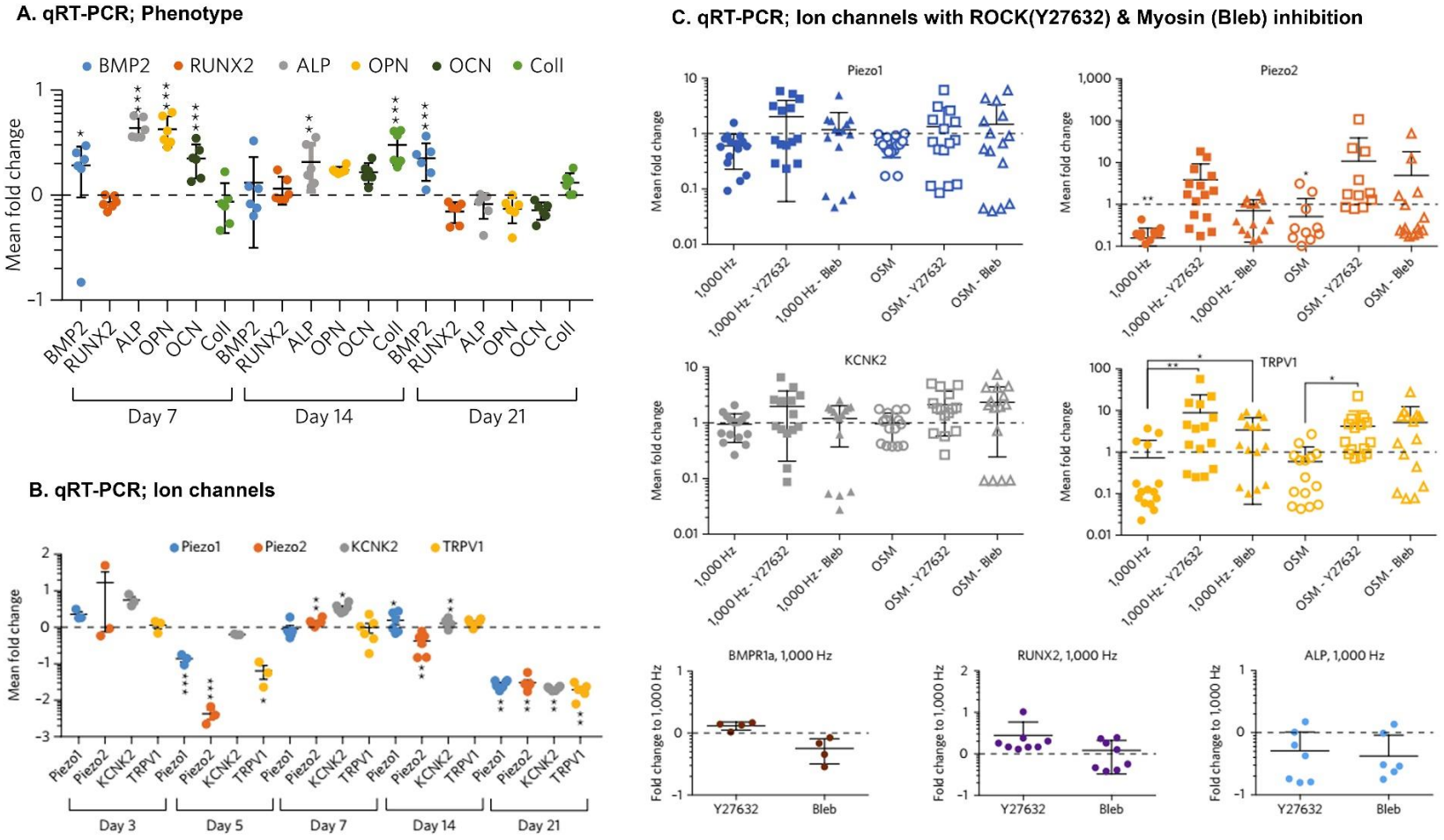

Figure 4.2 Previous study of NS induced 3D osteogenesis

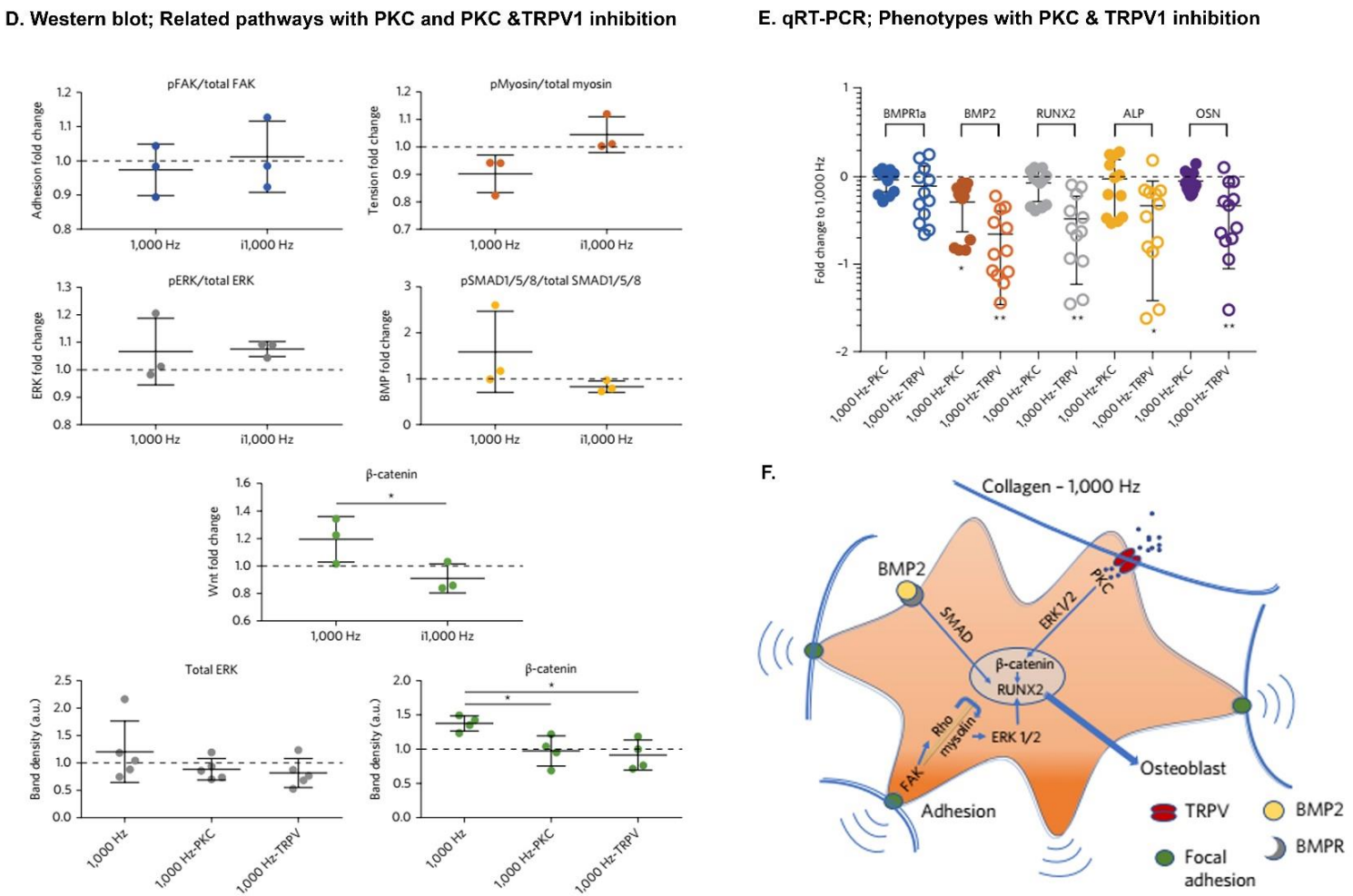

Figure 4.3 Previous study of NS induced 3D osteogenesis (continue)

Figure 4.2-4.3 Previous study of NS induced 3D osteogenesis (continue)

A) qRT-PCR temporal gene study showed osteogenic gene upregulation (BMP2, ALP, OPN, OCN) at day 7. B) At day 5-7, piezo1/2 and TRPV1 respond to NS. C) TRPV1 links to ROCK and myosin pathways with no effect on osteogenesis (BMPR1a, RUNX2 and ALP). D) NS activated ß-catenin through PKC and TRPV1 showing by the decrease of ß-catenin after PKC and TRPV inhibition. E) TRPV1 affected on osteogenesis (showing in RUNX2, ALP and OSX) F) Diagram showed the pathways of NS induced osteogenesis (With permission of Tsimbouri et al., 2017 (Tsimbouri P.M., 2017))

4.1.3.2 Calcium homeostasis and signaling

Calcium ions are essential for many cellular activities (Stojilkovic, Tomić, Koshimizu, & Van Goor, 2000). Intracellular calcium is a key signal in modulating proliferation, differentiation or apoptosis (Humeau et al., 2017). Intracellular calcium concentration $[Ca^{2+}]_i$ is maintained within physiological levels for normal cellular functions. All sources of calcium, including $[Ca^{2+}]_i$, extracellular calcium concentration $[Ca^{2+}]_o$ and calcium ions in endoplasmic reticulum ($[Ca^{2+}]_e$) (Carafoli, 2002; Humeau et al., 2017; Nowycky & Thomas, 2002), are well-regulated through ion channels/transporters on the cell membrane.

In the resting stage, $[Ca^{2+}]_i$ (concentration~100 nM) is lower than $[Ca^{2+}]_o$ (concentration~2 mM). Na^+/Ca^{2+} exchangers (NCX) and Na^+/Ca^{2+}-K^+ exchangers (NCKX) play roles in maintaining Ca^{2+} at the cellular membrane. At endoplasmic reticulum (ER) (such as myocyte and cardiocyte), where is the cellular calcium storage, sarco/endoplasmic reticular Ca^{2+}-ATPase (SERCA) pumps Ca^{2+} into the ER while plasma membrane Ca^{2+}ATPase (PMCA) control the outflow (Clapham, 2007). However, in bone, osteoblast may use pannexin 3 (gap junction which locates at ER) to regulate intracellular calcium ions released from ER (Masaki Ishikawa et al., 2011; M. Ishikawa & Yamada, 2017).

In the excited state, which requires an increase of $[Ca^{2+}]_i$, calcium is initially released from the ER via ryanodine receptors (RyR). On cellular membrane, the stimuli such as hormones, neurotransmitters, etc activate G protein coupled receptors (GPCRs) and in turn activate phospholipase C (PLC) to hydrolyse phosphatidylinositol 4,5-

bisphosphate (PIP_2) to diacylglycerol (DAG) and inositol-1,4,5-triphosphate (IP3). IP3 binds to IP3 receptor at ER resulting release Ca^{2+} into cytosol (Humeau et al., 2017). Ca^{2+} and DAG activated PKC (K.-P. Huang, 1989). PKC subsequently activates voltage-gated (Raifman et al., 2017) (e.g. L-VGCCs), ligand-gated channels (Breitinger et al., 2018) and TRP channels (Bhave et al., 2003)) to allow influx of $[Ca^{2+}]_o$. $[Ca^{2+}]_i$ interacts with proteins in the cytoplasm in particular calmodulin and forms calcium-calmodulin complexs. In turn, these complexes activate many enzymes including calmodulin-dependent protein kinase (CaMKs) (Majd Zayzafoon, 2006). Ca2+-Calmodulin dependent kinase II (CaMKII) plays a role in osteblast differentiation (Y. H. Choi, Choi, Oh, & Lee, 2013; Majd Zayzafoon, 2006). CAMKII promotes phosphorylation of ERK via Ras-Raf-1(Illario et al., 2003) and enhances osterix expression (Y. H. Choi et al., 2013) **(Figure 4.4)**.

Furthermore, calcium signaling between cells through gap junctions is also important for cell function. In MSCs, pannexin 3, intercellular gap junction, activates intracellular calcium driving osteogenesis (M. Ishikawa & Yamada, 2017). Thus, understanding the calcium homeostasis among intra- and extracellular- and ER can help identifying the NS activated pathways.

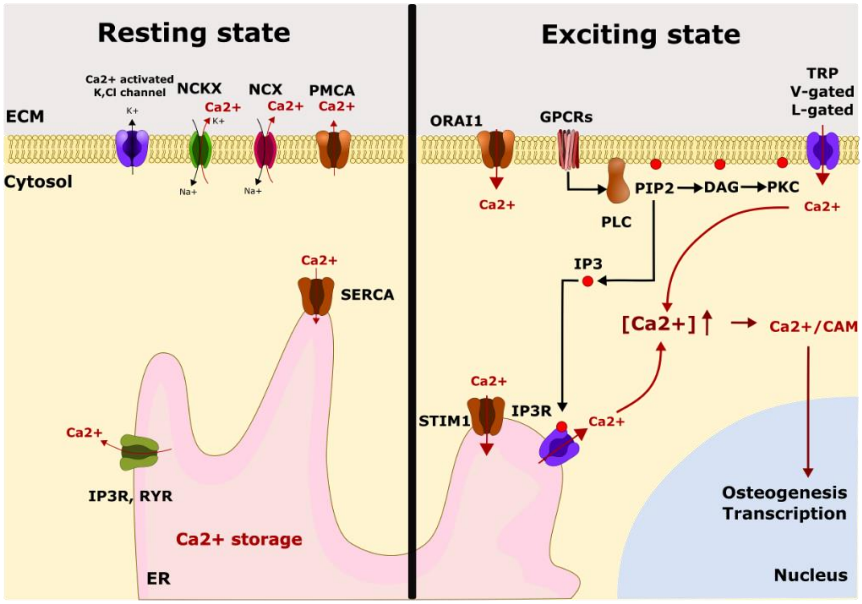

Figure 4.4 Calcium homeostasis

In the resting state, [Ca2+]i is maintained at low level by ion channels on the cellular membrane (such as Na+/Ca2+ exchangers; NCX, Na+/Ca2+-K+ exchanger; NCKX and plasma

membrane Ca2+ATPase PMCA) and endoplasmic reticulum (e.g. sarcoendoplasmic reticular Ca2+-ATPase; SERCA). In the excited state, stimuli or agonists activate G-protein-coupled receptors (GPCRs; sensing to pain, itch and inflammation) (Geppetti, Veldhuis, Lieu, & Bunnett, 2015), which in turn, activate phospholipases (e.g. PLCβ, PLA2). PLC cleaves PIP2 into diacylglycerol (DAG) and 1,4,5-inositol triphosphate (IP3). IP3 diffuses in the cytosol and binds to IP3 receptor on the ER, subsequently, allowing calcium ion release into the cytoplasm and resulting in the increase of $[Ca^{2+}]_i$ (Clapham, 2007; Geppetti et al., 2015). $[Ca^{2+}]_i$ activate kinases (e.g. PKC, tyrosine kinases). DAG binds to intracellular calcium and activates PKC. PKC then phosphorylates calcium ion channels e.g. TRPV1, 4 and transient receptor potential ankyrin1 (TRPA1) (Geppetti et al., 2015).

4.1.3.3 Mechanical stimulation induced calcium signaling.

From the literature, mechanical stimulation can increase intracellular calcium (Demer, Wortham, Dirksen, & Sanderson, 1993; Sharma et al., 1995). However, some literature reported that mechanical stimulation alone may not increase the influx of extracellular calcium due to the rigorous control of ions transportation through ion channels (Chabbert, Geleoc, Lehouelleur, & Sans, 1994). Theorectically, mechanical stimulation may affect ion chanels directly (e.g. piezos) or indirectly through changes in cytoskeletal tension. For example, in airway smooth muscle, integrin formation activates myosin light chain (both kinase and phosphatase) phosphorylation and in turn increases intracellular calcium (Tran & Teoh, 2014). If NS was considered as a mechanical stimuli driving osteogenesis through calcium signaling activation, mechanosensitive ion channels (on cellular membrane) would be the target to study.

Calcium ion channels are important sites controlling intracellular calcium by allowing extracellular calcium ion influx as well as calcium storing and releasing from ER (Clapham, 2007; Monteith, Prevarskaya, & Roberts-Thomson, 2017). There are many types of calcium ion channels on cellular membrane such as stretching ion channels, voltage-gate channels, etc. Therefore, understanding calcium ion channels functions is crucial for regulating intracellular calcium concentration. Calcium ion channels which potentially link to osteogenesis are summarized in **Table 4.1**.

If NS is considered as a “force” (stretching or tethering), two hypotheses can be raised. Firstly, ion channels may be directly controlled by NS. The NS force possibly opens the channels by itself through applying force to the lipid membrane (Martinac & Poole, 2018) e.g. piezo1/2 channels. Secondly, NS may be indirectly controlled via cytoskeleton (Martinac & Poole, 2018) e.g. TRPV channels. The change of cytoskeletal tension, in turn, may increase the stretching force to the ion channels. If NS was considered as other form such as pain, itch or heat, then the NS may modulate through the TRP-GPCR axis. GPCRs can activate TRPs via phospholipases (PLC/PLA-PIP2-TRPagonist) or kinases (PKC/PKA-pTRP) **(Figure 4.5).**

Table 4.1 Current evidences of calcium ions related to osteogenesis

Calcium ion channels types	Examples of channels	Stimuli	References
Voltage sensitive calcium channels; VSCC	L-types, Ca_V 1.2	Depolarized membrane potential	(C. Cao et al., 2017; J. Li, Duncan, Burr, & Turner, 2002; Y. Z. Tan et al., 2019)
TRP channels	TRPP (polycystin1,2)	pH, voltage, phosphorylation	(Dalagiorgou, Basdra, & Papavassiliou, 2010; Dalagiorgou et al.,
	TRPV1	Nanovibration	(Tsimbouri P.M., 2017)
	TRPV4	Oscillatory fluid shear (primary cilia)	(Michele A. Corrigan et al., 2018; H.-p. Lee, Stowers, & Chaudhuri, 2019)
	TRPM7	Membrane tension	(Xiao et al., 2015)
Piezos	Piezo1	Hydrostatic pressure	(A. Sugimoto et al., 2017)

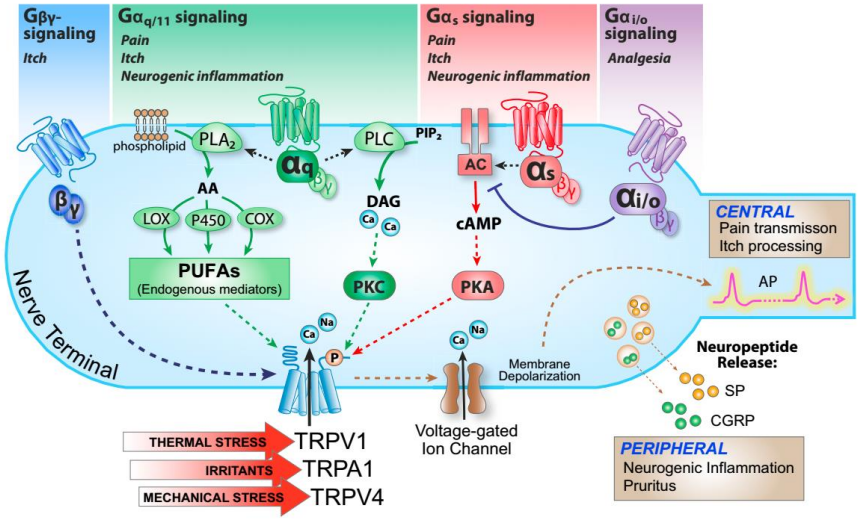

Figure 4.5 G-protein couples receptor and TRP receptors

GPCRs activate phospholipases or kinases. For phospholipases, GPCRs activate PLA2-AA-PUFAs while PLC links to PIP3-DAG-PKC. For kinases, GPCRs stimulate AC-cAMP-PKA.(AA; arachidonic acid, AC; adenylate cyclase, cAMP; adenyl cyclase pathway, PUFA; polyunsaturated fatty acid) (With permission of Geppetti et al., 2015 (Geppetti et al., 2015)).

In the next section, mechanosensitive ion channels and non-mechanosensitive channels are reviewed.

4.1.3.4 Calcium ion channels

4.1.3.4.1 TRP channels

Transient receptor potential (TRP) is a calcium and sodium ions channel, sensitive to temperature and pain (Caterina et al., 1997). TRP consists of 7 subfamilies of ion channels including canonical (TRPC), melastatin (TRPM), vanilloid (TRPV), polycystin (TRPP), Ankyrin (TRPA), mucolipin (TRPML) and (NomPC-like (TRPN). Focusing only on TRPV, TRPV consists of 6 members (TRPV1-6) **(Table 4.2)**. TRPV1-4 are nocireceptors. TRPV1 is highly expressed in normal cells (but reduced in cancer cells). TRPs can be regulated by protein kinase A, C and G (Ramsey, Delling, & Clapham, 2006) e.g. PKC affects sensitization of TRPV1 (Premkumar & Ahern, 2000) and TRPV4 (Peng et al., 2010). TRP is not a mechanically sensitive channel. However, stretching-induced actin polymerization can enhance calcium influx through the channels found in TRPV2 and 4 (S. Ito et al., 2010). Considering Tsimbouri et al's paper (Tsimbouri P.M., 2017), the result

showed that NS involved TRPV1 and TRPV1 did not link to ROCK nor myosin. Thus, it suggested that NS induced TRPV1 is possibly activated through GPCRs (this was not investigated in the paper).

4.1.3.4.2 TRPA1 channel

TRPA1 is member of TRP channels sensing irritants causing pain (García-Añoveros & Nagata, 2007). TRPA1 can be activated by inflammatory cytokines such as IL1ß, IL6, Nitric oxide (NO), H_2O_2 , prostaglandin and ROS through cysteine residues at the amino N terminus of TRPA1 (Hinman, Chuang, Bautista, & Julius, 2006; Nummenmaa et al., 2016; N. Takahashi et al., 2008; C. Xu, Luo, He, Montell, & Perrimon, 2017). Currently, there is no evidence showing that mechanical force directly activates TRPA1 in MSCs (García-Añoveros & Nagata, 2007). However, in hair cells, TRPA1 is considered as one of the mechanosensitive transduction channels (Corey et al., 2004).

Table 4.2 TRPVs family; types of channels

TRP family	Types	Mechanical stimulation /Functions	References
TRPV1	Thermosensitive	Temperature and pH	(Huynh et al., 2014)
TRPV2	Thermosensitive	Heat, innate immunity	(Huynh et al., 2014; Link et al., 2010)
TRPV3	Thermosensitive	Temperature, sense to Ca^{2+}/CaM	(Hasan & Zhang, 2018; Huynh et al., 2014)
TRPV4	Thermosensitive	Oscillatory fluid shear Mechanical stimulation	(M. A. Corrigan et al., 2018)
TRPV5	Epithelial calcium homeostasis	Calcium reabsorption in kidney	(Hughes et al., 2018; Huynh et al., 2014)
TRPV6	Epithelial calcium homeostasis	Parathyroid hormones and Vitamin D3	(Hasan & Zhang, 2018; Huynh et al., 2014)

4.1.3.4.3 Piezo1 and 2 ion channels.

Piezo1 and 2 are more sensitive to stress than TRPV1 (Bavi et al., 2017). Piezo1 responded to stretching, cell indentation, shear fluid, stiffness, etc (Nourse & Pathak, 2017). While Piezo2, found at nerve endings, was sensitive to light touch and sensed rapidly-adapting mechanical activated stimulation (Coste et al., 2010). Piezo1 is sensitive to stretch and interacts with the cytoskeleton which allows calcium influx into cytoplasm (Miyamoto et al., 2014; Nourse & Pathak, 2017). Increase of intracellular calcium potentially, in turn, modulates or coactivates Yes-associated protein (YAP) nuclear translocation (Franklin, Ghosh, Shi, & Liphardt, 2019). Accumulation of YAP can drive cell differentiation (Dobrokhotov, Samsonov, Sokabe, & Hirata, 2018; Elosegui-Artola et al., 2017; Y. Sun, Shao, Xue, & Fu, 2016). Mechanical stimulation through the Piezo1 channel can induce osteogenesis in MSCs. For example, hydrostatic pressure stimulation modulated piezo1 expression and enhanced BMP2 production driving osteoblast differentiation (A. Sugimoto et al., 2017).

4.1.3.4.4 Calcium sensing receptor (CaSR)

CaSR is a G protein-coupled receptor responding to calcium regulatory hormone (e.g. parathyroid hormone) to maintain calcium homeostasis (extracellular calcium) (Theman & Collins, 2009). CaSR is sensitive to extracellular calcium, however, the mechanism of CaSR sensing extracellular calcium is unknown (Dvorak et al., 2004). CaSR can be activated through GPCRs-PLC-DAG-PKC (Rodland, 2003); it is not a mechanosensitive channel. However, if NS can modulate CaSR sensing to extracellular calcium, it might regulate intracellular calcium concentration.

4.1.3.5 Interplay among calcium signaling, MAPK and β-catenin pathways

Calcium signaling relays signals from various first messengers and also modulates abundant intracellular pathways. Based on our current evidence of NS induced 3D osteogenesis (Tsimbouri P.M., 2017), interaction between calcium signaling-ERK1/2, calcium signaling-β-catenin and β-catenin-ERK1/2 pathways were discussed in order to predict the possible route of NS effect **(Figure 4.6)**.

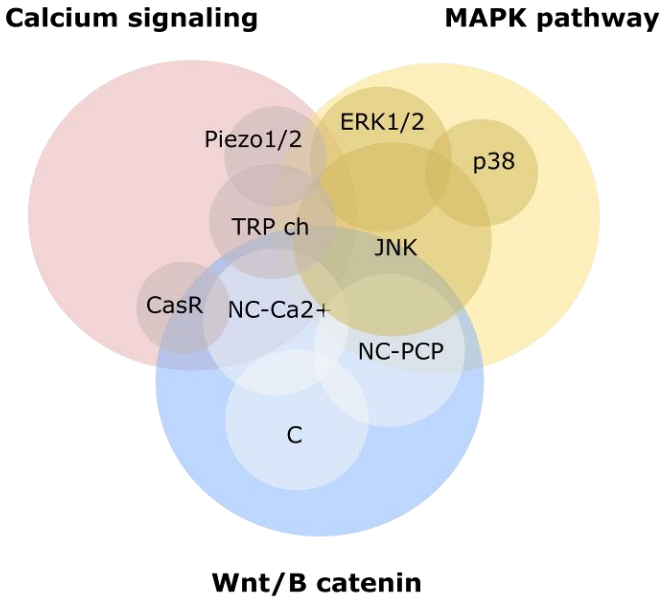

Figure 4.6 Interaction among calcium signaling, MAPK and Wnt/β-catenin pathway

The diagram showing the interaction among calcium signaling, MAPK and β-catenin. Considering calcium ion channels, CaSR and TRP channels involve PKC, thus, link to NC/Ca^{2+}. TRP-Piezo1/2 can be tethered/stretched by cytoskeletal tension changes thus MAPK is co-activated. In the MAPK pathway, JNK is involved in both NC/Ca^{2+} and NC-PCP. All canonical and non-canonical-Wnt signaling can crosstalk (Y. Zhang, Pizzute, & Pei, 2014) (NC; Noncanonical, C; Canonical, PCP; planar-cell polarity).

4.1.3.5.1 Calcium signaling and ERK1/2 pathway

Calcium signaling can mediate various cellular pathways including the ERK1/2 (member of MAPK) cascade (Chuderland & Seger, 2008). Calcium signaling can be coactivated by hormones, transcription factors through many receptors e.g. G protein receptor ($G_{q/11}$-coupled receptors) (Gudermann, Grosse, & Schultz, 2000). Calcium signaling interacts with proteins of the ERK1/2 pathways e.g. Ras proteins (Chuderland & Seger, 2008). Calcium is also involved in cell cycle regulation via the ERK1/2 dependent NFκB pathway (Sée, Rajala, Spiller, & White, 2004).

4.1.3.5.2 Calcium signaling and β-catenin pathway

Wnt pathways play an important role in cell growth, differentitation and apoptosis (Krishnan et al., 2006). Wnt pathways are important in driving MSCs into osteogenesis (J. H. Kim et al., 2013; G. Liu et al., 2009). Wnt also affects BMP2 induced osteogenesis (Y. Chen et al., 2007). Wnt/β-catenin consists of three pathways; canonical (β-catenin related regulation of gene transcription) and 2 non-canonical routes. These are non β-catenin related and Wnt planar cell polarlity (PCP) regulating cell polarity, cytoskeleton and Wnt/calcium which links to intracellular calcium signaling (Y. Zhang et al., 2014). Canonical Wnt can sense mechanical stimulation by coactivation of low density lipoprotein-related receptor-5 and -6 (LRP5, LRP6) (K. S. Kang & Robling, 2015). It is known that mechanical stimulation can, via Wnt5a, induced the Wnt canonical pathway (H.-D. Fu et al., 2016; Gu et al., 2018). For Tsimbouri et al, (Figure 4.1) (Tsimbouri P.M., 2017), Wnt canonical pathway (β-catenin related) thus was hypothesized to be modulated by the NS effect.

4.1.3.5.3 Canonical β-catenin and ERK1/2 crosstalking

Wnt canonical (β-catenin related) pathway affects transcription and interacts with MAPK. Focusing only ERK1/2, Wnt itself can activate ERK1/2. For example, Wnt3a activates ERK1/2 through Raf1-MEK-ERK cascade (M.-S. Yun, Kim, Jeon, Lee, & Choi, 2005; Zeller, Hammer, Kirschnick, & Braeuning, 2013). On the other hand, ERK1/2 also affects Wnt pathway. MAPK (ERK1/2, JNK, p38) can phosphorylate PPPS/TP clusters of LRP6 which promote canonical Wnt expression (Červenka et al., 2011).

4.1.3.6 NS and other possible pathways driving osteogenesis

4.1.3.6.1 BMP2-SMAD1/5 pathways

Mechanical stimulation can enhance BMP2 production. BMP2 promotes RUNX2 via Smad1/5 (Javed et al., 2008), osterix via Msx2-RUNX2 (Matsubara et al., 2008), OCN via RUNX2 mediated Atf6 (Jang et al., 2012), OPN via ERK1/2 (X. Yang et al., 2009) and also ALP expression (L. Wang et al., 2010). In previous publication, Tsimbouri et al illustrated the upregulation of BMP2 during 3 week NS (Tsimbouri P.M., 2017). Thus, it is interesting that NS possibly enhances BMP2 secretion driving osteogenic phenotypes.

4.1.3.6.2 Adhesion-cytoskeletal tension

It has been shown that cytoskeletal tension regulation promotes osteogenesis (McBeath et al., 2004). NS enhances 2D osteogenesis linking to cytoskeletal tension regulation via the Rho-ROCK pathway (Nikukar et al., 2013). However, it seems less dependent in 3D culture (Tsimbouri P.M., 2017). Investigating the roles of cytoskeleton in NS induced 3D osteogenesis (starting at ECM synthesis, focal adhesion formation and the ROCK pathway) could help to clarify the NS mechanism. Most osteogenic induced signaling, such as TGFß (Creely, DiMari, Howe, & Haralson, 1992; Sato, 2006) and BMP2 (Takuwa, Ohse, Wang, Wozney, & Yamashita, 1991) pathways, enhance collagen synthesis. Integrins form focal adhesion complexes and transfer mechanical signal through actin into the nucleus. RhoA-ROCK activation crosstalks with ERK1/2 driving subsequent RUNX2 phosphorylation (Dalby et al., 2014; Khatiwala et al., 2009). Thus, if NS enhances Col1A and integrins production as well as involves ROCK pathway, it suggests that NS potentially regulates cytoskeletal tension for 3D osteogenesis.

4.2 Aims and objectives

1. To identify the NS stimulating amplitude which can induce 3D osteogenesis in 1.8 mg/ml collagen hydrogel.

2. To investigate the effect of high amplitude stimulation (90 nm, N90) in mechanical and biological aspects.

3. To further study the biological pathways activating by high amplitude NS (N90).

4.3 Methodology and experimental design

4.3.1 Interferometry

The 1.8 mg/ml collagen type I hydrogels (2.5 ml) with 1.5 ml media were prepared 2 days before the measurement. T5000 model was used to study the relationship between frequency-voltage and voltage-

surface displacement amplitude. The measurement technique was explained in Chapter 2, section 2.4.

4.3.2 Alamar Blue assay

Stro1 selected MSCs seeded in 1.8 mg/ml collagen hydrogels with 4 $x10^4$ cells/ml density were prepared. NS was stimulated with 30 nm and 90 nm for 2 weeks. The technique and calculation of percentage of alamar blue reduction was shown in Chapter 2, section 2.6

4.3.3 qRT-PCR and ROCK inhibition study

Stro1 selected MSCs seeded collagen hydrogels with 4 $x10^4$ cells/ml density were prepared and stimulated with NS. The RNA purification using Trizol and chloroform, RNA isolation, cDNA synthesis and qRT-PCR techniques were explained in chapter 2, section 2.8. To study the ROCK pathway, 10 μM of Y-27632 (Tocris) in media was prepared. Changing media with inhibitor was started on day 2 and then every 2 days. Details were shown in chapter 2, section 2.12.

4.3.4 Western blot

To study protein expression, 4 x 10^4 cells/ml of Stro1 selected MSC in 1.8 mg/ml collagen hydrogel were prepared and NS for 7 days. After culture for 7 days, all samples were digested. Protein extraction and western blot technique were shown in Chapter 2, section 2.9.

4.3.5 Protein antibody microarrays

The 4 x 10^4 cells/ml of Stro1 selected MSC in 1.8 mg/ml collagen hydrogel were prepared and stimulated for 7 and 14 days. After the samples were digested with collagenase, the total protein was quantified using micro BCA kit (Pierce, ThermoFisher). The technique was explained in chapter 2, section 2.13.

4.4 Results

4.4.1 Frequency and amplitude selection

To study the effect of amplitude and frequency on osteogenesis, hMSCs seeded in 1.8 mg/ml collagen hydrogels were stimulated with various frequencies and amplitudes of NS. At 1000 Hz and (19.69 Vpp), measured amplitudes of all 24 wells (both 12 well plates) were grouped as N17 (N = nanodisplacement, mean 17.37 nm: SD 8.21 nm), N30 (mean 30.12 nm, SD 6.58 nm), N44 (mean 43.08 nm, SD 3.12nm), and N90 (mean 90 nm, SD 16.21). All hydrogels were then stimulated for 2 weeks and studied for phenotypical changes by qRT-PCR. After 2 weeks stimulation **(Figure 4.7)**, qRT-PCR showed some evidence of RUNX2 and osteonectin upregulation with a trend of PPARγ and nestin suppression in N90 while other tested frequencies and amplitudes showed more generalized gene upregulation patterns. Therefore, N90 was selected for further studies.

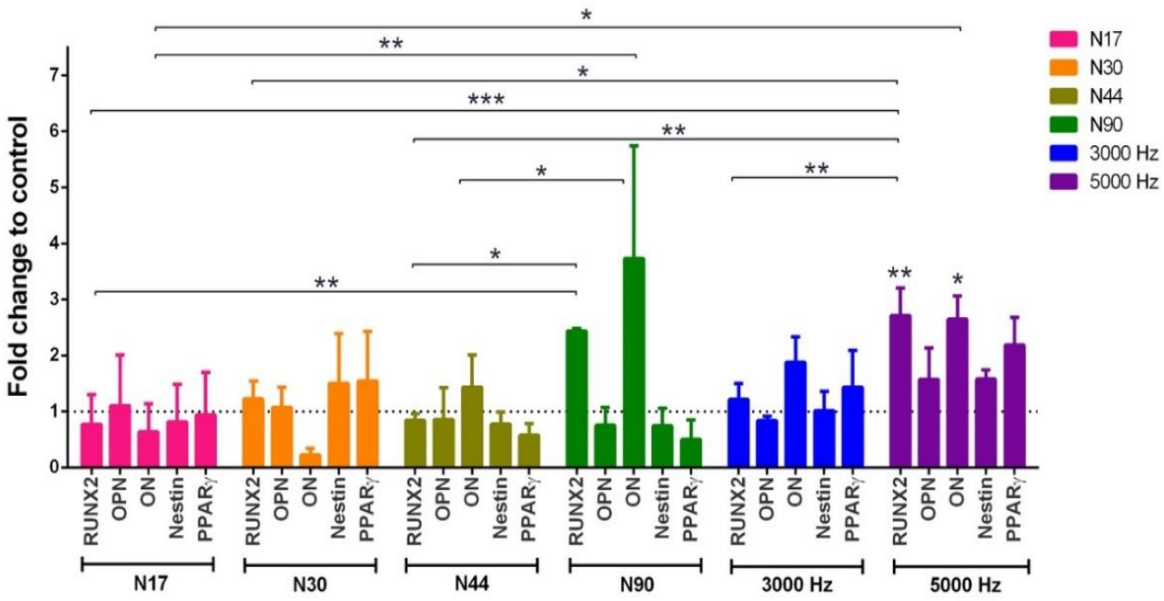

Figure 4.7 The selection of NS amplitude driving for 3D osteogenesis by qRT-PCR

RT-PCR after 2 weeks stimulation. Gels were exposed to 1000 Hz (average 17, 30, 44 and 90 nm), 3000 Hz and 5000 Hz (stimulated with 19.69 Vpp). Upregulation of RUNX2 and ON, as well as PPARɣ and nestin suppression was seen in N90 group

(mean±SD, n=2-4, * P≤ 0.05, ** P≤ 0.01, *** P≤ 0.001, Two-way ANOVA, Tukey's post hoc test).

4.4.2 Mechanical response of hydrogel to nanovibrational stimulation

In order to study the effect of high amplitude stimulation (N90), the efficacy of bioreactors generating amplitude required validation, including the precision of amplitude (section 4.4.2.1), the reliability of amplitude control by voltage (section 4.4.2.2) and investigating the resonant frequency of the culture plate system (section 4.4.2.3).

4.4.2.1 High amplitude (N90) bioreactor validation

To examine the reliability of the stimulating amplitude generated by the bioreactor, the standard (NTB 4003) 30 nm amplitude bioreactor and the N90 (T5000) 90 nm amplitude bioreactor were used for validation. Displacement amplitudes were measured by the interferometer at the centre area on the surface of wells and gels. The results showed that amplitude of gel was significantly higher than that of the well plate, but within expected ranges. The mean value of gel displacement amplitude of N30 was 35.83 nm (SD 1.77 nm) while mean value of amplitude of N90 was 93.94 nm (SD 13.06 nm) **(Figure 4.8)**.

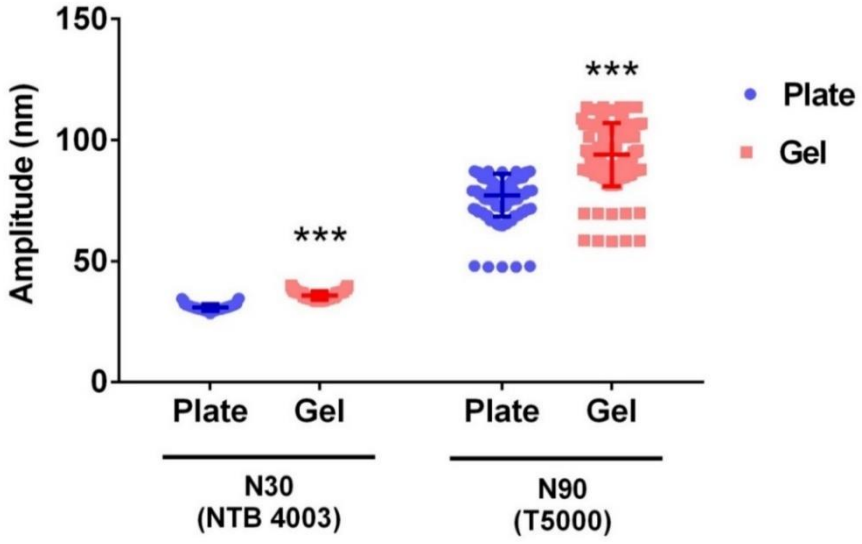

Figure 4.8 NS-amplitude validation of NS bioreactor

Comparing N30 and N90 on the NTB 4003 vs T5000 bioreactors. Both bioreactors generated reliable amplitudes. The

displacement amplitude of the hydrogel was significantly increased compared to the well plate in both N30 and N90 (mean±SD, n=24, * P≤ 0.05, ** P≤ 0.01, *** P≤ 0.001 Mann-Whitney test).

4.4.2.2 Effect of increasing amplitude and hydrogel displacement

To validate the stimulating voltage for high amplitude stimulation, 1.8 mg/ml hydrogels were prepared. The surface displacement of 5 wells (2D) and 5 hydrogels (3D) were measured at the same point by interferometer using the N90, T5000 bioreactor. The graph of surface displacement and stimulating voltage was plotted. The displayed graph of AC signal pattern on oscilloscope was observed during increasing the stimulating voltage. Considering the AC signaling pattern shown by the oscilloscope, distortion of the output signal was noted at 31.64 Vpp indicating the saturaturation point of amplitude by the bioreactor system. Thus, N90 (stimulation by using 19.69 Vpp) can be used as high amplitude stimulation due to having a normal AC signal pattern (Vpp was less than 31.64 Vpp and AC signal pattern is normal). In **Figure 4.9**, the relationship between stimulating voltage and surface amplitude is a linear pattern upto 30 Vpp. Therefore, the bioreactor can generate precise- and reliable-high amplitudes (at 19.69 Vpp).

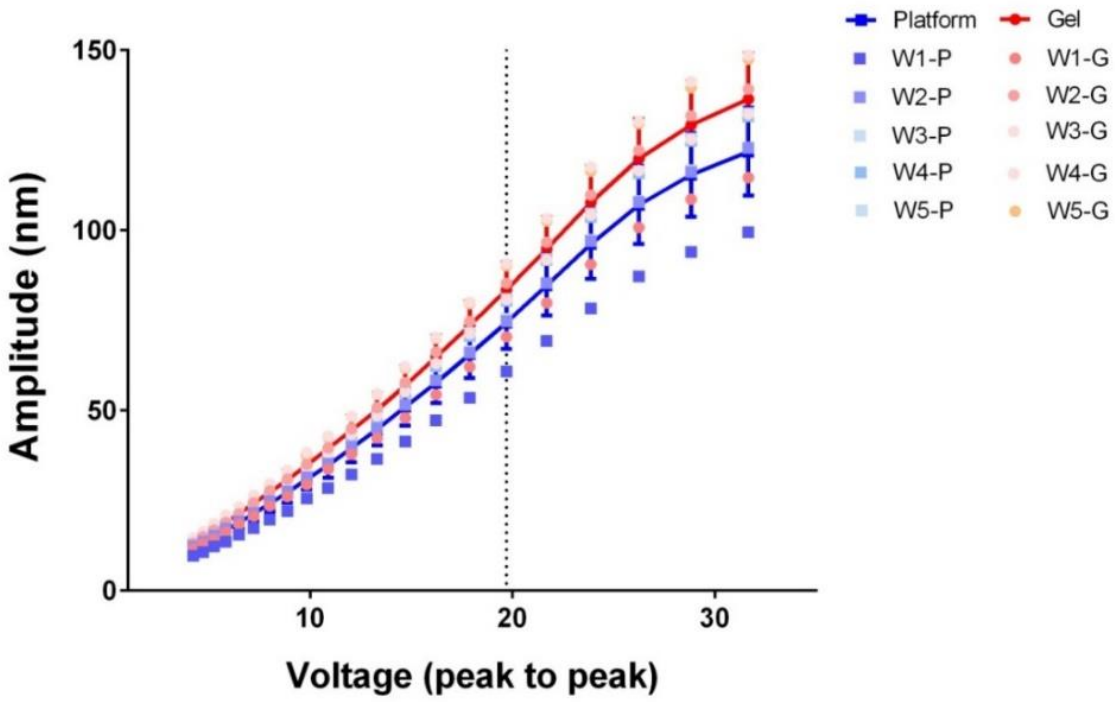

Figure 4.9 The effect of increasing stimulating voltage on NS amplitude

The linear correlation of voltage-amplitude was found upto 31.64 Vpp. Thus, N90 (at 19.69 Vpp) is reliable and precise (mean±SD, n=5, W; well, P; platform, G; hydrogel).

4.4.2.3 Resonance frequency and hydrogel-12 well plate system on nanvibrational bioreactor

The relationship between frequency and amplitude was measured on the surface of 1.8 mg/ml hydrogels at the centre and edge points in 12 well plates. The resonant frequency ranged approximately 2,250-2,750 Hz. Thus, it confirmed that there was no resonance effect during the stimulation at 1000 Hz. There was no significant difference of amplitude between the centre and edge of the gels at 1000 Hz **(Figure 4.10)**.

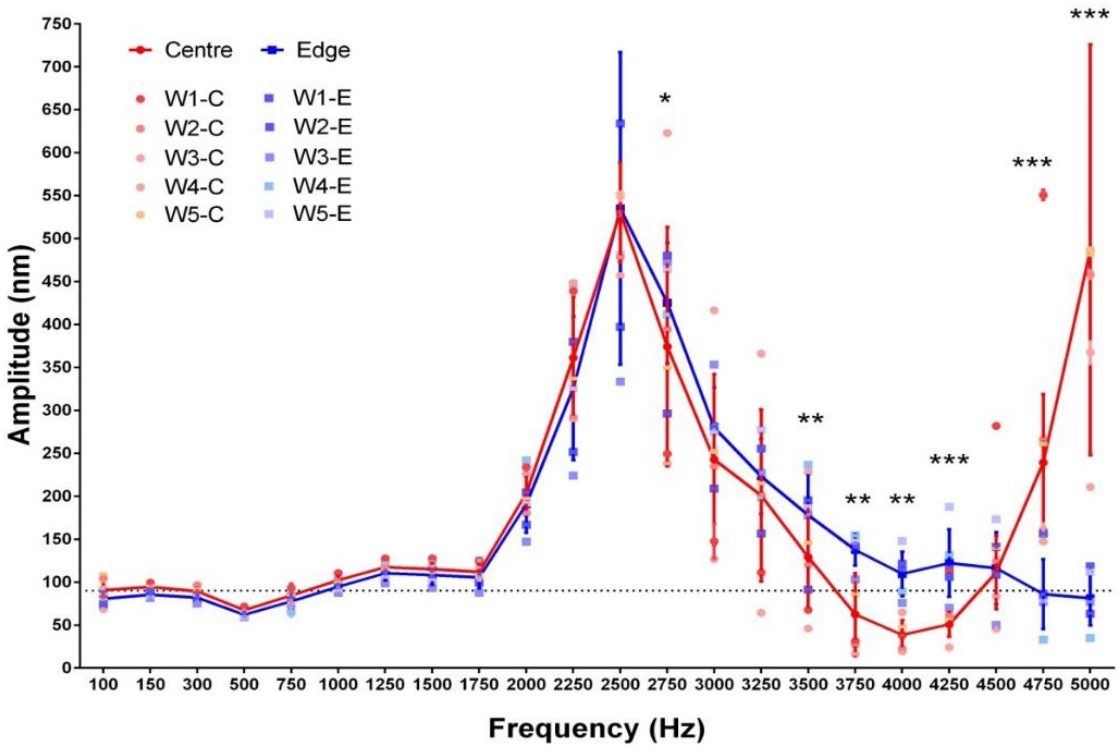

Figure 4.10 Relationship between frequency and amplitude in 12 well plate

At 1000 Hz, hydrogel displacement is reliable and precise. Effect of resonance (at 2500 Hz) amplified the stimulating amplitudes resulting in high variation (high SD value) in both the centre and edge areas (mean±SD, n=5, T5000, 19.69 Vpp, * P≤ 0.05, ** P≤ 0.01, *** P≤ 0.001, Two-way ANOVA, Sidak post hoc test, W; well, C; centre, E; edge).

4.4.3 Biological response of MSCs to high amplitude nanovibrational stimulation

Biological effects of high amplitude NS were investigated for viability, effect on osteogenic differentiation induction in gene and protein levels and the involved cellular pathways.

4.4.3.1 High amplitude and cell viability

After 2 weeks of NS, alamar blue study was peformed. Both standard (N30) and high amplitude (N90) showed no difference to unstimulated control and osteogenic media **(Figure 4.11)**.

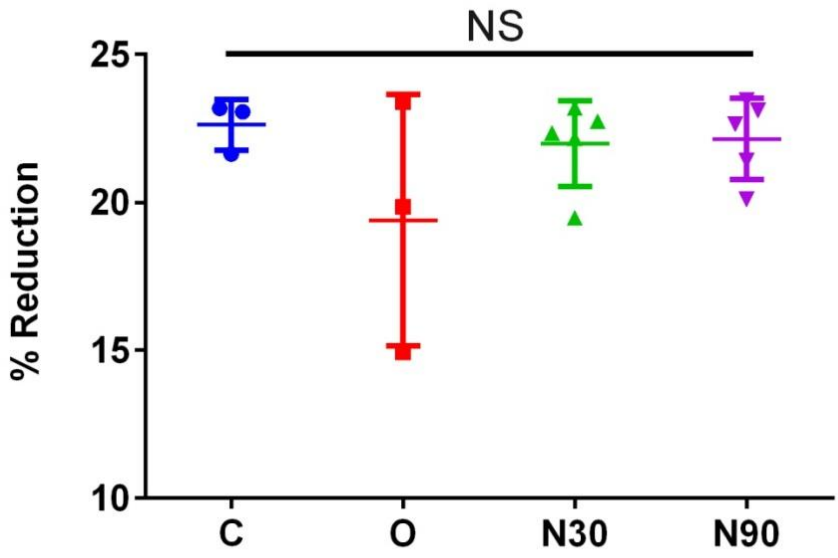

Figure 4.11 Alamar blue assays in N30 and N90 at 2 week

Alamar blue study showed no significant difference between all groups indicating that high amplitude stimulation (N90) was safe for MSCs (mean±SD, n=3-4, Stro1+ MSCs, NS= no significant difference, One-way ANOVA, Tukey's post hoc test, C; control, O; osteogenic media, N30; 30 nm, N90; 90 nm).

4.4.3.2 Nanovibrational stimulation enhance 3D osteogenesis

The effect of high amplitude nanovibrational stimulation in osteogenic induction were then studied in Stro1+ MSCs seeded in hydrogels. To study the effect of N90 on gene expression, qRT-PCR was investigated at day 7 and 9. At day 7, osteogenic gene expression was not obviously presented, and only OSX upregulation was found. At day 9, N90 induced osteogenic gene expression including RUNX2 (major transcription factor for osteogenesis), OSX, ON, ALP, OPN and OCN. PPARγ (fat gene expression) increased from day 7 to 9 but there was no change compared to control **(Figure 4.12)**. Therefore, day 9 is the suitable time point showing the obvious NS effect and was selected to study a single time point in gene expression.

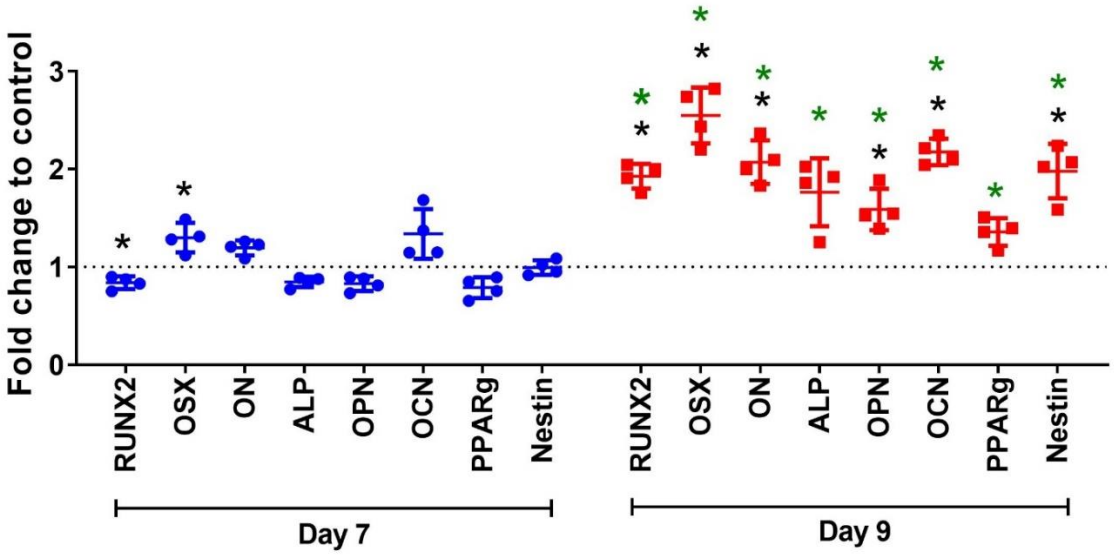

Figure 4.12 Gene expression comparing between day7 and 9 in N90

After stimulation with N90 at 1000 Hz for 7 days, only OSX was significantly increased. Interestingly, at day9, N90 enhanced osteogenic gene expression. PPARɣ (fat) suppression was noted. (mean±SD, n=4, * P≤ 0.05, Stro1+ MSCs, green asterix; comparing between day7 and 9 using Mann-Whitney test, black asterix; comparing to control using Mann-Whitney test).

Comparing between N30 and N90 after stimulating for 9 days, N90 promoted greater osteogenic gene expression (RUNX2, OSX, ON, OPN, OCN) than N30. Adipogenesis suppression was found in both N30 and N90 **(Figure 4.13)**.

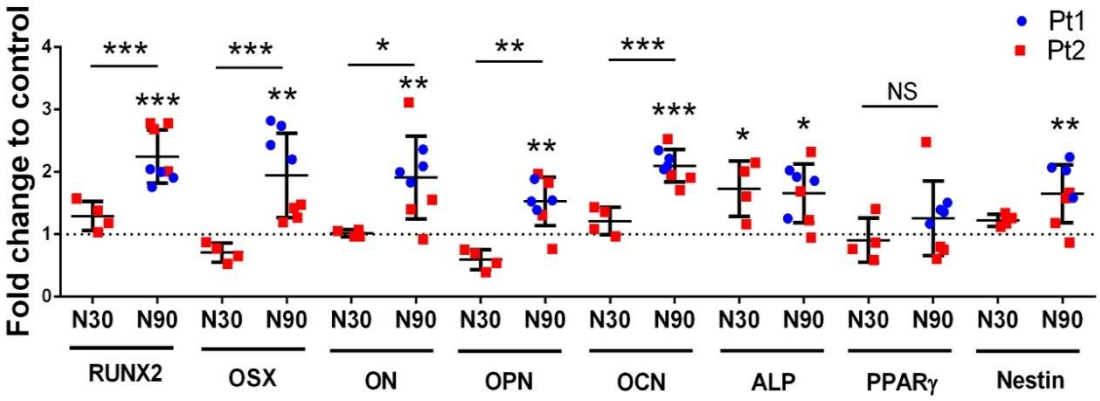

Figure 4.13 Osteogenic gene expression comparing between N30 and N90 at day 9

The qRT-PCR at day 9 comparing N30 and N90. High amplitude stimulation (N90) significantly increased RUNX2, OSX, ON, OPN and OCN while N30 showed less osteogenic induction (mean±SD, n=4, * P≤ 0.05, ** P≤ 0.01, *** P≤ 0.001, One-way ANOVA, Tukey's post hoc test, Pt1-2; patient 1-2).

4.4.3.3 Protein expression

To study protein level osteogenesis, western blot and densitometry were performed at day7. Again, N90 significantly enhanced pRUNX2/RUNX2 upregulation greater than N30 **(Figure 4.14A-B)**. Interestingly, this result corresponded to gene level **(Figure 4.12-4.13).**

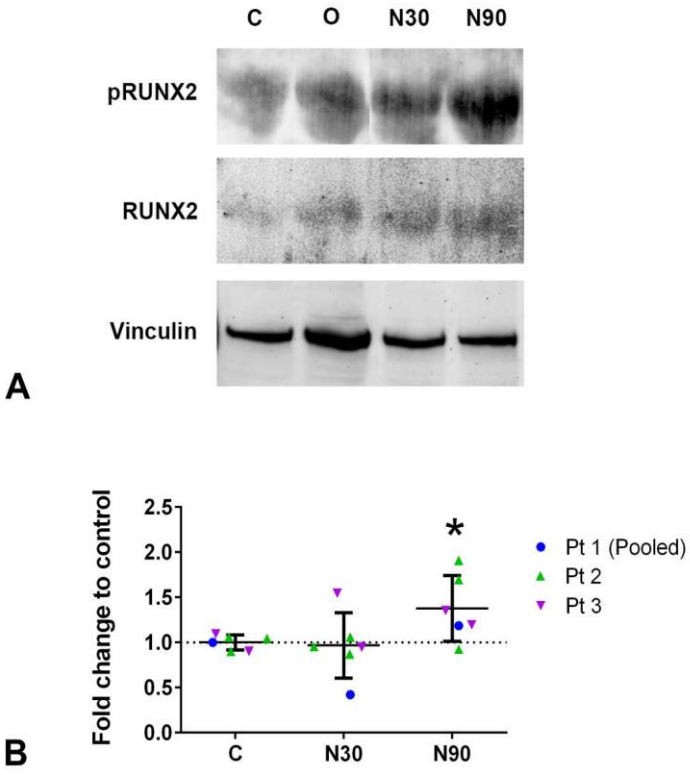

Figure 4.14 RUNX2 protein expression comparing between N30 and N90 at day 7

Western blot after 1 week stimulation; A. Phospho RUNX2 was upregulated in N30 and N90 (representative blot). B. Western blot densitometry showed significant upregulation of pRUNX2/RUNX2 for N90 comparing to control (mean±SD, 3 patients, n=3, * P≤ 0.05, Mann-Whitney test, Pt1-3; patient1-3).

4.4.3.4 Temporal gene study

To investigate whether NS may change the osteogenic gene expression pattern, a temporal gene study by qRT-PCR was performed at day 7, 14 and 21. These results elucidate that N90 provides greater enhanced osteogenic gene expression than N30. The pattern of N90 induced osteogenic gene expression corresponded to normal osteogenic gene expression pattern (Lian & Stein, 1992; Stein et al., 1991; Stein et al., 2004; J. L. Yang et al., 2014). RUNX2 and OSX were found at 1-2 week, playing a role in committing preosteoblasts to immature osteoblasts (J. L. Yang et al., 2014). OPN and OCN increased at week 2 and 3 for

mineralization (Lian & Stein, 1992; Stein et al., 1991). ALP and ON expression increased at week 1-2 **(Figure 4.15)**.

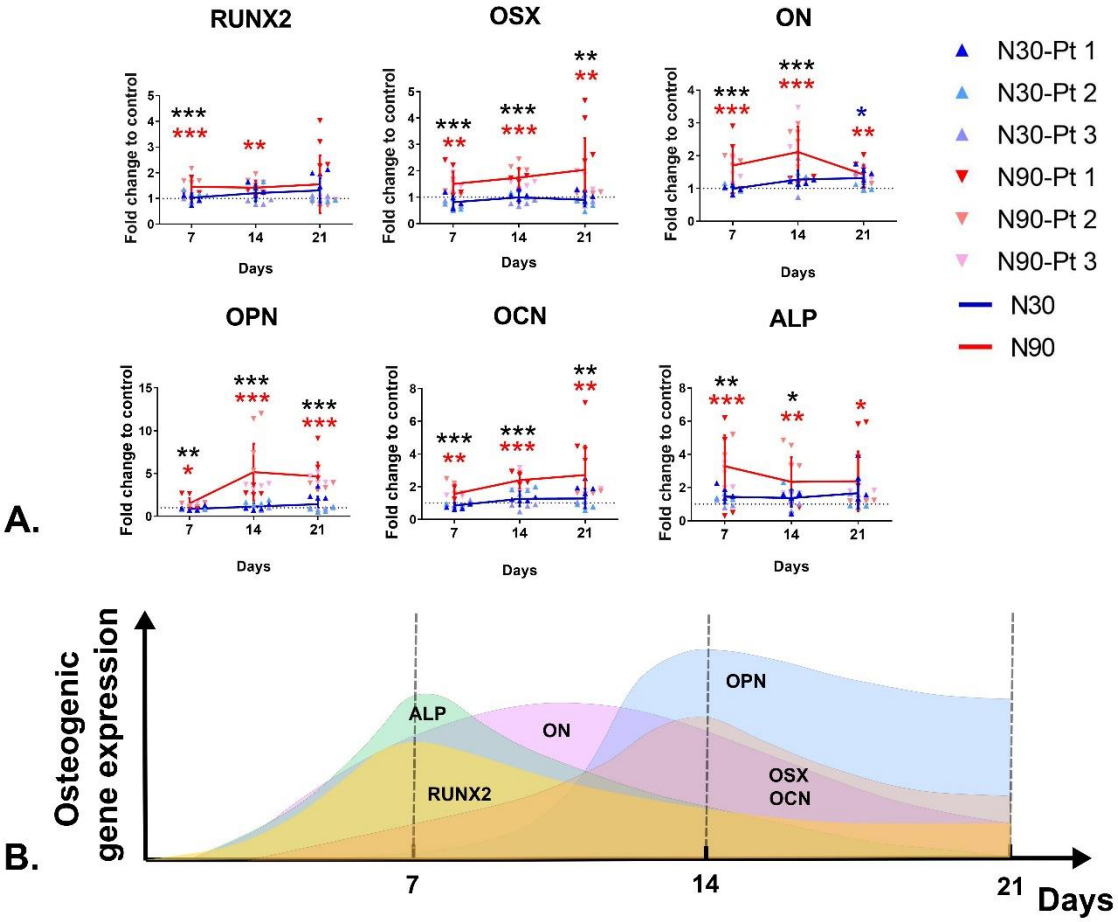

Figure 4.15 Temporal gene analysis comparing between N30 and N90 during day 7-21

A) N90 showed greater osteogenic gene expression over N30. RUNX2 increased at week 1. OSX and ON tended to increase and reached a peak at week 2. OPN and OCN increased at week 2 and 3. ALP was maximal at week 1. Overall, NS induced osteogenic gene expression pattern which corresponded to normal osteogenic gene pattern (mean±SD, 3 patients, n=4, * P≤ 0.05, ** P≤ 0.01, *** P≤ 0.001, One way-ANOVA, Tukey's post hoc test, asterix; blue= significant difference of N30, red=significant difference of N90, black= significant difference comparing between N30 vs N90, Pt1-3; patient1-3).

B) Diagram showing trends of the temporal gene study for N90.

4.4.4 Nanovibrational stimulation and related pathways

Understanding the NS induced 3D osteogenesis is crucial. As aformentioned, Tsimbouri et al proposed that NS drives 3D osteogenesis mainly through TRPV1, PKC and β-catenin (Tsimbouri P.M., 2017) while Nikukar et al showed that NS induced 2D osteogenesis via ROCK-ERK1/2 pathway (Nikukar et al., 2013). Thus, in this section, NS related osteogenic pathways including calcium signaling, BMP2- and cytoskeletal related pathways were investigated.

4.4.4.1 Investigating in calcium-, BMP2-and cytoskeletal-related pathways in gene expression

Osteogenesis pathways including BMP2-SMAD5, ion channels (including TRPV1, Piezos, CasR protein receptors), as well as ERK1/2 (which is MAPK member) were studied by qRT-PCR at day 9. The results showed that BMP2-SMAD1, TRPV1-Piezo2-CaSR and ERK1 expression was significantly upregulated, indicating that N90 potentially induced 3D osteogenesis through BMP2 and calcium signaling pathways **(Figure 4.16).**

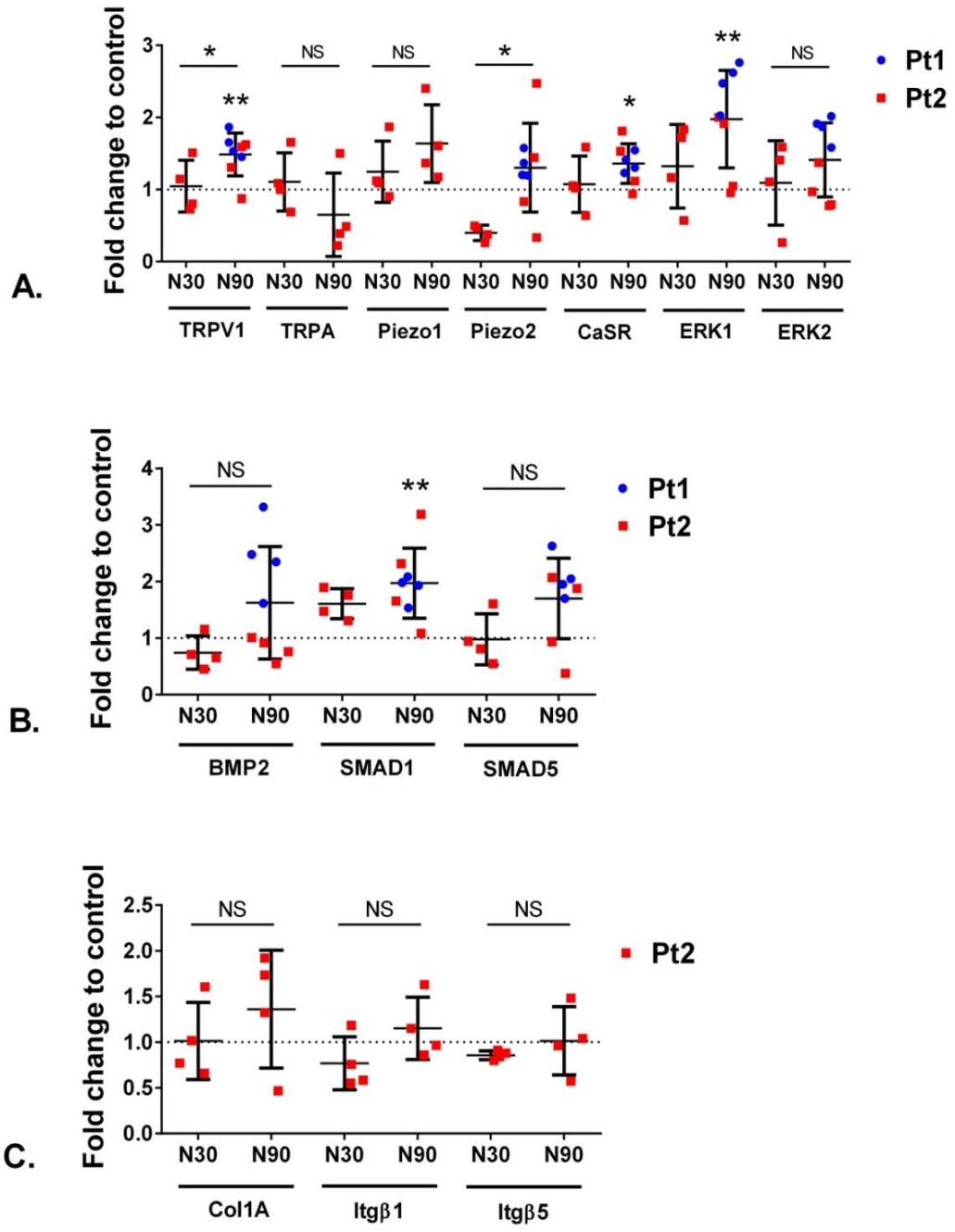

Figure 4.16 Gene expression of NS activated pathways compared between N30 and N90 at day 9

RT-PCR at day 9 showed N90 activated BMP2-SMAD1, calcium signaling (TRPV1-Piezo2) and ERK1 pathways (mean±SD, n=4, * P≤ 0.05, ** P≤ 0.01, *** P≤ 0.001, One-way ANOVA, Tukey's post hoc test, Pt1-2; patient 1-2).

4.4.4.2 ROCK pathways and osteogenesis in 2D vs 3D nanovibrational stimulation

The previous study by Nikukar et al demonstrated that NS enhances 2D osteogenesis via ROCK pathway (Nikukar et al., 2013). To study the effect of N30 vs N90 on ROCK pathway, MSCs were cultured in 2D for 7 day. The ratio of pRUNX2/RUNX2 was studied by In-Cell western assay. The 10 μM of Y-27632 (ROCK inhibitor) was added at day 2 and day 5. At day 4, pRUNX2/RUNX2 significantly decreased in N90, indicating that ROCK pathway links to RUNX2 expression. However, no significant difference was noted at day 7. Therefore, ROCK pathway might influece 2D osteogenesis, especially for N90, in the very early stages of committment (day4) **(Figure 4.17)**.

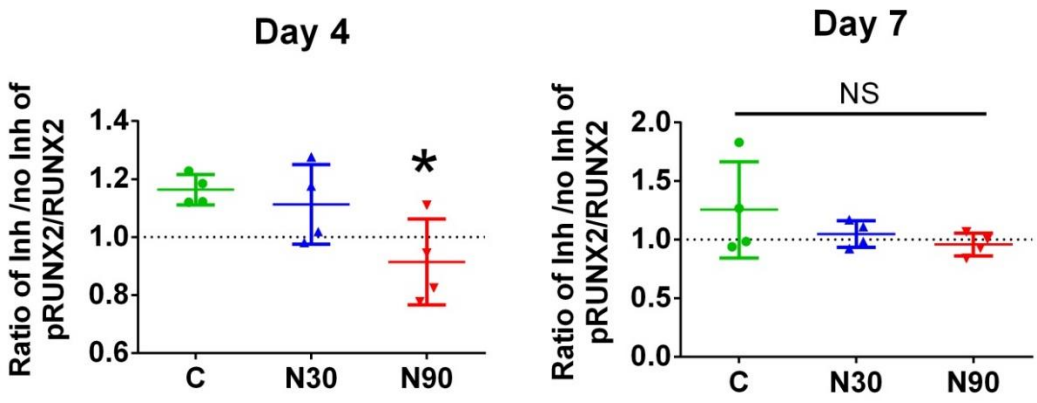

Figure 4.17 RUNX2 protein expression with ROCK pathway inhibition in 2D culture

In-Cell Western assay of pRUNX2/RUNX2 with ROCK pathway inhibition for 2D osteogenesis. At day 4, the ROCK pathway was significantly involved in osteogenesis in the early phase (day 4). Effect of ROCK pathway was reduced at day 7 (Mean±SD, n=4, * P≤ 0.05, ** P≤ 0.01, *** P≤ 0.001, One-way ANOVA, Tukey's post hoc test).

To investigate the role of ROCK pathways in 3D osteogenesis, 10 μM of Y-27632 (ROCK inhibitor) supplemented in the media was changed every 2 days (starting from day 2), and qRT-PCR was performed at day 9. The decrease of the RUNX2 ratio between with and without inhibitor (less than 1) was noted in N90, indicating that ROCK pathway may also tend to enhance to RUNX2 expression in 3D NS osteogenesis. Moreover, a significant ROCK-linked decrease of OSX expression was

noted in the N30 group (but not in N90), indicating that the ROCK pathway is involved in N30 driven osteogenesis **(Figure 4.18).**

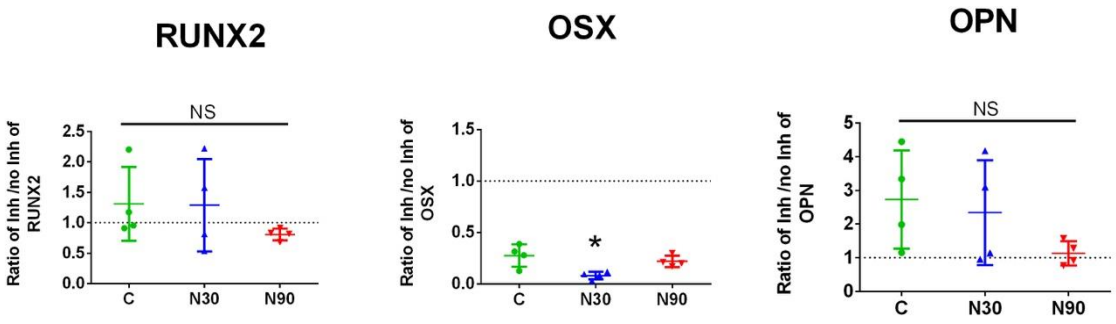

Figure 4.18 Osteogenic gene expression with ROCK pathway inhibition in 3D culture

qRT-PCR with Y-27632 (ROCK inhibition) was performed at day 9. ROCK pathways significantly involved in OSX gene expression in N30 group at day 9. No significant change was found in RUNX2 and OPN gene expression (mean±SD, n=4, * P≤ 0.05, ** P≤ 0.01, *** P≤ 0.001, One-way ANOVA, Tukey's post hoc test).

4.4.4.3 Protein expression by protein arrays

To further investigate the NS induced pathways at protein level, a protein array was performed. MSCs were stimulated with standard (N30) and high amplitude stimulation (N90) for 7 days. N30 activated cellular membrane receptors such as integrins and BMP2. Increase of collagen protein production was also noted. High stimulating amplitude (N90), however, showed the activation of ion channel proteins on cellular membranes such as TRPA1, TRPV1, Piezo1,2, and L-type calcium channel. **(Figure 4.19**). Interestingly, protein array

results corresponded to qRT-PCR showing the upregulation of TRPV1 and piezo2 in gene level **(Figure 4.16A).**

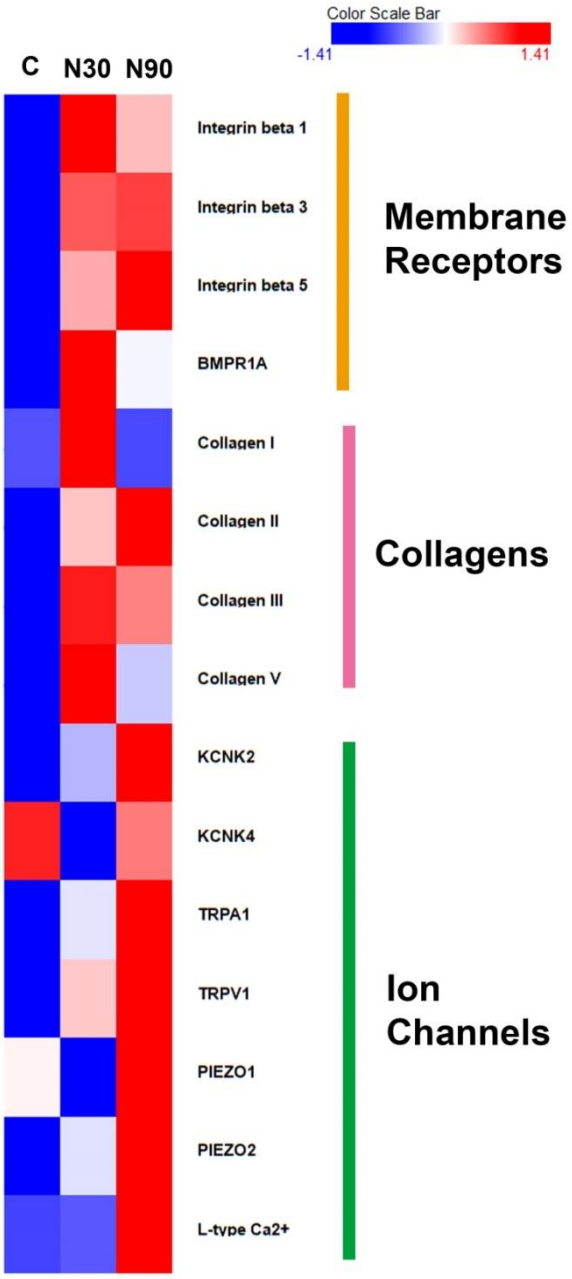

Figure 4.19 Protein expression of NS activated pathways at day 7

From protein array at day 7, standard NS amplitude (N30) activated ECM proteins including integrins and collagens. Interestingly, High amplitude NS (N90) not only triggered ECM protein production but also activated stretching ion channels

proteins such as TRPV1, Piezo1, 2, and L-type calcium ion channels.

4.5 Discussion

4.5.1 High amplitude nanovibration stimulation enhances osteognesis and pathway activation

At day 9, osteogenic genes (RUNX2, OSX, ALP, OPN and OCN) were significantly upregulated in the N90 group **(Figure 4.12)**. Regarding the gene expression in N90, it might be implied that stimulated MSCs are committed to preosteoblasts (by the effect of RUNX2 and osterix) and became immature osteoblasts (by the evidence of RUNX2, OPN and OCN upregulation at day 9). At the protein level, the evidence of pRUNX2/RUNX2 upregulation **(Figure 4.14)**, again, affirmed that N90 provided a better osteogenic induction effect than N30 which coresponded to activated pathways at the gene level for N90 **(Figure 4.16)**. The activation of N90-induced calcium ion-related (TRPV1, Piezo1, ERK1) and BMP2-related (BMP2, SMAD1) genes and proteins indicated that N90 may link to calcium signaling and BMP2 pathways.

In a temporal gene study **(Figure 4.15)**, again, N90 showed better osteogenic induction during 3 weeks of stimulation. The temporal gene study of N90 corresponded to Yang et al who studied the temporal gene expression for nanotopography induced osteogenesis (J. Yang et al., 2014). RUNX2 and OSX upregulation was found in week 1-2 for osteogenic commitment of MSCs. OCN and OPN were then increased at week 2-3 for ECM production and mineralization. However, the early increase of ALP at week 1 was noted which correlated to Tsimbouri et al's study showing the upregulation of ALP and OPN in 1 week by N30 induction (Tsimbouri P.M., 2017). The early upregulation of ALP in N90 was observed and possibly relate to mineralization initiation (Stefkova, Prochazkova, & Pachernik, 2015). In a physiologically-relevant osteogenic gene expression pattern, ALP was produced in low levels at week 1 and progressively increase at week 2-3 (Hoemann, El-Gabalawy, & McKee, 2009). To explain why the early upregulation of ALP and OPN was found in week 1, three hypotheses were drawn. Firstly, NS may directly activate calcium channels such as TRPV1, Piezo1/2, and L-type calcium channels especially in week1 resulting in the influx of extracellular calcium. The increase of intracellular calcium may induce OPN (You et al.,

2001) and possibly enhance ALP secretion (Iannotti, Naidu, Noguchi, Hunt, & Brighton, 1994).

BMP2 secretion in week1 could be another cause. NS possibly promotes BMP2 secretion in the early phase (shown in (Tsimbouri P.M., 2017) and **Figure 4.2A, 4.16B)**, and may increase intracellular calcium and ALP expression (W. Xu et al., 2016). This hypothesis coresponded to Tsimbouri's study reporting that the effect of NS links to calcium signaling (Tsimbouri P.M., 2017). Morover, NS also induce BMP2 as well as links to TRPV1 and PKC which is the mediator of the calcium signaling pathway **(Figure 4.3 D-E)**.

Another hypothesis could be drawn based on the metabolomic data, NS may induce low grade oxidative stress e.g. reactive oxygen species (ROS). This stress, in turn, induced endoplasmic reticulum (ER) stress (J. K. Kim et al., 2016) in early phase (day 7), thus, enhancing ALP upregulation (Furmanik & Shanahan, 2018). NS induced ROS hypothesis possibly linked to calcium ions. ROS can control calcium homeostasis and affects on mitochondria and ER functions. ROS induces ER to release calcium ions from ER into the cytosol (Görlach, Bertram, Hudecova, & Krizanova, 2015). ROS may generally enhance ion channels upregulation in protein arrays such as TRPV1 (Chuang & Lin, 2009), TRPA1(Nicholas, Yuan, Brookes, Spencer, & Zagorodnyuk, 2017; C. Xu et al., 2017), L-type Ca^{2+} channels (L. Yang et al., 2013) and, furthermore, it may enhance collagen synthesis (Boin et al., 2014) showing in protein array **(Figure 4.19)**. Effect of ROS on MSCs is a double-edged sword, low level of ROS suits for osteogenesis and proliferation (C. H. Byon et al., 2008; Choe et al., 2012). However, high doses of ROS reduce differentiation (Atashi et al., 2015; C. H. Lin, Li, Cheng, & Yen, 2018; J. Tan et al., 2015). Further discussion of ROS and osteogenesis are discussed in **chapter 5**.

4.5.2 The hypothesized pathways and crosstalk activated by NS; possible interaction between calcium signaling-BMP2-cytoskeleton.

It is difficult to conclude that NS directly activate calcium ion channels or that calcium ion channels are the secondary responders from other activated pathways. The possible pathways, activated by NS, are summarized in **Figure 4.20**. NS is potentially involved in calcium ion channel expression/function (directly activated or indirectly activated by cytoskeleton or by reducing channel sensitization by ROS and inflammatory cytokines) or involves GPCRs

which might be overlooked as mechanosensor (Connelly et al., 2015). Increased intracellular calcium activate PKC (K.-P. Huang, 1989) in turn phosphorylates TRPV1 allowing calcium influx (Studer & McNaughton, 2010). Cacium/CAM complex might then activate CaMKs promoting differentiation (Y. H. Choi et al., 2013; Illario et al., 2003). NS also enhanced BMP2 signalling via SMAD1/5 pathway driving osteogenesis. BMP2 also increases intracellular calcium promoting osteogenesis (W. Xu et al., 2016). Cytoskeletal tension appears to play a role in 3D osteogenesis via integrins-ROCK pathway. ERK1/2 was possibly mediated by cytoskeleton, crosstalking of calcium signaling as well as crosstalking between canonical and non-cannonical Wnt. Joining the dots on all of these pathways remains to be done.

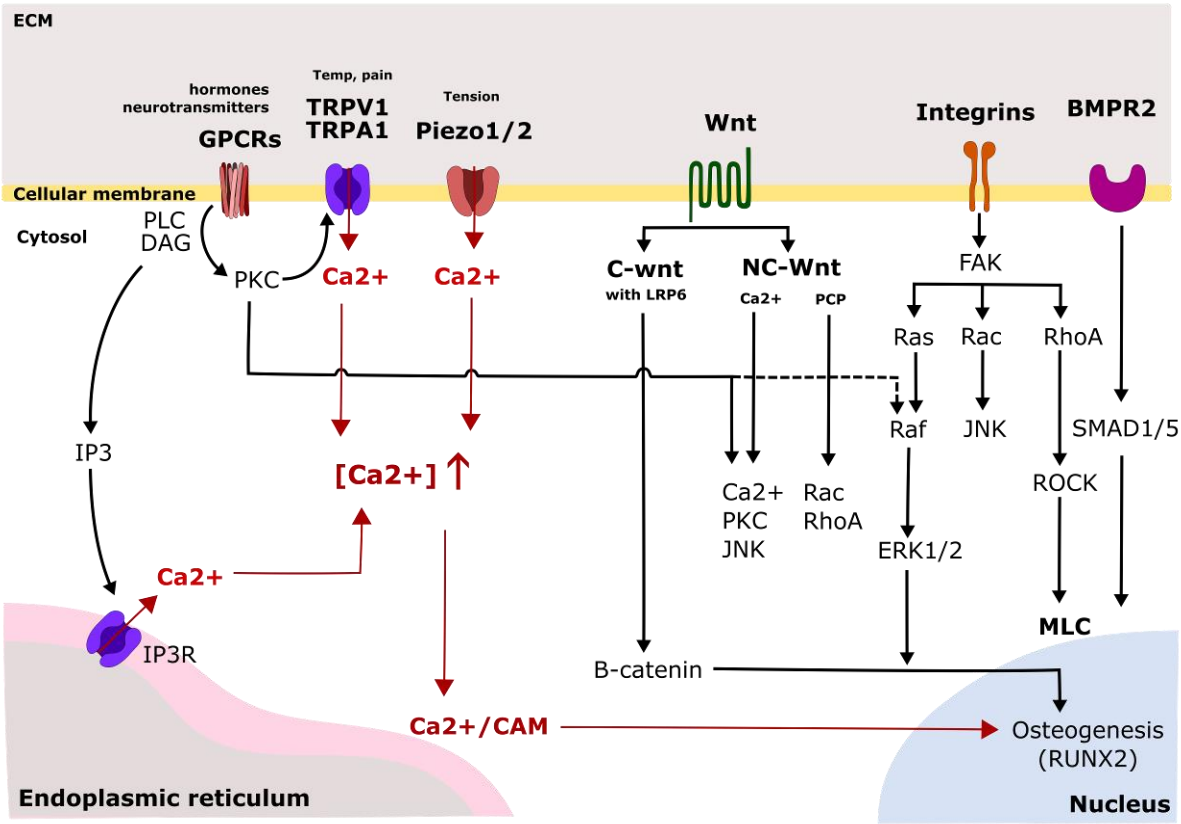

Figure 4.20 Extended hypothesis of NS induced 3D osteogenesis

(refer to section 4.5.2)

4.6 Conclusion

NS with high amplitude stimulation (90 nm) was safe for MSCs and enhanced 3D osteogenesis in gene and protein levels. In a temporal gene study, N90 induced 3D osteogenesis corresponding to an osteogenic gene expression pattern. N90 appeared to drive 3D osteogenesis through multiple biological pathways including BMP-smad1/5, calcium signaling (through TRPV1, piezo2, CaSR) and ROCK pathways.

Chapter 5 The effect of high amplitude nanovibrational stimulation on MSC metabolomics and inflammatory response

Chapter 5 The effect of high amplitude nanovibrational stimulation on MSC metabolomics and inflammatory response

5.1 Introduction

5.1.1 Metabolic changes in MSC status

It is known that metabolomic changes reflect cellular status such as proliferation, differentiation, oxidative stress or apoptosis (Wanet, Arnould, Najimi, & Renard, 2015). Thus, understanding the metabolomic changes, during proliferation, differentiation and exposure to external stimuli, could help to interpret how MSCs respond to NS.

In physiological conditions, MSCs require bioenergy from glycolysis and fatty acid β-oxidation for maintaining self-renewal (K. Ito & Suda, 2014). During differentiation, MSCs develop different metabolic patterns. For example, chondroblastic differentiation mainly uses glycolysis under hypoxic conditions (Pattappa, Heywood, de Bruijn, & Lee, 2011). However, osteoblastic differentiation likely requires energy from oxidative phosphorylation (OXPHOS) in normoxic conditions; reactive oxygen species (ROS) are thus produced at low levels (Shum, White, Mills, Bentley, & Eliseev, 2016). Adipogenic differentiation requires OXPHOS for differentiation from pre-adipocyte to adipocyte; ROS is produced at high levels (Shyh-Chang et al., 2013). It is noted that the Phosphoinositide 3-kinase/Protein kinase B/mammalian target of rapamycin (PI3K-AKT-mTOR) pathway is important for bioenergetic regulation maintaining cellular homeostasis (K. Ito & Ito, 2016).

5.1.1.1 Glycolysis, oxidative phosphorylation: from quiescence to differentiation

MSCs require high energy to maintain functions such as differentiation or proliferation. Glucose metabolism plays an important role in undifferentiated and differentiated cells. The oxygen niche is another

key regulator for glycolysis and oxidative phosphorylation (Ziello, Jovin, & Huang, 2007).

It had been known that HIF1α regulates glycolysis and oxidative phosphorylation in responding to oxygen concentration. HIF1α activates pyruvate dehydrogenase kinase 1 (PDK1) in turn inactivating pyruvate dehydrogenase (PDH). A decrease in PDH reduces the conversion of pyruvate to acetyl-CoA, thus, suppressing tricarboxylic acid cycle (TCA) cycle (J.-w. Kim, Tchernyshyov, Semenza, & Dang, 2006). HIF1α is increased in the hypoxic niche resulting in activation of glycolysis and reduction of OXPHOS. High levels of HIF1α are found in undifferentiated cells in the niche (Shum et al., 2016). In normoxic conditions, where MSCs are e.g. osteogenically induced, HIF1α is downregulated and thus OXPHOS is activated (Palomaki et al., 2013) **(Figure 5.1)**. HIF1α is thus a determinant of stem cell fate along osteogenic, angiogenic or chondrogenic lineages. Moreover, HIFs also crosstalk with many signaling pathways such as TGF/Smad and Wnt/Catenin pathways (Ozturk, Hobiger, Despot-Slade, Pichler, & Zenobi-Wong, 2017; S. M. Watt, Tsaknakis, Forde, & Carpenter, 2009). In hypoxic condition, HIF1α is best known to promote angiogenesis through vascular endothelial growth factors (VEGFs) signaling result (Drager et al., 2015). However, VEGF-D also regulates osteoblast maturation via VEGF receptor 3 (VEGFR3) (Orlandini et al., 2006).

5.1.1.2 Lipid metabolism in MSCs

Lipid metabolism is essential for cell homeostasis maintaining the equilibrium between anabolism (lipogenesis) and catabolism (generating ATP) (Kuo & Ann, 2018); lipids are important sources of ATP. In quiescent stem cells, fatty acids are catabolized by β-oxidation into acetyl-CoA then used to generate ATP via TCA cycle. In proliferative stem cells, Acetyl-CoA is used to synthesize polyunsaturated fatty acids or complex fatty acids such as the phospholipid membrane (Folmes, Park, & Terzic, 2013).

5.1.1.3 Amino acid metabolism; role of glutamine in MSCs

Glutamine metabolism is important for cell survival as it is the main nitrogen source for nucleotide synthesis. During cell differentiation which requires high energy, reactive oxygen species (ROS) are produced. Glutamine balances cellular redox acting as an antioxidant (Mates, Perez-Gomez, Nunez de Castro, Asenjo, & Marquez, 2002). In hypoxic conditions, the TCA cycle is limited in generating ATP by HIF1-α. HIF1-α reduces pyruvate dehydrogenase (PDH), thus reduces the conversion of pyruvate to acetyl-CoA. Subsequently, glycolysis is the main source of energy in hypoxia. Glutamine is converted to glutamate and α-ketoglutarate which in turn enters TCA cycle for ATP production (Michalak, Mackowska-Kedziora, Sobolewski, & Wozniak, 2015) **(Figure 5.1)**.

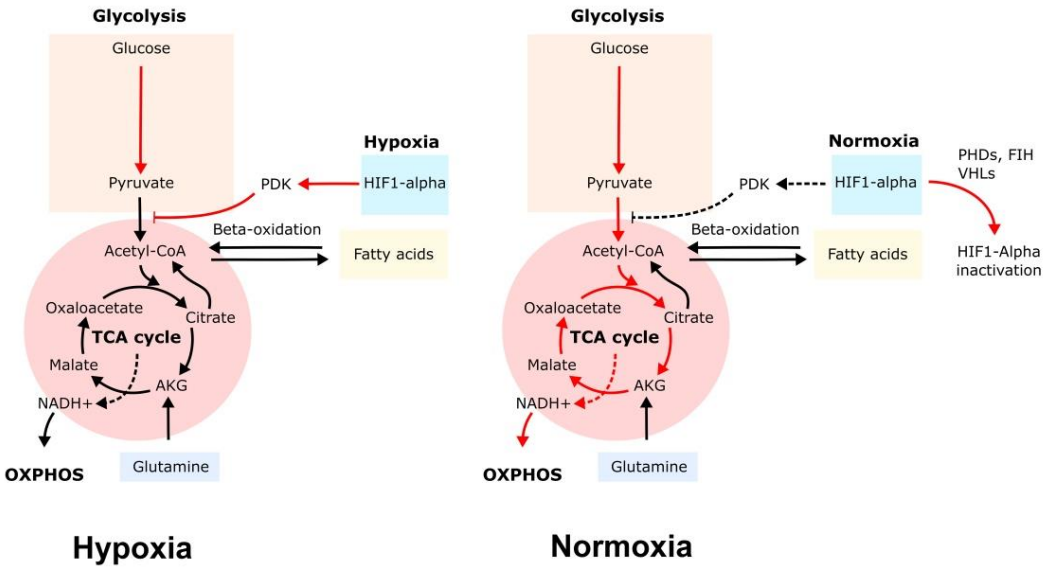

Figure 5.1 Glycolysis, oxidative phosphorylation and HIF1-α

In hypoxic conditions, HIF1- α activates pyruvate dehydrogenase kinase 1 (PDK1) to inhibit PDH reducing the conversion of pyruvate to Acetyl-CoA. Glycolysis therefore is mainly used during the quiescent state. In normoxic conditions, HIF1- α is degraded by prolyl hydroxylases (PHDs), factor inhibiting HIF-1 (FIH) and Von Hippel-Lindau ubiquitin ligase complex (VHLs). Pyruvate from glycolysis is converted to Acetyl-CoA which, in turn, enters TCA cycle and oxidative phosphorylation (K. Ito & Suda, 2014; Y. Liu & Ma, 2015; Mahon, Hirota, & Semenza, 2001).

5.1.2 Can NS-induced osteogenesis with low grade oxidative stress?

From current evidence, mechanical stimulation can induce osteogenesis (P. L. Fu et al., 2017; X. Huang et al., 2018) but it may also produce oxidative stress (Chapman et al., 2005; Sharifpanah, Behr, Wartenberg, & Sauer, 2016). Optimal reactive oxygen species (ROS) drive differentiation (Choe et al., 2012) while over stimulation (high level of ROS) can suppress differentiation and may affect cell survival (Chang Hyun Byon et al., 2008; Jufri, Mohamedali, Avolio, & Baker, 2015; J. Tan et al., 2015). There are many studies that show that mechanical stimulations may link to oxidative stress (Chapman et al., 2005; J. J. Cheng, Wung, Chao, & Wang, 1998; Hong et al., 2015; Schmelter, Ateghang, Helmig, Wartenberg, & Sauer, 2006; Sharifpanah et al., 2016). For example, cyclic stretch produces ROS at the plasma membrane (by NADPH oxidase) or via the mitochondrial respiratory chain. ROS is involved in multiple cell functions including cellular contraction (via ion channels), cell growth, cellular apoptosis (via cyclins, CDK) and inflammation (via e.g. NFκB) (Birukov, 2009). NS can be considered as a mechanical stimulus, thus, it possibly generates oxidative stress. Thus, if ROS is found during NS, this possibly hints the clue of NS induced osteogenesis.

5.1.3 ROS: sources and REDOX balance

ROS are oxygen free radicals e.g. peroxides, superoxide, etc., produced by cellular metabolism (Murphy, 2009). ROS metabolites maintain redox homeostasis (Droge, 2002). ROS are mainly produced by mitochondria from the electron transport chain (Murphy, 2009) but can also be produced at the cellular membrane where external stimuli such as bacteria or mechanical stimulation (e.g. cyclic stretch (Liang et al., 2019)) act. At the cellular membrane, NADPH oxidase (NOX) plays important roles in ROS generation (Bigarella, Liang, & Ghaffari, 2014).

ROS is controlled by antioxidative responses in cells. In acute response, ROS is counterbalanced by enzymes. For example, superoxide dismutase (SOD) can convert ROS to H_2O and O_2 (Mittal, Siddiqui, Tran, Reddy, & Malik, 2014). Glutathione also scavenges ROS by oxidation (Droge, 2002). Chronic ROS production triggers the nuclear factor erythroid 2-related factor2 (Nrf2) gene for antioxidant

response (Ma, 2013). This activates MAPK, p53 and NFκB for cell survival in a long-term response (Martindale & Holbrook, 2002).

At the physiological level, ROS enhances stem cell proliferation and differentiation. In high oxidative stress conditions, ROS can lead to mitochondrial dysfunction, induce DNA damage and apoptosis (Maryanovich & Gross, 2013). ROS is also directly involved in redox signaling and protein functions such through NFκB, HIF1α, FOXO, mTOR, AKT which in turn, regulate glycolysis and oxidative phosphorylation (Bai et al., 2005; Bigarella et al., 2014; Murphy, 2009).

5.1.4 Metabolomic changes of MSCs in oxidative stress conditions

As aforementioned, MSCs maintain *in vivo* potency using glycolysis under hypoxic niche conditions. In osteogenically differentiating MSCs, OXPHOS is activated (Shyh-Chang et al., 2013). SOD and catalase are increased to control ROS (C. T. Chen, Shih, Kuo, Lee, & Wei, 2008). In the early differentiation stage, ROS is produced at physiological levels, enhancing molecular signaling to help driving differentiation and proliferation (Droge, 2002). In high energetic process such as proliferation, ROS can temporally increase but it then reverts to normal levels (Droge, 2002; Shyh-Chang & Ng, 2017).

In oxidative stress conditions where ROS accumulation can damage cellular organs, cells scavenge ROS using enzymes and redox signaling as sentinel mechanisms maintaining normal cellular functions and reduce ROS. Glycolysis is also shifted to pentose phosphate pathway (PPP).

5.1.4.1 The shift of OXPHOS to glycolysis and pentose phosphate pathways in oxidative stress conditions

In oxidative stress conditions, cells use a redox balancing system to reduce mitochondrial injury from high levels of ROS. Cells reduce ATP production from the TCA cycle by diverting glycolysis to PPP (Kuehne et al., 2015). The PPP generates NADPH, pentoses and ribose from G-6 phosphate; ribose-5-phosphate is a precursor for DNA, RNA synthesis and NADPH formation (Perl, Hanczko, Telarico, Oaks, & Landas, 2011). By redox balancing, PPP reduces oxidative stress by converting H_2O_2 to H_2O using glutathione peroxidase (Bigarella et al., 2014). Some

literature mentions that shifting to PPP may be an early sign of tumorigenesis before shifting to aerobic glycolysis-dependent mechanisms (Warburg effect) (E. S. Cho, Cha, Kim, Kim, & Yook, 2018; Kuehne et al., 2015).

5.1.4.2 Effect of ROS on amino acids and lipids

ROS oxidizes proteins causing hydroxylation of aromatic amino acids as well as nitration, nitrosylation and sulfoxidation, in turn, resulting in protein degradation and dysfunction (Stadtman & Levine, 2003). Moreover, L-glutamine also links with ROS. L-glutamine is a precursor of glutathione (GSH). GSH plays role in redox balance reducing ROS. GSH is oxidized to glutathione disulfide (GSSG) by converting H_2O_2 to H_2O (Mailloux, McBride, & Harper, 2013). Aspartate, a non-essential amino acid, is another source of ATP from mitochondrial oxidation (Pi et al., 2014). Aspartate is a known antioxidant. However, evidence and mechanism of aspartate on ROS reduction is scarce and remains unclear (J. Duan et al., 2016).

Considering lipids, LC-PUFAs are important as they are ATP sources and precursors of phospholipids (Maulucci et al., 2016). LC-PUFAs are also antioxidants (via Nrf-2/HO-1 pathway) (Kusunoki et al., 2013; Richard, Kefi, Barbe, Bausero, & Visioli, 2008). However, in oxidative stress conditions, ROS can peroxidize PUFAs, lipoproteins and damage oxidative membrane (H. Arai, 2014; Ayala, Muñoz, & Argüelles, 2014).

5.1.5 mTOR-AMPK-Akt pathway regulates metabolism in oxidative stress conditions.

It has been shown that the mTOR-AMPK-Akt pathway links to cellular metabolism, redox balancing, autophagy and cell survival (Y. Zhao et al., 2017). Zhao et al contributed a good summary of the interaction between mTOR-AMPK-Akt and ROS as illustrated in **Figure 5.2 A-B**.

In low (physiological) stress conditions (with glucose deprivation), AMP-activated protein kinase (AMPK) pathway plays a catabolic role to produce energy together with anti-oxidant production (via Forkhead box class O; FOXO) as well as reduce anabolism (Y. Zhao et al., 2017). AMPK acts as an energy sensor for cells. AMPK suppresses protein synthesis (by inhibiting mTOR), fatty acid catabolism (by activating adipose triglyceride lipase; ATGL) and lipid synthesis (via inhibition of HMG-CoA reductase and acetyl-CoA-carboxylases; ACC1

and 2). AMPK increases glucose uptake (by TBC1D1 activate via GLUT1 and 4) and inhibits glycogen synthesis (inhibiting glycogen synthase) (Herzig & Shaw, 2018). AMPK also plays role in autophagy (via ULK1) (Mihaylova & Shaw, 2011). Interestingly, some studies have shown that AMPK may promote osteogenesis and mineralization (E. K. Kim et al., 2012; Yi Li, Su, Sun, Cai, & Deng, 2018).

In high stress conditions (shown by ROS accumulation), the Akt (protein kinase B) pathway plays a role by initiating cell survival and anti-apoptotic pathways as well as promotes anabolism (Y. Zhao et al., 2017). mTOR (considered as a nutrient sensor) is a member of PI3K kinase family (Saxton & Sabatini, 2017). mTOR is regulated by both AMPK (inhibitory effect) and Akt (stimulating effect) thus balancing between catabolism and anabolism (Hahn-Windgassen et al., 2005; Saxton & Sabatini, 2017). Akt activation provides anti-apoptotic function and increases glucose uptake (Y. Zhao et al., 2017) as well as resists an oxidative stress (L. Wang, Chen, Sternberg, & Cai, 2008).

Akt activated-mTOR increases protein synthesis and decreases autophagy (Saxton & Sabatini, 2017).

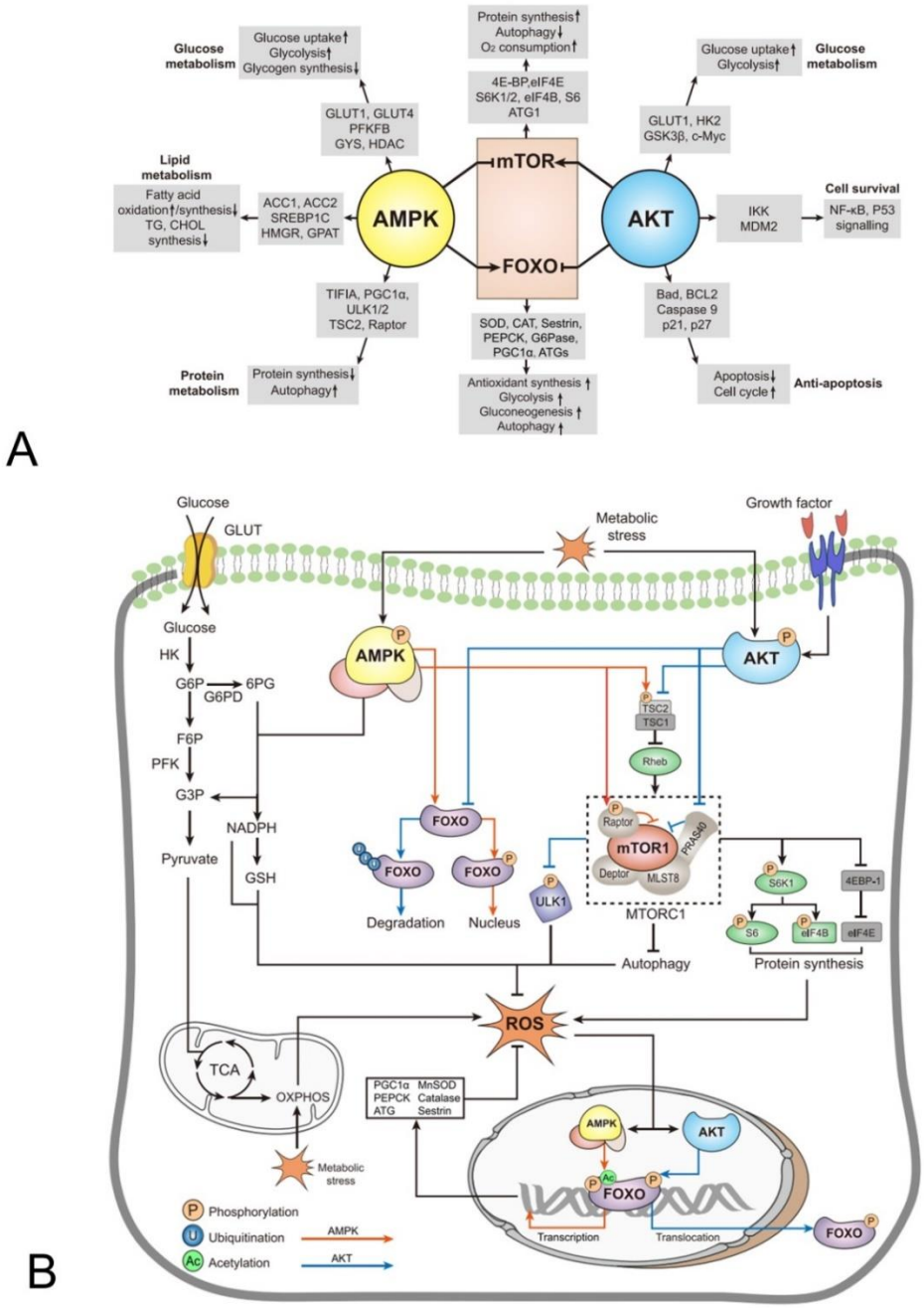

Figure 5.2 mTOR mTOR-AMPK-Akt signaling pathway and oxidative stress

A) AMPK, Akt, mTOR and FOXO interaction. In summary, AMPK promotes energy production by increasing catabolism (increase fatty acid oxidation, glycolysis) and reducing anabolism (reduce protein and fatty acid synthesis). Akt activation increases anabolism such as glycogen and protein

synthesis and promotes anti-apoptosis. mTOR is activated by Akt but inhibited by AMPK. FOXO is controlled by AMPK and Akt.

B) mTOR-AMPK-Akt pathways and ROS regulation; Akt-AMPK affects on mTOR (AMPK inhibits while Akt activates mTOR). Activated mTOR promotes protein synthesis and decrease autophagy. AMPK-FOXO promotes anti-oxidants synthesis and shift glycolysis to PPP in order to reduce ROS

5.1.6 Oxidative stress and interaction among lipid rafts, NAPDH oxidase and ROS on the cellular membrane

It has been proposed that NS may 'flutter' cellular membranes (Childs et al., 2016). Theoretically, ROS can also be generated at the cellular membrane by NADPH oxidase (NOX). Indeed, much signaling emanating from the cellular membrane is linked to lipid rafts. Thus, understanding the lipid raft-oxidative stress relationship is important.

Lipid rafts (LR or membrane rafts) are microdomain clusters on the cellular membrane which consist of phospholipids, sphingolipids and sterols. LRs interact with proteins (e.g. receptors) providing biological functions such as redox signaling. LR functions depend on the major proteins in rafts e.g. calcium channel rafts (functioned as ion channels activity), GPCR rafts (GPCR cellular signaling), and raft-cytoskeleton (Fas signaling) (Jin, Zhou, Katirai, & Li, 2011).

LR also plays crucial roles on NOX controlling redox signaling by forming NOX-lipid rafts platform (Ushio-Fukai, 2006). At the cellular membrane, ROS can be generated by NADPH oxidase (NOX) which can be found in physiological and pathological conditions (Bedard & Krause, 2007). NOX-dependent ROS oxidises cysteine residues activating many transcription factor such as NFkB and Ras as well as inducing TNFα and TGFβ1 (Bedard & Krause, 2007). Moreover, NOX can be activated by calcium signaling. NOX can regulate calcium channels (L-type channels, stored-operated calcium channels, Ca^{2+} ATPase pump) resulting in increased intracellular calcium (Bedard & Krause, 2007).

5.1.7 Interplays between ROS and inflammatory pathways

Inflammation is a major cause of oxidative stress (Chatterjee, 2016) and, as has been discussed, ROS can induce inflammation (Biswas, 2016) Thus, It is difficult to specify whether ROS or inflammation firstly triggers these inflammation-ROS signals. If the process is started with inflammation induced ROS production, the inflammation may be initiated as MSCs are exposed to stimuli such as bacteria or tissue injury. These inflammasomes, in turn, activate ROS production from mitochondria and the cellular membrane (via NADPH oxidase) together with inducing ER stress and calcium influx. These signals then activate thioredoxin-binding protein and NLRP3 to produce IL-1β (Abais, Xia, Zhang, Boini, & Li, 2015). However, oxidative stress can also induce inflammation by itself. Chronic ROS exposure can activate NFκB which is a sensor of oxidative stress that links cell survival pathways (Morgan & Liu, 2011; Oliveira-Marques, Marinho, Cyrne, & Antunes, 2009; T. Wang et al., 2002), it also activates TNFα (Blaser, Dostert, Mak, & Brenner, 2016), IL-1β (via NLRP3) (Abais et al., 2015; Chang Hyun Byon et al., 2008), caspases (Higuchi, Honda, Proske, & Yeh, 1998) as well as activator protein 1 (AP-1; links to cell growth or apoptosis) (Ferreira Mendes, Caramona, Carvalho, & Lopes, 2003). These signals explain why inflammatory cascades are activated (Lugrin, Rosenblatt-Velin, Parapanov, & Liaudet, 2014; Reuter,

Gupta, Chaturvedi, & Aggarwal, 2010). The cycle of ROS-inflammation is illustrated in **Figure 5.3**.

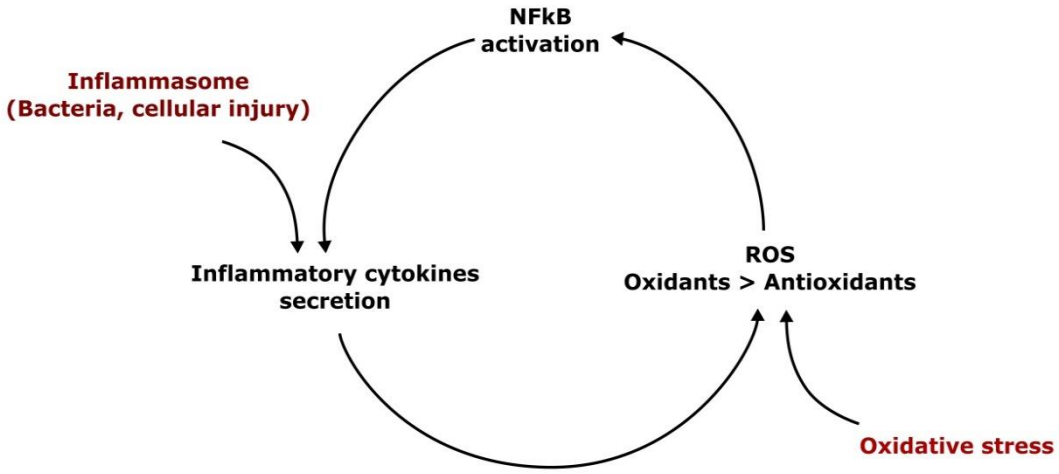

Figure 5.3 Vicious cycle of ROS and inflammatory response

ROS can induce inflammation. However, inflammation also enhances ROS production. Uncontrolled inflammasomes or oxidative stress, drive this cycle leading to apoptosis.

5.1.8 MSCs play roles in inflammation

Theoretically, inflammatory cells exposed to exogenous (pathogen) or endogenous (soft tissue damage) stimuli present pathogen-associated or damaged associated molecular patterns (PAMPs or DAMPs) which can be recognized by pattern recognition receptors (PRRs) e.g. Toll-like (TLRs on the cell membrane) and NOD-like (NLRs in cytoplasm) receptors. Both receptors activate NFκB signaling pathway which is a major inflammatory regulator producing inflammatory cytokines (Lugrin et al., 2014).

MSCs also have TLRs which can respond to DAMPs (e.g. heat shock protein; HSP60, HSP70) and PAMPs (e.g. bacteria) (Shirjang, Mansoori, Solali, Hagh, & Shamsasenjan, 2017). Regarding MSC polarization, MSCs can express pro-inflammatory or anti-inflammatory phenotype depending on environments (Bernardo & Fibbe, 2013). In an inflammatory environment, MSCs interact with other MSCs through TLR secreting TGFβ, PGE2, NO and indoleamine 2,3-dioxygenase (IDO) (Mellor, Lemos, & Huang, 2017; Putra et al., 2018). Moreover, MSCs also produce IL-6 to convert monocytes to M2 macrophages which, in

turn, produce IL-10 giving anti-inflammatory effects (Bernardo & Fibbe, 2013).

5.1.8.1 Inflammation and metabolomics; role of long chain polyunsaturated fatty acids (LC-PUFAs) and inflammation

Long chain polyunsaturated fatty acids (LC-PUFAs), are essential fatty acids derived from linolenic and linoleic acid desaturation and elongation. LC-PUFAs consist of n-3 and n-6 fatty acids (or omega-3 and omega-6). Omega-3 is known to be anti-inflammatory while omega-6 is pro-inflammatory (Borges, Santos Fde, Telles, Correia, & Lanna, 2014).

Omega-3 and omega-6 require Δ5-desaturase to synthesize LC-PUFAs; Omega-6 requires Δ5-desaturase to produce arachidonic acid (AA) which synthesizes high grade inflammatory metabolites (e.g. thromboxane, prostaglandins) by cyclooxygenase (COX) and lipoxygenase (LOX). Whlile omega-3s such as eicosapentaenoic acid (EPA) and docosahexaenoic acid (DHA) also use Δ5-desaturase to synthesize low grade inflammatory metabolites by COX and LOX (e.g. leukotrienes) (Kruger, Coetzee, Haag, & Weiler, 2010). Increased levels of n-3 PUFAs competitively use Δ5-desaturase with n-6 PUFAs to synthesize eicosanoids. Thus, there is evidence that omega-3 PUFAs may indicate a shift of high to low grade synthesis reducing inflammation level (Calder, 2001).

PUFAs might enhance osteogenic differentiation depending on their levels (Martinez-Ramirez et al., 2007). Optimal (low) level of PUFAs may promote TGFβ1 and insulin like growth factor (IGF) which are essential for differentiation (Kruger et al., 2010). However, some evidence has shown that DHA could inhibit alkaline phosphatase expression but did not involve mineralization studied in MC3T3-1 osteoblast-like cells (Coetzee, Haag, & Kruger, 2009). Moreover, omega-3 also has antioxidative effects (through Nrf2-HO-1) (Giordano & Visioli, 2014; Kusunoki et al., 2013; Richard et al., 2008). Interestingly, PUFAs can also regulate TRP channels via PKC (Ciardo & Ferrer-Montiel, 2017; Sisignano, Bennett, Geisslinger, & Scholich,

2014). As NS may activate osteogenesis via TRPV1, thus, the role of PUFAs during NS should be investigated.

5.2 Aims and objectives

1. To study the metabolomic response of MSCs on high amplitude NS.

2. To study the effect of high amplitude stimulation in 3D osteogenesis in terms of biological response.

3. To Identify related inflammatory pathways which are involved in osteogenic differentiation

5.3 Methodology and experimental design

5.3.1 Metabolomics

Stro1-selected MSCs seeded with 4 x10^4 cells/ml density in 1.8 mg/ml collagen hydrogels were stimulated with N30 and N90. After 1 and 2 week, NS the gels were homogenized on ice, and metabolites were then extracted using a Chloroform/Methanol/water (1:3:1 ratio) extraction buffer. Samples were agitated on a shaker at 4°C for 1 hour and in turn centrifuged at 13,000xg at 4°C for 5 minutes. Supernatants were transferred to and analysed by the Glasgow Polyomics team. Hydrophilic interaction liquid chromatography-mass spectrometry was performed (Dionex, UltiMate 3000 RSCL system, Thermo Fisher Scientific, Hemel Hempstead, UK) using a ZIC-pHILIC column (150 mm x 4.6 mm, 5 μm. column, Merck Sequant). The datasets were processed using XCMS (peak picking), MzMatch (filter and grouping), IDEOM (post processing filtering and identification). Metaboanalyst was used to generate heatmaps and PCA analysis. KEGG database and Ingenuity Pathway Analysis (IPA) software were used for metabolomic pathway analysis.

5.3.2 qRT-PCR and protein inhibition test

In all qRT-PCR studies, 4 x10^4 cells/ml of Stro1-selected MSCs seeded in 1.8 mg/ml collagen hydrogels was prepared and stimulated with N30 and N90. For the temporal gene study, the samples were

harvested at day 7, 14 and 21. The samples were digested with collagenase. The techniques of RNA extraction and purification as well as cDNA synthesis were mentioned in **Chapter 2 section 2.8.** For qRT-PCR with the inhibition test, hydrogels were stimulated for 9 days. All inhibitors (ERK1/2, JNK, p38, TNFα, NFκB inhibitors) were mixed with basal media which were changed at day 2, 5 and 8. The functional concentration of inhibitors in media was shown in **chapter 2 section 2.12.**

5.3.3 In-Cell Western with protein inhibition test

Stro1-selected MSCs were seeded in 24 well-plates with the density of 10,000 cells/well. MSCs then were stimulated with N30 and N90 for 7 days. Culture media was added with ERK1/2, JNK, p38, TNFα, and NFκB inhibitors (functional concentration of inhibitors in media was shown in **Chapter 2, section 2.12**). Media was changed at day 2 and day 5. In-Cell Westerns were performed at day 7 (technique described in **chapter 2 section 2.10**).

5.3.4 ROS measurement by DCF-DA with flow cytometry

Stro1-selected MSCs seeded with 4 $x10^4$ cells/ml density in 1.8 mg/ml collagen hydrogels were stimulated with N30 and N90 for 7 day. The samples were incubated in 2.5 mg/ml collagenase for 1 hour and were then centrifuged at 200xg for 4 minutes. Following that, the cell pellets were incubated for 1 hour in 2 uM 2',7'- dichlorodihydrogen-fluorescein diacetate (H_2DCF-DA, Invitrogen) in phenol red free media (Sigma, D5030). In the positive control group, 500 uM hydrogen peroxide was added. After incubation, the samples were then centrifuged and resuspended in 250 ul of flow cytometry buffer (2% FBS, 2 mM EDTA in PBS) and transferred to 96 well plates. Resuspended MSCs in 96 well plates were incubated for 30 minutes. Signal of H_2DCF-DA fluorescein was detected by using flow cytometry at 492-295 nm of excitation and 517-527 nm of emission.

5.3.5 Mitotracker

Stro1-selected MSCs with 4 $x10^4$ cells/ml of density in hydrogels were prepared. After 7 days stimulation, samples were digested using collagenase D. Cells were centrifuged to obtain pellets and resuspended with 100 nM final concentration of Mitotracker Green (FM, M7514, Invitrogen). The incubation lasted for 45 minutes and the

cells were then resuspended in prewarmed flow cytometry buffer (2% FBS, 2 mM EDTA in PBS). Flow cytometry was done immediately to detect fluorescence emission at 490 nm of excitation and 516 nm of emission.

5.3.6 Mitochondrial activity measurement (JC-1)

To study the mitochondrial activity, Stro1-selected MSCs with 4 $x10^4$ cells/ml of density in hydrogels were stimulated with NS for 7 days. The samples were harvested at day 7 and digested in collagenase D for 1 hour. After centrifuging the cell pellets were treated with 2 uM (final concentration) of 5',6,6'-tetrachloro-1,1',3,3'-tetraehyl-benzimidazolylcarbocyanine iodide (JC1, M34152, Molecular probes) for 30 minutes at 37°C. In the control group, 50 uM (final concentration) of CCCP was added and incubated at 37°C for 5 minutes. The mitochondria membrane potential was detected by flow cytometry. The fluorescence emissions were measured at green (529 nm) and red (590 nm) channels.

5.4 Results and discussion

5.4.1 Metabolomic assessment

In this study, metabolomics was used to search the NS-induced activation of bioenergetic-based pathways. Overall, metabolomic changes were firstly analysed broadly in order to scope out where more specific study should be focused. Then, interesting metabolites related to energy synthesis and oxidative stress pathways were selected and analysed in more depth. To correlate metabolomic results with biochemical signaling, the IPA software was used to create predicted activated networks from total metabolite data vs control.

5.4.1.1 Clustered metabolite assessment

To identify associated metabolites of MSCs responding to NS, major nutrient metabolisms including carbohydrate, amino acid and lipid metabolism were studied. Metaboanalyst was used to identify overall metabolomic changes. Heatmaps showed that N30 and N90 increased the activated metabolites, especially in lipid metabolism **(Figure 5.4 and 5.5).** Principle component analysis (PCA) showed the most obvious changes. There is clear clustering of the samples into different, isolated groups in lipid metabolism at week 2, suggesting discrete metabolite phenotypes for each sample at this time point. However, amino acid metabolome of N90 was still clustered together **(Figure 5.6 and 5.7).**

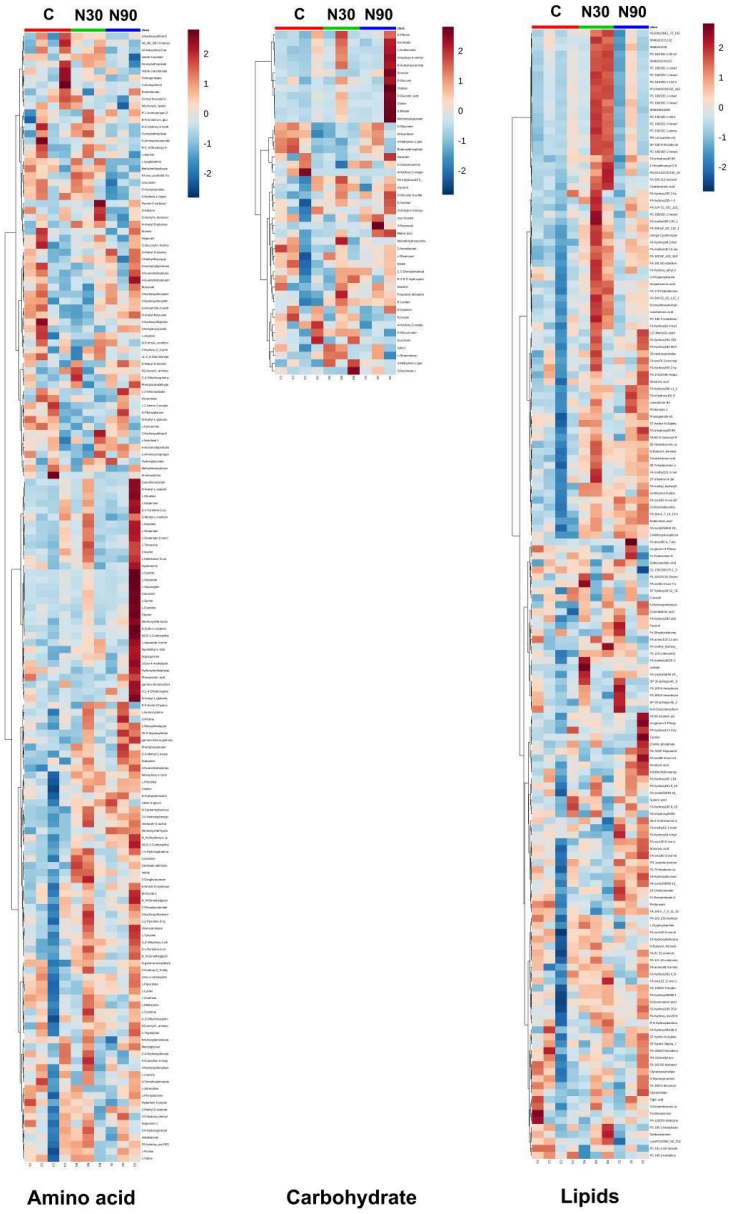

Figure 5.4 Heatmap at week 1 of NS

Amino acid, carbohydrate and lipid metabolism after 1 week of Stro1 selected MSCs being seeded in 1.8 mg/ml collagen hydrogels analysed by Metaboanalyst. Although there was only a small change in carbohydrate and amino acid metabolism in response to N30 and N90, the lipid metabolism demonstrated the greatest changes particularly in N90 group (n=3-4; red and blue representing up and down regulation respectively, C=control, N30= 30 nm amplitude N90= 90 nm amplitude).

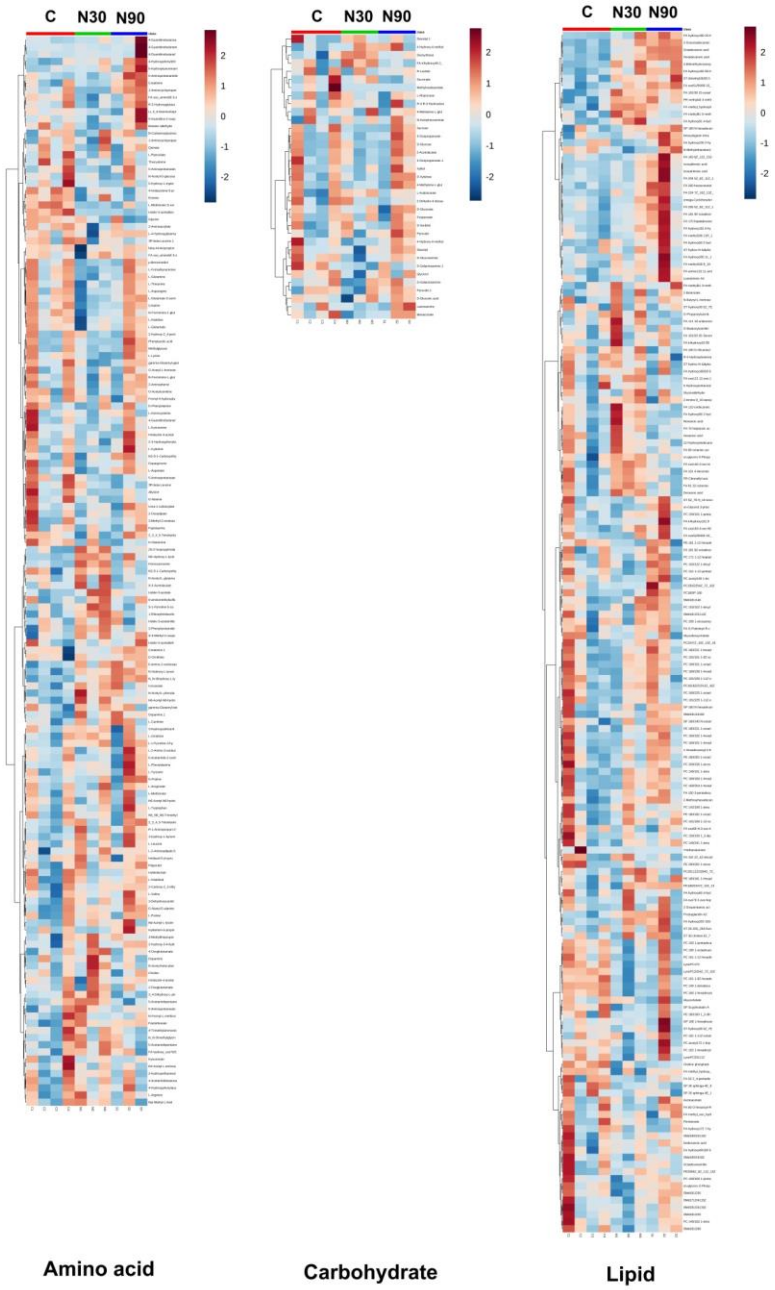

Figure 5.5 Heatmap at week 2 of NS

The lipid metabolism showed an increase in metabolite abundance in response to N90. No obvious change in amino acid and carbohydrate metabolites (n=3-4; red and blue representing up and down regulation respectively, C=control, N30= 30 nm stimulating amplitude N90= 90 nm stimulating amplitude).

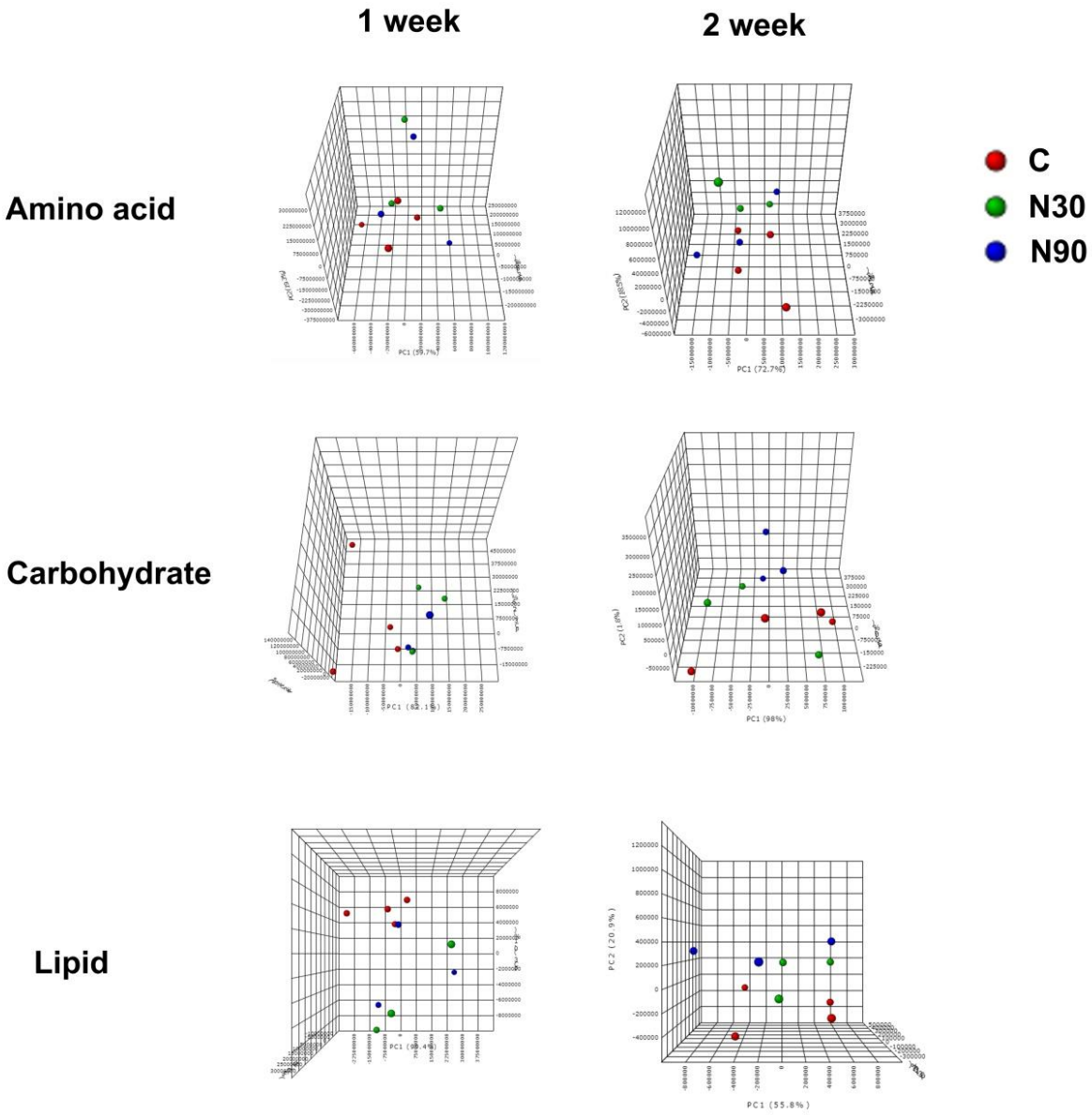

Figure 5.6 3D Principle component analysis

3D Principle component analysis of carbohydrate, amino acid and lipid metabolism at 1 and 2 week time points; Lipid showed the most discrete metabolome in response to N90 at 1 and 2 weeks. Only minor changes in carbohydrate and amino acid metabolism (n=3-4).

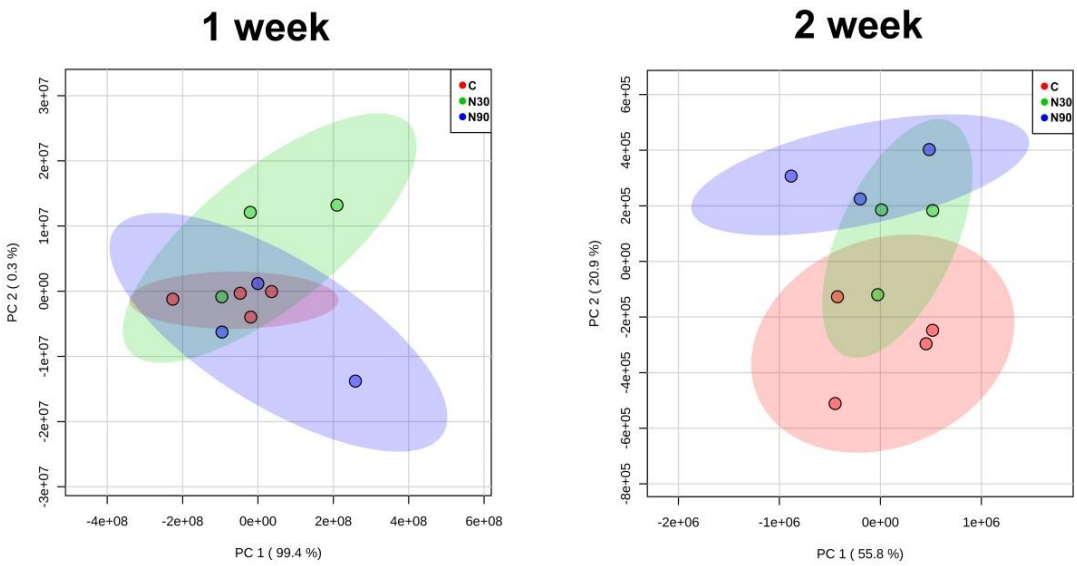

Figure 5.7 2D Principle component analysis of lipid metabolites

Considering only lipid metabolites at week 1, the lipid metabolites of all groups remain clustered together. At week 2, the N90 metabolites showed a clear separation from the control group indicating that NS (especially N90) involved lipid metabolism (n=3-4).

5.4.1.2 Metabolomic profile assessment

In order to spotlight specific metabolite pathways linking to osteogenesis, the selection of metabolites involving glycolysis, pentose phosphate pathway, TCA cycle, oxidative phosphorylation (OXPHOS), L-, and L-aromatic amino acid, Long-chain polyunsaturated fatty acids (LC-PUFAs) and β-oxidation was performed. These metabolites were selected from the IDEOM file. Metaboanalyst software was used to generate the heatmaps.

At week 1, the heatmap in figure 5.8 displayed that the metabolites of N90 group are an increased PPP product (ribose) with decreased pyruvate indicating that MSCs responded to oxidative stress by controlling redox balancing. Active metabolites of TCA cycle were found suggesting that MSCs required rapid energy through amino acid (via glutamine), lipids (via β-oxidation) and glycerol-3-phosphate (G3P) shuttle. The increase of LC-PUFAs was found only in N30 group.

Thus, it was hypothesised that N30 may synthesised LC-PUFAs possibly aiming for anti-inflammatory effect **(Figure 5.8)**.

Overall, from week1-2 **(Table AII.1)**, N90 slightly increased pentose phosphate pathway products (**Figure AII.2 and AII.3**), LCPU-FAs (precursor of inflammatory metabolites; **Figure AII.8**), β-oxidation (lipid catabolism; **Figure AII.9**), L-amino acid (linking to calcium sensing receptor; **Figure AII.6**) as well as glycerol-3-phosphate shuttle (relating to rapid ATP production) and OXPHOS (linking to reactive oxygen species and osteogenesis; **Figure AII.5**). Further details are shown in **Appendix II.**

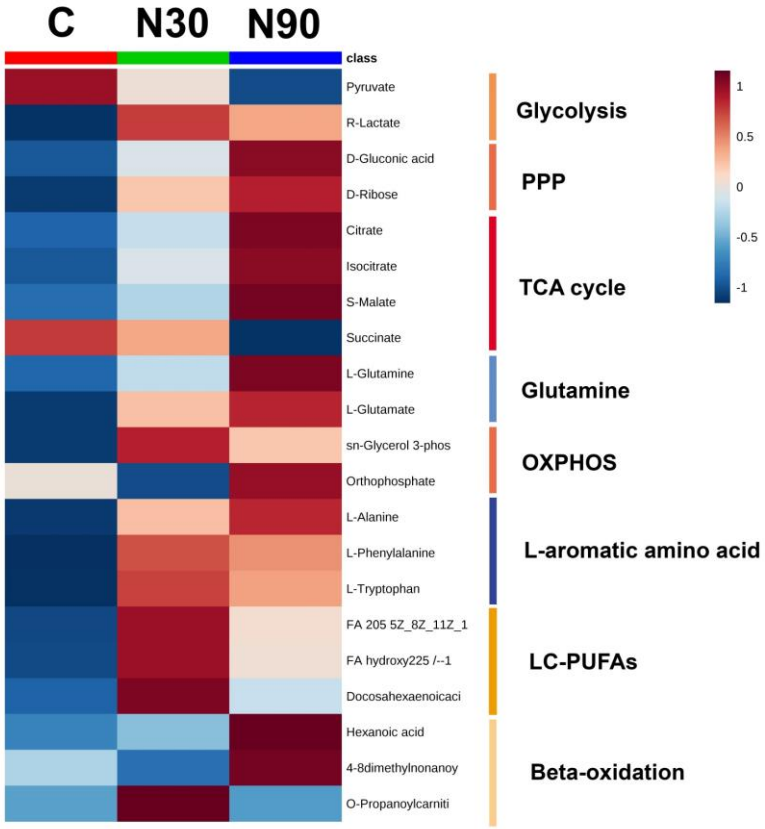

Figure 5.8 Heatmaps at week 1 of main nutrient pathways.

At week 1, active metabolites in TCA cycle were found indicating that N90 is an energetic process. MSCs required rapid energy from β-oxidation and G3P shuttle. Increased PPP suggested that redox balancing was involved to reduce oxidative stress (N=3).

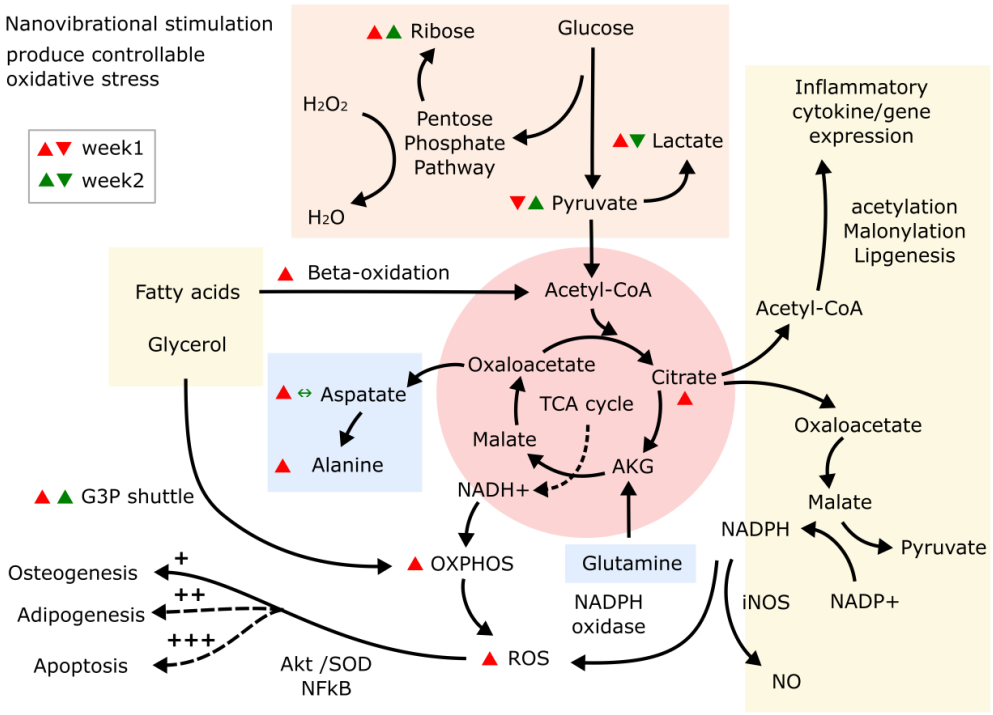

Figure 5.9 Metabolomic change during high amplitude stimulation at week 1 and 2

N90 activated energetic pathways such as OXPHOS, glycerol-3-phosphate shuttle and β-oxidation. Metabolic pathways were potentially slightly modulated to reduce oxidative stress (indicated by activation of PPP).

5.4.1.3 Predicted activated networks after 1 week stimulation

The IPA software was then used to link metabolomics to biochemical pathways through prediction analysis. After 1 week stimulation **(Figure 5.10)**, N30 was predicted to enhance ERK1/2 and superoxide dismutase (SOD) indicating that N30 produced slight oxidative stress which was counterbalanced by SOD. In the N90 group, the activation of SOD, phosphatidylinositol-3 kinase (PI3K or Akt) and NFκB were indicated. SOD, Akt (antiapoptotic function), and NFκB (cell survival signaling) are linked to antioxidant function (C. T. Chen et al., 2008; L. Wang et al., 2015). These data indicate that N90 possibly provides higher levels of oxidative stress compared to N30 and required higher level of counterbalance mechanism to reduce cellular stress maintaining cell survivals.

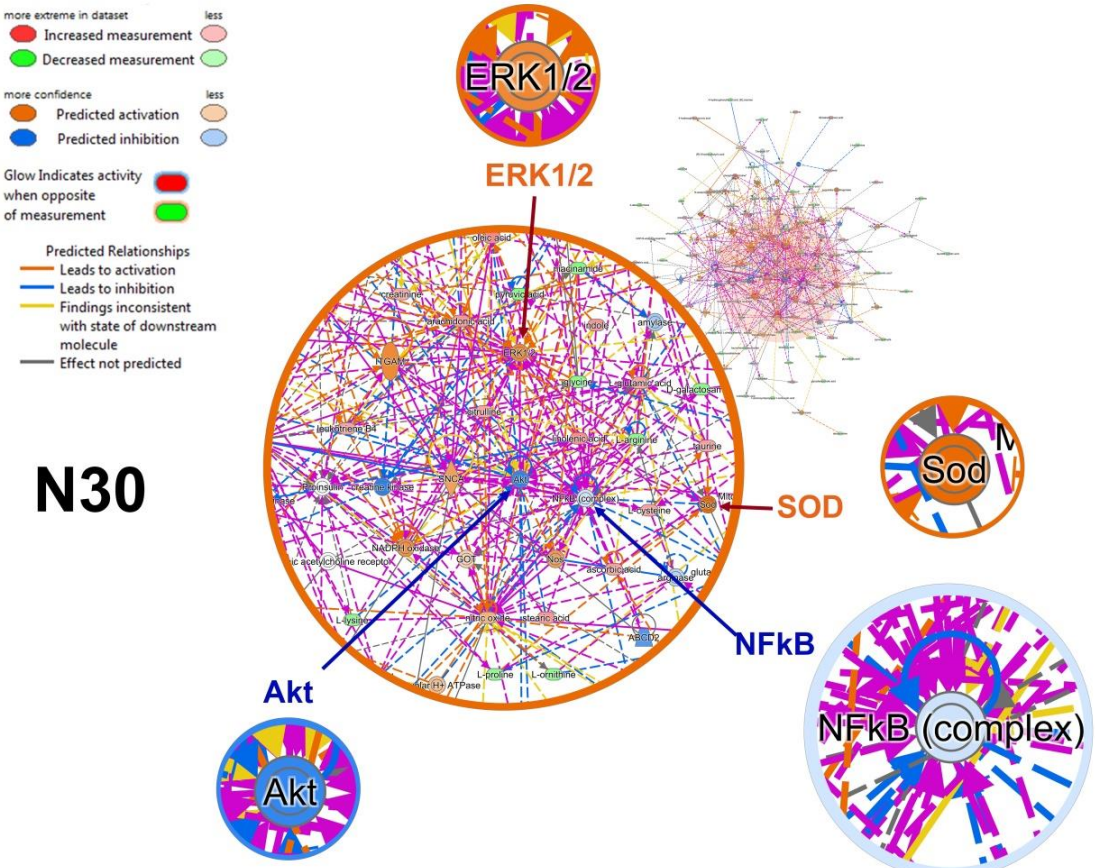
more extreme in dataset
less
Increased measurement
Decreased measurement
more confidence
less
Predicted activation
Predicted inhibition
Glow Indicates activity when opposite of measurement
Predicted Relationships
Leads to activation
Leads to inhibition
Findings inconsistent with state of downstream molecule
Effect not predicted
N30
ERK1/2
ERK1/2
SOD
NFkB
Akt
Akt
Sod
NFkB (complex)

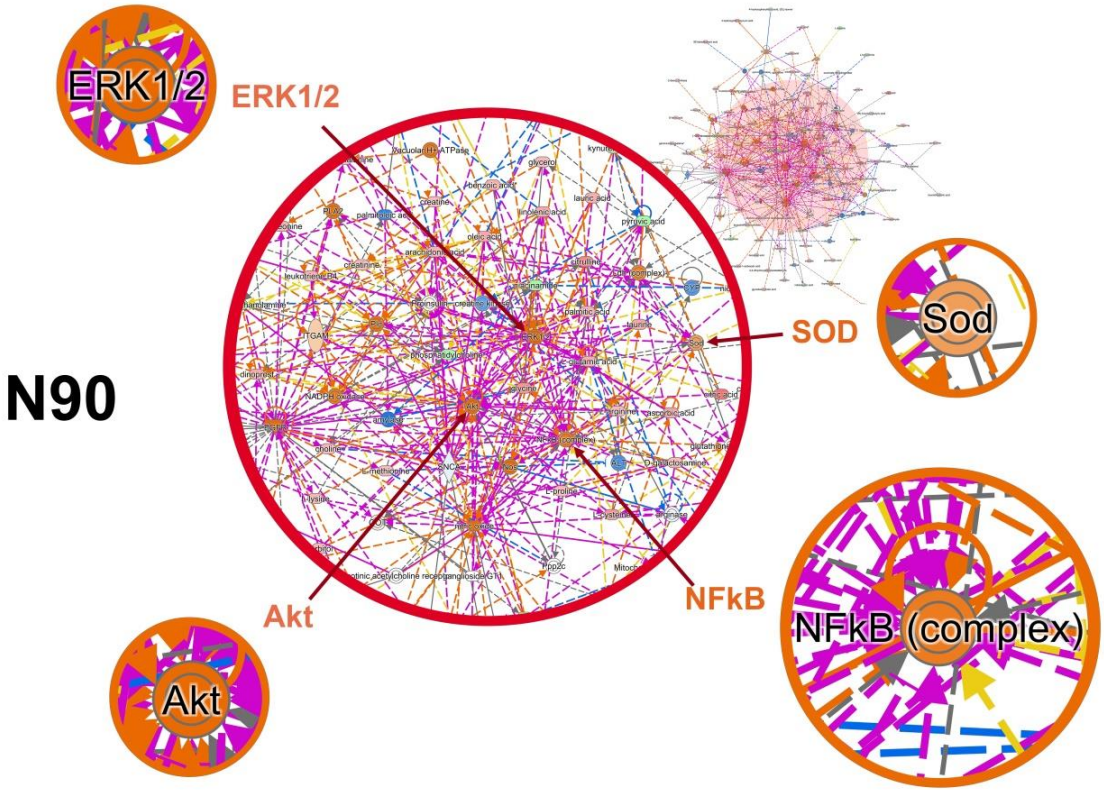
N90
ERK1/2
ERK1/2
SOD
NFkB
Akt
Akt
Sod
NFkB (complex)

Figure 5.10 Networks with predicted activation at week 1

NS, both N30 and N90, activate the ERK1/2 pathway which is crucial for osteogenesis. Stimulation with 30 and 90 nm both generated controllable cellular stress. N30 and N90 activated SOD for ROS reduction. Increasing stimulating amplitude (N90) also triggered Akt and NFκB. This can be interpreted that N90 produced the higher level of counterbalance system such as NFκB, SOD, Nitric oxide synthase (NOS) and Akt aiming for anti-apoptosis. (n=3-4, Networks were merged from the top 4 pathways of N30 and N90; scores/focus molecules were 47/24, 47/24, 45/23, and 42/22 respectively).

At 2 weeks, a predicted increased response in antioxidant mechanism was found in both N30 and N90. In the N30 group, IL-1β and Akt activation was noted compared to week1. The degree of NFκB and Akt activation in N90 were increased at 2 weeks **(Figure 5.11)**. This result indicated that increased duration of stimulation possibly enhanced oxidative stress as a function of time.

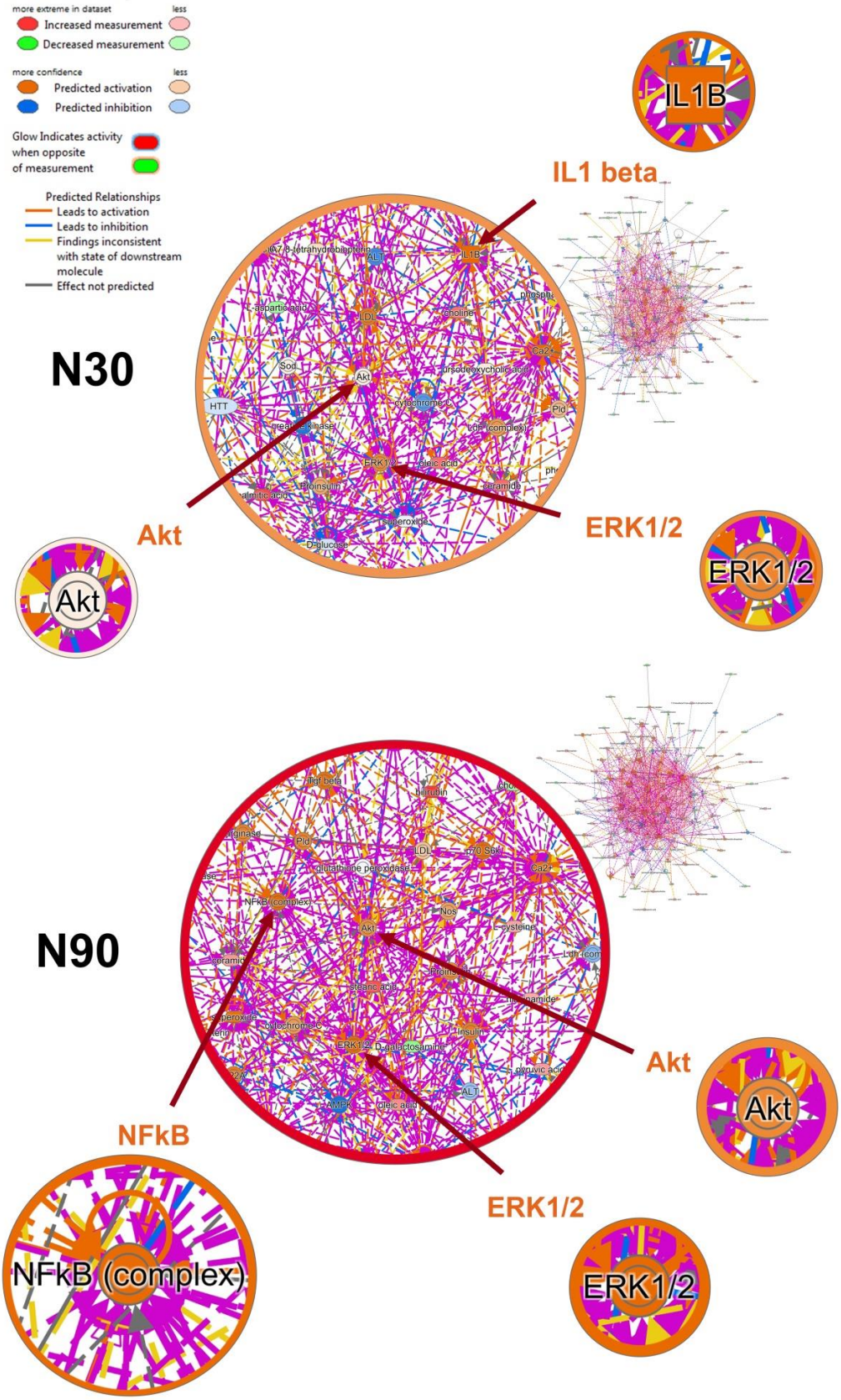
more extreme in dataset
less
Increased measurement
Decreased measurement
more confidence
less
Predicted activation
Predicted inhibition
Glow Indicates activity when opposite of measurement
Predicted Relationships
Leads to activation
Leads to inhibition
Findings inconsistent with state of downstream molecule
Effect not predicted
IL1B
IL1 beta
N30
Akt
ERK1/2
Akt
ERK1/2
N90
Akt
NFkB
ERK1/2
NFkB (complex)
Akt
ERK1/2

Figure 5.11 Predicted activated networks at week 2

Compared to week1, an increase in antioxidative pathways was found. In the N30 group, Akt, ERK1/2 and IL-1β activation was newly noted from week1. Predicted activation of NFκB, Akt and ERK1/2 was increased compared to week1 in N90 (n=3-4, Networks were merged from the top 4 pathways of N30 and N90; N30 score/focus molecules were 52/25, 49/24, 38/20, and 28/16; N90 were 51/25, 49/24, 38/20, and 26/15 respectively).

5.4.2 Nanovibrational stimulation effect on reactive oxygen species and mitochondrial activity

From the previous section, NS possibly enhances oxidative stress. Slight increase of PPP (gluconic acid, ribose) and glycolytic (pyruvate, lactate) pathways may link to redox balancing in oxidative stress condition (E. S. Cho et al., 2018; Kuehne et al., 2015). Moreover, small increases of LC-PUFAs may promote ROS reduction. Therefore, the evidence of ROS production was analysed and quantified.

5.4.2.1 Molecular and functional pathway analysis

The IPA software was again used to predict and compare molecular and functional pathways in aspect of oxidative stress. At 1 and 2 weeks, heatmaps of activation Z-score showed NS activated inflammatory metabolites and reactive oxygen species (ROS). Increased stimulating amplitude (N90) showed higher activation of ROS production and cellular stress **(Figure 5.12)**.

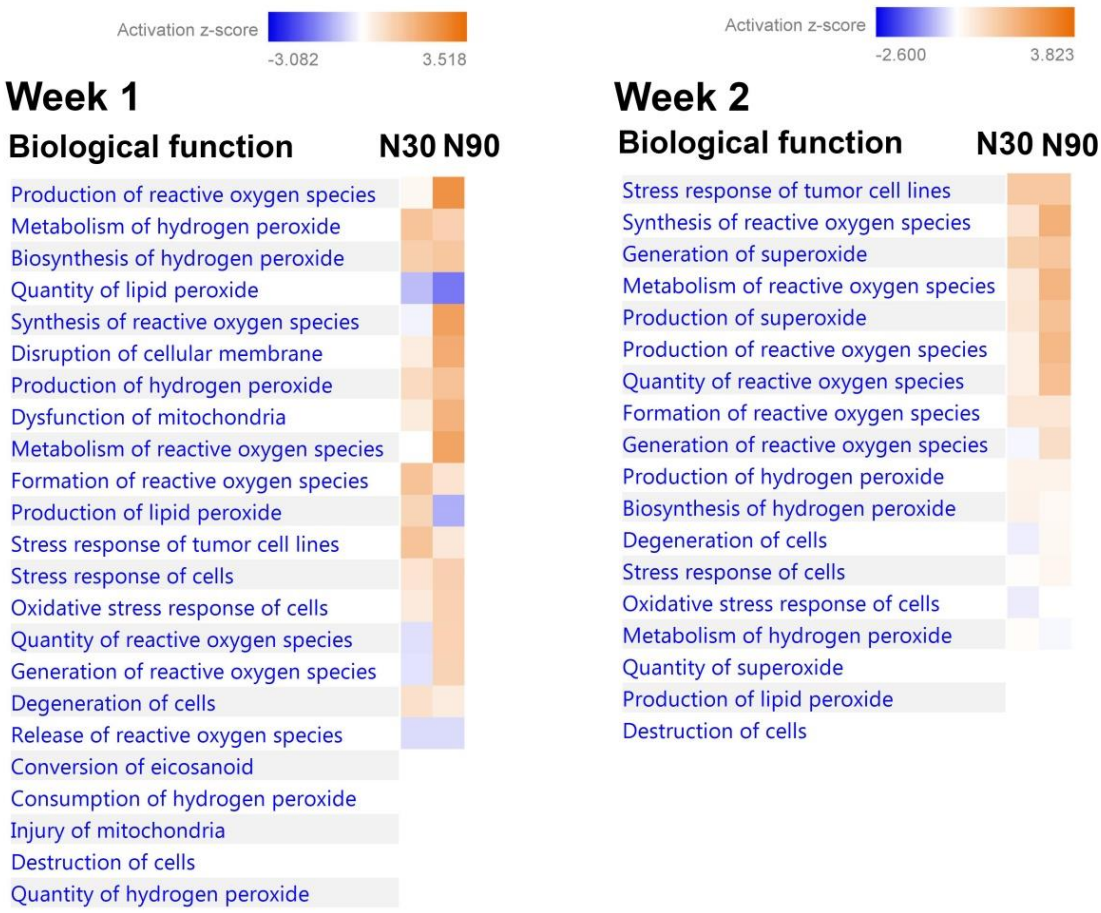

Figure 5.12 Heatmap of activation z-score of molecular and cellular function in respect to cellular stress and ROS production at weeks 1 and 2

N90 indicated greater ROS production and cellular stress in both 1 and 2 week cultures. The heatmap gradient was scaled from blue (representing inhibition) to orange (activation) whereas z score >2.0, predicted activation Z score <-2.0 predicted inhibition (n=3-4).

To further investigate the ROS-production related metabolites, IPA was used to generate the metabolite network of ROS production. Interestingly, high amplitude stimulation (N90) increased ROS production linked metabolites compared to N30 **(Figure 5.13).**

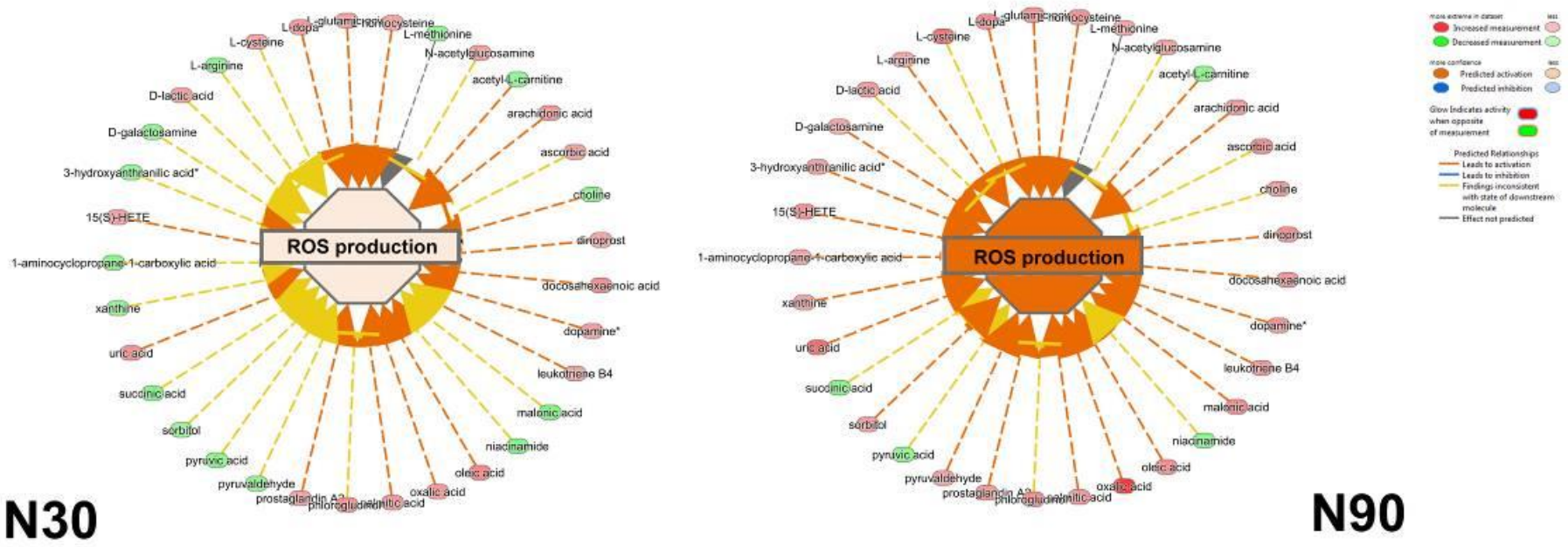

Figure 5.13 Related metabolites of ROS production in N30 and N90 at week 1

High amplitude stimulation (N90) increased active ROS production related metabolites compared to N30. (n=3-4, Orange representing predicted functional activation while blue showing the predicted inactivation, green and red representing increase and decrease measurement respectively).

IPA was used to generate heatmaps of metabolites relating to ROS production. The increase of the stimulating amplitude (N90) activated stronger signals and involved higher number of ROS related metabolites such as malonic acid, which has mitochondrial toxicity and induces ROS production (Fernandez-Gomez et al., 2005). Palmitic acid, which induces oxidative stress by involving intracellular calcium balance, was found to be increased at week 2 (Nissar, Sharma, & Tasduq, 2015). The increase of uric acid in N90 may play a role as antioxidant (Glantzounis, Tsimoyiannis, Kappas, & Galaris, 2005) **(Figure 5.14).**

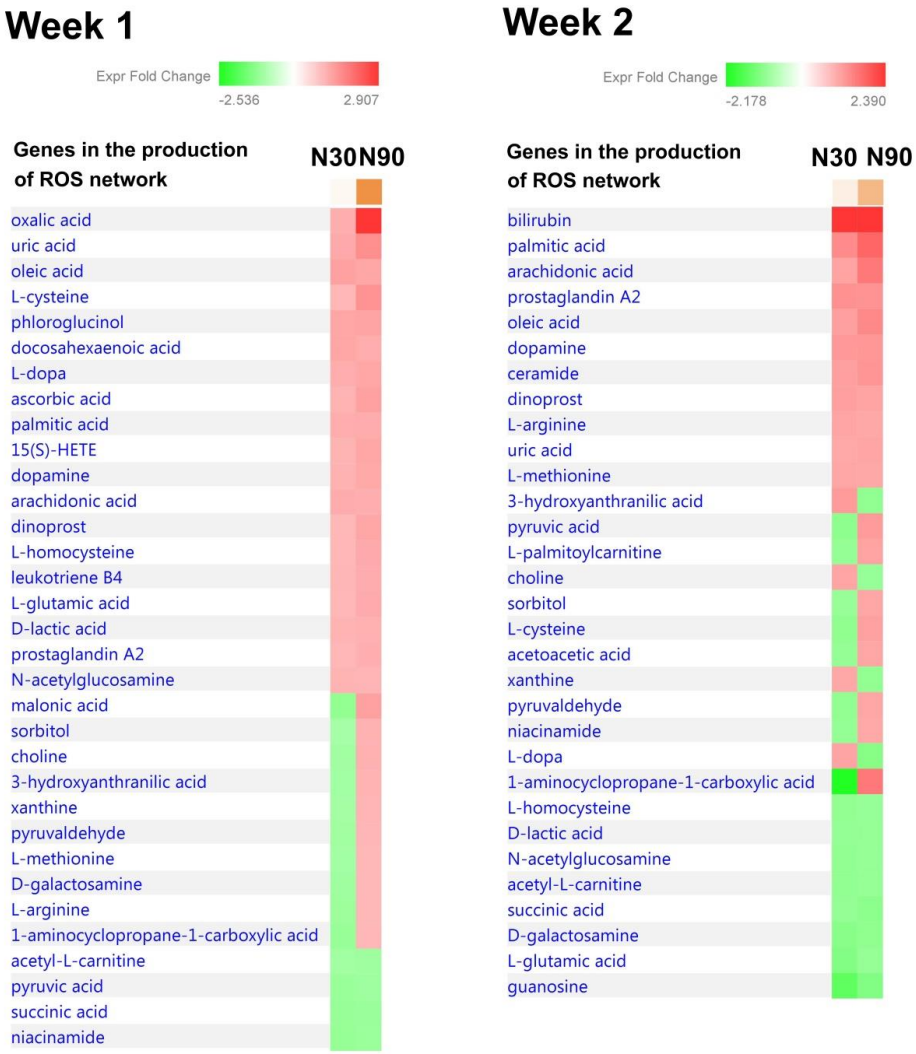

Figure 5.14 Heatmap metabolites related to ROS at 1 and 2 week.

High amplitude stimulation (N90) increased active metabolites related to ROS production. (n=3-4, Red; increased measurement; green; decreased measurement).

5.4.2.2 Reactive oxygen specie measurement

To measure ROS production, Stro1 selected MSCs in 1.8mg/ml collagen were prepared and stimulated with N30 and N90 for 7 days. The 2'-7 dichlorodihydrofluorescein diacetate (DCF-DA) fluorescein was used to quantify ROS production. Flow-cytometry was performed to detect the labelled cells at day 7. A significant increase of ROS production was noted in N90 compared to control **(Figure 5.15)**.

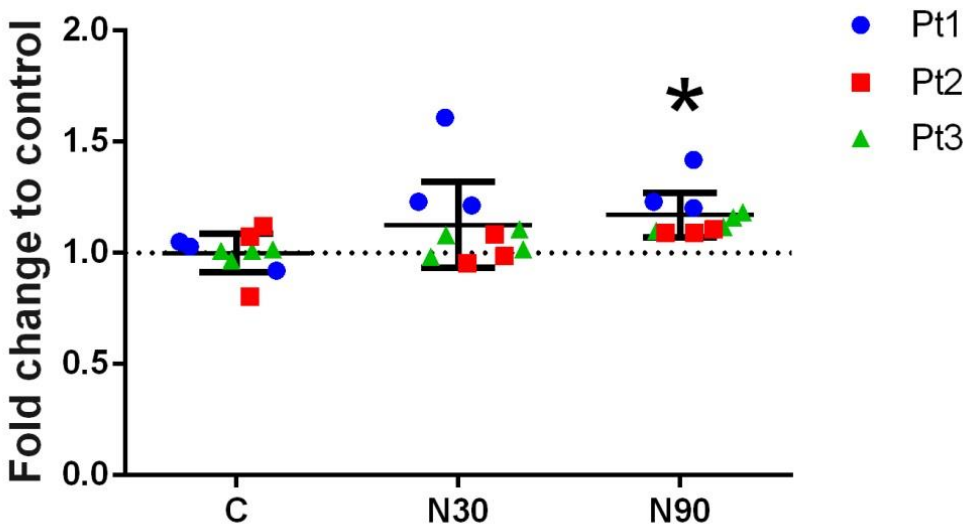

Figure 5.15 Reactive oxygen species measurement

By using DCF-DA fluorescein and flow cytometry, high amplitude stimulation (N90) was seen to significantly increase cellular ROS production corresponding to my previous metabolomic study (mean±SD, n=3-4, 3 patients (Pt 1-3), * P≤ 0.5, one-way ANOVA, Tukey's post hoc test, Pt1-3; patient 1-3).

5.4.2.3 The effect of Nanovibrational stimulation induced reactive oxygen species on 3D ostegenesis

It is known that controllable ROS enhances osteogenesis but uncontrollable ROS suppresses osteogenesis (M. Arai et al., 2007; Atashi et al., 2015; C. H. Byon et al., 2008). Therefore, the effect of ROS on 3D osteogenesis during NS was studied by qRT-PCR with ROS inhibition (N-acetyl cysteine; NAC) for 9 days of culture. The ratio to control of qRT-PCR with ROS inhibitor for RUNX2 and OSX were calculated. This ratio represented RUNX2 and OSX which are affected by the ROS-independent pathways. After that, the ratio to control of RUNX2 and OSX without ROS inhibition (thus, representing RUNX2 and OSX which were derived from the total pathway; both ROS dependent and independent pathways) was also calculated. The effect of ROS on RUNX2 (or OSX) expression was calculated from the difference of RUNX2 (or OSX) from total pathway to RUNX2 (or OSX) from ROS independent pathway. To interpret the results, positive outcomes represented enhancing- while negative outcomes mean reducing RUNX2 (or OSX) expression.

In the N30 group, RUNX2 and OSX downregulation was noted after inhibiting ROS **(Figure 5.16A, right)**. Together with RUNX2 and OSX outcomes in **Figure 5.16B** showing positive values, N30-induced ROS enhanced RUNX2 and OSX expression at day 9. Considering N90, N90 significantly promoted RUNX2 and OSX expression **(Figure 5.16A, left)**. However, an increase of ratio to control of RUNX2 and OSX was noted after inhibiting ROS **(Figure 5.16, right)** as well as ROS effect of N90 were noted in negative value (**Figure 5.16B)**. Thus, N90-induced ROS slightly reduced RUNX2 and OSX expression. Even though

ROS negatively affected RUNX2 and OSX expression, N90 still highly induced RUNX2 and OSX expression **(Figure 5.16A, left)**.

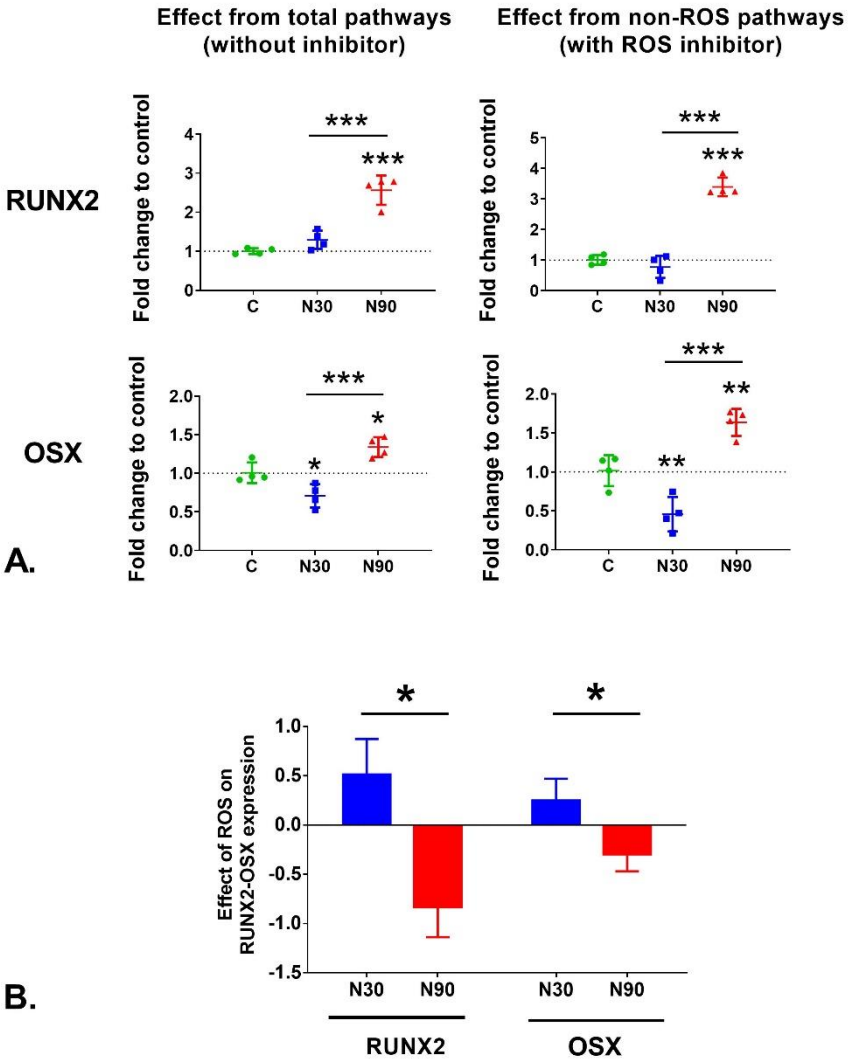

Figure 5.16 The effect of ROS on RUNX2 and OSX expression by qRT-PCR with ROS inhibition at day 9.

A) N90 significantly induced RUNX2 and OSX expression (left). After inhibiting ROS with N-acetyl cysteine, an increase of ratio to control of RUNX2 and OSX indicated that ROS slightly reduced RUNX2 and OSX expressions. In N30 group, RUNX2 and OSX expression was reduced after inhibiting ROS, which indicated that N30-induced ROS was important for RUNX2 and OSX expression (mean±SD, n=4, * P≤ 0.05, ** P≤ 0.01, *** P≤ 0.001, one way ANOVA, Tukey's post hoc test).

B) The effect of ROS on RUNX2 and OSX; positive value of N30 and negative value of N90, suggested that N30-induced ROS

enhanced while N90-induced ROS reduced osteogenesis (mean±SD, n=4, * P≤ 0.05, Mann-Whitney test).

5.4.3 NS and mitochondrial activity

Metabolomic studies showed that NS involved ß-oxidation metabolites **(Figure 5.8 - 5.9)**. Thus, investigating mitochondrial activity may indicate whether MSCs require high energy for differentiation. Mitotracker and JC1 fluorescein dye were used to quantify mitochondrial activity measured by flow cytometry. At day 9, no significant changes were found indicating that mitochondrial activity is normal during NS **(Figure 5.17A-B)**. Therefore, it was hypothesized that N90 may affect nutrient sources for energy production. MSCs may require more energy from fatty acids by increasing catabolism (β-oxidation) through the AMPK pathway (Herzig & Shaw, 2018; Lipovka & Konhilas, 2015).

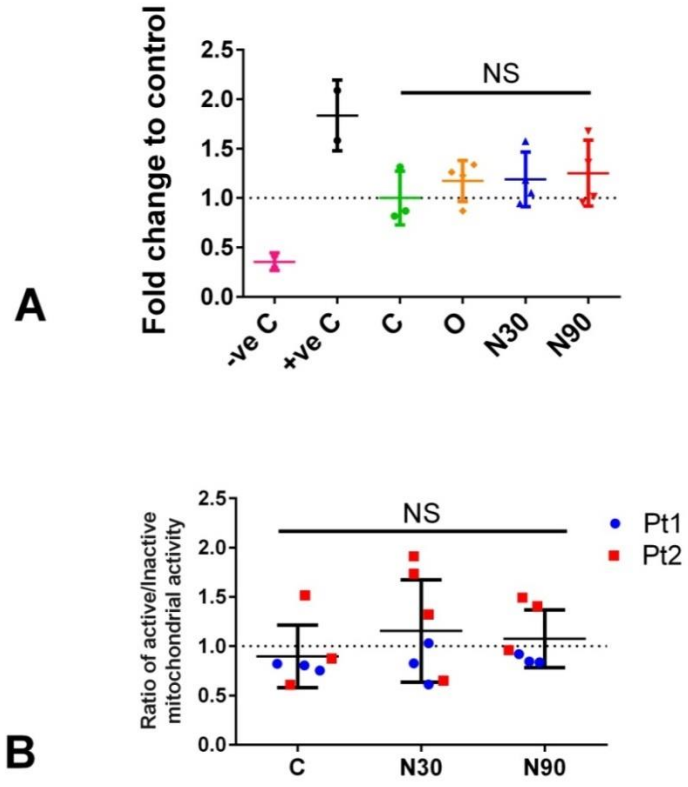

Figure 5.17 Mitochondrial mass and activity studied by mitotracker and JC1 fluorescein dye.

A. Mitotracker stain showed no difference in mitochondrial mass (mean±SD, n=3-4, 1 patients, One-way ANOVA, Tukey's post hoc, negative control was induced by CCCP, positive control was

induced by H_2O_2) B. JC1 staining showed no difference in mitochondrial activity (mean±SD, n=3-4, 2 patients, Pt1-2; patient 1-2, one-way ANOVA, Tukey's post hoc test).

5.4.4 NS induced inflammation in 3D osteogenesis

To investigate the hypothesis that NS-induced inflammation is essential for bone healing. qRT-PCR was used to investigate the inflammatory gene expression at day 9 (**Figure 5.18**). Interestingly, qRT-PCR showed the first clues of NS induced inflammation by the increased expression of TNFα and IL-6 transcripts. Concomitantly, increased NFκB expression indicated that cell survival pathways were also potentially activated.

IL-1β which is a coupled inflammatory cytokine to TNFα (Oppenheim, Matsushima, Yoshimura, Leonard, & Neta, 1989) and commonly found in the bone healing process was then investigated using ELISA. The level of IL-1β, however, was unable to be detected. It is thus likely that transcript changes are not fully reflected at protein level and it is undetectable; it could be postulated that this indicatives very low levels of inflammation that may help in bone healing.

Next, the BMP2-induced osteogenesis signaling pathway was also investigated based on the hypothesis that IL-6 mediated inflammation may induce BMP2 secretion, in turn, activates SMAD1/5 to enhance osteogenesis (M. Sun et al., 2017; W. Yang et al., 2013). As postulated, the result showed evidence of increased BMP2 (between N30 and N90) and SMAD1/5 gene upregulation (compared to control). The MAPK signaling pathway study provided evidence of ERK1/2 and JNK activation. This clue hinted that NS not only activated osteogenic gene expression but also relayed the signals for basic cellular regulation (proliferation, differentiation or apoptosis) responding to extracellular stimuli, however, it did not produce large amounts of cytokines at the protein level.

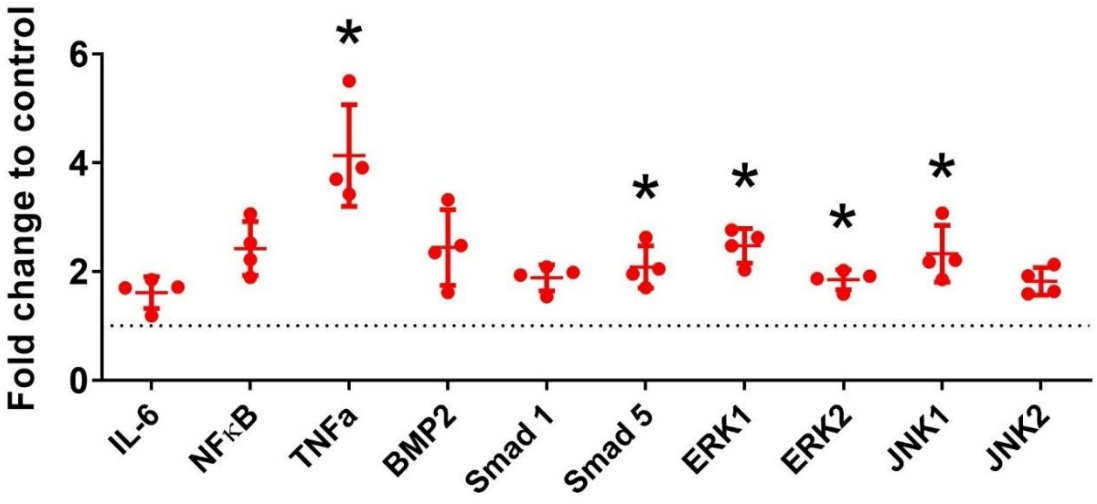

Figure 5.18 Inflammatory gene response in 3D-N90.

qRT-PCR at day 9 showed IL-6 (between NS groups) and TNFα (compared to control for N90) gene upregulation which are inflammatory cytokines. NFκB upregulation was also noted suggesting that MSCs produced NFκB reducing death signaling pathways. Upregulation of BMP2 and SMAD1/5 gene expression may imply that N90 enhances osteogenesis through a BMP2-SMAD1/5-mediated pathway. Activation of MAPK pathway gene expression including ERK1/2, JNK1/2 can be interpreted that NS signal was regulated by MAPK signaling hubs in order to select the appropriate cellular response such as differentiation or inflammation (Mean±SD, n=4, * P≤ 0.5, ** P≤ 0.01, *** P≤ 0.001, Mann-Whitney test).

5.4.5 NS-induced Inflammation may affect 2D osteogenesis in the early phase

To determine the effect of inflammation on 2D osteogenesis, In-Cell Western assay was used. Protein inhibition tests, which are associated to inflammation-related osteogenesis pathways, were investigated including MAPK pathways (ERK, JNK, p38), TNFα and NFκB. All inhibitors were added at day 2 and day 4. The ratio of phosphorylated RUNX2 to total RUNX2 was quantified at day 4 and 7 respectively. While this is not a particularly sensitive test, it was chosen as it is quantitative and at the protein level. It can determine activated osteogenesis and it fits with the time course in which we could use the inhibitors. The result showed that NS successfully induced 2D osteogenesis at day 7 while there was no increase in pRUNX2/RUNX2 at day 4 (**Figure 5.19**). This could be explained as day 4 was a very early time point to detect RUNX2 expression under NS.

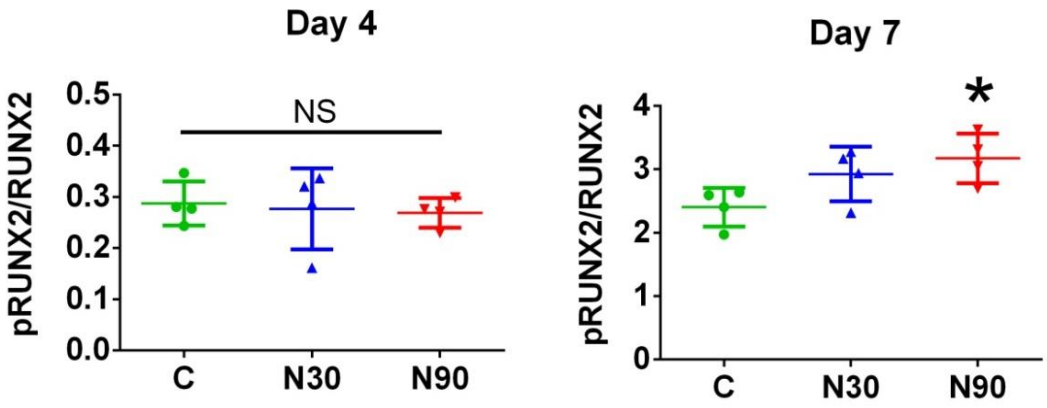

Figure 5.19 Nanovibrational stimulation in 2D osteogenesis

NS showed the success of 2D osteogenic induction at day 7 by In-Cell Western study. The significant increase of pRUNX2/RUNX2 in N90 group was noted (Mean±SD, n=4, * P≤ 0.5, ** P≤ 0.01, *** P≤ 0.001, one-way ANOVA, Tukey's post hoc test).

Next, protein inhibition analysis was used to identify which pathways linked to osteogenesis determed by the pRUNX2/ RUNX2 expression. The pRUNX2/RUNX2 was used to calculate the ratio (R) of group with inhibitor to group without inhibitor. Therefore, if R > 1 (pRUNX2/RUNX2 expression in inhibitor group is > than in the non-inhibited group), representing that pathways suppress osteogenesis as the inhibition increased pRUNX2/ RUNX2 expression. If R=1 or close to 1 (the inhibitor group is the same as the non-inhibited group), it means

that the pathways investigated did not affect pRUNX2/RUNX2 expression. However, if R<1 (inhibited group < non inhibited group) the inhibition of the pathway reduced pRUNX2/RUNX2 expression. Thus, it could be interpreted that the studied pathway promotes osteogenesis.

At day 4 (**Figure 5.20**), the only effect the assay was sensitive enough to detect was that NFκB inhibition significantly decreased pRUNX2/RUNX2 protein expression representing that NFκB was important for 2D osteogenesis with N90 stimulation. This result may be interpreted as that NFκB is potentially important for RUNX2, perhaps by optimizing inflammatory response to improve osteogenesis; this ties in with increased NFκB expression **(Figure 5.17)**.

At day 7 (**Figure 5.20**), as interpreted from the inhibition studies the MAPK pathway (ERK1/2, JNK, p38) and NFκB negatively affected RUNX2 expression in all groups. NS provided an increase of osteogenesis trend via ERK1/2 (R trend towards to 1 in N90 group).

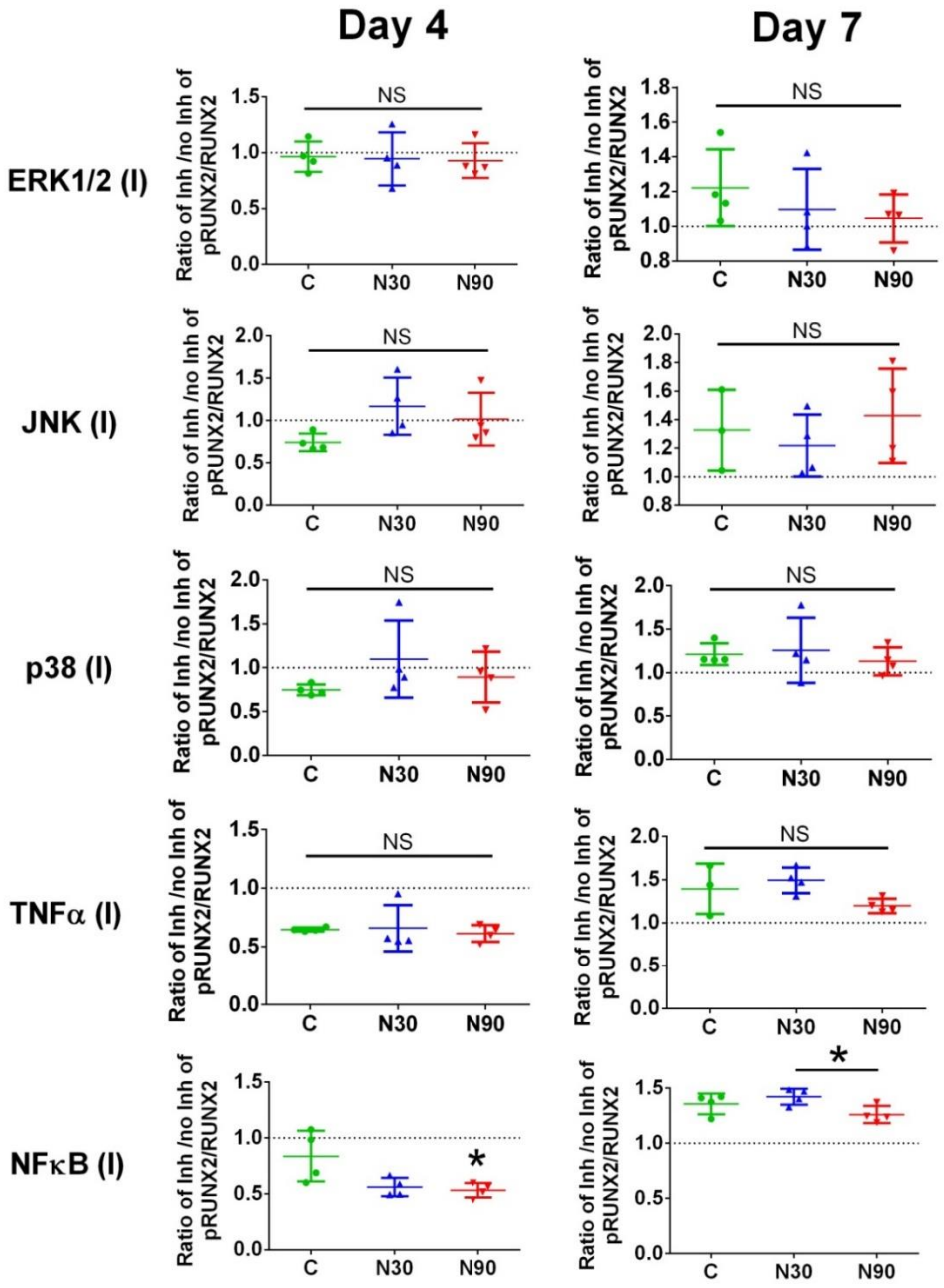

Figure 5.20. Effect of inhibition of inflammation pathways on 2D osteogenesis.

In-Cell Western study of pRUNX2/RUNX2 expression in the presence of inhibitors at day 4 and day 7. A) At day 4, very early phase, NFκB significantly affected osteogenesis in the N90 group (R <1). No other pathway changed with inhibition (Mean±SD, n=4, * P≤ 0.5, ** P≤ 0.01, *** P≤ 0.001, one-way ANOVA, Tukey's post hoc test).

5.4.6 Nanovibrational stimulation also involved inflammatory pathways in 3D osteogenesis

From the 2D inhibition study, the results showed that MAPK, TNFα and NFκB expression during osteogenesis were dynamically changed at different time points. To study the relationship of inflammation and nanovibration induced 3D osteogenesis, qRT-PCR with MAPK (ERK1/2, JNK and p38), TNFα and NFκB inhibitors was performed at day 9. The ratio of the group with inhibitor to that without inhibitor (R) was calculated based on $2^{\Delta\Delta ct}$ technique (Livak & Schmittgen, 2001). Thus, R >1 representing pathways that reduce osteogenesis. On the other hand, R<1 meant that pathway promotes osteogenic gene expression.

In **Figure 5.21**, JNK, p38 and NFκB inhibition showed the decreased trend of RUNX2 gene expression in N90 group. The ratio being less than 1 of p38 in all group indicated that p38 promoted RUNX2 expression and NS possibly enhanced RUNX2 expression via p38 showing in the decrease trend after inhibiting p38. Reduction of RUNX2 expression in NS comparing to control group was also found after inhibiting JNK and NFκB. The results indicated that JNK and NFκB played positive roles for RUNX2 expression.

MAPK (ERK1/2, JNK and p38), TNFα and NFκB pathways; all of these pathways tended to enhance OSX gene expression. However, the effect of NS was not obviously seen linking to OSX expression. Considering the NS effect on OPN, NS seemed to link to NFκB and p38 in OPN expression by showing the decrease trend of OPN expression in the NS group.

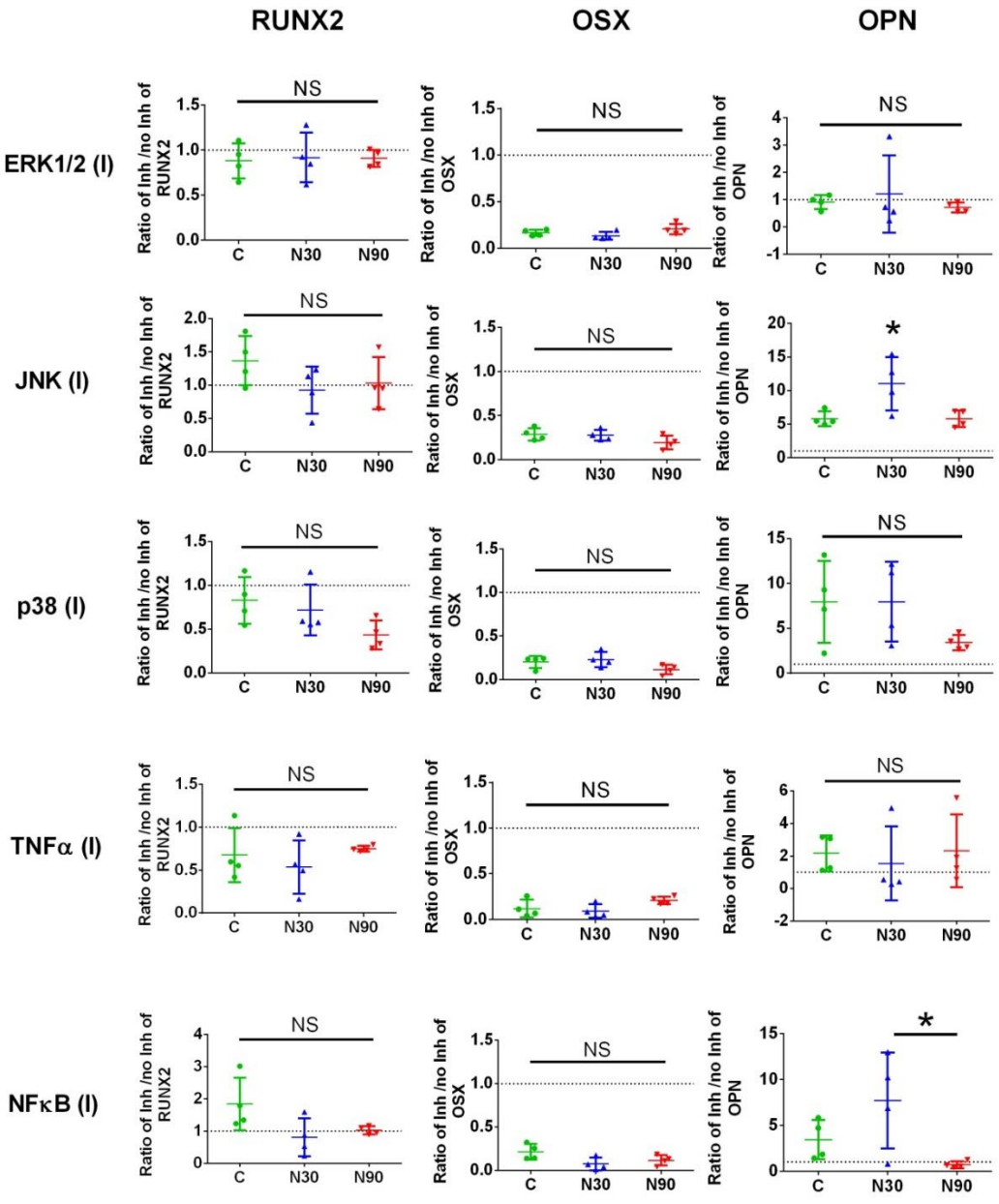

Figure 5.21 The effect of nanovibrational stimulation induced inflammation in 3D osteogenesis

qRT-PCR with inhibitors at day 9 indicated that JNK, p38 and NFκB promote RUNX2 expression. MAPK, TNFα and NFκB promote OSX expression (R<1). However, no obviously NS effects involved OSX gene expression. OPN is possibly enhanced by p38 and NFκB (Mean±SD, n=4, * P≤ 0.5, ** P≤ 0.01, *** P≤ 0.001, one-way ANOVA, Tukey's post hoc test).

To simply identify the roles of pathways of interest (POI; MAPKs, NFκB, and TNFα) on osteogenesis, RT-PCR data with inhibitors at day 9 was re-calculated. The difference between total pathways and POI-independent pathways was calculated for the effect of POI on RUNX2 and OSX expression. Positive value means enhancing while negative means suppressing osteogenesis **(Figure 5.22A)**. Corresponding to **Figure 5.21**, JNK, p38 and NFκB were positive thus enhancing- while TNFα and ROS were negative values thus suppressing osteogenesis **(Figure 5.22A)**. These results can possibly be explained by the response of NFκB in oxidative stress (J. L. Luo, Kamata, & Karin, 2005; T. Wang et al., 2002). In oxidative stress condition or inflammation, it is known that TNFα can activate NFκB to produce signals in order to reduce oxidative stress (ROS and TNFα) and also involved MAPK via JNK and p38 (Lingappan, 2018; Nakano, 2004; L. Wang et al., 2012). These survival pathways aim to reduce apoptotic signals (Nakano,

2004). Simple diagram of mechanotransduction with NFκB and MAPK involvement under oxidative stress were shown in **Figure 5.22B**.

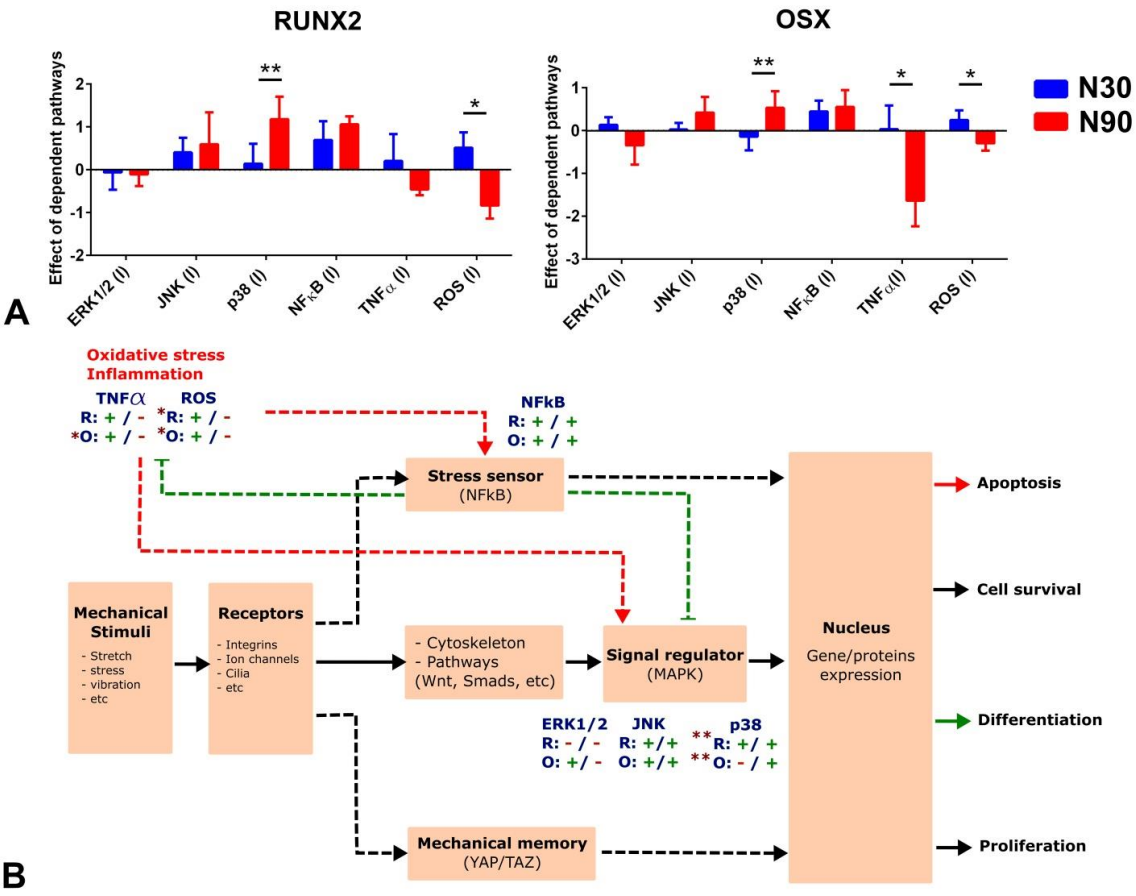

Figure 5.22 Role of MAPKs, NFκB and TNFα on RUNX2 and OSX expression

A. The effect of POI graph showed that JNK p38 and NFκB promote RUNX2 and OSX expression while TNFα and ROS reduced RUNX2 and OSX expression. (Mean±SD, n=4, * P≤ 0.5, ** P≤ 0.01, paired-t-test)
B. Simple diagram showed the effect of NFκB on TNFα and ROS in oxidative stress during mechanical stimulation.

To investigate whether inflammation is controllable, a temporal gene study of IL-6 and NFκB by qRT-PCR was performed at day 7, 14 and 21. IL-6 and NFκB levels in N90 were higher than those in N30. IL-6 and NFκB expression peaked at week 2 and tended to reduce at week 3 indicating that inflammation was controllable **(Figure 5.23).** Correlating this data with the temporal study of phenotype showing

successful osteogenic induction **(Figure 4.15)**, we propose that NS induced inflammation is controllable and suitable for osteogenesis.

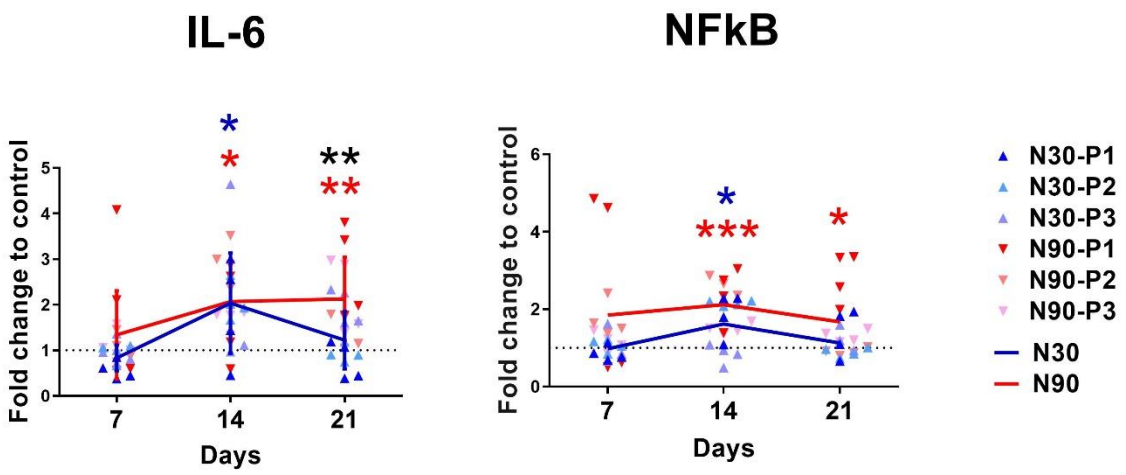

Figure 5.23 Temporal gene analysis of IL-6 and NFκB

Temporal study of IL-6 and NFκB showed that NS possibly produces inflammation, but that it is controllable. IL-6 and NFκB expression peaked at week 2 and tended to decrease at week 3 (Mean±SD, n=4, 3 patients, 4=replicates, * P≤ 0.5, ** P≤ 0.01, *** P≤ 0.001, one-way ANOVA, Tukey's post hoc test, Pt1-3; patient 1-3, blue asterix; compared N30 to control, red Asterix; compared N90 to control, black Asterix; compared N30 to N90).

5.4.7 The balance between osteogenesis and inflammation in NS induced 3D osteogenesis

Occasionally, we found a non-responding patient sample (approx. 1 in 20 according to whole lab data). If NS can produce inflammation, thus, prestimulating the inflammatory status of MSCs could affect NS outcomes. To prove this hypothesis, qRT-PCR in a non-responding patient was performed at day 9. Initial phenotype after NS showed the expected no change in osteogenic gene expression in NS group (N30 and N90); RUNX2 was even significantly downregulated in N30 **(Figure 5.24).**

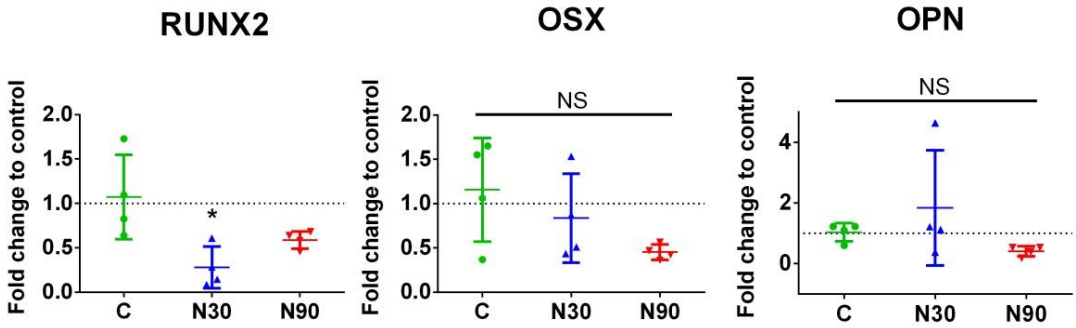

Figure 5.24 Failure of NS induced 3D osteogenesis

qRT-PCR at day 9, showing data from a non-responding patient (Mean ± SD, n=4, * P≤ 0.5, ** P≤ 0.01, *** P≤ 0.001, one-way ANOVA, Tukey's post hoc test).

To investigate the cause of osteogenic induction failure in the patient whose cells did not respond to NS, qRT-PCR with cultures grown using MAPK, TNFα and NFκB inhibitors was performed at day 9. Considering the significant decrease of RUNX2 expression in the N30 group (**Figure 5.25**), JNK and NFκB were seen to be repressing RUNX2 expression, and hence osteogenesis. ERK 1/2 was also seen to inhibit osteogenesis through OSX expression. Inhibition of p38 MAPK appeared to increase osteogenesis as seen by repression of pRUNX with p38 inhibition (**Figure 5.25**).

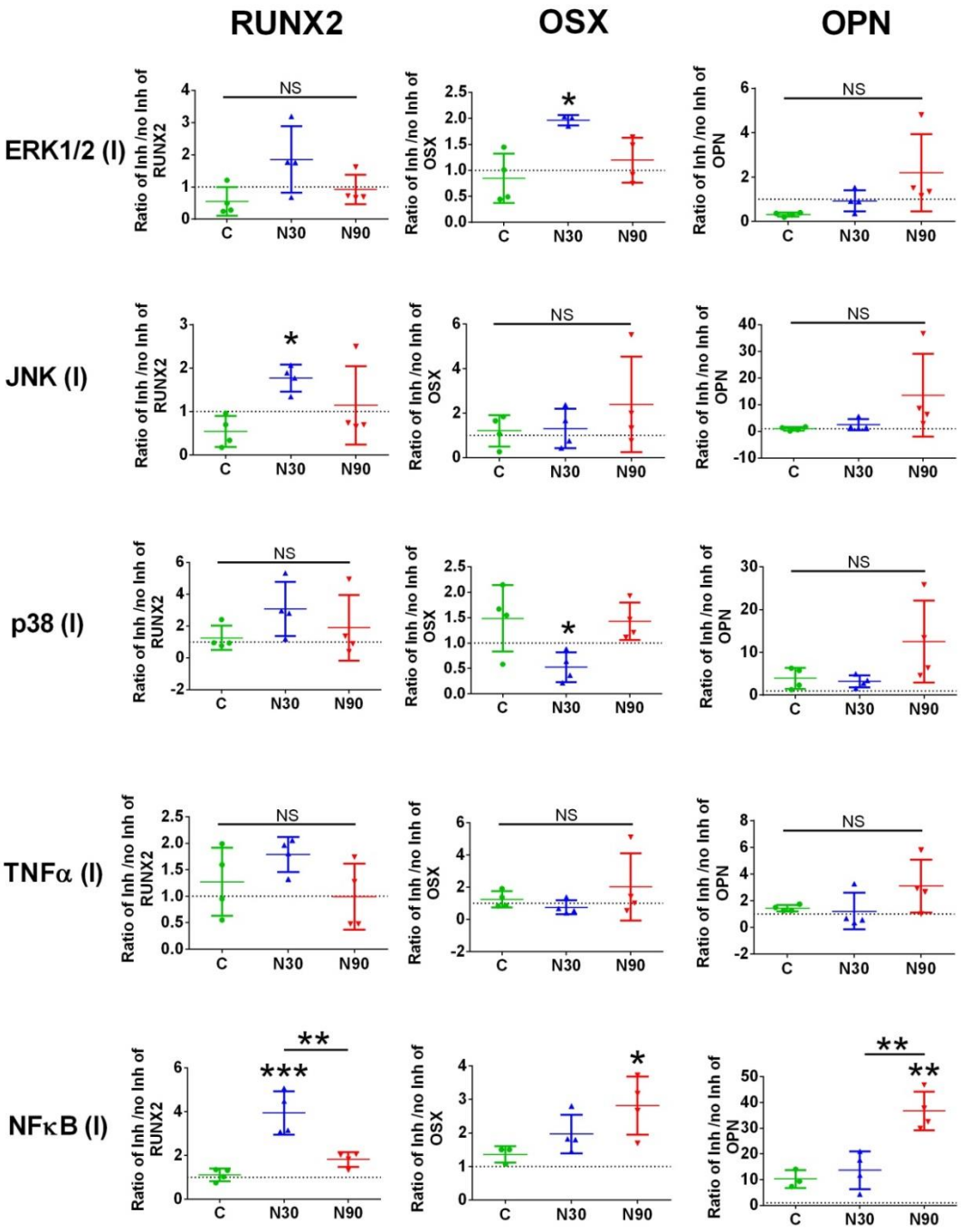

Figure 5.25 3D NS and inflammatory pathway studies with inhibition of biochemical pathways in a non-responding patient

qRT-PCR at day 9, the inhibition of MAPK pathway (ERK1/2, JNK, p38), TNFα and NFκB increased the RUNX2 expression in the N30 group. R>1 indicates that MAPK, TNFα and NFκB pathways are inhibiting RUNX2 expression at this time point. Considering the OPN response, only NFκB inhibition significantly increased OPN gene expression. The OSX expression slightly differed from

RUNX2 and OPN. ERK1/2 and NFκB were seen to significantly reduce expression while p38 is indicated to enhance OSX gene expression (Mean ± SD, n=4, * P≤ 0.5, ** P≤ 0.01, *** P≤ 0.001, one-way ANOVA, Tukey's post hoc test).

To determine the level of NFκB gene expression as it had strong effect in reducing osteogenesis for N30 (RUNX2) and N90 (OPN and OSX) in this non-responding patient, qRT-PCR for NFκB with/without NS and together with/without inhibitor (TPCA-1) compared to non-stimulated control without inhibitor were investigated at day 9. Surprisingly, a significant reduction of NFκB gene expression was found in both the N30 and N90 groups with expression of NFκB reduced below that of the inhibitor on the control group (**Figure 5.26**). It was hypothesized that the suppression of NFκB gene expression was affected by the negative feedback loop (Renner & Schmitz, 2009). In the NS group, long term exposure of higher level of NFκB may result in significantly greater suppression of NFκB gene expression. Moreover, inflammation could also affect on level of NFκB. Stimulating with low magnitude stimulation (such as NS) may inhibit NFκB signaling pathways in cells with pre-existing low inflammation (Agarwal et al., 2003; Dossumbekova et al., 2007; Madhavan et al., 2007; J. Nam et al., 2009).

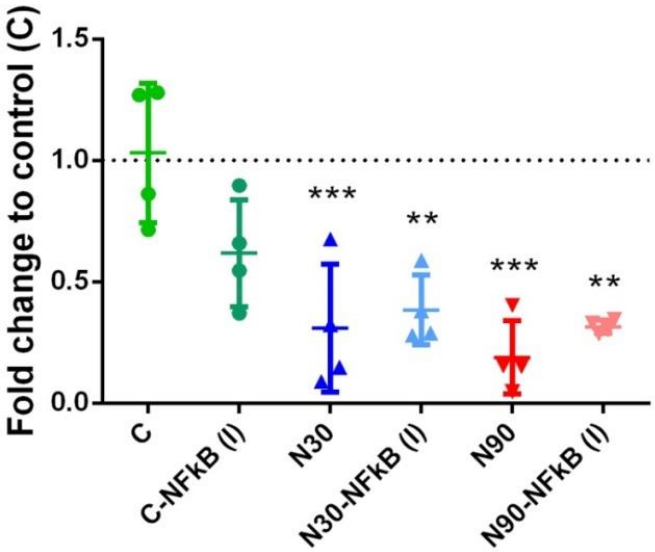

Figure 5.26 NFκB level was controlled by negative feedback loop in failure of nanovibration-induced osteogenesis

RT-PCR at day 9 showed that NFκB of stimulated group (N30 and N90) was less than that of non-stimulated control group. Addition of NFκB Inhibitor in N30 and N90 did not change the gene expression as it was already very low. (Mean ± SD, n=4, * P≤ 0.5, ** P≤ 0.01, *** P≤ 0.001, one-way ANOVA, Tukey's post hoc test).

5.5 Discussion

5.5.1 Nanovibrational stimulation: what we have learnt from metabolomics

From clustering metabolome analysis, NS mainly affected lipid metabolism after 1 and 2 weeks of stimulation **(Figure 5.4 - 5.7)**. Smaller metabolome shifts from N30- and N90-NS were noted in amino acid and carbohydrate metabolism compared to control. Lipid metabolism is pivotal for stem cell differentiation due to its bioenergetic roles through fatty acid catabolism as well as producing precursor metabolites which are necessary for diverse cytokine synthesis such as arachidonic acid and prostaglandins (Burke & Weiler, 2002).

Carbohydrate metabolism, specifically glycolysis, is important for stem cell self-renewal and maintenance. In the process of osteogenic differentiation of MSCs, the role of glycolysis remains inconclusive. Some evidence indicates that the role of glycolysis is reduced in differentiated cells (C. T. Chen et al., 2008; Fillmore et al., 2015; Pattappa et al., 2011; Shyh-Chang et al., 2013). However, Shum et al shows that there is no difference in glycolysis level between osteogenic differentiated cells and undifferentiated cells (Shum et al., 2016). In our results, pyruvate tended to increase at 2 weeks but there was no significant difference of pyruvate level at both 1 and 2 weeks. The upregulation of lactate was noted at 1 week but was decreased by 2 weeks. All data indicated that NS did not obviously change the glycolysis pathway. Theoretically, increase of lactate may indicate aerobic glycolysis, explained by the Warburg effect (H. Lu, Forbes, & Verma, 2002). Even though the cues from glycolysis-related metabolites might not reveal the stage of cell development, the success of NS induced osteogenesis as shown in chapter 4 has

supported that nanovibration induced MSCs differentiate from preosteoblast to immature osteoblasts by week 2.

Although NS insignificantly changed carbohydrate metabolism, the increase of orthophosphate in N90, as well as the increase of sn-glycerol-3-phosphate shuttle in N30 and N90 groups **(Figure AII.5)**, suggesting that NS driven osteogenesis is an energetic process. Activation of the glycerol-3-phosphate shuttle represents that cells require expenditure of ATP by shifting complex I of OXPHOS (Mracek, Drahota, & Houstek, 2013). Increased activity of OXPHOS is linked to greater reactive oxygen species (ROS) production (Huttemann, Lee, Samavati, Yu, & Doan, 2007). Furthermore, increased glycerol-3-phosphate shuttle activity is associated with high ROS production (Mracek, Pecinova, Vrbacky, Drahota, & Houstek, 2009). OXPHOS with low levels of ROS promotes osteoblastic differentiation while high OXPHOS with high ROS promotes adipogenesis (C. T. Chen et al., 2008; Shyh-Chang et al., 2013). Our previous gene expression study showed the upregulation of osteogenic gene expression over adipogenic gene expression ($PPAR_{\gamma}$) at day 9 **(Figure 4.12 and 4.13)**. Therefore, it was reasonable to hypothesise that N90 affected osteogenesis and produced an optimal level of ROS at 1 week.

The effect of NS is possibly linked to amino acid metabolism. Previous literature showed that L-type and aromatic L-amino acids can activate the calcium-sensing receptor (CaSR) which controls calcium metabolism (Conigrave, Mun, & Lok, 2007). Calcium influx in turn actives the ERK1/2 pathway and PKC resulting in osteoblast differentiation and proliferation (MacDonell, Hamrick, & Isales, 2016). Our results showed the increase of L-type and L-aromatic amino acids in N90 corresponded to CaSR gene expression. Generally, CaSR takes an important role in intracellular calcium regulation. CaSR responds to extracellular calcium ion levels, parathyroid hormone, amino acid and pH changes (Theman & Collins, 2009). It was hypothesised that NS slightly increased amino acid and may subsequently upregulates CaSR. This requires investigation.

Lipid metabolism is important for cell proliferation and differentiation. To explore the relationship of NS and lipid metabolism on osteoblast differentiation, firstly, long-chain polyunsaturated fatty acids (LC-PUFAs) are considered. LC-PUFAs are derived from essential fatty acids such as linoleic acid and alpha-linolenic acid (omega-3 fatty acid) desaturating to eicosapentaenoic acid (EPA),

docosapentaenoic acid (DPA), and docosahexaenoic acid (DHA). These PUFAs are precursors of inflammatory metabolites such as arachidonic acid (AA), cyclooxygenase (COX), thromboxanes (TXA) which play pivotal roles on osteoblast and osteoclast development (Kruger et al., 2010). Many reports show that PUFAs improve bone synthesis in *in vitro* and *in vivo* studies (Jeromson, Gallagher, Galloway, & Hamilton, 2015; Kruger & Schollum, 2005). EPA supplements link to low grade inflammatory metabolites synthesis such as leukotriene 5 via cyclooxygenase (COX). The use of COX competitively inhibits high-grade inflammatory metabolite synthesis (such as PGE2, TXA2) from AA (Borges et al., 2014). However, some studies show adverse effects of long term exposure of AA and DHA in osteogenic gene expression (Coetzee et al., 2009).

In this study, a slightly increase of EPA, DPA and DHA after NS at 1 and 2 weeks was found **(Figure AII.8)** meaning that NS could promote PUFA synthesis and this might link to the increase of inflammatory metabolite synthesis. In respect to energy production via lipid catabolism, β-oxidation-related metabolites were further investigated which were found in the experiments including hexanoic acid, 4-8 dimethylnonanoylcarnitine and O-propanoylcarnitine. N30 and N90 showed slightly increases of hexanoic acid and 4-8 dimethylnonanoylcarnitine levels. However, there was no significant change of TCA cycle metabolites **(Figure AII.4)**. Therefore, NS might slightly affect ATP production but evidence is week and needs more investigation. The current literature of these metabolites is very limited.

5.5.2 Metabolomics perspective; nanovibrational stimulation possibly promotes osteogenesis through an inflammation process

The related biological pathways of NS were analyzed by IPA software. At 1 and 2 weeks of stimulation, the ERK1/2 pathway **(Figure 5.10 - 5.11)** had predicted activation in N90 which corresponded to PCR showing gene upregulation **(Figure 4.15A)**. It is likely that ERK1/2 plays a pivotal role in NS induced osteogenesis (Tsimbouri P.M., 2017).

Nitric oxide synthase (NOS) also had predicted activation in the N30 and N90 group at 1 and 2 weeks **(Figure 5.10-5.11)**. NOS is an enzyme that produces nitric oxide (NO). Nitric oxide controls intracellular homeostasis (Klein-Nulend, van Oers, Bakker, & Bacabac, 2014). NOS

can be produced by endothelial cells (eNOS), the central nervous system (nNOS) or induced by inflammation (iNOS) (Saura, Tarin, & Zaragoza, 2010). Many studies elucidate the importance of NO in osteoblast proliferation and differentiation (Fox & Chow, 1998; Samuels, Perry, Gibson, Colley, & Tobias, 2001), e.g. NO mediates the ERK1/2 pathway resulting in osteogenesis (Saura et al., 2010; S. Wang et al., 2006; H. Y. Yun, Dawson, & Dawson, 1999) as well as promoting bone healing by increasing blood flow from vasodilation (R. E. Tomlinson, Shoghi, & Silva, 2014). However, overproduction of iNOS can induce osteoblast apoptosis possibly linked to ROS and cytochrome C (Ho, Chen, Chiu, Tai, & Chen, 2005).

NS could be linked to inflammation through reactive oxygen species (ROS). ROS is a product of mitochondrial oxidative phosphorylation. Optimal ROS levels directly control MSC osteogenic differentiation (Q. Q. Li, Gao, Chen, & Guan, 2017). Excessive ROS production can reduce osteogenesis and promote adipogenesis as well as induce cell dysfunction and apoptosis (Atashi et al., 2015; Circu & Aw, 2010; Wanet et al., 2015). The Akt pathway and superoxide dismutase pathway (SOD) take on important roles to counter inflammatory metabolites overproduction. Insulin growth factor (IGFs) can activates Akt pathway and promotes osteoblast differentiation though BMP2 (Mukherjee & Rotwein, 2009; Pramojanee, Phimphilai, Chattipakorn, & Chattipakorn, 2014). The Akt pathway counterbalances ROS overproduction improving inflammation capacity and subsequently promoting osteogenesis (L. Wang et al., 2015). Not only does the Akt pathway reduce ROS, but also superoxide dismutase (SOD) represses inflammatory metabolites. SOD takes a role to convert superoxide anions (O_2-) to hydrogen peroxide (H_2O_2) and then H_2O and O_2 by catalase and glutathione peroxidase (C. T. Chen et al., 2008).

At 1 week stimulation **(Figure 5.10)**, IPA indicated that the Akt pathway seemed to be activated, potentially to counterbalance inflammation in N90, while SOD was activated in N30 and N90. Therefore, NS could promote osteogenesis together with increasing of oxidative stress. In N90 group, Akt and NFκB were activated in N90 but not N30 suggesting that N90 can switch on survival pathways (Akt and NFκB) resulting in increase intracellular signaling. Thus, it was hypothesised that stimulation with high amplitude NS (N90) possibly provides osteogenic induction over that of N30 due to activation of

the Akt pathway which could enhance osteogenesis by itself while N30 activated only SOD.

At 2 weeks, N30 started to trigger Akt and interleukin-1β while greater levels of activation of Akt, ERK1/2 and NFκB were noted in N90. The results indicated that NS effect may be accumulated with time. The effect of NFκB on osteogenic differentiation is not well known. Activation of NFκB seems to provide negative effect on osteogenesis (Boyce, Yao, & Xing, 2010; Chang et al., 2013). However, from our results, NFκB tended to provide positive effect on RUNX2 expression during NS (**Figure 5.21**).

Overall, NS promoted osteogenesis shown through gene, protein and metabolomic studies. Lipids showed the highest change responded to NS. Oxidative stress was slightly generated during NS but it was controllable. The conclusion of metabolite changes is illustrated in **Figure 5.27.**

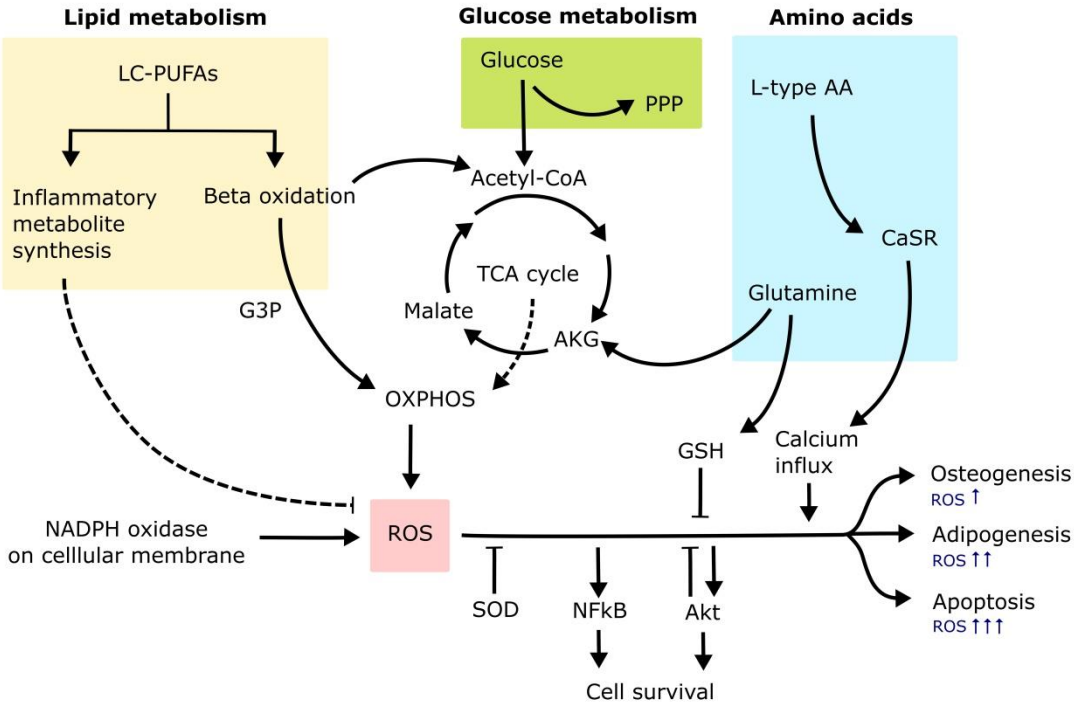

Figure 5.27 Summary of metabolomic change during NS

Lipid metabolism showed the greatest change possibly linked to PUFA synthesis which produces inflammatory metabolites as well as slightly enhanced β-oxidation producing energy. PPP may be involved in redox balancing. Oxidative phosphorylation was increased in parallel with glycerol-3-phosphate shuttle

activation and possibly, in turn, produced ROS. ROS may also be produced on the cell membrane by NAPDH oxidase. ROS was counterbalanced by SOD. ROS activated NFκB and Akt to maintain cell survival. NS also increased L-type amino acid which may subsequently upregulated calcium signaling receptor (CaSR), allowing calcium influx. (G3P= glycerol-3-phosphate shuttle)

5.5.3 Inflammation in normal bone healing process vs nanovibrational stimulation

NS induces osteogenesis mimicking the normal bone healing process. In the normal bone healing process, inflammation is the first phase that occurs at the fracture site. Neutrophils produce cytokines such as TNFα to recruit inflammatory cells to eliminate the pathogens, prepare the fracture niche and recruit osteoprogenitor cells pooling at the fracture site (F. Loi et al., 2016). Pro-inflammatory cytokines including IL-1, IL-6 and BMP2 trigger MSCs to become osteoblasts (F. Loi et al., 2016). NFκB and RANKL can activate osteoclast differentiation (through RANK) thus preparing for the remodeling phase (Abu-Amer, 2013). However, in tissue engineering, high levels of inflammation are critical hurdles for stem cell differentiation controlled by mechanical induction or prosthesis (Gibon, Lu, Nathan, & Goodman, 2017). Thus, mimicking the mechanical stimuli which can directly enhance osteogenesis with low level activation of inflammation is challenging. Considering the results, NS promoted inflammatory cytokines corresponding to the normal bone healing process (**Figure 5.28**). In this study, Stro1-selected human MSCs were used which are osteoblast precursors (Dennis et al., 2002). NS induced inflammatory cytokines to be produced by the MSCs (Kyurkchiev et al., 2014) as other inflammatory cell types were not present in the culture.

In normal bone healing, bone fractures produce an inflammation triggerring healing process (F. Loi et al., 2016). NS promoted inflammatory modulators at an early time point, day 7. The inflammatory cytokines were then suppressed by intracellular signaling pathways which may corresponded to normal bone healing stage (F. Loi et al., 2016).

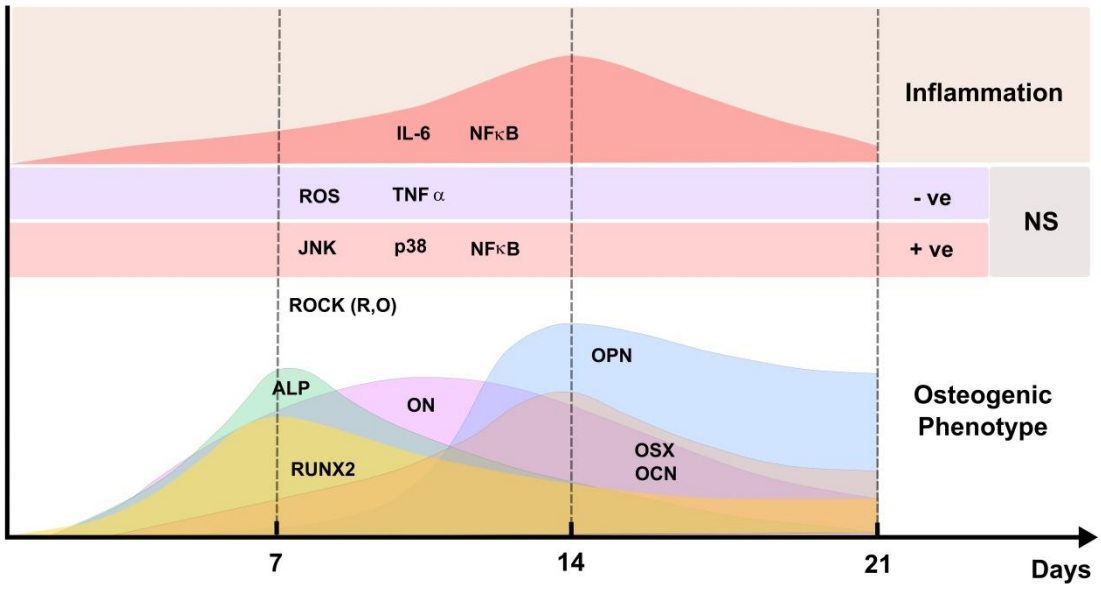

Figure 5.28 Conclusion of N90 effect on phenotype and inflammatory pathway

N90 promoted osteogenesis which corresponded to normal osteogenic pathway. In early phase (day 9), JNK, p38 and NFκB enhanced while TNFα and ROS slightly reduced osteogenic induction. Inflammatory response (IL-6 and NFκB), peaking at week 2, may help promoting mineralization.

5.5.4 Osteogenic pathway in nanovibrational stimulation; mechanotransduction-metabolite-inflammation

Based upon our knowledge, NS potentially enhances osteogenesis via multiple pathways. From this studies, the effect of NS-induced osteogenesis can be placed into mechano-transduction, inflammation and metabolite 'bins'. These major pathways all work downstream of the MAPK signaling hub which determine the appropriate cellular responses to these stimuli such as proliferation, differentiation and apoptosis.

5.5.4.1 Mechanotransduction perspective

Considering the mechanotransduction aspect, our previous publication (Tsimbouri P.M., 2017) showed that NS induced osteogenesis through 1) ion channels TRPV1-PKC-β-catenin pathway, 2) BMP2-SMAD1/5 and 3) Integrin-ROCK pathway. These pathways

operate through ERK1/2 to trigger RUNX2 phosphorylation and osteogenesis.

5.5.4.2 Inflammation perspective

As aformentioned, NS induced low levels of MSC driven inflammation during early culture (week1-2). The inflammation subsided by week 3 suggesting that it was a well-controlled inflammatory response and thus enhanced osteogenesis. Inflammation is a double-edged sword for osteogenesis. Low grade inflammation is essential for mineralization. Inflammation induces MSCs to produce OPN which, in turn, promotes mineralization via binding to the growing apatite mineral (F. Kahles, H. M. Findeisen, & D. Bruemmer, 2014). While high grade inflammation suppresses osteogenesis, and promotes osteoclastogenesis (Knapik et al., 2014). In this study, NS induced IL-6 and TNFα production. IL-6 can induce osteogenesis via the BMP2-SMAD1/5 pathway (M. Sun et al., 2017) whose gene upregulation was noted in Chapter 4 **(Figure 4.12 and 4.14)**.

The effect of TNFα on osteogenesis varies by dose, duration and starting phase. Short-term exposure with a low dose of TNFα can enhance osteogenesis while long-term exposure of TNFα inhibits mineralization (Daniele et al., 2017; H. Huang et al., 2011). Hess et al., showed that the addition of TNFα enhances ALP expression (Hess, Ushmorov, Fiedler, Brenner, & Wirth, 2009). TNFα can stimulate IL-6 secretion that, in turn, can induce bone activating BMP2 production (De Cesaris et al., 1998). TNFα does not effect on differentiation in pre-committed MSCs but does promote mineralization and osteogenesis in committed MSCs (Croes et al., 2015). Daniele et al., also confirmed that TNFα did not affect proliferation and differentiation in undifferentiated cells but that it is involved in early phase of osteogenic differentiation (Daniele et al., 2017). High levels of TNFα, however, suppress osteogenesis. In this study, TNFα was produced in the early phase only suggesting a role in enhancing osteogenesis.

The MAPK signaling pathway plays an important role in cell response and is activated by extracellular stimuli such as adhesion, stress, growth factors and cytokines. The MAPK pathway regulates cellular responses such as proliferation, differentiation, inflammation and apoptosis (W. Zhang & Liu, 2002; Y. Zhang et al., 2014). MAPK signaling requires to be balanced in optimal levels for enhancing

osteogenesis while higher levels suppress osteogenesis (Rodriguez-Carballo et al., 2016).

Intracellular ERK1/2 is involved in many cellular functions. ERK1/2 and mechanically-induced osteogenesis may associate with differentiation stages. Prolonged mechanical stimulation might desensitize ERK1/2 and thus reduce phosphorylated, active, ERK1/2 (Jansen et al., 2004). ERK itself can also activate osteoclast function thus promoting osteoclastogenesis (Rodriguez-Carballo et al., 2016). Considering the effect of NS, it was previously shown that NS can induce ERK1/2 related osteogenic pathway through 1) TRPV1-PKC-ERK1/2 -β-catenin and 2) Integrin-FAK-ROCK-ERK1/2 pathways (Tsimbouri P.M., 2017). On the other hand, NS may also activate ERK1/2 through TNFα induced inflammation. Thus, 3D osteogenesis required the great balancing harmony of osteogenic enhancing signals.

The role of JNK in osteogenesis is less clear. JNK can be activated by TNFα (Papa, Zazzeroni, Pham, Bubici, & Franzoso, 2004) and NFκB (A. Lin, 2003). In our study, N90 activated only JNK1 during osteogenesis **(Figure 5.18)** which tended to enhance osteogenesis **(Figure 5.21)**. However, in our non-responding patient, JNK significantly suppressed RUNX2 expression **(Figure 5.25)**. This implies that pre-inflamed cells with high levels of TNFα, JNK and NFκB suppress osteogenesis.

P38 is also known to have roles in osteoblast differentiation (Rodriguez-Carballo et al., 2016). In this inhibition study **(Figure 5.22)**, p38 significantly enhanced not only RUNX2 but also OSX gene expression in 3D osteogenesis of N90. This result corresponded to Wang et al affirming p38 mediated OSX for osteogenic differentiation (X. Y. Wang, Goh, & Li, 2007). Activation of p38 can phosphorylate various osteogenic transcription factors. Interestingly, signaling axis such as 1) BMP/TGFβ-p38-β-catenin or 2) WNT-p38-β-catenin (Rodriguez-Carballo et al., 2016) could worth further investigation.

NFκB pathway is crucial for cell survival. NFκB can be activated by inflammatory cytokines such as IL-1, IL-6 and TNFα through classic and alternative pathways (Lawrence, 2009). The activation of NFκB counterbalances the cell death pathway for cell survival (J. L. Luo et al., 2005). NFκB can also function as an antiproliferative protein, thus determining growth arrest, differentiation or cell death (Imran & Lim, 2013). NFκB pathways result in antioxidant (e.g. Mn SOD, catalase) and oxidant (e.g. iNOS, COX2, LOX2) production (Morgan & Liu, 2011).

Moreover, NFκB can crosstalk with ROS. NFκB can mediate RANK ligand induced osteoclastogenesis (Abu-Amer, 2013). Thus, the upregulation of NFκB in early phase by NS probably promoted osteoclast differentiation preparing for bone remodeling in later phase. This osteoclastogenesis hypothesis may be worth further study.

5.5.4.3 Metabolomic perspective

Our metabolomics study indicated that NS produced low grade inflammation. The evidence of long chain polysaturated fatty acid synthesis (LC-PUFAs) and reactive oxygen species (ROS) production were found. TCA cycle showed a slightly increase trend of TCA metabolite in NS group. Interestingly, NADPH oxidase was also found in N90 group. It is known that NADPH oxidase is related to ROS production at the plasma membrane (Fisher, 2009). Thus, it could be hypothesized that NS may directly affect the plasma membrane e.g. by fluttering the cell membrane. Considering the predicted activated network, the network showed the activation of NADPH oxidase, ERK1/2, Akt, NFκB, NOS, SOD with N90 stimulation; these signals were predicted at much lower levels with N30 stimulation **(Figure 5.10 - 5.11)**. This could be interpreted that stimulating amplitude (approximate range from 40-100 nm) may involve or activate the inflammatory signal or ROS product at the cellular membrane. This activation then induces the counterbalance signaling. The "switch on" of counterbalance signaling may concomitantly activate the osteogenic differentiation pathway as well.

5.5.5 Cellular Yin-yang; the balance between osteogenesis and inflammation in nanovibrational stimulation.

The balance between osteogenesis and inflammation at each time point appears to be the key to stimulate osteogenesis by mechanical stimuli. Adequate duration and intensity of stimuli will commit MSC differentiation to osteoblasts and produce slight inflammation (with benefit for mineralization). Over inflammatory response reduces osteogenesis and, in the literature, has been linked to increased adipogenesis or suppressed differentiation or apoptosis. The pathways enhancing or suppressing osteogenesis which might be induced by NS are summarised in **Table 5.1**.

Table 5.1 Summary of potential NS pathways

	Pathways/ Effects	References	In this thesis
Enhanced osteogenesis	**1)** Cytoskeletal involvement Integrin-FAK-ROCK-ERK1/2	(Tsimbouri P.M., 2017)	✓
	2) BMP2 BMP2-SMAD1/5	(Tsimbouri P.M., 2017)	✓
	3) Stretching ion channels TRPV1-PKC-β-catenin	(Tsimbouri P.M., 2017)	✓
	4) Inflammation IL-6-BMP2-SMAD1/5 TNFα- NFκB? -(BMP2-OSX-RUNX2)	(Hess et al., 2009; Osta, Benedetti, & Miossec, 2014; M. Sun et al., 2017)	✓
	5) ROS (controllable)	(Atashi et al., 2015)	✓
	6) **Others** such as - **Fluid flow** (questionable) (PC-1-JAK2/STAT3-RUNX2) - Heat activation	(Dalagiorgou et al., 2017) (E. Chen, Xue, Zhang, Lin, & Pan, 2015; Ota et al., 2017)	-
Suppressed osteogenesis	**1)** **NFκB** degraded β-catenin	(Chang et al., 2013; N. Wang et al., 2016).	-
	2) **MAPK** inhibits SMAD1/5	(R. L. Huang, Yuan, Tu, Zou, & Li, 2014; Mao et al., 2016)	-
	3) TNFα	(R. L. Huang et al., 2014; Lencel, Delplace, Hardouin, & Magne, 2011; Osta et al., 2014)	✓
	4) ROS (high level)	(Atashi et al., 2015)	✓

To simplify the interaction of NS related pathways, the mechanotransduction-metabolite-inflammation theory was used to illustrate signaling maps caused by mechanical stimulating cues, inflammation and metabolites. The example of signaling pathways in optimal stimulation and in high oxidative stress are shown in **Figure 5.29-5.30**

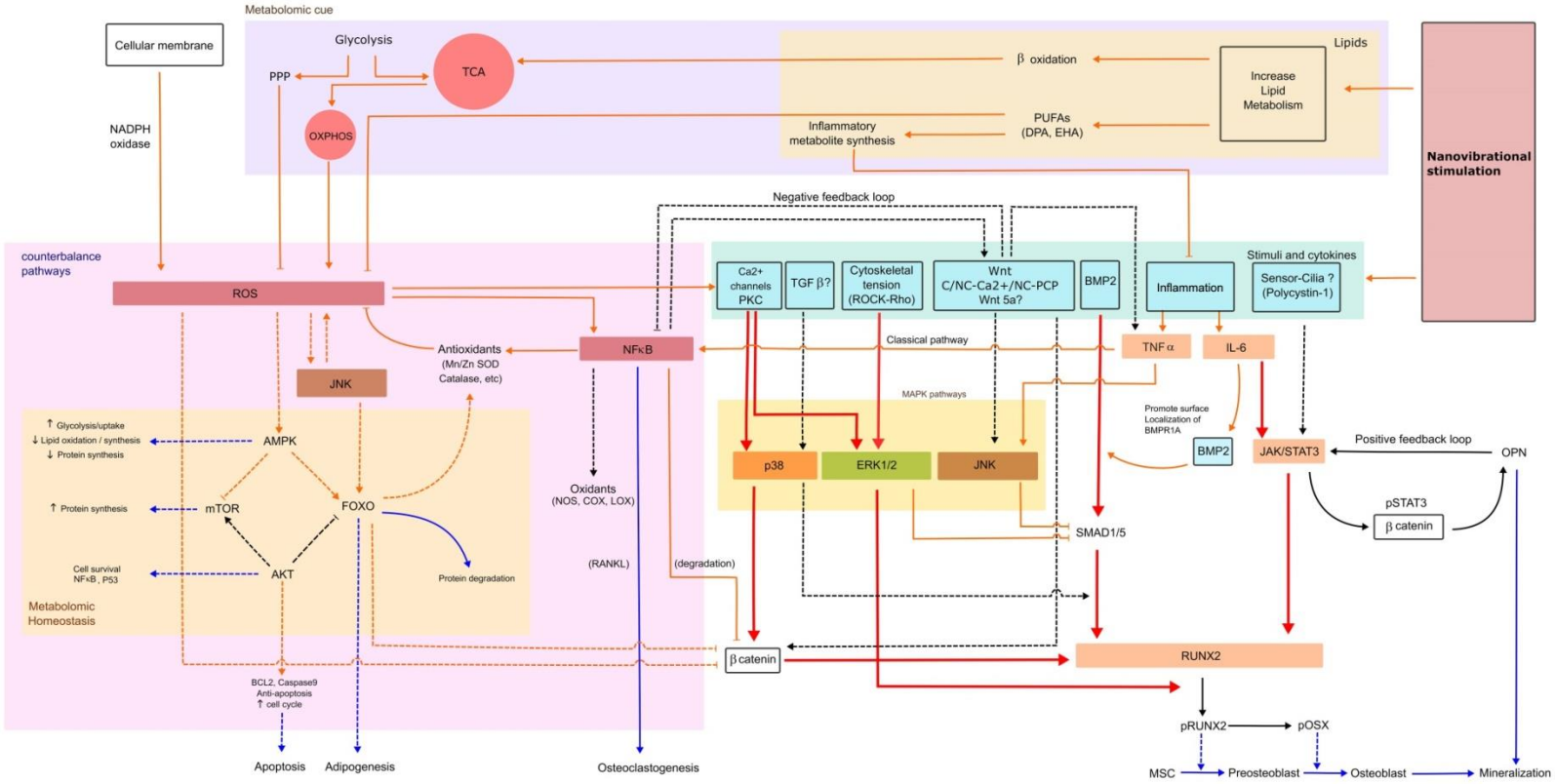

Figure 5.29 The hypothesis of NS involved pathway with optimal intensity of NS.

Inflammation effect on osteogenesis is greater than its negative effects (contributing by inflammation, TNFα, ROS and NFκB (Red line = high level expression, Orange line = low level expression, dense line = proved pathways, dot line = theorectical pathway, blue line = phenotype/ result expression).

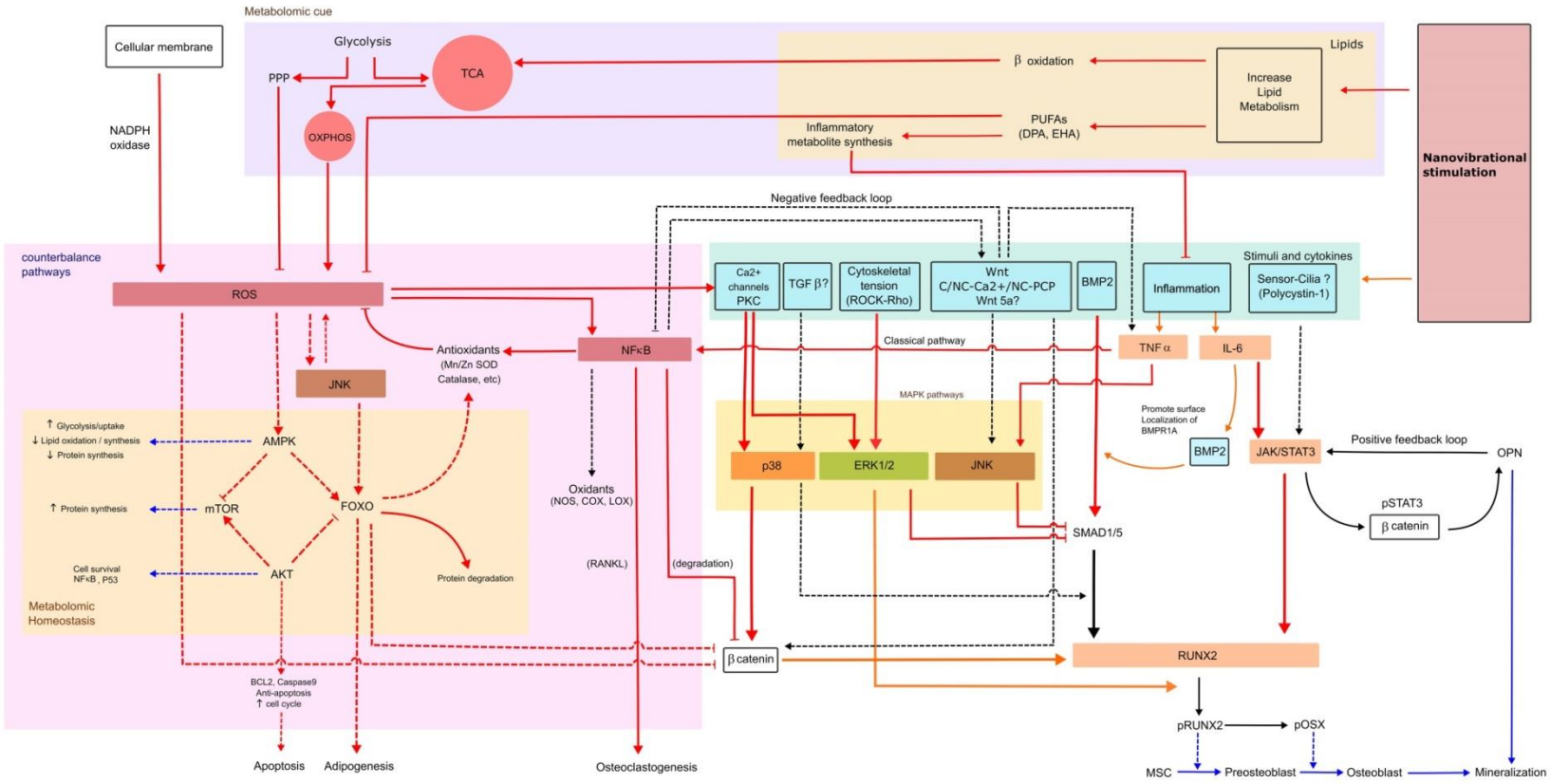

Figure 5.30 The hypothesis of NS involved pathway in high oxidative stress condition

Over stimulation or poor cell quality (resulting in high level of NFκB and TNFα baseline level), these conditions suppress osteogenesis (Red line = high level expression, Orange line = low level expression, dense line = proved pathways, dot line = theoretical pathway, blue line = phenotype/ result expression).

5.6 Conclusion

Nanovibrational stimulation involved lipid metabolism and produced controllable ROS which enhance osteogenesis. NS also induced controllable inflammatory response (IL-6 and TNFα) promoting 3D osteogenesis. A good balance between osteogenic enhanced niche and oxidative stress-inflammation is crucial to achieve the osteogenic induction.

Chapter 6 Composites for nanovibrational stimulation using in bone tissue engineering

Chapter 6 Composites for nanovibrational stimulation using in bone tissue engineering

6.1 Introduction

Natural hydrogels, such as collagen, are widely used for tissue engineering (Antoine, Vlachos, & Rylander, 2015). However, improving the mechanical properties of natural hydrogel such as collagen, gelatin, etc for bone tissue engineering is challenging. In chapter 3, it was shown that soft collagen hydrogels were unable to resist cell traction forces resulting in hydrogel contraction. Moreover, the degradation time of soft collagen hydrogels do not correspond to bone regeneration (Helary et al., 2011). Crosslinking techniques can improve physical properties (Sundararaghavan et al., 2008) and extend the degradation time of hydrogels (Lang, Spousta, & Lyubovitsky, 2015; McGann et al., 2015). However, these techniques provide cytotoxicity issues for MSC culture (Fessel et al., 2014; J. C. Lee et al., 2011; X. Yang et al., 2013).

Rigid scaffolds provide better mechanical properties than hydrogels. However, nutrient and oxygen transfer in hydrogels is superior than in dense, rigid scaffolds (Zohreh Izadifar, Xiongbiao Chen, & William Kulyk, 2012; Rouwkema et al., 2010). There are many techniques to produce rigid collagen scaffolds such as electrospinning (Jha et al., 2011; Law et al., 2017), freeze drying (Kane & Roeder, 2012; Kane et al., 2015; Schoof, Apel, Heschel, & Rau, 2001), etc. However, loading cells into these rigid scaffolds are inevitably performed after the scaffolds were prepared. Thus, it is difficult to achieve homogenous cell distribution together with 3D cellular response within 3D scaffolds (Weilun Sun et al., 2012).

To combine advantages of rigid scaffold and hydrogel together, biphasic scaffold is composed of rigid constructs inside hydrogels providing composite architecture while the MSCs reside in the hydrogel component as a 3D cellular niche. From the current evidence, many techniques have been proposed using the biphasic scaffold concept. For example, Tanaka et al proposed combination of a hydrogel and rigid internal construct by compositing Poly L-lactic acid (PLLA) scaffolds into atelocollagen for cartilage tissue

engineering (Y. Tanaka et al., 2010). Furthermore, the concept of a combination between gel phase and rigid phase were also integrated into a 3D printed bioprinting scaffolds approach. Hydrogels were used as the ECM for stem cells in the 3D bioprinting process. PCL was also printed as a rigid component for maintaining scaffold shape (H. W. Kang et al., 2016).

Considering a different issue, it is questionable whether MSCs can maintain their osteogenic phenotype after NS is finished. Moreover, it is known that materials can regulate cell fate. Stiff materials promote osteogenesis while soft materials enhance adipogenesis (Engler et al., 2006). Therefore, loading MSCs in soft collagen hydrogel may reverse NS induced osteogenic phenotype. Theoretically, adequate dose and duration of mechanical stimulation allows MSCs to differentiate and memorize their fates without phenotypic reversibility after stimuli is terminated (C. Yang et al., 2014).

In this chapter, biphasic scaffold compositing of collagen hydrogels with freeze dried collagen sponge was introduced. This composite combined the advantage of hydrogel and sponge together. The hydrogel allows nanovibrational force transmission and nutrient transfer, while the collagen sponge supports the composite structure, preventing hydrogel contraction and improves handleability (important for clinic). Mechanical properties, hydrogel contraction and mechanical response of cell-hydrogel-sponge composite (CHSC) during N90 stimulation were optimised. Biological responses including viability and phenotype expression were investigated. Finally, the optimal NS duration for osteogenesis and phenotypical memory was also studied.

6.2 Aims and objectives.

1 To develop a CHSC that suits the NS bioreactor

2 To investigate mechanical properties of CHSCs and study how CHSCs responded to NS.

3 To evaluate the biological responses of MSCs to CHSCs as well as investigate the phenotype expression of MSCs in CHSCs after NS.

4 To optimise the NS duration and dose for MSCs in CHSCs which can induce osteogenesis as well as maintain phenotype after NS was removed.

6.3 Methodology and experimental design

6.3.1 Freeze dried collagen sponge preparation

To prepare the collagen sponges, 5% weight of bovine tendon powder (Collagen solution, UK) was used. The 0.001 M of HCl with pH 3 was added and then homogenized with homogenizer (TissueRuptor, Qiagen) on ice. The mixed composites were then molded in polystyrene cell culture inserts (0.4 μm Polyethylene terephthalate; PET, membrane, 12 well plate diameter, Greiner bio-one, Austria) and in turn frozen at -80°C for 10 hours. Freeze drying was done at -110°C, Vapor pressure at 0 mBar, for 20 hours (VirTis, SP industries, USA). Freeze dried collagen sponges were sterilised by UV light exposure for 1 hour.

6.3.2 Cell-hydrogel-sponge composite preparation

To prepare the CHSCs, sponges were placed at the centre of 12 well plates and were weighted down by placing a screw nut on top of the sponges. 1.8 mg/ml collagen hydrogels were prepared by using rat-tail collagen type I (5mg/ml, First Link, UK). 10xDMEM (First link, UK) and Fetal bovine serum (Fisher Scientific) was used as cell medium supplement. 0.1M sodium hydroxide (Fluka, UK) was added for pH titration by phenol red indicator and pH paper. After the pH titration, MSCs were added in the hydrogel mixture and 2.5 ml of MSCs-hydrogel mixture was decanted around the sponges. Gelation was allowed at pH 7.7 - 8.0 and in a 37°C incubator. Following the cell-hydrogels

gelation, 0.5 ml of secondary hydrogels (1.8 mg/ml) without cells were aliquoted on top the composite. The CHSCs were then transferred for stimulation on the NS bioreactor. When the stimulation time ended, the CHSCs were detached from the culture wells by spatula allowing CHSC contraction before removed for further analysis **(Figure 6.1).**

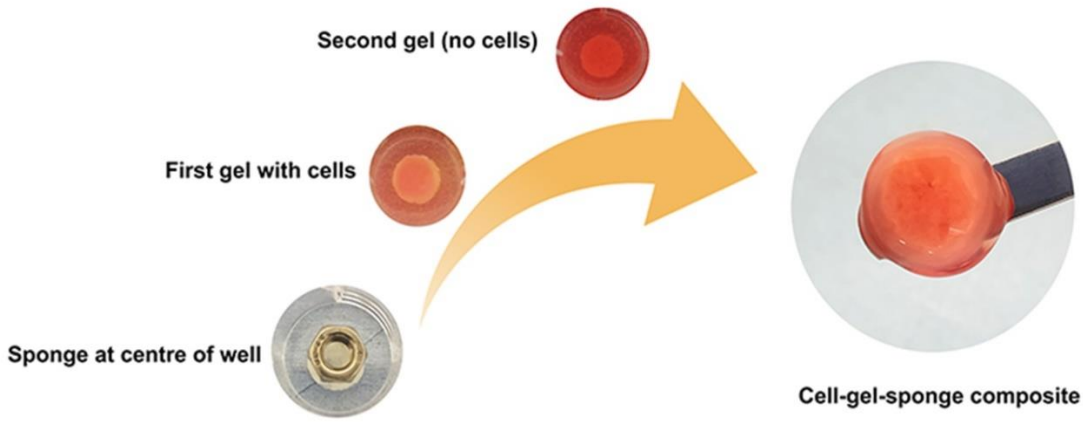

Figure 6.1 Cells-hydrogel-sponge composite preparation

To prepare CHSC, sponges were placed at the centre of wells. Cells were mixed with 1.8 mg/ml collagen hydrogel and then aliquoted into wells. After gels were set, hydrogels were then aliquoted on top to cover the composite.

6.3.3 CHSC contraction and time lapse microscopy

To observe the CHSC contraction, top view images of gel-sponge composite were taken every 1-2 days. The surface area of the gels was measured using ImageJ software. To evaluate cell migration, CHSCs were cultured for 6 and 10 days. CHSCs were imaged using a 10x objective lens at 120 sec intervals for 24 hours at 37°C. Cell velocity and migration directions were analysed using imageJ plugin (manual tracking) and Chemotaxis and Migration tool (Ibidi).

6.3.4 Compression test

The collagen sponges (5% of dry weight) were prepared (sample height 4 mm, radius 5.5 mm) and placed on the base of the compression testing machine (Zwick-Roell, Z2.0, Germany). Compression velocity

was set at 1mm/min. Samples were compressed for 2 mm distance. Stress-strain graphs were plotted to identify the linear range which represented the elastic property of the collagen sponges. The elastic modulus was then calculated by Microsoft Excel software using data within the elastic range **(Figure 6.2)**.

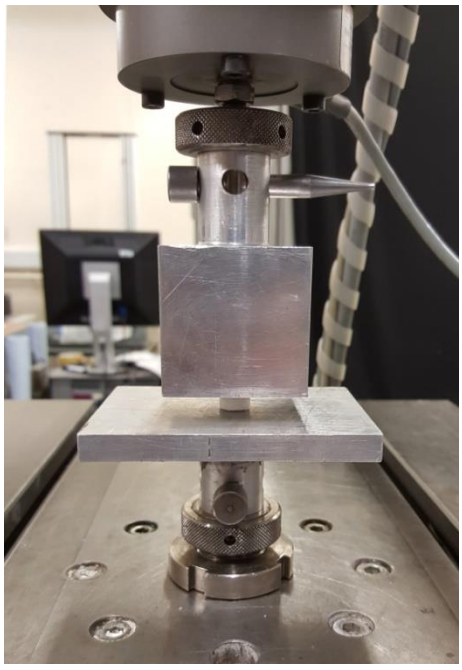

Figure 6.2 Compression test of collagen sponge

Collagen was placed on the base of the compression testing machine. Compression test was performed for 2 mm with 1 mm/min velocity.

6.3.5 Cryosection

After CHSCs were stimulated with NS, the samples were fixed in 4% formadehyde and infused in 30% sucrose in PBS for cryoprotection, overnight at 4°C. The samples were then transferred to embedding molds and O.C.T. (Tissue-Tek, Sakura) was aliquoted to cover the samples. The samples were then frozen in liquid nitrogen and kept at -80°C. The frozen samples were then sliced into 60 mm thickness and attached onto adhesive slides (9597, Tissue-Tek, Sakura, Netherlands). Immunofluorescent staining was then carried out. Techniques were explained in chapter 2 section 2.11.

6.3.6 Scanning electron microscopy (SEM)

The samples were prepared for SEM using the sputter coating technique. The samples were mounted onto SEM stubs using double sided conductive tape and silver paint. They were then coated with Gold/ Palladium (approximately 10-20 nm) using a SEM coating system (Q150T ES, Quorum, UK). The samples were viewed on a JEOL6400. SEM running at 10 kV and Tif image captured using Olympus Scandium Software. Porosity diameter was analysed by ImageJ software.

6.4 Results

6.4.1 Mechanical validation

The studies of porous characteristics (by SEM), mechanical properties of CHSCs, as well as reproducibility of CHSC composite preparation were conducted. The pattern of CHSCs responding to NS was also studied.

6.4.1.1 Characteristics, SEM and CHSC

The 5% weight of freeze dried collagen sponges were prepared in order to study the effect of NS on biphasic scaffolds. The average pore size was 227.74 mm (SD 72.93) **(Figure 6.3 A-D)**, and the average elastic modulus of the dry collagen sponge was 1.08 MPa (SD 0.29) measured by compression testing (Zwick-Roell, compression rate 1 mm/min) **(Appendix III)**. CHSC was lift up with spatula for a simple inspection.

CHSC was maintained its shape and handleable in both pre- and post-contraction **(Figure 6.3 E)**.

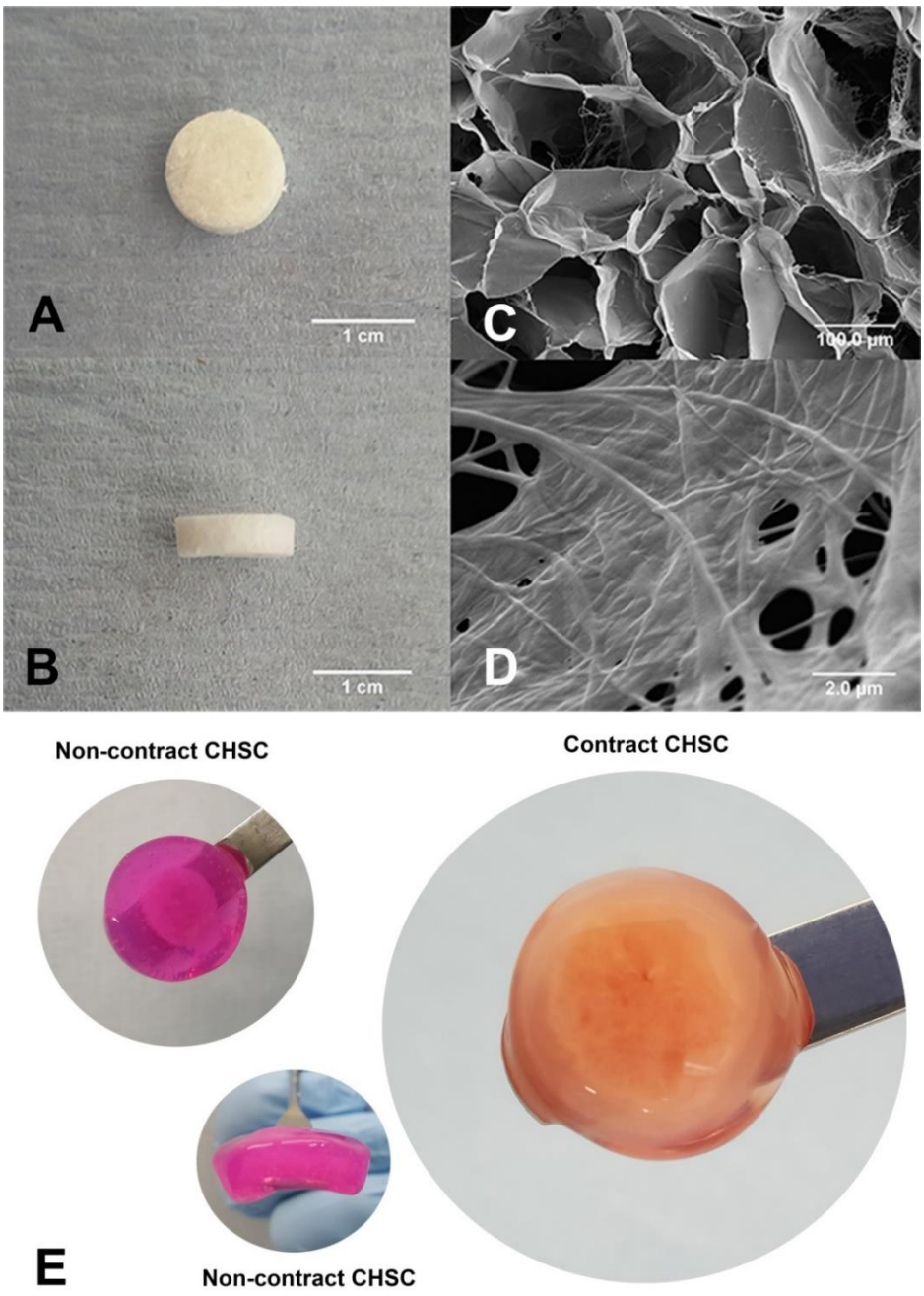

Figure 6.3 Sponge characteristics, SEM and CHSC

The 5% weight freeze-dried collagen sponges were prepared (A-B). SEM showed the homogeneous porosity of the collagen sponge (magnification c; 200x, d; 10,000x) (C-D). CHSC was maintained its shape (E).

6.4.1.2 Hydrogel contraction

Initially, the "one-week NS protocol" was developed to evaluate the reproducibility of CHSC contraction. To study CHSC contraction progression, Stro1-selected MSCs were mixed in collagen hydrogels at different cell concentrations (4x, 10x and 20x10^4 cells/ml) and prepared as CHSCs. After NS for 7 days, the hydrogel component was detached from the wells and cultured for a further 14 days **(Figure 6.4)**. At day 9, all CHSCs in all groups started to contract until the gels touched the sponge. Increasing the number of cells seeded had some effect on hydrogel contraction, but no effect of NS on CHSC contraction was found **(Figure 6.5)**.

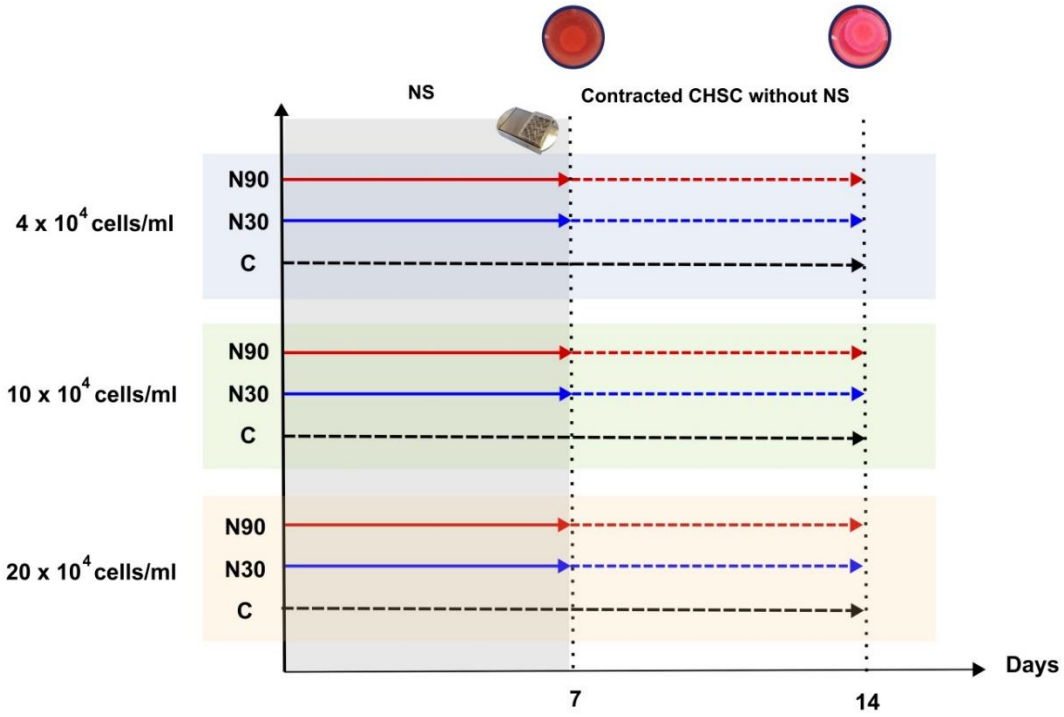

Figure 6.4 Diagram of hydrogel contraction study

To test the "one-week NS protocol", three different cell concentration groups (4x, 10x and 20x10^4 cells/ml) were stimulated with N30 and N90 for 7 days. At day 7, CHSCs were detached and continuously cultured until day 14.

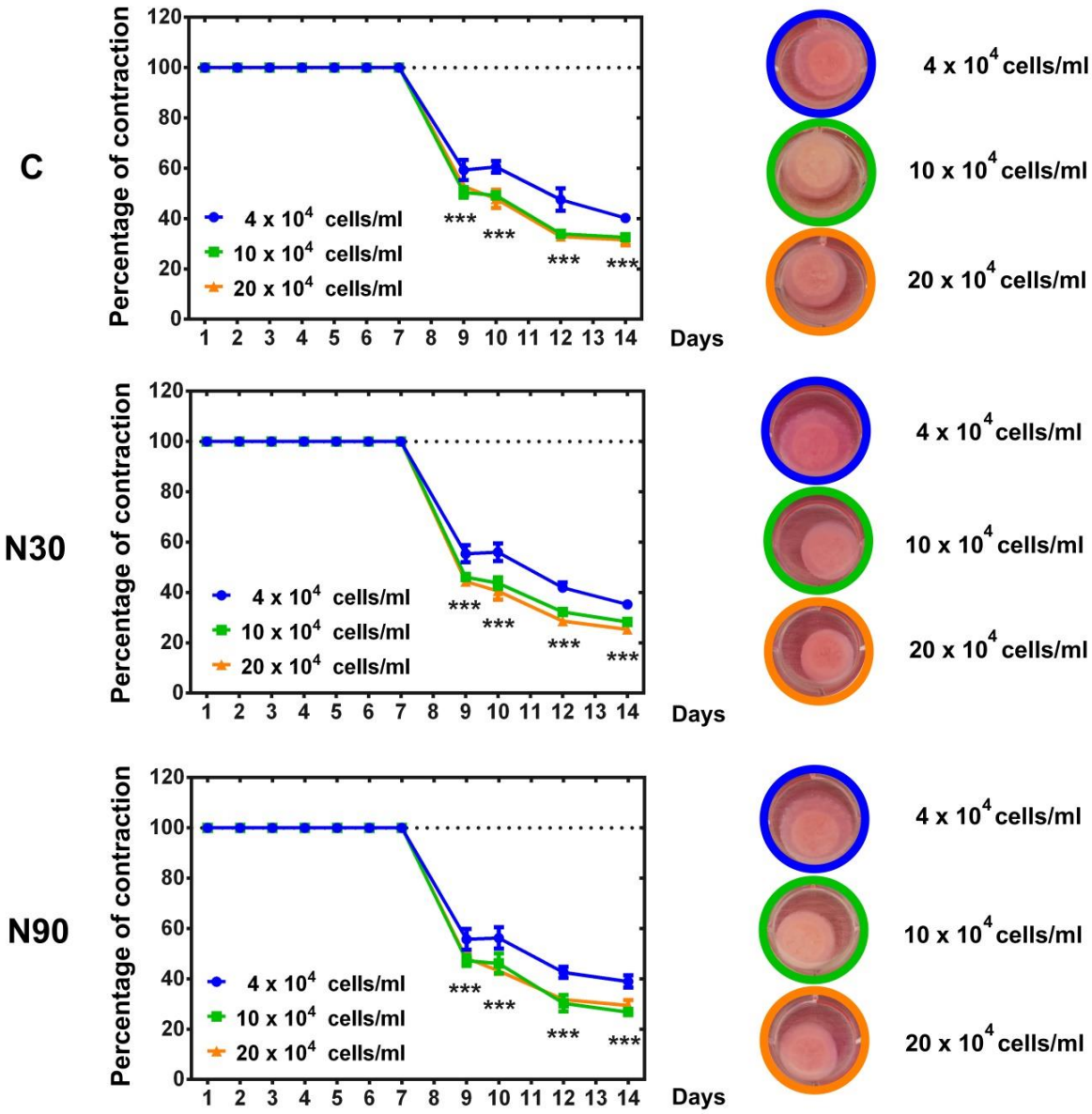

Figure 6.5 CHSC contraction observation

CHSC contraction was observed between day 7 and 14. At day 7, CHSCs were detached from the culture plates. All CHSCs started to contract at day 9; the hydrogels were significantly contracted in the 10x and 20x10^4 cells/ml groups comparing to the 4x10^4 cells/ml group. This result implies that the high cell numbers possibly increased the cell pulling force (mean±SD, n=4, *= P≤ 0.05; ** = P≤ 0.01; *** = P≤ 0.001, Two-way ANOVA, Tukey's post hoc test).

6.4.1.3 Displacement amplitude in hydrogel-sponge composite

To confirm that the cells would feel the vibrations in the hydrogel-sponge composite during NS, the hydrogel displacement amplitudes were measured at the centre of the hydrogel (at the sponge area) and hydrogel periphery (where MSCs were seeded). **Figure 6.6A** shows that the NS bioreactor generated reliable CHSC displacement amplitudes within the elastic range of the hydrogel; increasing voltage increased the CHSC surface displacement in a linear manner. The CHSC surface amplitude at the sponge area (centre of CHSC) was always slightly higher than the gel area (peripheral area) **(Figure 6.6 B-C).** A graph of frequency (Hz) - amplitude validation was plotted in order to study the resonance phenomenon of hydrogel-sponge composite **(Figure 6.7)**. A reduction of CHSC resonance frequency was noted (at 1,250 Hz) when comparing to hydrogels without sponge (at 2,250 Hz).

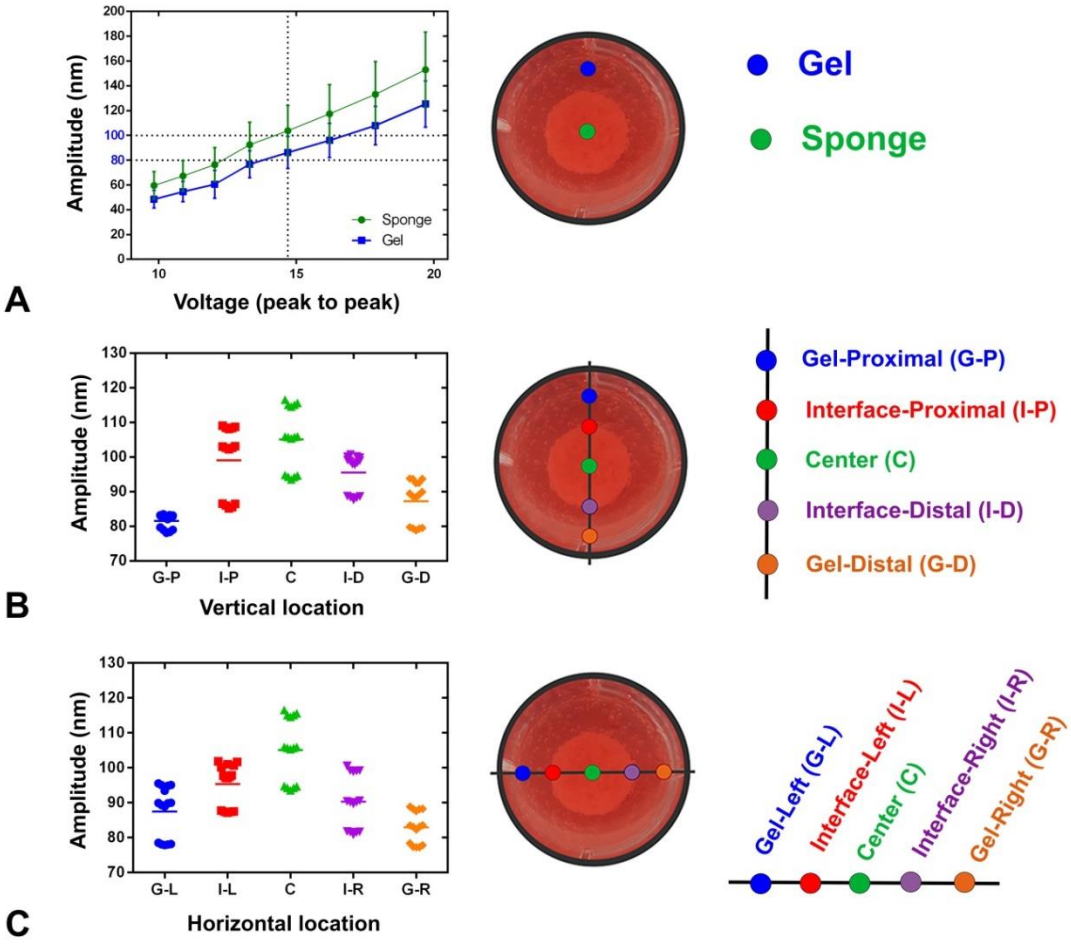

Figure 6.6 Amplitude validation of CHSC during NS

Voltage (peak to peak)-amplitude validation (A); Linear pattern of the relationship between amplitude-voltage represented that nanovibrational stimulating bioreactor was reliable and desired frequency was tunable within the elastic range of the hydrogel. Hydrogel displacement along vertical (B) and horizontal (C) lines showed that the peak of amplitude located at the centre of hydrogel-sponge composite (C; centre, D; distal, G; gel area, I; interface between gel and sponge, L; left, P; proximal, R; right).

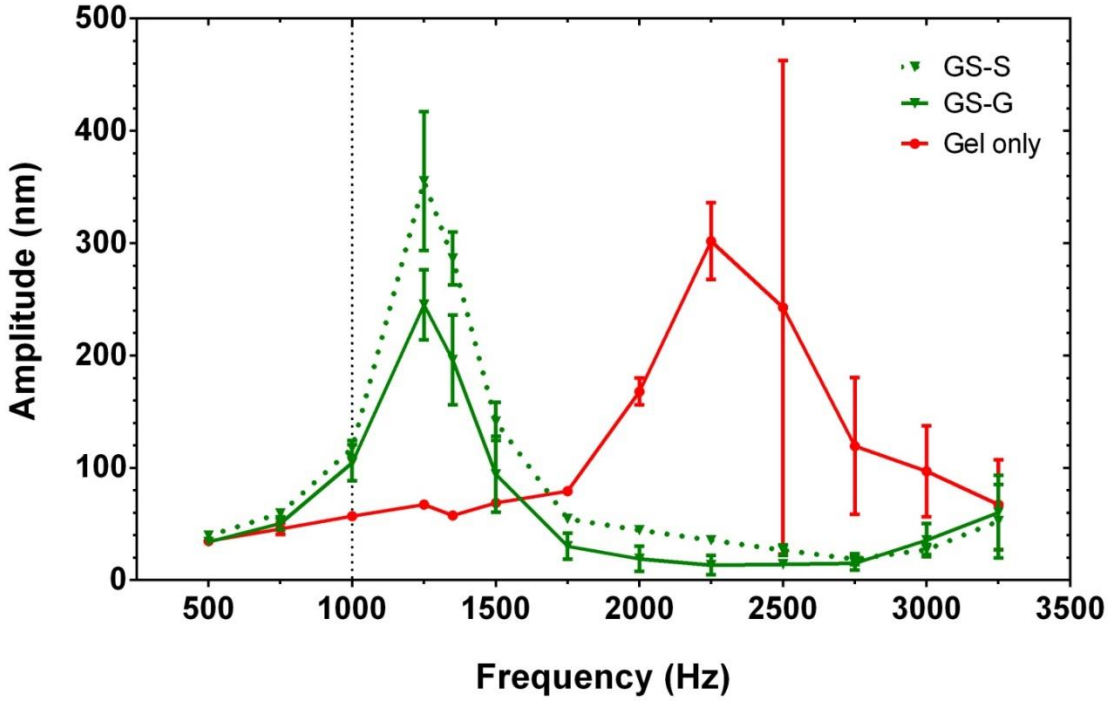

Figure 6.7 Frequency-amplitude validation by interferometry

Frequency-amplitude validation. Decrease of resonance frequency in gel-sponge composites (green) comparing to the hydrogel without sponge group was noted (red) which followed the rule of simple harmonic motion. In both gel and the hydrogel-sponge composites, NS still showed a good fidelity at 1000 Hz stimulation. GS; gel-sponge composite, G; gel area (peripheral area), S; sponge area (centre area).

6.4.2 Biological validation of cells-hydrogel-sponge composite

Next, the biological response of CHSCs as well as biocompatibility were carried out. Firstly, the interaction between cells and the sponge in the composite was tested. Cell behaviors in the CHSC, such as cell migration and velocity were studied. Moreover, biocompatibility was also tested by Alamar Blue assay. Utmostly, MSC phenotype of NS induced CHSCs was investigated.

6.4.2.1 Time lapse microscopy

To investigate cell viability in pre- and post-contracted CHSC, $4x10^4$ cells/ml of MSCs were seeded into CHSCs. Time-lapse microscopy images were taken at day 6 (pre-contracted) and 10 (post-contracted) for 24 hours. Cell migration velocity in the pre-contracted CHSCs was significantly higher than that in the post-contracted CHSCs **(Figure 6.8).** Chemotaxis plots and rose plots illustrated that cells favored migration towards the sponge in both pre- and post-contracted gels **(Figure 6.9)**.

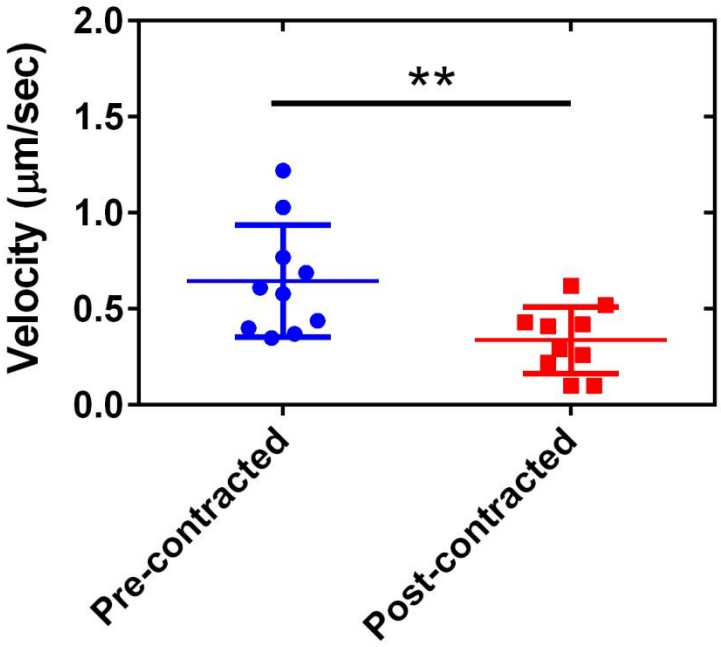

Figure 6.8 Effect of CHSC contraction on cell migration velocity

Comparison of cell migration velocity in pre-contracted and post contracted hydrogels showing that cell velocity decreased in the contracted hydrogels (n=10) (mean±SD, n=10, *= P≤ 0.05; ** = P≤ 0.01; *** = P≤ 0.001, paired t-test)

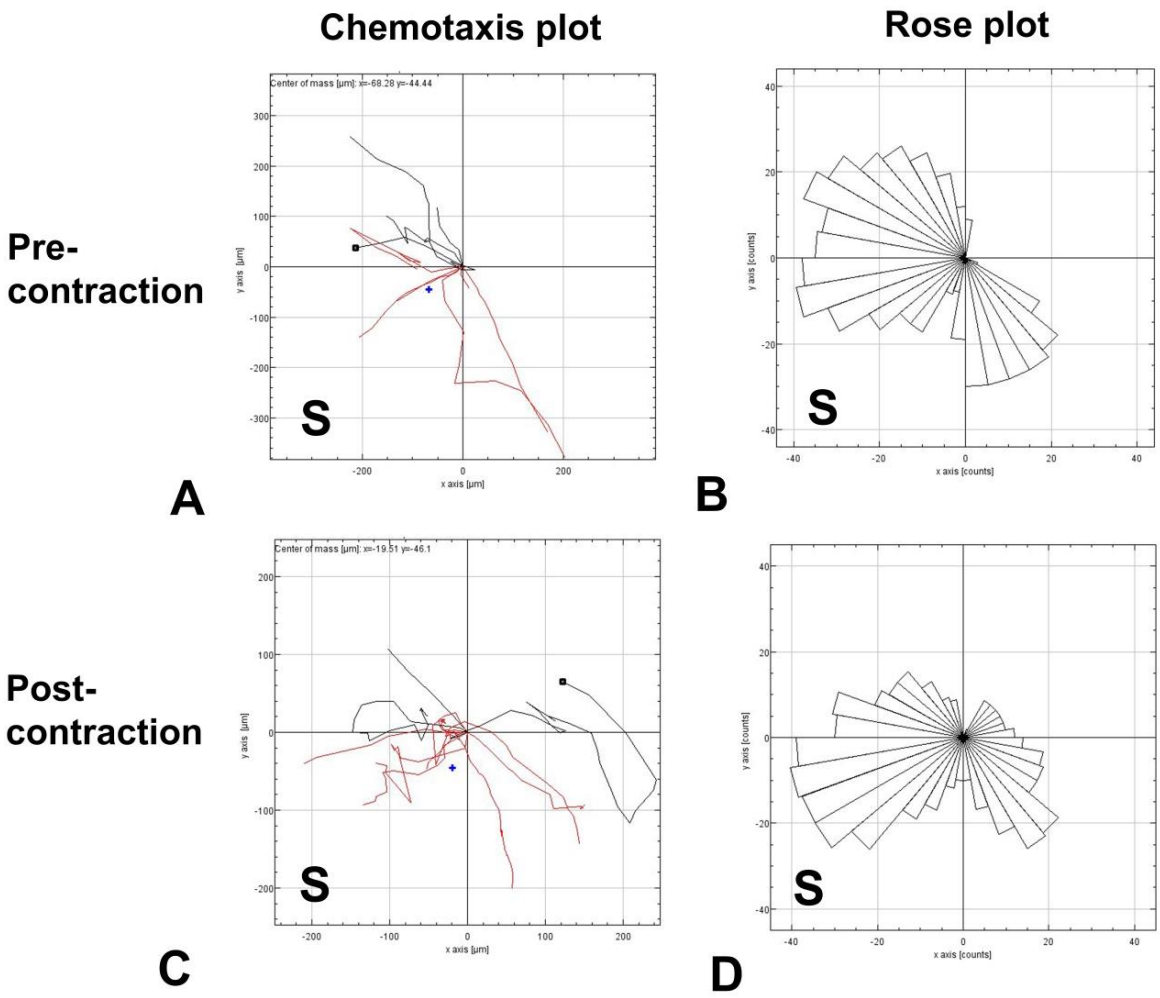

Figure 6.9 Cell movement direction

Chemotaxis and rose plots demonstrated that cells tended to migrate toward the sponge in non NS-stimulated CHSCs. (n=10, red line; counts the upward direction, black line; counts the downward direction, +; center of migration, S; collagen sponge in CHSCs).

6.4.2.2 Cell characteristics at hydrogel-sponge junction

As MSCs in the CHSCs tended to migrate toward the sponge **(Figure 6.9)**, it was decided to look closer. Thus, 4x10^4 cells/ml of MSCs were seeded into CHSCs and cultured for 14 days without NS. Microscopy showed that MSCs tended to move toward to the sponge in pre-contracted CHSCs. In contracted CHSCs, MSCs attached onto the sponge **(Figure 6.10 A-B)**. Next, CHSC cryosections were studied to identify MSCs inside the sponge. The 10^4 cells/ml of MSCs seeded into CHSCs and cultured for 1 week without NS. CHSCs contraction was allowed at day 7. At day14, contracted MSC seeded CHSCs were sliced by cryosection and immunofluorescence stains (myosin IIa, actin and DAPI) were carried out. Microscopy showed that MSCs attached onto sponges. Red stained cells (actin) could be seen inside the sponges **(Figure 6.10 C-D)**.

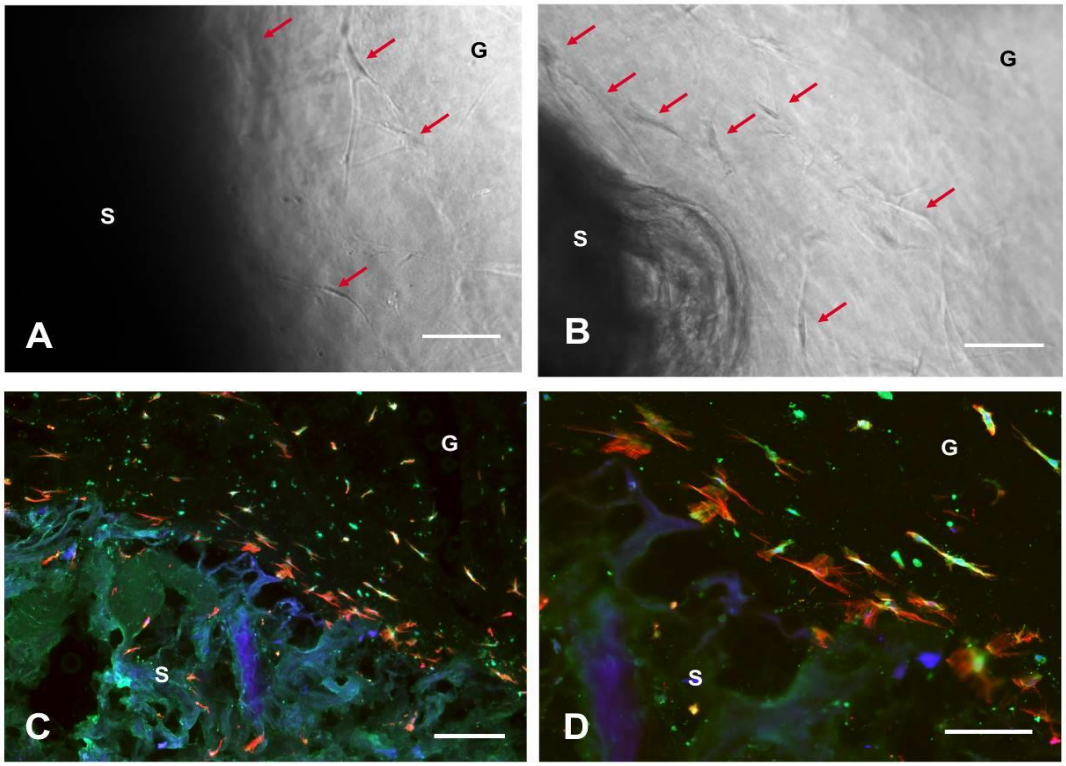

Figure 6.10 Microscopy and cryosection of gel-sponge

A-B Microscopy of the gel-sponge composite. Stro1 selected MSCs at day7 (A) in precontracted CHSCs showed that MSCs were viable and tended to move toward the sponge (20x magnification, scale bar 100 µm). At day 12 (B), in contracted

CHSCs, viable MSCs were still seen in the hydrogel (20x magnification, scale bar 100 µm).
C-D Gel-sponge cryosections. Cryosections of the contracted CHSCs at day 14 showed MSCs attached onto the sponge. (C; 4x magnification; scalebar 300 µm, D; 10x magnification; scale bar 150 µm, Green; myosinIIa, Red; actin, Blue; DAPI, S; sponge, G; hydrogel)

6.4.2.3 Alamar Blue study

Stro-selected MSCs seeded with different cell concentrations (4x, 10x, 20 x 10^4 cells/ml) into CHSCs were prepared to investigate biocompatibility using the alamar blue assay. The 1-week NS was performed as in **Figure 6.4**. The Alamar Blue study **(Figure 6.11A-C)**, representing both viability and metabolic activity, emphasized again that CHSCs were compatible for MSCs. Interestingly, the percentage of alamar blue reduction in the contracted CHSCs was significantly higher than in the non-contracted CHSCs **(Figure 6.11A).** This could be interpreted that MSCs in the contracted CHSCs are more active than cells in non-contracted CHSCs. During NS (day 6), the increase in the percentage of alamar blue reduction compared to non-stimulated controls indicated that NS enhanced cellular metabolic activity **(Figure 6.11B).** This activity remained in the N90 group after stopping stimulation (day 11) **(Figure 6.11C).** Construct loading with a high number of cells produced greater metabolic activity than lower concentrations.

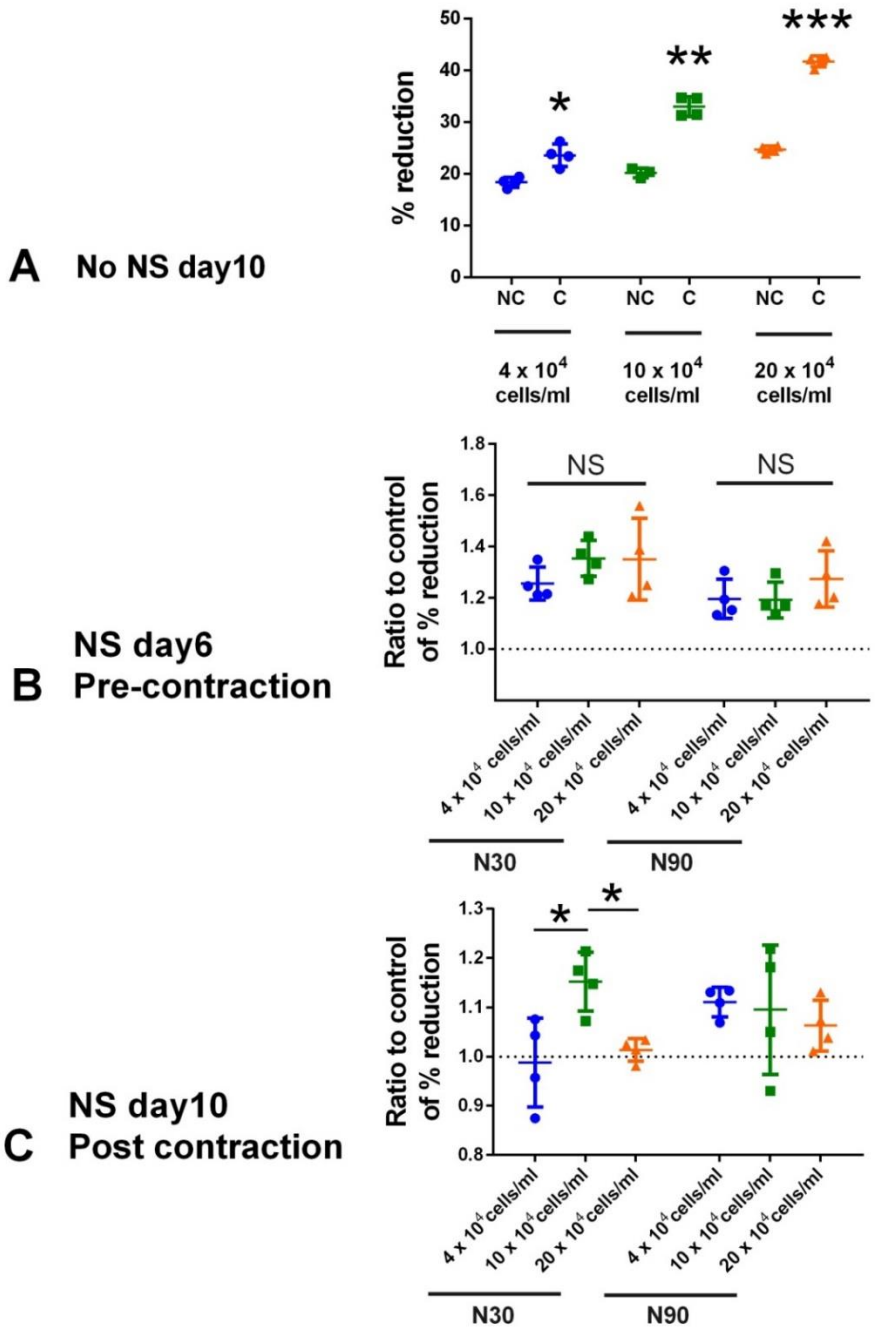

Figure 6.11 Alamar blue study in CHSC

A) Comparing contracted and non-contracted CHSCs at day 10, metabolic activity in the contracted CHSCs was higher than that in the non-contracted CHSCs, indicating that MSCs are more active in the contracted CHSCs. (mean±SD, n=4, *= P≤ 0.05; ** = P≤ 0.01; *** = P≤ 0.001, pair t test).

B) Considering NS in pre-contracted CHSCs at day 6, NS enhanced metabolic activity compared to control (non-

contracted CHSC) (mean±SD, n=4, *= P≤ 0.05; ** = P≤ 0.01; *** = P≤ 0.001, one-way ANOVA, Tukey's post hoc test).

C) After stopping the stimulation at day 7, metabolic activities in all groups were reduced at day 10. Interestingly, the activity in N90 group was the same compared to control (contracted CHSC) (n=4, *= P≤ 0.05; ** = P≤ 0.01; *** = P≤ 0.001, one-way ANOVA, Tukey's post hoc test).

6.4.2.4 Temporal gene analysis

Next, a temporal gene study was performed to select an adequate dose of NS which can commit MSCs for osteoblastic differentiation. The $4x10^4$ cells/ml of Stro1-selected MSCs/ml in CHSCs was prepared. MSCs in CHSCs were stimulated with NS for 7, 14 and 21 days without detachment, therefore, there was no hydrogel contraction. RUNX2 and OSX upregulation were found at week 1 for osteogenic commitment. OPN was upregulated in week 2-3. The N90 group provided better osteogenic induction than the N30 group **(Figure 6.12A)**. Considering inflammation, IL-6 upregulation was noted at week 1 indicating that MSCs produced an inflammatory response. However, the inflammation was reduced in week 2-3. This suggests a controllable inflammatory response that is beneficial for osteogenesis. NFκB was produced at week 1 and again was reduced by week 2-3 corresponding to IL-6 level and supporting the controlled inflammation hypothesis **(Figure 6.12B)**. The summary diagram of NS induced phenotype and inflammatory response is shown in **Figure 6.12C**.

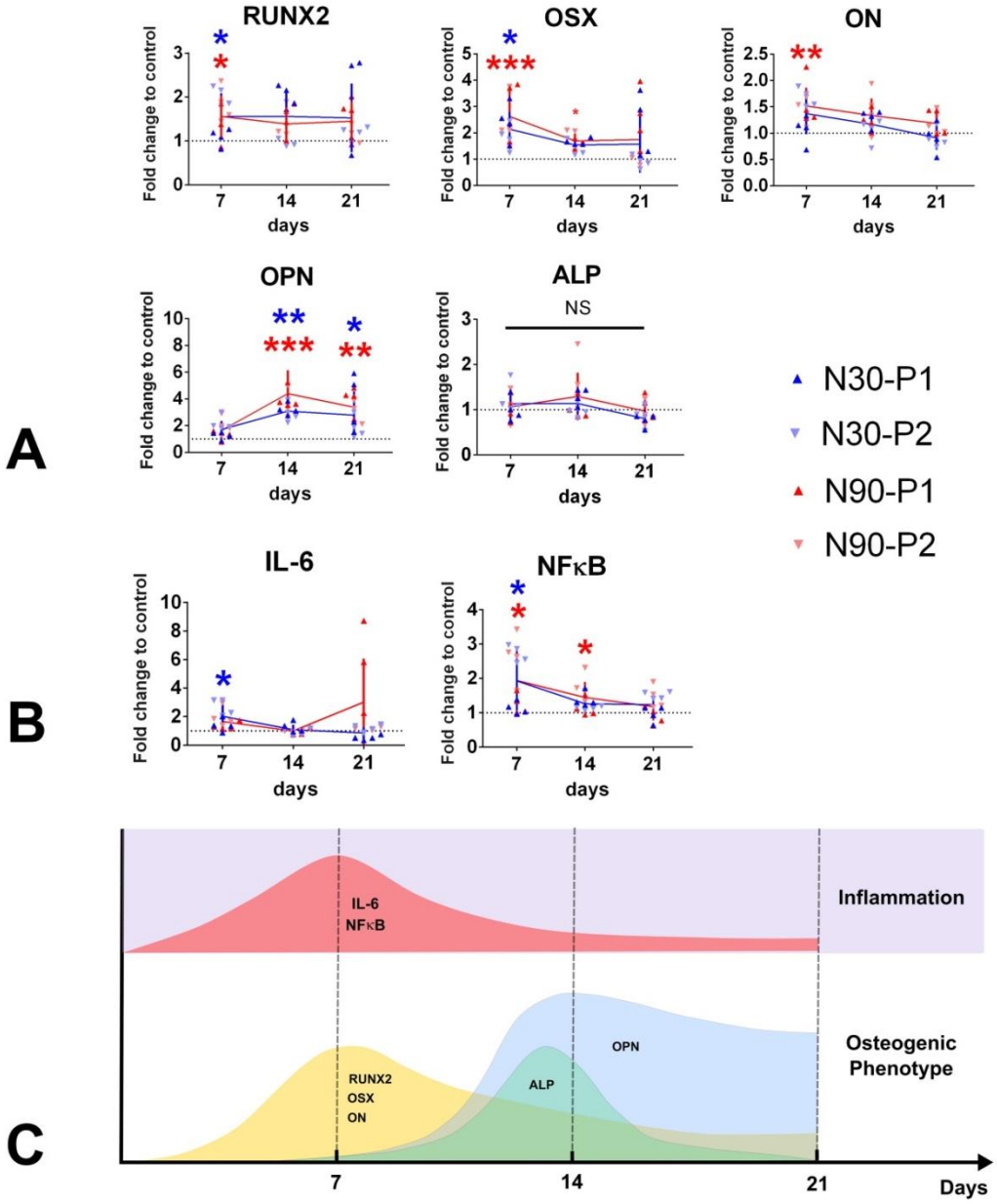

Figure 6.12 Temporal gene study at day 7-21

NS induced osteogenic gene expression. RUNX2, OSX and ON were upregulated at week 1 for osteogenic commitment while OPN was increased at week 2-3 (A). Inflammation (linked to IL-6 and NFκB levels) was found at week 1 but decreased at week 2-3 indicating that inflammation is controllable (B). A diagram illustrating the relationship between phenotype and inflammatory response (C) (mean±SD, P1-2; patient 1-2, * = P≤ 0.05; ** = P≤ 0.01; *** = P≤ 0.001, n=3, One way ANOVA, Tukey's post hoc test).

6.4.3 Nanovibrational stimulation and phenotypic memory

Maintaining the osteogenic phenotype of MSCs after NS is important for translation into clinics and clinical applications. From the temporal gene study above **(Figure 6.12)**, it was shown that 1-2 weeks of NS possibly provided an adequate dose triggerring osteogenic gene expression. To study whether MSCs can memorize their osteogenic commitments or if their phenotypes were reversible, models of 1- and 2-week NS were created for a phenotypic memory test. CHSCs contraction was allowed after 7 or 14 days and phenotypes were then tested after an additional week (after 7 days of NS) or 2 weeks (after 2 weeks of NS) after the end of NS. The outcomes could suggest the best process for clinical translation in the future production of a handlable, osteogenic scaffold where contraction isues have been considered.

6.4.3.1 Gene expression (1 week-NS and qRT-PCR at week 2)

As the effects of cell seeding number and duration of NS on osteogenic phenotype expression and cell fate memory are unknown, three different cell concentrations (4x, 10x and $20x10^4$ cells/ml) of Stro1 selected MSCs seeded in CHSCs were prepared. CHSCs were nanovibrated for 1 week. After this stimulation, hydrogels were allowed to contract onto the sponge by detaching them from the wells. CHSC cultures were then maintained in incubator for a further week. At week 2, phenotypic studies were performed by qRT-PCR. The increased trend of osteogenic gene upregulation in N90 group including osterix, osteonectin, osteopontin and alkaline phosphatase were noted but they were not significant. Theoretically, cell-seeding concentration can affect differentiation. Bitar M et al, showed a cell density of 10^6-10^7 cells/ml can increase RUNX2 and osteonectin transcriptions (Bitar et al., 2008). However, no significant effect of cell seeding concentration on osteogenic induction was noted **(Figure 6.13)**. As loading MSCs with $4x10^4$ cells/ml in CHSCs used less cell but

provided the best osteogenic induction, this was selected to go forwards.

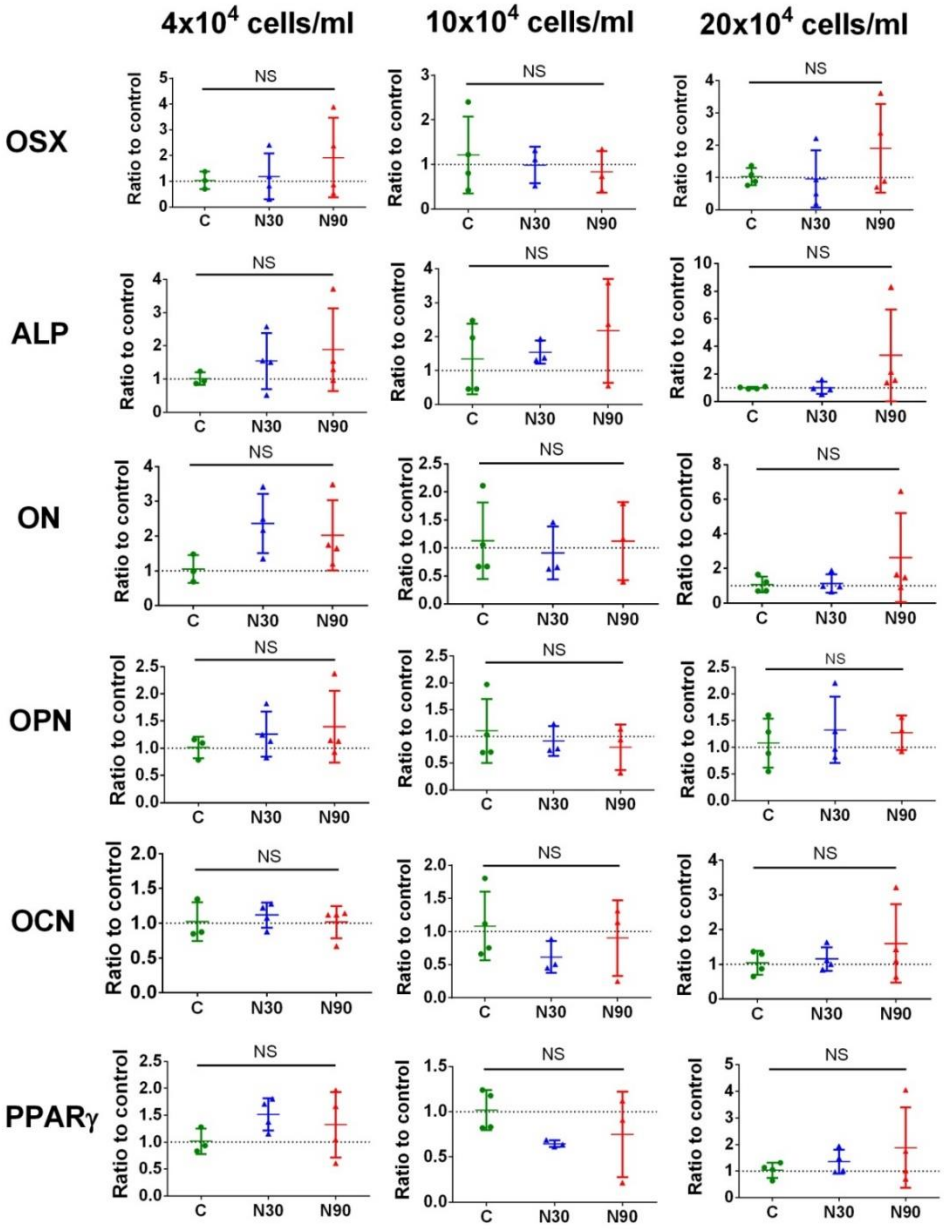

Figure 6.13 qRT-PCR at week 2 after 1 week-NS

qRT-PCR at day 14 showed the trend of osterix, alkaline phosphatase, osteonectin and osteopontin gene upregulation in N30 and N90 groups. No significant effect of cell concentration on osteogenic gene expression was noted. The $4x10^4$ cell/ml appeared to provide the best osteogenic induction results (mean±SD, n=4, * = P≤ 0.05; ** = P≤ 0.01; *** = P≤ 0.001, Tukey post hoc test, Dunn's post hoc test).

6.4.3.2 Gene expression (2 week-NS and qRT-PCR at week 4)

The previous experiment showed that 1 week-NS can produce only a very slight evidence of osteogenesis in CHSCs **(Figure 6.13)**, the next experiment was designed to increase duration of stimulation to 2 weeks. The $4x10^4$ cells/ml of Stro1-selected MSCs seeded in CHSCs were used in this study. After 2 weeks of stimulation, hydrogels were allowed to contract onto the sponge and then cultured without stimulation up to 4 weeks. qRT-PCR at week 4 showed RUNX2 and osteonectin (ON) were significantly increased in N90 group **(Figure 6.14)**. This result indicated that 2 week-NS with N90 triggered osteogenic commitment driving MSCs into preosteoblasts. ALP, OPN and OCN expression were not changed **(Figure 6.14)**. ALP plays a role in hydrolysing organic to inorganic phosphate. Thus, no induction of ALP may affect mineralization through inorganic phosphate reduction (Orimo, 2010; Siffert, 1951). As the increase trend of OPN was found at week 2-3 in previous temporal gene study **(Figure 6.12)**, the lack of change in OPN and OCN at week 4 **(Figure 6.14)** may also affect bone remodelling (Icer & Gezmen-Karadag, 2018).

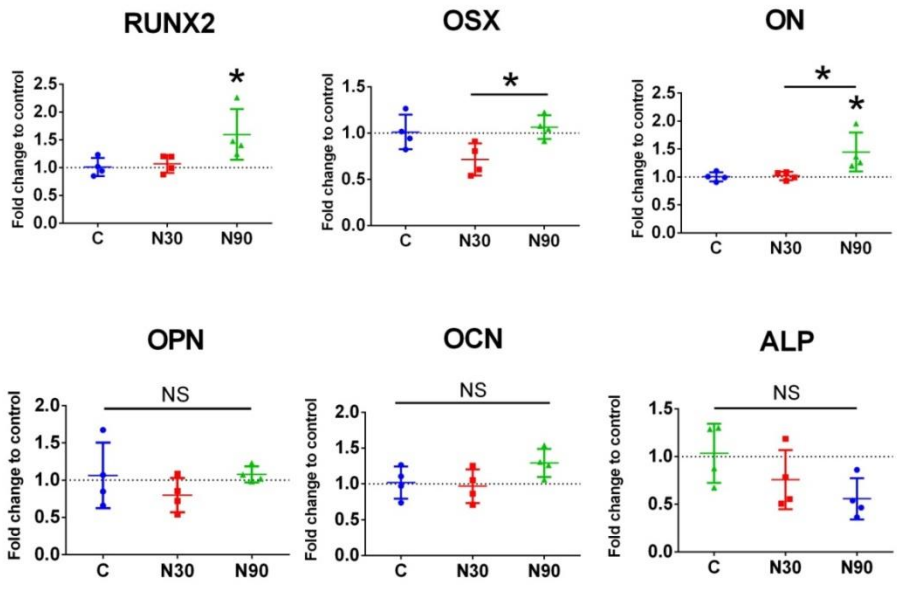

Figure 6.14 qRT-PCR at week 4 after 2 weeks-NS

Only RUNX2 and ON were significantly upregulated in N90. The result indicated that N90 potentially committed MSCs to preosteoblasts in this regime. (mean ± SD, n=4, * = P≤ 0.05; ** = P≤ 0.01; *** = P≤ 0.001, One way ANOVA, Tukey's post hoc test).

6.4.3.3 Protein expression (2 weeks-NS and western blot at week 3)

As qRT-PCR at week 4 (after 2 weeks-NS) showed low levels of OPN, this was investigated further and OPN expression at week 3, after 2 weeks of NS, was conducted. The $4x10^4$ cells/ml of Stro1-selected MSCs seeded in CHSCs was stimulated for 2 weeks. After that CHSCs were detached allowing hydrogel contraction onto the sponge and cultured for a further week without NS. Western blots were performed at week 3. An increased, non-significant, trend of OPN was found in the N90 group **(Figure 6.15).**

Summarising the NS memory tests, 2 week-N90 stimulation can induce osteogenic gene expression showing the successful up-regulation of RUNX2 (week 1) and osterix (week 2) **(Figure 6.12)**. This result indicates that MSCs are slowed in their progression and are possibly at the preosteoblast stage after the stimulation and rest. Summary diagram was shown in **Figure 6.16**.

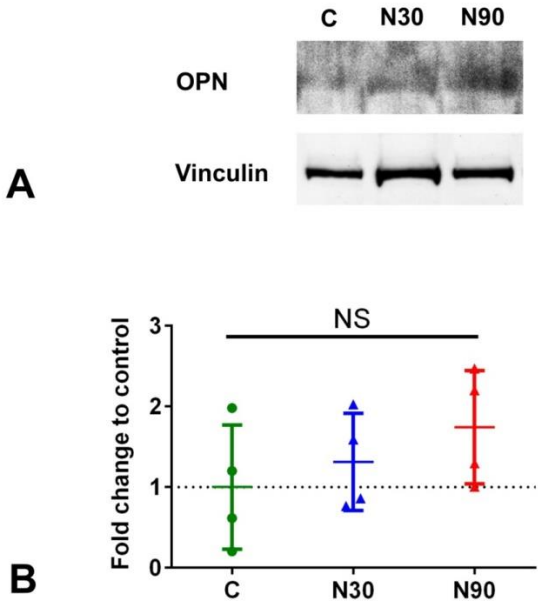

Figure 6.15 Western blot of osteopontin at week 3 post 2 week-NS

After 2 weeks of NS, CHSCs contraction was allowed. Western blot study showed a trend of OPN protein upregulation in N90 at week 3. The result indicated that after 2 week-NS, MSCs possibly

memorized osteogenic expression upto week 3 (mean±SD, n=4, One-way ANOVA, Tukey's post hoc test).

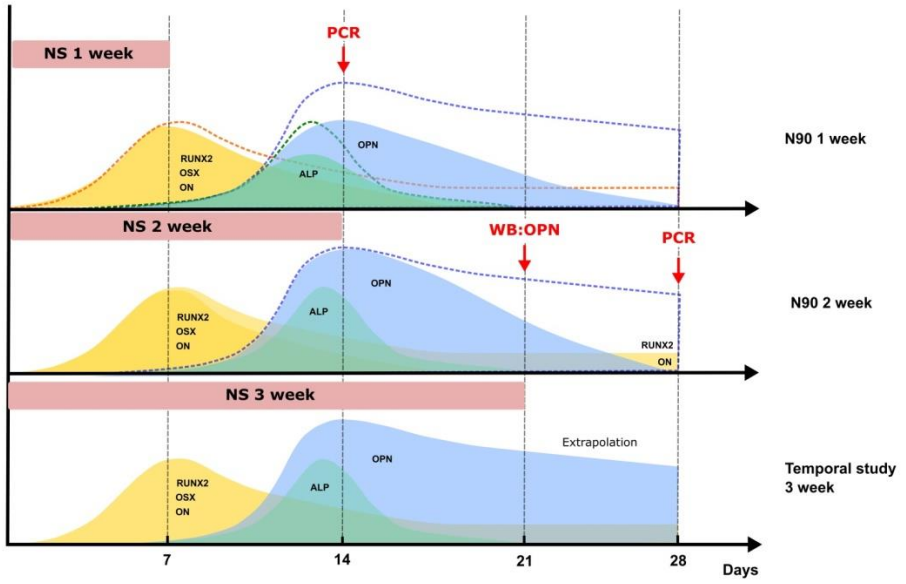

Figure 6.16 The summary of phenotypic memory test after stimulating with 1 week- and 2 weeks- N90 protocol in CHSC.

Stimulating with 1 week-N90 was inadequate to induce osteogenesis. Interestingly, 2 weeks of N90 stimulation was possibly adequate to commit MSCs at preosteoblast stage showing by significant upregulations of RUNX2 and ON at week 4.

6.5 Discussion

6.5.1 CHSC; the clinical application model for NS and rationale of 1-2 week NS protocol.

Collagen type I hydrogels provide a range of biological advantages (Antoine, Vlachos, & Rylander, 2014). Hydrogel stiffness is compatible with a hematoma which is formed in the initial phase of fracture healing (Ryan et al., 1999). The increase in cell number by collagen supporting proliferation (Chinnapaka Somaiah et al., 2015) as well as permitting differentiation, increase cell contractile force, known to be important for osteogenesis (Darinka D. Klumpers, Xuanhe Zhao, David J. Mooney, & Theo H. Smit, 2013; Kumar, Placone, & Engler, 2017), but that can result in gel contraction. This contraction, at the

wrong time can be problematic as once detached, the vibrations do not transmit faithfully.

The CHSC combined the advantages of hydrogel and sponge together. Hydrogels provide biological advantages such as allowing the distribution of nutrients, growth factors and oxygen, which are essential for the cell differentiation process (Hesse et al., 2010). Preparing cells in hydrogels can prevent cell sedimentation onto the bottom of the tissue culture wells, therefore improving MSCs distribution and attachment onto the sponge. On the other hand, the rigid sponge improves mechanical property of the scaffold. The sponge inside the hydrogel can also act to stop further hydrogel contraction, maintaining composite structure and extending the degradation time. Thus, control of contraction using the sponge results in a more handleable structure. Moreover, gel contraction can increase spatial cell-to-cell interaction (D. D. Klumpers, X. Zhao, D. J. Mooney, & T. H. Smit, 2013). In our study, the hydrogel creates the bonding to the rim of tissue culture wells. This hydrogel-well bonding, however, can be overcome by cell traction forces. Therefore, the time of hydrogel contraction can be chosen by controlling the force balance at the rim of well plate and hydrogel. At 2-3 days after hydrogel detachment, the hydrogels had contracted onto the sponges. The results showed that CHSC contraction can be made to be controllable and reproducible **(Figure 6.5)**.

Next, the protocol that would allow the stimulated MSCs in CHSCs to be used for clinical application, was developed. The “1 week-NS protocol” was initially tested by stimulating CHSCs for 1 week with high amplitude stimulation (N90; 90 nm). The rationale is based on trauma patient scenario and the theory of cell mechanical memory after adequate exposure of mechanical stimulation (approximately 10 days) that results in irreversible phenotype (C. Yang et al., 2014). However, only a trend rather than statistical difference at this time point was observed. Next, NS duration was extended to 2 weeks. Phenotypical study at week 4 showed that MSCs were committed to preosteoblasts as shown by enhanced RUNX2 and OSX expression.

However, evidence of mineralization (by ALP) and remodelling (by OPN) were not obviously found.

6.5.2 Nanovibrational stimulation and mechanical response of CHSCs

In this study, collagen sponges were produced to study the effects of NS in CHSCs. It was demonstrated that the NS bioreactor is reliable with CHSCs and generates tunable stimulating amplitude by adjusting the voltage **(Figure 6.6A)**. **Figure 6.6B and C** possibly explained that the CHSCs vibrated as circular membrane (e.g. a drumhead) in a standing wave pattern with greatest displacement at the centre. It was also found that incorporating the sponge into hydrogel changed the resonance frequency (**Figure 6.7**). To explain this phenomenon, it can be implied that during NS, the hydrogel is displaced in the culture plate well, driven by the stimulating frequency (1,000 Hz) without energy loss and thus each hydrogel is displaced with its own natural frequency in a simple harmonic motion. The natural frequency of hydrogels can be explained by the equation below.

$$f = \frac{1}{2\pi}\sqrt{\frac{k}{m}} \qquad (1)$$

Therefore, the change of mass (m) or elastic property (spring constant; k) results in changes in the hydrogel natural frequency. The resonance phenomenon represents that the external stimulating frequency (NS) equal to the natural frequency of the system resulting in amplification of gel displacement amplitude and showing a high peak of gel displacement. From **Figure 6.7**, the addition of sponge into the hydrogel increases mass (m) of the stimulated composite. Consequently, it reduces the natural frequency of the CHSC representing the reduction of resonance frequency.

The change of amplitude in the CHSC during NS can be explained by Newton's second law and Hooke's law as follows;

Newton's second law;	F	= ma
Hooke's law;	F	= -kx
Therefore,	ma	= -kx

(2)

Regarding equation (2), the increase of mass (m) amplifies the displacement of object (x). In a hydrogel without the sponge, the stimulation with 19.69 Vpp generated 91 nm average hydrogel displacement while in the CHSC (addition of mass [sponge] into the system), amplitude was increased to approximately 150 nm at the sponge zone **(Figure 6.6A)**.

As aforementioned, the variation of amplitude due to changing the composite can be solved by tuning the stimulating voltage. At 1000 Hz, amplitude in CHSC was slightly increased compared to hydrogels alone, but it is reproducible without random vibrations occurring and can be tuned to achieve a 90 nm average.

6.5.3 Biological response in CHSCs; cell concentration, cell differentiation and phenotype memory theory

In this study, it was demonstrated that CHSCs using the hydrogel contraction concept are biocompatible in terms of cell viability. Some literature has shown that the effect of gel contraction can provide unfavorable results such as cell apoptosis (Y. K. Zhu et al., 2001). However, in this study, the contraction was limited using the sponge and the effect of gel contraction was tested at three different cell concentrations. The Alamar Blue assay indicated that cell activity of the contracted CHSCs increased compared to that of the non-contracted CHSCs **(figure 6.11A)**. It was also noted that MSCs tended to migrate toward the sponge in pre- and post-contracted CHSCs **(figure 6.9 - 6.10)**.

During NS, the increase of percentage of Alamar Blue reduction indicated that NS is an energetic process. Alamar Blue can be reduced by NADPH, FADH and cytochromes (Ehrbar et al., 2011). These

cofactors are involved in catabolism and anabolism. Together with the data in chapter 5, it was found that NS involved in lipid metabolism as well as increased osteogenic phenotype. Thus, we could imply that NS in the CHSCs potentially drives the cell differentiation process.

Again, in this study, the contracted CHSCs had higher cell metabolic activity compared to non-contracted CHSCs **(Figure 6.11A).** It was hypothesised that this change was linked to energy consumption of MSCs in order to migrate within the higher dense 3D matrix (contracted hydrogel). Microscopic images showed cell migration velocity in the pre-contracted CHSC was significantly faster than those in the post-contracted CHSCs. From the literature, it has been previously shown that contracted collagen hydrogels provide a dense collagen fiber architecture, driving cells to consume greater ATP during migration compared to pre-contracted gels (Zanotelli et al., 2018). Also in 3D matrices, matrix stiffness and pore size have been shown to affect cell differentiation (Petrie & Yamada, 2015). Cells form focal adhesions in direct correlation to increasing stiffness and transfer mechanotransductive signals to the nucleus. Stiff surfaces can induce MSC osteogenesis while soft surfaces direct MSC towards adipogenesis (Engler et al., 2006). During cell migration through small pores, cells are squeezed and subsequently transfer mechanical signal to their nuclei (Fruleux & Hawkins, 2016; Petrie & Yamada, 2015). The increase of matrix stiffness could increase the reaction force interaction to the cell nucleus enhancing YAP (Yes-associated protein) influx (Dalby, Garcia, & Salmeron-Sanchez, 2018). YAP/TAZ is a pathway which links to differentiation control by mechanical cues (Codelia, Sun, & Irvine, 2014; J. X. Pan et al., 2018; Piccolo, Dupont, & Cordenonsi, 2014). This concept triggered our curiosity to further study the effect of the contracted CHSCs on MSCs differentiation. It was hypothesised that the reduction of pore size in contracted hydrogels might modulate cell differentiation by directly deforming nuclear shape as well as relatively increasing cytoskeletal tension during migration. Moreover, the increase of metabolic activity in the contracted hydrogel might be related to the increase of oxygen consumption, ROS production and oxidative phosphorylation consequently affecting MSC differentiation e.g. osteogenesis (Arakaki, Yamashita, Niimi, & Yamazaki, 2013). Theoretically, the matrix stiffness which can drive osteogenesis, is very rigid (25-40 kPa) (Engler et al., 2006). However, some literature reports the effect of 3D collagen hydrogel contraction on driving osteogenesis (D. D.

Klumpers et al., 2013). In our study, the effect of hydrogel contraction onto the sponge was initially aimed at improving handleability and extending the material degradation time.

From the temporal gene study **(Figure 6.12)**, nanovibration sucessfully promoted osteogenic gene expression in CHSCs. However, the evidence of osteogenic phenotype was less clear than that of the constant NS **(Figure 6.13, 6.14)**. In theory, adequate duration and intensity of mechanical stimulation can commit an irreversible phenotype and NS is considered to be a mechanical stimulation (Tsimbouri P.M., 2017). Cells sense the mechanical environment using their cytoskeletons. Mechanical signals are transfered to the nucleus via actin and myosin by cytoskeletal tension change (K. H. Vining & D. J. Mooney, 2017). YAP/TAZ is important for mechanosensing and phenotype memory. YAP transfers mechanical signal via Rho-GTPase-dependent translocation to the nucleus (Driscoll, Cosgrove, Heo, Shurden, & Mauck, 2015). Influx and accumulation of YAP into the nucleus initiates the onset of osteogenic differentiation. Force intensity and duration link to YAP transport through the nuclear pores. Sufficient force allows YAP nuclear translocation into the nucleus (Elosegui-Artola et al., 2017; Panciera, Azzolin, Cordenonsi, & Piccolo, 2017). Exposure to adequate duration and intensity of mechanical stimulation thus results in irreversible phenotype (C. Yang et al., 2014) while inadequate force stimulation causes phenotype reversibility (Cui et al., 2015). The hypothesis of NS effect on cell memory is shown in **Figure 6.17**. Further studies of NS effect on YAP/TAZ pathway would need to be performed in future work.

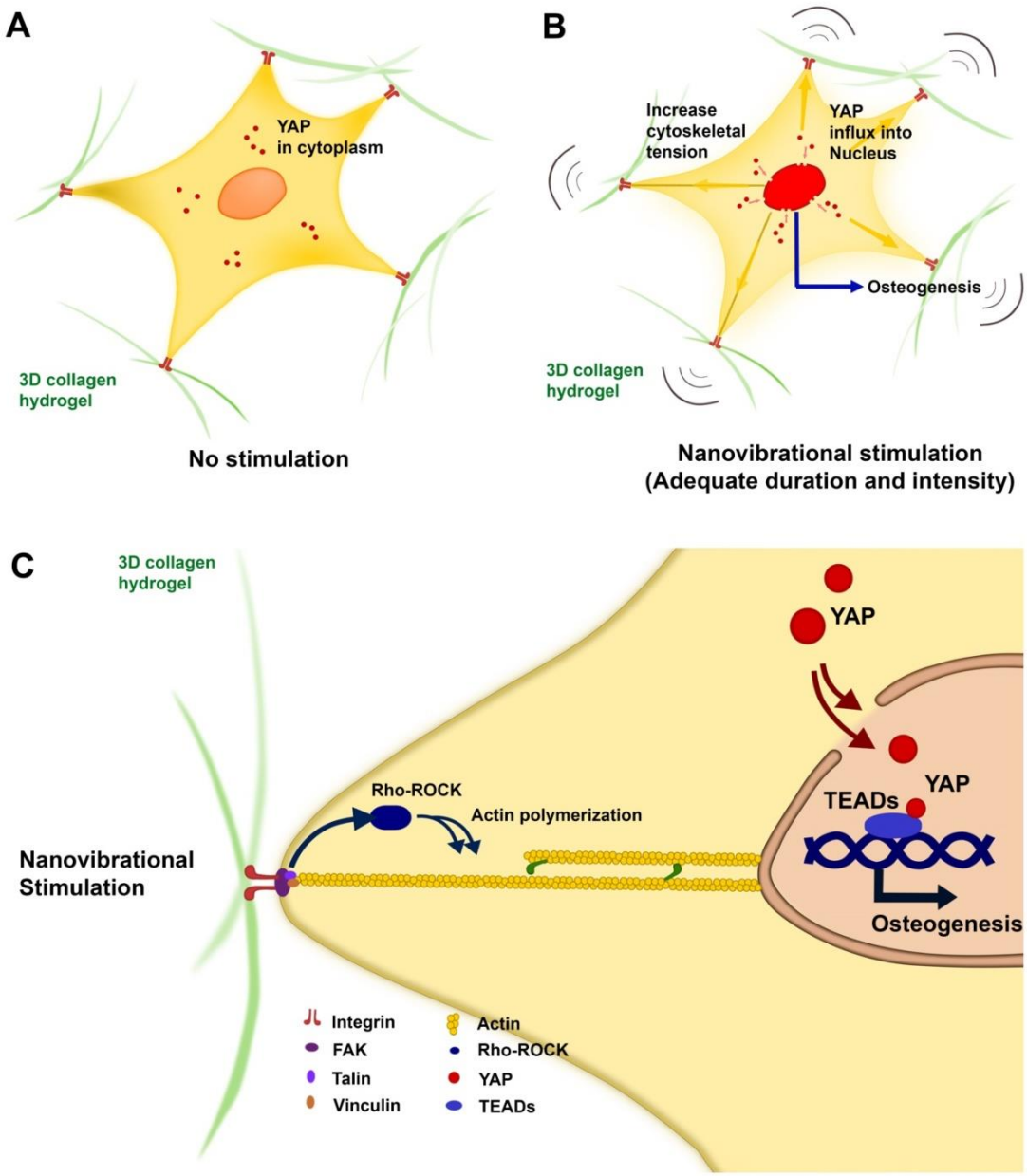

Figure 6.17 Hypothesis of mechanical memory and nanovibrational stimulation for 3D osteogenesis

A) In non-stimulated MSCs, YAP remains in the cytoplasm. B) With adequate stimulation amplitude and duration, NS potentially increased cytoskeletal tension, in turn, there was an enhanced YAP influx into the nucleus thus driving osteogenesis. C) During NS, MSCs attach to the ECM via focal adhesions including integrins, which then enhance the Rho-ROCK pathway for actin polymerization and myosin II activation (Parsons, Horwitz, & Schwartz, 2010). The increase of cytoskeletal tension could stretch nuclear pores resulting in YAP influx into

the nucleus (Elosegui-Artola et al., 2017). Subsequently, YAP coactivated with TEA domain-containing sequence-specific transcription factors (TEADs) drive osteogenesis

6.6 Conclusion

We are stepping towards translation of NS into a handlable format and trying to workout a robust and short NS protocol. Our composite is safe for cell viability and allows a controllable nanovibrational force transmission. NS enhanced osteogenic gene expression in the CHSCs. An extension of the duration of stimulation may improve phenotype expression without reversibility.

Chapter 7 General discussion and conclusion

Chapter 7 General discussion and conclusion

7.1 General discussion

In this section, interesting issues are discussed to help identifying further studies in the future. The ideas and concepts of improving the NS protocol and introducing scaffolds into clinics are also proposed.

7.1.1 Amplitude, frequency or accerelation (g); which parameter should be focused on?

Low-magnitude high-frequency vibration (LMHFV) for osteogenic induction is studied with use of a diverse range of stimulating protocols **(Chapter1, Table 1.4)**. Considering the literature, osteogenic induction has been achieved using 0.3 g of acceleration but with varying frequencies and amplitudes (Lau et al., 2011; Marędziak et al., 2017; Mehta et al., 2018; Q. Zhao et al., 2017; Y. Zhou et al., 2011) **(Chapter1, Table 1.4)**. Interestingly, in this thesis, increasing the NS amplitude from 30 nm (0.12 g at 1000 Hz (Tsimbouri P.M., 2017)) to 90 nm (0.36 g at 1000 Hz) showed significantly increased osteogenesis where the acceleration corresponded to those of other LMHFV protocols. Considering the theory of simple harmonic motion (Garrett, 2017; Kett, 1982; "Simple harmonic motion," 2007), the relationship between accerelation, stimulating amplitude and frequency are shown in the equation below.

$$A = (a)(2\pi f)^2$$

Where A = acceleration (1g = 9.81 ms^{-2})

a = amplitude

f = frequency

From the equation, squaring of a slight increase of frequency results in a large change of acceleration while an increase of amplitude directly corresponds to the acceleration in a linear pattern (when using a constant frequency). As shown in the phenotypic and metabolomic studies, the change of NS amplitude on the nanoscale (from 30 to 90 nm) can display the alteration of cellular response from low (by N30) to high levels (by N90) of osteogenesis. Thus, nanoscale

amplitude or acceleration is a good parameter to consider for further studies.

7.1.2 Mechanisms and pathways

This study clearly elucidated that NS induces osteogenesis through multiple pathways, not only by a single pathway. It was hypothesised that high amplitude stimulation probably generates multiple stimuli such as stretching on the cell membrane, fluid shearing or heat, which in turn induces osteogenesis through various types of cellular membrane receptors. Simultaneously, high amplitude stimulation also produces low grade inflammation which is important to promote mineralization and recruit precursor cells for enhancing osseointegration and vascularization into scaffolds in the *in vivo* phase. The high amplitude stimulation also produces low level of controllable ROS. However, the overall outcome of NS favors high levels of osteogenesis.

7.1.3 Oxidative stress and Inflammation

In chapter 5, it was shown that NS induces oxidative stress and low-grade inflammation without reducing osteogenesis. However, oxidative stress and inflammation are double-edged swords. Controllable and low-grade ROS enhances diverse intracellular signalling pathways including osteogenic signals (Atashi et al., 2015) while uncontrollable or chronic ROS exposure induces detrimental effects such as cell senescence and DNA damage (Droge, 2002) as well as suppressing osteogenesis but inducing adipogenesis (M. Arai et al., 2007; C. H. Lin et al., 2018); low levels of inflammation enhance osteogenesis (R. L. Huang et al., 2018; Y. Li, Backesjo, Haldosen, & Lindgren, 2008; M. Sun et al., 2017) but chronic or high levels can suppress osteogenesis (Lacey et al., 2009). As NS amplitude is adjustable and stimulating duration is controllable, the effect of long-term exposure and high intensity of NS should be conducted to define an upper limit of stimulation.

To overcome the current strategy of bone defect treatments, such as distraction osteogenesis provides a good treatment outcome but takes a long time and is costly, NS needs to rapidly enhance osteogenesis. Increasing NS amplitude beyond 90 nm aiming to gain quicker and higher osteogenic phenotype expression could be trialed. As shown by

our results, the increase of NS amplitude concomitantly induced greater oxidative stress and inflammation. Thus, pre-treating MSCs with anti-inflammatory (e.g. NSAIDs) or anti-ROS (e.g. N-acetyl cysteine; NAC) drugs may help controlling inflammation and oxidative stress in very high amplitude stimulation (>90 nm). Some evidence showed that NAC may improve osteogenesis (Ji, Liu, Zhao, & Zhang, 2011; Yamada et al., 2013). However, NSAIDs treatment may reduce bone formation (I. Pountos, Georgouli, Calori, & Giannoudis, 2012; Ippokratis Pountos et al., 2011; Yoon et al., 2010), thus pre-treatment inflammation protocols need to be considered with care. Patterning of NS stimulation with resting intervals is another option to balance the oxidative stress products if the study of 3D osteogenesis in the hydrogel with very high amplitude stimulation (>90 nm) is carried out to accelerate osteogenic gene expression. The phenotypic studies of NS stimulation-resting intervals are needed to avoid either overdose stimulation (from long duration of very high intensity NS exposure) resulting cell apoptosis or phenotypic reversibility (from a long time of NS free-interval) ending up with osteogenic induction failure.

7.1.4 Reversibility and gel-sponge composite

It was shown that the cell-hydrogel-sponge composite (CHSC) concept is possible for osteogenesis and the 2 week-N90 stimulation is adequate for preosteoblast commitment. However, OPN which is important for mineralization and bone remodelling (Lund et al., 2009; P. J. Thurner et al., 2010) was downregulated at week 3 **(Figure 6.15)**. Optimistically, the decrease of OPN is possibly compensated by the host-inflammatory response at the surgical site after post scaffold implantation surgery. Considering an induced membrane surgical technique or Masquelet technique (two-step surgery which allows the host to create a self membrane pouch for autograft implantation (Giannoudis et al., 2011)), this membrane secretes transcription factors such as BMP2, TGFβ and inflammatory cytokines including IL-6 (Toth et al., 2019). OPN plays a role not only in regulating osteoclast function but also affecting inflammatory cells (Florian Kahles, Hannes M. Findeisen, & Dennis Bruemmer, 2014). Further, it is known that IL-6 can upregulate OPN expression, as it is found in macrophages (Uchibori et al., 2017). Thus, in post scaffold-implantation surgery, if the host generates an optimal inflammation (in turn producing optimal level of IL-1β and IL-6), we could extrapolate that OPN (enhanced by the inflammatory niche) may continuously promote the

remodelling process of mineralized scaffold in *in vivo* study (Florian Kahles et al., 2014; Lund et al., 2009; P. J. Thurner et al., 2010).

7.1.5 Cell sources and quality

Regarding this thesis, the success of NS induced osteogenesis is strongly related to 'cell quality', and pre-stimulated MSC status affects the stimulation outcome. A high degree of subculturing (more than passage 3) risked poor osteogenic responses. Moreover, cell senescence, over density/overgrowth of cell culture, high passages can change NFκB level (Hellweg, Arenz, Bogner, Schmitz, & Baumstark-Khan, 2006). To minimise this problem, developing cell status screening techniques or protocols (before NS) may improve NS induction outcomes and save costs from failed experiments.

Stem cell seeded scaffolds for large bone defect treatment is challenging as it requires an extremely large number of cells. However, autologous bone graft sources, commonly derived from iliac crest, are inadequate. Other cell types such as iPSCs and ESCs may be alternative options for NS in the future.

7.1.6 Future design scaffolds for NS

The concept of the biphasic scaffold is an upcoming trend in bone tissue engineering providing both structural support (via the rigid phase) and biological enhancement (via the hydrogel phase). Our cell-gel-sponge composite is a simple model which can be implemented with various type of scaffolds such as 3D bioprinted scaffolds. However, changing the scaffold form and structure can change the cell response pathways; thus, biological responses analysis needs to be repeated.

Developing bone scaffolds for clinical applications is challenging. They need to provide not only the mechanical support but also the biological advantages. Moreover, they have to contribute to osteogenic and angiogenic inductions. Together with NS, the scaffolds may be supplemented with growth factors such as BMP2 and VEGF for fast driving of osteogenesis and vascular formation. As bone loss often results in open fractures, the wound is regularly exposed to microorganisms (Otchwemah et al., 2015) and is prone to be infected (Guerra, Gregio, Bernardi, & Castro, 2017). Developing scaffolds,

which allow NS to enhance osteogenesis and provide an antibacterial effect, is an ideal target in the future (Nair, Kretlow, Mikos, & Kasper, 2011).

7.2 Conclusion

7.2.1 Increased concentration improves hydrogel handleability

Hydrogel contraction is an obstacle in allowing adequate doses of NS for inducing 3D osteogenesis of MSCs within the NS bioreactor. In chapter 3, three strategies including in-gel scaffolds, collagen concentration optimization and genipin crosslinking were trialed to improving hydrogel properties. In conclusion, the in-gel scaffold was discontinued as it did not prevent contraction and was less feasible for potential clinical application. Genipin was also discounted as its cytotoxicity was an unwanted side effect though it could improve hydrogel stiffness. Increasing collagen concentration from 0.8 mg/ml to 1.8 mg/ml was seen to delay hydrogel contraction. This simple approach allows a straight forward strategy.

7.2.2 High amplitude nanovibrational stimulation enhances osteogenesis through multiple pathways

High amplitude stimulation (N90) showed better osteogenic induction than the standard amplitude used in the group (N30). High amplitude stimulation increased osteogenic gene and protein expression at day 9 and did not effect MSC viability. From a temporal gene study, N90 induced osteogenic gene expression corresponding to a normal osteogenic pattern. N90 significantly induced TRPV1, piezo2, ion channels and ERK1 which corresponded well to Tsimbouri et al (Tsimbouri P.M., 2017) showing that N30 stimulates TRPV1-PKC-β-catenin to induce bone differentiation in MSCs (Tsimbouri P.M., 2017). N90 stimulation tended to involve the BMP2-SMAD1/5 and ROCK pathways in 3D culture suggesting that high stimulating amplitude

possibly activated more osteogenic pathways through BMP2 and cytoskeletal tension regulations.

7.2.3 NS enhanced osteogenesis and produced controllable oxidative stress and inflammation

The metabolomic study showed that N90 stimulation involved lipid metabolism and produced low levels of oxidative stress which is well regulated through redox balancing and counterregulatory responses such as superoxide dismutase enzyme (a ROS reducing enzyme), NFκB and Akt (anti-apoptosis mechanisms). The evidence of inflammatory responses (such as IL-6, TNFα) was found during N90 NS. Through protein inhibition tests, it was shown that MAPK (JNK, p38) and NFkB positively correlated to RUNX2 and OSX gene expressions. It was hypothesised that N90 enhanced osteogenesis through JNK and p38 MAPK activation. NFκB was produced to control oxidative stress and inflammation. In conclusion, N90 enhances osteogenesis though multiple pathways with low levels of ROS and inflammation.

7.2.4 Cell-hydrogel-sponge composite potential for clinical use

From our study, we proposed the CHSC to use with the NS bioreactor. CHSCs are reproducible and handlable in the clinic. CHSCs allowed NS force transmission and produced reliable stimulating amplitudes. Contracted CHSCs did not adversely effect MSC viability. Temporal gene studies showed that NS promoted osteogenesis corresponding to the normal osteogenic pattern. It was found that 2 week-NS in CHSCs possibly maintained osteogenic phenotype. The results can be used to develop the NS protocol for osteogenic induction without phenotypic reversibility and could be useful in *in vivo* studies and clinics in the future.

Appendix I

Appendix I

Protein antibody microarray

Processed by Dr Marc Antoni Fernandez-Yague, Centre for Research in Medical devices, National University of Ireland, Galway.

Protein samples were labeled with Alexa Fluor 555 carboxylic acid succinimidyl ester (Life Technologies, CA, USA). Excess label was removed and buffer was exchanged with PBS, pH 7.4, by centrifugation through 3 kDa molecular weight cutoff filters. Absorbance at 555 and 280 nm was measured for labeled samples and calculations were performed according to the manufacturer's instructions using an arbitrary extinction coefficient of 100 000 and molecular mass of 100 000 to enable quantification of relative protein concentration and label substitution efficiency. All commercial antibodies **(Table AI.1)** were buffer exchanged into PBS and quantified by bicinchoninic acid (BCA) assay. Antibodies were diluted to print concentration in PBS and printed in six replicates on Nexterion H amine reactive, hydrogel coated glass slides (Schott AG, Mainz, Germany) using a SciFLEXARRAYER S3 piezoelectric printer (Scienion, Berlin, Germany) under constant humidity (62% +/− 2%) at 20°C. Each feature was printed using ≈1 nL of diluted antibody using an uncoated 90 µm glass nozzle with eight replicated subarrays per microarray slide. After printing, slides were incubated in a humidity chamber overnight at room temperature to facilitate complete conjugation. The slides were then blocked in 100×10^{-3} m ethanolamine in 50×10^{-3} m sodium borate, pH 8.0, for 1 h at room temperature. Slides were washed in PBS with 0.05% Tween 20 (PBS-T) three times for 2 minutes each wash followed by one wash in PBS, dried by centrifugation (470 × g, 5 min), and then stored with desiccant at 4 °C until use. Incubations were carried out in the dark. Microarray slides were incubated essentially as previously described. Initially, one labeled sample was titrated (2.5–15 µg mL^{-1}) for optimal signal to noise ratio and all samples were subsequently incubated for 1 h at 23 °C at 9 µg mL^{-1} in Tris-buffered saline (TBS; 20×10^{-3} m Tris-HCl, 100×10^{-3} m NaCl, 1×10^{-3} m $CaCl_2$, 1×10^{-3} m MgCl2, pH 7.2) with 0.05% Tween 20 (TBS-T). All microarray experiments were carried out using three replicate slides. Alexa Fluor 555 labeled mesenchymal stem cells lysate (10 µg mL^{-1}) were incubated in two separate subarrays on every slide to confirm retained antibody performance and printing,

respectively. After incubation, slides were washed three times in TBS-T for 2 minutes per wash, once in TBS and then centrifuged dry as above. Dried slides were scanned immediately on an Agilent G2505 microarray scanner using the Cy3 channel (532 nm excitation, 90% photomultiplier tubes (PMT), 5 µm resolution) and the intensity data were saved as a .tif file. Antibody microarrays were verified to remain active for at least 2 weeks after printing, and all incubations were carried out within that timeframe. Data extraction from .tif files was performed essentially as previously described. Data were normalized to the mean of three replicate microarray slides (subarray-by-subarray using subarray total intensity, n = 3, 18 data points).

Table AI. 1 List of commercial antibodies used in the protein antibody microarray

Probe	Concentration (mg/mL)	Information	Company	Stock conc (mg/mL)	Cat. no.	Lot	Species
Integrin β1	1	Integrin β1 [EPR1040Y] 100µl (0.157 mg/ml)	Abcam®	3.54	ab134179	GR97005-9	Rabbit
Integrin β3	0.1	Integrin β3 [crc54]	Abcam®	0.17	ab34409	GR31565-1	Rabbit
Integrin β5	<0.002	Integrin β5	Cell signalling®	<0.002	D24A5	3629S	Rabbit
BMPR1A	1	BMPR1A 800 µg	ThermoFisher®	12.71	PA5-11856	SH30123J	
Collagen I	1	Collagen I [EPR7785] 100 µl (0.875 mg/ml)	Abcam®	1.72	ab138492	GR247379-29	Rabbit
Collagen II	0.25	Collagen II [2B1.5] 250 µl (0.2 mg/ml)	Abcam®	2.29	ab185430	GR322394-1	Mouse
Collagen III	0.5	Collagen III 100 µg (1mg/ml)	Abcam®	1.03	ab7778	GR312095-3	Rabbit
Collagen V	1	Collagen V 100 µg (1mg/ml)	Abcam®	1.86	ab7046	GR255156-3	Rabbit
KCNK2	1	TREK-1 Antibody (C-20)	SantaCruz®	4.84	sc-11557		
KCNK4	0.02	KCNK4 100 µl (0.5mg/ml)	Abcam®	0.02	ab81367	GR193770-5	Rabbit
TRPA1	0.5	ANKTM1 (C-19)	SantaCruz®	5.45	sc-32353	-	Goat
TRPV1	1	VR1 (H-150)	SantaCruz®	6.06	sc-20813	-	Rabbit
PIEZO1	1	PIEZO1 Antibody (N-15)	SantaCruz®	3.13	sc-164319	-	Goat
PIEZO2	1	PIEZO2 Antibody (G-20)	SantaCruz®	2.99	sc-84763	-	Goat
L-type Ca^{2+}	0.5	Anticorps L-type Ca^{2+} CP α1C (H-280)	SantaCruz®	4.98	sc-25686	-	Rabbit
β-actin	1, 0.25, 0.5, 0.75, 2	IBA1	WAKO®	2.56	019-19741	-	Rabbit

Appendix II

Appendix II

Metabolomic profile assessment

Metabolite selection of glycolysis, PPP, TCA cycle, OXPHOS, L-, L-aromatic amino acid, LC-PUFAs and β-oxidation was performed. These metabolites were carried out using IDEOM. Metabolite intensities were then relatively compared as fold change. Statistical change and P-value were calculated using Graphpad software. The summarized data is shown in **Table AII.1.**

Table AII. 1 Metabolite profile analysis at 1 and 2 weeks of NS

Pathways	week	Metabolites	Metabolite change	Interpretation	Figure
Glycolysis	1	Pyruvate	(NS)	-	A1
	2	Pyruvate	(T)↑ N90	NS may increase energy consumption	A1
	1	Lactate	(T)↑ N30, N90	NS may increase energy consumption	A1
	2	Lactate	(NS)	-	A1
Pentose Phosphate Pathway (PPP)	1	D-gluconic acid	(T)↑ N90	NS may involve PPP	A2
	2	D-gluconic acid	(NS)	-	A2
	1	D-ribose	(NS)	-	A2
	2	D-ribose	(T)↑ N30, N90	NS may involve PPP	A2
TCA cycle	1	Citrate	(T)↑ N90	NS effect	A4
	1	Isocitrate	(T)↑ N90	NS effect	A4
	1	Succinate	(NS)	-	A4
	1	S-malate	(T)↑ N90	NS effect	A4
	2	Succinate	(NS)	-	A4
OXPHOS	1	Sn-Glycerol-3-phosphate	(T)↑ N30, N90	NS effect	A5
	2	Sn-Glycerol-3-phosphate	(T)↑ N90	NS effect	A5
	1	Orthophosphate	(T)↑ N90	NS effect	A5
L-, L-aromatic amino acid	1	L-alanine	(T)↑ N90	NS effect	A6
	1,2	L-phynylalanine	(NS)	-	A6
	1,2	L-tryptophan	(NS)	-	A6
LCPU-FAs	1	Eicosapentaenoic acid	(T)↑ N30, N90	NS effect	A8
	1	Docosapentaenoic acid	(T)↑ N90	NS effect	A8
	1	Docosahexaenoic acid	(T)↑ N90	NS effect	A8
	2	Eicosapentaenoic acid	(T)↑ N90	NS effect	A8
β-oxidation	1	Hexanoic acid	(T)↑ N90	NS effect	A9
	1	4-8 dimethylnonanoylcarnitine	(T)↑ N90	NS effect	A9
	1	O-propanoylcarnitine	(NS)	-	A9
	2	Hexanoic acid	(NS)	-	A9
	2	4-8 dimethylnonanoylcarnitine	(T)↑ N90	NS effect	A9
	2	O-propanoylcarnitine	(NS)	-	A9

↓ decrease; ↑ increase; (S) Statistic significance, (T) Trend, LC-PUFAs= long-chain polyunsaturated fatty acid, NS= nanovibrational stimulation, OXPHOS=oxidative phosphorylation, PPP; Pentose phosphate pathway

Carbohydrate metabolism at 1 and 2 week.

To study effect of NS on carbohydrate metabolism, metabolites involving the glycolysis pathway and TCA cycle were focused. It was found that there were no significant differences in the TCA cycle and glycolysis metabolites of NS group compared to control. Interestingly, lactate tended to increase in N90 at week 1 but reduced at week 2. Pyruvate tended to increase at week 2. This result indicated that MSCs still used glycolysis in N90 **(Figure AII.1)**. Increase trend of ribose and gluconic acid indicated that PPP was involved **(Figure AII.2-3)**. N90 also involved TCA cycle (by increasing trend of citrate, isocitrate and malate in N90) **(Figure AII.4)**.

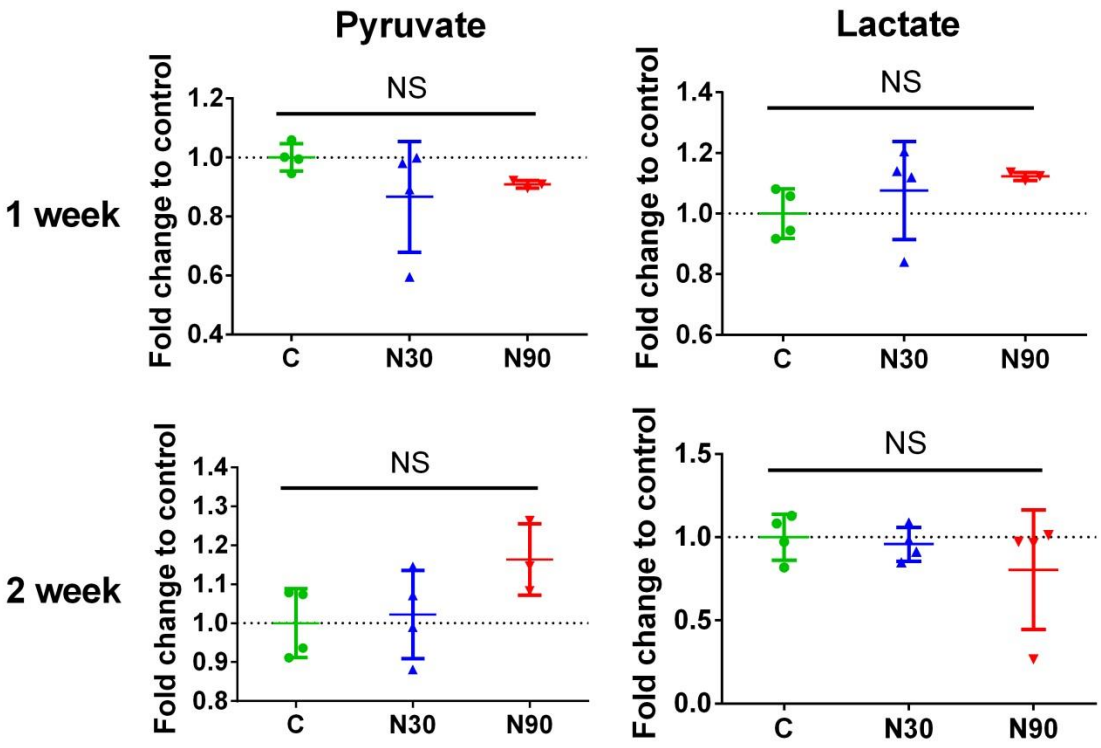

Figure AII. 1 Glycolysis and glucose metabolism

In N90 group, pyruvate tended to increase at week 2 while lactate increased at week 1. The results indicated that MSCs

still produced energy via glycolysis (mean±SD, n=4, * P≤ 0.5, ** P≤ 0.01, *** P≤ 0.001, one-way ANOVA, Tukey's post hoc test).

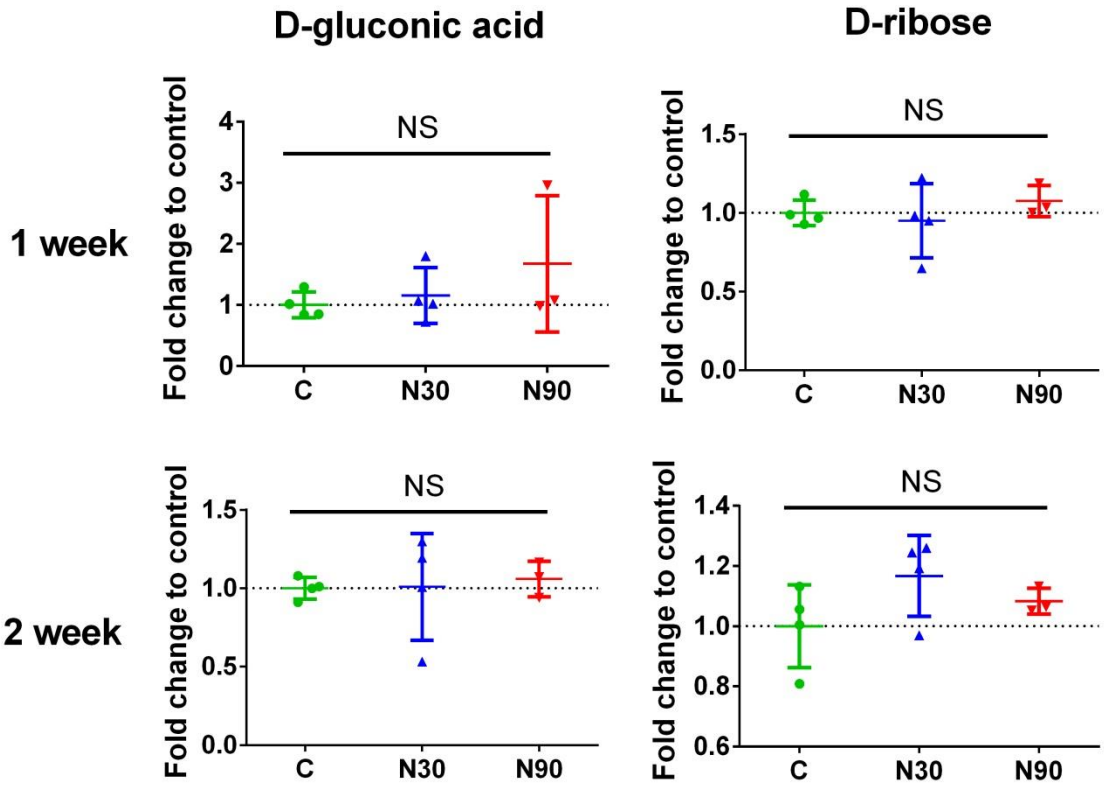

Figure AII. 2 Pentose phosphate pathway

D-gluconic acid and D-ribose were increased in N90 at week 1 and 2. The result may implied that PPP was involved in redox balancing during oxidative stress (mean±SD, n=4, * P≤ 0.5, ** P≤ 0.01, *** P≤ 0.001, one-way ANOVA, Tukey's post hoc test).

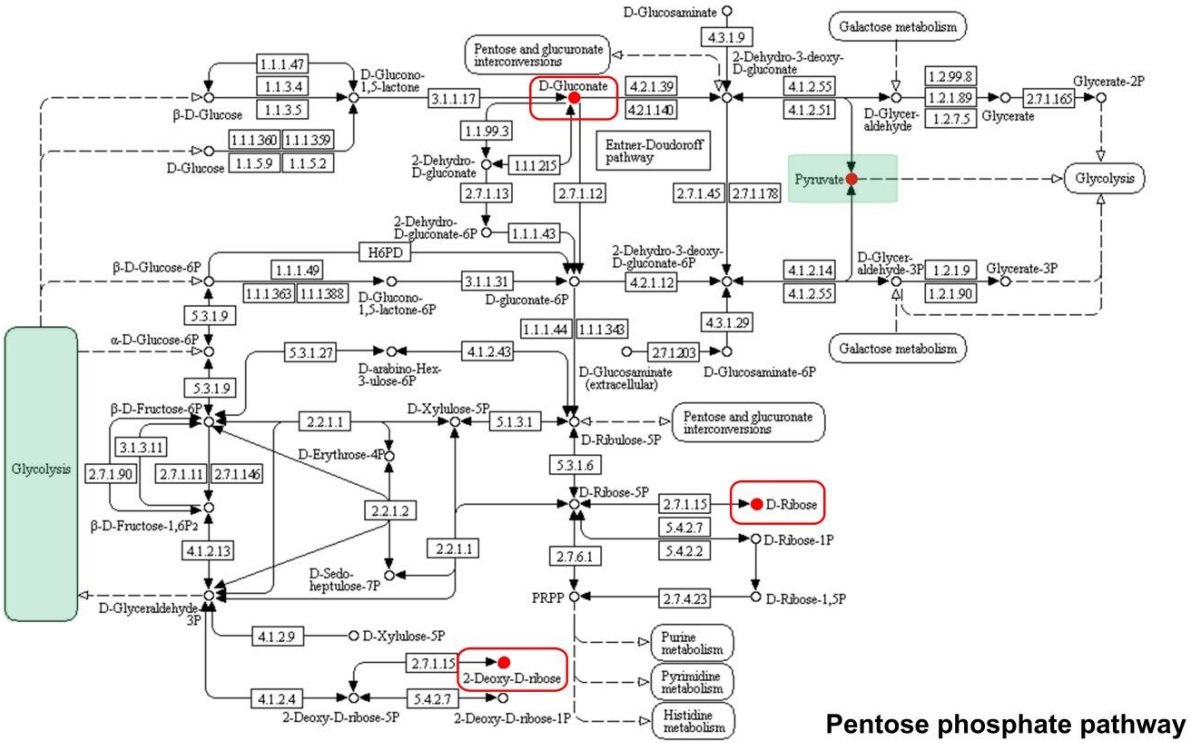

Figure AII. 3 Pentose phosphate pathway KEGG pathway

KEGG pathway shown shifting of glycolysis to pentose phosphate pathway (PPP). D-ribose and D-gluconate, which are PPP metabolites were identified in the map (n=4).

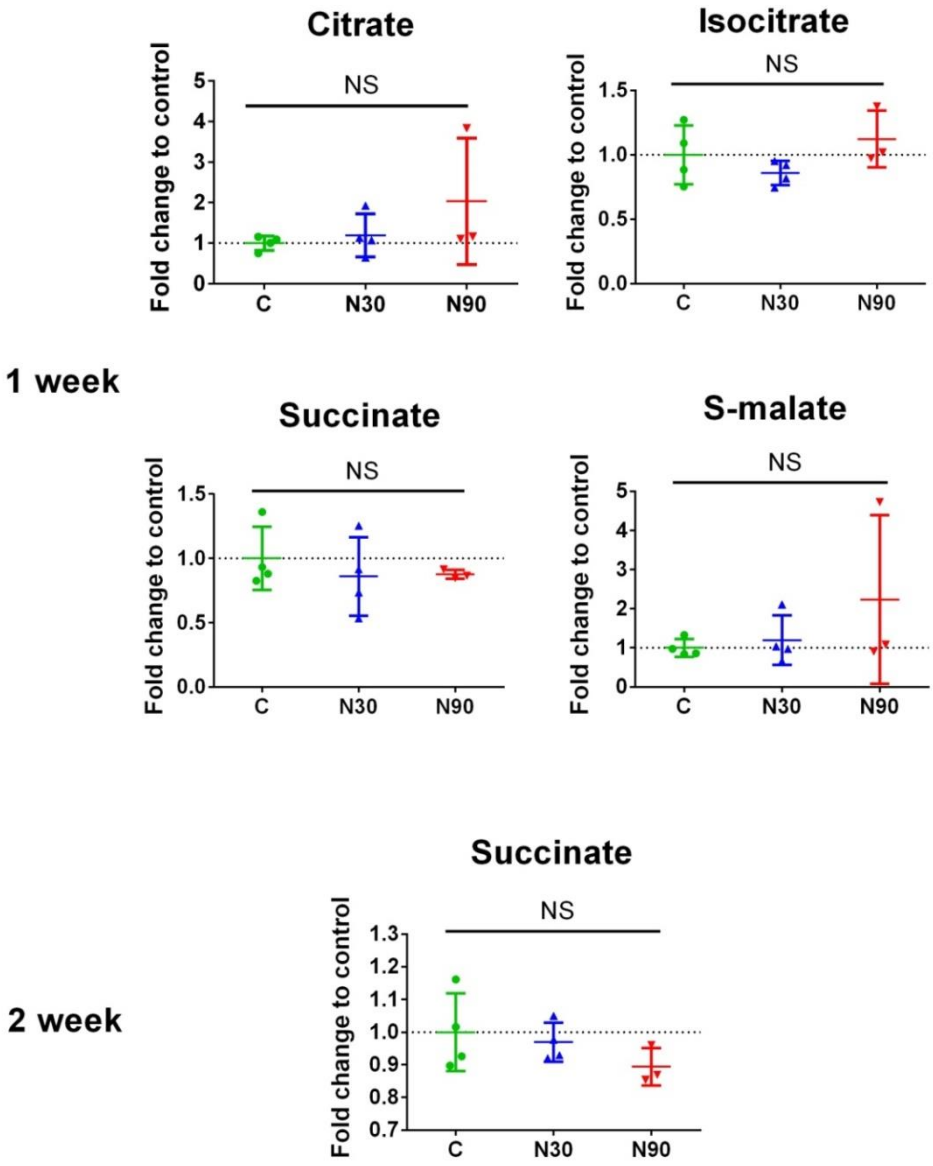

Figure AII. 4 TCA cycle metabolites.

N90 tend to increase citrate, isocitrate and malate indicating that N90 involved in TCA cycle generating ATP. The increase of isocitrate may protect cells from oxidative stress (J. Yang et al., 2017) (mean±SD, n=4, * P≤ 0.5, ** P≤ 0.01, *** P≤ 0.001, one-way ANOVA, Tukey's post hoc test).

Oxidative phosphorylation and nanovibrational stimulation

It has been known that oxidative phosphorylation (OXPHOS) is important for stem cell differentiation (Atashi et al., 2015; Q. Q. Li et al., 2017). OXPHOS produces reactive oxygen species (ROS) which can damage cells and affect cell aging. However, the optimal level of ROS promotes osteogenesis (Shyh-Chang et al., 2013). From our results, nanovibrational stimulation showed slightly increase of glycerol-3-phosphate shuttle at 1 week **(Figure AII.5)** representing that nanovibration required rapid energy bypassing the complete OXPHOS process. Glycerol-3-phosphate shuttle is the junction linking the oxidative phosphorylation, glycolysis and fatty acid metabolism together (Mracek et al., 2013). Furthermore, the increase of orthophosphate level in N90 group was found. This represented that MSCs required higher energy during the stimulation. Orthophosphate is the metabolite involving in OXPHOS for ATP synthesis at complex V in mitochondria (Huttemann et al., 2007) **(Figure AII.5)**.

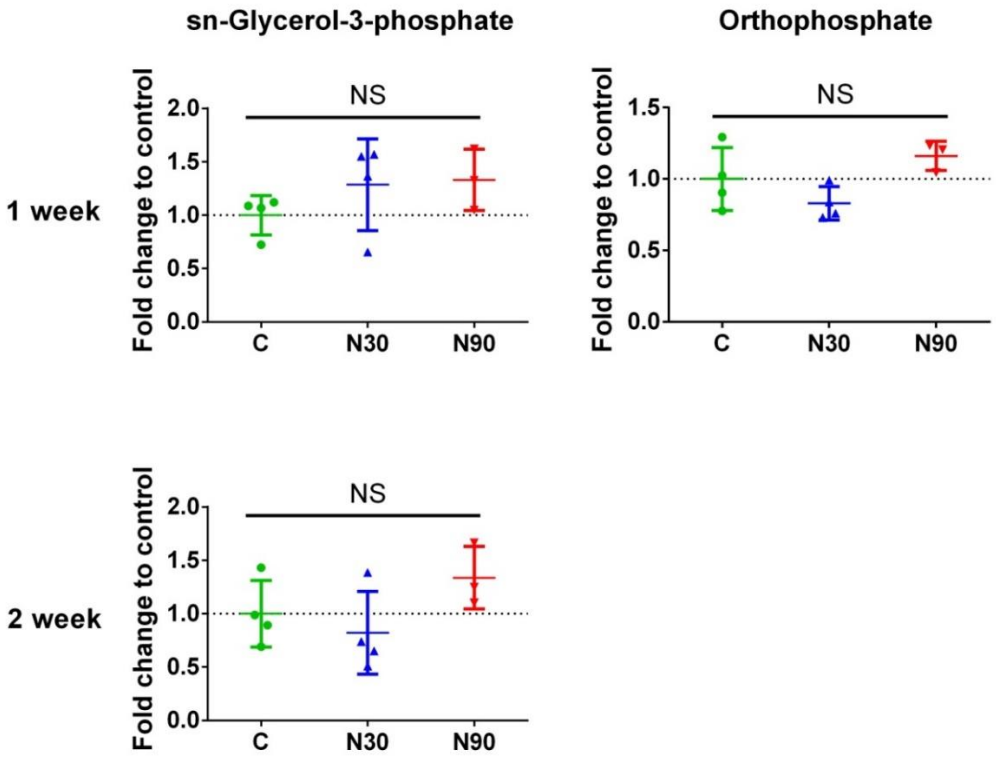

Figure AII. 5 Oxidative phosphorylation metabolites.

At 1 week stimulation, (A) sn-Glycerol-3-phosphate, which is a metabolite involving in glycerol-3-phosphate shuttle, slightly increased in N30 and N90 group. Glycerol-3-phosphate shuttle was activated requiring rapid energy production (bypass complex I of electron transport chain). (B) Orthophosphate level, involving complex V of OXPHOS, showed an increase trend in N90 group. It was hypothesized that nanovibrational stimulation increased lipid catabolism siphoning pathway through Glycerol-3-phosphate shuttle and in turn activated OXPHOS (Mracek et al., 2013; Nsiah-Sefaa & McKenzie, 2016) (mean±SD, n=4, * P≤ 0.5, ** P≤ 0.01, *** P≤ 0.001, one-way ANOVA, Tukey's post hoc test).

Amino acid metabolism: Roles of L-type, L-aromatic amino acid and calcium sensing receptor at 1 and 2 weeks.

To further explore the effect of nanovibrational stimulation, L-type and L-aromatic amino acids which might linked to osteogenic differentiation through Calcium sensing receptor (CaSR) (Conigrave et al., 2007) were studied. CaSR is a G-protein coupled receptor class III which responds to extracellular amino acid change (Conigrave & Hampson, 2006). Therefore, if L- or L-aromatic amino acid increases, CaSR in turn is possibly upregulated. However, it was found that only L-alanine **(Figure AII.6)** showed the increase trend after N90 which corresponded to CaSR gene upregulation showing in chapter 4 **(Figure 4.17)**.

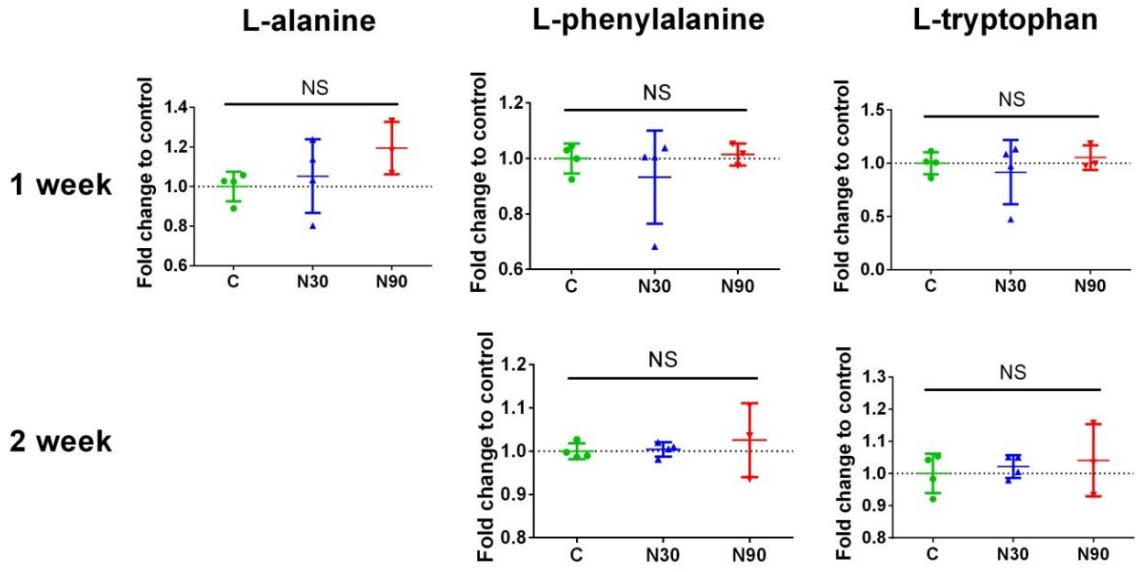

Figure AII. 6 L- and L-aromatic amino acid.

L- and L-aromatic amino acid associating to CaSR. Only, L-alanine showed the significant upregulation after N90 for 1 week (A) (mean±SD, n=4, * P≤ 0.5, ** P≤ 0.01, *** P≤ 0.001, one-way ANOVA, Tukey's post hoc test).

Glutamine and aspartate

Glutamine and aspatate also play a role in reducing oxidative stress (J. Duan et al., 2016; Mates et al., 2002). The increase trend of glutamine and aspartate were noted in N90 group at 1 week **(Figure AII.7)**.

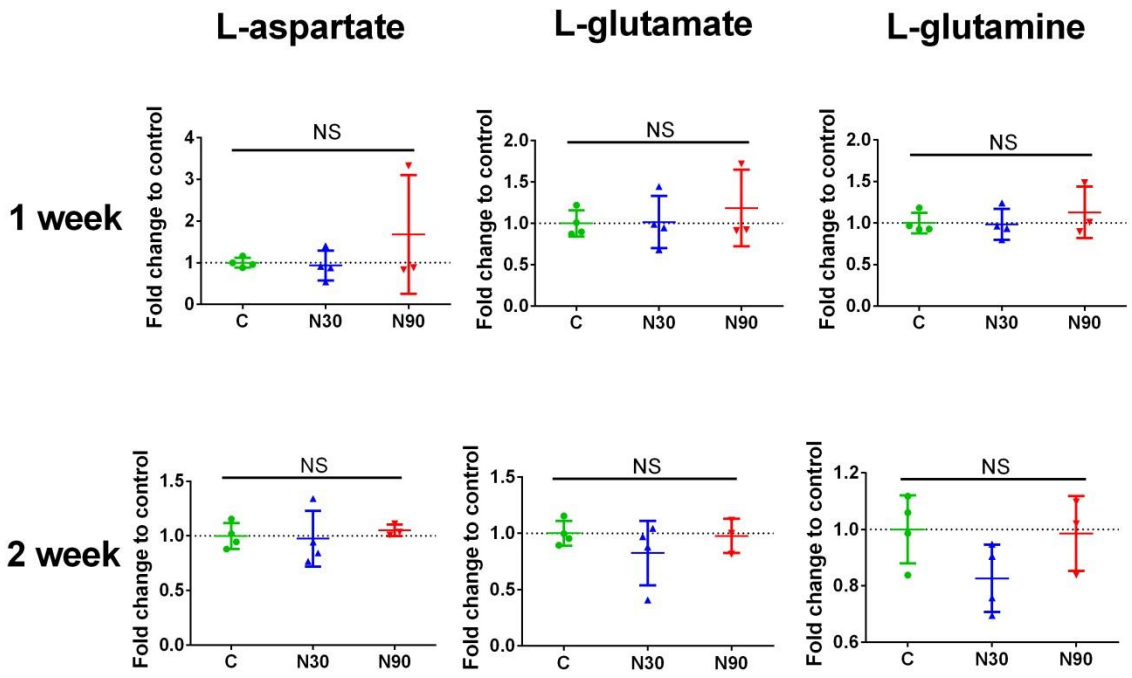

Figure AII. 7 Glutamine and aspartate

The increase of glutamine and aspartate indicates that MSCs possibly produce these metabolites protecting cells from oxidative stress (mean±SD, n=4, * P≤ 0.5, ** P≤ 0.01, *** P≤ 0.001, one-way ANOVA, Tukey's post hoc test).

Lipid metabolism: Long-chain polyunsaturated fatty acids and nanovibrational stimulation at 1 and 2 weeks.

Many literatures support the effect of long-chain polyunsaturated fatty acid (LCPU-FAs) metabolism on osteoblast proliferation and differentiation (Burke & Weiler, 2002; Damsgaard, Molgaard, Matthiessen, Gyldenlove, & Lauritzen, 2012; Jeromson et al., 2015; Kruger et al., 2010; Watkins, Li, Lippman, & Feng, 2003). Therefore, LCPU-FAs metabolites including eicosapentaenoic acid (EPA),

docosapentaenoic acid (DPA) and docohexanoic acid (DHA) were studied at 1 and 2 weeks. The slightly increase of LCPU-FAs was found in N30 and N90 groups at 1 and 2 weeks **(Figure AII.8)**.

To link the effect of NS with cellular energy consumption through lipid metabolism, lipid metabolites relating to β-oxidation were therefore considered. It was found that NS increased hexanoic acid and 4-8 dimethylnonanoyl carnitine while there was no change of O-propanoylcarnitine (or Propionyl L-carnitine) levels **(Figure AII.9)**.

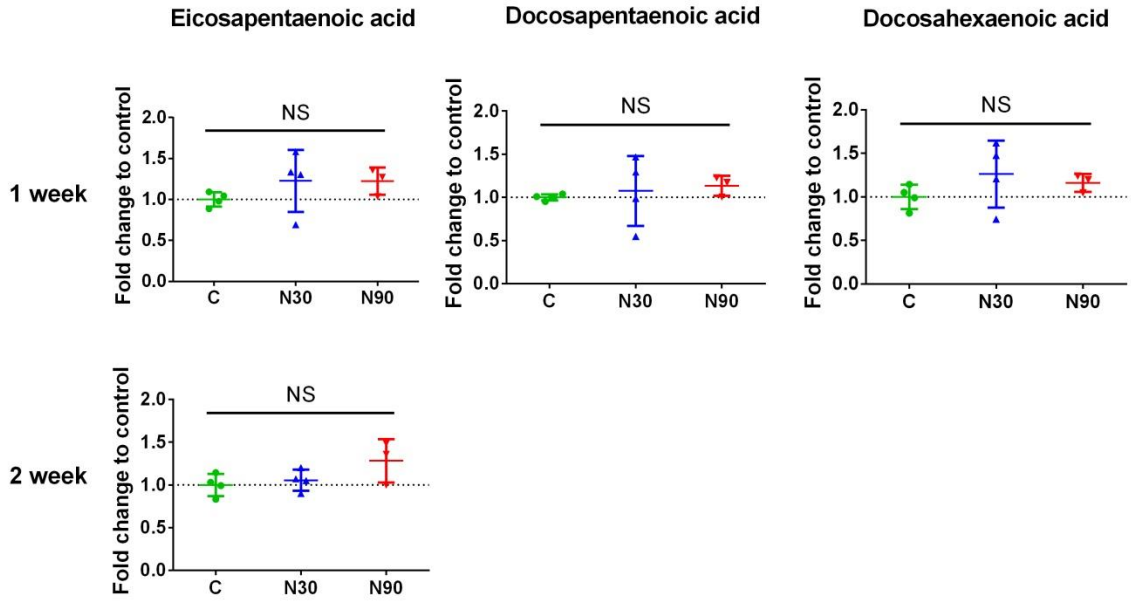

Figure AII. 8 Long chain poly unsaturated fatty acids

Metabolites of LCPU-FAs were studied. Increasing trend of PUFAs synthesis was found in both N30 and N90 stimulations (mean±SD, n=4, * P≤ 0.5, ** P≤ 0.01, *** P≤ 0.001, one-way ANOVA, Tukey's post hoc test).

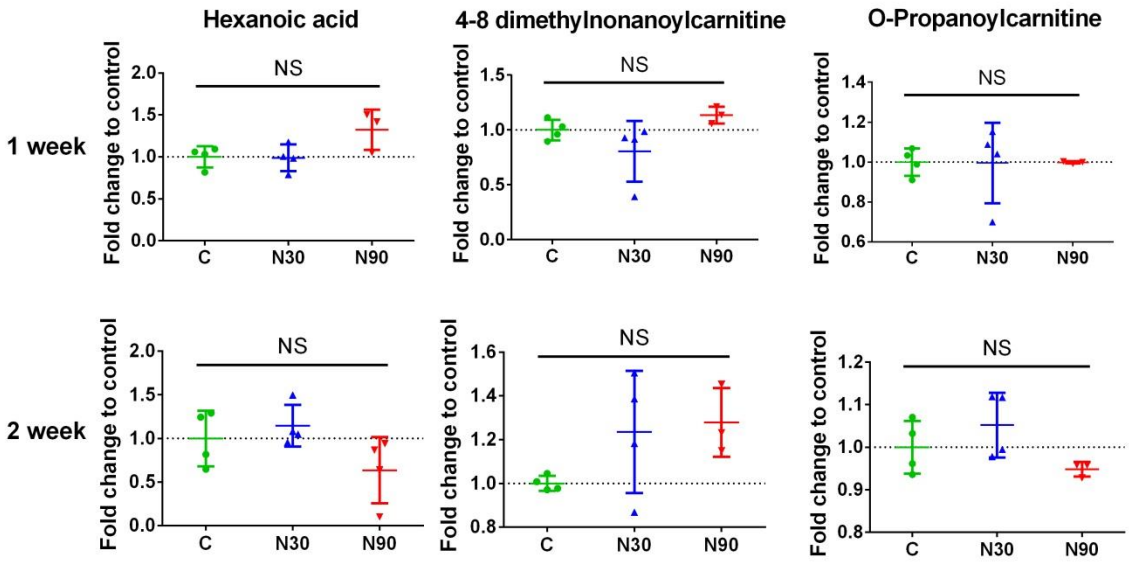

Figure AII. 9 β-oxidation of lipids

NS increased hexanoic acid and dimethylnonanoylcartinine levels. This evidence possibly implied that cells required more ATPs via fatty acid oxidation responded to NS. No change of O-propanoylcarnitine was found (mean±SD, n=4, * P≤ 0.5, ** P≤ 0.01, *** P≤ 0.001, one-way ANOVA, Tukey's post hoc test).

Appendix III

Appendix III

Compression test

After 5% collagen sponges were prepared (n=9), compression tests were then performed. Stress-strain graph were plotted to identify the elastic range of sponges. The slopes of the selected linear range (0.05-0.1 of strain) were calculated representing Young's modulus (material stiffness, mPA) (**Figure AIII.1, Table AIII.1**).

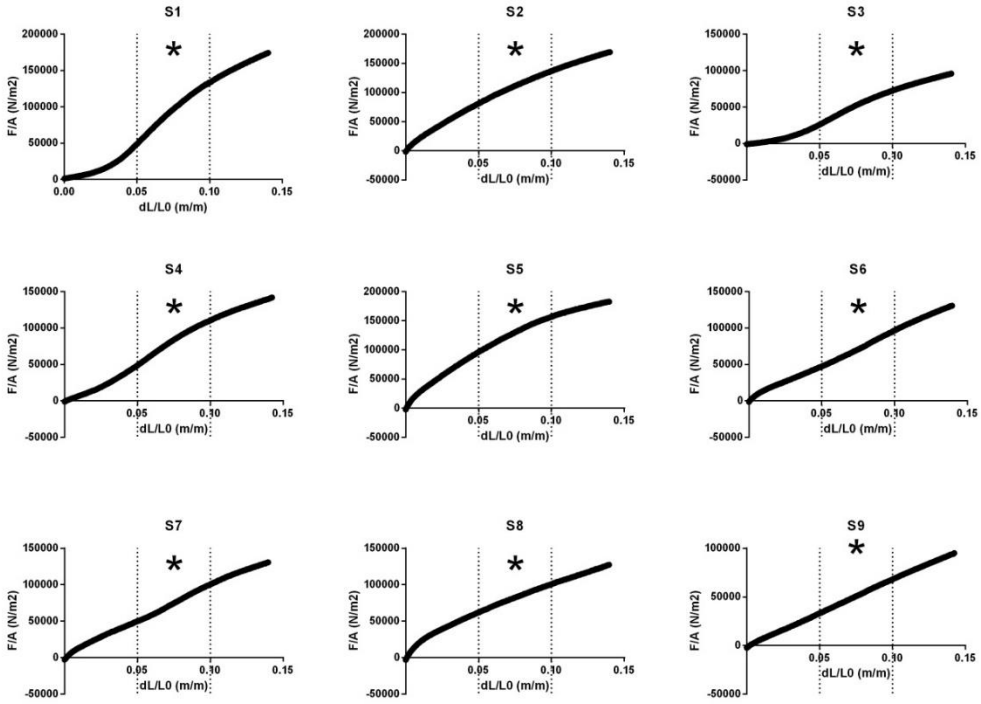

Figure AIII. 1 Stress-strain plot of compression test

Graph plotted between force (N) and changing (delta) length (mm) of compression test study. Linear relationship of the stress-strain graphs was identified which indicated the elastic range of collagen sponge. The range of altered length from 0.05- 0.1 of strain (ΔL/L0) were chosen for Young's modulus calculation (asterix; selected range for Young's modulus calculation).

Table AIII. 1 Young modulus (MPa) of each sample

Samples	Young modulus (Elastic modulus, MPa)
S1	1.705
S2	1.105
S3	0.893293
S4	1.251
S5	1.22
S6	1.001
S7	1.051
S8	0.769168
S9	0.704246
Ave	1.077745222
SD	0.299957153

References

Abais, J. M., Xia, M., Zhang, Y., Boini, K. M., & Li, P.-L. (2015). Redox regulation of NLRP3 inflammasomes: ROS as trigger or effector? *Antioxid Redox Signal, 22*(13), 1111-1129. doi:10.1089/ars.2014.5994

Abu-Amer, Y. (2013). NF-kappaB signaling and bone resorption. *Osteoporos Int, 24*(9), 2377-2386. doi:10.1007/s00198-013-2313-x

Achilli, M., & Mantovani, D. (2010). Tailoring Mechanical Properties of Collagen-Based Scaffolds for Vascular Tissue Engineering: The Effects of pH, Temperature and Ionic Strength on Gelation. *Polymers, 2*(4), 664-680. doi:10.3390/polym2040664

Agarwal, S., Long, P., Seyedain, A., Piesco, N., Shree, A., & Gassner, R. (2003). A central role for the nuclear factor-kappaB pathway in anti-inflammatory and proinflammatory actions of mechanical strain. *FASEB J, 17*(8), 899-901. doi:10.1096/fj.02-0901fje

Ahn, K. S., & Aggarwal, B. B. (2005). Transcription factor NF-kappaB: a sensor for smoke and stress signals. *Ann N Y Acad Sci, 1056*, 218-233. doi:10.1196/annals.1352.026

Akman, A. C., Seda Tigli, R., Gumusderelioglu, M., & Nohutcu, R. M. (2010). Bone morphogenetic protein-6-loaded chitosan scaffolds enhance the osteoblastic characteristics of MC3T3-E1 cells. *Artif Organs, 34*(1), 65-74. doi:10.1111/j.1525-1594.2009.00798.x

Aktuglu, K., Erol, K., & Vahabi, A. (2019). Ilizarov bone transport and treatment of critical-sized tibial bone defects: a narrative review. *Journal of orthopaedics and traumatology : official journal of the Italian Society of Orthopaedics and Traumatology, 20*(1), 22-22. doi:10.1186/s10195-019-0527-1

Al-Munajjed, A. A., & O'Brien, F. J. (2009). Influence of a novel calcium-phosphate coating on the mechanical properties of highly porous

collagen scaffolds for bone repair. *J Mech Behav Biomed Mater, 2*(2), 138-146. doi:10.1016/j.jmbbm.2008.05.001

Albarran-Juarez, J., Iring, A., Wang, S., Joseph, S., Grimm, M., Strilic, B., . . . Offermanns, S. (2018). Piezo1 and Gq/G11 promote endothelial inflammation depending on flow pattern and integrin activation. *J Exp Med, 215*(10), 2655-2672. doi:10.1084/jem.20180483

Alizadeh-Osgouei, M., Li, Y., & Wen, C. (2018). A comprehensive review of biodegradable synthetic polymer-ceramic composites and their manufacture for biomedical applications. *Bioactive materials, 4*(1), 22-36. doi:10.1016/j.bioactmat.2018.11.003

Amini, A. R., Wallace, J. S., & Nukavarapu, S. P. (2011). Short-term and long-term effects of orthopedic biodegradable implants. *J Long Term Eff Med Implants, 21*(2), 93-122.

Anderson, H. C. (1995). Molecular biology of matrix vesicles. *Clin Orthop Relat Res*(314), 266-280.

Anghelina, M., Sjostrom, D., Perera, P., Nam, J., Knobloch, T., & Agarwal, S. (2008). Regulation of biomechanical signals by NF-kappaB transcription factors in chondrocytes. *Biorheology, 45*(3-4), 245-256.

Ann, E. J., Kim, H. Y., Choi, Y. H., Kim, M. Y., Mo, J. S., Jung, J., . . . Park, H. S. (2011). Inhibition of Notch1 signaling by Runx2 during osteoblast differentiation. *J Bone Miner Res, 26*(2), 317-330. doi:10.1002/jbmr.227

Antoine, E. E., Vlachos, P. P., & Rylander, M. N. (2014). Review of collagen I hydrogels for bioengineered tissue microenvironments: characterization of mechanics, structure, and transport. *Tissue Eng Part B Rev, 20*(6), 683-696. doi:10.1089/ten.TEB.2014.0086

Antoine, E. E., Vlachos, P. P., & Rylander, M. N. (2015). Tunable collagen I hydrogels for engineered physiological tissue micro-

environments. *PLoS One, 10*(3), e0122500. doi:10.1371/journal.pone.0122500

Arai, H. (2014). Oxidative Modification of Lipoproteins. In Y. Kato (Ed.), *Lipid Hydroperoxide-Derived Modification of Biomolecules* (pp. 103-114). Dordrecht: Springer Netherlands.

Arai, M., Shibata, Y., Pugdee, K., Abiko, Y., & Ogata, Y. (2007). Effects of reactive oxygen species (ROS) on antioxidant system and osteoblastic differentiation in MC3T3-E1 cells. *Iubmb Life, 59*(1), 27-33. doi:10.1080/15216540601156188

Arakaki, N., Yamashita, A., Niimi, S., & Yamazaki, T. (2013). Involvement of reactive oxygen species in osteoblastic differentiation of MC3T3-E1 cells accompanied by mitochondrial morphological dynamics. *Biomed Res, 34*(3), 161-166.

Ardeshirylajimi, A., Soleimani, M., Hosseinkhani, S., Parivar, K., & Yaghmaei, P. (2014). A comparative study of osteogenic differentiation human induced pluripotent stem cells and adipose tissue derived mesenchymal stem cells. *Cell journal, 16*(3), 235-244.

Arpornmaeklong, P., Brown, S. E., Wang, Z., & Krebsbach, P. H. (2009). Phenotypic Characterization, Osteoblastic Differentiation, and Bone Regeneration Capacity of Human Embryonic Stem Cell-Derived Mesenchymal Stem Cells. *Stem Cells and Development, 18*(7), 955-968. doi:10.1089/scd.2008.0310

Arumugam, B., Vairamani, M., Partridge, N. C., & Selvamurugan, N. (2017). Characterization of Runx2 phosphorylation sites required for TGF-beta1-mediated stimulation of matrix metalloproteinase-13 expression in osteoblastic cells. *Journal of Cellular Physiology*. doi:10.1002/jcp.25964

Ash, H. E., & Unsworth, A. (2000). Design of a surface replacement prosthesis for the proximal interphalangeal joint. *Proceedings of the Institution of Mechanical Engineers Part H-Journal of*

Engineering in Medicine, 214(H2), 151-163. doi:Doi 10.1243/0954411001535327

Ashley, J. W., Ahn, J., & Hankenson, K. D. (2015). Notch signaling promotes osteoclast maturation and resorptive activity. *Journal of Cellular Biochemistry, 116*(11), 2598-2609. doi:10.1002/jcb.25205

Atashi, F., Modarressi, A., & Pepper, M. S. (2015). The role of reactive oxygen species in mesenchymal stem cell adipogenic and osteogenic differentiation: a review. *Stem Cells Dev, 24*(10), 1150-1163. doi:10.1089/scd.2014.0484

Atherton, P., Stutchbury, B., Jethwa, D., & Ballestrem, C. (2016). Mechanosensitive components of integrin adhesions: Role of vinculin. *Exp Cell Res, 343*(1), 21-27. doi:https://doi.org/10.1016/j.yexcr.2015.11.017

Ayala, A., Muñoz, M. F., & Argüelles, S. (2014). Lipid peroxidation: production, metabolism, and signaling mechanisms of malondialdehyde and 4-hydroxy-2-nonenal. *Oxidative Medicine and Cellular Longevity, 2014*, 360438-360438. doi:10.1155/2014/360438

Bai, X. C., Lu, D., Liu, A. L., Zhang, Z. M., Li, X. M., Zou, Z. P., . . . Luo, S. Q. (2005). Reactive oxygen species stimulates receptor activator of NF-kappaB ligand expression in osteoblast. *J Biol Chem, 280*(17), 17497-17506. doi:10.1074/jbc.M409332200

Baker, B. M., & Chen, C. S. (2012). Deconstructing the third dimension: how 3D culture microenvironments alter cellular cues. *J Cell Sci, 125*(Pt 13), 3015-3024. doi:10.1242/jcs.079509

Baldwin, P., Li, D. J., Auston, D. A., Mir, H. S., Yoon, R. S., & Koval, K. J. (2019). Autograft, Allograft, and Bone Graft Substitutes: Clinical Evidence and Indications for Use in the Setting of Orthopaedic

Trauma Surgery. *Journal of Orthopaedic Trauma, 33*(4), 203-213. doi:10.1097/bot.0000000000001420

Barbáchano, A., Larriba, M. J., Ferrer-Mayorga, G., Muñoz, A., & González-Sancho, J. M. (2014). Wnt Pathway at a Glance: From the Deep of the Crypts to the Current Ways of Targeting. In E. Grande & L. Antón Aparicio (Eds.), *Stem Cells in Cancer: Should We Believe or Not?* (pp. 85-106). Dordrecht: Springer Netherlands.

Barczyk, M., Carracedo, S., & Gullberg, D. (2010). Integrins. *Cell Tissue Res, 339*(1), 269-280. doi:10.1007/s00441-009-0834-6

Bastami, F., Nazeman, P., Moslemi, H., Rezai Rad, M., Sharifi, K., & Khojasteh, A. (2017). Induced pluripotent stem cells as a new getaway for bone tissue engineering: A systematic review. *Cell Proliferation, 50*(2), e12321. doi:10.1111/cpr.12321

Bavi, N., Nikolaev, Y. A., Bavi, O., Ridone, P., Martinac, A. D., Nakayama, Y., . . . Martinac, B. (2017). Principles of Mechanosensing at the Membrane Interface. In R. M. Epand & J.-M. Ruysschaert (Eds.), *The Biophysics of Cell Membranes: Biological Consequences* (pp. 85-119). Singapore: Springer Singapore.

Beazley, K. E., & Nurminskaya, M. (2014). BMP2 cross-linked by transglutaminase 2 to collagen-plla scaffold promotes osteogenic differentiation in mesenchymal stem cells. *Biotechnol Lett, 36*(9), 1901-1907. doi:10.1007/s10529-014-1551-0

Beck, G. R., Jr., & Knecht, N. (2003). Osteopontin regulation by inorganic phosphate is ERK1/2-, protein kinase C-, and

proteasome-dependent. *J Biol Chem, 278*(43), 41921-41929. doi:10.1074/jbc.M304470200

Becker, D., Blase, C., Bereiter-Hahn, J., & Jendrach, M. (2005). TRPV4 exhibits a functional role in cell-volume regulation. *J Cell Sci, 118*(11), 2435-2440. doi:10.1242/jcs.02372

Bedard, K., & Krause, K.-H. (2007). The NOX Family of ROS-Generating NADPH Oxidases: Physiology and Pathophysiology. *Physiological Reviews, 87*(1), 245-313. doi:10.1152/physrev.00044.2005

Bell, E. (2000). CHAPTER 16 - ORGANOTYPIC AND HISTIOTYPIC MODELS OF ENGINEERED TISSUES. In R. P. Lanza, R. Langer, & J. Vacanti (Eds.), *Principles of Tissue Engineering (Second Edition)* (pp. 181-193). San Diego: Academic Press.

Beningo, K. A., Dembo, M., & Wang, Y. L. (2004). Responses of fibroblasts to anchorage of dorsal extracellular matrix receptors. *Proc Natl Acad Sci U S A, 101*(52), 18024-18029. doi:10.1073/pnas.0405747102

Bernardo, M. E., & Fibbe, W. E. (2013). Mesenchymal stromal cells: sensors and switchers of inflammation. *Cell Stem Cell, 13*(4), 392-402. doi:10.1016/j.stem.2013.09.006

Bettina M. Willie, A. P., Katharina Schmidt-Bleek, Amaia Cipitria, Manav Mehta,, & Patrick Strube, J. L., Britt Wildemann, Peter Fratzlbc and Georg Duda. (2010). Designing biomimetic scaffolds for bone regeneration: why aim for a copy of

mature tissue properties if nature uses a different approach. *The Royal Society of Chemistry, 6*, 4976–4987.

Bhardwaj, A., Ganesan, N., Tachibana, K., Rajapakshe, K., Albarracin, C. T., Gunaratne, P. H., . . . Bedrosian, I. (2015). Annexin A1 Preferentially Predicts Poor Prognosis of Basal-Like Breast Cancer

Patients by Activating mTOR-S6 Signaling. *PLoS One, 10*(5), e0127678. doi:10.1371/journal.pone.0127678

Bhardwaj, A., Rosen, D., Liu, M., Liu, Y., Hao, Q., Ganesan, N., . . . Bedrosian, I. (2014). Suppression of Akt-mTOR pathway-a novel component of oncogene induced DNA damage response barrier in breast tumorigenesis. *PLoS One, 9*(5), e97076. doi:10.1371/journal.pone.0097076

Bhave, G., Hu, H.-J., Glauner, K. S., Zhu, W., Wang, H., Brasier, D. J., . . . Gereau, R. W. (2003). Protein kinase C phosphorylation sensitizes but does not activate the capsaicin receptor transient receptor potential vanilloid 1 (TRPV1). *Proceedings of the National Academy of Sciences, 100*(21), 12480-12485. doi:10.1073/pnas.2032100100

Bi, L., Cao, Z., Hu, Y., Song, Y., Yu, L., Yang, B., . . . Han, Y. (2011). Effects of different cross-linking conditions on the properties of genipin-cross-linked chitosan/collagen scaffolds for cartilage tissue engineering. *J Mater Sci Mater Med, 22*(1), 51-62. doi:10.1007/s10856-010-4177-3

Bigarella, C. L., Liang, R., & Ghaffari, S. (2014). Stem cells and the impact of ROS signaling. *Development, 141*(22), 4206-4218. doi:10.1242/dev.107086

Birukov, K. G. (2009). Cyclic stretch, reactive oxygen species, and vascular remodeling. *Antioxid Redox Signal, 11*(7), 1651-1667. doi:10.1089/ARS.2008.2390

Biswas, S. K. (2016). Does the Interdependence between Oxidative Stress and Inflammation Explain the Antioxidant Paradox? *Oxidative Medicine and Cellular Longevity*. doi:10.1155/2016/5698931

Bitar, M., Brown, R. A., Salih, V., Kidane, A. G., Knowles, J. C., & Nazhat, S. N. (2008). Effect of cell density on osteoblastic differentiation and matrix degradation of biomimetic dense

collagen scaffolds. *Biomacromolecules, 9*(1), 129-135. doi:10.1021/bm701112w

Bladh, L. G., Johansson-Haque, K., Rafter, I., Nilsson, S., & Okret, S. (2009). Inhibition of extracellular signal-regulated kinase (ERK) signaling participates in repression of nuclear factor (NF)-kappaB activity by glucocorticoids. *Biochim Biophys Acta, 1793*(3), 439-446. doi:10.1016/j.bbamcr.2008.11.013

Blaser, H., Dostert, C., Mak, T. W., & Brenner, D. (2016). TNF and ROS Crosstalk in Inflammation. *Trends in Cell Biology, 26*(4), 249-261. doi:https://doi.org/10.1016/j.tcb.2015.12.002

Boast, S., & Stern, C. D. (2013). Simple methods for generating neural, bone and endodermal cell types from chick embryonic stem cells. *Stem Cell Res, 10*(1), 20-28. doi:10.1016/j.scr.2012.08.008

Bodle, J., Hamouda, M. S., Cai, S., Williams, R. B., Bernacki, S. H., & Loboa, E. G. (2019). Primary Cilia Exhibit Mechanosensitivity to Cyclic Tensile Strain and Lineage-Dependent Expression in Adipose-Derived Stem Cells. *Sci Rep, 9*(1), 8009-8009. doi:10.1038/s41598-019-43351-y

Bodle, J. C., Rubenstein, C. D., Phillips, M. E., Bernacki, S. H., Qi, J., Banes, A. J., & Loboa, E. G. (2013). Primary cilia: the chemical antenna regulating human adipose-derived stem cell osteogenesis. *PLoS One, 8*(5), e62554. doi:10.1371/journal.pone.0062554

Boin, F., Erre, G. L., Posadino, A. M., Cossu, A., Giordo, R., Spinetti, G., . . . Pintus, G. (2014). Oxidative stress-dependent activation of collagen synthesis is induced in human pulmonary smooth muscle cells by sera from patients with scleroderma-associated pulmonary hypertension. *Orphanet Journal of Rare Diseases, 9*(1), 123. doi:10.1186/s13023-014-0123-7

Boonrungsiman, S., Gentleman, E., Carzaniga, R., Evans, N. D., McComb, D. W., Porter, A. E., & Stevens, M. M. (2012). The role of intracellular calcium phosphate in osteoblast-mediated bone

apatite formation. *Proceedings of the National Academy of Sciences, 109*(35), 14170-14175. doi:10.1073/pnas.1208916109

Borges, M. C., Santos Fde, M., Telles, R. W., Correia, M. I., & Lanna, C. C. (2014). [Polyunsaturated omega-3 fatty acids and systemic lupus erythematosus: what do we know?]. *Rev Bras Reumatol, 54*(6), 459-466. doi:10.1016/j.rbr.2013.12.002

Bouletreau, P. J., Warren, S. M., & Longaker, M. T. (2002). The molecular biology of distraction osteogenesis. *J Craniomaxillofac Surg, 30*(1), 1-11. doi:10.1054/jcms.2001.0263

Boyce, B. F., Yao, Z., & Xing, L. (2010). Functions of nuclear factor kappaB in bone. *Annals of the New York Academy of Sciences, 1192*, 367-375. doi:10.1111/j.1749-6632.2009.05315.x

Boyle, W. J., Simonet, W. S., & Lacey, D. L. (2003). Osteoclast differentiation and activation. *Nature, 423*(6937), 337-342. doi:10.1038/nature01658

Brakebusch, C., & Fassler, R. (2003). The integrin-actin connection, an eternal love affair. *EMBO J, 22*(10), 2324-2333. doi:10.1093/emboj/cdg245

Breitinger, U., Bahnassawy, L. M., Janzen, D., Roemer, V., Becker, C.-M., Villmann, C., & Breitinger, H.-G. (2018). PKA and PKC Modulators Affect Ion Channel Function and Internalization of Recombinant Alpha1 and Alpha1-Beta Glycine Receptors. *Frontiers in Molecular Neuroscience, 11*(154). doi:10.3389/fnmol.2018.00154

Brown, P. T., Squire, M. W., & Li, W. J. (2014). Characterization and evaluation of mesenchymal stem cells derived from human

embryonic stem cells and bone marrow. *Cell Tissue Res, 358*(1), 149-164. doi:10.1007/s00441-014-1926-5

Bruderer, M., Richards, R. G., Alini, M., & Stoddart, M. J. (2014). Role and regulation of RUNX2 in osteogenesis. *Eur Cell Mater, 28*, 269-286.

Buj-Corral, I., Bagheri, A., & Petit-Rojo, O. (2018). 3D Printing of Porous Scaffolds with Controlled Porosity and Pore Size Values. *Materials (Basel, Switzerland), 11*(9), 1532. doi:10.3390/ma11091532

Burger, E. H., Klein-Nulend, J., & Veldhuijzen, J. P. (1992). Mechanical stress and osteogenesis in vitro. *J Bone Miner Res, 7 Suppl 2*, S397-401. doi:10.1002/jbmr.5650071406

Burke, A., & Weiler, H. (2002). The effect of prostaglandin E(2) (PGE(2)) and long-chain polyunsaturated fatty acids (LC PUFA) on bone formation in piglets: a model for bone growth in nutritional investigation. *Prostaglandins Leukot Essent Fatty Acids, 67*(4), 229-235.

Burridge, K., & Wennerberg, K. (2004). Rho and Rac take center stage. *Cell, 116*(2), 167-179.

Butler, M. F., Ng, Y. F., & Pudney, P. D. A. (2003). Mechanism and kinetics of the crosslinking reaction between biopolymers containing primary amine groups and genipin. *Journal of Polymer Science Part a-Polymer Chemistry, 41*(24), 3941-3953. doi:10.1002/pola.10960

Byon, C. H., Javed, A., Dai, Q., Kappes, J. C., Clemens, T. L., Darley-Usmar, V. M., . . . Chen, Y. (2008). Oxidative stress induces vascular calcification through modulation of the osteogenic transcription factor Runx2 by AKT signaling. *J Biol Chem, 283*(22), 15319-15327. doi:10.1074/jbc.M800021200

Byon, C. H., Javed, A., Dai, Q., Kappes, J. C., Clemens, T. L., Darley-Usmar, V. M., . . . Chen, Y. (2008). Oxidative stress induces vascular calcification through modulation of the osteogenic

transcription factor Runx2 by AKT signaling. *J Biol Chem, 283*(22), 15319-15327. doi:10.1074/jbc.M800021200

Calder, P. C. (2001). Polyunsaturated fatty acids, inflammation, and immunity. *Lipids, 36*(9), 1007-1024.

Campbell, I. D., & Humphries, M. J. (2011). Integrin structure, activation, and interactions. *Cold Spring Harbor Perspectives in Biology, 3*(3), a004994. doi:10.1101/cshperspect.a004994

Campos, F., Bonhome-Espinosa, A. B., Vizcaino, G., Rodriguez, I. A., Duran-Herrera, D., Lopez-Lopez, M. T., . . . Carriel, V. (2018). Generation of genipin cross-linked fibrin-agarose hydrogel tissue-like models for tissue engineering applications. *Biomed Mater, 13*(2), 025021. doi:10.1088/1748-605X/aa9ad2

Cao, C., Ren, Y., Barnett, A. S., Mirando, A. J., Rouse, D., Mun, S. H., . . . Pitt, G. S. (2017). Increased Ca2+ signaling through CaV1.2 promotes bone formation and prevents estrogen deficiency–induced bone loss. *Jci Insight, 2*(22). doi:10.1172/jci.insight.95512

Cao, H., Feng, Q., Xu, W., Li, X., Kang, Z., Ren, Y., & Du, L. (2010). Genipin induced apoptosis associated with activation of the c-Jun NH2-terminal kinase and p53 protein in HeLa cells. *Biol Pharm Bull, 33*(8), 1343-1348.

Carafoli, E. (2002). Calcium signaling: a tale for all seasons. *Proc Natl Acad Sci U S A, 99*(3), 1115-1122. doi:10.1073/pnas.032427999

Carragee, E. J., Hurwitz, E. L., & Weiner, B. K. (2011). A critical review of recombinant human bone morphogenetic protein-2 trials in spinal surgery: emerging safety concerns and lessons learned. *Spine Journal, 11*(6), 471-491. doi:10.1016/j.spinee.2011.04.023

Caterina, M. J., Schumacher, M. A., Tominaga, M., Rosen, T. A., Levine, J. D., & Julius, D. (1997). The capsaicin receptor: a heat-activated

ion channel in the pain pathway. *Nature, 389*(6653), 816-824. doi:10.1038/39807

Červenka, I., Wolf, J., Mašek, J., Krejci, P., Wilcox, W. R., Kozubík, A., . . . Bryja, V. (2011). Mitogen-activated protein kinases promote WNT/beta-catenin signaling via phosphorylation of LRP6. *Molecular and Cellular Biology, 31*(1), 179-189. doi:10.1128/MCB.00550-10

Chabbert, C., Geleoc, G., Lehouelleur, J., & Sans, A. (1994). Intracellular Calcium Variations Evoked by Mechanical Stimulation of Mammalian Isolated Vestibular Type-I Hair-Cells. *Pflugers Archiv-European Journal of Physiology, 427*(1-2), 162-168. doi:Doi 10.1007/Bf00585956

Chang, J., Liu, F., Lee, M., Wu, B., Ting, K., Zara, J. N., . . . Wang, C. Y. (2013). NF-kappaB inhibits osteogenic differentiation of mesenchymal stem cells by promoting beta-catenin degradation. *Proc Natl Acad Sci U S A, 110*(23), 9469-9474. doi:10.1073/pnas.1300532110

Chapman, K. E., Sinclair, S. E., Zhuang, D., Hassid, A., Desai, L. P., & Waters, C. M. (2005). Cyclic mechanical strain increases reactive oxygen species production in pulmonary epithelial cells. *Am J Physiol Lung Cell Mol Physiol, 289*(5), L834-841. doi:10.1152/ajplung.00069.2005

Chatterjee, S. (2016). Oxidative Stress, Inflammation, and Disease. *Oxidative Stress and Biomaterials*, 35-58. doi:10.1016/B978-0-12-803269-5.00002-4

Cheema, U., Rong, Z. M., Kirresh, O., MacRobert, A. J., Vadgama, P., & Brown, R. A. (2012). Oxygen diffusion through collagen scaffolds at defined densities: implications for cell survival in tissue models. *J Tissue Eng Regen Med, 6*(1), 77-84. doi:10.1002/term.402

Chen, B., Lin, T., Yang, X., Li, Y., Xie, D., Zheng, W., . . . Tan, X. (2016). Low-magnitude, high-frequency vibration promotes the adhesion and the osteogenic differentiation of bone marrow-derived

mesenchymal stem cells cultured on a hydroxyapatite-coated surface: The direct role of Wnt/beta-catenin signaling pathway activation. *Int J Mol Med, 38*(5), 1531-1540. doi:10.3892/ijmm.2016.2757

Chen, C. T., Shih, Y. R., Kuo, T. K., Lee, O. K., & Wei, Y. H. (2008). Coordinated changes of mitochondrial biogenesis and antioxidant enzymes during osteogenic differentiation of human mesenchymal stem cells. *Stem Cells, 26*(4), 960-968. doi:10.1634/stemcells.2007-0509

Chen, E., Xue, D., Zhang, W., Lin, F., & Pan, Z. (2015). Extracellular heat shock protein 70 promotes osteogenesis of human mesenchymal stem cells through activation of the ERK signaling pathway. *Febs Letters, 589*(24 Pt B), 4088-4096. doi:10.1016/j.febslet.2015.11.021

Chen, F., Bi, D., Cheng, C., Ma, S., Liu, Y., & Cheng, K. (2019). Bone morphogenetic protein 7 enhances the osteogenic differentiation of human dermal-derived CD105+ fibroblast cells through the Smad and MAPK pathways. *International journal of molecular medicine, 43*(1), 37-46. doi:10.3892/ijmm.2018.3938

Chen, G., Deng, C., & Li, Y. P. (2012). TGF-beta and BMP signaling in osteoblast differentiation and bone formation. *Int J Biol Sci, 8*(2), 272-288. doi:10.7150/ijbs.2929

Chen, J. C., & Jacobs, C. R. (2013). Mechanically induced osteogenic lineage commitment of stem cells. *Stem Cell Res Ther, 4*. doi:10.1186/Scrt318

Chen, Q. Z., Thompson, I. D., & Boccaccini, A. R. (2006). 45S5 Bioglass®-derived glass–ceramic scaffolds for bone tissue engineering. *Biomaterials, 27*(11), 2414-2425. doi:https://doi.org/10.1016/j.biomaterials.2005.11.025

Chen, W. C., Zhou, H. Z., Weir, M. D., Tang, M. H., Bao, C. Y., & Xu, H. H. K. (2013). Human Embryonic Stem Cell-Derived Mesenchymal Stem Cell Seeding on Calcium Phosphate Cement-Chitosan-RGD

Scaffold for Bone Repair. *Tissue Engineering Part A, 19*(7-8), 915-927. doi:10.1089/ten.tea.2012.0172

Chen, X., He, F., Zhong, D. Y., & Luo, Z. P. (2015). Acoustic-frequency vibratory stimulation regulates the balance between osteogenesis and adipogenesis of human bone marrow-derived mesenchymal stem cells. *Biomed Res Int, 2015*, 540731. doi:10.1155/2015/540731

Chen, X., Wang, Z., Duan, N., Zhu, G., Schwarz, E. M., & Xie, C. (2018). Osteoblast-osteoclast interactions. *Connect Tissue Res, 59*(2), 99-107. doi:10.1080/03008207.2017.1290085

Chen, Y., Chen, S., Kawazoe, N., & Chen, G. (2018). Promoted Angiogenesis and Osteogenesis by Dexamethasone-loaded Calcium Phosphate Nanoparticles/Collagen Composite Scaffolds with Microgroove Networks. *Sci Rep, 8*(1), 14143. doi:10.1038/s41598-018-32495-y

Chen, Y., Kawazoe, N., & Chen, G. (2018). Preparation of dexamethasone-loaded biphasic calcium phosphate nanoparticles/collagen porous composite scaffolds for bone tissue engineering. *Acta Biomater, 67*, 341-353. doi:10.1016/j.actbio.2017.12.004

Chen, Y., Whetstone, H. C., Youn, A., Nadesan, P., Chow, E. C. Y., Lin, A. C., & Alman, B. A. (2007). beta-catenin signaling pathway is crucial for bone morphogenetic protein 2 to induce new bone formation. *Journal of Biological Chemistry, 282*(1), 526-533. doi:10.1074/jbc.M602700200

Cheng, J. J., Wung, B. S., Chao, Y. J., & Wang, D. L. (1998). Cyclic strain-induced reactive oxygen species involved in ICAM-1 gene induction in endothelial cells. *Hypertension, 31*(1), 125-130.

Cheng, Z. A., Alba-Perez, A., Gonzalez-Garcia, C., Donnelly, H., Llopis-Hernandez, V., Jayawarna, V., . . . Salmeron-Sanchez, M. (2019). Nanoscale Coatings for Ultralow Dose BMP-2-Driven Regeneration

of Critical-Sized Bone Defects. *Adv Sci (Weinh), 6*(2), 1800361. doi:10.1002/advs.201800361

Chieh, H. F., Sun, Y., Liao, J. D., Su, F. C., Zhao, C., Amadio, P. C., & An, K. N. (2010). Effects of cell concentration and collagen concentration on contraction kinetics and mechanical properties in a bone marrow stromal cell-collagen construct. *J Biomed Mater Res A, 93*(3), 1132-1139. doi:10.1002/jbm.a.32606

Childs, P. G., Boyle, C. A., Pemberton, G. D., Nikukar, H., Curtis, A. S., Dalby, M. J., & Reid, S. (2015). Use of nanoscale mechanical stimulation for control and manipulation of cell behaviour. *Acta Biomater*. doi:10.1016/j.actbio.2015.11.045

Childs, P. G., Boyle, C. A., Pemberton, G. D., Nikukar, H., Curtis, A. S., Henriquez, F. L., . . . Reid, S. (2016). Use of nanoscale mechanical stimulation for control and manipulation of cell behaviour. *Acta Biomater, 34*, 159-168. doi:10.1016/j.actbio.2015.11.045

Cho, E. S., Cha, Y. H., Kim, H. S., Kim, N. H., & Yook, J. I. (2018). The Pentose Phosphate Pathway as a Potential Target for Cancer Therapy. *Biomolecules & Therapeutics, 26*(1), 29-38. doi:10.4062/biomolther.2017.179

Cho, S., Irianto, J., & Discher, D. E. (2017). Mechanosensing by the nucleus: From pathways to scaling relationships. *The Journal of Cell Biology, 216*(2), 305-315. doi:10.1083/jcb.201610042

Choe, Y., Yu, J. Y., Son, Y. O., Park, S. M., Kim, J. G., Shi, X., & Lee, J. C. (2012). Continuously generated H2O2 stimulates the proliferation and osteoblastic differentiation of human periodontal ligament fibroblasts. *Journal of Cellular Biochemistry, 113*(4), 1426-1436. doi:10.1002/jcb.24017

Choi, H. D., & Chae, S. M. (2018). Comparison of efficacy and safety of combination therapy with statins and omega-3 fatty acids versus statin monotherapy in patients with dyslipidemia: A systematic

review and meta-analysis. *Medicine (Baltimore), 97*(50), e13593. doi:10.1097/md.0000000000013593

Choi, K. M., Seo, Y. K., Yoon, H. H., Song, K. Y., Kwon, S. Y., Lee, H. S., & Park, J. K. (2008). Effect of ascorbic acid on bone marrow-derived mesenchymal stem cell proliferation and differentiation. *J Biosci Bioeng, 105*(6), 586-594. doi:10.1263/jbb.105.586

Choi, Y. H., Choi, J. H., Oh, J. W., & Lee, K. Y. (2013). Calmodulin-dependent kinase II regulates osteoblast differentiation through regulation of Osterix. *Biochem Biophys Res Commun, 432*(2), 248-255. doi:10.1016/j.bbrc.2013.02.005

Christou, C., Oliver, R. A., Yu, Y., & Walsh, W. R. (2014). The Masquelet technique for membrane induction and the healing of ovine critical sized segmental defects. *PLoS One, 9*(12), e114122-e114122. doi:10.1371/journal.pone.0114122

Chuang, H.-h., & Lin, S. (2009). Oxidative challenges sensitize the capsaicin receptor by covalent cysteine modification. *Proceedings of the National Academy of Sciences, 106*(47), 20097-20102. doi:10.1073/pnas.0902675106

Chuderland, D., & Seger, R. (2008). Calcium regulates ERK signaling by modulating its protein-protein interactions. *Communicative & Integrative Biology, 1*(1), 4-5. doi:10.4161/cib.1.1.6107

Chung, C. H., Golub, E. E., Forbes, E., Tokuoka, T., & Shapiro, I. M. (1992). Mechanism of action of beta-glycerophosphate on bone cell mineralization. *Calcif Tissue Int, 51*(4), 305-311.

Ciardo, M. G., & Ferrer-Montiel, A. (2017). Lipids as central modulators of sensory TRP channels. *Biochimica Et Biophysica Acta-*

Biomembranes, 1859(9), 1615-1628. doi:10.1016/j.bbamem.2017.04.012

Circu, M. L., & Aw, T. Y. (2010). Reactive oxygen species, cellular redox systems, and apoptosis. *Free Radic Biol Med, 48*(6), 749-762. doi:10.1016/j.freeradbiomed.2009.12.022

Claes, L., Eckert-Hubner, K., & Augat, P. (2003). The fracture gap size influences the local vascularization and tissue differentiation in callus healing. *Langenbecks Arch Surg, 388*(5), 316-322. doi:10.1007/s00423-003-0396-0

Claes, L., Recknagel, S., & Ignatius, A. (2012). Fracture healing under healthy and inflammatory conditions. *Nat Rev Rheumatol, 8*(3), 133-143. doi:10.1038/nrrheum.2012.1

Clapham, D. E. (2007). Calcium signaling. *Cell, 131*(6), 1047-1058. doi:10.1016/j.cell.2007.11.028

Clarke, B. (2008). Normal Bone Anatomy and Physiology. *Clinical Journal of the American Society of Nephrology, 3*(Supplement 3), S131-S139. doi:10.2215/cjn.04151206

Codelia, V. A., Sun, G., & Irvine, K. D. (2014). Regulation of YAP by mechanical strain through Jnk and Hippo signaling. *Curr Biol, 24*(17), 2012-2017. doi:10.1016/j.cub.2014.07.034

Coetzee, M., Haag, M., & Kruger, M. C. (2009). Effects of arachidonic acid and docosahexaenoic acid on differentiation and

mineralization of MC3T3-E1 osteoblast-like cells. *Cell Biochem Funct, 27*(1), 3-11. doi:10.1002/cbf.1526

Collu, G. M., Hidalgo-Sastre, A., & Brennan, K. (2014). Wnt-Notch signalling crosstalk in development and disease. *Cell Mol Life Sci, 71*(18), 3553-3567. doi:10.1007/s00018-014-1644-x

Conigrave, A. D., & Hampson, D. R. (2006). Broad-spectrum L-amino acid sensing by class 3 G-protein-coupled receptors. *Trends Endocrinol Metab, 17*(10), 398-407. doi:10.1016/j.tem.2006.10.012

Conigrave, A. D., Mun, H. C., & Lok, H. C. (2007). Aromatic L-amino acids activate the calcium-sensing receptor. *J Nutr, 137*(6 Suppl 1), 1524S-1527S; discussion 1548S.

Connelly, T., Yu, Y., Grosmaitre, X., Wang, J., Santarelli, L. C., Savigner, A., . . . Ma, M. (2015). G protein-coupled odorant receptors underlie mechanosensitivity in mammalian olfactory sensory neurons. *Proceedings of the National Academy of Sciences, 112*(2), 590-595. doi:10.1073/pnas.1418515112

Conway, J. D., Shabtai, L., Bauernschub, A., & Specht, S. C. (2014). BMP-7 versus BMP-2 for the treatment of long bone nonunion. *Orthopedics, 37*(12), e1049-1057. doi:10.3928/01477447-20141124-50

Cook, S. D., Salkeld, S. L., Patron, L. P., & Rueger, D. C. (2000). Preclinical and Clinical Evaluation of Osteogenic Protein-1 (BMP-7) in Bony Sites. In D. L. Wise, J. D. Gresser, D. J. Trantolo, M. V. Cattaneo, K.-U. Lewandrowski, & M. J. Yaszemski (Eds.), *Biomaterials Engineering and Devices: Human Applications: Volume 1 Fundamentals and Vascular and Carrier Applications* (pp. 267-277). Totowa, NJ: Humana Press.

Corey, D. P., García-Añoveros, J., Holt, J. R., Kwan, K. Y., Lin, S.-Y., Vollrath, M. A., . . . Zhang, D.-S. (2004). TRPA1 is a candidate for

the mechanosensitive transduction channel of vertebrate hair cells. *Nature, 432*(7018), 723-730. doi:10.1038/nature03066

Corrigan, M. A., Johnson, G. P., Stavenschi, E., Riffault, M., Labour, M.-N., & Hoey, D. A. (2018). TRPV4-mediates oscillatory fluid shear mechanotransduction in mesenchymal stem cells in part via the primary cilium. *Sci Rep, 8*(1), 3824-3824. doi:10.1038/s41598-018-22174-3

Corrigan, M. A., Johnson, G. P., Stavenschi, E., Riffault, M., Labour, M. N., & Hoey, D. A. (2018). TRPV4-mediates oscillatory fluid shear mechanotransduction in mesenchymal stem cells in part via the primary cilium. *Sci Rep, 8*. doi:10.1038/s41598-018-22174-3

Coste, B., Mathur, J., Schmidt, M., Earley, T. J., Ranade, S., Petrus, M. J., . . . Patapoutian, A. (2010). Piezo1 and Piezo2 are essential components of distinct mechanically activated cation channels. *Science, 330*(6000), 55-60. doi:10.1126/science.1193270

Coste, B., Xiao, B., Santos, J. S., Syeda, R., Grandl, J., Spencer, K. S., . . . Patapoutian, A. (2012). Piezo proteins are pore-forming subunits of mechanically activated channels. *Nature, 483*(7388), 176-181. doi:10.1038/nature10812

Cowan, K. J., & Storey, K. B. (2003). Mitogen-activated protein kinases: new signaling pathways functioning in cellular responses to environmental stress. *Journal of Experimental Biology, 206*(7), 1107-1115. doi:10.1242/jeb.00220

Cox, C. D., Bae, C., Ziegler, L., Hartley, S., Nikolova-Krstevski, V., Rohde, P. R., . . . Martinac, B. (2016). Removal of the mechanoprotective influence of the cytoskeleton reveals PIEZO1 is

gated by bilayer tension. *Nat Commun, 7*, 10366. doi:10.1038/ncomms10366

Cox, C. D., Bavi, N., & Martinac, B. (2017). Origin of the Force: The Force-From-Lipids Principle Applied to Piezo Channels. *Curr Top Membr, 79*, 59-96. doi:10.1016/bs.ctm.2016.09.001

Creely, J. J., DiMari, S. J., Howe, A. M., & Haralson, M. A. (1992). Effects of transforming growth factor-beta on collagen synthesis by normal rat kidney epithelial cells. *Am J Pathol, 140*(1), 45-55.

Crippa, S., & Bernardo, M. E. (2018). Mesenchymal Stromal Cells: Role in the BM Niche and in the Support of Hematopoietic Stem Cell Transplantation. *Hemasphere, 2*(6), e151. doi:10.1097/hs9.0000000000000151

Croes, M., Oner, F. C., Kruyt, M. C., Blokhuis, T. J., Bastian, O., Dhert, W. J., & Alblas, J. (2015). Proinflammatory Mediators Enhance the Osteogenesis of Human Mesenchymal Stem Cells after Lineage Commitment. *PLoS One, 10*(7), e0132781. doi:10.1371/journal.pone.0132781

Cui, Y., Hameed, F. M., Yang, B., Lee, K., Pan, C. Q., Park, S., & Sheetz, M. (2015). Cyclic stretching of soft substrates induces spreading and growth. *Nat Commun, 6*, 6333. doi:10.1038/ncomms7333

Curtis, A. S., Reid, S., Martin, I., Vaidyanathan, R., Smith, C. A., Nikukar, H., & Dalby, M. J. (2013). Cell interactions at the nanoscale: piezoelectric stimulation. *IEEE Trans Nanobioscience, 12*(3), 247-254. doi:10.1109/TNB.2013.2257837

Curtis, A. S., & Tsimbouri, P. M. (2014). Epigenesis: roles of nanotopography, nanoforces and nanovibration. *Expert Review of*

Medical Devices, 11(4), 417-423. doi:10.1586/17434440.2014.916205

Dahl, K. N., Ribeiro, A. J. S., & Lammerding, J. (2008). Nuclear Shape, Mechanics, and Mechanotransduction. *Circulation Research, 102*(11), 1307-1318. doi:doi:10.1161/CIRCRESAHA.108.173989

Dai, Z. Q., Wang, R., Ling, S. K., Wan, Y. M., & Li, Y. H. (2007). Simulated microgravity inhibits the proliferation and osteogenesis of rat bone marrow mesenchymal stem cells. *Cell Prolif, 40*(5), 671-684. doi:10.1111/j.1365-2184.2007.00461.x

Dalagiorgou, G., Basdra, E. K., & Papavassiliou, A. G. (2010). Polycystin-1: function as a mechanosensor. *Int J Biochem Cell Biol, 42*(10), 1610-1613. doi:10.1016/j.biocel.2010.06.017

Dalagiorgou, G., Piperi, C., Adamopoulos, C., Georgopoulou, U., Gargalionis, A. N., Spyropoulou, A., . . . Papavassiliou, A. G. (2017). Mechanosensor polycystin-1 potentiates differentiation of human osteoblastic cells by upregulating Runx2 expression via induction of JAK2/STAT3 signaling axis. *Cell Mol Life Sci, 74*(5), 921-936. doi:10.1007/s00018-016-2394-8

Dalby, M. J., Gadegaard, N., & Oreffo, R. O. (2014). Harnessing nanotopography and integrin-matrix interactions to influence stem cell fate. *Nat Mater, 13*(6), 558-569. doi:10.1038/nmat3980

Dalby, M. J., Gadegaard, N., Tare, R., Andar, A., Riehle, M. O., Herzyk, P., . . . Oreffo, R. O. (2007). The control of human mesenchymal cell differentiation using nanoscale symmetry and disorder. *Nat Mater, 6*(12), 997-1003. doi:10.1038/nmat2013

Dalby, M. J., Garcia, A. J., & Salmeron-Sanchez, M. (2018). Receptor control in mesenchymal stem cell engineering. *Nature Reviews Materials, 3*(3). doi:10.1038/natrevmats.2017.91

Damsgaard, C. T., Molgaard, C., Matthiessen, J., Gyldenlove, S. N., & Lauritzen, L. (2012). The effects of n-3 long-chain polyunsaturated

fatty acids on bone formation and growth factors in adolescent boys. *Pediatr Res, 71*(6), 713-719. doi:10.1038/pr.2012.28

Daniele, S., Natali, L., Giacomelli, C., Campiglia, P., Novellino, E., Martini, C., & Trincavelli, M. L. (2017). Osteogenesis Is Improved by Low Tumor Necrosis Factor Alpha Concentration through the Modulation of Gs-Coupled Receptor Signals. *Molecular and Cellular Biology, 37*(8). doi:10.1128/MCB.00442-16

Davison, M. J., McMurray, R. J., Smith, C. A., Dalby, M. J., & Meek, R. D. (2016). Nanopit-induced osteoprogenitor cell differentiation: The effect of nanopit depth. *J Tissue Eng, 7*, 2041731416652778. doi:10.1177/2041731416652778

De Cesaris, P., Starace, D., Riccioli, A., Padula, F., Filippini, A., & Ziparo, E. (1998). Tumor necrosis factor-alpha induces interleukin-6 production and integrin ligand expression by distinct transduction pathways. *J Biol Chem, 273*(13), 7566-7571.

Demer, L. L., Wortham, C. M., Dirksen, E. R., & Sanderson, M. J. (1993). Mechanical stimulation induces intercellular calcium signaling in bovine aortic endothelial cells. *American Journal of Physiology-Heart and Circulatory Physiology, 264*(6), H2094-H2102. doi:10.1152/ajpheart.1993.264.6.H2094

Dennis, J. E., Carbillet, J. P., Caplan, A. I., & Charbord, P. (2002). The STRO-1+ marrow cell population is multipotential. *Cells Tissues Organs, 170*(2-3), 73-82.

Dickson, K. M., Bhakar, A. L., & Barker, P. A. (2004). TRAF6-dependent NF-kB transcriptional activity during mouse development. *Dev Dyn, 231*(1), 122-127. doi:10.1002/dvdy.20110

Dilogo, I. H., Primaputra, M. R. A., Pawitan, J. A., & Liem, I. K. (2017). Modified Masquelet technique using allogeneic umbilical cord-derived mesenchymal stem cells for infected non-union femoral shaft fracture with a 12 cm bone defect: A case report.

International journal of surgery case reports, 34, 11-16. doi:10.1016/j.ijscr.2017.03.002

Ding, M., & Wang, X. (2017). Antagonism between Hedgehog and Wnt signaling pathways regulates tumorigenicity. *Oncol Lett, 14*(6), 6327-6333. doi:10.3892/ol.2017.7030

Ding, S., Li, J. R., Luo, C., Li, L., Yang, G., & Zhou, S. B. (2013). Synergistic effect of released dexamethasone and surface nanoroughness on mesenchymal stem cell differentiation. *Biomaterials Science, 1*(10), 1091-1100. doi:10.1039/c3bm60095e

Dingal, P. C., & Discher, D. E. (2014). Systems mechanobiology: tension-inhibited protein turnover is sufficient to physically control gene circuits. *Biophys J, 107*(11), 2734-2743. doi:10.1016/j.bpj.2014.10.042

Doan, T. K. P., Park, K. S., Kim, H. K., Park, D. S., Kim, J. H., & Yoon, T. R. (2012). Inhibition of JNK and ERK Pathways by SP600125-and U0126-Enhanced Osteogenic Differentiation of Bone Marrow Stromal Cells. *Tissue Engineering and Regenerative Medicine, 9*(6), 283-294. doi:10.1007/s13770-012-0352-6

Dobrokhotov, O., Samsonov, M., Sokabe, M., & Hirata, H. (2018). Mechanoregulation and pathology of YAP/TAZ via Hippo and non-Hippo mechanisms. *Clin Transl Med, 7*(1), 23. doi:10.1186/s40169-018-0202-9

Dominici, M., Le Blanc, K., Mueller, I., Slaper-Cortenbach, I., Marini, F., Krause, D., . . . Horwitz, E. (2006). Minimal criteria for defining multipotent mesenchymal stromal cells. The International Society for Cellular Therapy position statement. *Cytotherapy, 8*(4), 315-317. doi:10.1080/14653240600855905

Donnelly, H., Salmeron-Sanchez, M., & Dalby, M. J. (2018). Designing stem cell niches for differentiation and self-renewal. *Journal of*

The Royal Society Interface, 15(145), 20180388. doi:doi:10.1098/rsif.2018.0388

Dossumbekova, A., Anghelina, M., Madhavan, S., He, L., Quan, N., Knobloch, T., & Agarwal, S. (2007). Biomechanical signals inhibit IKK activity to attenuate NF-kappaB transcription activity in inflamed chondrocytes. *Arthritis Rheum, 56*(10), 3284-3296. doi:10.1002/art.22933

Doyle, A. D. (2016). Generation of 3D Collagen Gels with Controlled Diverse Architectures. *Curr Protoc Cell Biol, 72*, 10 20 11-10 20 16. doi:10.1002/cpcb.9

Drager, J., Harvey, E. J., & Barralet, J. (2015). Hypoxia signalling manipulation for bone regeneration. *Expert Rev Mol Med, 17*, e6. doi:10.1017/erm.2015.4

Driscoll, T. P., Cosgrove, B. D., Heo, S. J., Shurden, Z. E., & Mauck, R. L. (2015). Cytoskeletal to Nuclear Strain Transfer Regulates YAP Signaling in Mesenchymal Stem Cells. *Biophys J, 108*(12), 2783-2793. doi:10.1016/j.bpj.2015.05.010

Droge, W. (2002). Free radicals in the physiological control of cell function. *Physiological Reviews, 82*(1), 47-95. doi:10.1152/physrev.00018.2001

Du, J., Zu, Y., Li, J., Du, S., Xu, Y., Zhang, L., . . . Yang, C. (2016). Extracellular matrix stiffness dictates Wnt expression through integrin pathway. *Sci Rep, 6*, 20395. doi:10.1038/srep20395

Duan, J., Yin, J., Ren, W., Liu, T., Cui, Z., Huang, X., . . . Yin, Y. (2016). Dietary supplementation with l-glutamate and l-aspartate alleviates oxidative stress in weaned piglets challenged with hydrogen peroxide. *Amino Acids, 48*(1), 53-64. doi:10.1007/s00726-015-2065-3

Duan, X., & Sheardown, H. (2006). Dendrimer crosslinked collagen as a corneal tissue engineering scaffold: mechanical properties and

corneal epithelial cell interactions. *Biomaterials, 27*(26), 4608-4617. doi:10.1016/j.biomaterials.2006.04.022

Ducy, P., Desbois, C., Boyce, B., Pinero, G., Story, B., Dunstan, C., . . . Karsenty, G. (1996). Increased bone formation in osteocalcin-deficient mice. *Nature, 382*(6590), 448-452. doi:DOI 10.1038/382448a0

Dumanian, Z. P., Tollemar, V., Ye, J., Lu, M., Zhu, Y., Liao, J., . . . Reid, R. R. (2017). Repair of critical sized cranial defects with BMP9-transduced calvarial cells delivered in a thermoresponsive scaffold. *PLoS One, 12*(3), e0172327. doi:10.1371/journal.pone.0172327

Dvorak, M. M., Siddiqua, A., Ward, D. T., Carter, D. H., Dallas, S. L., Nemeth, E. F., & Riccardi, D. (2004). Physiological changes in extracellular calcium concentration directly control osteoblast function in the absence of calciotropic hormones. *Proc Natl Acad Sci U S A, 101*(14), 5140-5145. doi:10.1073/pnas.0306141101

Ehrbar, M., Sala, A., Lienemann, P., Ranga, A., Mosiewicz, K., Bittermann, A., . . . Lutolf, M. P. (2011). Elucidating the role of matrix stiffness in 3D cell migration and remodeling. *Biophys J, 100*(2), 284-293. doi:10.1016/j.bpj.2010.11.082

Eijken, M., Meijer, I. M., Westbroek, I., Koedam, M., Chiba, H., Uitterlinden, A. G., . . . van Leeuwen, J. P. (2008). Wnt signaling acts and is regulated in a human osteoblast differentiation dependent manner. *Journal of Cellular Biochemistry, 104*(2), 568-579. doi:10.1002/jcb.21651

Einhorn, T. A., & Gerstenfeld, L. C. (2015). Fracture healing: mechanisms and interventions. *Nat Rev Rheumatol, 11*(1), 45-54. doi:10.1038/nrrheum.2014.164

El Bialy, I., Jiskoot, W., & Reza Nejadnik, M. (2017). Formulation, Delivery and Stability of Bone Morphogenetic Proteins for Effective

Bone Regeneration. *Pharmaceutical research, 34*(6), 1152-1170. doi:10.1007/s11095-017-2147-x

Elliott, D. S., Newman, K. J., Forward, D. P., Hahn, D. M., Ollivere, B., Kojima, K., . . . Moran, C. G. (2016). A unified theory of bone healing and nonunion: BHN theory. *Bone Joint J, 98-b*(7), 884-891. doi:10.1302/0301-620x.98b7.36061

Elosegui-Artola, A., Andreu, I., Beedle, A. E. M., Lezamiz, A., Uroz, M., Kosmalska, A. J., . . . Roca-Cusachs, P. (2017). Force Triggers YAP Nuclear Entry by Regulating Transport across Nuclear Pores. *Cell, 171*(6), 1397-1410 e1314. doi:10.1016/j.cell.2017.10.008

Engler, A. J., Sen, S., Sweeney, H. L., & Discher, D. E. (2006). Matrix elasticity directs stem cell lineage specification. *Cell, 126*(4), 677-689. doi:10.1016/j.cell.2006.06.044

Eriksen, E. F. (2010). Cellular mechanisms of bone remodeling. *Reviews in endocrine & metabolic disorders, 11*(4), 219-227. doi:10.1007/s11154-010-9153-1

Faikrua, A., Jeenapongsa, R., Sila-asna, M., & Viyoch, J. (2009). Properties of beta-glycerol phosphate/collagen/chitosan blend scaffolds for application in skin tissue engineering. *Scienceasia, 35*(3), 247-254. doi:10.2306/scienceasia1513-1874.2009.35.247

Faust, U., Hampe, N., Rubner, W., Kirchgessner, N., Safran, S., Hoffmann, B., & Merkel, R. (2011). Cyclic stress at mHz frequencies aligns fibroblasts in direction of zero strain. *PLoS One, 6*(12), e28963. doi:10.1371/journal.pone.0028963

Fernandez-Gomez, F. J., Galindo, M. F., Gómez-Lázaro, M., Yuste, V. J., Comella, J. X., Aguirre, N., & Jordán, J. (2005). Malonate induces cell death via mitochondrial potential collapse and delayed

swelling through an ROS-dependent pathway. *Br J Pharmacol, 144*(4), 528-537. doi:10.1038/sj.bjp.0706069

Ferreira, A. M., Gentile, P., Chiono, V., & Ciardelli, G. (2012). Collagen for bone tissue regeneration. *Acta Biomater, 8*(9), 3191-3200. doi:10.1016/j.actbio.2012.06.014

Ferreira Mendes, A., Caramona, M. M., Carvalho, A. P., & Lopes, M. C. (2003). Hydrogen peroxide mediates interleukin-1ß-induced AP-1 activation in articular chondrocytes: Implications for the regulation of iNOS expression. *Cell Biology and Toxicology, 19*(4), 203-214. doi:10.1023/B:CBTO.0000003730.21261.fa

Fessel, G., Cadby, J., Wunderli, S., van Weeren, R., & Snedeker, J. G. (2014). Dose- and time-dependent effects of genipin crosslinking on cell viability and tissue mechanics - toward clinical application for tendon repair. *Acta Biomater, 10*(5), 1897-1906. doi:10.1016/j.actbio.2013.12.048

Fillmore, N., Huqi, A., Jaswal, J. S., Mori, J., Paulin, R., Haromy, A., . . . Lopaschuk, G. D. (2015). Effect of fatty acids on human bone marrow mesenchymal stem cell energy metabolism and survival. *PLoS One, 10*(3), e0120257. doi:10.1371/journal.pone.0120257

Fisher, A. B. (2009). Redox signaling across cell membranes. *Antioxid Redox Signal, 11*(6), 1349-1356. doi:10.1089/ARS.2008.2378

Fliefel, R., Ehrenfeld, M., & Otto, S. (2018). Induced pluripotent stem cells (iPSCs) as a new source of bone in reconstructive surgery: A systematic review and meta-analysis of preclinical studies. *J Tissue Eng Regen Med, 12*(7), 1780-1797. doi:10.1002/term.2697

Fliefel, R., Popov, C., Troltzsch, M., Kuhnisch, J., Ehrenfeld, M., & Otto, S. (2016). Mesenchymal stem cell proliferation and mineralization but not osteogenic differentiation are strongly affected by

extracellular pH. *J Craniomaxillofac Surg, 44*(6), 715-724. doi:10.1016/j.jcms.2016.03.003

Folmes, C. D., Park, S., & Terzic, A. (2013). Lipid metabolism greases the stem cell engine. *Cell Metabolism, 17*(2), 153-155. doi:10.1016/j.cmet.2013.01.010

Fox, S. W., & Chow, J. W. (1998). Nitric oxide synthase expression in bone cells. *Bone, 23*(1), 1-6.

Franklin, J. M., Ghosh, R. P., Shi, Q., & Liphardt, J. T. (2019). Concerted localization resets precede YAP-dependent transcription. *bioRxiv*, 539049. doi:10.1101/539049

Frenette, P. S., Pinho, S., Lucas, D., & Scheiermann, C. (2013). Mesenchymal stem cell: keystone of the hematopoietic stem cell niche and a stepping-stone for regenerative medicine. *Annu Rev Immunol, 31*, 285-316. doi:10.1146/annurev-immunol-032712-095919

Fruleux, A., & Hawkins, R. J. (2016). Physical role for the nucleus in cell migration. *J Phys Condens Matter, 28*(36), 363002. doi:10.1088/0953-8984/28/36/363002

Fu, H.-D., Wang, B.-K., Wan, Z.-Q., Lin, H., Chang, M.-L., & Han, G.-L. (2016). Wnt5a mediated canonical Wnt signaling pathway activation in orthodontic tooth movement: possible role in the tension force-induced bone formation. *Journal of Molecular Histology, 47*(5), 455-466. doi:10.1007/s10735-016-9687-y

Fu, P. L., Chen, S., Ding, Z. R., Cong, R. J., Shao, J. H., Zhang, L., & Qian, Q. R. (2017). Mechanical stimulation promotes osteogenic and chondrogenic differentiation of synovial mesenchymal stem cells through BMP-2. *International Journal of Clinical and Experimental Medicine, 10*(2), 2842-2849.

Fu, T., Liang, P., Song, J., Wang, J., Zhou, P., Tang, Y., . . . Huang, E. (2019). Matrigel Scaffolding Enhances BMP9-induced Bone

Formation in Dental Follicle Stem/Precursor Cells. *Int J Med Sci, 16*(4), 567-575. doi:10.7150/ijms.30801

Furmanik, M., & Shanahan, C. M. (2018). ER stress regulates alkaline phosphatase gene expression in vascular smooth muscle cells via an ATF4-dependent mechanism. *BMC Research Notes, 11*(1), 483. doi:10.1186/s13104-018-3582-4

G.D., P. (2015). *Osteoblastogenic differentiation of mesenchymal stem cells through nanoscale stimulation: The concept of a novel 3D osteogenic bioreactor*. (Doctor of Philosophy), University of Glasgow.

Gao, H. Q., Zhai, M. M., Wang, P., Zhang, X. H., Cai, J., Chen, X. F., . . . Jing, D. (2017). Low-level mechanical vibration enhances osteoblastogenesis via a canonical Wnt signaling-associated mechanism. *Molecular Medicine Reports, 16*(1), 317-324. doi:10.3892/mmr.2017.6608

Gao, J., Fu, S., Zeng, Z., Li, F., Niu, Q., Jing, D., & Feng, X. (2016). Cyclic stretch promotes osteogenesis-related gene expression in osteoblast-like cells through a cofilin-associated mechanism. *Molecular medicine reports, 14*(1), 218-224. doi:10.3892/mmr.2016.5239

Gao, X., Xu, C., Asada, N., & Frenette, P. S. (2018). The hematopoietic stem cell niche: from embryo to adult. *Development, 145*(2), dev139691. doi:10.1242/dev.139691

García-Añoveros, J., & Nagata, K. (2007). TRPA1. In V. Flockerzi & B. Nilius (Eds.), *Transient Receptor Potential (TRP) Channels* (pp. 347-362). Berlin, Heidelberg: Springer Berlin Heidelberg.

Garcia-Gareta, E., Coathup, M. J., & Blunn, G. W. (2015). Osteoinduction of bone grafting materials for bone repair and regeneration. *Bone, 81*, 112-121. doi:10.1016/j.bone.2015.07.007

Garrett, S. L. (2017). The Simple Harmonic Oscillator *Understanding Acoustics: An Experimentalist's View of Acoustics and Vibration* (pp. 69-152). Cham: Springer International Publishing.

Garrison, K. R., Donell, S., Ryder, J., Shemilt, I., Mugford, M., Harvey, I., & Song, F. (2007). Clinical effectiveness and cost-effectiveness of bone morphogenetic proteins in the non-healing of fractures and spinal fusion: a systematic review. *Health Technol Assess, 11*(30), 1-150, iii-iv.

Ge, C., Xiao, G., Jiang, D., Yang, Q., Hatch, N. E., Roca, H., & Franceschi, R. T. (2009). Identification and functional characterization of ERK/MAPK phosphorylation sites in the Runx2 transcription factor. *J Biol Chem, 284*(47), 32533-32543. doi:10.1074/jbc.M109.040980

Geppetti, P., Veldhuis, Nicholas A., Lieu, T., & Bunnett, Nigel W. (2015). G Protein-Coupled Receptors: Dynamic Machines for Signaling Pain and Itch. *Neuron, 88*(4), 635-649. doi:https://doi.org/10.1016/j.neuron.2015.11.001

Ghiasi, M. S., Chen, J., Vaziri, A., Rodriguez, E. K., & Nazarian, A. (2017). Bone fracture healing in mechanobiological modeling: A review of principles and methods. *Bone Rep, 6*, 87-100. doi:10.1016/j.bonr.2017.03.002

Giannoudis, P. V., Einhorn, T. A., & Marsh, D. (2007). Fracture healing: the diamond concept. *Injury, 38 Suppl 4*, S3-6.

Giannoudis, P. V., Faour, O., Goff, T., Kanakaris, N., & Dimitriou, R. (2011). Masquelet technique for the treatment of bone defects: tips-tricks and future directions. *Injury, 42*(6), 591-598. doi:10.1016/j.injury.2011.03.036

Giannoudis, P. V., Hak, D., Sanders, D., Donohoe, E., Tosounidis, T., & Bahney, C. (2015). Inflammation, Bone Healing, and Anti-Inflammatory Drugs: An Update. *Journal of Orthopaedic Trauma, 29 Suppl 12*, S6-9. doi:10.1097/bot.0000000000000465

Gibon, E., Lu, L. Y., Nathan, K., & Goodman, S. B. (2017). Inflammation, ageing, and bone regeneration. *J Orthop Translat, 10*, 28-35. doi:10.1016/j.jot.2017.04.002

Giordano, E., & Visioli, F. (2014). Long-chain omega 3 fatty acids: Molecular bases of potential antioxidant actions. *Prostaglandins, Leukotrienes and Essential Fatty Acids, 90*(1), 1-4. doi:https://doi.org/10.1016/j.plefa.2013.11.002

Glantzounis, G. K., Tsimoyiannis, E. C., Kappas, A. M., & Galaris, D. A. (2005). Uric acid and oxidative stress. *Curr Pharm Des, 11*(32), 4145-4151.

Golji, J., & Mofrad, M. R. (2013). The interaction of vinculin with actin. *PLoS Comput Biol, 9*(4), e1002995. doi:10.1371/journal.pcbi.1002995

Görlach, A., Bertram, K., Hudecova, S., & Krizanova, O. (2015). Calcium and ROS: A mutual interplay. *Redox Biology, 6*, 260-271. doi:10.1016/j.redox.2015.08.010

Grieben, M., Pike, A. C. W., Shintre, C. A., Venturi, E., El-Ajouz, S., Tessitore, A., . . . Carpenter, E. P. (2016). Structure of the polycystic kidney disease TRP channel Polycystin-2 (PC2). *Nature Structural &Amp; Molecular Biology, 24*, 114. doi:10.1038/nsmb.3343

Grottkau, B. E., Yang, X., Zhang, L., Ye, L., & Lin, Y. (2013). Comparison of Effects of Mechanical Stretching on Osteogenic Potential of ASCs and BMSCs. *Bone Research, 1*, 282. doi:10.4248/BR201303006

Gu, Q., Tian, H., Zhang, K., Chen, D., Chen, D., Wang, X., & Zhao, J. (2018). Wnt5a/FZD4 Mediates the Mechanical Stretch-Induced Osteogenic Differentiation of Bone Mesenchymal Stem Cells.

Cellular Physiology and Biochemistry, 48(1), 215-226. doi:10.1159/000491721

Gudermann, T., Grosse, R., & Schultz, G. (2000). Contribution of receptor/G protein signaling to cell growth and transformation. *Naunyn-Schmiedeberg's Archives of Pharmacology, 361*(4), 345-362. doi:10.1007/s002109900208

Guerra, M. T. E., Gregio, F. M., Bernardi, A., & Castro, C. C. d. (2017). Infection rate in adult patients with open fractures treated at the emergency hospital and at the ULBRA university hospital in Canoas, Rio Grande do Sul, Brazil. *Revista brasileira de ortopedia, 52*(5), 544-548. doi:10.1016/j.rboe.2017.08.012

Guilluy, C., Garcia-Mata, R., & Burridge, K. (2011). Rho protein crosstalk: another social network? *Trends in Cell Biology, 21*(12), 718-726. doi:10.1016/j.tcb.2011.08.002

Guilluy, C., Osborne, L. D., Van Landeghem, L., Sharek, L., Superfine, R., Garcia-Mata, R., & Burridge, K. (2014). Isolated nuclei adapt to force and reveal a mechanotransduction pathway in the nucleus. *Nat Cell Biol, 16*(4), 376-381. doi:10.1038/ncb2927

Guo, J. L., Kim, Y. S., Xie, V. Y., Smith, B. T., Watson, E., Lam, J., . . . Mikos, A. G. (2019). Modular, tissue-specific, and biodegradable hydrogel cross-linkers for tissue engineering. *Sci Adv, 5*(6), eaaw7396. doi:10.1126/sciadv.aaw7396

Gutierrez-Aranda, I., Ramos-Mejia, V., Bueno, C., Munoz-Lopez, M., Real, P. J., Mácia, A., . . . Menendez, P. (2010). Human induced pluripotent stem cells develop teratoma more efficiently and faster than human embryonic stem cells regardless the site of injection. *Stem cells (Dayton, Ohio), 28*(9), 1568-1570. doi:10.1002/stem.471

Haffner-Luntzer, M., Lackner, I., Liedert, A., Fischer, V., & Ignatius, A. (2018). Effects of low-magnitude high-frequency vibration on osteoblasts are dependent on estrogen receptor alpha signaling and cytoskeletal remodeling. *Biochem Biophys Res Commun, 503*(4), 2678-2684. doi:10.1016/j.bbrc.2018.08.023

Hahn-Windgassen, A., Nogueira, V., Chen, C. C., Skeen, J. E., Sonenberg, N., & Hay, N. (2005). Akt activates the mammalian target of rapamycin by regulating cellular ATP level and AMPK activity. *J Biol Chem, 280*(37), 32081-32089. doi:10.1074/jbc.M502876200

Hamidouche, Z., Hay, E., Vaudin, P., Charbord, P., Schule, R., Marie, P. J., & Fromigue, O. (2008). FHL2 mediates dexamethasone-induced mesenchymal cell differentiation into osteoblasts by activating Wnt/beta-catenin signaling-dependent Runx2 expression. *FASEB J, 22*(11), 3813-3822. doi:10.1096/fj.08-106302

Hara, M., Tabata, K., Suzuki, T., Do, M.-K. Q., Mizunoya, W., Nakamura, M., . . . Tatsumi, R. (2012). Calcium influx through a possible coupling of cation channels impacts skeletal muscle satellite cell activation in response to mechanical stretch. *American Journal of Physiology-Cell Physiology, 302*(12), C1741-C1750. doi:10.1152/ajpcell.00068.2012

Hartsock, A., & Nelson, W. J. (2008). Adherens and tight junctions: Structure, function and connections to the actin cytoskeleton. *Biochimica et Biophysica Acta (BBA) - Biomembranes, 1778*(3), 660-669. doi:https://doi.org/10.1016/j.bbamem.2007.07.012

Hasan, R., & Zhang, X. (2018). Ca(2+) Regulation of TRP Ion Channels. *International Journal of Molecular Sciences, 19*(4), 1256. doi:10.3390/ijms19041256

Hasegawa, D., Wada, N., Yoshida, S., Mitarai, H., Arima, M., Tomokiyo, A., . . . Maeda, H. (2018). Wnt5a suppresses osteoblastic differentiation of human periodontal ligament stem cell-like cells

via Ror2/JNK signaling. *Journal of Cellular Physiology, 233*(2), 1752-1762. doi:10.1002/jcp.26086

Hassan, M. Q., Tare, R. S., Lee, S. H., Mandeville, M., Morasso, M. I., Javed, A., . . . Lian, J. B. (2006). BMP2 commitment to the osteogenic lineage involves activation of Runx2 by DLX3 and a homeodomain transcriptional network. *J Biol Chem, 281*(52), 40515-40526. doi:10.1074/jbc.M604508200

Hayward, P., Kalmar, T., & Martinez Arias, A. (2008). Wnt/Notch signalling and information processing during development. *Development, 135*(3), 411-424. doi:10.1242/dev.000505

Helary, C., Abed, A., Mosser, G., Louedec, L., Meddahi-Pellé, A., & Giraud-Guille, M. M. (2011). Synthesis and in vivo integration of improved concentrated collagen hydrogels. *J Tissue Eng Regen Med, 5*(3), 248-252. doi:10.1002/term.326

Hellweg, C. E., Arenz, A., Bogner, S., Schmitz, C., & Baumstark-Khan, C. (2006). Activation of nuclear factor kappa B by different agents: influence of culture conditions in a cell-based assay. *Ann N Y Acad Sci, 1091*, 191-204. doi:10.1196/annals.1378.066

Heo, J. S., Choi, Y., Kim, H. S., & Kim, H. O. (2016). Comparison of molecular profiles of human mesenchymal stem cells derived from bone marrow, umbilical cord blood, placenta and adipose tissue. *International Journal of Molecular Medicine, 37*(1), 115-125. doi:10.3892/ijmm.2015.2413

Herzig, S., & Shaw, R. J. (2018). AMPK: guardian of metabolism and mitochondrial homeostasis. *Nat Rev Mol Cell Biol, 19*(2), 121-135. doi:10.1038/nrm.2017.95

Hess, K., Ushmorov, A., Fiedler, J., Brenner, R. E., & Wirth, T. (2009). TNFalpha promotes osteogenic differentiation of human mesenchymal stem cells by triggering the NF-kappaB signaling pathway. *Bone, 45*(2), 367-376. doi:10.1016/j.bone.2009.04.252

Hesse, E., Hefferan, T. E., Tarara, J. E., Haasper, C., Meller, R., Krettek, C., . . . Yaszemski, M. J. (2010). Collagen type I hydrogel allows migration, proliferation, and osteogenic differentiation of rat bone marrow stromal cells. *J Biomed Mater Res A, 94*(2), 442-449. doi:10.1002/jbm.a.32696

Higuchi, M., Honda, T., Proske, R. J., & Yeh, E. T. H. (1998). Regulation of reactive oxygen species-induced apoptosis and necrosis by caspase 3-like proteases. *Oncogene, 17*(21), 2753-2760. doi:10.1038/sj.onc.1202211

Hilton, M. J., Tu, X., Wu, X., Bai, S., Zhao, H., Kobayashi, T., . . . Long, F. (2008). Notch signaling maintains bone marrow mesenchymal progenitors by suppressing osteoblast differentiation. *Nature Medicine, 14*, 306. doi:10.1038/nm1716

Hinman, A., Chuang, H.-h., Bautista, D. M., & Julius, D. (2006). TRP channel activation by reversible covalent modification. *Proceedings of the National Academy of Sciences, 103*(51), 19564. doi:10.1073/pnas.0609598103

Ho, W. P., Chen, T. L., Chiu, W. T., Tai, Y. T., & Chen, R. M. (2005). Nitric oxide induces osteoblast apoptosis through a mitochondria-dependent pathway. *Ann N Y Acad Sci, 1042*, 460-470. doi:10.1196/annals.1338.039

Hoang, Q. Q., Sicheri, F., Howard, A. J., & Yang, D. S. (2003). Bone recognition mechanism of porcine osteocalcin from crystal structure. *Nature, 425*(6961), 977-980. doi:10.1038/nature02079

Hoemann, C. D., El-Gabalawy, H., & McKee, M. D. (2009). In vitro osteogenesis assays: influence of the primary cell source on alkaline phosphatase activity and mineralization. *Pathol Biol (Paris), 57*(4), 318-323. doi:10.1016/j.patbio.2008.06.004

Hoey, D. A., Tormey, S., Ramcharan, S., O'Brien, F. J., & Jacobs, C. R. (2012). Primary cilia-mediated mechanotransduction in human mesenchymal stem cells. *Stem Cells, 30*(11), 2561-2570. doi:10.1002/stem.1235

Hoffman, B. D., Grashoff, C., & Schwartz, M. A. (2011). Dynamic molecular processes mediate cellular mechanotransduction. *Nature, 475*(7356), 316-323. doi:10.1038/nature10316

Holmes, D. (2017). Closing the gap. *Nature, 550*, S194. doi:10.1038/550S194a

Hong, S., Li, H., Wu, D., Li, B., Liu, C., Guo, W., . . . Yang, Q. (2015). Oxidative damage to human parametrial ligament fibroblasts induced by mechanical stress. *Mol Med Rep, 12*(4), 5342-5348. doi:10.3892/mmr.2015.4115

Hu, W., Wang, Z., Xiao, Y., Zhang, S., & Wang, J. (2019). Advances in crosslinking strategies of biomedical hydrogels. *Biomater Sci, 7*(3), 843-855. doi:10.1039/c8bm01246f

Huang, H., Zhao, N., Xu, X., Xu, Y., Li, S., Zhang, J., & Yang, P. (2011). Dose-specific effects of tumor necrosis factor alpha on osteogenic differentiation of mesenchymal stem cells. *Cell Prolif, 44*(5), 420-427. doi:10.1111/j.1365-2184.2011.00769.x

Huang, J., Grater, S. V., Corbellini, F., Rinck, S., Bock, E., Kemkemer, R., . . . Spatz, J. P. (2009). Impact of order and disorder in RGD

nanopatterns on cell adhesion. *Nano Lett, 9*(3), 1111-1116. doi:10.1021/nl803548b

Huang, K.-P. (1989). The mechanism of protein kinase C activation. *Trends in Neurosciences, 12*(11), 425-432. doi:https://doi.org/10.1016/0166-2236(89)90091-X

Huang, R. L., Sun, Y., Ho, C. K., Liu, K., Tang, Q. Q., Xie, Y., & Li, Q. (2018). IL-6 potentiates BMP-2-induced osteogenesis and adipogenesis via two different BMPR1A-mediated pathways. *Cell Death Dis, 9*(2), 144. doi:10.1038/s41419-017-0126-0

Huang, R. L., Yuan, Y., Tu, J., Zou, G. M., & Li, Q. (2014). Opposing TNF-alpha/IL-1beta- and BMP-2-activated MAPK signaling pathways converge on Runx2 to regulate BMP-2-induced osteoblastic differentiation. *Cell Death Dis, 5*, e1187. doi:10.1038/cddis.2014.101

Huang, W., Yang, S., Shao, J., & Li, Y. P. (2007). Signaling and transcriptional regulation in osteoblast commitment and differentiation. *Front Biosci, 12*, 3068-3092.

Huang, X., Das, R., Patel, A., & Duc Nguyen, T. (2018). Physical Stimulations for Bone and Cartilage Regeneration. *Regenerative Engineering and Translational Medicine, 4*(4), 216-237. doi:10.1007/s40883-018-0064-0

Huebsch, N., Arany, P. R., Mao, A. S., Shvartsman, D., Ali, O. A., Bencherif, S. A., . . . Mooney, D. J. (2010). Harnessing traction-mediated manipulation of the cell/matrix interface to control stem-cell fate. *Nat Mater, 9*(6), 518-526. doi:10.1038/nmat2732

Hughes, T. E. T., Pumroy, R. A., Yazici, A. T., Kasimova, M. A., Fluck, E. C., Huynh, K. W., . . . Moiseenkova-Bell, V. Y. (2018). Structural insights on TRPV5 gating by endogenous modulators. *Nat Commun, 9*(1), 4198. doi:10.1038/s41467-018-06753-6

Humeau, J., Bravo-San Pedro, J. M., Vitale, I., Nunez, L., Villalobos, C., Kroemer, G., & Senovilla, L. (2017). Calcium signaling and cell

cycle: Progression or death. *Cell Calcium*. doi:10.1016/j.ceca.2017.07.006

Huttemann, M., Lee, I., Samavati, L., Yu, H., & Doan, J. W. (2007). Regulation of mitochondrial oxidative phosphorylation through cell signaling. *Biochim Biophys Acta, 1773*(12), 1701-1720.

Huynh, K. W., Cohen, M. R., Chakrapani, S., Holdaway, H. A., Stewart, P. L., & Moiseenkova-Bell, V. Y. (2014). Structural Insight into the Assembly of TRPV Channels. *Structure, 22*(2), 260-268. doi:10.1016/j.str.2013.11.008

Iannotti, J. P., Naidu, S., Noguchi, Y., Hunt, R. M., & Brighton, C. T. (1994). Growth plate matrix vesicle biogenesis. The role of intracellular calcium. *Clin Orthop Relat Res*(306), 222-229.

Icer, M. A., & Gezmen-Karadag, M. (2018). The multiple functions and mechanisms of osteopontin. *Clin Biochem, 59*, 17-24. doi:10.1016/j.clinbiochem.2018.07.003

Illario, M., Cavallo, A. L., Bayer, K. U., Di Matola, T., Fenzi, G., Rossi, G., & Vitale, M. (2003). Calcium/calmodulin-dependent protein kinase II binds to Raf-1 and modulates integrin-stimulated ERK activation. *J Biol Chem, 278*(46), 45101-45108. doi:10.1074/jbc.M305355200

Illich, D. J., Demir, N., Stojkovic, M., Scheer, M., Rothamel, D., Neugebauer, J., . . . Zoller, J. E. (2011). Concise Review: Induced Pluripotent Stem Cells and Lineage Reprogramming: Prospects for Bone Regeneration. *Stem Cells, 29*(4), 555-563. doi:10.1002/stem.611

Imran, M., & Lim, I. K. (2013). Regulation of Btg2(/TIS21/PC3) expression via reactive oxygen species-protein kinase C-NuFkappaBeta pathway under stress conditions. *Cell Signal, 25*(12), 2400-2412. doi:10.1016/j.cellsig.2013.07.015

Inui, S., Minami, K., Ito, E., Imaizumi, H., Mori, S., Koizumi, M., . . . Matsuura, N. (2017). Irradiation strongly reduces tumorigenesis of

human induced pluripotent stem cells. *Journal of Radiation Research, 58*(4), 430-438. doi:10.1093/jrr/rrw124

Ishikawa, M., Iwamoto, T., Nakamura, T., Doyle, A., Fukumoto, S., & Yamada, Y. (2011). Pannexin 3 functions as an ER Ca(2+) channel, hemichannel, and gap junction to promote osteoblast differentiation. *The Journal of Cell Biology, 193*(7), 1257-1274. doi:10.1083/jcb.201101050

Ishikawa, M., & Yamada, Y. (2017). The Role of Pannexin 3 in Bone Biology. *J Dent Res, 96*(4), 372-379. doi:10.1177/0022034516678203

Ito, K., & Ito, K. (2016). Metabolism and the Control of Cell Fate Decisions and Stem Cell Renewal. *Annu Rev Cell Dev Biol, 32*, 399-409. doi:10.1146/annurev-cellbio-111315-125134

Ito, K., & Suda, T. (2014). Metabolic requirements for the maintenance of self-renewing stem cells. *Nat Rev Mol Cell Biol, 15*(4), 243-256. doi:10.1038/nrm3772

Ito, S., Suki, B., Kume, H., Numaguchi, Y., Ishii, M., Iwaki, M., . . . Sokabe, M. (2010). Actin cytoskeleton regulates stretch-activated Ca2+ influx in human pulmonary microvascular endothelial cells. *Am J Respir Cell Mol Biol, 43*(1), 26-34. doi:10.1165/rcmb.2009-0073OC

Ito, Y., Kimura, T., Ago, Y., Nam, K., Hiraku, K., Miyazaki, K., . . . Kishida, A. (2011). Nano-vibration effect on cell adhesion and its shape. *Biomed Mater Eng, 21*(3), 149-158. doi:10.3233/bme-2011-0664

Itonaga, I., Sabokbar, A., Sun, S. G., Kudo, O., Danks, L., Ferguson, D., . . . Athanasou, N. A. (2004). Transforming growth factor-beta

induces osteoclast formation in the absence of RANKL. *Bone, 34*(1), 57-64.

Izadifar, Z., Chen, X., & Kulyk, W. (2012). Strategic design and fabrication of engineered scaffolds for articular cartilage repair. *J Funct Biomater, 3*(4), 799-838. doi:10.3390/jfb3040799

Izadifar, Z., Chen, X., & Kulyk, W. (2012). Strategic design and fabrication of engineered scaffolds for articular cartilage repair. *J Funct Biomater, 3*(4), 799-838. doi:10.3390/jfb3040799

Izadpanah, R., Schächtele, D. J., Pfnür, A. B., Lin, D., Slakey, D. P., Kadowitz, P. J., & Alt, E. U. (2015). The impact of statins on biological characteristics of stem cells provides a novel explanation for their pleiotropic beneficial and adverse clinical effects. *American Journal of Physiology-Cell Physiology, 309*(8), C522-C531. doi:10.1152/ajpcell.00406.2014

James, A. W. (2013). Review of Signaling Pathways Governing MSC Osteogenic and Adipogenic Differentiation. *Scientifica (Cairo), 2013*, 684736. doi:10.1155/2013/684736

James, A. W., Leucht, P., Levi, B., Carre, A. L., Xu, Y., Helms, J. A., & Longaker, M. T. (2010). Sonic Hedgehog influences the balance of osteogenesis and adipogenesis in mouse adipose-derived stromal cells. *Tissue Eng Part A, 16*(8), 2605-2616. doi:10.1089/ten.TEA.2010.0048

Jang, W. G., Kim, E. J., Kim, D. K., Ryoo, H. M., Lee, K. B., Kim, S. H., . . . Koh, J. T. (2012). BMP2 protein regulates osteocalcin expression via Runx2-mediated Atf6 gene transcription. *J Biol Chem, 287*(2), 905-915. doi:10.1074/jbc.M111.253187

Jansen, J. H., Weyts, F. A., Westbroek, I., Jahr, H., Chiba, H., Pols, H. A., . . . Weinans, H. (2004). Stretch-induced phosphorylation of

ERK1/2 depends on differentiation stage of osteoblasts. *Journal of Cellular Biochemistry, 93*(3), 542-551. doi:10.1002/jcb.20162

Javed, A., Bae, J. S., Afzal, F., Gutierrez, S., Pratap, J., Zaidi, S. K., . . . Lian, J. B. (2008). Structural coupling of Smad and Runx2 for execution of the BMP2 osteogenic signal. *J Biol Chem, 283*(13), 8412-8422. doi:10.1074/jbc.M705578200

Javed, A., Chen, H., & Ghori, F. Y. (2010). Genetic and transcriptional control of bone formation. *Oral Maxillofac Surg Clin North Am, 22*(3), 283-293, v. doi:10.1016/j.coms.2010.05.001

Jeromson, S., Gallagher, I. J., Galloway, S. D., & Hamilton, D. L. (2015). Omega-3 Fatty Acids and Skeletal Muscle Health. *Mar Drugs, 13*(11), 6977-7004. doi:10.3390/md13116977

Jetta, D., Gottlieb, P. A., Verma, D., Sachs, F., & Hua, S. Z. (2019). Shear stress-induced nuclear shrinkage through activation of Piezo1 channels in epithelial cells. *J Cell Sci, 132*(11), jcs226076. doi:10.1242/jcs.226076

Jha, B. S., Ayres, C. E., Bowman, J. R., Telemeco, T. A., Sell, S. A., Bowlin, G. L., & Simpson, D. G. (2011). Electrospun Collagen: A Tissue Engineering Scaffold with Unique Functional Properties in a Wide Variety of Applications. *Journal of Nanomaterials*. doi:10.1155/2011/348268

Ji, H., Liu, Y., Zhao, X., & Zhang, M. (2011). N-acetyl-L-cysteine enhances the osteogenic differentiation and inhibits the adipogenic differentiation through up regulation of Wnt 5a and down regulation of PPARG in bone marrow stromal cells. *Biomed Pharmacother, 65*(5), 369-374. doi:10.1016/j.biopha.2011.04.020

Jia, Y. Y., Li, F., Geng, N., Gong, P., Huang, S. J., Meng, L. X., . . . Ban, Y. (2014). Fluid flow modulates the expression of genes involved in

the Wnt signaling pathway in osteoblasts in 3D culture conditions. *Int J Mol Med, 33*(5), 1282-1288. doi:10.3892/ijmm.2014.1694

Jiang, H., & Grinnell, F. (2005). Cell-matrix entanglement and mechanical anchorage of fibroblasts in three-dimensional collagen matrices. *Mol Biol Cell, 16*(11), 5070-5076. doi:10.1091/mbc.E05-01-0007

Jin, S., Zhou, F., Katirai, F., & Li, P. L. (2011). Lipid raft redox signaling: molecular mechanisms in health and disease. *Antioxid Redox Signal, 15*(4), 1043-1083. doi:10.1089/ars.2010.3619

Jing, D., Tong, S., Zhai, M., Li, X., Cai, J., Wu, Y., . . . Luo, E. (2015). Effect of low-level mechanical vibration on osteogenesis and osseointegration of porous titanium implants in the repair of long bone defects. *Sci Rep, 5*, 17134. doi:10.1038/srep17134

John, A., Varma, H. K., & Kumari, T. V. (2003). Surface reactivity of calcium phosphate based ceramics in a cell culture system. *J Biomater Appl, 18*(1), 63-78.

Johnson, M. L. (2004). The high bone mass family--the role of Wnt/Lrp5 signaling in the regulation of bone mass. *J Musculoskelet Neuronal Interact, 4*(2), 135-138.

Jufri, N. F., Mohamedali, A., Avolio, A., & Baker, M. S. (2015). Mechanical stretch: physiological and pathological implications for human vascular endothelial cells. *Vasc Cell, 7*, 8. doi:10.1186/s13221-015-0033-z

Jung, G.-Y., Park, Y.-J., & Han, J.-S. (2010). Effects of HA released calcium ion on osteoblast differentiation. *Journal of Materials Science: Materials in Medicine, 21*(5), 1649-1654. doi:10.1007/s10856-010-4011-y

Kahles, F., Findeisen, H. M., & Bruemmer, D. (2014). Osteopontin: A novel regulator at the cross roads of inflammation, obesity and

diabetes. *Molecular Metabolism, 3*(4), 384-393. doi:10.1016/j.molmet.2014.03.004

Kahles, F., Findeisen, H. M., & Bruemmer, D. (2014). Osteopontin: A novel regulator at the cross roads of inflammation, obesity and diabetes. *Mol Metab, 3*(4), 384-393. doi:10.1016/j.molmet.2014.03.004

Kane, R. J., & Roeder, R. K. (2012). Effects of hydroxyapatite reinforcement on the architecture and mechanical properties of freeze-dried collagen scaffolds. *J Mech Behav Biomed Mater, 7*, 41-49. doi:10.1016/j.jmbbm.2011.09.010

Kane, R. J., Weiss-Bilka, H. E., Meagher, M. J., Liu, Y., Gargac, J. A., Niebur, G. L., . . . Roeder, R. K. (2015). Hydroxyapatite reinforced collagen scaffolds with improved architecture and mechanical properties. *Acta Biomater, 17*, 16-25. doi:10.1016/j.actbio.2015.01.031

Kang, H. W., Lee, S. J., Ko, I. K., Kengla, C., Yoo, J. J., & Atala, A. (2016). A 3D bioprinting system to produce human-scale tissue constructs with structural integrity. *Nat Biotechnol, 34*(3), 312-319. doi:10.1038/nbt.3413

Kang, K. S., & Robling, A. G. (2015). New Insights into Wnt–Lrp5/6–β-Catenin Signaling in Mechanotransduction. *Frontiers in Endocrinology, 5*(246). doi:10.3389/fendo.2014.00246

Kanno, T., Takahashi, T., Tsujisawa, T., Ariyoshi, W., & Nishihara, T. (2007). Mechanical stress-mediated Runx2 activation is dependent on Ras/ERK1/2 MAPK signaling in osteoblasts. *Journal of Cellular Biochemistry, 101*(5), 1266-1277. doi:10.1002/jcb.21249

Karageorgiou, V., & Kaplan, D. (2005). Porosity of 3D biomaterial scaffolds and osteogenesis. *Biomaterials, 26*(27), 5474-5491. doi:10.1016/j.biomaterials.2005.02.002

Kargozar, S., Mozafari, M., Hamzehlou, S., Brouki Milan, P., Kim, H.-W., & Baino, F. (2019). Bone Tissue Engineering Using Human Cells: A

Comprehensive Review on Recent Trends, Current Prospects, and Recommendations. *Applied Sciences, 9*(1), 174.

Kaunas, R., Usami, S., & Chien, S. (2006). Regulation of stretch-induced JNK activation by stress fiber orientation. *Cell Signal, 18*(11), 1924-1931. doi:10.1016/j.cellsig.2006.02.008

Kempton, S. J., McCarthy, J. E., & Afifi, A. M. (2014). A systematic review of distraction osteogenesis in hand surgery: what are the benefits, complication rates, and duration of treatment? *Plast Reconstr Surg, 133*(5), 1120-1130. doi:10.1097/prs.0000000000000247

Kessler, C. B., & Delany, A. M. (2007). Increased Notch 1 expression and attenuated stimulatory G protein coupling to adenylyl cyclase in osteonectin-null osteoblasts. *Endocrinology, 148*(4), 1666-1674. doi:10.1210/en.2006-0443

Kett, P. W. (1982). Simple harmonic motion (C16) *Motor Vehicle Science Part 2* (pp. 349-367). Dordrecht: Springer Netherlands.

Khatau, S. B., Hale, C. M., Stewart-Hutchinson, P. J., Patel, M. S., Stewart, C. L., Searson, P. C., . . . Wirtz, D. (2009). A perinuclear actin cap regulates nuclear shape. *Proceedings of the National Academy of Sciences, 106*(45), 19017-19022. doi:10.1073/pnas.0908686106

Khatiwala, C. B., Kim, P. D., Peyton, S. R., & Putnam, A. J. (2009). ECM compliance regulates osteogenesis by influencing MAPK signaling downstream of RhoA and ROCK. *J Bone Miner Res, 24*(5), 886-898. doi:10.1359/jbmr.081240

Khurana, J. S., & Safadi, F. F. (2010). Bone Structure, Development and Bone Biology *Essentials in Bone and Soft-Tissue Pathology* (pp. 1-15). Boston, MA: Springer US.

Kilian, K. A., Bugarija, B., Lahn, B. T., & Mrksich, M. (2010). Geometric cues for directing the differentiation of mesenchymal stem cells.

Proc Natl Acad Sci U S A, 107(11), 4872-4877. doi:10.1073/pnas.0903269107

Kim, B. C., Kim, H. G., Lee, S. A., Lim, S., Park, E. H., Kim, S. J., & Lim, C. J. (2005). Genipin-induced apoptosis in hepatoma cells is mediated by reactive oxygen species/c-Jun NH2-terminal kinase-dependent activation of mitochondrial pathway. *Biochem Pharmacol, 70*(9), 1398-1407. doi:10.1016/j.bcp.2005.07.025

Kim, E. K., Lim, S., Park, J. M., Seo, J. K., Kim, J. H., Kim, K. T., . . . Suh, P. G. (2012). Human mesenchymal stem cell differentiation to the osteogenic or adipogenic lineage is regulated by AMP-activated protein kinase. *Journal of Cellular Physiology, 227*(4), 1680-1687. doi:10.1002/jcp.22892

Kim, E. S., Jeong, C. S., & Moon, A. (2012). Genipin, a constituent of Gardenia jasminoides Ellis, induces apoptosis and inhibits invasion in MDA-MB-231 breast cancer cells. *Oncol Rep, 27*(2), 567-572. doi:10.3892/or.2011.1508

Kim, J.-w., Tchernyshyov, I., Semenza, G. L., & Dang, C. V. (2006). HIF-1-mediated expression of pyruvate dehydrogenase kinase: A metabolic switch required for cellular adaptation to hypoxia. *Cell Metabolism, 3*(3), 177-185. doi:https://doi.org/10.1016/j.cmet.2006.02.002

Kim, J. H., Liu, X., Wang, J., Chen, X., Zhang, H., Kim, S. H., . . . He, T. C. (2013). Wnt signaling in bone formation and its therapeutic potential for bone diseases. *Ther Adv Musculoskelet Dis, 5*(1), 13-31. doi:10.1177/1759720X12466608

Kim, J. K., Kang, K. A., Ryu, Y. S., Piao, M. J., Han, X., Oh, M. C., . . . Hyun, J. W. (2016). Induction of Endoplasmic Reticulum Stress via Reactive Oxygen Species Mediated by Luteolin in Melanoma Cells. *Anticancer Res, 36*(5), 2281-2289.

Kim, K. M., Choi, Y. J., Hwang, J. H., Kim, A. R., Cho, H. J., Hwang, E. S., . . . Hong, J. H. (2014). Shear stress induced by an interstitial level of slow flow increases the osteogenic differentiation of

mesenchymal stem cells through TAZ activation. *PLoS One, 9*(3), e92427. doi:10.1371/journal.pone.0092427

King, N. M. P., & Perrin, J. (2014). Ethical issues in stem cell research and therapy. *Stem Cell Res Ther, 5*(4), 85. doi:10.1186/scrt474

Kironde, E., Sekimpi, P., Kajja, I., & Mubiri, P. (2019). Prevalence and patterns of traumatic bone loss following open long bone fractures at Mulago Hospital. *OTA International, 2*(1), e015. doi:10.1097/oi9.0000000000000015

Klein-Nulend, J., van Oers, R. F., Bakker, A. D., & Bacabac, R. G. (2014). Nitric oxide signaling in mechanical adaptation of bone. *Osteoporos Int, 25*(5), 1427-1437. doi:10.1007/s00198-013-2590-4

Klumpers, D. D., Zhao, X., Mooney, D. J., & Smit, T. H. (2013). Cell mediated contraction in 3D cell-matrix constructs leads to spatially regulated osteogenic differentiation. *Integrative biology : quantitative biosciences from nano to macro, 5*(9), 1174-1183. doi:10.1039/c3ib40038g

Klumpers, D. D., Zhao, X., Mooney, D. J., & Smit, T. H. (2013). Cell mediated contraction in 3D cell-matrix constructs leads to spatially regulated osteogenic differentiation. *Integr Biol (Camb), 5*(9), 1174-1183. doi:10.1039/c3ib40038g

Knapik, D. M., Perera, P., Nam, J., Blazek, A. D., Rath, B., Leblebicioglu, B., . . . Agarwal, S. (2014). Mechanosignaling in bone health, trauma and inflammation. *Antioxid Redox Signal, 20*(6), 970-985. doi:10.1089/ars.2013.5467

Knippenberg, M., Helder, M. N., Zandieh Doulabi, B., Wuisman, P. I., & Klein-Nulend, J. (2006). Osteogenesis versus chondrogenesis by BMP-2 and BMP-7 in adipose stem cells. *Biochem Biophys Res Commun, 342*(3), 902-908. doi:10.1016/j.bbrc.2006.02.052

Knippenberg, M., Helder, M. N., Zandieh Doulabi, B., Wuisman, P. I. J. M., & Klein-Nulend, J. (2006). Osteogenesis versus chondrogenesis by BMP-2 and BMP-7 in adipose stem cells. *Biochem Biophys Res*

Commun, 342(3), 902-908. doi:https://doi.org/10.1016/j.bbrc.2006.02.052

Kobayashi, Y., Thirukonda, G. J., Nakamura, Y., Koide, M., Yamashita, T., Uehara, S., . . . Takahashi, N. (2015). Wnt16 regulates osteoclast differentiation in conjunction with Wnt5a. *Biochem Biophys Res Commun, 463*(4), 1278-1283. doi:10.1016/j.bbrc.2015.06.102

Kobayashi, Y., Uehara, S., Koide, M., & Takahashi, N. (2015). The regulation of osteoclast differentiation by Wnt signals. *Bonekey Rep, 4*, 713. doi:10.1038/bonekey.2015.82

Kobayashi, Y., Uehara, S., Koide, M., & Takahashi, N. (2015). The regulation of osteoclast differentiation by Wnt signals. *Bonekey Rep, 4*, 713-713. doi:10.1038/bonekey.2015.82

Kobayashi, Y., Uehara, S., & Udagawa, N. (2018). Roles of non-canonical Wnt signaling pathways in bone resorption. *Journal of Oral Biosciences, 60*(2), 31-35. doi:https://doi.org/10.1016/j.job.2018.03.001

Komori, T. (2010). Regulation of Osteoblast Differentiation by Runx2. *Osteoimmunology: Interactions of the Immune and Skeletal Systems Ii, 658*, 43-49. doi:10.1007/978-1-4419-1050-9_5

Komori, T. (2019). Regulation of Proliferation, Differentiation and Functions of Osteoblasts by Runx2. *Int J Mol Sci, 20*(7). doi:10.3390/ijms20071694

Kopf, J., Petersen, A., Duda, G. N., & Knaus, P. (2012). BMP2 and mechanical loading cooperatively regulate immediate early signalling events in the BMP pathway. *BMC Biology, 10*(1), 37. doi:10.1186/1741-7007-10-37

Krishnan, V., Bryant, H. U., & Macdougald, O. A. (2006). Regulation of bone mass by Wnt signaling. *J Clin Invest, 116*(5), 1202-1209. doi:10.1172/JCI28551

Kruger, M. C., Coetzee, M., Haag, M., & Weiler, H. (2010). Long-chain polyunsaturated fatty acids: selected mechanisms of action on bone. *Prog Lipid Res, 49*(4), 438-449. doi:10.1016/j.plipres.2010.06.002

Kruger, M. C., & Schollum, L. M. (2005). Is docosahexaenoic acid more effective than eicosapentaenoic acid for increasing calcium bioavailability? *Prostaglandins Leukotrienes and Essential Fatty Acids, 73*(5), 327-334. doi:10.1016/j.plefa.2005.08.001

Kuehne, A., Emmert, H., Soehle, J., Winnefeld, M., Fischer, F., Wenck, H., . . . Zamboni, N. (2015). Acute Activation of Oxidative Pentose Phosphate Pathway as First-Line Response to Oxidative Stress in Human Skin Cells. *Molecular Cell, 59*(3), 359-371. doi:https://doi.org/10.1016/j.molcel.2015.06.017

Kuhn, L. T., Liu, Y. X., Boyd, N. L., Dennis, J. E., Jiang, X., Xin, X. N., . . . Goldberg, A. J. (2014). Developmental-Like Bone Regeneration by Human Embryonic Stem Cell-Derived Mesenchymal Cells. *Tissue Engineering Part A, 20*(1-2), 365-377. doi:10.1089/ten.tea.2013.0321

Kular, J. K., Basu, S., & Sharma, R. I. (2014). The extracellular matrix: Structure, composition, age-related differences, tools for analysis and applications for tissue engineering. *J Tissue Eng, 5*, 2041731414557112. doi:10.1177/2041731414557112

Kumar, A., Placone, J. K., & Engler, A. J. (2017). Understanding the extracellular forces that determine cell fate and maintenance. *Development, 144*(23), 4261-4270. doi:10.1242/dev.158469

Kunze, K. G., Hofstetter, H., Posalaky, I., & Winkler, B. (1981). Changes in blood-flow in the bones after osteotomy and osteosynthesis. *Unfallchirurgie, 7*(3), 169-180.

Kuo, C.-Y., & Ann, D. K. (2018). When fats commit crimes: fatty acid metabolism, cancer stemness and therapeutic resistance. *Cancer communications (London, England), 38*(1), 47-47. doi:10.1186/s40880-018-0317-9

Kupcsik, L., Meurya, T., Flury, M., Stoddart, M., & Alini, M. (2009). Statin-induced calcification in human mesenchymal stem cells is cell death related. *Journal of Cellular and Molecular Medicine, 13*(11-12), 4465-4473. doi:10.1111/j.1582-4934.2008.00545.x

Kusunoki, C., Yang, L., Yoshizaki, T., Nakagawa, F., Ishikado, A., Kondo, M., . . . Maegawa, H. (2013). Omega-3 polyunsaturated fatty acid has an anti-oxidant effect via the Nrf-2/HO-1 pathway in 3T3-L1 adipocytes. *Biochem Biophys Res Commun, 430*(1), 225-230. doi:https://doi.org/10.1016/j.bbrc.2012.10.115

Kwon, Y. W., Heo, S. C., Jeong, G. O., Yoon, J. W., Mo, W. M., Lee, M. J., . . . Kim, J. H. (2013). Tumor necrosis factor-alpha-activated mesenchymal stem cells promote endothelial progenitor cell homing and angiogenesis. *Biochim Biophys Acta, 1832*(12), 2136-2144. doi:10.1016/j.bbadis.2013.08.002

Kyurkchiev, D., Bochev, I., Ivanova-Todorova, E., Mourdjeva, M., Oreshkova, T., Belemezova, K., & Kyurkchiev, S. (2014). Secretion of immunoregulatory cytokines by mesenchymal stem cells. *World J Stem Cells, 6*(5), 552-570. doi:10.4252/wjsc.v6.i5.552

L., B. A. L., C., B. J., J., M. S., A., F. M., & Baldy, d. R. F. (2010). Complications associated with distraction osteogenesis for infected nonunion of the femoral shaft in the presence of a bone defect. *The Journal of Bone and Joint Surgery. British volume, 92-B*(4), 565-570. doi:10.1302/0301-620x.92b4.23475

Lacey, D. C., Simmons, P. J., Graves, S. E., & Hamilton, J. A. (2009). Proinflammatory cytokines inhibit osteogenic differentiation from

stem cells: implications for bone repair during inflammation. *Osteoarthritis Cartilage, 17*(6), 735-742. doi:10.1016/j.joca.2008.11.011

Lachowski, D., Cortes, E., Robinson, B., Rice, A., Rombouts, K., & Del Rio Hernandez, A. E. (2018). FAK controls the mechanical activation of YAP, a transcriptional regulator required for durotaxis. *FASEB J, 32*(2), 1099-1107. doi:10.1096/fj.201700721R

Lamb, J. A., Ventura, J. J., Hess, P., Flavell, R. A., & Davis, R. J. (2003). JunD mediates survival signaling by the JNK signal transduction pathway. *Mol Cell, 11*(6), 1479-1489.

Lamplot, J. D., Denduluri, S., Liu, X., Wang, J., Yin, L., Li, R., . . . He, T.-C. (2013). Major Signaling Pathways Regulating the Proliferation and Differentiation of Mesenchymal Stem Cells. In R. C. Zhao (Ed.), *Essentials of Mesenchymal Stem Cell Biology and Its Clinical Translation* (pp. 75-100). Dordrecht: Springer Netherlands.

Lane, S. W., Williams, D. A., & Watt, F. M. (2014). Modulating the stem cell niche for tissue regeneration. *Nat Biotechnol, 32*(8), 795-803. doi:10.1038/nbt.2978

Lang, X., Spousta, M. J., & Lyubovitsky, J. G. (2015). *Detecting the collagen-based hydrogels degradation by multiphoton microscopy (MPM)* (Vol. 9329): SPIE.

Langenbach, F., & Handschel, J. (2013). Effects of dexamethasone, ascorbic acid and beta-glycerophosphate on the osteogenic differentiation of stem cells in vitro. *Stem Cell Res Ther, 4*. doi:10.1186/1757-6512-4-117

Lascombes, P., Popkov, D., Huber, H., Haumont, T., & Journeau, P. (2012). Classification of complications after progressive long bone lengthening: Proposal for a new classification. *Orthopaedics &*

Traumatology: Surgery & Research, 98(6), 629-637. doi:https://doi.org/10.1016/j.otsr.2012.05.010

Lau, E., Lee, W. D., Li, J., Xiao, A., Davies, J. E., Wu, Q., . . . You, L. (2011). Effect of low-magnitude, high-frequency vibration on osteogenic differentiation of rat mesenchymal stromal cells. *J Orthop Res, 29*(7), 1075-1080. doi:10.1002/jor.21334

Law, J. X., Liau, L. L., Saim, A., Yang, Y., & Idrus, R. (2017). Electrospun Collagen Nanofibers and Their Applications in Skin Tissue Engineering. *Tissue Engineering and Regenerative Medicine, 14*(6), 699-718. doi:10.1007/s13770-017-0075-9

Lawrence, T. (2009). The nuclear factor NF-kappaB pathway in inflammation. *Cold Spring Harb Perspect Biol, 1*(6), a001651. doi:10.1101/cshperspect.a001651

Lawson, C. D., & Burridge, K. (2014). The on-off relationship of Rho and Rac during integrin-mediated adhesion and cell migration. *Small GTPases, 5*(1), e27958. doi:10.4161/sgtp.27958

Lee, H.-p., Stowers, R., & Chaudhuri, O. (2019). Volume expansion and TRPV4 activation regulate stem cell fate in three-dimensional microenvironments. *Nat Commun, 10*(1), 529. doi:10.1038/s41467-019-08465-x

Lee, J. C., Ahn, K. S., Jeong, S. J., Jung, J. H., Kwon, T. R., Rhee, Y. H., . . . Kim, S. H. (2011). Signal transducer and activator of transcription 3 pathway mediates genipin-induced apoptosis in U266 multiple myeloma cells. *Journal of Cellular Biochemistry, 112*(6), 1552-1562. doi:10.1002/jcb.23077

Lee, K. L., Guevarra, M. D., Nguyen, A. M., Chua, M. C., Wang, Y., & Jacobs, C. R. (2015). The primary cilium functions as a mechanical

and calcium signaling nexus. *Cilia, 4*, 7. doi:10.1186/s13630-015-0016-y

Lee, K. Y., & Mooney, D. J. (2001). Hydrogels for tissue engineering. *Chemical Reviews, 101*(7), 1869-1879.

Lee, K. Y., & Mooney, D. J. (2012). Alginate: properties and biomedical applications. *Prog Polym Sci, 37*(1), 106-126. doi:10.1016/j.progpolymsci.2011.06.003

Lee, M. H., Kwon, T. G., Park, H. S., Wozney, J. M., & Ryoo, H. M. (2003). BMP-2-induced Osterix expression is mediated by Dlx5 but is independent of Runx2. *Biochem Biophys Res Commun, 309*(3), 689-694.

Lee, S.-Y., & Long, F. (2018). Notch signaling suppresses glucose metabolism in mesenchymal progenitors to restrict osteoblast differentiation. *The Journal of Clinical Investigation, 128*(12), 5573-5586. doi:10.1172/JCI96221

Lencel, P., Delplace, S., Hardouin, P., & Magne, D. (2011). TNF-alpha stimulates alkaline phosphatase and mineralization through PPARgamma inhibition in human osteoblasts. *Bone, 48*(2), 242-249. doi:10.1016/j.bone.2010.09.001

Lerner, A., Fodor, L., Stein, H., Soudry, M., Peled, I. J., & Ullmann, Y. (2005). Extreme bone lengthening using distraction osteogenesis after trauma: a case report. *Journal of Orthopaedic Trauma, 19*(6), 420-424.

Lévesque, J. P., Helwani, F. M., & Winkler, I. G. (2010). The endosteal 'osteoblastic' niche and its role in hematopoietic stem cell homing and mobilization. *Leukemia, 24*(12), 1979-1992. doi:10.1038/leu.2010.214

Lewis, A. H., & Grandl, J. (2015). Mechanical sensitivity of Piezo1 ion channels can be tuned by cellular membrane tension. *Elife, 4,* e12088. doi:10.7554/eLife.12088

Li, D.-Q., Pakala, S. B., Reddy, S. D. N., Ohshiro, K., Zhang, J.-X., Wang, L., . . . Kumar, R. (2011). Bidirectional autoregulatory mechanism of metastasis-associated protein 1-alternative reading frame pathway in oncogenesis. *Proceedings of the National Academy of Sciences, 108*(21), 8791-8796. doi:10.1073/pnas.1018389108

Li, J., Duncan, R. L., Burr, D. B., & Turner, C. H. (2002). L-type calcium channels mediate mechanically induced bone formation in vivo. *J Bone Miner Res, 17*(10), 1795-1800. doi:10.1359/jbmr.2002.17.10.1795

Li, J., Kacena, M. A., & Stocum, D. L. (2019). Chapter 12 - Fracture Healing. In D. B. Burr & M. R. Allen (Eds.), *Basic and Applied Bone Biology (Second Edition)* (pp. 235-253): Academic Press.

Li, Q. Q., Gao, Z. W., Chen, Y., & Guan, M. X. (2017). The role of mitochondria in osteogenic, adipogenic and chondrogenic differentiation of mesenchymal stem cells. *Protein & Cell, 8*(6), 439-445. doi:10.1007/s13238-017-0385-7

Li, X., Wang, Y., Wang, Z., Qi, Y., Li, L., Zhang, P., . . . Huang, Y. (2018). Composite PLA/PEG/nHA/Dexamethasone Scaffold Prepared by 3D Printing for Bone Regeneration. *Macromol Biosci, 18*(6), e1800068. doi:10.1002/mabi.201800068

Li, Y., Backesjo, C. M., Haldosen, L. A., & Lindgren, U. (2008). IL-6 receptor expression and IL-6 effects change during osteoblast differentiation. *Cytokine, 43*(2), 165-173. doi:10.1016/j.cyto.2008.05.007

Li, Y., Meng, Y., & Yu, X. (2019). The Unique Metabolic Characteristics of Bone Marrow Adipose Tissue. *Frontiers in Endocrinology, 10*(69). doi:10.3389/fendo.2019.00069

Li, Y., Su, J., Sun, W., Cai, L., & Deng, Z. (2018). AMP-activated protein kinase stimulates osteoblast differentiation and mineralization through autophagy induction. *International journal of molecular medicine, 41*(5), 2535-2544. doi:10.3892/ijmm.2018.3498

Lian, J. B., & Stein, G. S. (1992). Concepts of osteoblast growth and differentiation: basis for modulation of bone cell development and tissue formation. *Crit Rev Oral Biol Med, 3*(3), 269-305.

Lian, J. B., Stein, G. S., Owen, T. A., Aronow, M., Tassinari, M. S., Pockwinse, S., & Bortell, R. (1991). Cell Structure and Gene-Expression - Contributions of the Extracellular-Matrix to Regulation of Osteoblast Growth and Differentiation. *Molecular Basis of Human Cancer /, 209*, 39-71.

Liang, X., Wang, Z., Gao, M., Wu, S., Zhang, J., Liu, Q., . . . Liu, W. (2019). Cyclic stretch induced oxidative stress by mitochondrial and NADPH oxidase in retinal pigment epithelial cells. *BMC Ophthalmol, 19*(1), 79. doi:10.1186/s12886-019-1087-0

Lienau, J., Schell, H., Muchow, S., & Duda, G. N. (2004). Initial Vascularization Is Influenced by Fixation Stability in Bone Healing. *Calcif Tissue Int, 74*, S55-S55.

Lilly, A. J., Johnson, W. E., & Bunce, C. M. (2011). The haematopoietic stem cell niche: new insights into the mechanisms regulating haematopoietic stem cell behaviour. *Stem Cells Int, 2011*, 274564. doi:10.4061/2011/274564

Lin, A. (2003). Activation of the JNK signaling pathway: breaking the brake on apoptosis. *Bioessays, 25*(1), 17-24. doi:10.1002/bies.10204

Lin, C. H., Li, N. T., Cheng, H. S., & Yen, M. L. (2018). Oxidative stress induces imbalance of adipogenic/osteoblastic lineage commitment in mesenchymal stem cells through decreasing SIRT1 functions.

Journal of Cellular and Molecular Medicine, 22(2), 786-796. doi:10.1111/jcmm.13356

Lin, F. X., Zheng, G. Z., Chang, B., Chen, R. C., Zhang, Q. H., Xie, P., . . . Li, X. D. (2018). Connexin 43 Modulates Osteogenic Differentiation of Bone Marrow Stromal Cells Through GSK-3beta/Beta-Catenin Signaling Pathways. *Cellular Physiology and Biochemistry, 47*(1), 161-175. doi:10.1159/000489763

Lin, G., Liu, G., Banie, L., Wang, G., Ning, H., Lue, T. F., & Lin, C. S. (2011). Tissue distribution of mesenchymal stem cell marker Stro-1. *Stem Cells Dev, 20*(10), 1747-1752. doi:10.1089/scd.2010.0564

Lin, S., & Gu, L. (2015). Influence of Crosslink Density and Stiffness on Mechanical Properties of Type I Collagen Gel. *Materials (Basel), 8*(2), 551-560. doi:10.3390/ma8020551

Lingappan, K. (2018). NF-kappaB in Oxidative Stress. *Curr Opin Toxicol, 7*, 81-86. doi:10.1016/j.cotox.2017.11.002

Link, T. M., Park, U., Vonakis, B. M., Raben, D. M., Soloski, M. J., & Caterina, M. J. (2010). TRPV2 has a pivotal role in macrophage particle binding and phagocytosis. *Nat Immunol, 11*(3), 232-239. doi:10.1038/ni.1842

Lipovka, Y., & Konhilas, J. P. (2015). AMP-Activated Protein Kinase Signalling in Cancer and Cardiac Hypertrophy. *Cardiovascular pharmacology: open access, 4*(3), 154.

Liu, G., Vijayakumar, S., Grumolato, L., Arroyave, R., Qiao, H., Akiri, G., & Aaronson, S. A. (2009). Canonical Wnts function as potent regulators of osteogenesis by human mesenchymal stem cells. *The Journal of Cell Biology, 185*(1), 67-75. doi:10.1083/jcb.200810137

Liu, J., Minemoto, Y., & Lin, A. (2004). c-Jun N-terminal protein kinase 1 (JNK1), but not JNK2, is essential for tumor necrosis factor alpha-induced c-Jun kinase activation and apoptosis. *Mol Cell Biol, 24*(24), 10844-10856. doi:10.1128/MCB.24.24.10844-10856.2004

u, M., Zeng, X., Ma, C., Yi, H., Ali, Z., Mou, X., . . . He, N. (2017). Injectable hydrogels for cartilage and bone tissue engineering. *Bone Res, 5*, 17014. doi:10.1038/boneres.2017.14

Liu, P., Ping, Y., Ma, M., Zhang, D., Liu, C., Zaidi, S., . . . Zaidi, M. (2016). Anabolic actions of Notch on mature bone. *Proceedings of the National Academy of Sciences, 113*(15), E2152-E2161. doi:10.1073/pnas.1603399113

Liu, T., Li, J., Shao, Z., Ma, K., Zhang, Z., Wang, B., & Zhang, Y. (2018). Encapsulation of mesenchymal stem cells in chitosan/beta-glycerophosphate hydrogel for seeding on a novel calcium phosphate cement scaffold. *Med Eng Phys, 56*, 9-15. doi:10.1016/j.medengphy.2018.03.003

Liu, T., Zhang, L., Joo, D., & Sun, S. C. (2017). NF-kappaB signaling in inflammation. *Signal Transduct Target Ther, 2*. doi:10.1038/sigtrans.2017.23

Liu, W., Zhang, L., Xuan, K., Hu, C., Li, L., Zhang, Y., . . . Jin, Y. (2018). Alkaline Phosphatase Controls Lineage Switching of Mesenchymal Stem Cells by Regulating the LRP6/GSK3beta Complex in Hypophosphatasia. *Theranostics, 8*(20), 5575-5592. doi:10.7150/thno.27372

Liu, Y., & Ma, T. (2015). Metabolic regulation of mesenchymal stem cell in expansion and therapeutic application. *Biotechnol Prog, 31*(2), 468-481. doi:10.1002/btpr.2034Livak, K. J., & Schmittgen, T. D. (2001). Analysis of relative gene expression data using real-time quantitative PCR and the 2(-Delta Delta C(T)) Method. *Methods, 25*(4), 402-408. doi:10.1006/meth.2001.1262

Llopis-Hernández, V., Cantini, M., González-García, C., Cheng, Z. A., Yang, J., Tsimbouri, P. M., . . . Salmerón-Sánchez, M. (2016). Material-driven fibronectin assembly for high-efficiency presentation of growth factors. *Science Advances, 2*(8), e1600188. doi:10.1126/sciadv.1600188

Lo, B., & Parham, L. (2009). Ethical issues in stem cell research. *Endocrine Reviews, 30*(3), 204-213. doi:10.1210/er.2008-0031

Loh, Q. L., & Choong, C. (2013). Three-dimensional scaffolds for tissue engineering applications: role of porosity and pore size. *Tissue Eng Part B Rev, 19*(6), 485-502. doi:10.1089/ten.TEB.2012.0437

Loi, F., Córdova, L. A., Pajarinen, J., Lin, T.-h., Yao, Z., & Goodman, S. B. (2016). Inflammation, fracture and bone repair. *Bone, 86*, 119-130. doi:10.1016/j.bone.2016.02.020

Loi, F., Cordova, L. A., Pajarinen, J., Lin, T. H., Yao, Z., & Goodman, S. B. (2016). Inflammation, fracture and bone repair. *Bone, 86*, 119-130. doi:10.1016/j.bone.2016.02.020

Lopes, M. S., Jardini, A. L., & Maciel, R. (2012). Poly (lactic acid) production for tissue engineering applications. *Chisa 2012, 42*, 1402-1413. doi:10.1016/j.proeng.2012.07.534

Lozito, T. P., Kolf, C. M., & Tuan, R. S. (2009). Microenvironmental Regulation of Adult Mesenchymal Stem Cells. In V. K. Rajasekhar & M. C. Vemuri (Eds.), *Regulatory Networks in Stem Cells* (pp. 185-210). Totowa, NJ: Humana Press.

Lu, H., Forbes, R. A., & Verma, A. (2002). Hypoxia-inducible factor 1 activation by aerobic glycolysis implicates the Warburg effect in carcinogenesis. *J Biol Chem, 277*(26), 23111-23115. doi:10.1074/jbc.M202487200

Lu, Y., Fukuda, K., Liu, Y., Kumagai, N., & Nishida, T. (2004). Dexamethasone inhibition of IL-1-induced collagen degradation by corneal fibroblasts in three-dimensional culture. *Invest Ophthalmol Vis Sci, 45*(9), 2998-3004. doi:10.1167/iovs.04-0051

Lugrin, J., Rosenblatt-Velin, N., Parapanov, R., & Liaudet, L. (2014). The role of oxidative stress during inflammatory processes. *Biol Chem, 395*(2), 203-230. doi:10.1515/hsz-2013-0241

Lund, S. A., Giachelli, C. M., & Scatena, M. (2009). The role of osteopontin in inflammatory processes. *J Cell Commun Signal, 3*(3-4), 311-322. doi:10.1007/s12079-009-0068-0

Luo, J. L., Kamata, H., & Karin, M. (2005). IKK/NF-kappaB signaling: balancing life and death--a new approach to cancer therapy. *J Clin Invest, 115*(10), 2625-2632. doi:10.1172/JCI26322

Luo, Z., Shang, X., Zhang, H., Wang, G., Massey, P. A., Barton, S. R., . . . Dong, Y. (2019). Notch Signaling in Osteogenesis, Osteoclastogenesis, and Angiogenesis. *Am J Pathol, 189*(8), 1495-1500. doi:https://doi.org/10.1016/j.ajpath.2019.05.005

Lv, F. J., Tuan, R. S., Cheung, K. M., & Leung, V. Y. (2014). Concise review: the surface markers and identity of human mesenchymal stem cells. *Stem Cells, 32*(6), 1408-1419. doi:10.1002/stem.1681

Lv, H., Li, L., Sun, M., Zhang, Y., Chen, L., Rong, Y., & Li, Y. (2015). Mechanism of regulation of stem cell differentiation by matrix stiffness. *Stem Cell Res Ther, 6*, 103. doi:10.1186/s13287-015-0083-4

Ma, Q. (2013). Role of nrf2 in oxidative stress and toxicity. *Annual review of pharmacology and toxicology, 53*, 401-426. doi:10.1146/annurev-pharmtox-011112-140320

MacDonell, R., Hamrick, M. W., & Isales, C. M. (2016). Protein/amino-acid modulation of bone cell function. *Bonekey Rep, 5*, 827. doi:10.1038/bonekey.2016.58

Madhavan, S., Anghelina, M., Sjostrom, D., Dossumbekova, A., Guttridge, D. C., & Agarwal, S. (2007). Biomechanical Signals Suppress TAK1 Activation to Inhibit NF-κB Transcriptional Activation in Fibrochondrocytes. *The Journal of Immunology, 179*(9), 6246-6254. doi:10.4049/jimmunol.179.9.6246

Maeda, K., Kobayashi, Y., Udagawa, N., Uehara, S., Ishihara, A., Mizoguchi, T., . . . Takahashi, N. (2012). Wnt5a-Ror2 signaling between osteoblast-lineage cells and osteoclast precursors

enhances osteoclastogenesis. *Nat Med, 18*(3), 405-412. doi:10.1038/nm.2653

Maeda, S., Hayashi, M., Komiya, S., Imamura, T., & Miyazono, K. (2004). Endogenous TGF-ß signaling suppresses maturation of osteoblastic mesenchymal cells. *The EMBO Journal, 23*(3), 552-563. doi:10.1038/sj.emboj.7600067

Mahon, P. C., Hirota, K., & Semenza, G. L. (2001). FIH-1: a novel protein that interacts with HIF-1alpha and VHL to mediate repression of HIF-1 transcriptional activity. *Genes Dev, 15*(20), 2675-2686. doi:10.1101/gad.924501

Mailloux, R. J., McBride, S. L., & Harper, M. E. (2013). Unearthing the secrets of mitochondrial ROS and glutathione in bioenergetics. *Trends Biochem Sci, 38*(12), 592-602. doi:10.1016/j.tibs.2013.09.001

Malone, A. M., Anderson, C. T., Tummala, P., Kwon, R. Y., Johnston, T. R., Stearns, T., & Jacobs, C. R. (2007). Primary cilia mediate mechanosensing in bone cells by a calcium-independent mechanism. *Proc Natl Acad Sci U S A, 104*(33), 13325-13330. doi:10.1073/pnas.0700636104

Mao, C. Y., Wang, Y. G., Zhang, X., Zheng, X. Y., Tang, T. T., & Lu, E. Y. (2016). Double-edged-sword effect of IL-1beta on the osteogenesis of periodontal ligament stem cells via crosstalk between the NF-kappaB, MAPK and BMP/Smad signaling pathways. *Cell Death Dis, 7*, e2296. doi:10.1038/cddis.2016.204

Marędziak, M., Lewandowski, D., Tomaszewski, K. A., Kubiak, K., & Marycz, K. (2017). The Effect of Low-Magnitude Low-Frequency Vibrations (LMLF) on Osteogenic Differentiation Potential of Human Adipose Derived Mesenchymal Stem Cells. *Cellular and Molecular Bioengineering, 10*(6), 549-562. doi:10.1007/s12195-017-0501-z

Marenzana, M., & Arnett, T. R. (2013). The Key Role of the Blood Supply to Bone. *Bone Research, 1*(3), 203-215. doi:10.4248/BR201303001

Marolt, D., Campos, I. M., Bhumiratana, S., Koren, A., Petridis, P., Zhang, G. P., . . . Vunjak-Novakovic, G. (2012). Engineering bone tissue from human embryonic stem cells. *Proc Natl Acad Sci U S A, 109*(22), 8705-8709. doi:10.1073/pnas.1201830109

Marsell, R., & Einhorn, T. A. (2011). The biology of fracture healing. *Injury, 42*(6), 551-555. doi:10.1016/j.injury.2011.03.031

Marshall, S. J., Bayne, S. C., Baier, R., Tomsia, A. P., & Marshall, G. W. (2010). A review of adhesion science. *Dent Mater, 26*(2), e11-16. doi:10.1016/j.dental.2009.11.157

Martinac, B., & Poole, K. (2018). Mechanically activated ion channels. *Int J Biochem Cell Biol, 97*, 104-107. doi:10.1016/j.biocel.2018.02.011

Martindale, J. L., & Holbrook, N. J. (2002). Cellular response to oxidative stress: Signaling for suicide and survival*. *Journal of Cellular Physiology, 192*(1), 1-15. doi:10.1002/jcp.10119

Martinez-Ramirez, M. J., Palma, S., Martinez-Gonzalez, M. A., Delgado-Martinez, A. D., de la Fuente, C., & Delgado-Rodriguez, M. (2007). Dietary fat intake and the risk of osteoporotic fractures in the elderly. *Eur J Clin Nutr, 61*(9), 1114-1120. doi:10.1038/sj.ejcn.1602624

Marupanthorn, K., Tantrawatpan, C., Kheolamai, P., Tantikanlayaporn, D., & Manochantr, S. (2017). Bone morphogenetic protein-2 enhances the osteogenic differentiation capacity of mesenchymal stromal cells derived from human bone marrow and umbilical cord. *International journal of molecular medicine, 39*(3), 654-662. doi:10.3892/ijmm.2017.2872

Maryanovich, M., & Gross, A. (2013). A ROS rheostat for cell fate regulation. *Trends in Cell Biology, 23*(3), 129-134. doi:10.1016/j.tcb.2012.09.007

Marycz, K., Lewandowski, D., Tomaszewski, K. A., Henry, B. M., Golec, E. B., & Marędziak, M. (2016). Low-frequency, low-magnitude

vibrations (LFLM) enhances chondrogenic differentiation potential of human adipose derived mesenchymal stromal stem cells (hASCs). *PeerJ, 4*, e1637. doi:10.7717/peerj.1637

Mason, B. N., Starchenko, A., Williams, R. M., Bonassar, L. J., & Reinhart-King, C. A. (2013). Tuning three-dimensional collagen matrix stiffness independently of collagen concentration modulates endothelial cell behavior. *Acta Biomater, 9*(1), 4635-4644. doi:10.1016/j.actbio.2012.08.007

Masquelet, A., Kanakaris, N. K., Obert, L., Stafford, P., & Giannoudis, P. V. (2019). Bone Repair Using the Masquelet Technique. *J Bone Joint Surg Am, 101*(11), 1024-1036. doi:10.2106/jbjs.18.00842

Masquelet, A. C. (2003). Muscle reconstruction in reconstructive surgery: soft tissue repair and long bone reconstruction. *Langenbecks Arch Surg, 388*(5), 344-346. doi:10.1007/s00423-003-0379-1

Masquelet, A. C., & Begue, T. (2010). The concept of induced membrane for reconstruction of long bone defects. *Orthop Clin North Am, 41*(1), 27-37; table of contents. doi:10.1016/j.ocl.2009.07.011

Mates, J. M., Perez-Gomez, C., Nunez de Castro, I., Asenjo, M., & Marquez, J. (2002). Glutamine and its relationship with intracellular redox status, oxidative stress and cell proliferation/death. *Int J Biochem Cell Biol, 34*(5), 439-458.

Matsubara, T., Kida, K., Yamaguchi, A., Hata, K., Ichida, F., Meguro, H., . . . Yoneda, T. (2008). BMP2 regulates Osterix through Msx2 and Runx2 during osteoblast differentiation. *J Biol Chem, 283*(43), 29119-29125. doi:10.1074/jbc.M801774200

Matsumoto, H., Yamamoto, Y., Shiota, M., Kuruma, H., Beraldi, E., Matsuyama, H., . . . Gleave, M. (2013). Cotargeting Androgen Receptor and Clusterin Delays Castrate-Resistant Prostate Cancer Progression by Inhibiting Adaptive Stress Response and AR Stability.

Cancer Research, 73(16), 5206-5217. doi:10.1158/0008-5472.can-13-0359

Matsunobu, T., Torigoe, K., Ishikawa, M., de Vega, S., Kulkarni, A. B., Iwamoto, Y., & Yamada, Y. (2009). Critical roles of the TGF-beta type I receptor ALK5 in perichondrial formation and function, cartilage integrity, and osteoblast differentiation during growth plate development. *Dev Biol, 332*(2), 325-338. doi:10.1016/j.ydbio.2009.06.002

Matthews, J. A., Wnek, G. E., Simpson, D. G., & Bowlin, G. L. (2002). Electrospinning of collagen nanofibers. *Biomacromolecules, 3*(2), 232-238.

Maulucci, G., Cohen, O., Daniel, B., Sansone, A., Petropoulou, P. I., Filou, S., . . . Sasson, S. (2016). Fatty acid-related modulations of membrane fluidity in cells: detection and implications. *Free radical research, 50*(sup1), S40-s50. doi:10.1080/10715762.2016.1231403

Mazzali, M., Kipari, T., Ophascharoensuk, V., Wesson, J. A., Johnson, R., & Hughes, J. (2002). Osteopontin--a molecule for all seasons. *QJM, 95*(1), 3-13.

McBeath, R., Pirone, D. M., Nelson, C. M., Bhadriraju, K., & Chen, C. S. (2004). Cell shape, cytoskeletal tension, and RhoA regulate stem cell lineage commitment. *Dev Cell, 6*(4), 483-495.

McClarren, B., & Olabisi, R. (2018). Strain and Vibration in Mesenchymal Stem Cells. *International Journal of Biomaterials*. doi:10.1155/2018/8686794

McClarren, B., & Olabisi, R. (2018). Strain and Vibration in Mesenchymal Stem Cells. *International Journal of Biomaterials, 2018*, 13. doi:10.1155/2018/8686794

McGann, M. E., Bonitsky, C. M., Jackson, M. L., Ovaert, T. C., Trippel, S. B., & Wagner, D. R. (2015). Genipin crosslinking of cartilage

enhances resistance to biochemical degradation and mechanical wear. *J Orthop Res, 33*(11), 1571-1579. doi:10.1002/jor.22939

McMurray, R. J., Gadegaard, N., Tsimbouri, P. M., Burgess, K. V., McNamara, L. E., Tare, R., . . . Dalby, M. J. (2011). Nanoscale surfaces for the long-term maintenance of mesenchymal stem cell phenotype and multipotency. *Nat Mater, 10*(8), 637-644. doi:10.1038/NMAT3058

McNamara, L. E., Sjostrom, T., Seunarine, K., Meek, R. D., Su, B., & Dalby, M. J. (2014). Investigation of the limits of nanoscale filopodial interactions. *J Tissue Eng, 5*, 2041731414536177. doi:10.1177/2041731414536177

Mebratu, Y., & Tesfaigzi, Y. (2009). How ERK1/2 activation controls cell proliferation and cell death is subcellular localization the answer? *Cell Cycle, 8*(8), 1168-1175. doi:DOI 10.4161/cc.8.8.8147

Medvedev, S. P., Shevchenko, A. I., & Zakian, S. M. (2010). Induced Pluripotent Stem Cells: Problems and Advantages when Applying them in Regenerative Medicine. *Acta naturae, 2*(2), 18-28.

Meeson, R., Moazen, M., Sanghani-Kerai, A., Osagie-Clouard, L., Coathup, M., & Blunn, G. (2019). The influence of gap size on the development of fracture union with a micro external fixator. *Journal of the Mechanical Behavior of Biomedical Materials, 99*, 161-168. doi:https://doi.org/10.1016/j.jmbbm.2019.07.015

Mehta, S., McClarren, B., Aijaz, A., Chalaby, R., Cook-Chennault, K., & Olabisi, R. M. (2018). The effect of low-magnitude, high-frequency vibration on poly(ethylene glycol)-microencapsulated mesenchymal stem cells. *J Tissue Eng, 9*, 2041731418800101-2041731418800101. doi:10.1177/2041731418800101

Melchiorri, A. J., Nguyen, B.-N. B., & Fisher, J. P. (2014). Mesenchymal stem cells: roles and relationships in vascularization. *Tissue*

engineering. Part B, Reviews, 20(3), 218-228. doi:10.1089/ten.TEB.2013.0541

Meleti, Z., Shapiro, I. M., & Adams, C. S. (2000). Inorganic phosphate induces apoptosis of osteoblast-like cells in culture. *Bone, 27*(3), 359-366.

Mellor, A. L., Lemos, H., & Huang, L. (2017). Indoleamine 2,3-Dioxygenase and Tolerance: Where Are We Now? *Frontiers in Immunology, 8*, 1360-1360. doi:10.3389/fimmu.2017.01360

Meyers, J., Craig, J., & Odde, D. J. (2006). Potential for control of signaling pathways via cell size and shape. *Curr Biol, 16*(17), 1685-1693. doi:10.1016/j.cub.2006.07.056

Michalak, K. P., Mackowska-Kedziora, A., Sobolewski, B., & Wozniak, P. (2015). Key Roles of Glutamine Pathways in Reprogramming the Cancer Metabolism. *Oxidative Medicine and Cellular Longevity, 2015*, 964321. doi:10.1155/2015/964321

Mihaylova, M. M., & Shaw, R. J. (2011). The AMPK signalling pathway coordinates cell growth, autophagy and metabolism. *Nature Cell Biology, 13*(9), 1016-1023. doi:10.1038/ncb2329

Mitchell, A., Wanczyk, H., Jensen, T., & Finck, C. (2019). Assessment of iPSC teratogenicity throughout directed differentiation toward an alveolar-like phenotype. *Differentiation, 105*, 45-53. doi:https://doi.org/10.1016/j.diff.2019.01.003

Mittal, M., Siddiqui, M. R., Tran, K., Reddy, S. P., & Malik, A. B. (2014). Reactive oxygen species in inflammation and tissue injury. *Antioxid Redox Signal, 20*(7), 1126-1167. doi:10.1089/ars.2012.5149

Miyagawa, S., & Sawa, Y. (2018). Building a new strategy for treating heart failure using Induced Pluripotent Stem Cells. *Journal of Cardiology, 72*(6), 445-448. doi:10.1016/j.jjcc.2018.05.002

Miyamoto, T., Mochizuki, T., Nakagomi, H., Kira, S., Watanabe, M., Takayama, Y., . . . Tominaga, M. (2014). Functional Role for Piezo1 in Stretch-evoked Ca2+ Influx and ATP Release in Urothelial Cell Cultures. *Journal of Biological Chemistry, 289*(23), 16565-16575. doi:10.1074/jbc.M113.528638

Mohyeldin, A., Garzón-Muvdi, T., & Quiñones-Hinojosa, A. (2010). Oxygen in Stem Cell Biology: A Critical Component of the Stem Cell Niche. *Cell Stem Cell, 7*(2), 150-161. doi:https://doi.org/10.1016/j.stem.2010.07.007

Monfoulet, L. E., Becquart, P., Marchat, D., Vandamme, K., Bourguignon, M., Pacard, E., . . . Logeart-Avramoglou, D. (2014). The pH in the microenvironment of human mesenchymal stem cells is a critical factor for optimal osteogenesis in tissue-engineered constructs. *Tissue Eng Part A, 20*(13-14), 1827-1840. doi:10.1089/ten.TEA.2013.0500

Monteith, G. R., Prevarskaya, N., & Roberts-Thomson, S. J. (2017). The calcium–cancer signalling nexus. *Nature Reviews Cancer, 17*, 367. doi:10.1038/nrc.2017.18

Moorer, M. C., & Stains, J. P. (2017). Connexin43 and the Intercellular Signaling Network Regulating Skeletal Remodeling. *Curr Osteoporos Rep, 15*(1), 24-31. doi:10.1007/s11914-017-0345-4

Morgan, M. J., & Liu, Z. G. (2011). Crosstalk of reactive oxygen species and NF-kappaB signaling. *Cell Res, 21*(1), 103-115. doi:10.1038/cr.2010.178

Morris, C. (2011). Voltage-Gated Channel Mechanosensitivity: Fact or Friction? *Frontiers in Physiology, 2*(25). doi:10.3389/fphys.2011.00025

Mottaghitalab, F., Hosseinkhani, H., Shokrgozar, M. A., Mao, C. B., Yang, M. Y., & Farokhi, M. (2015). Silk as a potential candidate for bone

tissue engineering. *Journal of Controlled Release, 215*, 112-128. doi:10.1016/j.jconrel.2015.07.031

Moverare-Skrtic, S., Henning, P., Liu, X., Nagano, K., Saito, H., Borjesson, A. E., . . . Ohlsson, C. (2014). Osteoblast-derived WNT16 represses osteoclastogenesis and prevents cortical bone fragility fractures. *Nat Med, 20*(11), 1279-1288. doi:10.1038/nm.3654

Mracek, T., Drahota, Z., & Houstek, J. (2013). The function and the role of the mitochondrial glycerol-3-phosphate dehydrogenase in mammalian tissues. *Biochim Biophys Acta, 1827*(3), 401-410. doi:10.1016/j.bbabio.2012.11.014

Mracek, T., Pecinova, A., Vrbacky, M., Drahota, Z., & Houstek, J. (2009). High efficiency of ROS production by glycerophosphate dehydrogenase in mammalian mitochondria. *Arch Biochem Biophys, 481*(1), 30-36. doi:10.1016/j.abb.2008.10.011

Mukherjee, A., & Rotwein, P. (2009). Akt promotes BMP2-mediated osteoblast differentiation and bone development. *J Cell Sci, 122*(Pt 5), 716-726. doi:10.1242/jcs.042770

Murdoch, A. H., Mathias, K. J., & Smith, F. W. (2002). Measurement of the bony anatomy of the humerus using magnetic resonance imaging. *Proceedings of the Institution of Mechanical Engineers Part H-Journal of Engineering in Medicine, 216*(H1), 31-35. doi:Doi 10.1243/0954411021536252

Murphy, M. P. (2009). How mitochondria produce reactive oxygen species. *Biochemical Journal, 417*, 1-13. doi:10.1042/Bj20081386

Musunuru, K., Sheikh, F., Gupta, R. M., Houser, S. R., Maher, K. O., Milan, D. J., . . . Wu, J. C. (2018). Induced Pluripotent Stem Cells for Cardiovascular Disease Modeling and Precision Medicine: A Scientific Statement From the American Heart Association.

Circulation: Genomic and Precision Medicine, 11(1), e000043. doi:doi:10.1161/HCG.0000000000000043

Muzzarelli, R. A., El Mehtedi, M., Bottegoni, C., Aquili, A., & Gigante, A. (2015). Genipin-Crosslinked Chitosan Gels and Scaffolds for Tissue Engineering and Regeneration of Cartilage and Bone. *Mar Drugs, 13*(12), 7314-7338. doi:10.3390/md13127068

Nair, M. B., Kretlow, J. D., Mikos, A. G., & Kasper, F. K. (2011). Infection and tissue engineering in segmental bone defects--a mini review. *Current opinion in biotechnology, 22*(5), 721-725. doi:10.1016/j.copbio.2011.02.005

Naito, H., Yoshimura, M., Mizuno, T., Takasawa, S., Tojo, T., & Taniguchi, S. (2013). The advantages of three-dimensional culture in a collagen hydrogel for stem cell differentiation. *J Biomed Mater Res A, 101*(10), 2838-2845. doi:10.1002/jbm.a.34578

Nakano, H. (2004). Signaling crosstalk between NF-kappaB and JNK. *Trends Immunol, 25*(8), 402-405. doi:10.1016/j.it.2004.05.007

Nakashima, K., Zhou, X., Kunkel, G., Zhang, Z., Deng, J. M., Behringer, R. R., & de Crombrugghe, B. (2002). The novel zinc finger-containing transcription factor osterix is required for osteoblast differentiation and bone formation. *Cell, 108*(1), 17-29.

Nam, J., Aguda, B. D., Rath, B., & Agarwal, S. (2009). Biomechanical thresholds regulate inflammation through the NF-kappaB pathway: experiments and modeling. *PLoS One, 4*(4), e5262. doi:10.1371/journal.pone.0005262

Nam, K., Kimura, T., Funamoto, S., & Kishida, A. (2010a). Preparation of a collagen/polymer hybrid gel designed for tissue membranes. Part I: controlling the polymer-collagen cross-linking process using an ethanol/water co-solvent. *Acta Biomater, 6*(2), 403-408. doi:10.1016/j.actbio.2009.06.021

Nam, K., Kimura, T., Funamoto, S., & Kishida, A. (2010b). Preparation of a collagen/polymer hybrid gel for tissue membranes. Part II: in

vitro and in vivo biological properties of the collagen gels. *Acta Biomater, 6*(2), 409-417. doi:10.1016/j.actbio.2009.06.022

Nayak, P. S., Wang, Y., Najrana, T., Priolo, L. M., Rios, M., Shaw, S. K., & Sanchez-Esteban, J. (2015). Mechanotransduction via TRPV4 regulates inflammation and differentiation in fetal mouse distal lung epithelial cells. *Respiratory Research, 16*(1), 60. doi:10.1186/s12931-015-0224-4

Neumann, J., & Gottschalk, K.-E. (2016). The integrin–talin complex under force. *Protein Engineering, Design and Selection, 29*(11), 503-512. doi:10.1093/protein/gzw031

Niccolai, F., Di Mento, L., Mocchi, M., & Berlusconi, M. (2018). Modified Masquelet's technique with nail and allograft: A case report. *Injury, 49 Suppl 4*, S21-s24. doi:10.1016/j.injury.2018.11.040

Nicholas, S., Yuan, S. Y., Brookes, S. J., Spencer, N. J., & Zagorodnyuk, V. P. (2017). Hydrogen peroxide preferentially activates capsaicin-sensitive high threshold afferents via TRPA1 channels in the guinea pig bladder. *Br J Pharmacol, 174*(2), 126-138. doi:10.1111/bph.13661

Niehrs, C. (2012). The complex world of WNT receptor signalling. *Nature Reviews Molecular Cell Biology, 13*, 767. doi:10.1038/nrm3470

Nikukar, H. (2013). *Nanomechanotransduction of Human Mesenchymal Stem Cells an Application of Medical Nanobiotechnology*. (Doctor of Philosophy), University of Glasgow.

Nikukar, H., Reid, S., Tsimbouri, P. M., Riehle, M. O., Curtis, A. S., & Dalby, M. J. (2013). Osteogenesis of mesenchymal stem cells by nanoscale mechanotransduction. *ACS Nano, 7*(3), 2758-2767. doi:10.1021/nn400202j

Ning, C. Y., Wang, S. Y., Zhu, Y., Zhong, M. L., Lin, X., Zhang, Y., . . . Mao, C. B. (2016). Ti nanorod arrays with a medium density

significantly promote osteogenesis and osteointegration. *Sci Rep, 6*. doi:10.1038/srep19047

Nissar, A. U., Sharma, L., & Tasduq, S. A. (2015). Palmitic acid induced lipotoxicity is associated with altered lipid metabolism, enhanced CYP450 2E1 and intracellular calcium mediated ER stress in human hepatoma cells. *Toxicology Research, 4*(5), 1344-1358. doi:10.1039/c5tx00101c

Norwitz, N. G., Mota, A. S., Misra, M., & Ackerman, K. E. (2019). LRP5, Bone Density, and Mechanical Stress: A Case Report and Literature Review. *Frontiers in Endocrinology, 10*(184). doi:10.3389/fendo.2019.00184

Nourse, J. L., & Pathak, M. M. (2017). How cells channel their stress: Interplay between Piezo1 and the cytoskeleton. *Seminars in Cell & Developmental Biology, 71*, 3-12. doi:10.1016/j.semcdb.2017.06.018

Nowycky, M. C., & Thomas, A. P. (2002). Intracellular calcium signaling. *J Cell Sci, 115*(Pt 19), 3715-3716. doi:10.1242/jcs.00078

Nsiah-Sefaa, A., & McKenzie, M. (2016). Combined defects in oxidative phosphorylation and fatty acid beta-oxidation in mitochondrial disease. *Bioscience Reports, 36*. doi:10.1042/BSR20150295

Nummenmaa, E., Hämäläinen, M., Moilanen, L. J., Paukkeri, E.-L., Nieminen, R. M., Moilanen, T., . . . Moilanen, E. (2016). Transient receptor potential ankyrin 1 (TRPA1) is functionally expressed in primary human osteoarthritic chondrocytes. *Arthritis Research & Therapy, 18*(1), 185. doi:10.1186/s13075-016-1080-4

Oeckinghaus, A., & Ghosh, S. (2009). The NF-kappaB family of transcription factors and its regulation. *Cold Spring Harbor Perspectives in Biology, 1*(4), a000034-a000034. doi:10.1101/cshperspect.a000034

Ogura, T., Sakaguchi, H., Miyamoto, S., & Takahashi, J. (2018). Three-dimensional induction of dorsal, intermediate and ventral spinal

cord tissues from human pluripotent stem cells. *Development, 145*(16), dev162214. doi:10.1242/dev.162214

Ohba, S. (2016). Hedgehog Signaling in Endochondral Ossification. *Journal of developmental biology, 4*(2), 20. doi:10.3390/jdb4020020

Okamoto, M., Udagawa, N., Uehara, S., Maeda, K., Yamashita, T., Nakamichi, Y., . . . Kobayashi, Y. (2014). Noncanonical Wnt5a enhances Wnt/β-catenin signaling during osteoblastogenesis. *Sci Rep, 4*, 4493. doi:10.1038/srep04493

Olivares-Navarrete, R., Lee, E. M., Smith, K., Hyzy, S. L., Doroudi, M., Williams, J. K., . . . Schwartz, Z. (2017). Substrate Stiffness Controls Osteoblastic and Chondrocytic Differentiation of Mesenchymal Stem Cells without Exogenous Stimuli. *PLoS One, 12*(1), e0170312. doi:10.1371/journal.pone.0170312

Oliveira-Marques, V., Marinho, H. S., Cyrne, L., & Antunes, F. (2009). Role of hydrogen peroxide in NF-kappaB activation: from inducer to modulator. *Antioxid Redox Signal, 11*(9), 2223-2243. doi:10.1089/ARS.2009.2601

Ongaro, A., Pellati, A., Bagheri, L., Rizzo, P., Caliceti, C., Massari, L., & De Mattei, M. (2016). Characterization of Notch Signaling During Osteogenic Differentiation in Human Osteosarcoma Cell Line MG63. *Journal of Cellular Physiology, 231*(12), 2652-2663. doi:10.1002/jcp.25366

Onuki, Y., Bhardwaj, U., Papadimitrakopoulos, F., & Burgess, D. J. (2008). A review of the biocompatibility of implantable devices: current challenges to overcome foreign body response. *J Diabetes Sci Technol, 2*(6), 1003-1015. doi:10.1177/193229680800200610

Oppenheim, J. J., Matsushima, K., Yoshimura, T., Leonard, E. J., & Neta, R. (1989). Relationship between Interleukin-1 (Il1), Tumor

Necrosis Factor (Tnf) and a Neutrophil Attracting Peptide (Nap-1). *Agents and Actions, 26*(1-2), 134-140. doi:Doi 10.1007/Bf02126586

Orimo, H. (2010). The mechanism of mineralization and the role of alkaline phosphatase in health and disease. *J Nippon Med Sch, 77*(1), 4-12.

Orlandini, M., Spreafico, A., Bardelli, M., Rocchigiani, M., Salameh, A., Nucciotti, S., . . . Oliviero, S. (2006). Vascular endothelial growth factor-D activates VEGFR-3 expressed in osteoblasts inducing their differentiation. *J Biol Chem, 281*(26), 17961-17967. doi:10.1074/jbc.M600413200

Oryan, A., Kamali, A., & Moshiri, A. (2015). Potential mechanisms and applications of statins on osteogenesis: Current modalities, conflicts and future directions. *Journal of Controlled Release, 215*, 12-24. doi:10.1016/j.jconrel.2015.07.022

Osta, B., Benedetti, G., & Miossec, P. (2014). Classical and Paradoxical Effects of TNF-alpha on Bone Homeostasis. *Front Immunol, 5*, 48. doi:10.3389/fimmu.2014.00048

Ota, T., Nishida, Y., Ikuta, K., Kato, R., Kozawa, E., Hamada, S., . . . Ishiguro, N. (2017). Heat-stimuli-enhanced osteogenesis using clinically available biomaterials. *PLoS One, 12*(7), e0181404. doi:10.1371/journal.pone.0181404

Otchwemah, R., Grams, V., Tjardes, T., Shafizadeh, S., Bathis, H., Maegele, M., . . . Probst, C. (2015). Bacterial contamination of open fractures - pathogens, antibiotic resistances and therapeutic regimes in four hospitals of the trauma network Cologne, Germany. *Injury, 46 Suppl 4*, S104-108. doi:10.1016/s0020-1383(15)30027-9

Ozturk, E., Hobiger, S., Despot-Slade, E., Pichler, M., & Zenobi-Wong, M. (2017). Hypoxia regulates RhoA and Wnt/beta-catenin signaling in a context-dependent way to control re-differentiation of

chondrocytes. *Sci Rep, 7*(1), 9032. doi:10.1038/s41598-017-09505-6

Paley, D. (1990). Problems, obstacles, and complications of limb lengthening by the Ilizarov technique. *Clin Orthop Relat Res*(250), 81-104.

Palomaki, S., Pietila, M., Laitinen, S., Pesala, J., Sormunen, R., Lehenkari, P., & Koivunen, P. (2013). HIF-1alpha is upregulated in human mesenchymal stem cells. *Stem Cells, 31*(9), 1902-1909. doi:10.1002/stem.1435

Pan, H. H., Xie, Y. T., Li, K., Hu, D. D., Zhao, J., Zheng, X. B., & Tang, T. T. (2015). ROCK-regulated synergistic effect of macropore/nanowire topography on cytoskeletal distribution and cell differentiation. *Rsc Advances, 5*(123), 101834-101842. doi:10.1039/c5ra19691d

Pan, J. X., Xiong, L., Zhao, K., Zeng, P., Wang, B., Tang, F. L., . . . Xiong, W. C. (2018). YAP promotes osteogenesis and suppresses adipogenic differentiation by regulating beta-catenin signaling. *Bone Res, 6*, 18. doi:10.1038/s41413-018-0018-7

Panciera, T., Azzolin, L., Cordenonsi, M., & Piccolo, S. (2017). Mechanobiology of YAP and TAZ in physiology and disease. *Nat Rev Mol Cell Biol, 18*(12), 758-770. doi:10.1038/nrm.2017.87

Papa, S., Zazzeroni, F., Pham, C. G., Bubici, C., & Franzoso, G. (2004). Linking JNK signaling to NF-kappaB: a key to survival. *J Cell Sci, 117*(Pt 22), 5197-5208. doi:10.1242/jcs.01483

Parekh, S. H., Chatterjee, K., Lin-Gibson, S., Moore, N. M., Cicerone, M. T., Young, M. F., & Simon, C. G., Jr. (2011). Modulus-driven differentiation of marrow stromal cells in 3D scaffolds that is independent of myosin-based cytoskeletal tension. *Biomaterials, 32*(9), 2256-2264. doi:10.1016/j.biomaterials.2010.11.065

Park, M. H., Moon, H. J., Park, J. H., Shinde, U. P., Ko du, Y., & Jeong, B. (2015). PEG-Poly(L-alanine) thermogel as a 3D scaffold of bone-

marrow-derived mesenchymal stem cells. *Macromol Biosci, 15*(4), 464-472. doi:10.1002/mabi.201400426

Parsons, J. T., Horwitz, A. R., & Schwartz, M. A. (2010). Cell adhesion: integrating cytoskeletal dynamics and cellular tension. *Nat Rev Mol Cell Biol, 11*(9), 633-643. doi:10.1038/nrm2957

Pathak, M. M., Nourse, J. L., Tran, T., Hwe, J., Arulmoli, J., Le, D. T., . . . Tombola, F. (2014). Stretch-activated ion channel Piezo1 directs lineage choice in human neural stem cells. *Proc Natl Acad Sci U S A, 111*(45), 16148-16153. doi:10.1073/pnas.1409802111

Pattappa, G., Heywood, H. K., de Bruijn, J. D., & Lee, D. A. (2011). The metabolism of human mesenchymal stem cells during proliferation and differentiation. *Journal of Cellular Physiology, 226*(10), 2562-2570. doi:10.1002/jcp.22605

Pelissier, P., Masquelet, A. C., Bareille, R., Pelissier, S. M., & Amedee, J. (2004). Induced membranes secrete growth factors including vascular and osteoinductive factors and could stimulate bone regeneration. *J Orthop Res, 22*(1), 73-79. doi:10.1016/S0736-0266(03)00165-7

Pemberton, G. D., Childs, P., Reid, S., Nikukar, H., Tsimbouri, P. M., Gadegaard, N., . . . Dalby, M. J. (2015). Nanoscale stimulation of osteoblastogenesis from mesenchymal stem cells: nanotopography and nanokicking. *Nanomedicine (Lond), 10*(4), 547-560. doi:10.2217/nnm.14.134

Peng, H., Lewandrowski, U., Muller, B., Sickmann, A., Walz, G., & Wegierski, T. (2010). Identification of a Protein Kinase C-dependent phosphorylation site involved in sensitization of TRPV4 channel. *Biochem Biophys Res Commun, 391*(4), 1721-1725. doi:10.1016/j.bbrc.2009.12.140

Perl, A., Hanczko, R., Telarico, T., Oaks, Z., & Landas, S. (2011). Oxidative stress, inflammation and carcinogenesis are controlled

through the pentose phosphate pathway by transaldolase. *Trends Mol Med, 17*(7), 395-403. doi:10.1016/j.molmed.2011.01.014

Perren, S. M. (2002). Evolution of the internal fixation of long bone fractures - The scientific basis of biological internal fixation: Choosing a new balance between stability and biology. *Journal of Bone and Joint Surgery-British Volume, 84b*(8), 1093-1110. doi:Doi 10.1302/0301-620x.84b8.13752

Petrie, R. J., & Yamada, K. M. (2015). Fibroblasts Lead the Way: A Unified View of 3D Cell Motility. *Trends in Cell Biology, 25*(11), 666-674. doi:10.1016/j.tcb.2015.07.013

Phimphilai, M., Zhao, Z., Boules, H., Roca, H., & Franceschi, R. T. (2006). BMP signaling is required for RUNX2-dependent induction of the osteoblast phenotype. *J Bone Miner Res, 21*(4), 637-646. doi:10.1359/jbmr.060109

Pi, D., Liu, Y., Shi, H., Li, S., Odle, J., Lin, X., . . . Leng, W. (2014). Dietary supplementation of aspartate enhances intestinal integrity and energy status in weanling piglets after lipopolysaccharide challenge. *The Journal of Nutritional Biochemistry, 25*(4), 456-462. doi:https://doi.org/10.1016/j.jnutbio.2013.12.006

Piccolo, S., Dupont, S., & Cordenonsi, M. (2014). The Biology of Yap/Taz: Hippo Signaling and Beyond. *Physiological Reviews, 94*(4), 1287-1312. doi:10.1152/physrev.00005.2014

Pilkington, M. F., Sims, S. M., & Dixon, S. J. (2001). Transforming growth factor-beta induces osteoclast ruffling and chemotaxis: potential role in osteoclast recruitment. *J Bone Miner Res, 16*(7), 1237-1247. doi:10.1359/jbmr.2001.16.7.1237

Plant, T. D., & Strotmann, R. (2007). TRPV4. In V. Flockerzi & B. Nilius (Eds.), *Transient Receptor Potential (TRP) Channels* (pp. 189-205). Berlin, Heidelberg: Springer Berlin Heidelberg.

Plotnikov, A., Zehorai, E., Procaccia, S., & Seger, R. (2011). The MAPK cascades: signaling components, nuclear roles and mechanisms of

nuclear translocation. *Biochim Biophys Acta, 1813*(9), 1619-1633. doi:10.1016/j.bbamcr.2010.12.012

Porter, R. M., Huckle, W. R., & Goldstein, A. S. (2003). Effect of dexamethasone withdrawal on osteoblastic differentiation of bone marrow stromal cells. *Journal of Cellular Biochemistry, 90*(1), 13-22. doi:10.1002/jcb.10592

Pountos, I., Georgouli, T., Calori, G. M., & Giannoudis, P. V. (2012). Do Nonsteroidal Anti-Inflammatory Drugs Affect Bone Healing? A Critical Analysis. *Scientific World Journal*. doi:10.1100/2012/606404

Pountos, I., Giannoudis, P. V., Jones, E., English, A., Churchman, S., Field, S., . . . McGonagle, D. (2011). NSAIDS inhibit in vitro MSC chondrogenesis but not osteogenesis: implications for mechanism of bone formation inhibition in man. *Journal of Cellular and Molecular Medicine, 15*(3), 525-534. doi:10.1111/j.1582-4934.2010.01006.x

Pramojanee, S. N., Phimphilai, M., Chattipakorn, N., & Chattipakorn, S. C. (2014). Possible roles of insulin signaling in osteoblasts. *Endocrine Research, 39*(4), 144-151. doi:10.3109/07435800.2013.879168

Premkumar, L. S., & Ahern, G. P. (2000). Induction of vanilloid receptor channel activity by protein kinase C. *Nature, 408*(6815), 985-990. doi:10.1038/35050121

Price, L. S., Leng, J., Schwartz, M. A., & Bokoch, G. M. (1998). Activation of Rac and Cdc42 by integrins mediates cell spreading. *Mol Biol Cell, 9*(7), 1863-1871. doi:10.1091/mbc.9.7.1863

Provenzano, P. P., & Keely, P. J. (2011). Mechanical signaling through the cytoskeleton regulates cell proliferation by coordinated focal

adhesion and Rho GTPase signaling. *J Cell Sci, 124*(Pt 8), 1195-1205. doi:10.1242/jcs.067009

Putra, A., Ridwan, F. B., Putridewi, A. I., Kustiyah, A. R., Wirastuti, K., Sadyah, N. A. C., . . . Munir, D. (2018). The Role of TNF-α induced MSCs on Suppressive Inflammation by Increasing TGF-ß and IL-10. *Open access Macedonian journal of medical sciences, 6*(10), 1779-1783. doi:10.3889/oamjms.2018.404

Qian, W., Gong, L., Cui, X., Zhang, Z., Bajpai, A., Liu, C., . . . Chen, W. (2017). Nanotopographic Regulation of Human Mesenchymal Stem Cell Osteogenesis. *ACS Appl Mater Interfaces, 9*(48), 41794-41806. doi:10.1021/acsami.7b16314

R., M., M., H., A., E., & I., P. (2017). Induced membrane technique for treating tibial defects gives mixed results. *The Bone & Joint Journal, 99-B*(5), 680-685. doi:10.1302/0301-620x.99b5.bjj-2016-0694.r2

Rafat, M., Li, F., Fagerholm, P., Lagali, N. S., Watsky, M. A., Munger, R., . . . Griffith, M. (2008). PEG-stabilized carbodiimide crosslinked collagen-chitosan hydrogels for corneal tissue engineering. *Biomaterials, 29*(29), 3960-3972. doi:10.1016/j.biomaterials.2008.06.017

Rahman, M. S., Akhtar, N., Jamil, H. M., Banik, R. S., & Asaduzzaman, S. M. (2015). TGF-beta/BMP signaling and other molecular events: regulation of osteoblastogenesis and bone formation. *Bone Res, 3*, 15005. doi:10.1038/boneres.2015.5

Raic, A., Rödling, L., Kalbacher, H., & Lee-Thedieck, C. (2014). Biomimetic macroporous PEG hydrogels as 3D scaffolds for the multiplication of human hematopoietic stem and progenitor cells. *Biomaterials, 35*(3), 929-940. doi:https://doi.org/10.1016/j.biomaterials.2013.10.038

Raifman, T. K., Kumar, P., Haase, H., Klussmann, E., Dascal, N., & Weiss, S. (2017). Protein kinase C enhances plasma membrane

expression of cardiac L-type calcium channel, CaV1.2. *Channels (Austin), 11*(6), 604-615. doi:10.1080/19336950.2017.1369636

Ramsey, I. S., Delling, M., & Clapham, D. E. (2006). An introduction to TRP channels. *Annu Rev Physiol, 68*, 619-647. doi:10.1146/annurev.physiol.68.040204.100431

Rappaz, B., Barbul, A., Hoffmann, A., Boss, D., Korenstein, R., Depeursinge, C., . . . Marquet, P. (2009). Spatial analysis of erythrocyte membrane fluctuations by digital holographic microscopy. *Blood Cells Mol Dis, 42*(3), 228-232. doi:10.1016/j.bcmd.2009.01.018

Rath, B., Nam, J., Knobloch, T. J., Lannutti, J. J., & Agarwal, S. (2008). Compressive forces induce osteogenic gene expression in calvarial osteoblasts. *J Biomech, 41*(5), 1095-1103. doi:10.1016/j.jbiomech.2007.11.024

Rauch, A., Seitz, S., Baschant, U., Schilling, A. F., Illing, A., Stride, B., . . . Tuckermann, J. P. (2010). Glucocorticoids suppress bone formation by attenuating osteoblast differentiation via the monomeric glucocorticoid receptor. *Cell Metabolism, 11*(6), 517-531. doi:10.1016/j.cmet.2010.05.005

Razzaque, M. S., Soegiarto, D. W., Chang, D., Long, F., & Lanske, B. (2005). Conditional deletion of Indian hedgehog from collagen type 2alpha1-expressing cells results in abnormal endochondral bone formation. *J Pathol, 207*(4), 453-461. doi:10.1002/path.1870

Rebelatto, C. K., Aguiar, A. M., Moretao, M. P., Senegaglia, A. C., Hansen, P., Barchiki, F., . . . Correa, A. (2008). Dissimilar differentiation of mesenchymal stem cells from bone marrow, umbilical cord blood, and adipose tissue. *Experimental Biology and Medicine, 233*(7), 901-913. doi:10.3181/0712-Rm-356

Regard, J. B., Zhong, Z., Williams, B. O., & Yang, Y. (2012). Wnt signaling in bone development and disease: making stronger bone

with Wnts. *Cold Spring Harb Perspect Biol, 4*(12). doi:10.1101/cshperspect.a007997

Renner, F., & Schmitz, M. L. (2009). Autoregulatory feedback loops terminating the NF-kappaB response. *Trends Biochem Sci, 34*(3), 128-135. doi:10.1016/j.tibs.2008.12.003

Retting, K. N., Song, B., Yoon, B. S., & Lyons, K. M. (2009). BMP canonical Smad signaling through Smad1 and Smad5 is required for endochondral bone formation. *Development, 136*(7), 1093-1104. doi:10.1242/dev.029926

Reuter, S., Gupta, S. C., Chaturvedi, M. M., & Aggarwal, B. B. (2010). Oxidative stress, inflammation, and cancer: how are they linked? *Free Radic Biol Med, 49*(11), 1603-1616. doi:10.1016/j.freeradbiomed.2010.09.006

Richard, D., Kefi, K., Barbe, U., Bausero, P., & Visioli, F. (2008). Polyunsaturated fatty acids as antioxidants. *Pharmacological Research, 57*(6), 451-455. doi:https://doi.org/10.1016/j.phrs.2008.05.002

Riera-Borrull, M., Cuevas, V. D., Alonso, B., Vega, M. A., Joven, J., Izquierdo, E., & Corbí, Á. L. (2017). Palmitate Conditions Macrophages for Enhanced Responses toward Inflammatory Stimuli via JNK Activation. *The Journal of Immunology, 199*(11), 3858-3869. doi:10.4049/jimmunol.1700845

Rocio Servin-Vences, M., Moroni, M., Lewin, G. R., & Poole, K. (2017). Direct measurement of TRPV4 and PIEZO1 activity reveals multiple mechanotransduction pathways in chondrocytes. *Elife, 6*, e21074. doi:10.7554/eLife.21074

Rodda, S. J., & McMahon, A. P. (2006). Distinct roles for Hedgehog and canonical Wnt signaling in specification, differentiation and

maintenance of osteoblast progenitors. *Development, 133*(16), 3231-3244. doi:10.1242/dev.02480

Rodland, K. D. (2003). Calcium Receptor-mediated Signaling. In N. Chattopadhyay & E. M. Brown (Eds.), *Calcium-Sensing Receptor* (pp. 53-67). Boston, MA: Springer US.

Rodriguez-Carballo, E., Gamez, B., & Ventura, F. (2016). p38 MAPK Signaling in Osteoblast Differentiation. *Front Cell Dev Biol, 4*, 40. doi:10.3389/fcell.2016.00040

Rosset, E. M., & Bradshaw, A. D. (2016). SPARC/osteonectin in mineralized tissue. *Matrix biology : journal of the International Society for Matrix Biology, 52-54*, 78-87. doi:10.1016/j.matbio.2016.02.001

Rouwkema, J., Koopman, B. F. J. M., van Blitterswijk, C. A., Dhert, W. J. A., & Malda, J. (2010). Supply of Nutrients to Cells in Engineered Tissues. *Biotechnology and Genetic Engineering Reviews, Vol 26, 26*, 163-177.

Rucci, N. (2008). Molecular biology of bone remodelling. *Clinical cases in mineral and bone metabolism : the official journal of the Italian Society of Osteoporosis, Mineral Metabolism, and Skeletal Diseases, 5*(1), 49-56.

Ryan, E. A., Mockros, L. F., Weisel, J. W., & Lorand, L. (1999). Structural origins of fibrin clot rheology. *Biophys J, 77*(5), 2813-2826. doi:10.1016/S0006-3495(99)77113-4

S.D., B., T.A., Z., H.S., S., S.E., H., & Sofamor, D. d. (2002). THE USE OF BMP-2 IN INTERBODY FUSION CAGES: DEFINITIVE EVIDENCE OF OSTEOINDUCTION IN HUMANS. *Orthopaedic Proceedings, 84-B*(SUPP_III), 216-216. doi:10.1302/0301-620X.84BSUPP_III.0840216a

Sachs, F. (2010). Stretch-activated ion channels: what are they? *Physiology (Bethesda), 25*(1), 50-56. doi:10.1152/physiol.00042.2009

Safadi, F. F., Barbe, M. F., Abdelmagid, S. M., Rico, M. C., Aswad, R. A., Litvin, J., & Popoff, S. N. (2009). Bone Structure, Development and Bone Biology. In J. S. Khurana (Ed.), *Bone Pathology* (pp. 1-50). Totowa, NJ: Humana Press.

Salkın, H., Gönen, Z. B., Ergen, E., Bahar, D., & Çetin, M. (2019). Effects of TGF-ß1 Overexpression on Biological Characteristics of Human Dental Pulp-derived Mesenchymal Stromal Cells. *International journal of stem cells, 12*(1), 170-182. doi:10.15283/ijsc18051

Samavedi, S., Whittington, A. R., & Goldstein, A. S. (2013). Calcium phosphate ceramics in bone tissue engineering: a review of properties and their influence on cell behavior. *Acta Biomater, 9*(9), 8037-8045. doi:10.1016/j.actbio.2013.06.014

Samuels, A., Perry, M. J., Gibson, R. L., Colley, S., & Tobias, J. H. (2001). Role of endothelial nitric oxide synthase in estrogen-induced osteogenesis. *Bone, 29*(1), 24-29.

Sangani, R., Periyasamy-Thandavan, S., Pathania, R., Ahmad, S., Kutiyanawalla, A., Kolhe, R., . . . Fulzele, S. (2015). The crucial role of vitamin C and its transporter (SVCT2) in bone marrow stromal cell autophagy and apoptosis. *Stem Cell Res, 15*(2), 312-321. doi:https://doi.org/10.1016/j.scr.2015.06.002

Sato, M. (2006). Upregulation of the Wnt/beta-catenin pathway induced by transforming growth factor-beta in hypertrophic scars and keloids. *Acta Derm Venereol, 86*(4), 300-307. doi:10.2340/00015555-0101

Saunders, M. M., You, J., Zhou, Z., Li, Z., Yellowley, C. E., Kunze, E. L., . . . Donahue, H. J. (2003). Fluid flow-induced prostaglandin E2

response of osteoblastic ROS 17/2.8 cells is gap junction-mediated and independent of cytosolic calcium. *Bone, 32*(4), 350-356.

Saura, M., Tarin, C., & Zaragoza, C. (2010). Recent insights into the implication of nitric oxide in osteoblast differentiation and proliferation during bone development. *ScientificWorldJournal, 10*, 624-632. doi:10.1100/tsw.2010.58

Saxton, R. A., & Sabatini, D. M. (2017). mTOR Signaling in Growth, Metabolism, and Disease. *Cell, 168*(6), 960-976. doi:https://doi.org/10.1016/j.cell.2017.02.004

Schaller, M. D. (2010). Cellular functions of FAK kinases: insight into molecular mechanisms and novel functions. *J Cell Sci, 123*(7), 1007-1013. doi:10.1242/jcs.045112

Scherer, G. W. (1989a). Mechanics of Syneresis .1. Theory. *Journal of Non-Crystalline Solids, 108*(1), 18-27. doi:Doi 10.1016/0022-3093(89)90328-1

Scherer, G. W. (1989b). Mechanics of Syneresis .2. Experimental-Study. *Journal of Non-Crystalline Solids, 108*(1), 28-36. doi:Doi 10.1016/0022-3093(89)90329-3

Schipani, E. (2006). Hypoxia and HIF-1 alpha in chondrogenesis. *Skeletal Development and Remodeling in Health, Disease, and Aging, 1068*, 66-73. doi:10.1196/annals.1346.009

Schmelter, M., Ateghang, B., Helmig, S., Wartenberg, M., & Sauer, H. (2006). Embryonic stem cells utilize reactive oxygen species as transducers of mechanical strain-induced cardiovascular differentiation. *Faseb Journal, 20*(8), 1182-+. doi:10.1096/fj.05-4723fje

Schmidt, J. B., Chen, K., & Tranquillo, R. T. (2016). Effects of Intermittent and Incremental Cyclic Stretch on ERK Signaling and

Collagen Production in Engineered Tissue. *Cell Mol Bioeng, 9*(1), 55-64. doi:10.1007/s12195-015-0415-6

Schoof, H., Apel, J., Heschel, I., & Rau, G. (2001). Control of pore structure and size in freeze-dried collagen sponges. *J Biomed Mater Res, 58*(4), 352-357.

Sée, V., Rajala, N. K. M., Spiller, D. G., & White, M. R. H. (2004). Calcium-dependent regulation of the cell cycle via a novel MAPK–NF-κB pathway in Swiss 3T3 cells. *The Journal of Cell Biology, 166*(5), 661-672. doi:10.1083/jcb.200402136

Sen, B., Xie, Z., Case, N., Styner, M., Rubin, C. T., & Rubin, J. (2011). Mechanical signal influence on mesenchymal stem cell fate is enhanced by incorporation of refractory periods into the loading regimen. *J Biomech, 44*(4), 593-599. doi:10.1016/j.jbiomech.2010.11.022

Serra, T., Mateos-Timoneda, M. A., Planell, J. A., & Navarro, M. (2013). 3D printed PLA-based scaffolds: a versatile tool in regenerative medicine. *Organogenesis, 9*(4), 239-244. doi:10.4161/org.26048

Shalhoub, V., Conlon, D., Tassinari, M., Quinn, C., Partridge, N., Stein, G. S., & Lian, J. B. (1992). Glucocorticoids promote development of the osteoblast phenotype by selectively modulating expression of cell growth and differentiation associated genes. *Journal of Cellular Biochemistry, 50*(4), 425-440. doi:10.1002/jcb.240500411

Sharaf-Eldin, W. E., Abu-Shahba, N., Mahmoud, M., & El-Badri, N. (2016). The Modulatory Effects of Mesenchymal Stem Cells on Osteoclastogenesis. *Stem Cells International, 2016*, 1908365-1908365. doi:10.1155/2016/1908365

Sharifpanah, F., Behr, S., Wartenberg, M., & Sauer, H. (2016). Mechanical strain stimulates vasculogenesis and expression of angiogenesis guidance molecules of embryonic stem cells through elevation of intracellular calcium, reactive oxygen species and

nitric oxide generation. *Biochim Biophys Acta, 1863*(12), 3096-3105. doi:10.1016/j.bbamcr.2016.10.001

Sharma, R. V., Chapleau, M. W., Hajduczok, G., Wachtel, R. E., Waite, L. J., Bhalla, R. C., & Abboud, F. M. (1995). Mechanical stimulation increases intracellular calcium concentration in nodose sensory neurons. *Neuroscience, 66*(2), 433-441.

Shibasaki, K. (2016). TRPV4 ion channel as important cell sensors. *J Anesth, 30*(6), 1014-1019. doi:10.1007/s00540-016-2225-y

Shih, Y. R., Tseng, K. F., Lai, H. Y., Lin, C. H., & Lee, O. K. (2011). Matrix stiffness regulation of integrin-mediated mechanotransduction during osteogenic differentiation of human mesenchymal stem cells. *J Bone Miner Res, 26*(4), 730-738. doi:10.1002/jbmr.278

Shim, J. H., Kim, J. Y., Park, M., Park, J., & Cho, D. W. (2011). Development of a hybrid scaffold with synthetic biomaterials and hydrogel using solid freeform fabrication technology. *Biofabrication, 3*(3), 034102. doi:10.1088/1758-5082/3/3/034102

Shimer, A. L., Oner, F. C., & Vaccaro, A. R. (2009). Spinal reconstruction and bone morphogenetic proteins: open questions. *Injury, 40 Suppl 3*, S32-38. doi:10.1016/S0020-1383(09)70009-9

Shirjang, S., Mansoori, B., Solali, S., Hagh, M. F., & Shamsasenjan, K. (2017). Toll-like receptors as a key regulator of mesenchymal stem cell function: An up-to-date review. *Cellular Immunology, 315*, 1-10. doi:https://doi.org/10.1016/j.cellimm.2016.12.005

Shum, L. C., White, N. S., Mills, B. N., Bentley, K. L., & Eliseev, R. A. (2016). Energy Metabolism in Mesenchymal Stem Cells During Osteogenic Differentiation. *Stem Cells Dev, 25*(2), 114-122. doi:10.1089/scd.2015.0193

Shyh-Chang, N., Daley, G. Q., & Cantley, L. C. (2013). Stem cell metabolism in tissue development and aging. *Development, 140*(12), 2535-2547. doi:10.1242/dev.091777

Shyh-Chang, N., & Ng, H. H. (2017). The metabolic programming of stem cells. *Genes Dev, 31*(4), 336-346. doi:10.1101/gad.293167.116

Siffert, R. S. (1951). The Role of Alkaline Phosphatase in Osteogenesis. *Journal of Experimental Medicine, 93*(5), 415-&. doi:DOI 10.1084/jem.93.5.415

. Simple harmonic motion. (2007). In J. W. Gooch (Ed.), *Encyclopedic Dictionary of Polymers* (pp. 887-888). New York, NY: Springer New York.

Sisignano, M., Bennett, D. L., Geisslinger, G., & Scholich, K. (2014). TRP-channels as key integrators of lipid pathways in nociceptive neurons. *Prog Lipid Res, 53*, 93-107. doi:10.1016/j.plipres.2013.11.002

Sjostrom, T., Dalby, M. J., Hart, A., Tare, R., Oreffo, R. O., & Su, B. (2009). Fabrication of pillar-like titania nanostructures on titanium and their interactions with human skeletal stem cells. *Acta Biomater, 5*(5), 1433-1441. doi:10.1016/j.actbio.2009.01.007

Smith, E., Redman, R. A., Logg, C. R., Coetzee, G. A., Kasahara, N., & Frenkel, B. (2000). Glucocorticoids inhibit developmental stage-specific osteoblast cell cycle. Dissociation of cyclin A-cyclin-dependent kinase 2 from E2F4-p130 complexes. *J Biol Chem, 275*(26), 19992-20001. doi:10.1074/jbc.M001758200

Somaiah, C., Kumar, A., Mawrie, D., Sharma, A., Patil, S. D., Bhattacharyya, J., . . . Jaganathan, B. G. (2015). Collagen Promotes Higher Adhesion, Survival and Proliferation of Mesenchymal Stem Cells. *PLoS One, 10*(12), e0145068-e0145068. doi:10.1371/journal.pone.0145068

Somaiah, C., Kumar, A., Mawrie, D., Sharma, A., Patil, S. D., Bhattacharyya, J., . . . Jaganathan, B. G. (2015). Collagen

Promotes Higher Adhesion, Survival and Proliferation of Mesenchymal Stem Cells. *PLoS One, 10*(12), e0145068. doi:10.1371/journal.pone.0145068

Song, L., Li, Z. Y., Liu, W. P., & Zhao, M. R. (2015). Crosstalk between Wnt/beta-catenin and Hedgehog/Gli signaling pathways in colon cancer and implications for therapy. *Cancer Biol Ther, 16*(1), 1-7. doi:10.4161/15384047.2014.972215

Spiegelberg, B., Parratt, T., Dheerendra, S. K., Khan, W. S., Jennings, R., & Marsh, D. R. (2010). Ilizarov principles of deformity correction. *Annals of the Royal College of Surgeons of England, 92*(2), 101-105. doi:10.1308/003588410X12518836439326

Stadtman, E. R., & Levine, R. L. (2003). Free radical-mediated oxidation of free amino acids and amino acid residues in proteins. *Amino Acids, 25*(3-4), 207-218. doi:10.1007/s00726-003-0011-2

Stafford, P. R., & Norris, B. L. (2010). Reamer-irrigator-aspirator bone graft and bi Masquelet technique for segmental bone defect nonunions: a review of 25 cases. *Injury, 41 Suppl 2*, S72-77. doi:10.1016/S0020-1383(10)70014-0

Stanton, M. M., Samitier, J., & Sanchez, S. (2015). Bioprinting of 3D hydrogels. *Lab Chip, 15*(15), 3111-3115. doi:10.1039/c5lc90069g

Stefkova, K., Prochazkova, J., & Pachernik, J. (2015). Alkaline phosphatase in stem cells. *Stem Cells Int, 2015*, 628368. doi:10.1155/2015/628368

Stein, G. S., Lian, J. B., Owen, T. A., Stein, J. L., Tassinari, M., Vanwijnen, A., . . . Holthuis, J. (1991). Cell Structure and the Regulation of Genes-Controlling Proliferation and Differentiation - the Nuclear Matrix and Cytoskeleton. *Molecular Basis of Human Cancer /, 209*, 1-38.

Stein, G. S., Lian, J. B., van Wijnen, A. J., Stein, J. L., Montecino, M., Javed, A., . . . Pockwinse, S. M. (2004). Runx2 control of organization, assembly and activity of the regulatory machinery for

skeletal gene expression. *Oncogene, 23*(24), 4315-4329. doi:10.1038/sj.onc.1207676

Steward, A. J., & Kelly, D. J. (2015). Mechanical regulation of mesenchymal stem cell differentiation. *Journal of anatomy, 227*(6), 717-731. doi:10.1111/joa.12243

Stojilkovic, S. S., Tomić, M., Koshimizu, T.-a., & Van Goor, F. (2000). Calcium Ions as Intracellular Messengers. In P. M. Conn & A. R. Means (Eds.), *Principles of Molecular Regulation* (pp. 149-185). Totowa, NJ: Humana Press.

Stolberg, S., & McCloskey, K. E. (2009). Can shear stress direct stem cell fate? *Biotechnol Prog, 25*(1), 10-19. doi:10.1002/btpr.124

Studer, M., & McNaughton, P. A. (2010). Modulation of single-channel properties of TRPV1 by phosphorylation. *J Physiol, 588*(Pt 19), 3743-3756. doi:10.1113/jphysiol.2010.190611

Sugarman, J. (2008). Ethical issues in stem cell research and treatment. *Cell Research, 18*, S176. doi:10.1038/cr.2008.266

Sugimoto, A., Miyazaki, A., Kawarabayashi, K., Shono, M., Akazawa, Y., Hasegawa, T., . . . Iwamoto, T. (2017). Piezo type mechanosensitive ion channel component 1 functions as a regulator of the cell fate determination of mesenchymal stem cells. *Sci Rep, 7*(1), 17696-17696. doi:10.1038/s41598-017-18089-0

Sugimoto, A., Miyazaki, A., Kawarabayashi, K., Shono, M., Akazawa, Y., Hasegawa, T., . . . Iwamoto, T. (2017). Piezo type mechanosensitive ion channel component 1 functions as a regulator of the cell fate determination of mesenchymal stem cells. *Sci Rep, 7*(1), 17696. doi:10.1038/s41598-017-18089-0

Suk, M. (2008). Use of recombinant human BMP-2 in orthopedic trauma. In S. Vukicevic & K. T. Sampath (Eds.), *Bone Morphogenetic*

Proteins: From Local to Systemic Therapeutics (pp. 25-42). Basel: Birkhäuser Basel.

Sun, F., Jiang, Y., Xu, Y., Shi, H., Zhang, S., Liu, X., . . . Zhong, C. (2016). Genipin cross-linked decellularized tracheal tubular matrix for tracheal tissue engineering applications. *Sci Rep, 6*, 24429. doi:10.1038/srep24429

Sun, M., Chang, Q., Xin, M., Wang, Q., Li, H., & Qian, J. (2017). Endogenous bone morphogenetic protein 2 plays a role in vascular smooth muscle cell calcification induced by interleukin 6 in vitro. *Int J Immunopathol Pharmacol, 30*(3), 227-237. doi:10.1177/0394632016689571

Sun, W., Chi, S., Li, Y., Ling, S., Tan, Y., Xu, Y., . . . Li, Y. (2019). The mechanosensitive Piezo1 channel is required for bone formation. *Elife, 8*. doi:10.7554/eLife.47454

Sun, W., Tiemessen, D. M., Sloff, M., Lammers, R. J., de Mulder, E. L. W., Hilborn, J., . . . Oosterwijk, E. (2012). Improving the cell distribution in collagen-coated poly-caprolactone knittings. *Tissue engineering. Part C, Methods, 18*(10), 731-739. doi:10.1089/ten.TEC.2011.0593

Sun, Y., Shao, Y., Xue, X., & Fu, J. (2016). Emerging Roles of YAP/TAZ in Mechanobiology. In S. Chien, A. J. Engler, & P. Y. Wang (Eds.), *Molecular and Cellular Mechanobiology* (pp. 83-96). New York, NY: Springer New York.

Sundararaghavan, H. G., Monteiro, G. A., Lapin, N. A., Chabal, Y. J., Miksan, J. R., & Shreiber, D. I. (2008). Genipin-induced changes in collagen gels: correlation of mechanical properties to fluorescence. *J Biomed Mater Res A, 87*(2), 308-320. doi:10.1002/jbm.a.31715

Suzuki, R., Nemoto, E., & Shimauchi, H. (2014). Cyclic tensile force up-regulates BMP-2 expression through MAP kinase and COX-2/PGE2

signaling pathways in human periodontal ligament cells. *Exp Cell Res, 323*(1), 232-241. doi:10.1016/j.yexcr.2014.02.013

Swift, J., & Discher, D. E. (2014). The nuclear lamina is mechano-responsive to ECM elasticity in mature tissue. *J Cell Sci, 127*(Pt 14), 3005-3015. doi:10.1242/jcs.149203

Swift, J., Ivanovska, I. L., Buxboim, A., Harada, T., Dingal, P. C., Pinter, J., . . . Discher, D. E. (2013). Nuclear lamin-A scales with tissue stiffness and enhances matrix-directed differentiation. *Science, 341*(6149), 1240104. doi:10.1126/science.1240104

Syeda, R., Florendo, M. N., Cox, C. D., Kefauver, J. M., Santos, J. S., Martinac, B., & Patapoutian, A. (2016). Piezo1 Channels Are Inherently Mechanosensitive. *Cell Rep, 17*(7), 1739-1746. doi:10.1016/j.celrep.2016.10.033

Takahashi, K., Tanabe, K., Ohnuki, M., Narita, M., Ichisaka, T., Tomoda, K., & Yamanaka, S. (2007). Induction of pluripotent stem cells from adult human fibroblasts by defined factors. *Cell, 131*(5), 861-872. doi:10.1016/j.cell.2007.11.019

Takahashi, K., & Yamanaka, S. (2006). Induction of pluripotent stem cells from mouse embryonic and adult fibroblast cultures by defined factors. *Cell, 126*(4), 663-676. doi:10.1016/j.cell.2006.07.024

Takahashi, N., Mizuno, Y., Kozai, D., Yamamoto, S., Kiyonaka, S., Shibata, T., . . . Mori, Y. (2008). Molecular characterization of TRPA1 channel activation by cysteine-reactive inflammatory mediators. *Channels, 2*(4), 287-298. doi:10.4161/chan.2.4.6745

Takuwa, Y., Ohse, C., Wang, E. A., Wozney, J. M., & Yamashita, K. (1991). Bone morphogenetic protein-2 stimulates alkaline phosphatase activity and collagen synthesis in cultured osteoblastic cells, MC3T3-E1. *Biochem Biophys Res Commun, 174*(1), 96-101. doi:https://doi.org/10.1016/0006-291X(91)90490-X

Tamma, R., & Ribatti, D. (2017). Bone Niches, Hematopoietic Stem Cells, and Vessel Formation. *International Journal of Molecular Sciences, 18*(1), 151. doi:10.3390/ijms18010151

Tan, F., Huang, Y., Pei, Q., Liu, H., Pei, H., & Zhu, H. (2018). Matrix stiffness mediates stemness characteristics via activating the Yes-associated protein in colorectal cancer cells. *Journal of Cellular Biochemistry*. doi:10.1002/jcb.27532

Tan, J., Xu, X., Tong, Z., Lin, J., Yu, Q., Lin, Y., & Kuang, W. (2015). Decreased osteogenesis of adult mesenchymal stem cells by reactive oxygen species under cyclic stretch: a possible mechanism of age related osteoporosis. *Bone Res, 3*, 15003. doi:10.1038/boneres.2015.3

Tan, Y. Z., Fei, D. D., He, X. N., Dai, J. M., Xu, R. C., Xu, X. Y., . . . Li, B. (2019). L-type voltage-gated calcium channels in stem cells and tissue engineering. *Cell Prolif*, e12623. doi:10.1111/cpr.12623

Tanaka, H., Matsumura, I., Ezoe, S., Satoh, Y., Sakamaki, T., Albanese, C., . . . Kanakura, Y. (2002). E2F1 and c-Myc potentiate apoptosis through inhibition of NF-kappaB activity that facilitates MnSOD-mediated ROS elimination. *Mol Cell, 9*(5), 1017-1029.

Tanaka, Y., Yamaoka, H., Nishizawa, S., Nagata, S., Ogasawara, T., Asawa, Y., . . . Hoshi, K. (2010). The optimization of porous polymeric scaffolds for chondrocyte/atelocollagen based tissue-engineered cartilage. *Biomaterials, 31*(16), 4506-4516. doi:10.1016/j.biomaterials.2010.02.028

Tang, M., Peng, Z., Mai, Z., Chen, L., Mao, Q., Chen, Z., . . . Ai, H. (2014). Fluid shear stress stimulates osteogenic differentiation of human periodontal ligament cells via the extracellular signal-regulated kinase 1/2 and p38 mitogen-activated protein kinase signaling pathways. *J Periodontol, 85*(12), 1806-1813. doi:10.1902/jop.2014.140244

Tang, Y., Wu, X., Lei, W., Pang, L., Wan, C., Shi, Z., . . . Cao, X. (2009). TGF-beta1-induced migration of bone mesenchymal stem cells

couples bone resorption with formation. *Nat Med, 15*(7), 757-765. doi:10.1038/nm.1979

Tasli, P. N., Aydin, S., Yalvac, M. E., & Sahin, F. (2014). Bmp 2 and bmp 7 induce odonto- and osteogenesis of human tooth germ stem cells. *Appl Biochem Biotechnol, 172*(6), 3016-3025. doi:10.1007/s12010-013-0706-0

Taşlı, P. N., Aydın, S., Yalvaç, M. E., & Şahin, F. (2014). Bmp 2 and Bmp 7 Induce Odonto- And Osteogenesis of Human Tooth Germ Stem Cells. *Appl Biochem Biotechnol, 172*(6), 3016-3025. doi:10.1007/s12010-013-0706-0

Termine, J. D., Kleinman, H. K., Whitson, S. W., Conn, K. M., McGarvey, M. L., & Martin, G. R. (1981). Osteonectin, a bone-specific protein linking mineral to collagen. *Cell, 26*(1 Pt 1), 99-105.

Theman, T. A., & Collins, M. T. (2009). The role of the calcium-sensing receptor in bone biology and pathophysiology. *Curr Pharm Biotechnol, 10*(3), 289-301.

Thurner, P. J., Chen, C. G., Ionova-Martin, S., Sun, L., Harman, A., Porter, A., . . . Alliston, T. (2010). Osteopontin deficiency increases bone fragility but preserves bone mass. *Bone, 46*(6), 1564-1573. doi:10.1016/j.bone.2010.02.014

Thurner, P. J., Chen, C. G., Ionova-Martin, S., Sun, L., Harman, A., Porter, A., . . . Alliston, T. (2010). Osteopontin deficiency increases bone fragility but preserves bone mass. *Bone, 46*(6), 1564-1573. doi:10.1016/j.bone.2010.02.014

Tian, Z. H., Liu, W. T., & Li, G. Y. (2016). The microstructure and stability of collagen hydrogel cross-linked by glutaraldehyde. *Polymer Degradation and Stability, 130*, 264-270. doi:10.1016/j.polymdegradstab.2016.06.015

Tomlinson, R. E., Shoghi, K. I., & Silva, M. J. (2014). Nitric oxide-mediated vasodilation increases blood flow during the early stages

of stress fracture healing. *J Appl Physiol (1985), 116*(4), 416-424. doi:10.1152/japplphysiol.00957.2013

Tomlinson, R. E., & Silva, M. J. (2013). Skeletal Blood Flow in Bone Repair and Maintenance. *Bone Research, 1*(4), 311-322. doi:10.4248/BR201304002

Toth, Z., Roi, M., Evans, E., Watson, J. T., Nicolaou, D., & McBride-Gagyi, S. (2019). Masquelet Technique: Effects of Spacer Material and Micro-topography on Factor Expression and Bone Regeneration. *Ann Biomed Eng, 47*(1), 174-189. doi:10.1007/s10439-018-02137-5

Tran, T., & Teoh, C. M. (2014). Role of Integrins in the Regulation of Calcium Signaling. In Y.-X. Wang (Ed.), *Calcium Signaling In Airway Smooth Muscle Cells* (pp. 309-320). Cham: Springer International Publishing.

Tranquillo, R. T., Durrani, M. A., & Moon, A. G. (1992). Tissue engineering science: consequences of cell traction force. *Cytotechnology, 10*(3), 225-250. doi:10.1007/bf00146673

Trappmann, B., Gautrot, J. E., Connelly, J. T., Strange, D. G., Li, Y., Oyen, M. L., . . . Huck, W. T. (2012). Extracellular-matrix tethering regulates stem-cell fate. *Nat Mater, 11*(7), 642-649. doi:10.1038/nmat3339

Travlos, G. S. (2006). Normal Structure, Function, and Histology of the Bone Marrow. *Toxicologic Pathology, 34*(5), 548-565. doi:10.1080/01926230600939856

Tripathi, G., & Basu, B. (2012). A porous hydroxyapatite scaffold for bone tissue engineering: Physico-mechanical and biological evaluations. *Ceramics International, 38*(1), 341-349. doi:https://doi.org/10.1016/j.ceramint.2011.07.012

Tsiapla, A.-R., Karagkiozaki, V., Bakola, V., Pappa, F., Gkertsiou, P., Pavlidou, E., & Logothetidis, S. (2018). Biomimetic and biodegradable cellulose acetate scaffolds loaded with

dexamethasone for bone implants. *Beilstein Journal of Nanotechnology, 9*, 1986-1994. doi:10.3762/bjnano.9.189

Tsimbouri P.M., C. P. G., Pemberton G.D., Yang J, Jayawarna V., Orapiriyakul W., Burgess K., Gonzalez-Garcia C., Thomas D., Giraldo C.V., Biggs M.P., Curtis A.G., Salmeron-Sanchez M., Reid S., Dalby M.J. (2017). 3D osteogenesis of mesenchymal stem cells stimulated by nanovibrational bioreactor in vitro. *Nature Biomedical engineering, 1*, 758-770.

Tsimbouri, P. M., McMurray, R. J., Burgess, K. V., Alakpa, E. V., Reynolds, P. M., Murawski, K., . . . Dalby, M. J. (2012). Using Nanotopography and Metabolomics to Identify Biochemical Effectors of Multipotency. *ACS Nano, 6*(11), 10239-10249. doi:10.1021/nn304046m

Tzelepi, V., Tsamandas, A. C., Zolota, V., & Scopa, C. D. (2009). Bone Anatomy, Physiology and Function. In D. Kardamakis, V. Vassiliou, & E. Chow (Eds.), *Bone Metastases: A translational and clinical approach* (pp. 3-30). Dordrecht: Springer Netherlands.

Uchibori, T., Matsuda, K., Shimodaira, T., Sugano, M., Uehara, T., & Honda, T. (2017). IL-6 trans-signaling is another pathway to upregulate Osteopontin. *Cytokine, 90*, 88-95. doi:10.1016/j.cyto.2016.11.006

Undale, A., Fraser, D., Hefferan, T., Kopher, R. A., Herrick, J., Evans, G. L., . . . Khosla, S. (2011). Induction of Fracture Repair by Mesenchymal Cells Derived from Human Embryonic Stem Cells or Bone Marrow. *Journal of Orthopaedic Research, 29*(12), 1804-1811. doi:10.1002/jor.21480

Ushio-Fukai, M. (2006). Localizing NADPH Oxidase–Derived ROS. *Science's STKE, 2006*(349), re8-re8. doi:10.1126/stke.3492006re8

Valentin, J. E., Stewart-Akers, A. M., Gilbert, T. W., & Badylak, S. F. (2009). Macrophage participation in the degradation and

remodeling of extracellular matrix scaffolds. *Tissue Eng Part A, 15*(7), 1687-1694. doi:10.1089/ten.tea.2008.0419

Viateau, V., Bensidhoum, M., Guillemin, G., Petite, H., Hannouche, D., Anagnostou, F., & Pélissier, P. (2010). Use of the Induced Membrane Technique for Bone Tissue Engineering Purposes: Animal Studies. *Orthopedic Clinics, 41*(1), 49-56. doi:10.1016/j.ocl.2009.07.010

Vining, K. H., & Mooney, D. J. (2017). Mechanical forces direct stem cell behaviour in development and regeneration. *Nature Reviews Molecular Cell Biology, 18*, 728. doi:10.1038/nrm.2017.108

Vining, K. H., & Mooney, D. J. (2017). Mechanical forces direct stem cell behaviour in development and regeneration. *Nat Rev Mol Cell Biol, 18*(12), 728-742. doi:10.1038/nrm.2017.108

Vyklicka, L., Boukalova, S., Macikova, L., Chvojka, S., & Vlachova, V. (2017). The human transient receptor potential vanilloid 3 channel is sensitized via the ERK pathway. *J Biol Chem, 292*(51), 21083-21091. doi:10.1074/jbc.M117.801167

Wagner, W., Wein, F., Seckinger, A., Frankhauser, M., Wirkner, U., Krause, U., . . . Ho, A. D. (2005). Comparative characteristics of mesenchymal stem cells from human bone marrow, adipose tissue, and umbilical cord blood. *Experimental Hematology, 33*(11), 1402-1416. doi:10.1016/j.exphem.2005.07.003

Wanet, A., Arnould, T., Najimi, M., & Renard, P. (2015). Connecting Mitochondria, Metabolism, and Stem Cell Fate. *Stem Cells Dev, 24*(17), 1957-1971. doi:10.1089/scd.2015.0117

Wang, C., Cao, X., & Zhang, Y. (2017). A novel bioactive osteogenesis scaffold delivers ascorbic acid, β-glycerophosphate, and dexamethasone in vivo to promote bone regeneration. *Oncotarget, 8*(19), 31612-31625. doi:10.18632/oncotarget.15779

Wang, H., Sun, W., Ma, J. Q., Pan, Y. C., Wang, L., & Zhang, W. B. (2014). Polycystin-1 Mediates Mechanical Strain-Induced

Osteoblastic Mechanoresponses via Potentiation of Intracellular Calcium and Akt/beta-Catenin Pathway. *PLoS One, 9*(3). doi:10.1371/journal.pone.0091730

Wang, J., Yin, Q., Gu, S., Wu, Y., & Rui, Y. (2019). Induced membrane technique in the treatment of infectious bone defect: A clinical analysis. *Orthopaedics & Traumatology: Surgery & Research, 105*(3), 535-539. doi:https://doi.org/10.1016/j.otsr.2019.01.007

Wang, L., Chen, Y., Sternberg, P., & Cai, J. (2008). Essential roles of the PI3 kinase/Akt pathway in regulating Nrf2-dependent antioxidant functions in the RPE. *Invest Ophthalmol Vis Sci, 49*(4), 1671-1678. doi:10.1167/iovs.07-1099

Wang, L., Du, F. H., & Wang, X. D. (2008). TNF-alpha induces two distinct caspase-8 activation pathways. *Cell, 133*(4), 693-703. doi:10.1016/j.cell.2008.03.036

Wang, L., Li, J. Y., Zhang, X. Z., Liu, L., Wan, Z. M., Li, R. X., & Guo, Y. (2012). Involvement of p38MAPK/NF-kappaB signaling pathways in osteoblasts differentiation in response to mechanical stretch. *Ann Biomed Eng, 40*(9), 1884-1894. doi:10.1007/s10439-012-0548-x

Wang, L., Zhang, X., Guo, Y., Chen, X., Li, R., Liu, L., . . . Zhang, Y. (2010). Involvement of BMPs/Smad signaling pathway in mechanical response in osteoblasts. *Cellular Physiology and Biochemistry, 26*(6), 1093-1102. doi:10.1159/000323987

Wang, L., Zhao, X., Wei, B. Y., Liu, Y., Ma, X. Y., Wang, J., . . . Feng, Y. F. (2015). Insulin improves osteogenesis of titanium implants under diabetic conditions by inhibiting reactive oxygen species overproduction via the PI3K-Akt pathway. *Biochimie, 108*, 85-93. doi:10.1016/j.biochi.2014.10.004

Wang, N., Tytell, J. D., & Ingber, D. E. (2009). Mechanotransduction at a distance: mechanically coupling the extracellular matrix with the

nucleus. *Nature Reviews Molecular Cell Biology, 10*, 75. doi:10.1038/nrm2594

Wang, N., Zhou, Z., Wu, T., Liu, W., Yin, P., Pan, C., & Yu, X. (2016). TNF-alpha-induced NF-kappaB activation upregulates microRNA-150-3p and inhibits osteogenesis of mesenchymal stem cells by targeting beta-catenin. *Open Biol, 6*(3). doi:10.1098/rsob.150258

Wang, S., Zhang, J., Theel, S., Barb, J. J., Munson, P. J., & Danner, R. L. (2006). Nitric oxide activation of Erk1/2 regulates the stability and translation of mRNA transcripts containing CU-rich elements. *Nucleic Acids Res, 34*(10), 3044-3056. doi:10.1093/nar/gkl386

Wang, T., Zhang, X., & Li, J. J. (2002). The role of NF-kappaB in the regulation of cell stress responses. *Int Immunopharmacol, 2*(11), 1509-1520.

Wang, X., Chen, T. X., Leng, L., Fan, J. Q., Cao, K., Duan, Z. X., . . . Ren, Y. (2012). MIF Produced by Bone Marrow-Derived Macrophages Contributes to Teratoma Progression after Embryonic Stem Cell Transplantation. *Cancer Research, 72*(11), 2867-2878. doi:10.1158/0008-5472.Can-11-3247

Wang, X., Wei, F., Luo, F., Huang, K., & Xie, Z. (2015). Induction of granulation tissue for the secretion of growth factors and the promotion of bone defect repair. *J Orthop Surg Res, 10*, 147. doi:10.1186/s13018-015-0287-4

Wang, X. Y., Goh, C. H., & Li, B. J. (2007). p38 Mitogen-activated protein kinase regulates osteoblast differentiation through Osterix. *Endocrinology, 148*(4), 1629-1637. doi:10.1210/en.2006-1000

Wang, Y., Li, Y.-P., Paulson, C., Shao, J.-Z., Zhang, X., Wu, M., & Chen, W. (2014). Wnt and the Wnt signaling pathway in bone development and disease. *Frontiers in bioscience (Landmark edition), 19*, 379-407.

Wang, Y., Wan, C., Deng, L., Liu, X., Cao, X., Gilbert, S. R., . . . Clemens, T. L. (2007). The hypoxia-inducible factor alpha pathway couples

angiogenesis to osteogenesis during skeletal development. *J Clin Invest, 117*(6), 1616-1626. doi:10.1172/JCI31581

Watkins, B. A., Li, Y., Lippman, H. E., & Feng, S. (2003). Modulatory effect of omega-3 polyunsaturated fatty acids on osteoblast function and bone metabolism. *Prostaglandins Leukot Essent Fatty Acids, 68*(6), 387-398.

Watt, F. M., & Huck, W. T. S. (2013). Role of the extracellular matrix in regulating stem cell fate. *Nature Reviews Molecular Cell Biology, 14*, 467. doi:10.1038/nrm3620

Watt, S. M., Tsaknakis, G., Forde, S. P., & Carpenter, L. (2009). Stem Cells, Hypoxia and Hypoxia-Inducible Factors. In V. K. Rajasekhar & M. C. Vemuri (Eds.), *Regulatory Networks in Stem Cells* (pp. 211-231). Totowa, NJ: Humana Press.

Webb, K., Hlady, V., & Tresco, P. A. (1998). Relative importance of surface wettability and charged functional groups on NIH 3T3 fibroblast attachment, spreading, and cytoskeletal organization. *J Biomed Mater Res, 41*(3), 422-430. doi:10.1002/(sici)1097-4636(19980905)41:3<422::aid-jbm12>3.0.co;2-k

Wei, F., Qu, C., Song, T., Ding, G., Fan, Z., Liu, D., . . . Wang, S. (2012). Vitamin C treatment promotes mesenchymal stem cell sheet formation and tissue regeneration by elevating telomerase activity. *Journal of Cellular Physiology, 227*(9), 3216-3224. doi:10.1002/jcp.24012

Wei, J., & Karsenty, G. (2015). An overview of the metabolic functions of osteocalcin. *Curr Osteoporos Rep, 13*(3), 180-185. doi:10.1007/s11914-015-0267-y

Wen, J. H., Vincent, L. G., Fuhrmann, A., Choi, Y. S., Hribar, K. C., Taylor-Weiner, H., . . . Engler, A. J. (2014). Interplay of matrix

stiffness and protein tethering in stem cell differentiation. *Nat Mater, 13*(10), 979-987. doi:10.1038/nmat4051

Weston, C. R., & Davis, R. J. (2007). The JNK signal transduction pathway. *Curr Opin Cell Biol, 19*(2), 142-149. doi:10.1016/j.ceb.2007.02.001

Wolf, K., Te Lindert, M., Krause, M., Alexander, S., Te Riet, J., Willis, A. L., . . . Friedl, P. (2013). Physical limits of cell migration: control by ECM space and nuclear deformation and tuning by proteolysis and traction force. *J Cell Biol, 201*(7), 1069-1084. doi:10.1083/jcb.201210152

Wu, D., Ganatos, P., Spray, D. C., & Weinbaum, S. (2011). On the electrophysiological response of bone cells using a Stokesian fluid stimulus probe for delivery of quantifiable localized picoNewton level forces. *J Biomech, 44*(9), 1702-1708. doi:10.1016/j.jbiomech.2011.03.034

Wu, M., Chen, G., & Li, Y. P. (2016). TGF-beta and BMP signaling in osteoblast, skeletal development, and bone formation, homeostasis and disease. *Bone Res, 4*, 16009. doi:10.1038/boneres.2016.9

Wu, X., Black, L., Santacana-Laffitte, G., & Patrick, C. W., Jr. (2007). Preparation and assessment of glutaraldehyde-crosslinked collagen-chitosan hydrogels for adipose tissue engineering. *J Biomed Mater Res A, 81*(1), 59-65. doi:10.1002/jbm.a.31003

Xiao, E., Yang, H. Q., Gan, Y.-H., Duan, D.-H., He, L.-H., Guo, Y., . . . Zhang, Y. (2015). Brief Reports: TRPM7 Senses Mechanical Stimulation Inducing Osteogenesis in Human Bone Marrow Mesenchymal Stem Cells. *Stem Cells, 33*(2), 615-621. doi:10.1002/stem.1858

Xie, J., Bao, M., Bruekers, S. M. C., & Huck, W. T. S. (2017). Collagen Gels with Different Fibrillar Microarchitectures Elicit Different

Cellular Responses. *ACS Appl Mater Interfaces, 9*(23), 19630-19637. doi:10.1021/acsami.7b03883

Xu, C., Luo, J., He, L., Montell, C., & Perrimon, N. (2017). Oxidative stress induces stem cell proliferation via TRPA1/RyR-mediated Ca(2+) signaling in the Drosophila midgut. *Elife, 6*. doi:10.7554/eLife.22441

Xu, J., & Mosher, D. (2011). Fibronectin and Other Adhesive Glycoproteins. In R. P. Mecham (Ed.), *The Extracellular Matrix: an Overview* (pp. 41-75). Berlin, Heidelberg: Springer Berlin Heidelberg.

Xu, R., Zhang, C., Shin, D. Y., Kim, J. M., Lalani, S., Li, N., . . . Greenblatt, M. B. (2017). c-Jun N-Terminal Kinases (JNKs) Are Critical Mediators of Osteoblast Activity In Vivo. *J Bone Miner Res, 32*(9), 1811-1815. doi:10.1002/jbmr.3184

Xu, W., Liu, B., Liu, X., Chiang, M. Y., Li, B., Xu, Z., & Liao, X. (2016). Regulation of BMP2-induced intracellular calcium increases in osteoblasts. *J Orthop Res, 34*(10), 1725-1733. doi:10.1002/jor.23196

Xue, Z., Niu, L. Y., An, G., Guo, Y. S., Lv, S. C., & Ren, X. P. (2015). Expression of recombinant BMP-7 gene increased ossification activity in the rabbit bone mesenchymal stem cells. *Eur Rev Med Pharmacol Sci, 19*(16), 3056-3062.

Yamada, M., Tsukimura, N., Ikeda, T., Sugita, Y., Att, W., Kojima, N., . . . Ogawa, T. (2013). N-acetyl cysteine as an osteogenesis-enhancing molecule for bone regeneration. *Biomaterials, 34*(26), 6147-6156. doi:10.1016/j.biomaterials.2013.04.064

Yang, C., Tibbitt, M. W., Basta, L., & Anseth, K. S. (2014). Mechanical memory and dosing influence stem cell fate. *Nat Mater, 13*(6), 645-652. doi:10.1038/nmat3889

Yang, G., Crawford, R. C., & Wang, J. H. (2004). Proliferation and collagen production of human patellar tendon fibroblasts in

response to cyclic uniaxial stretching in serum-free conditions. *J Biomech, 37*(10), 1543-1550. doi:10.1016/j.jbiomech.2004.01.005

Yang, J., Andre, P., Ye, L., & Yang, Y.-Z. (2015). The Hedgehog signalling pathway in bone formation. *International Journal Of Oral Science, 7*, 73. doi:10.1038/ijos.2015.14

Yang, J., Kim, M. J., Yoon, W., Kim, E. Y., Kim, H., Lee, Y., . . . Koh, H. (2017). Isocitrate protects DJ-1 null dopaminergic cells from oxidative stress through NADP+-dependent isocitrate dehydrogenase (IDH). *PLoS Genet, 13*(8), e1006975. doi:10.1371/journal.pgen.1006975

Yang, J., McNamara, L. E., Gadegaard, N., Alakpa, E. V., Burgess, K. V., Meek, R. M., & Dalby, M. J. (2014). Nanotopographical induction of osteogenesis through adhesion, bone morphogenic protein cosignaling, and regulation of microRNAs. *ACS Nano, 8*(10), 9941-9953. doi:10.1021/nn504767g

Yang, J., Shi, P., Tu, M., Wang, Y., Liu, M., Fan, F., & Du, M. (2014). Bone morphogenetic proteins: Relationship between molecular structure and their osteogenic activity. *Food Science and Human Wellness, 3*(3), 127-135. doi:https://doi.org/10.1016/j.fshw.2014.12.002

Yang, J. L., McNamara, L. E., Gadegaard, N., Alakpa, E. V., Burgess, K. V., Meek, R. M. D., & Dalby, M. J. (2014). Nanotopographical Induction of Osteogenesis through Adhesion, Bone Morphogenic Protein Cosignaling, and Regulation of MicroRNAs. *ACS Nano, 8*(10), 9941-9953. doi:10.1021/nn504767g

Yang, L., Xu, J., Minobe, E., Yu, L., Feng, R., Kameyama, A., . . . Kameyama, M. (2013). Mechanisms underlying the modulation of L-type Ca2+ channel by hydrogen peroxide in guinea pig ventricular myocytes. *J Physiol Sci, 63*(6), 419-426. doi:10.1007/s12576-013-0279-2

Yang, W., Guo, D., Harris, M. A., Cui, Y., Gluhak-Heinrich, J., Wu, J., . . . Harris, S. E. (2013). Bmp2 in osteoblasts of periosteum and

trabecular bone links bone formation to vascularization and mesenchymal stem cells. *J Cell Sci, 126*(Pt 18), 4085-4098. doi:10.1242/jcs.118596

Yang, X., Meng, X., Su, X., Mauchley, D. C., Ao, L., Cleveland, J. C., Jr., & Fullerton, D. A. (2009). Bone morphogenic protein 2 induces Runx2 and osteopontin expression in human aortic valve interstitial cells: role of Smad1 and extracellular signal-regulated kinase 1/2. *J Thorac Cardiovasc Surg, 138*(4), 1008-1015. doi:10.1016/j.jtcvs.2009.06.024

Yang, X., Yao, J., Luo, Y., Han, Y., Wang, Z., & Du, L. (2013). P38 MAP kinase mediates apoptosis after genipin treatment in non-small-cell lung cancer H1299 cells via a mitochondrial apoptotic cascade. *J Pharmacol Sci, 121*(4), 272-281.

Yang, Y., Wang, B. K., Chang, M. L., Wan, Z. Q., & Han, G. L. (2018). Cyclic Stretch Enhances Osteogenic Differentiation of Human Periodontal Ligament Cells via YAP Activation. *Biomed Res Int, 2018*, 2174824. doi:10.1155/2018/2174824

Yao, M., Goult, B. T., Klapholz, B., Hu, X., Toseland, C. P., Guo, Y., . . . Yan, J. (2016). The mechanical response of talin. *Nat Commun, 7*, 11966. doi:10.1038/ncomms11966

Yasui, T., Kadono, Y., Nakamura, M., Oshima, Y., Matsumoto, T., Masuda, H., . . . Tanaka, S. (2011). Regulation of RANKL-induced osteoclastogenesis by TGF-beta through molecular interaction between Smad3 and Traf6. *J Bone Miner Res, 26*(7), 1447-1456. doi:10.1002/jbmr.357

Yavropoulou, M. P., & Yovos, J. G. (2016). The molecular basis of bone mechanotransduction. *J Musculoskelet Neuronal Interact, 16*(3), 221-236.

Yeh, L. C., Tsai, A. D., & Lee, J. C. (2002). Osteogenic protein-1 (OP-1, BMP-7) induces osteoblastic cell differentiation of the pluripotent

mesenchymal cell line C2C12. *Journal of Cellular Biochemistry, 87*(3), 292-304. doi:10.1002/jcb.10315

Yoo, J. S., Kim, Y. J., Kim, S. H., & Choi, S. H. (2011). Study on genipin: a new alternative natural crosslinking agent for fixing heterograft tissue. *Korean J Thorac Cardiovasc Surg, 44*(3), 197-207. doi:10.5090/kjtcs.2011.44.3.197

Yoon, D. S., Yoo, J. H., Kim, Y. H., Paik, S., Han, C. D., & Lee, J. W. (2010). The effects of COX-2 inhibitor during osteogenic differentiation of bone marrow-derived human mesenchymal stem cells. *Stem Cells Dev, 19*(10), 1523-1533. doi:10.1089/scd.2009.0393

Yoshikawa, H., Tamai, N., Murase, T., & Myoui, A. (2009). Interconnected porous hydroxyapatite ceramics for bone tissue engineering. *J R Soc Interface, 6 Suppl 3*, S341-348. doi:10.1098/rsif.2008.0425.focus

Yoshikawa, H., Tsumaki, N., & Myoui, A. (2009). Bone Biology: Development and Regeneration Mechanisms in Physiological and Pathological Conditions. In M. Santin (Ed.), *Strategies in Regenerative Medicine: Integrating Biology with Materials Design* (pp. 1-18). New York, NY: Springer New York.

You, J., Reilly, G. C., Zhen, X., Yellowley, C. E., Chen, Q., Donahue, H. J., & Jacobs, C. R. (2001). Osteopontin gene regulation by oscillatory fluid flow via intracellular calcium mobilization and activation of mitogen-activated protein kinase in MC3T3-E1 osteoblasts. *J Biol Chem, 276*(16), 13365-13371. doi:10.1074/jbc.M009846200

Yourek, G., McCormick, S. M., Mao, J. J., & Reilly, G. C. (2010). Shear stress induces osteogenic differentiation of human mesenchymal stem cells. *Regenerative medicine, 5*(5), 713-724. doi:10.2217/rme.10.60

Yousefi, A. M., Hoque, M. E., Prasad, R. G., & Uth, N. (2015). Current strategies in multiphasic scaffold design for osteochondral tissue

engineering: A review. *J Biomed Mater Res A, 103*(7), 2460-2481. doi:10.1002/jbm.a.35356

Yousefi, A. M., James, P. F., Akbarzadeh, R., Subramanian, A., Flavin, C., & Oudadesse, H. (2016). Prospect of Stem Cells in Bone Tissue Engineering: A Review. *Stem Cells Int, 2016*, 6180487. doi:10.1155/2016/6180487

Yu, W.-L., Sun, T.-W., Qi, C., Zhao, H.-K., Ding, Z.-Y., Zhang, Z.-W., . . . He, Y.-H. (2017). Enhanced osteogenesis and angiogenesis by mesoporous hydroxyapatite microspheres-derived simvastatin sustained release system for superior bone regeneration. *Sci Rep, 7*, 44129. doi:10.1038/srep44129

Yun, H. Y., Dawson, V. L., & Dawson, T. M. (1999). Glutamate-stimulated calcium activation of Ras/Erk pathway mediated by nitric oxide. *Diabetes Res Clin Pract, 45*(2-3), 113-115.

Yun, M.-S., Kim, S.-E., Jeon, S. H., Lee, J.-S., & Choi, K.-Y. (2005). Both ERK and Wnt/ß-catenin pathways are involved in Wnt3a-induced proliferation. *J Cell Sci, 118*(2), 313-322. doi:10.1242/jcs.01601

Zanotelli, M. R., Goldblatt, Z. E., Miller, J. P., Bordeleau, F., Li, J., VanderBurgh, J. A., . . . Reinhart-King, C. A. (2018). Regulation of ATP utilization during metastatic cell migration by collagen architecture. *Mol Biol Cell, 29*(1), 1-9. doi:10.1091/mbc.E17-01-0041

Zayzafoon, M. (2006). Calcium/calmodulin signaling controls osteoblast growth and differentiation. *Journal of Cellular Biochemistry, 97*(1), 56-70. doi:10.1002/jcb.20675

Zayzafoon, M., Gathings, W. E., & McDonald, J. M. (2004). Modeled microgravity inhibits osteogenic differentiation of human

mesenchymal stem cells and increases adipogenesis. *Endocrinology, 145*(5), 2421-2432. doi:10.1210/en.2003-1156

Zeller, E., Hammer, K., Kirschnick, M., & Braeuning, A. (2013). Mechanisms of RAS/β-catenin interactions. *Archives of Toxicology, 87*(4), 611-632. doi:10.1007/s00204-013-1035-3

Zhang, C. (2010). Transcriptional regulation of bone formation by the osteoblast-specific transcription factor Osx. *J Orthop Surg Res, 5*(1), 37. doi:10.1186/1749-799x-5-37

Zhang, J.-M., & An, J. (2007). Cytokines, inflammation, and pain. *International anesthesiology clinics, 45*(2), 27-37. doi:10.1097/AIA.0b013e318034194e

Zhang, T., Lin, S., Shao, X., Zhang, Q., Xue, C., Zhang, S., . . . Cai, X. (2017). Effect of matrix stiffness on osteoblast functionalization. *Cell Proliferation, 50*(3), e12338. doi:10.1111/cpr.12338

Zhang, W., & Liu, H. T. (2002). MAPK signal pathways in the regulation of cell proliferation in mammalian cells. *Cell Res, 12*(1), 9-18. doi:10.1038/sj.cr.7290105

Zhang, X., Yang, Y., Yao, J., Shao, Z., & Chen, X. (2014). Strong Collagen Hydrogels by Oxidized Dextran Modification. *ACS Sustainable Chemistry & Engineering, 2*(5), 1318-1324. doi:10.1021/sc500154t

Zhang, Y., Pizzute, T., & Pei, M. (2014). A review of crosstalk between MAPK and Wnt signals and its impact on cartilage regeneration. *Cell Tissue Res, 358*(3), 633-649. doi:10.1007/s00441-014-2010-x

Zhao, C., Li, Y., Wang, X., Zou, S., Hu, J., & Luo, E. (2017). The Effect of Uniaxial Mechanical Stretch on Wnt/beta-Catenin Pathway in Bone Mesenchymal Stem Cells. *J Craniofac Surg, 28*(1), 113-117. doi:10.1097/scs.0000000000003252

Zhao, Q., Lu, Y., Gan, X., & Yu, H. (2017). Low magnitude high frequency vibration promotes adipogenic differentiation of bone marrow

stem cells via P38 MAPK signal. *PLoS One, 12*(3), e0172954. doi:10.1371/journal.pone.0172954

Zhao, X., Han, Y., Li, J., Cai, B., Gao, H., Feng, W., . . . Li, D. (2017). BMP-2 immobilized PLGA/hydroxyapatite fibrous scaffold via polydopamine stimulates osteoblast growth. *Mater Sci Eng C Mater Biol Appl, 78*, 658-666. doi:10.1016/j.msec.2017.03.186

Zhao, Y., Hu, X., Liu, Y., Dong, S., Wen, Z., He, W., . . . Shi, M. (2017). ROS signaling under metabolic stress: cross-talk between AMPK and AKT pathway. *Mol Cancer, 16*(1), 79. doi:10.1186/s12943-017-0648-1

Zhou, S., Zu, Y., Sun, Z., Zhuang, F., & Yang, C. (2015). Effects of Hypergravity on Osteopontin Expression in Osteoblasts. *PLoS One, 10*(6), e0128846-e0128846. doi:10.1371/journal.pone.0128846

Zhou, Y., Guan, X., Liu, T., Wang, X., Yu, M., Yang, G., & Wang, H. (2015). Whole body vibration improves osseointegration by up-regulating osteoblastic activity but down-regulating osteoblast-mediated osteoclastogenesis via ERK1/2 pathway. *Bone, 71*, 17-24. doi:https://doi.org/10.1016/j.bone.2014.09.026

Zhou, Y., Guan, X., Zhu, Z., Gao, S., Zhang, C., Li, C., . . . Yu, H. (2011). Osteogenic differentiation of bone marrow-derived mesenchymal stromal cells on bone-derived scaffolds: effect of microvibration and role of ERK1/2 activation. *Eur Cell Mater, 22*, 12-25.

Zhu, S. Q., Pan, A. P., Zheng, L. Y., Wu, Y., & Xue, A. Q. (2018). Posterior scleral reinforcement using genipin-cross-linked sclera for macular hole retinal detachment in highly myopic eyes. *Br J Ophthalmol, 102*(12), 1701-1704. doi:10.1136/bjophthalmol-2017-311340

Zhu, S. Q., Zheng, L. Y., Pan, A. P., Yu, A. Y., Wang, Q. M., & Xue, A. Q. (2016). The efficacy and safety of posterior scleral reinforcement using genipin cross-linked sclera for macular detachment and retinoschisis in highly myopic eyes. *Br J*

Ophthalmol, 100(11), 1470-1475. doi:10.1136/bjophthalmol-2015-308087

Zhu, Y. K., Umino, T., Liu, X. D., Wang, H. J., Romberger, D. J., Spurzem, J. R., & Rennard, S. I. (2001). Contraction of fibroblast-containing collagen gels: initial collagen concentration regulates the degree of contraction and cell survival. *In Vitro Cell Dev Biol Anim, 37*(1), 10-16. doi:10.1290/1071-2690(2001)037<0010:COFCCG>2.0.CO;2

Ziello, J. E., Jovin, I. S., & Huang, Y. (2007). Hypoxia-Inducible Factor (HIF)-1 regulatory pathway and its potential for therapeutic intervention in malignancy and ischemia. *The Yale journal of biology and medicine, 80*(2), 51-60.

Zuidema, J. M., Rivet, C. J., Gilbert, R. J., & Morrison, F. A. (2014). A protocol for rheological characterization of hydrogels for tissue engineering strategies. *J Biomed Mater Res B Appl Biomater, 102*(5), 1063-1073. doi:10.1002/jbm.b.33088